



TECHNISCHE  
UNIVERSITÄT  
WIEN

# Dissertation

## **DIAZIRINE-FAD: A STABLE COFACTOR FOR BIOCATALYSTS AND A MOLECULAR PROBE**

ausgeführt zum Zwecke der Erlangung des akademischen Grades eines  
Doktors unter der Leitung von

**Prof. Dr. Marko D. Mihovilovic**

**&**

**Assoc. Prof. Dr. Florian Rudroff**

ausgeführt am

**Institut für Angewandte Synthesechemie, E163**

eingereicht an der Technischen Universität Wien

**Fakultät für Technische Chemie**

von

**Dipl. Ing. Bsc. Clemens Cziegler**

Feldmühlgasse 15, 1130 Wien

Wien, Oktober 2022

*"Let everything happen to you: Beauty and terror. Just keep going. No feeling is final."*

*- Rainer Maria Rilke*

Für meine Eltern.

# Declaration of contribution

The experimental work in chapter C IV was conducted by Dr. Su Ma, Dr. Erik Breslmayer, Dr. Florian Csarman from the University of Natural Resources and Life Sciences, Vienna, and the author. The experiments were supervised by Assoc. Prof. Dr. Roland Ludwig.



# Front Matter

## Table of Contents

Declaration of contribution	iv	
Front Matter	i	
Table of Contents	i	
Acknowledgments	vii	
Abstract	ix	
Kurzfassung	x	
<b>A</b>	<b>Synthetic schemes</b>	<b>12</b>
A I	Aliphatic diazirine building blocks	13
A II	Aromatic diazirine building blocks I	14
A III	Aromatic diazirine building blocks II	15
A IV	Adenosine building blocks—Protection of hydroxyl groups	16
A V	Esterification of adenosine I	17
A VI	Esterification of adenosine II	18
A VII	Deprotection of esters of adenosine	19
A VIII	Diazirine-FAD—Esters I	20
A IX	Diazirine-FAD—Esters II	21
A X	Adenosine building blocks—Amines I	22
A XI	Adenosine building blocks—Amines II	23
A XII	Amide building blocks I	24
A XIII	Amide building blocks II	25
A XIV	Adenosine building blocks—Amines with alteration of stereochemistry I	26
A XV	Adenosine building blocks—Amines with alteration of stereochemistry II	27
A XVI	Amide building blocks III	28
A XVII	Amide building blocks IV	29
A XVIII	Amide building blocks V	30
A XIX	Mono phosphates—Amides	30
A XX	Diazirine-FAD—Amides	34
A XXI	Fluorescent dyes	37
A XXII	Aminating reagent	37
A XXIII	Building blocks for modifications of the riboflavin moiety	38
<b>B</b>	<b>Introduction</b>	<b>39</b>
B I	Prelude	39
B II	A brief history of biocatalysis	40

<b>B III</b>	<b>Classification of enzymes</b>	<b>45</b>
<b>B IV</b>	<b>Cofactor-dependent enzymes</b>	<b>46</b>
B IV.1	Classification of cofactors	46
B IV.1.1	Inorganic cofactors	47
B IV.1.2	Organic cofactors	48
B IV.2	Flavin-dependent enzymes	54
B IV.2.1	Flavin derivatives and cofactors	55
B IV.2.2	Reactions and the classification of flavin-dependent enzymes	58
B IV.2.3	Flavin-dependent oxidases and dehydrogenases	60
B IV.2.4	Flavin-dependent monooxygenases	60
B IV.2.5	Flavin-dependent reductases	61
B IV.3	The GMC-type oxidase family and Baeyer-Villiger monooxygenases	61
B IV.3.1	The GMC-type oxidase family	62
B IV.3.1.1	Glucose oxidase	63
B IV.3.1.2	Mechanistic aspects of glucose oxidase	64
B IV.3.1.3	Applications of glucose oxidase	64
B IV.3.2	Cellobiose dehydrogenase	65
B IV.3.2.1	Mechanistic aspects of cellobiose dehydrogenase	66
B IV.3.2.2	Applications of cellobiose dehydrogenase	66
B IV.4	Baeyer-Villiger monooxygenases	67
B IV.4.1	The enzymatic mechanism of BVMOs	70
B IV.4.2	Structures of BVMOs	71
B IV.4.3	Applications of BVMOs	72
B IV.4.4	Cyclohexanone monooxygenase	72
<b>B V</b>	<b>The stability of enzymes</b>	<b>73</b>
B V.1	Thermodynamic versus kinetic stability	73
B V.1.1	Thermodynamic stability	73
B V.1.2	Kinetic stability	74
B V.2	The role of the flavin cofactor on enzymes' stability and activity	75
B V.2.1	Types of covalent flavin-protein bonds	75
B V.2.2	The redox potential of covalent flavoenzymes	79
B V.2.3	The structural integrity of flavoenzymes and retention of the flavin cofactor	80
B V.2.4	The formation of covalent flavin-protein bonds	81
B V.2.5	Artificial flavinylation	81
<b>B VI</b>	<b>Forming a new covalent bond (Photoaffinity labeling)</b>	<b>82</b>
B VI.1	Photoreactive groups used in photoaffinity labeling	83
B VI.1.1	Diazirines as a photoreactive group	85
B VI.1.2	Applications of diazirines in photoaffinity labeling studies	87
<b>B VII</b>	<b>Objective</b>	<b>93</b>
<b>C</b>	<b>Results and Discussion</b>	<b>95</b>
<b>C I</b>	<b>Synthesis of flavin adenine dinucleotide derivatives</b>	<b>95</b>
C I.1	Retrosynthetic analysis and theoretical considerations of the synthesis of flavin adenine dinucleotide analogs bearing diazirine groups	95
C I.2	Synthesis of FAD analogs	96
C I.3	Possible modifications of the adenosine building block	99
C I.3.1	Direct incorporation of the diazirine unit at the adenosine moiety	101
C I.3.2	Incorporation of the diazirine unit via an aliphatic and aromatic linker	102
C I.4	Possible modifications of the riboflavin building block	102
C I.4.1	Synthesis of riboflavin building blocks	103
<b>C II</b>	<b>Chemical synthesis of building blocks and intermediates towards the synthesis of diazirine-FADs</b>	<b>106</b>
C II.1	Synthesis of aliphatic diazirine linkers	106
C II.2	Synthesis of aromatic diazirine linkers	108
C II.3	Synthesis of a terminal diazirine as an alternative building block	111
C II.4	One-pot synthesis of diazirines from ketones and aldehydes	113
C II.5	Derivatization of adenosine — Synthesis of FAD analogs modified at the adenosine moiety	114
C II.5.1	Protection of the hydroxyl groups at the C-3' and C-5' positions of adenosine	114
C II.5.2	Protection of the hydroxyl groups at the C-2' and C-5' positions of adenosine	115
C II.5.3	Direct incorporation of a diazirine unit at the ribose moiety of adenosine	115

C II.5.4	Etherification of adenosine on the protected adenosine derivatives	116
C II.5.5	Esterification of protected adenosine	118
C II.5.6	Deprotection of protected adenosine ester analogs	120
C II.5.7	5'-O-Phosphorylation of ester analogs of adenosine	122
C II.5.8	The final step—Chemical coupling of adenosine esters with flavin mononucleotide	124
C II.6	Synthesis of amides of adenosine	129
<b>C III</b>	<b>Photolysis of diazirines—Obtaining first insights</b>	<b>150</b>
<b>C IV</b>	<b>Biochemical evaluation of diazidine-FAD analogs on flavoenzymes</b>	<b>159</b>
C IV.1	Glucose oxidase and cellubiose dehydrogenase	160
C IV.2	Cyclohexanone monooxygenase	171
<b>C V</b>	<b>Modifications of the riboflavin building block</b>	<b>178</b>
C V.1	Chemical synthesis of the riboflavin building block—First steps	179
C V.1.1	Protection of 4,5-dimethyl-1,2-phenylenediamine	179
C V.1.2	Protection of D-ribose	179
C V.1.3	Reductive amination	180
C V.1.4	Enzymatic conversion of riboflavin analogs to FAD	181
C V.1.4.1	Transformation of FAD synthetase gene into <i>E. coli</i> .	181
C V.1.4.2	Enzyme expression and purification	182
C V.1.4.3	The enzymatic reaction using purified FAD synthetase	182
<b>D</b>	<b>Conclusion</b>	<b>186</b>
<b>E</b>	<b>Experimental part</b>	<b>188</b>
<b>E I</b>	<b>Materials and methods—standard microbiological techniques</b>	<b>188</b>
E I.1	Standard buffer solutions and media	188
E I.1.1	Buffers	188
E I.1.2	Media	188
E I.1.2.1	Standard media	188
E I.1.2.2	Autoinduction media	189
E I.2	SDS-PAGE	189
E I.2.1	Gel staining	190
E I.3	Transformation of <i>E. coli</i> competent cell	190
E I.3.1	Heat shock transformation	190
E I.4	Growth of bacterial cells for enzyme expression and isolation	191
E I.4.1	CHMO	191
E I.4.2	FAD synthetase	191
E I.5	Enzyme purification	191
E I.5.1	CHMO	191
E I.5.2	FAD synthetase	192
E I.6	Deflavination and Reconstitution	192
E I.6.1	Deflavination of GOx and CDH	192
E I.6.2	Deflavination of CHMO	193
E I.6.3	Reconstitution	193
E I.7	Photolysis experiments	194
E I.7.1	Photolabeling of proteins with diazidine-comprising dyes	194
E I.7.2	Photolabeling of enzymes with diazidine-FADs	194
E I.8	Activity measurement	194
E I.8.1	ABTS-Assay	194
E I.8.2	DCIP-Assay	195
E I.8.3	NADPH-Assay	195
E I.9	Conversion reactions – Kinetic stability of CHMO	196
E I.10	Enzymatic FAD synthesis (FAD synthetase)	197
E I.11	Protein concentration	197
E I.11.1	Bradford-Assay	197
<b>E II</b>	<b>Materials and methods—chemical synthesis</b>	<b>198</b>
E II.1	NMR spectroscopy	198
E II.2	Chromatographic methods	198
E II.3	Melting point	200
E II.4	HR-MS	200
E II.5	Specific rotation	200

<b>E III</b>	<b>General operating proceducer (E°II)</b>	<b>200</b>
E III.1	General procedure A: Synthesis of esters of modified adenosines	200
E III.2	General procedure B: Synthesis of amides of modified adenosines	201
E III.3	General procedure C: Deprotection of TIPDS group	202
E III.4	General procedure D: Deprotection of TBDMS group	202
E III.5	General procedure E: Monophosphate synthesis—Selective phosphorylation of the 5'OH-group.	202
E III.6	General procedure F: Chemical coupling reaction—Modified flavin adenine dinucleotide synthesis	203
<b>E IV</b>	<b>Chemical synthesis</b>	<b>204</b>
E IV.1	Synthesis of aliphatic diazine building blocks	204
E IV.1.1	2-(3-Methyl-3 <i>H</i> -diazirin-3-yl)ethan-1-ol [3]	204
E IV.1.2	3-(2-Iodoethyl)-3-methyl-3 <i>H</i> -diazirine [5]	205
E IV.1.3	3-(2-Bromoethyl)-3-methyl-3 <i>H</i> -diazirine [6]	206
E IV.1.4	3-(3-Methyl-3 <i>H</i> -diazirin-3-yl)propanoic acid [9]	207
E IV.2	Synthesis of Staudinger reagent [57]	208
E IV.2.1	2-(Diphenylphosphaneyl)phenyl 3-(3-methyl-3 <i>H</i> -diazirin-3-yl)propanoate [57]	208
E IV.3	Synthesis of aminating reagent [23]	210
E IV.3.1	Ethyl ( <i>E</i> )- <i>N</i> -((mesitylsulfonyl)oxy)acetimidate [22]	210
E IV.3.2	<i>O</i> -(Mesitylsulfonyl)hydroxylamine [23]	211
E IV.4	Synthesis of aromatic diazine building blocks	212
E IV.4.1	((4-Bromobenzyl)oxy)( <i>tert</i> -butyl)dimethylsilane [11]	213
E IV.4.2	1-(4-((( <i>tert</i> -Butyldimethylsilyl)oxy)methyl)phenyl)-2,2,2-trifluoroethan-1-one [12]	214
E IV.4.3	( <i>Z</i> )-1-(4-((( <i>tert</i> -Butyldimethylsilyl)oxy)methyl)phenyl)-2,2,2-trifluoro- <i>N</i> -(trimethylsilyl)ethan-1-imine [13]	215
E IV.4.4	1-(4-((( <i>tert</i> -Butyldimethylsilyl)oxy)methyl)phenyl)-2,2,2-trifluoroethan-1-imine [14]	216
E IV.4.5	3-(4-((( <i>tert</i> -Butyldimethylsilyl)oxy)methyl)phenyl)-3-(trifluoromethyl)diaziridine [15]	217
E IV.4.6	3-(4-((( <i>tert</i> -Butyldimethylsilyl)oxy)methyl)phenyl)-3-(trifluoromethyl)-3 <i>H</i> -diazirine [16]	219
E IV.4.7	4-(3-(Trifluoromethyl)-3 <i>H</i> -diazirin-3-yl)phenyl)methanol [17]	220
E IV.4.8	4-(3-(Trifluoromethyl)-3 <i>H</i> -diazirin-3-yl)benzoic acid [18]	221
E IV.4.9	3-(4-(Iodomethyl)phenyl)-3-(trifluoromethyl)-3 <i>H</i> -diazirine [19]	222
E IV.5	Synthesis of alternative aromatic diazine building blocks	224
E IV.5.1	4-((3 <i>H</i> -Diazirin-3-yl)methyl)phenol [25]	224
E IV.5.2	<i>tert</i> -Butyl 2-(4-((3 <i>H</i> -diazirin-3-yl)methyl)phenoxy)acetate [27]	225
E IV.5.3	2-(4-((3 <i>H</i> -Diazirin-3-yl)methyl)phenoxy)acetic acid [28]	226
E IV.6	Synthesis of modified adeny building blocks	227
E IV.7	Synthesis of protected adenosine building blocks	228
E IV.7.1	(6 <i>aR</i> ,8 <i>R</i> ,9 <i>R</i> ,9 <i>aS</i> )-8-(6-Amino-9 <i>H</i> -purin-9-yl)-2,2,4,4-tetraisopropyltetrahydro-6 <i>H</i> -furo[3,2- $\eta$ ][1,3,5,2,4]trioxadisilocin-9-ol [1]	228
E IV.7.2	(2 <i>R</i> ,3 <i>R</i> ,4 <i>R</i> ,5 <i>R</i> )-5-(6-Amino-9 <i>H</i> -purin-9-yl)-4-(( <i>tert</i> -butyldimethylsilyl)oxy)-2-((( <i>tert</i> -butyldimethylsilyl)oxy)methyl)tetrahydrofuran-3-ol [30]	229
E IV.8	Synthesis of ester derivates of adenosine and FAD	231
E IV.8.1	(6 <i>aR</i> ,8 <i>R</i> ,9 <i>R</i> ,9 <i>aR</i> )-8-(6-Amino-9 <i>H</i> -purin-9-yl)-2,2,4,4-tetraisopropyltetrahydro-6 <i>H</i> -furo[3,2- $\eta$ ][1,3,5,2,4]trioxadisilocin-9-yl 3-(3-methyl-3 <i>H</i> -diazirin-3-yl)propanoate [31]	231
E IV.8.2	(6 <i>aR</i> ,8 <i>R</i> ,9 <i>R</i> ,9 <i>aR</i> )-8-(6-Amino-9 <i>H</i> -purin-9-yl)-2,2,4,4-tetraisopropyltetrahydro-6 <i>H</i> -furo[3,2- $\eta$ ][1,3,5,2,4]trioxadisilocin-9-yl 4-(3-(trifluoromethyl)-3 <i>H</i> -diazirin-3-yl)benzoate [32]	232
E IV.8.3	(2 <i>R</i> ,3 <i>R</i> ,4 <i>R</i> ,5 <i>R</i> )-5-(6-amino-9 <i>H</i> -purin-9-yl)-4-(( <i>tert</i> -butyldimethylsilyl)oxy)-2-((( <i>tert</i> -butyldimethylsilyl)oxy)methyl)tetrahydrofuran-3-yl 3-(3-methyl-3 <i>H</i> -diazirin-3-yl)propanoate [33]	234
E IV.8.4	(2 <i>R</i> ,3 <i>R</i> ,4 <i>R</i> ,5 <i>R</i> )-5-(6-Amino-9 <i>H</i> -purin-9-yl)-4-(( <i>tert</i> -butyldimethylsilyl)oxy)-2-((( <i>tert</i> -butyldimethylsilyl)oxy)methyl)tetrahydrofuran-3-yl 4-(3-(trifluoromethyl)-3 <i>H</i> -diazirin-3-yl)benzoate [34]	235
E IV.8.5	(2 <i>R</i> ,3 <i>S</i> ,4 <i>R</i> ,5 <i>R</i> )-5-(6-Amino-9 <i>H</i> -purin-9-yl)-4-hydroxy-2-(hydroxymethyl)tetrahydrofuran-3-yl 3-(3-methyl-3 <i>H</i> -diazirin-3-yl)propanoate [37]	237
E IV.8.6	(2 <i>R</i> ,3 <i>S</i> ,4 <i>R</i> ,5 <i>R</i> )-5-(6-Amino-9 <i>H</i> -purin-9-yl)-4-hydroxy-2-(hydroxymethyl)tetrahydrofuran-3-yl 4-(3-(trifluoromethyl)-3 <i>H</i> -diazirin-3-yl)benzoate [38]	238
E IV.8.7	(2 <i>R</i> ,3 <i>S</i> ,4 <i>R</i> ,5 <i>R</i> )-5-(6-Amino-9 <i>H</i> -purin-9-yl)-4-hydroxy-2-((phosphonoxy)methyl)tetrahydrofuran-3-yl 3-(3-methyl-3 <i>H</i> -diazirin-3-yl)propanoate [39]	240
E IV.8.8	(2 <i>R</i> ,3 <i>S</i> ,4 <i>R</i> ,5 <i>R</i> )-5-(6-Amino-9 <i>H</i> -purin-9-yl)-4-hydroxy-2-((phosphonoxy)methyl)tetrahydrofuran-3-yl 3-(3-methyl-3 <i>H</i> -diazirin-3-yl)propanoate [43]	242
E IV.8.9	(2 <i>R</i> ,3 <i>S</i> ,4 <i>R</i> ,5 <i>R</i> )-5-(6-Amino-9 <i>H</i> -purin-9-yl)-2-((((((((2 <i>R</i> ,3 <i>S</i> ,4 <i>S</i> )-5-(7,8-dimethyl-2,4-dioxo-3,4-dihydrobenzo[ <i>g</i> ]pteridin-10(2 <i>H</i> )-yl)-2,3,4-trihydroxypentyl)oxy)(hydroxy)phosphoryl)oxy)(hydroxy)phosphoryl)oxy)methyl)-4-hydroxytetrahydrofuran-3-yl 3-(3-methyl-3 <i>H</i> -diazirin-3-yl)propanoate	244
E IV.9	Synthesis of amide derivatives of adenosine	246
E IV.9.1	(6 <i>aR</i> ,8 <i>R</i> ,9 <i>aR</i> )-8-(6-Amino-9 <i>H</i> -purin-9-yl)-2,2,4,4-tetraisopropylidihydro-6 <i>H</i> -furo[3,2- $\eta$ ][1,3,5,2,4]trioxadisilocin-9(8 <i>H</i> )-one [44]	246

E IV.9.2	(6aR,8R,9S,9aS)-8-(6-Amino-9H-purin-9-yl)-2,2,4,4-tetraisopropyltetrahydro-6H-furo[3,2- f][1,3,5,2,4]trioxadisilocin-9-ol [45]	248
E IV.9.3	(6aR,8R,9S,9aR)-8-(6-Amino-9H-purin-9-yl)-2,2,4,4-tetraisopropyltetrahydro-6H-furo[3,2- f][1,3,5,2,4]trioxadisilocin-9-yl trifluoromethanesulfonate [46]	249
E IV.9.4	9-((6aR,8R,9R,9aS)-9-Azido-2,2,4,4-tetraisopropyltetrahydro-6H-furo[3,2-f][1,3,5,2,4]trioxadisilocin-8-yl)-9H- purin-6-amine [47]	251
E IV.9.5	9-((6aR,8R,9R,9aS)-9-Amino-2,2,4,4-tetraisopropyltetrahydro-6H-furo[3,2-f][1,3,5,2,4]trioxadisilocin-8-yl)- 9H-purin-6-amine [48]	252
E IV.9.6	(2R,3S,4R,5R)-5-(6-amino-9H-purin-9-yl)-4-azido-2-(hydroxymethyl)tetrahydrofuran-3-ol	254
E IV.9.7	(2R,3S,4R,5R)-4-amino-5-(6-Amino-9H-purin-9-yl)-2-(hydroxymethyl)tetrahydrofuran-3-ol	255
E IV.9.8	(2R,4S,5R)-5-(6-Amino-9H-purin-9-yl)-4-((tert-butylidimethylsilyloxy)-2-(((tert- butylidimethylsilyloxy)methyl)dihydrofuran-3(2H)-one [49]	256
E IV.9.9	(2R,3S,4R,5R)-5-(6-Amino-9H-purin-9-yl)-4-((tert-butylidimethylsilyloxy)-2-(((tert- butylidimethylsilyloxy)methyl)tetrahydrofuran-3-ol [50]	257
E IV.9.10	(2R,3S,4R,5R)-5-(6-Amino-9H-purin-9-yl)-4-((tert-butylidimethylsilyloxy)-2-(((tert- butylidimethylsilyloxy)methyl)tetrahydrofuran-3-yl trifluoromethanesulfonate [51]	259
E IV.9.11	9-((2R,3R,4R,5S)-4-Azido-3-((tert-butylidimethylsilyloxy)-5-(((tert- butylidimethylsilyloxy)methyl)tetrahydrofuran-2-yl)-9H-purin-6-amine [52]	260
E IV.9.12	9-((6aR,8R,9R,9aS)-9-Amino-2,2,4,4-tetraisopropyltetrahydro-6H-furo[3,2-f][1,3,5,2,4]trioxadisilocin-8-yl)- 9H-purin-6-amine [53]	262
E IV.9.13	(6aR,8R,9R,9aR)-8-(6-Amino-9H-purin-9-yl)-2,2,4,4-tetraisopropyltetrahydro-6H-furo[3,2- f][1,3,5,2,4]trioxadisilocin-9-yl trifluoromethanesulfonate [64]	263
E IV.9.14	9-((6aR,8R,9S,9aS)-9-Azido-2,2,4,4-tetraisopropyltetrahydro-6H-furo[3,2-f][1,3,5,2,4]trioxadisilocin-8-yl)-9H- purin-6-amine [65]	265
E IV.9.15	9-((6aR,8R,9S,9aS)-9-Amino-2,2,4,4-tetraisopropyltetrahydro-6H-furo[3,2-f][1,3,5,2,4]trioxadisilocin-8-yl)- 9H-purin-6-amine [66]	266
E IV.9.16	(2R,3R,4R,5R)-5-(6-Amino-9H-purin-9-yl)-4-((tert-butylidimethylsilyloxy)-2-(((tert- butylidimethylsilyloxy)methyl)tetrahydrofuran-3-yl trifluoromethanesulfonate [67]	268
E IV.9.17	9-((2R,3R,4S,5S)-4-Azido-3-((tert-butylidimethylsilyloxy)-5-(((tert- butylidimethylsilyloxy)methyl)tetrahydrofuran-2-yl)-9H-purin-6-amine [68]	269
E IV.9.18	9-((2R,3R,4S,5S)-4-Amino-3-((tert-butylidimethylsilyloxy)-5-(((tert- butylidimethylsilyloxy)methyl)tetrahydrofuran-2-yl)-9H-purin-6-amine [69]	271
E IV.9.19	N-((6aR,8R,9R,9aR)-8-(6-Amino-9H-purin-9-yl)-2,2,4,4-tetraisopropyltetrahydro-6H-furo[3,2- f][1,3,5,2,4]trioxadisilocin-9-yl 3-(3-methyl-3H-diazirin-3-yl)propanoate [59]	272
E IV.9.20	N-((6aR,8R,9S,9aS)-8-(6-Amino-9H-purin-9-yl)-2,2,4,4-tetraisopropyltetrahydro-6H-furo[3,2- f][1,3,5,2,4]trioxadisilocin-9-yl)-3-(3-methyl-3H-diazirin-3-yl)propanamide [70]	274
E IV.9.21	N-((6aR,8R,9S,9aS)-8-(6-Amino-9H-purin-9-yl)-2,2,4,4-tetraisopropyltetrahydro-6H-furo[3,2- f][1,3,5,2,4]trioxadisilocin-9-yl)-4-(3-(trifluoromethyl)-3H-diazirin-3-yl)benzamide [72]	276
E IV.9.22	N-((2S,3R,4R,5R)-5-(6-Amino-9H-purin-9-yl)-4-((tert-butylidimethylsilyloxy)-2-(((tert- butylidimethylsilyloxy)methyl)tetrahydrofuran-3-yl)-3-(3-methyl-3H-diazirin-3-yl)propanamide [61]	277
E IV.9.23	N-((2S,3R,4R,5R)-5-(6-Amino-9H-purin-9-yl)-4-((tert-butylidimethylsilyloxy)-2-(((tert- butylidimethylsilyloxy)methyl)tetrahydrofuran-3-yl)-4-(3-(trifluoromethyl)-3H-diazirin-3-yl)benzamide [63]	279
E IV.9.24	N-((2S,3S,4R,5R)-5-(6-Amino-9H-purin-9-yl)-4-((tert-butylidimethylsilyloxy)-2-(((tert- butylidimethylsilyloxy)methyl)tetrahydrofuran-3-yl)-3-(3-methyl-3H-diazirin-3-yl)propanamide [74]	280
E IV.9.25	N-((2S,3S,4R,5R)-5-(6-Amino-9H-purin-9-yl)-4-((tert-butylidimethylsilyloxy)-2-(((tert- butylidimethylsilyloxy)methyl)tetrahydrofuran-3-yl)-4-(3-(trifluoromethyl)-3H-diazirin-3-yl)benzamide [76]	281
E IV.9.26	N-((2R,3R,4S,5R)-2-(6-Amino-9H-purin-9-yl)-4-hydroxy-5-(hydroxymethyl)tetrahydrofuran-3-yl)-3-(3-methyl- 3H-diazirin-3-yl)propanamide [59]	283
E IV.9.27	N-((2R,3S,4S,5R)-2-(6-Amino-9H-purin-9-yl)-4-hydroxy-5-(hydroxymethyl)tetrahydrofuran-3-yl)-3-(3-methyl- 3H-diazirin-3-yl)propanamide [71]	284
E IV.9.28	N-((2R,3S,4S,5R)-2-(6-amino-9H-purin-9-yl)-4-hydroxy-5-(hydroxymethyl)tetrahydrofuran-3-yl)-4-(3- (trifluoromethyl)-3H-diazirin-3-yl)benzamide [73]	285
E IV.9.29	N-((2S,3S,4R,5R)-5-(6-Amino-9H-purin-9-yl)-4-hydroxy-2-(hydroxymethyl)tetrahydrofuran-3-yl)-3-(3-methyl- 3H-diazirin-3-yl)propanamide [61]	287
E IV.9.30	N-((2S,3S,4R,5R)-5-(6-Amino-9H-purin-9-yl)-4-hydroxy-2-(hydroxymethyl)tetrahydrofuran-3-yl)-4-(3- (trifluoromethyl)-3H-diazirin-3-yl)benzamide [63]	288
E IV.9.31	N-((2S,3R,4R,5R)-5-(6-Amino-9H-purin-9-yl)-4-hydroxy-2-(hydroxymethyl)tetrahydrofuran-3-yl)-3-(3-methyl- 3H-diazirin-3-yl)propanamide [75]	290
E IV.9.32	N-((2S,3R,4R,5R)-5-(6-Amino-9H-purin-9-yl)-4-hydroxy-2-(hydroxymethyl)tetrahydrofuran-3-yl)-4-(3- (trifluoromethyl)-3H-diazirin-3-yl)benzamide [77]	291
E IV.10	Synthesis of modified adenosine monophosphates—Amides	293
E IV.10.1	((2R,3S,4R,5R)-5-(6-Amino-9H-purin-9-yl)-3-hydroxy-4-(3-(3-methyl-3H-diazirin-3- yl)propanamido)tetrahydrofuran-2-yl)methyl dihydrogen phosphate [78]	293

E IV.10.2	((2 <i>R</i> ,3 <i>S</i> ,4 <i>S</i> ,5 <i>R</i> )-5-(6-Amino-9 <i>H</i> -purin-9-yl)-3-hydroxy-4-(3-(3-methyl-3 <i>H</i> -diazirin-3-yl)propanamido)tetrahydrofuran-2-yl)methyl dihydrogen phosphate [81]	294
E IV.10.3	((2 <i>R</i> ,3 <i>S</i> ,4 <i>S</i> ,5 <i>R</i> )-5-(6-Amino-9 <i>H</i> -purin-9-yl)-3-hydroxy-4-(4-(3-(trifluoromethyl)-3 <i>H</i> -diazirin-3-yl)benzamido)tetrahydrofuran-2-yl)methyl dihydrogen phosphate [82]	295
E IV.10.4	((2 <i>S</i> ,3 <i>S</i> ,4 <i>R</i> ,5 <i>R</i> )-5-(6-Amino-9 <i>H</i> -purin-9-yl)-4-hydroxy-3-(3-(3-methyl-3 <i>H</i> -diazirin-3-yl)propanamido)tetrahydrofuran-2-yl)methyl dihydrogen phosphate [79]	297
E IV.10.5	((2 <i>S</i> ,3 <i>S</i> ,4 <i>R</i> ,5 <i>R</i> )-5-(6-Amino-9 <i>H</i> -purin-9-yl)-4-hydroxy-3-(4-(3-(trifluoromethyl)-3 <i>H</i> -diazirin-3-yl)benzamido)tetrahydrofuran-2-yl)methyl dihydrogen phosphate [80]	298
E IV.10.6	((2 <i>S</i> ,3 <i>R</i> ,4 <i>R</i> ,5 <i>R</i> )-5-(6-Amino-9 <i>H</i> -purin-9-yl)-4-hydroxy-3-(3-(3-methyl-3 <i>H</i> -diazirin-3-yl)propanamido)tetrahydrofuran-2-yl)methyl dihydrogen phosphate [83]	300
E IV.11	Synthesis of modified flavin adenine dinucleotides—Amides	301
E IV.11.1	((2 <i>R</i> ,3 <i>S</i> ,4 <i>R</i> ,5 <i>R</i> )-5-(6-Amino-9 <i>H</i> -purin-9-yl)-3-hydroxy-4-(3-(3-methyl-3 <i>H</i> -diazirin-3-yl)propanamido)tetrahydrofuran-2-yl)methyl dihydrogen phosphate [85]	302
E IV.11.2	((2 <i>R</i> ,3 <i>S</i> ,4 <i>S</i> ,5 <i>R</i> )-5-(6-Amino-9 <i>H</i> -purin-9-yl)-3-hydroxy-4-(3-(3-methyl-3 <i>H</i> -diazirin-3-yl)propanamido)tetrahydrofuran-2-yl)methyl dihydrogen phosphate [88]	303
E IV.11.3	((2 <i>R</i> ,3 <i>S</i> ,4 <i>S</i> ,5 <i>R</i> )-5-(6-Amino-9 <i>H</i> -purin-9-yl)-3-hydroxy-4-(4-(3-(trifluoromethyl)-3 <i>H</i> -diazirin-3-yl)benzamido)tetrahydrofuran-2-yl)methyl dihydrogen phosphate [89]	305
E IV.11.4	((2 <i>S</i> ,3 <i>S</i> ,4 <i>R</i> ,5 <i>R</i> )-5-(6-Amino-9 <i>H</i> -purin-9-yl)-4-hydroxy-3-(3-(3-methyl-3 <i>H</i> -diazirin-3-yl)propanamido)tetrahydrofuran-2-yl)methyl dihydrogen phosphate [86]	307
E IV.11.5	((2 <i>S</i> ,3 <i>S</i> ,4 <i>R</i> ,5 <i>R</i> )-5-(6-Amino-9 <i>H</i> -purin-9-yl)-4-hydroxy-3-(4-(3-(trifluoromethyl)-3 <i>H</i> -diazirin-3-yl)benzamido)tetrahydrofuran-2-yl)methyl dihydrogen phosphate [87]	308
E IV.11.6	((2 <i>S</i> ,3 <i>R</i> ,4 <i>R</i> ,5 <i>R</i> )-5-(6-Amino-9 <i>H</i> -purin-9-yl)-4-hydroxy-3-(3-(3-methyl-3 <i>H</i> -diazirin-3-yl)propanamido)tetrahydrofuran-2-yl)methyl dihydrogen phosphate [90]	310
E IV.12	Synthesis of fluorescent dyes containing a diazirine linker	311
E IV.12.1	2-(3-Methyl-3 <i>H</i> -diazirin-3-yl)ethyl 2-(2,4,5,7-tetrabromo-3,6-dihydroxy-9 <i>H</i> -xanthen-9-yl)benzoate [92]	312
E IV.12.2	2-(3-Methyl-3 <i>H</i> -diazirin-3-yl)ethyl 2,3,4,5-tetrachloro-6-(6-hydroxy-2,4,5,7-tetraiodo-3-oxo-9,9a-dihydro-3 <i>H</i> -xanthen-9-yl)benzoate [94]	313
E IV.13	Synthesis of modified ribityl building block	314
E IV.13.1	<i>tert</i> -Butyl (2-amino-4,5-dimethylphenyl)carbamate [96]	314
E IV.13.2	(3 <i>aR</i> ,6 <i>R</i> ,6 <i>aR</i> )-6-(Hydroxymethyl)-2,2-dimethyltetrahydrofuro[3,4- <i>d</i> ][1,3]dioxol-4-ol [98]	316

<b>F</b>	<b>Appendix</b>	<b>318</b>
<b>F I</b>	<b>Curriculum vitae</b>	<b>319</b>
<b>F II</b>	<b>List of abbreviations</b>	<b>320</b>
<b>F III</b>	<b>References</b>	<b>321</b>



# Acknowledgments

Die letzten vier Jahre in denen ich an dieser Arbeit gearbeitet habe, stellen zweifelsohne eine der prägensten und lehrreichsten Zeiten in meinem Leben dar. Auf diesem Wege möchte ich den zahlreichen Menschen, die mich auf diesem Lebensabschnitt begleitet haben, bedanken.

Ein großer Dank gilt Marko D. Mihovilovic, der mich als Betreuer in allen Angelegenheiten unterstützte und mir sowohl für wissenschaftliche als auch bürokratische Fragestellungen immer zur Seite stand. Weiters möchte ich mich bei Ihm dafür bedanken, dass er mir dieses spannende und ambitionierte Projekt anvertraut hat und mir dabei stets den notwendigen Freiraum ließ, mich wissenschaftlich entfalten zu können. Er hielt auch in anspruchsvolleren Zeiten an dieser „crazy idea“ fest und konnte mich damit immer entsprechend motivieren. Vielen Dank, Marko!

Ebenfalls gilt mein aufrichtiger Dank Florian Rudroff, der mich nicht nur in meinem Hauptprojekt unterstützte, sondern mir auch kleinere Nebenprojekte anvertraute durch die ich meinen wissenschaftlichen Horizont beständig erweitern konnte.

Danken möchte ich Roland Ludwig für die gute Zusammenarbeit und die Bereitschaft, mich in seinem Labor mitarbeiten zu lassen. In diesem Zusammenhang möchte ich den drei Post-Docs Su Ma, Erik Breselmeyer und Florian Csarman für deren großartige Arbeit und das gute Zusammenwirken an der BOKU bedanken.

Ich bedanke mich beim Wiener Wissenschafts-, Forschungs- und Technologiefonds für die finanzielle Unterstützung in diesem Projekt.

Mein aufrichtiger Dank gilt einmal mehr Roland Ludwig und Uwe Bornscheuer für das Begutachten dieser Arbeit.

Mein Dank gilt Christian Stanetty, Markus Draskovits, Nicolas Kratena und Christoph Suster für das Messen meiner Proben am 600er NMR.

Ein großer Dank gilt Lydia Suchy, die mir bei der Enzym-Expression stets eine große Hilfe war.

Bedanken möchte ich mich bei Hamid Reza Mansouri Khosravi für die Unterstützung bei den Untersuchungen bezüglich des Enzyms FAD-Synthetase.

Weiters möchte ich Matthias Schittmayer-Schantl sowie Isabella Burger aus der Forschungsgruppe von Frau Prof. Birner-Grünberger für die zahlreichen massenspektrometrischen Analysen meinen Dank ausrichten.

Ebenso danken möchte ich Stephanie Steinberger für die Einschulung und das Messen von In-Gel Fluoresenz Proben in der Forschungsgruppe von Frau Prof. Marchetti-Deschmann.

Wenngleich mich die wissenschaftlichen Herausforderungen oft sehr gefordert haben, bin ich dennoch jeden Tag gerne ins Labor gekommen. Danken möchte ich hierfür meinen tollen Kolleg:innen der gesamten BSC-Forschungsgruppe, in der stets eine angenehme Atmosphäre herrschte. Danke für viele inspirierende und lustige Momente im Lab, an die ich gerne zurückdenke. Die Zeit mit Euch im Labor wird mir fehlen.

Meinen Freunden Felix, Luki, Moritz, Philipp und Ufuk danke ich für die Momente außerhalb des Labors.

Besonderer Dank gebührt meinen Eltern Eveline und Kurt, meinem Bruder Andreas und meiner Tante Gitti, die mich immer unterstützt und sich stets um mich gesorgt haben.

Die letzten Jahre wären ohne Dich bei Weitem nicht so lustig und schön gewesen. Danke, dass Du immer für mich da bist, Lena!



# Abstract

Flavin-dependent enzymes represent an extraordinary class of biocatalysts that is important to industry and life. However, although the flavin cofactors empower their tremendous transformations, their cofactor dependency is a limitation. Typically, the cofactors are non-covalently bound to the enzymes, and their dissociation results in the loss of the enzymes' activities and stabilities. This drawback of flavoenzymes compromises their applicability in biosensing and biocatalysis.

In this project, we aimed to develop a general approach for improving the stability of flavoenzymes by covalently binding the cofactor FAD to proteins of interest to impede the cofactor's dissociation. Based on the photoaffinity labeling technique, covalent anchoring of the cofactor should occur only using a light stimulus, which allows tethering at will and thus enables the correct incorporation of the cofactor.

Therefore, we designed and synthesized a set of six FAD analogs bearing a diazirine moiety to allow the photoinduced covalent attachment. Different flavoenzymes, including glucose oxidase (*Aspergillus niger*), glucose dehydrogenase (*Pichia pastoris*), and cyclohexanone monooxygenase (*Acinetobacter calcoaceticus* NCIMB9871), were selected as model enzymes, and suitable protocols for the preparation of apoenzymes and their efficient reconstitution with synthesized FAD analogs were established. The proper incorporation of FAD analogs was studied by specific activity assays, and the light-induced covalent anchoring was confirmed by in-gel fluorescence and mass analysis.

With all enzymes investigated, the activity could be restored by the reconstitution with synthetic FAD analogs, and the best specific activities were similar to the results of control experiments performed with native FAD. Ultimately, the stabilizing effect of the covalent modification was assessed by measuring the thermal and kinetic stability.

The light-induced covalent tethering of the FAD analogs prevents enzyme inactivation by cofactor loss and is considered a unique and novel approach for stabilizing flavoenzymes and enhancing their applicability in biocatalysis and biosensing.

# Kurzfassung

Flavinabhängige Enzyme repräsentieren eine außergewöhnliche Klasse an Biokatalysatoren, die für zahlreiche industrielle Anwendungen von großem Interesse sind, aber auch für alle Tiere, Pflanzen und Mikroorganismen eine besondere Bedeutung zukommt. In der Regel ist der Flavin-Kofaktor nicht kovalent an die Proteinstruktur gebunden. Hieraus resultiert der große Nachteil von Flavoenzymen, da durch die nicht-kovalente Anbindung der Kofaktor aus dem Proteinmolekül dissoziieren kann, wodurch es zu einer raschen Inaktivierung und Denaturierung des Enzyms kommt. Folglich ist die Anwendung von Flavoenzymen in der Biokatalyse für die Herstellung von medizinischen Wirkstoffen oder als Bestandteil in Biosensoren stark eingeschränkt.

In diesem Projekt konzentrierten wir uns auf die Entwicklung einer neuen Methodik zur Stabilisierung von flavinabhängigen Enzymen durch die kovalente Anbindung des FAD-Kofaktors an verschiedene für Biosensoren und Bioprozesse wichtige Enzyme. Inspiriert von der Methode der Photoaffinitätsmarkierung hatten wir das Ziel, die Ausbildung der kovalenten Anbindung nur durch Licht zu initiieren, wodurch die korrekte Einbettung und Anbindung des Kofaktors auf eine nicht invasive Art ermöglicht wird.

Um die photoinduzierte Anbindung zu realisieren, entwarfen und synthetisierten wir sechs FAD-Analoga mit der photolabilen Diazirine-Gruppe. In weiterer Folge entwickelten wir für die drei Modellenzyme Glucose-Oxidase (*Aspergillus niger*), Cellobiose-Dehydrogenase (*Pichia pastoris*) und Cyclohexanon-Monooxygenase (*Acinetobacter calcoaceticus* NCIMB9871) Methoden zur Deflavinierung und deren effizienten Rekonstitution mit den synthetisierten FAD-Derivaten. Die richtige Einbettung der FAD-Analoga wurde durch Messung der spezifischen Aktivitäten des jeweiligen Enzyms untersucht und die lichtinduzierte kovalente Anknüpfung konnte durch Fluoreszenzmessungen von SDS-PAGE Gelen sowie massenspektrometrischen Analysen experimentell bestätigt werden.

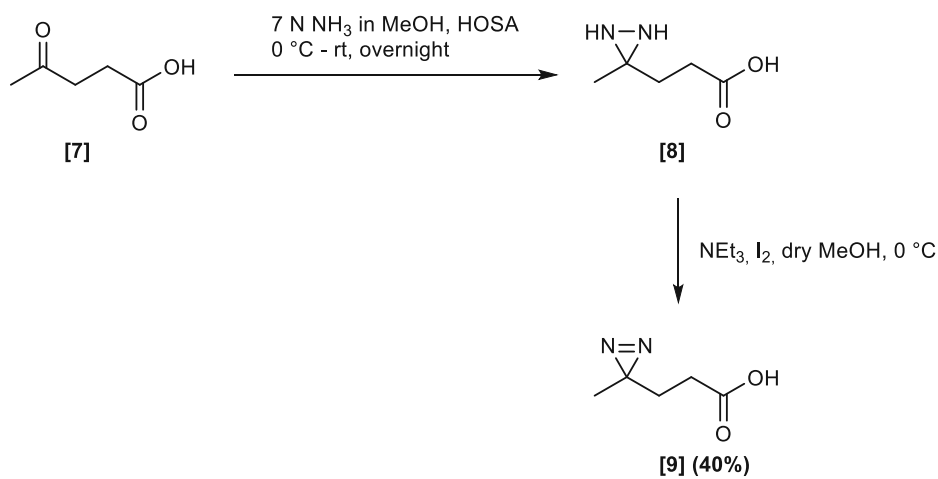
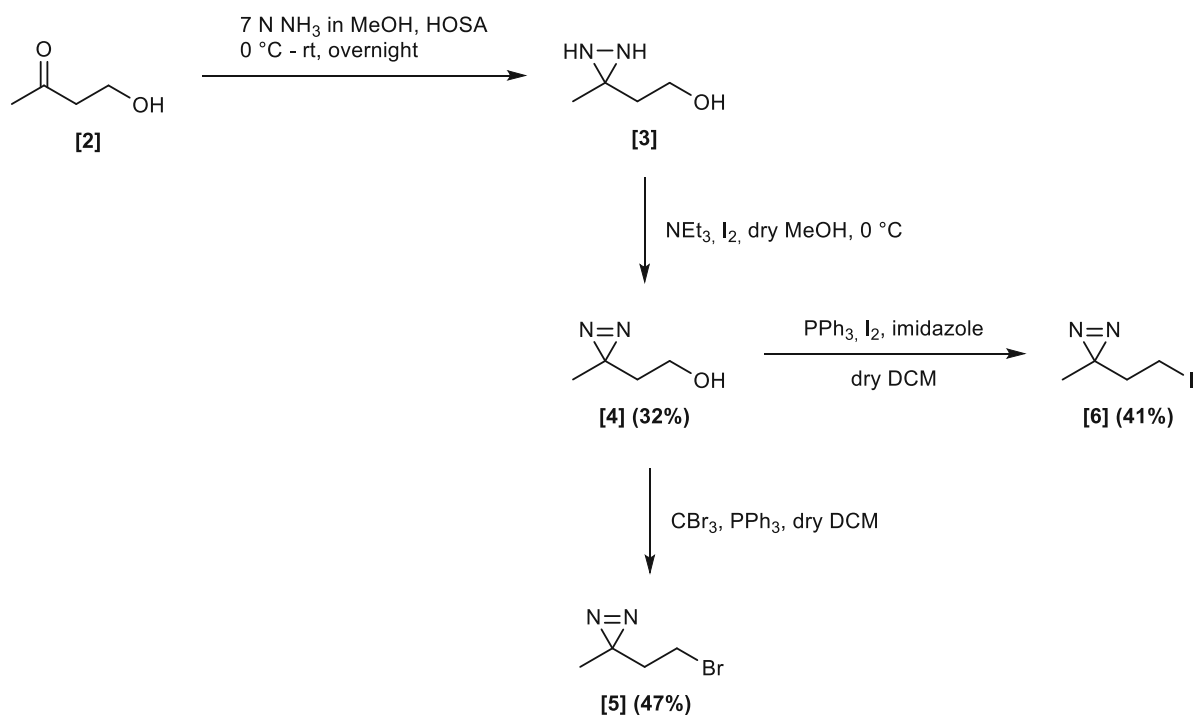
Von allen untersuchten Enzymen konnte die Aktivität durch die Rekonstitution mit den synthetischen FAD-Derivaten wiederhergestellt werden. Die besten spezifischen Aktivitäten waren vergleichbar mit den Ergebnissen von Kontrollexperimenten, die mit nativem FAD-Kofaktor durchgeführt worden sind. Abschließend wurde der stabilisierende Effekt der kovalenten Anbindung durch Messung der thermischen und kinetischen Stabilität untersucht.

Die lichtinduzierte Anknüpfung des Kofaktors FAD an Flavoenzymen verhindert dessen Dissoziation und stellt eine neuartige Methode zur Stabilisierung von Flavoproteinen dar, wodurch deren Einsatz in der Biokatalyse und in Biosensoren verbessert werden kann.

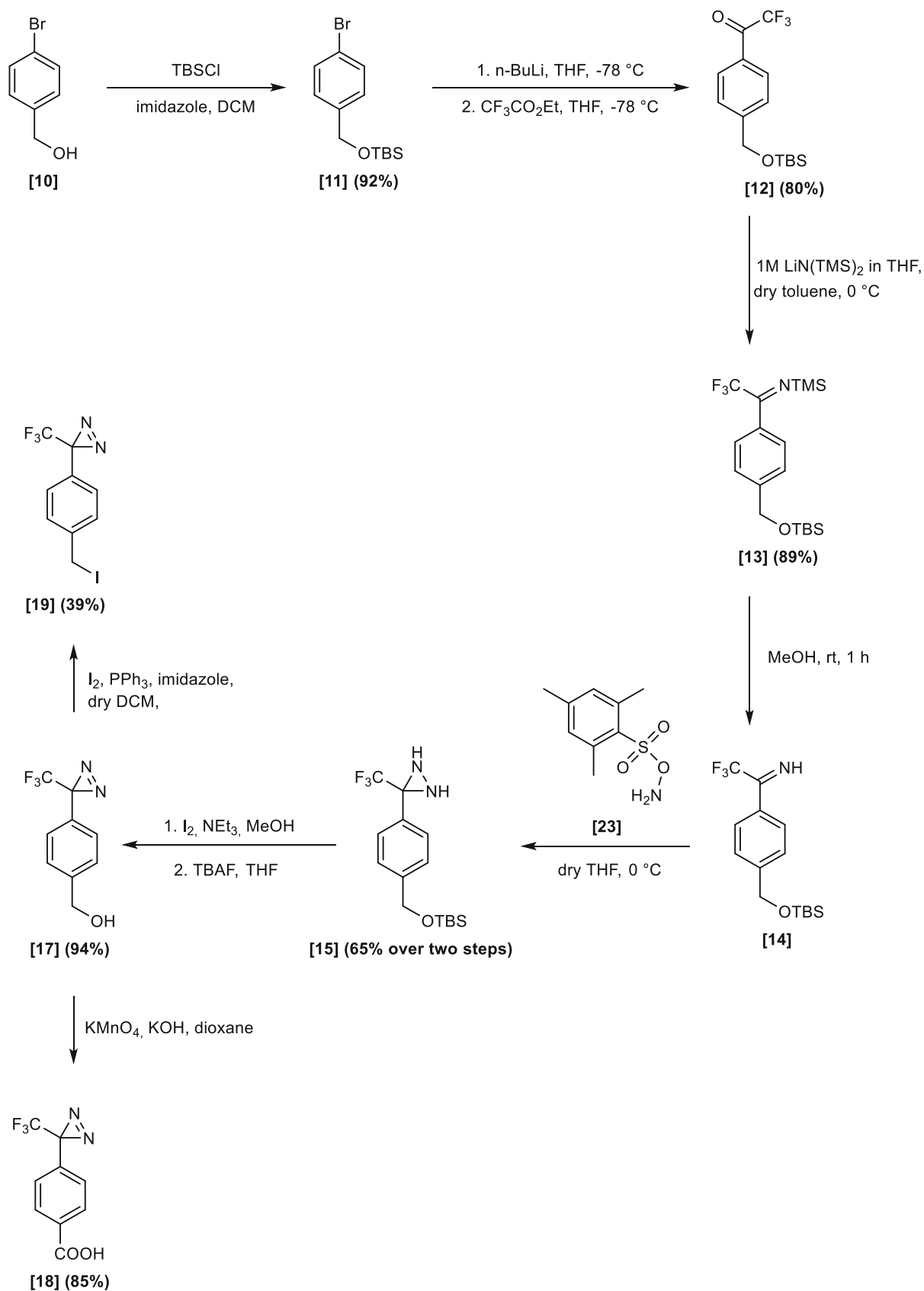
# A Synthetic schemes

All compounds prepared or used as starting materials in this thesis are numbered in bold Arabic numerals. Additionally, compounds unknown in the literature are underlined. Compounds referred to in the literature or presented hypothetically are numbered in bold Roman numerals.

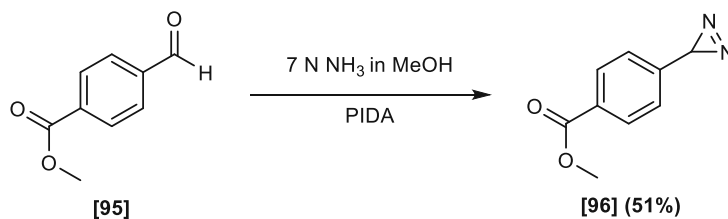
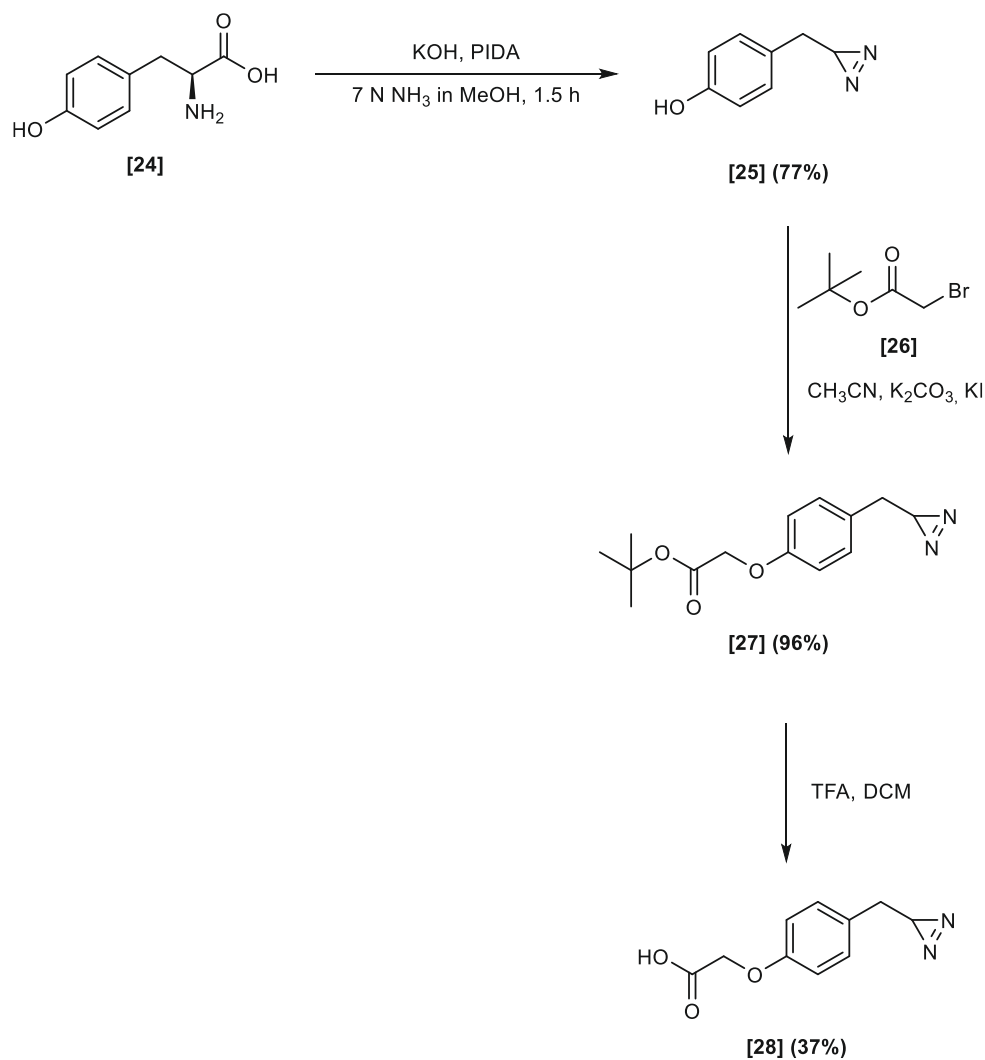
# A I Aliphatic diazirine building blocks



## A II Aromatic diazirine building blocks I

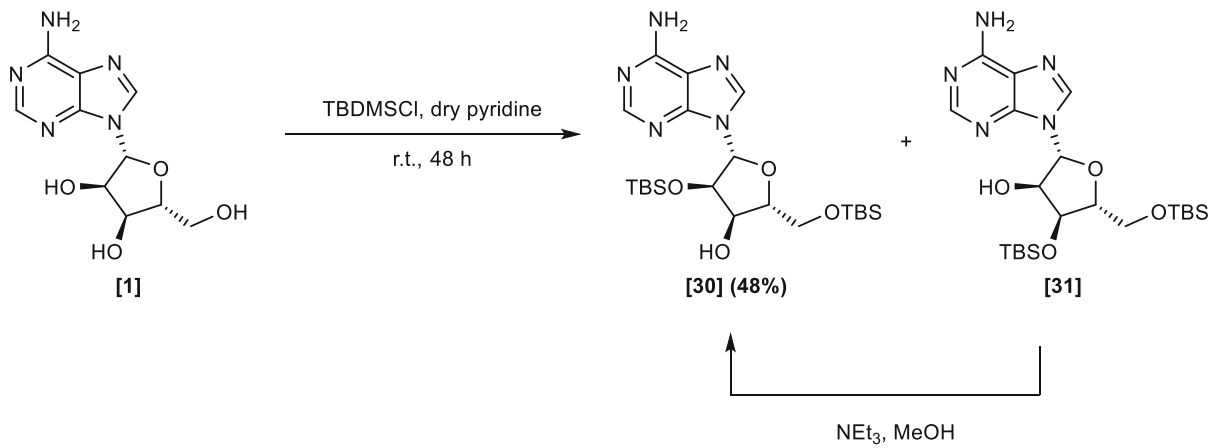
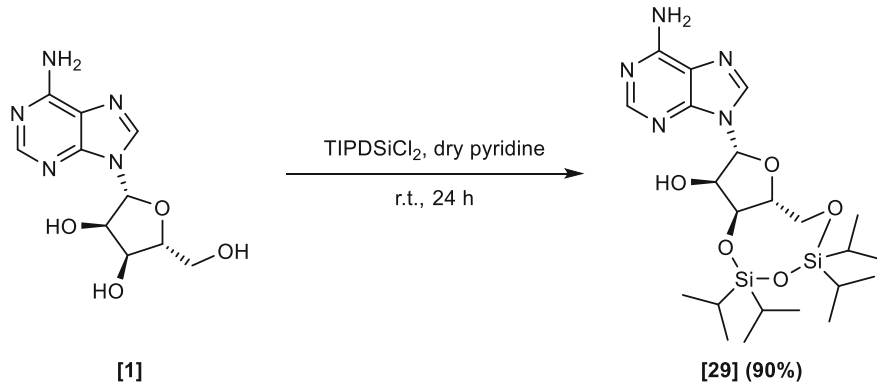


## A III Aromatic diazirine building blocks II



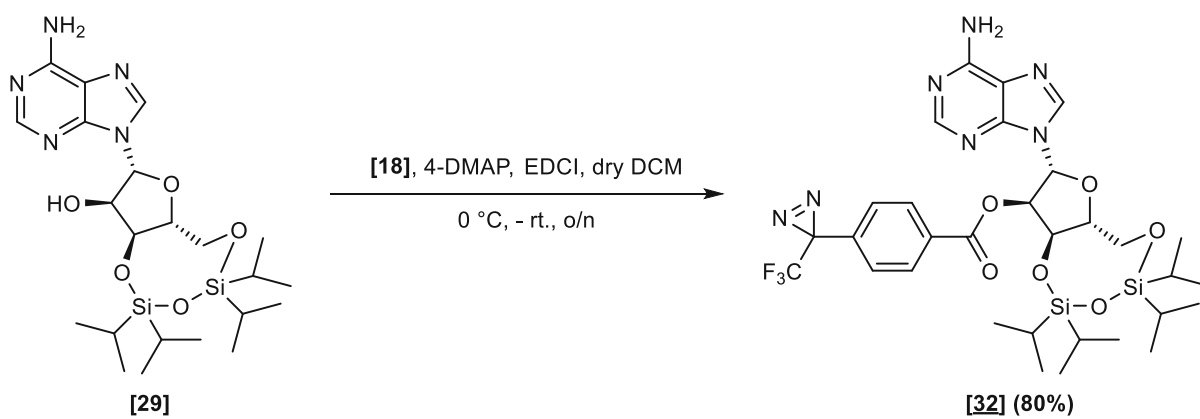
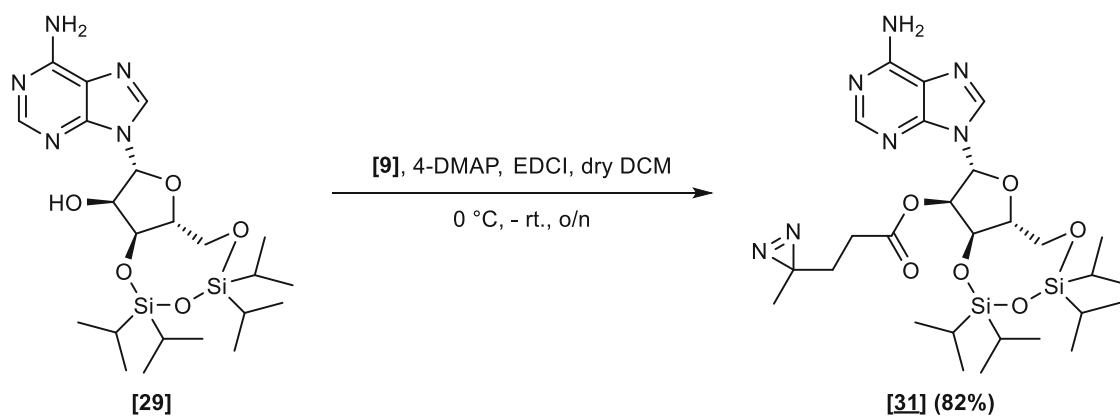
# A IV Adenosine building blocks—

## Protection of hydroxyl groups

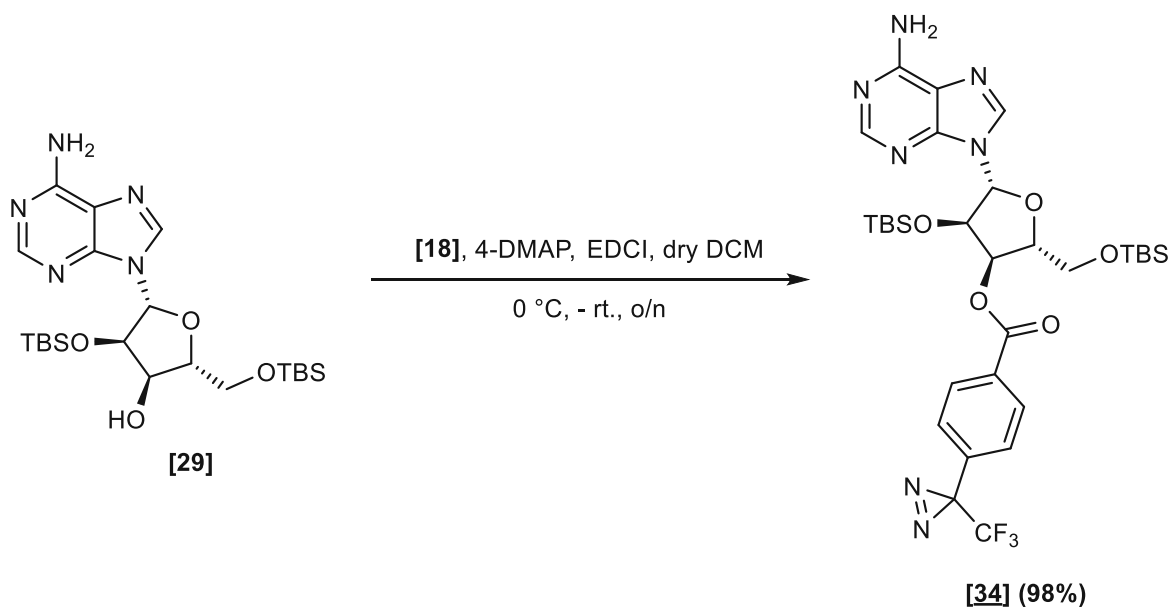
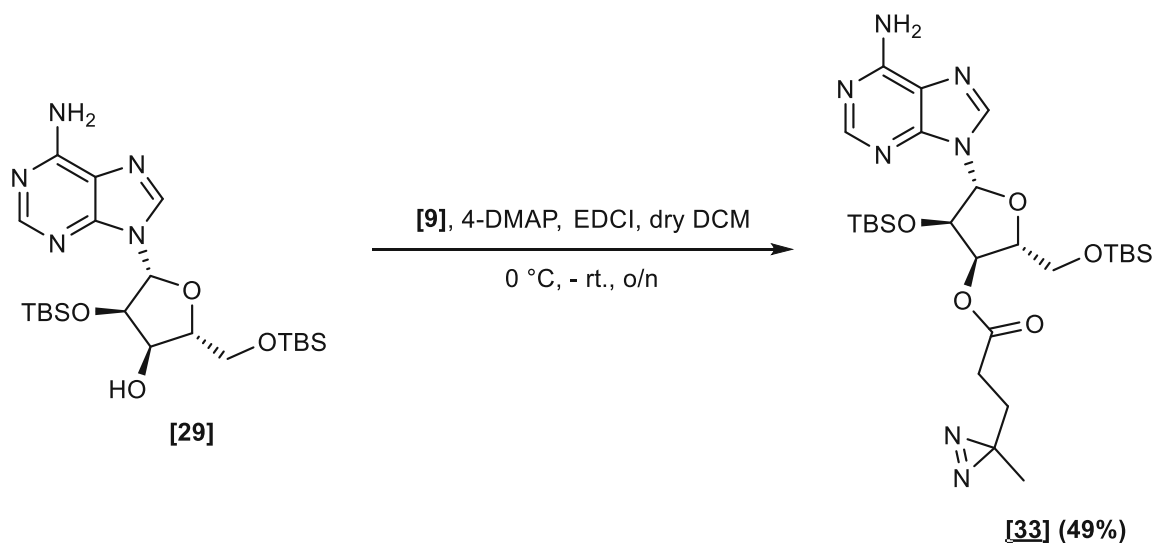




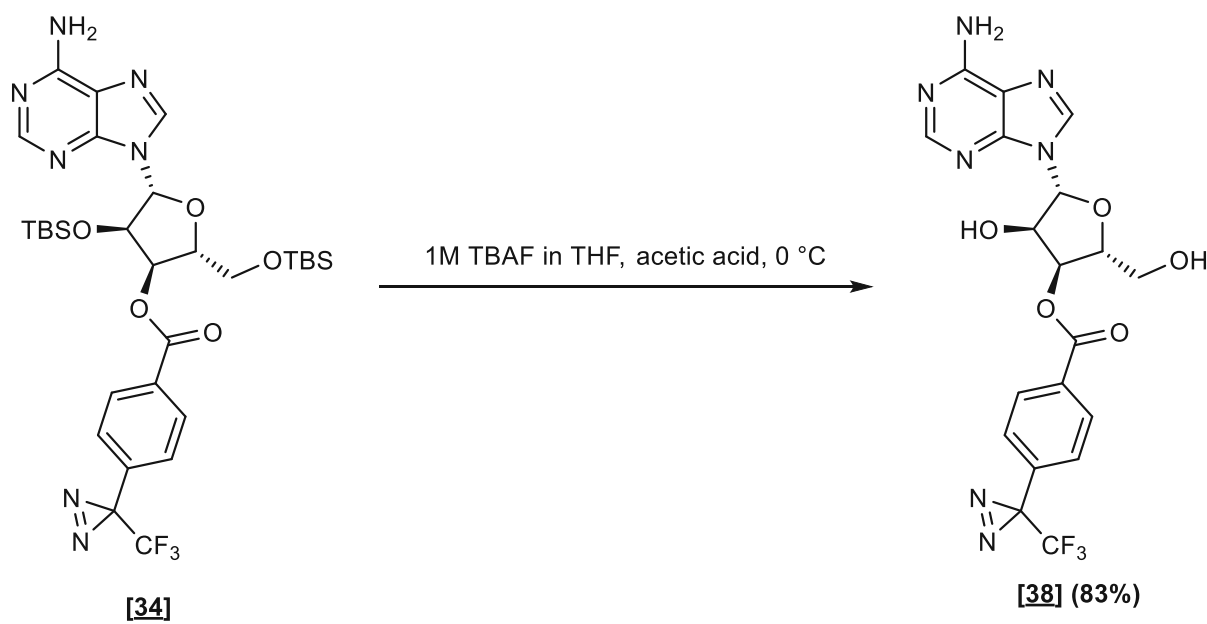
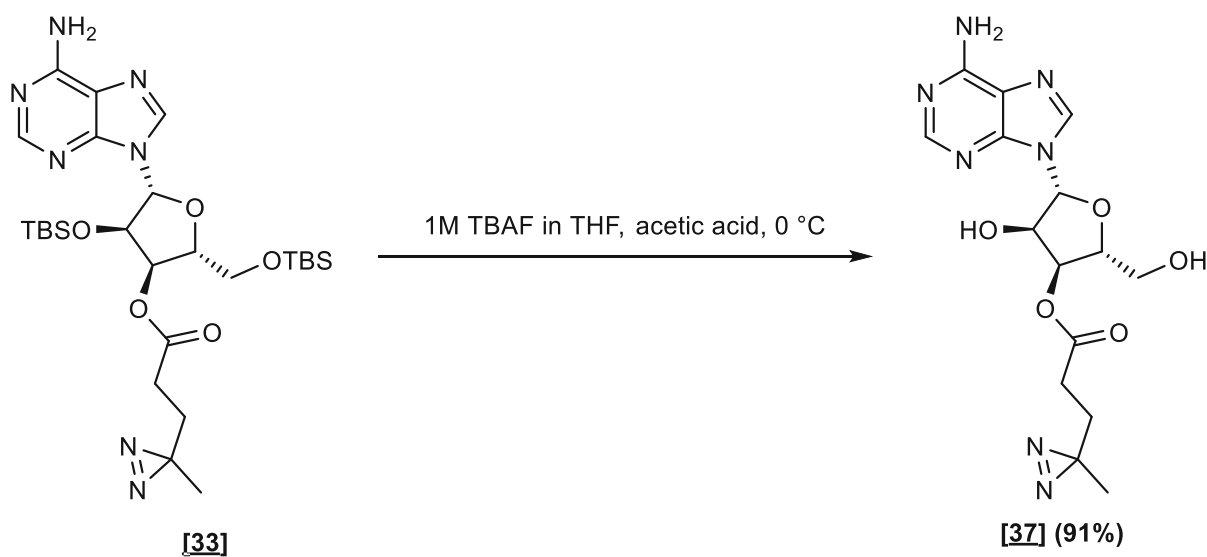
## A V Esterification of adenosine I



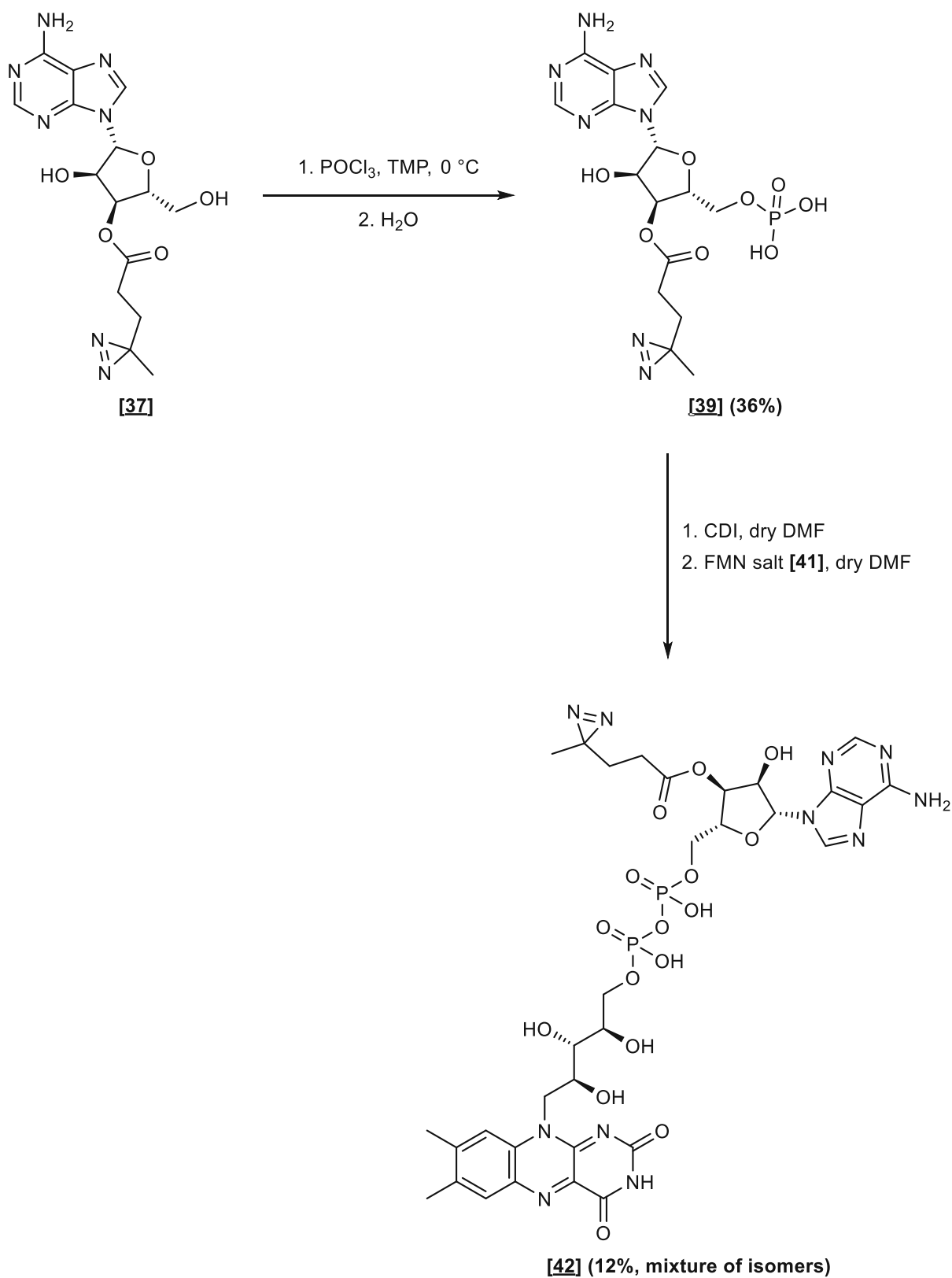
## A VI Esterification of adenosine II



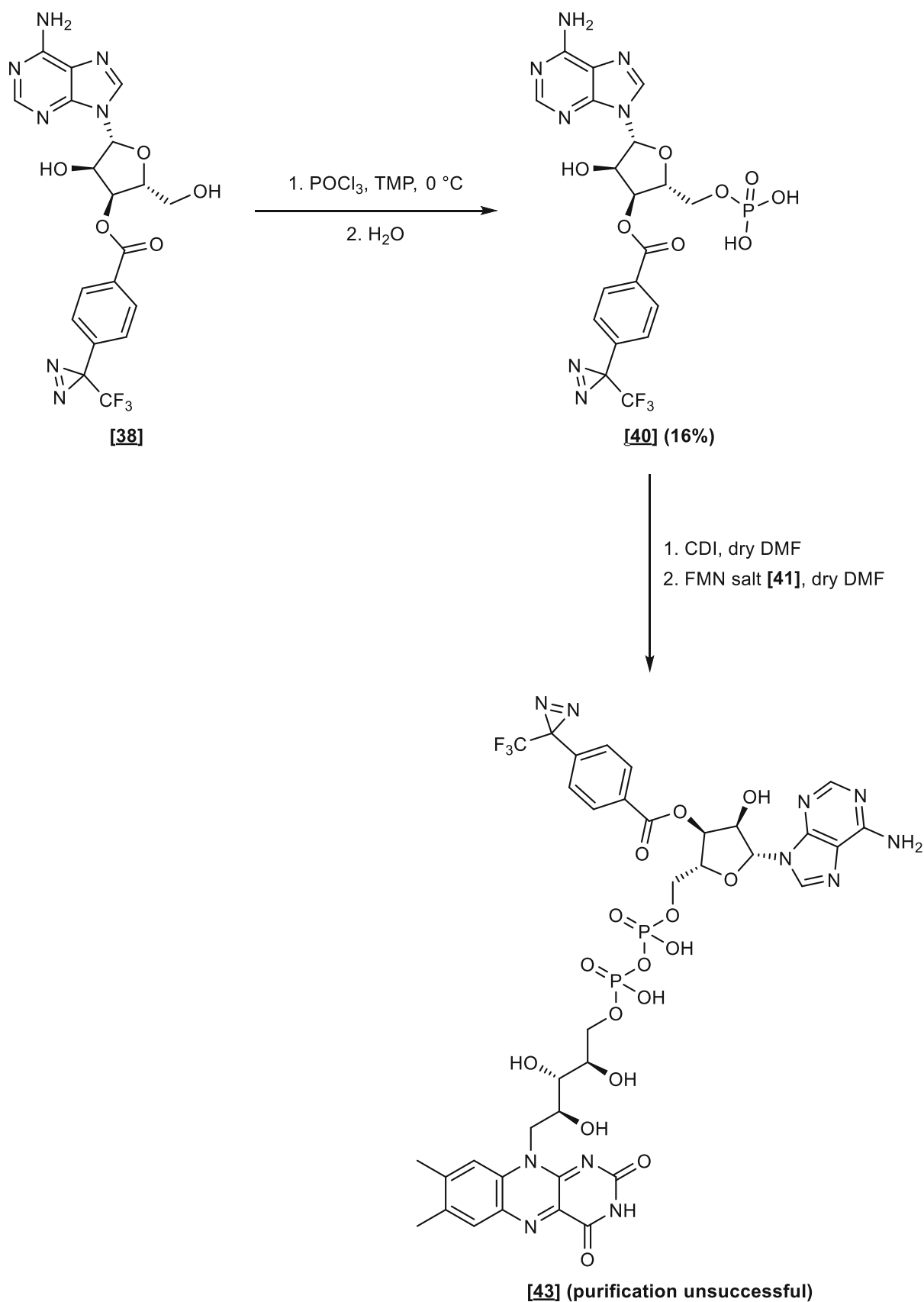
## A VII Deprotection of esters of adenosine



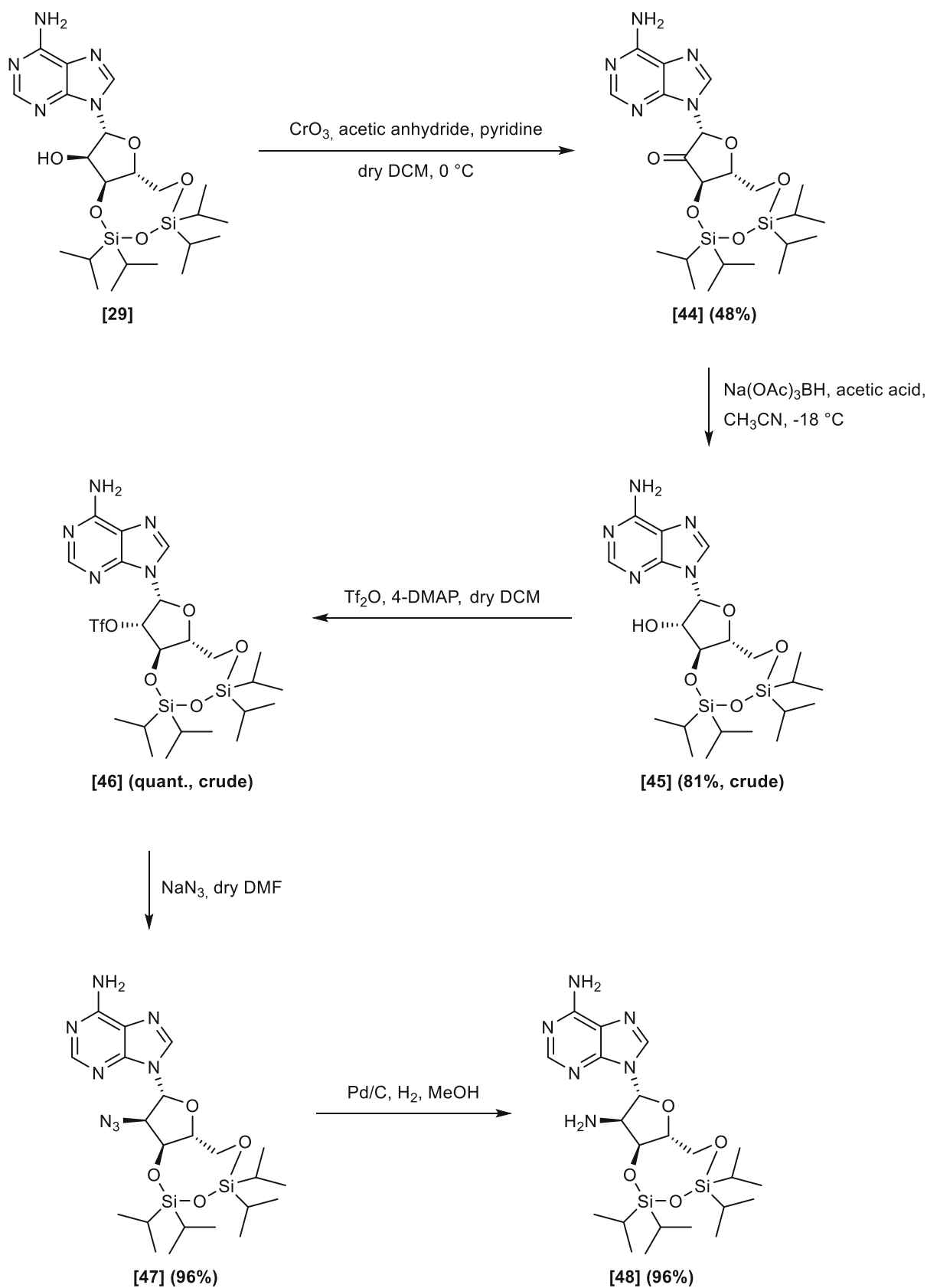
## A VIII Diazirine-FAD—Esters I



## A IX Diazirine-FAD—Esters II

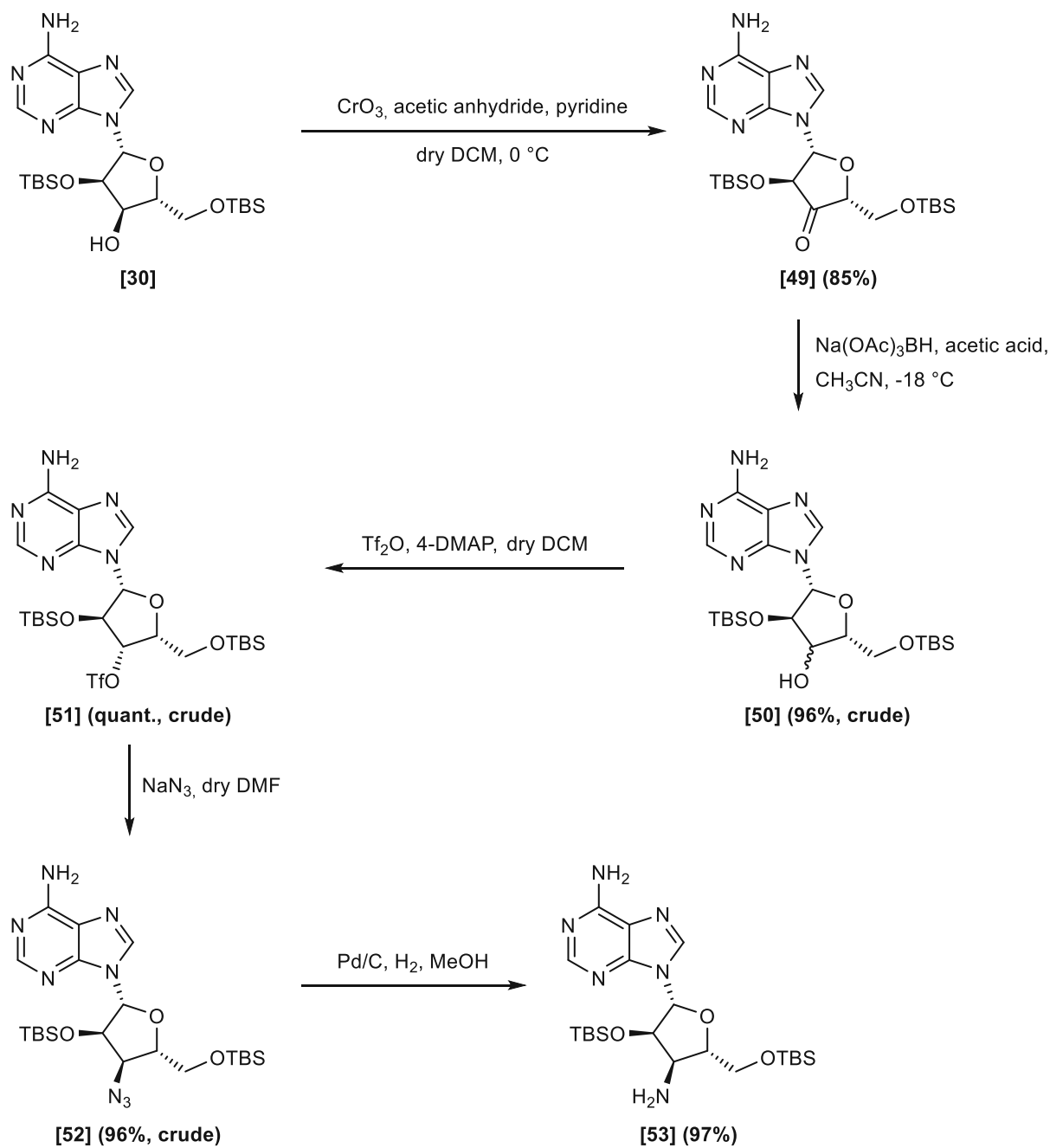


# A X Adenosine building blocks—Amines I

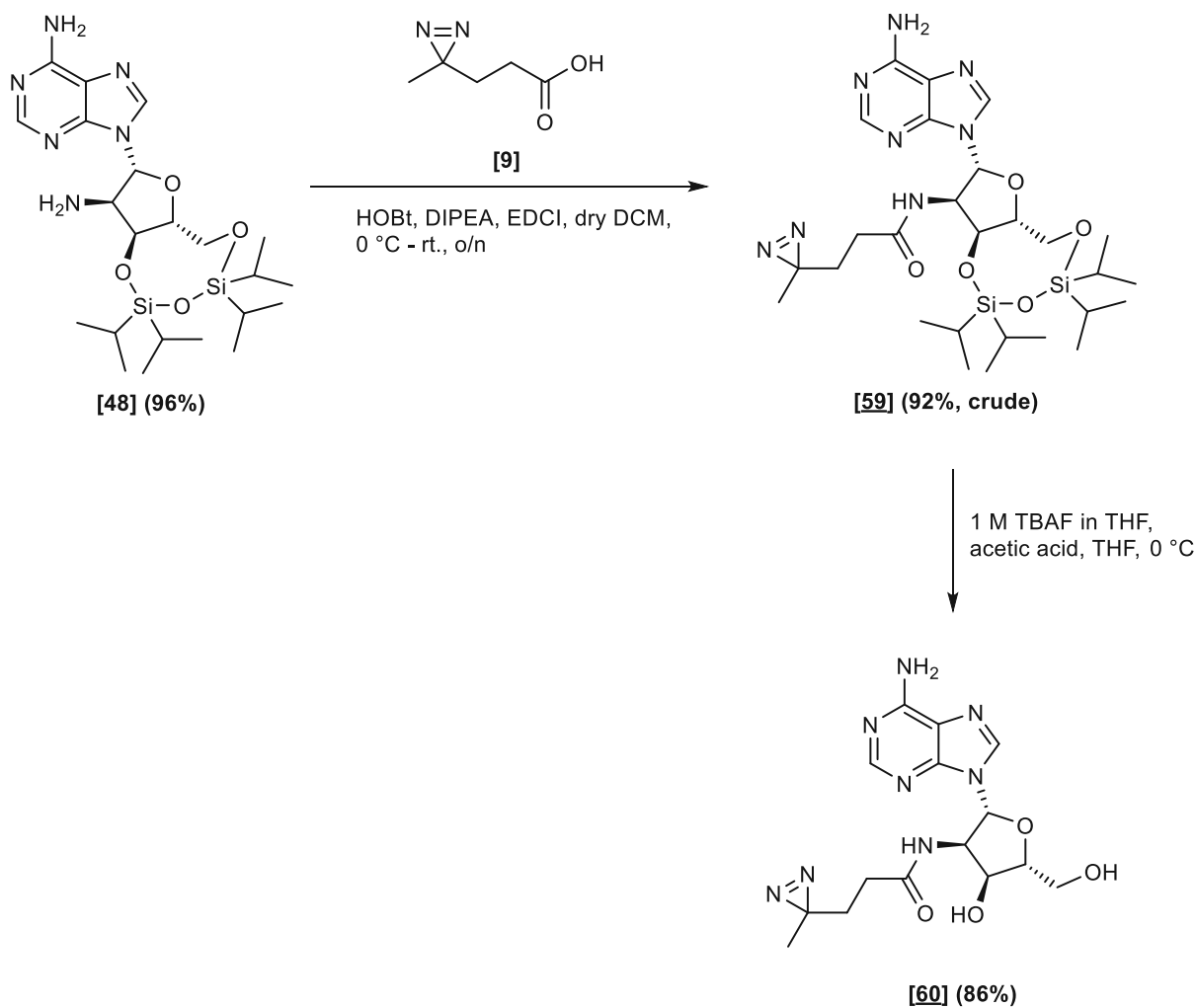


# A XI Adenosine building blocks—Amines

## II

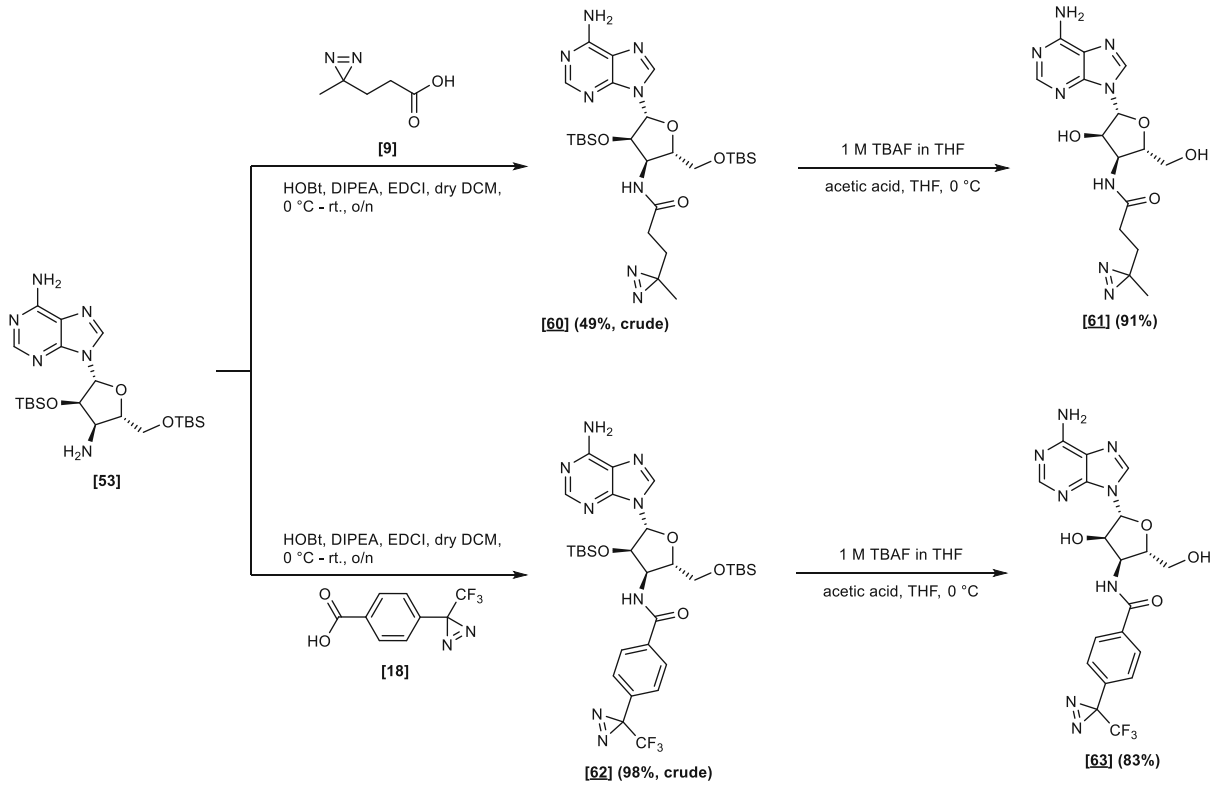


## A XII Amide building blocks I

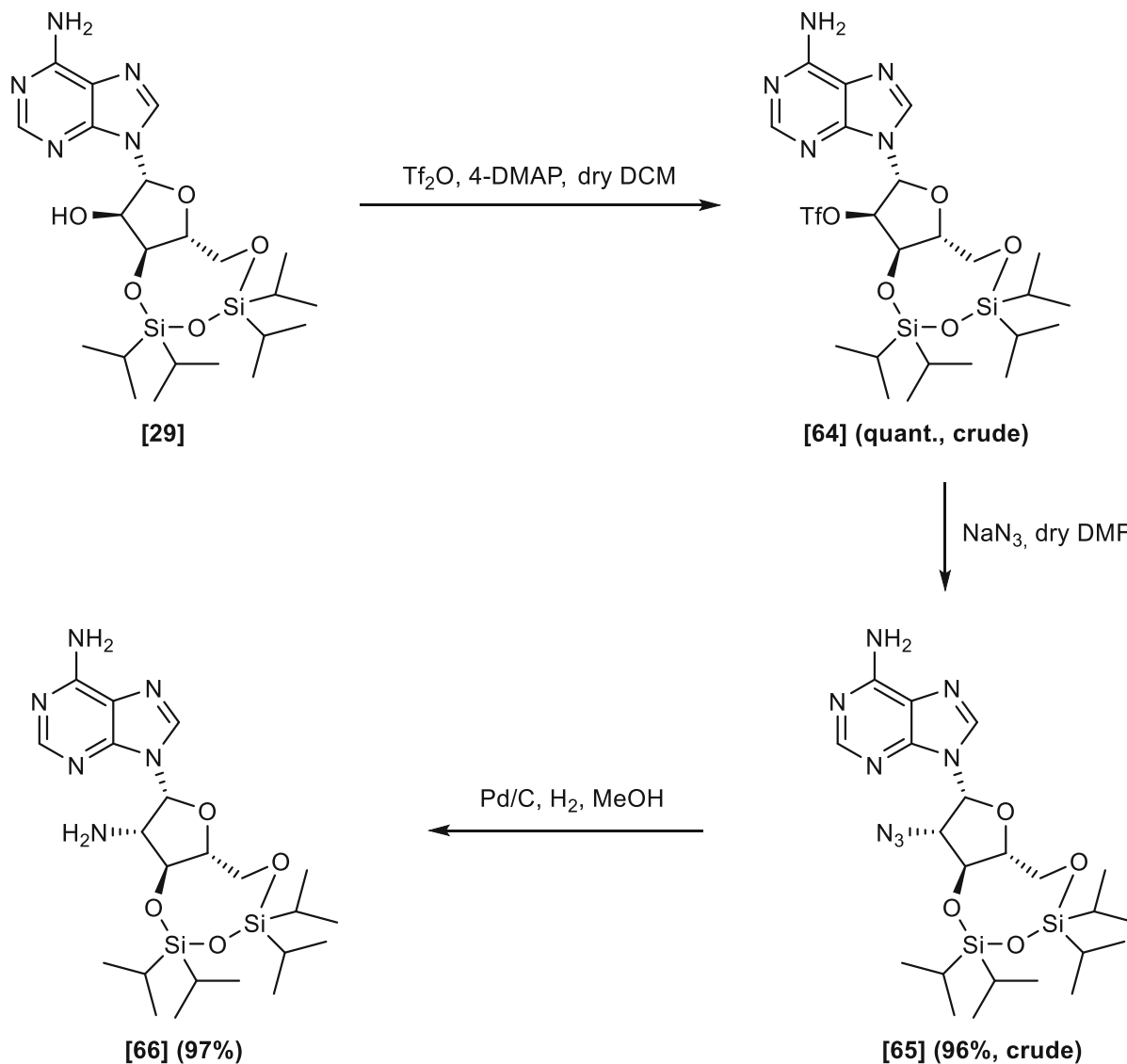




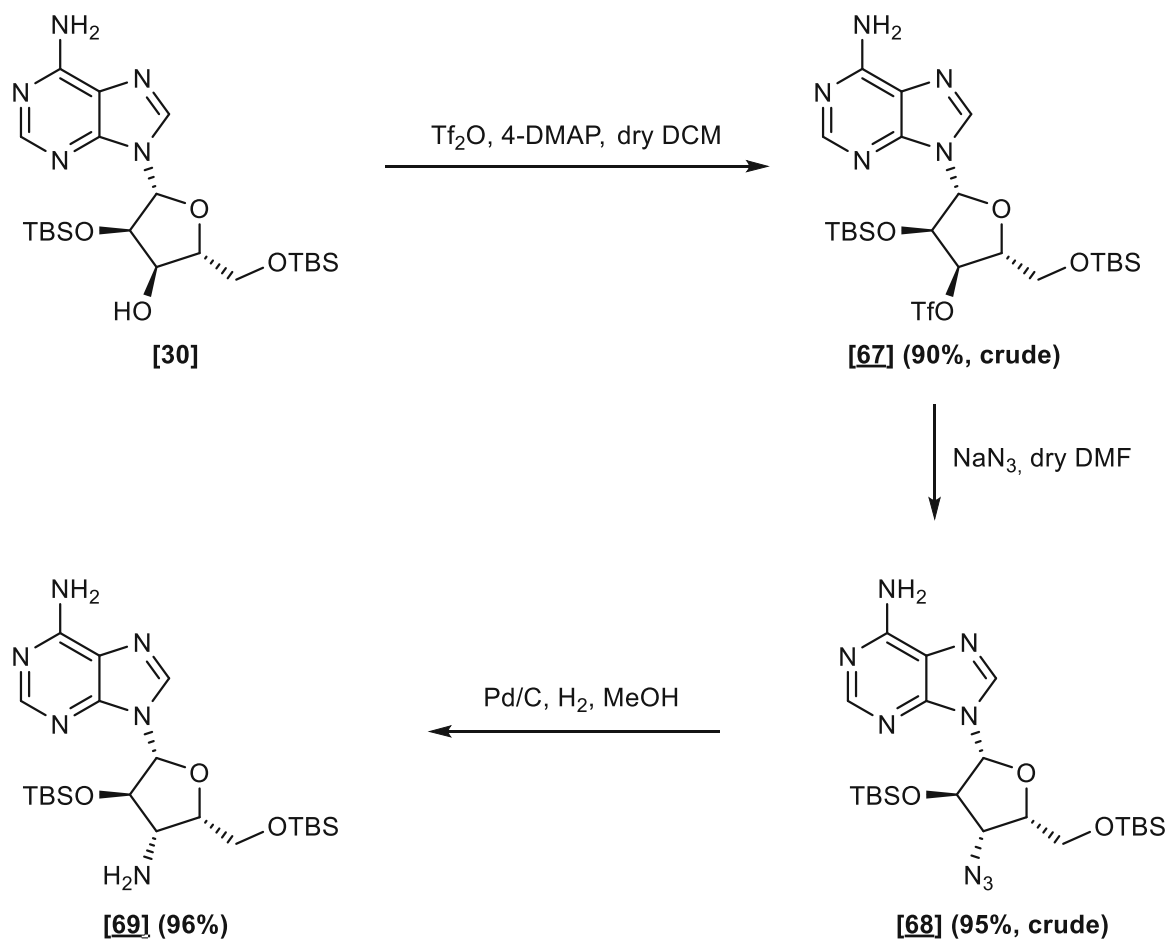
# A XIII Amide building blocks II



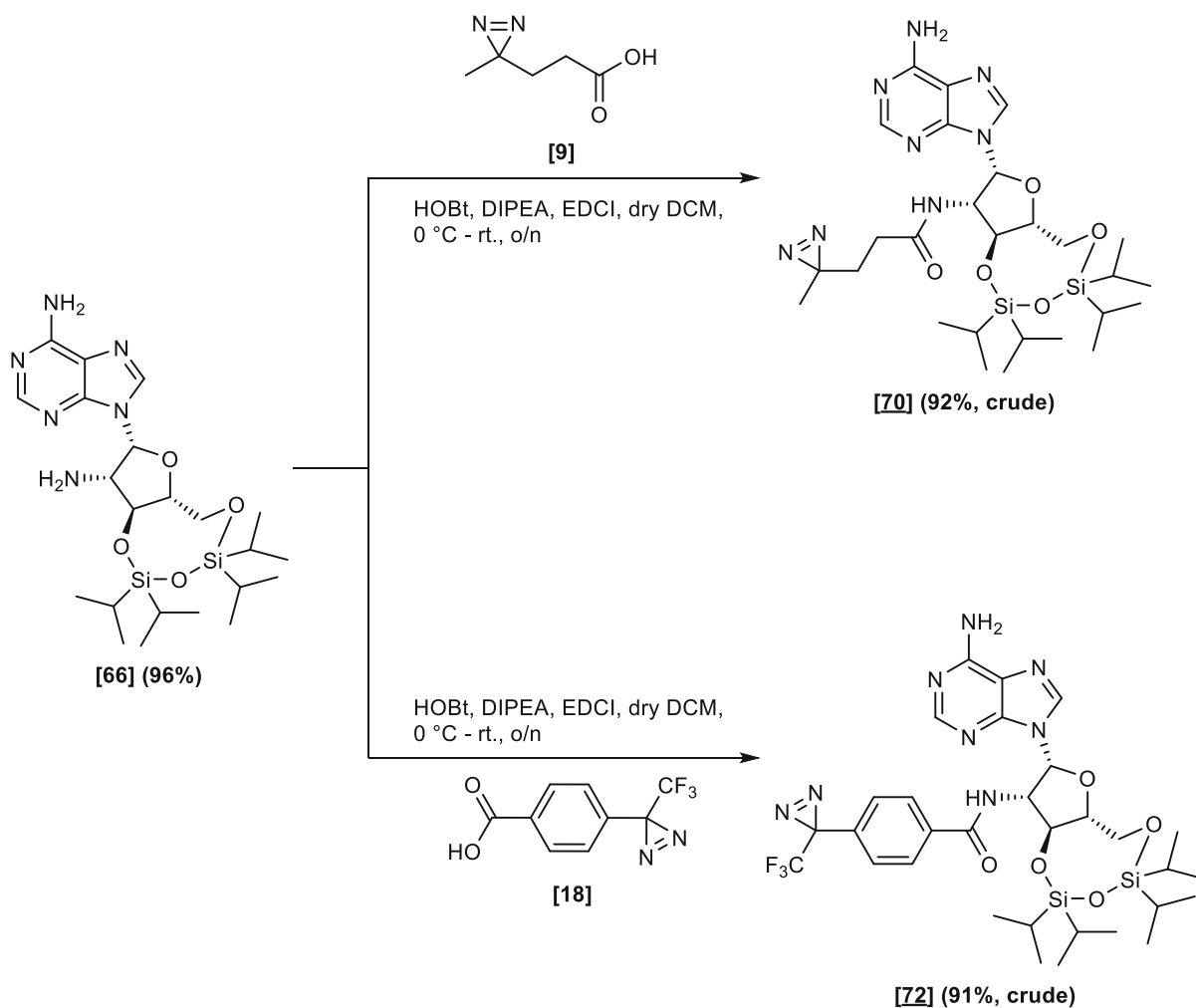
# A XIV Adenosine building blocks—Amines with alteration of stereochemistry I



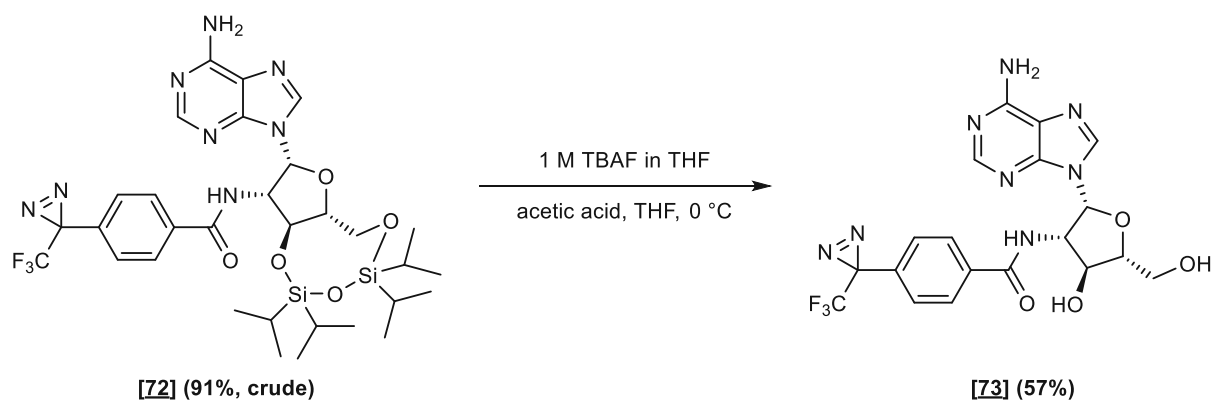
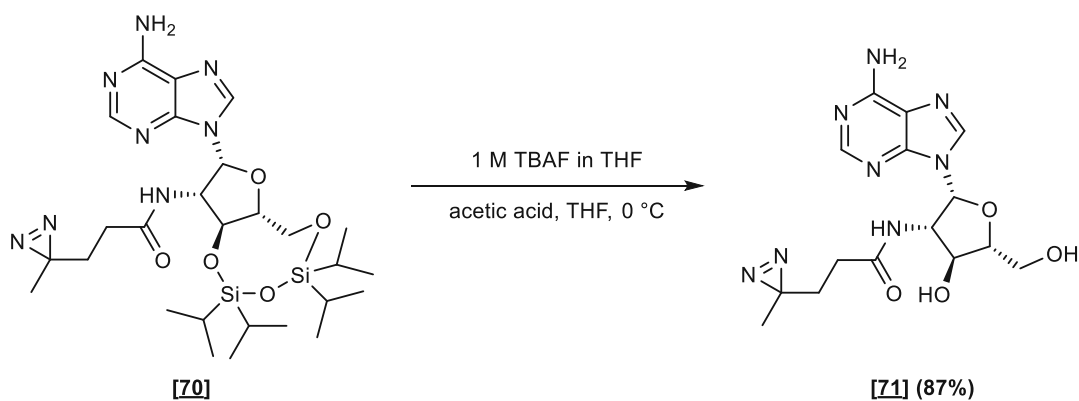
# A XV Adenosine building blocks—Amines with alteration of stereochemistry II



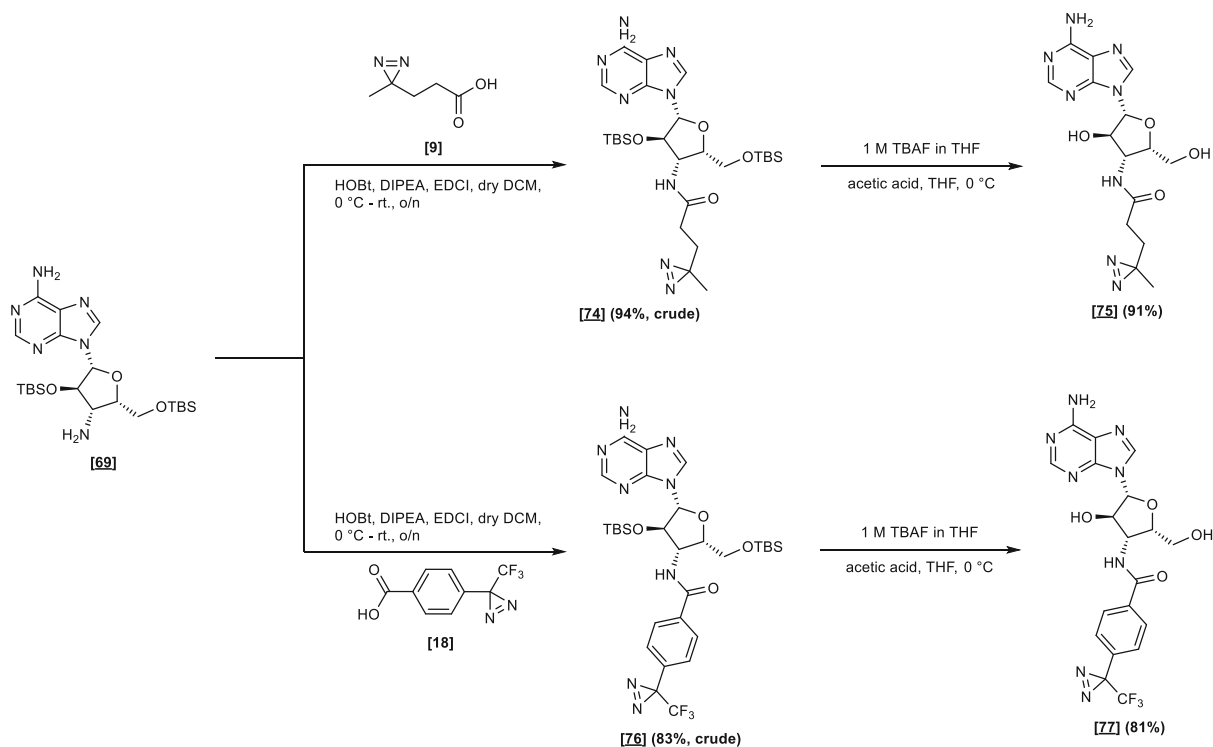
## A XVI Amide building blocks III



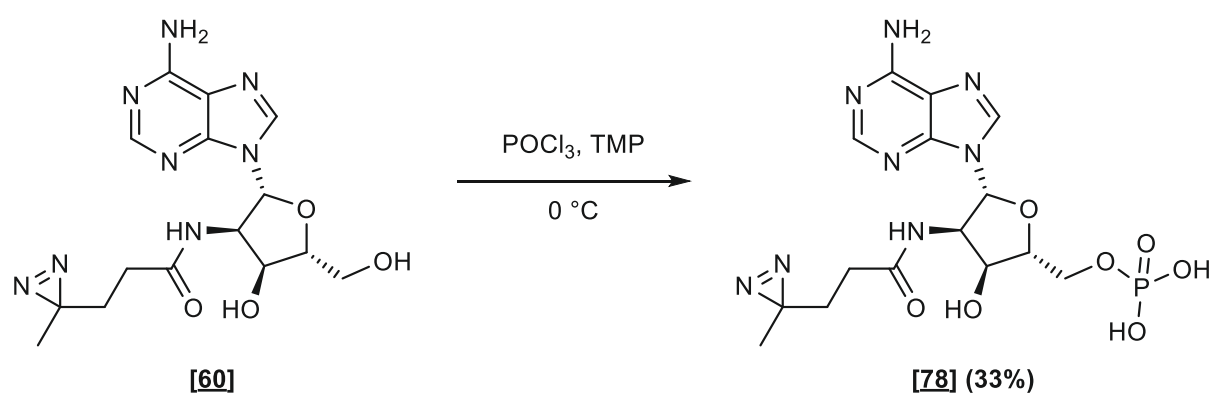
## A XVII Amide building blocks IV

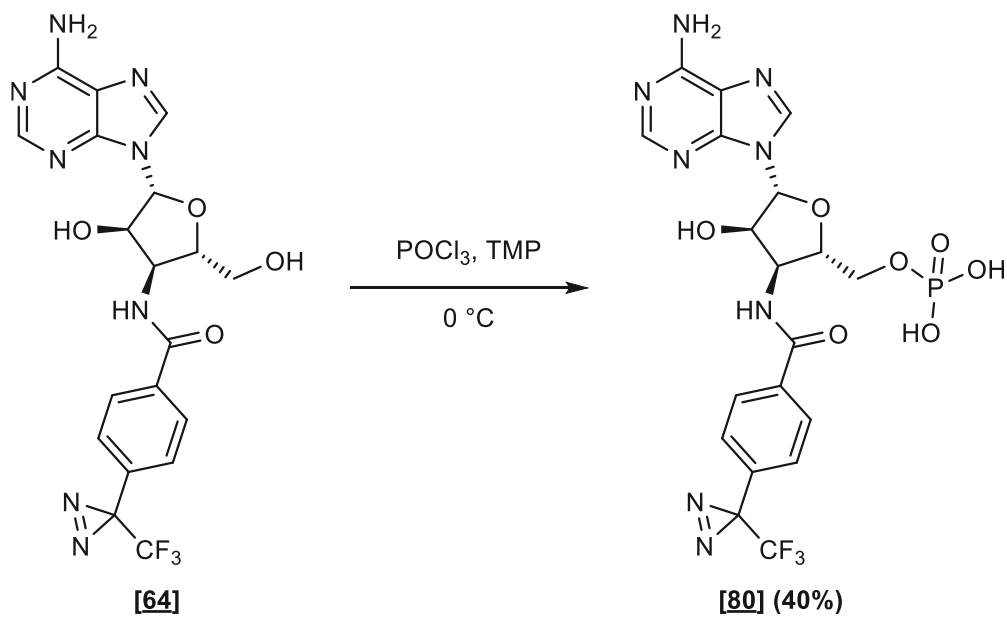
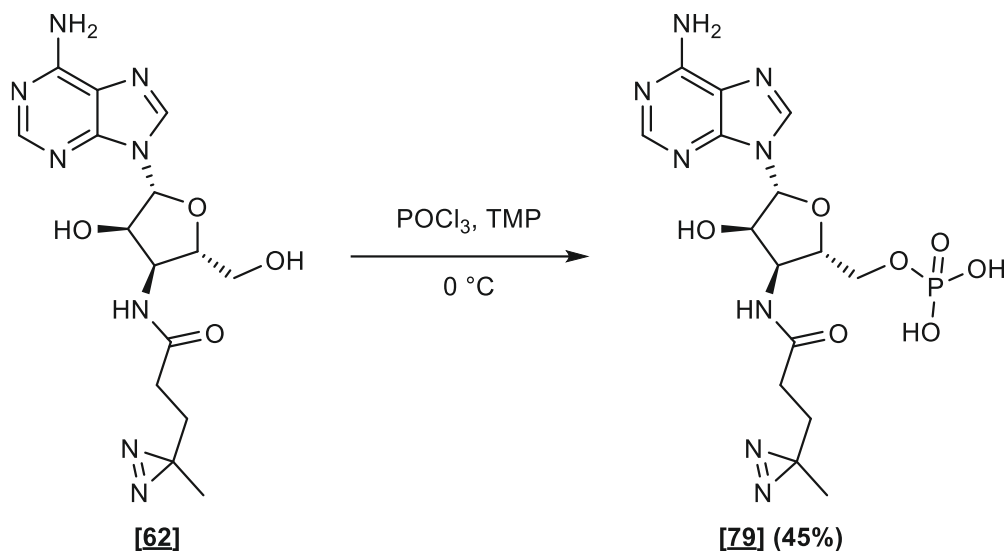


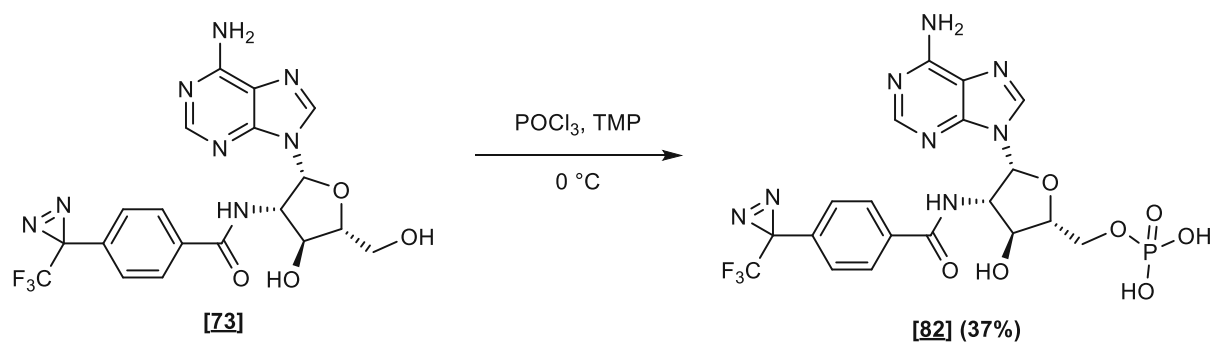
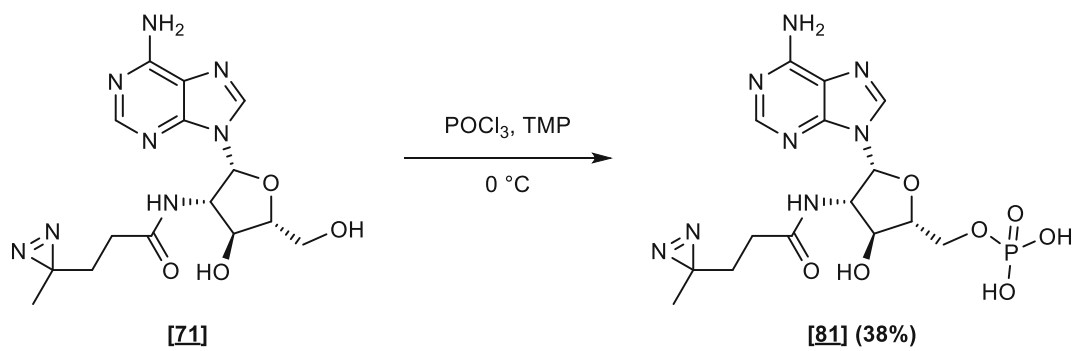
## A XVIII Amide building blocks V



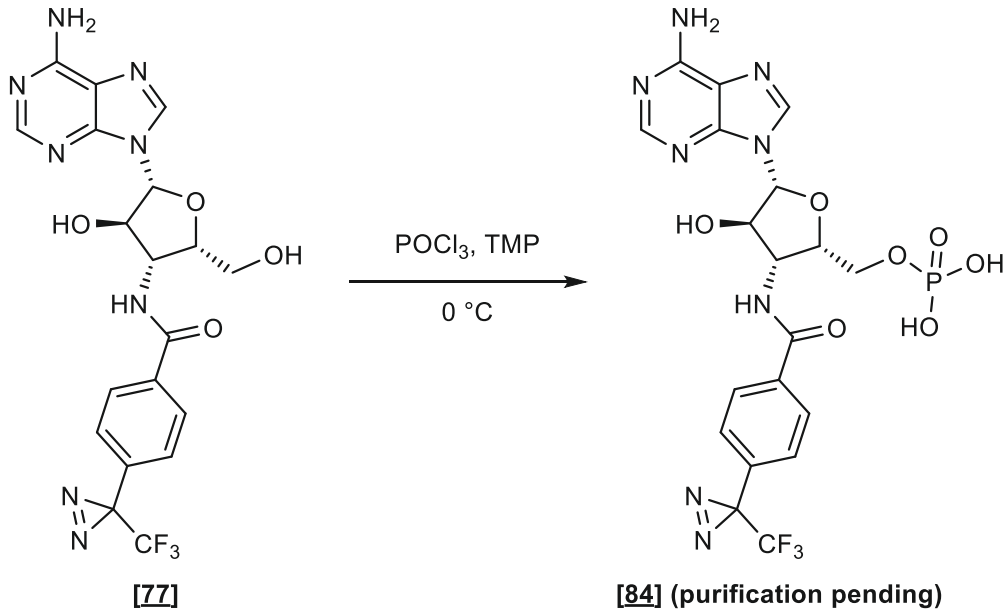
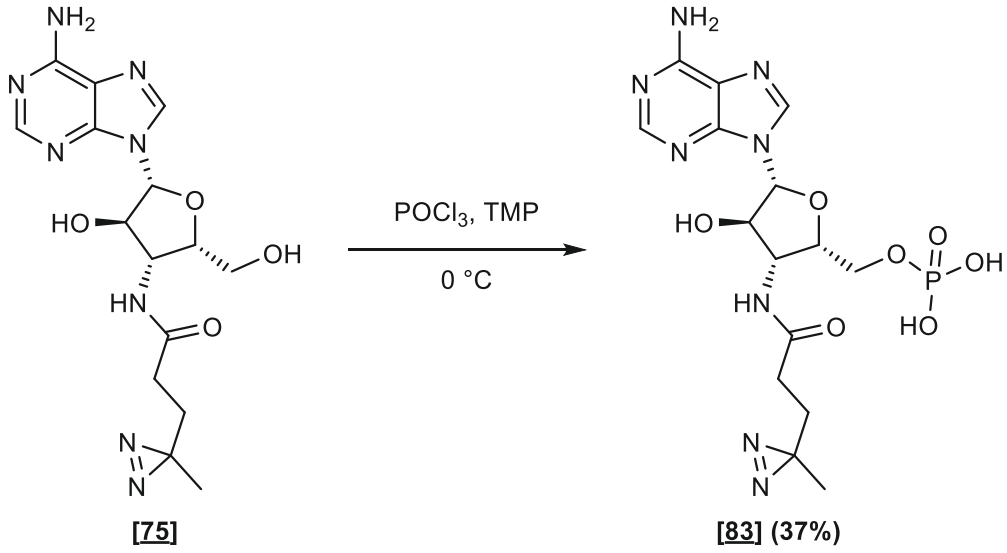
## A XIX Mono phosphates—Amides



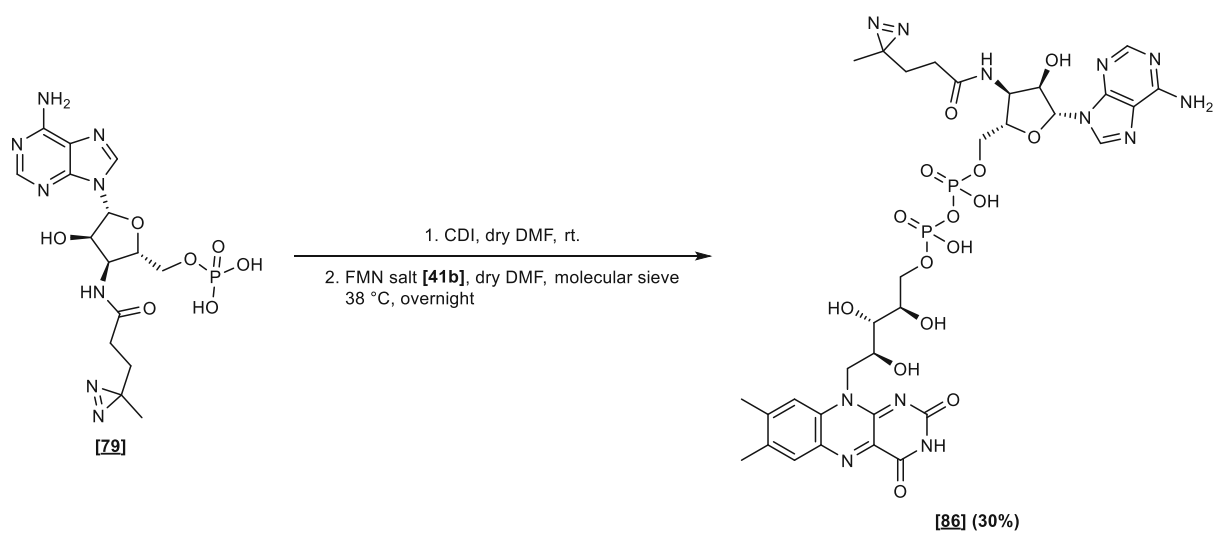
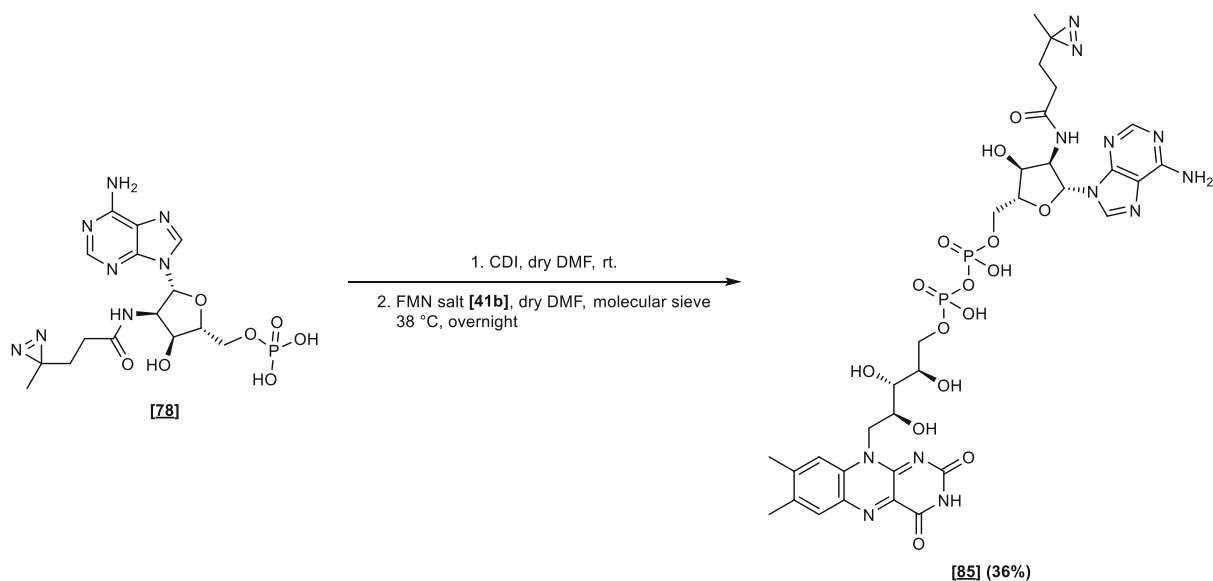


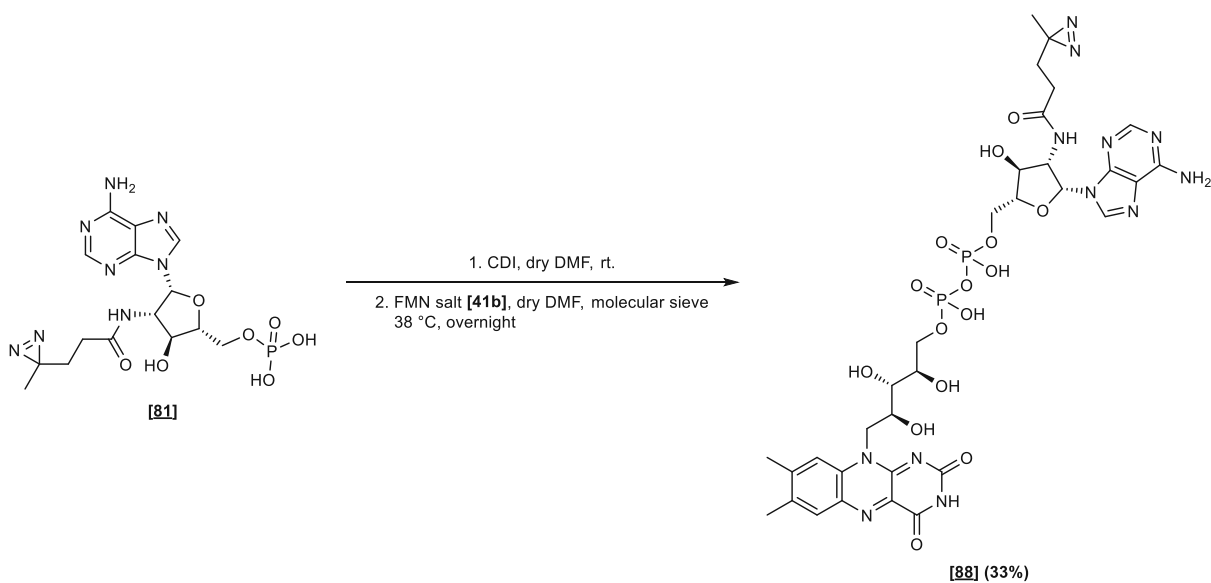
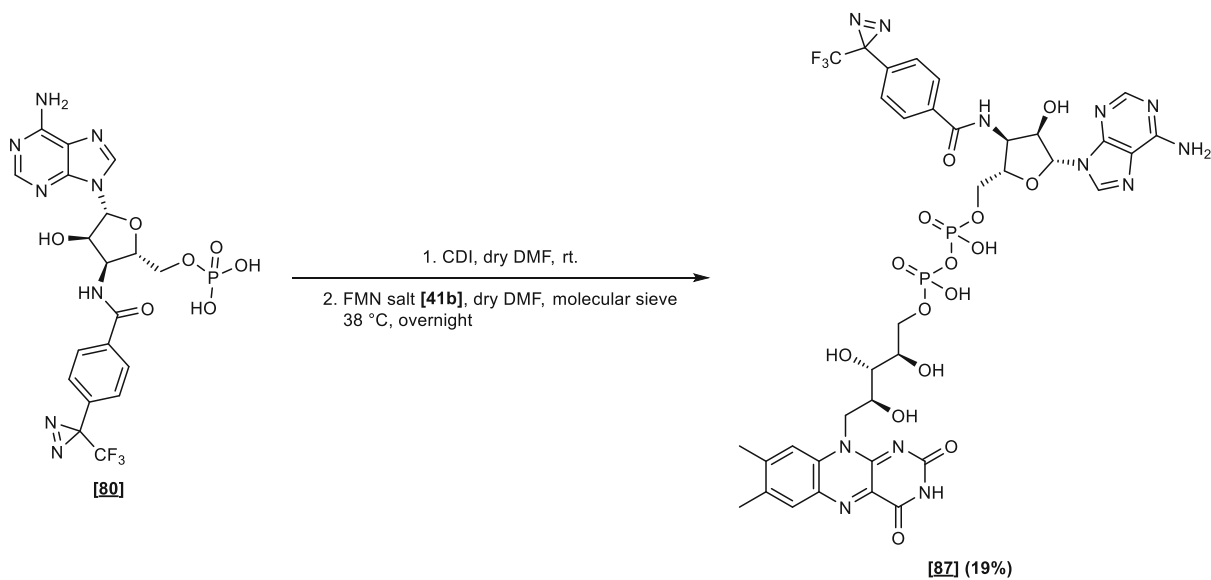


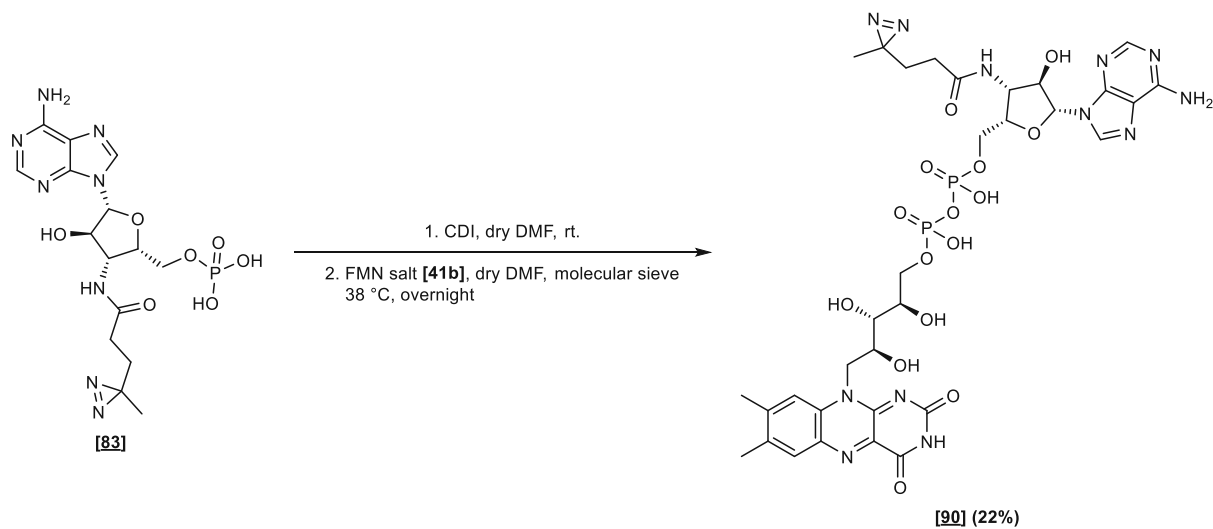
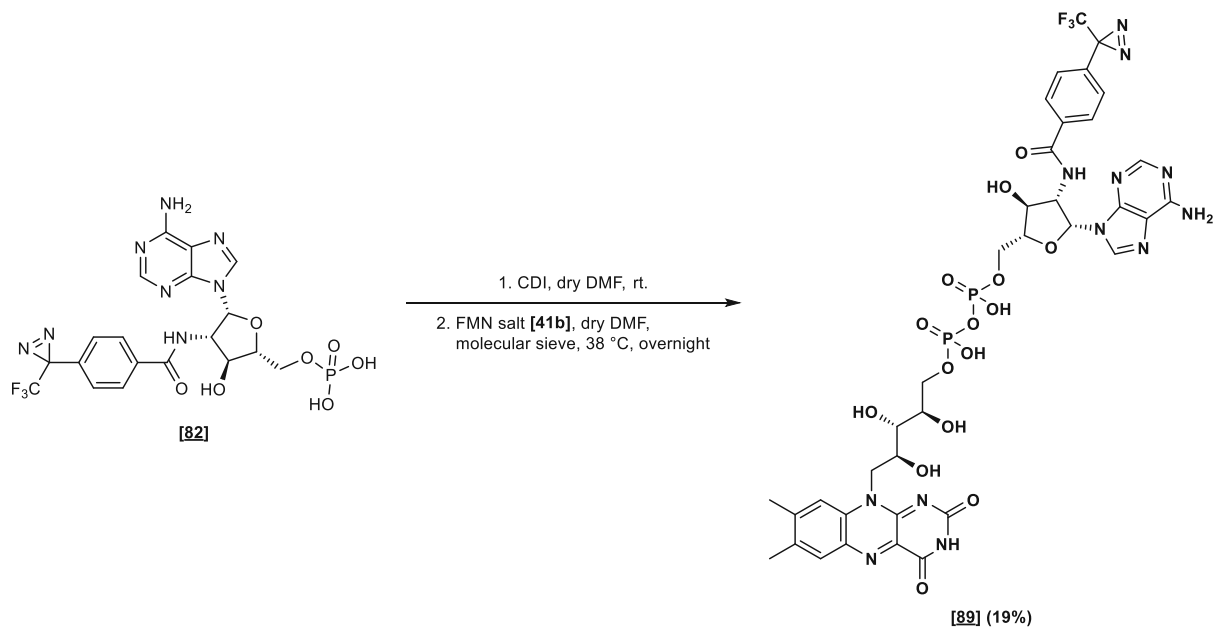




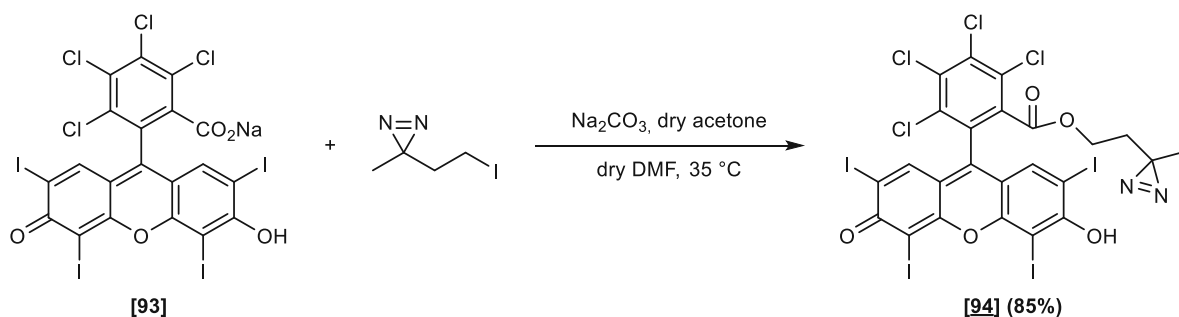
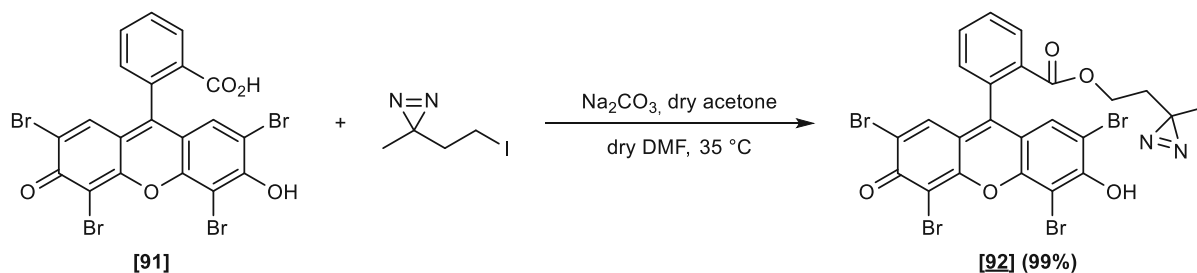
# A XX Diazirine-FAD—Amides



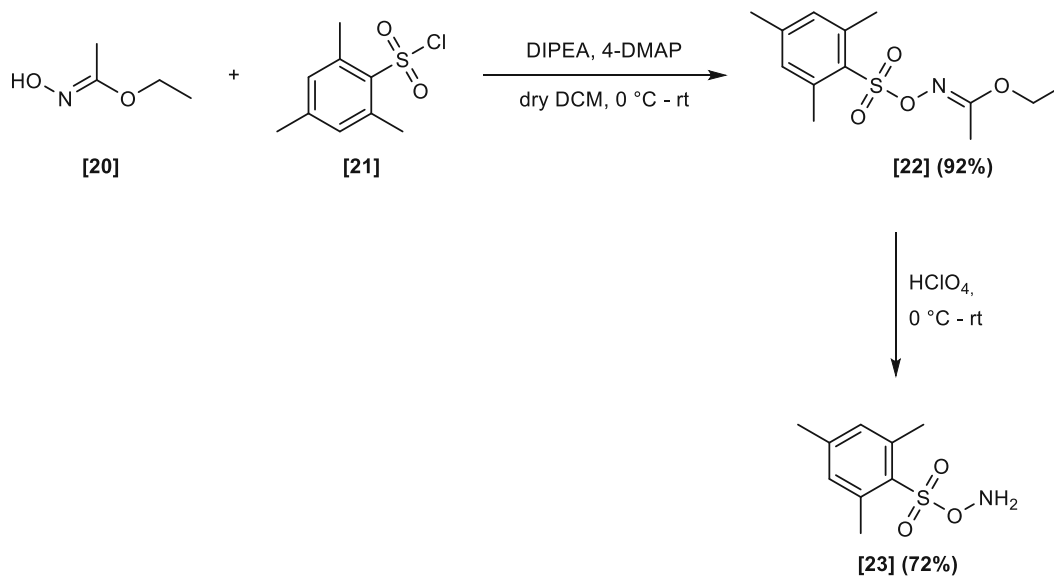




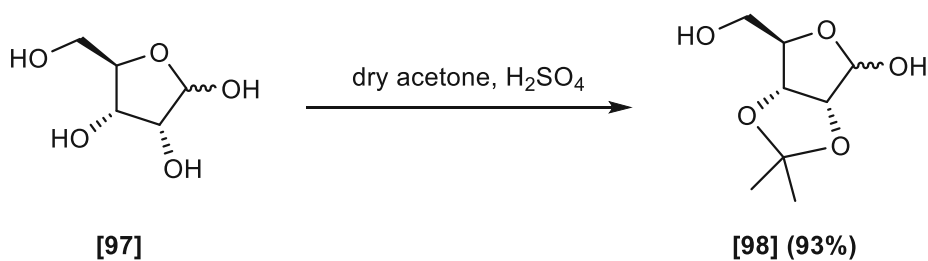
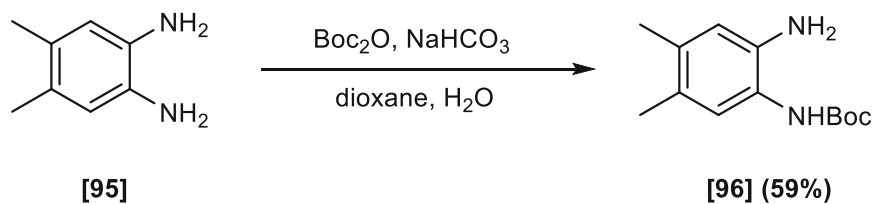
## A XXI Fluorescent dyes



## A XXII Aminating reagent



## A XXIII Building blocks for modifications of the riboflavin moiety



# B Introduction

The present thesis investigates the improved stability of flavoenzymes. To pursue this aim, analogs of flavin adenine dinucleotide containing a photoreactive group were synthesized to link the cofactor covalently to various enzymes. The activities and stabilities of these novel semi-synthetic enzymes were then determined.

## B I Prelude

Enzymes are nature's catalysts that facilitate biochemical reactions in living organisms.<sup>1</sup> In general, biological reactions occur under mild reaction conditions, such as moderate temperatures and atmospheric pressures and within aqueous solutions.<sup>2</sup> Enzymes can also be isolated from cells and used to catalyze a broad range of chemical transformations with high selectivity; thus, they are indispensable in current applications. For example, enzymes are used in washing powders and cleaning products,<sup>3,4</sup> and they play an important role in the production of various pharmaceuticals and fine chemicals.<sup>5</sup> They also hold a central role in analytical devices and assays that are used in multiple fields, including biomedical applications,<sup>6</sup> food safety monitoring,<sup>7</sup> and environmental pollutant detection.<sup>8</sup>

However, despite their many beneficial qualities, some naturally occurring enzymes are not feasible options for several applications due to their marginal stability. As enzymes have evolved to operate in a cellular environment, they typically are not stable under harsher reaction conditions, such as pH extremes and high temperatures. Furthermore, they do not tolerate the presence of organic solvents to a large extent.<sup>9</sup>

Consequently, great interest lies in improving enzyme stability, and several approaches (Figure 1) have been established to overcome issues related to enzyme instabilities, thereby realizing the true potential of enzymes in biocatalysis. In this thesis, we aim to increase the stability of cofactor-dependent enzymes using a genuinely novel chemical modification approach. This approach will provide valuable insights into the role of cofactors in enzyme stability and will provide a universal method for stabilizing cofactor-dependent enzymes to increase their adoption within the biocatalytic systems of various applications.

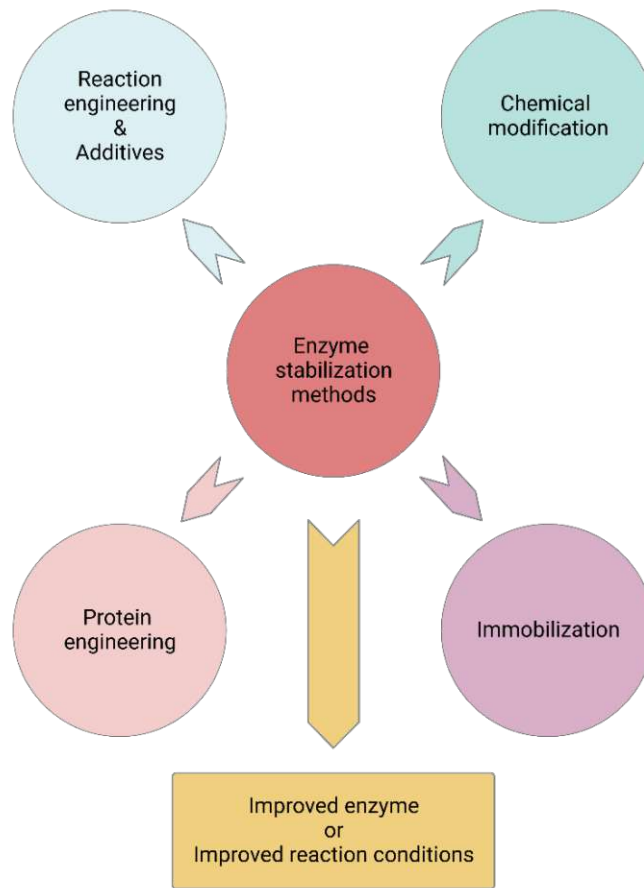


**Figure 1:** Strategies to improve the stability of enzymes.

## B II A brief history of biocatalysis

Biocatalysis describes the use of natural catalysts to achieve a desired conversion from a chosen substrate to the final product through the application of isolated enzymes or whole-cell systems.<sup>10</sup> Humans unknowingly used enzymes thousands of years ago in ancient Mesopotamia<sup>11</sup> and China<sup>12</sup> when they produced alcoholic drinks from sugars through fermentation. Subsequently, many milestones were achieved, shifting the use of enzymes from unintentional to intentional applications in modern society (Figure 2).



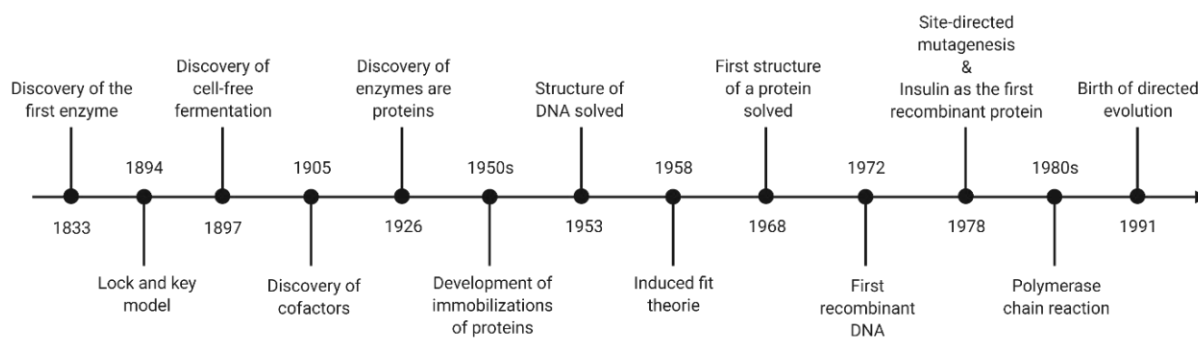


**Figure 2:** Timeline of significant developments in the field of biocatalysis.

The French chemist Anselme Payen discovered the first enzyme, diastase, in 1833.<sup>13</sup> However, the term *enzyme* was coined by the German physiologist Wilhelm Kühne in 1877 when he explained the capability of yeast to produce alcohol from sugars.<sup>14</sup> In 1897, Eduard Büchner discovered that sugars were fermented by a dead yeast extract, which until then had been thought to be performed only by a living organism. Büchner's results contradicted the vitalists' belief that a *life force* is necessary for these complex transformations, bringing about a new biochemical paradigm in which enzyme catalysis is a chemical process not necessarily related to the presence or action of living organisms.<sup>15,16</sup> Büchner named the enzyme attributed to the fermentation of sugars into ethanol and carbon dioxide *zymase* and believed that this soluble substance was undoubtedly a protein. However, in the early 1900s, the enzymes' chemical nature was still unknown. In 1926, James B. Sumner delivered proof that enzymes were, in fact, proteins by crystallizing the enzyme urease.<sup>16</sup> Subsequently, John H. Northrop and Wendell M. Stanley crystallized various other proteins, earning the Nobel Prize in 1946.<sup>17</sup>

By the early 1950s, a range of enzymes had been discovered, and some industrial applications had already been developed. These applications included German production of glycerol on a 1000 ton per month scale during World War I; condensation of acetaldehyde with benzaldehyde catalyzed by whole yeast to produce *L*-phenylacetylcarbinol, which acts as a precursor for *L*-ephedrine and other drugs, such as methamphetamine (patented in 1934<sup>18</sup>); and production of citric acid by the fungus *Aspergillus niger* in 1949.<sup>16</sup> Although many biocatalytic systems found applications in the industry, little was known about the mechanism by which the individual enzymes worked. Scholars agreed that the substrate must bind to the enzyme first to achieve a biochemical transformation; however, neither how the binding is accomplished nor how the chemical reaction occurs was known.

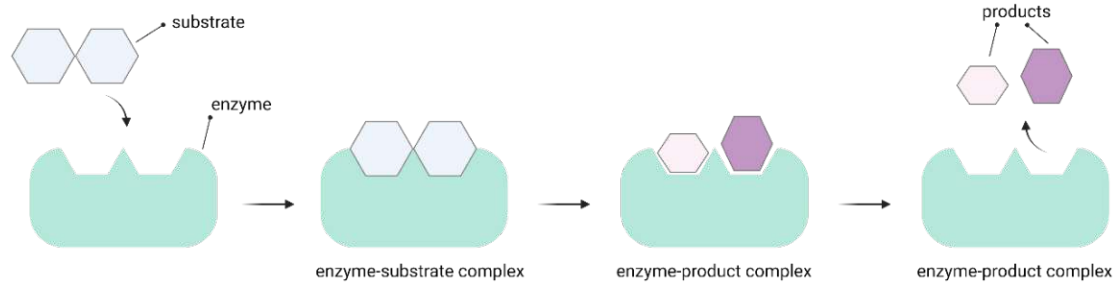
Emil Fischer's famous lock key model, created in 1894,<sup>19</sup> provides only a vague answer to questions regarding the binding and chemical reaction of enzymes. According to Fischer, enzymes exhibit a high degree of specificity to the substrates with which they react. He

proposed that similar to the way in which a lock fits a specific key, a specific substrate fits the shape of a specific enzyme. However, Fischer's model failed to describe the fact that enzymes do not always show complete specificity to only one type of substrate. In 1958, Daniel Koshland refined Fischer's model further and proposed the concept of induced fit,<sup>20</sup> which delivered a more accurate description of the enzyme structure. Since enzymes are relatively flexible, the enzyme's active site is constantly reshaped by interactions between the substrate and the enzyme (Figure 3).<sup>20</sup>

Although the induced fit model achieved a better understanding of how enzymes work, it nevertheless described protein interactions on an abstract level. In parallel to Fischer's and Koshland's work, a deeper understanding of the structure of proteins was built. In 1951, Frederick Sanger determined the complete amino acid sequence of bovine insulin, showing that proteins have a defined chemical composition consisting of a sequence of amino acids linked by amide bonds.<sup>21</sup> For this significant work, he was honored with his first Nobel Prize in 1958.

With the development of X-ray crystallography, further insights into the structure of proteins were gained. For example, John Kendrew and May Perutz solved the first structures of proteins using X-ray crystallography in 1958–1960.<sup>22</sup> In 1965, David C. Philips solved the structure of lysozyme with attached inhibitors, thus uncovering the location and residues of the active site.<sup>23</sup> The crystal structures of carboxypeptidase A with and without bound substrate glycyl-*L*-tyrosine revealed conformational changes of the enzyme as well as the key domains of the interactions between the substrate and enzyme.<sup>24</sup> These findings greatly impacted the understanding of how enzymes work at the atomic level, allowing enzymatic mechanisms to be further elucidated.<sup>25</sup>

### Lock-key model by Fischer



### Induced fit model by Koshland

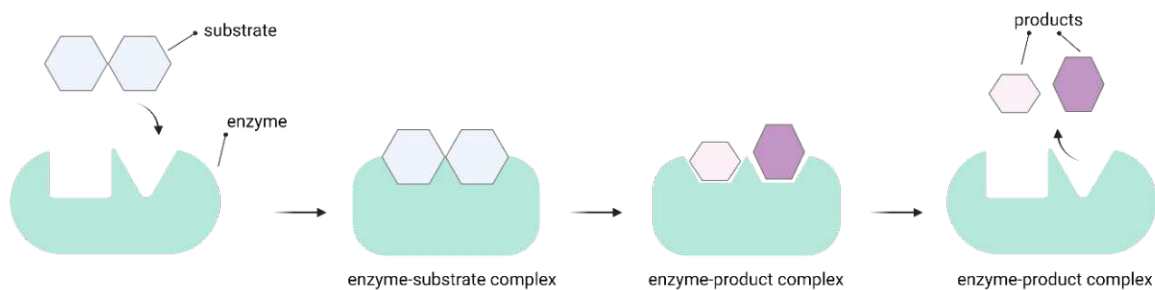


**Figure 3:** Comparison of the lock-key model by Fischer and the induced fit concept by Koshland.

Although great strides had been made to understand enzyme mechanisms, the use of biocatalysis, especially in industry, was still limited due to the low quantities of enzymes that could be obtained.<sup>16</sup> Immobilization of enzymes, which was discovered in the 1950s,<sup>15</sup> made applications in industrial processes more economical due to the ability to recycle applied enzymes. The two most important processes using this immobilization technique are the penicillin acylase process and the isomerization of glucose.<sup>15</sup>

However, for more widespread use of enzymes, protein production had to be increased, and the enzyme's active sites had to be changed. The establishment of nucleic acids as hereditary units and carriers of biological information, as well as the understanding of how to manipulate them, was key to solving these issues. Pioneering work by Avery on DNA as the chemical basis of chromosomes in 1944,<sup>26</sup> by Watson and Crick<sup>27</sup> on the postulated structure of DNA, and by Rosalind Franklin, who confirmed this structure using X-ray diffraction data, were important milestones in genetics and its molecular basis. However, their work did not immediately lead to technical innovations.

The observation of restriction enzymes in the 1970s finally led to the revolutionization of biocatalysis. The use of restriction enzymes enabled genes to be cut at specific locations and, thus, allowed any piece of DNA from any organism to be transferred into any other organism. Paul Berg reported the first so-called *recombinant* DNA in 1972.<sup>28</sup> From this time on, the DNA sequence of any enzyme of interest could be cloned and over-expressed in a suitable organism (e.g., *E. coli*) to produce the desired protein on a large scale for industrial applications.<sup>16</sup> Insulin was the first recombinant protein produced, and the commercial production of human insulin began in 1982.<sup>29</sup>

With new knowledge of enzymes and their mechanisms, as well as the availability of recombinant DNA techniques, the era of modern biocatalysis was heralded. Interest grew in improving the properties of enzymes, particularly their stability and (co)-solvent tolerance, or broadening their limited substrate scope. In 1978, Michael Smith reported a general method for site-directed mutagenesis<sup>30</sup> that allows specific, targeted changes (insertions, deletions, and substitutions) in double-stranded plasmid DNA.<sup>31</sup> Crucial for this method were the efficient syntheses of short oligonucleotides developed by Khorana<sup>32</sup> and Caruthers.<sup>33</sup> Another critical method that had a significant impact on the development of novel enzymes was the polymerase chain reaction. This technique, developed by Kary Mullis in the 1980s, enabled a large number of DNA sequence copies to be created from a single template.<sup>34</sup> Under optimal conditions, the replication of DNA through the polymerase is extremely specific; however, by modulation of the fidelity of the DNA polymerase through changed conditions, random mutations are introduced into the polymerase chain reaction (PCR) product. This method, termed error-prone PCR, was used by Frances Arnold in the early 1990s to create large libraries of mutants. In 1993, she created a variant of subtilisin E that was active in the organic solvent dimethylformamide (DMF) by introducing a total of 10 mutations using error-prone PCR.<sup>35</sup> Arnold was honored with the Nobel Prize in Chemistry in 2018 for her pioneering work in the field of directed evolution of enzymes.

In the following years, novel enzymes with improved thermo- and pH stability, altered substrate specificity and modified enantioselectivity, as well as enzymes that performed reactions not observed in nature, were created with the help of directed evolution. Thus, this method became a powerful tool for protein engineering.

## B III Classification of enzymes

Enzymes can be classified according to the reactions they catalyze.<sup>36</sup> The classification of enzymes follows the Enzyme Commission (EC) number, which was developed by the Union of Biochemistry and Molecular Biology in 1961. This nomenclature system identifies enzymes according to a unique four-digit code, or EC number, which is generated as follows:<sup>37</sup>

- The first number states the type of reaction being catalyzed by the enzyme.
- The second number provides the subclass, which mainly contains information about the type of compound or group involved.
- The third number indicates the sub-subclass, which specifies the type of reaction involved.
- The fourth number is the serial number of the enzyme within its sub-subclass.

Since 2018, the enzyme list has comprised seven classes of enzymes, as shown in Figure 4.

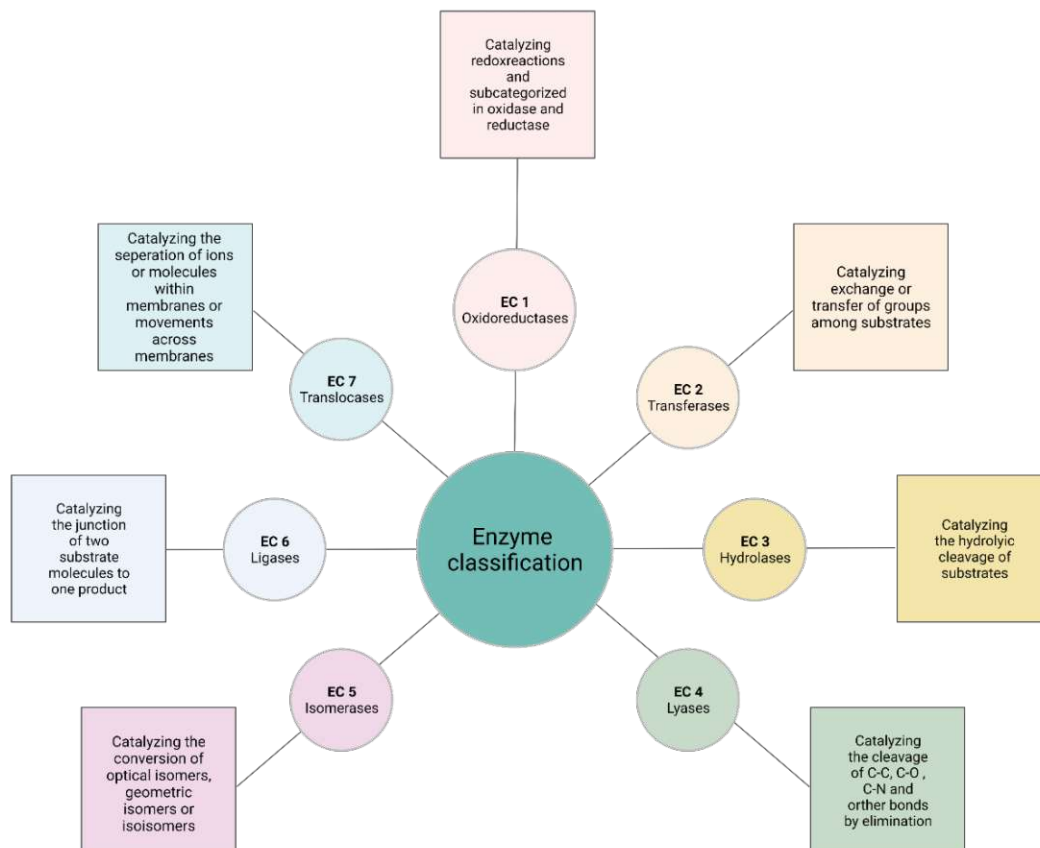


**Figure 4:** The seven classes of enzymes with the description of the catalyzed reactions.

## B IV Cofactor-dependent enzymes

Those enzymes constructed only of the 20 genetically encoded amino acids catalyze an astonishing range of reactions. However, many enzymes often depend on organic metabolites, metal ions, or metal-organic complexes to achieve certain types of activity. These species are known as cofactors, which have functional groups and properties that enable the protein-cofactor system to catalyze reactions that could not be achieved by the cofactor or the polypeptide backbone of the enzyme alone.<sup>38,39</sup> Thus, cofactors increase the portfolio of chemical reactions catalyzed by enzymes.

Although the chemical potential of a cofactor-dependent enzyme results from the cofactor chemistry, cofactors themselves are poorly catalytically active. For example, many cofactors do not feature a chiral center, while the introduction of chirality by amino acids in the active site of enzymes enables asymmetric biosynthesis.<sup>39</sup> Additionally, a given cofactor can often catalyze various chemical transformations. Thus, the flexible nature of proteins plays a crucial role in controlling and amplifying the reactivity of the cofactor by guiding the reactivity to one of many possible pathways.<sup>38</sup> In turn, cofactors are essential for the structural integrity of the protein; the presence of the cofactor is essential for the folding of the polypeptide chain and the stabilization of the native protein.<sup>40</sup>

The reaction mechanism of cofactor-dependent enzymes that promote catalysis have been studied thoroughly; in fact, the first mechanisms studied were those of enzymes employing cofactors since their structures were determined before the structure of whole proteins (see Figure 2).<sup>16</sup> Nicotinamide adenine dinucleotide (NAD<sup>+</sup>) was the first cofactor ever described, which was discovered in 1906 by Arthur Harden and William Young.<sup>41</sup> Hans-Euler-Chelpin identified the chemical composition of NAD<sup>+</sup> almost 25 years later.<sup>42</sup> The function of NAD<sup>+</sup> in hydride transfers was further unveiled by Otto Heinrich Warburg in 1936.<sup>43</sup> Subsequently, the structures of other important cofactors were discovered, such as pyridoxal<sup>44</sup> by Esmond Snell, ATP<sup>45,46</sup> and FAD<sup>47</sup> by Alexander Todd, and Vitamin B<sub>12</sub><sup>48,49</sup> by Dorothy Hodgkin.

### B IV.1 Classification of cofactors

According to the International Union of Pure and Applied Chemistry (IUPAC) Gold Book,<sup>50</sup> cofactors are "organic molecules ... or ions ... that are required by an enzyme [for] its activity." The definition also states that a "cofactor binds with its associated protein (the apoenzyme), which is functionally inactive, to form the active enzyme (holoenzyme)."<sup>50</sup> This definition can

be further refined in that cofactors must be present in the enzyme's active site to exclude allosteric regulations, where molecules do not play an active role in the catalytic cycle.<sup>51</sup> Organic cofactors are sometimes further divided into coenzymes, which are dissociable from the enzyme, and prosthetic groups, which are tightly bound to the enzyme's active site—either covalently or non-covalently.<sup>52</sup>

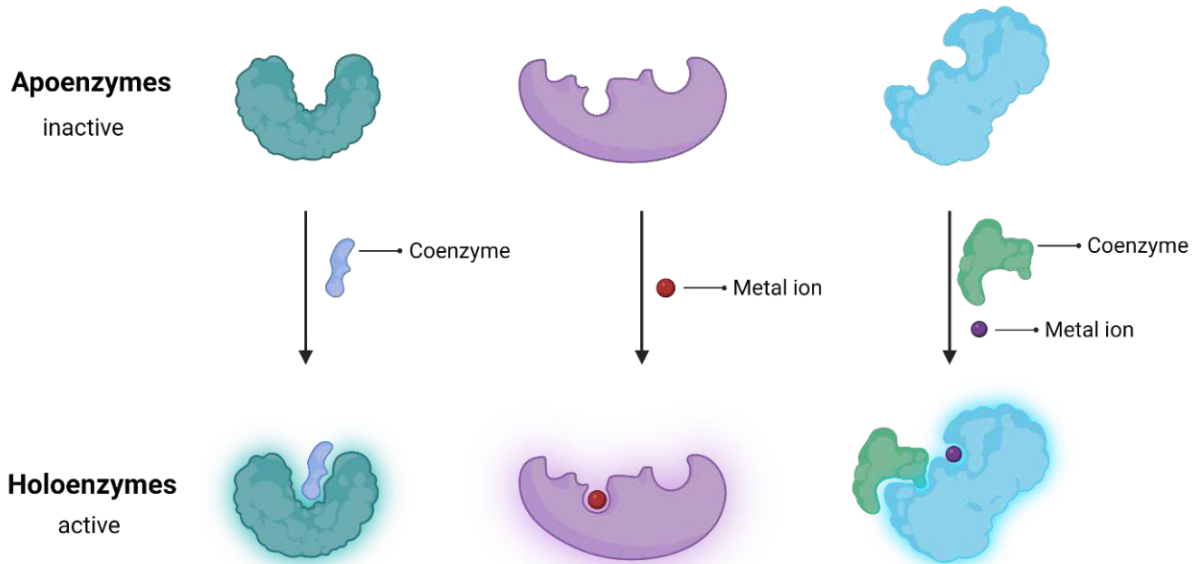


**Figure 5:** Comparison of apoenzyme and holoenzyme of different classes of cofactor-dependent enzymes. Cofactor-dependent enzymes unfold their catalytic potentials only when a cofactor binds to the enzyme's active site.

## B IV.1.1 Inorganic cofactors

A significant number of enzymes requires metal ions for catalytic activity. In 2008, Andreini *et al.* analyzed the role and distribution of metal ions using public databases and noted that about 40% of enzymes with known structures are metal-dependent.<sup>53</sup> They further identified 13 metal ions involved in catalytic transformations. As shown in Figure 6, magnesium is most often involved in the function of enzymes, followed by iron and zinc. The role of metal ions in enzymatic catalytic mechanisms can be roughly divided into two categories depending on whether the metal acts as a redox center or not.<sup>53</sup> In redox catalyzed reactions, the metal either is directly involved in the catalytic pathway by donating and accepting electrons to or from other reacting species or acts as an auxiliary by helping transfer electrons to or from the active site.<sup>54-57</sup>

When involved in non-redox catalytic transformations, the metal ion plays an essential role in activating reacting species or stabilizing the charges of intermediates and transition states. In



these cases, the metal ion acts as a Lewis acid by withdrawing electrons from the ligand atom of a substrate; this increases the electrophilicity of the substrate.<sup>58,59</sup> In another form of activation, the acidity of a proton in a substrate is increased through metal binding, resulting in electronic rearrangement of the substrate through the proton's transfer within the catalytic site.<sup>60</sup> Alternatively, releasing the proton from the substrate forms a reactive anionic species that can be attacked by a nucleophile. In most cases, the activated species is water that forms a hydroxide ion.<sup>61</sup> Another example of activation that plays a crucial role in terpene synthesis is the heterolytic cleavage of a C-O bond and the formation of a carbocation as a result of the coordination of the metal ion to the substrate.<sup>62</sup>

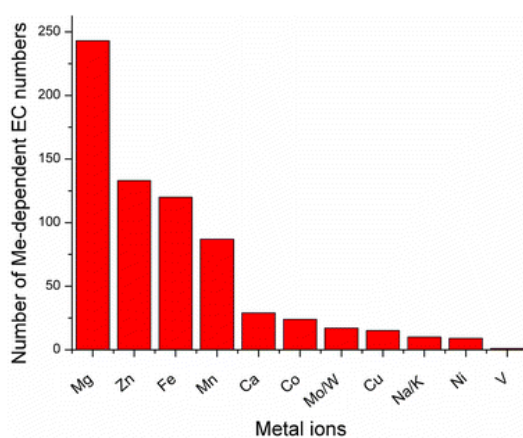


**Figure 6:** Occurrence of catalytic metal ions in enzymes. The figure is taken from reference.<sup>53</sup>

As mentioned above, metals play a role in electrostatic stabilization of intermediates and transition states. In these cases, the positively charged metal ion counterbalances local negative charges formed in the active site during the catalytic transformation.<sup>63</sup>

## B IV.1.2 Organic cofactors

Organic cofactors are relatively small molecules that bind either loosely or tightly to the enzyme to contribute to the catalytic transformation (see chapter B IV.1). A loosely bound cofactor is termed coenzyme, which binds to the apoenzyme's active site at the beginning of the catalytic cycle and leaves after each cycle. In contrast, a cofactor that is tightly bound to the enzyme—either covalently or non-covalently—remains at the active site during the catalytic cycle and cannot be removed from the holoenzyme without denaturing the protein and is called prosthetic group. However, the differentiation between loosely and tightly bound cofactors is



somewhat fluid, as seen in the examples of the cofactors  $\text{NAD}^{+64}$  and thiamine pyrophosphate,<sup>65</sup> which are loosely bound in some enzymes while tightly bound to others.

The structures of many organic cofactors are derived from biochemical metabolites and, thus, are composed of chemical moieties similar to compounds vital to life, such as vitamins, nucleotides, and amino acids.<sup>51</sup> Consequently, many studies have questioned how cofactors have evolved,<sup>66-70</sup> although at which stage during the evolutionary process cofactors did appear is highly debated. Cofactors are known to exert poor catalytic properties, and their full potential unfolds only in an evolved protein environment (see chapter B IV).

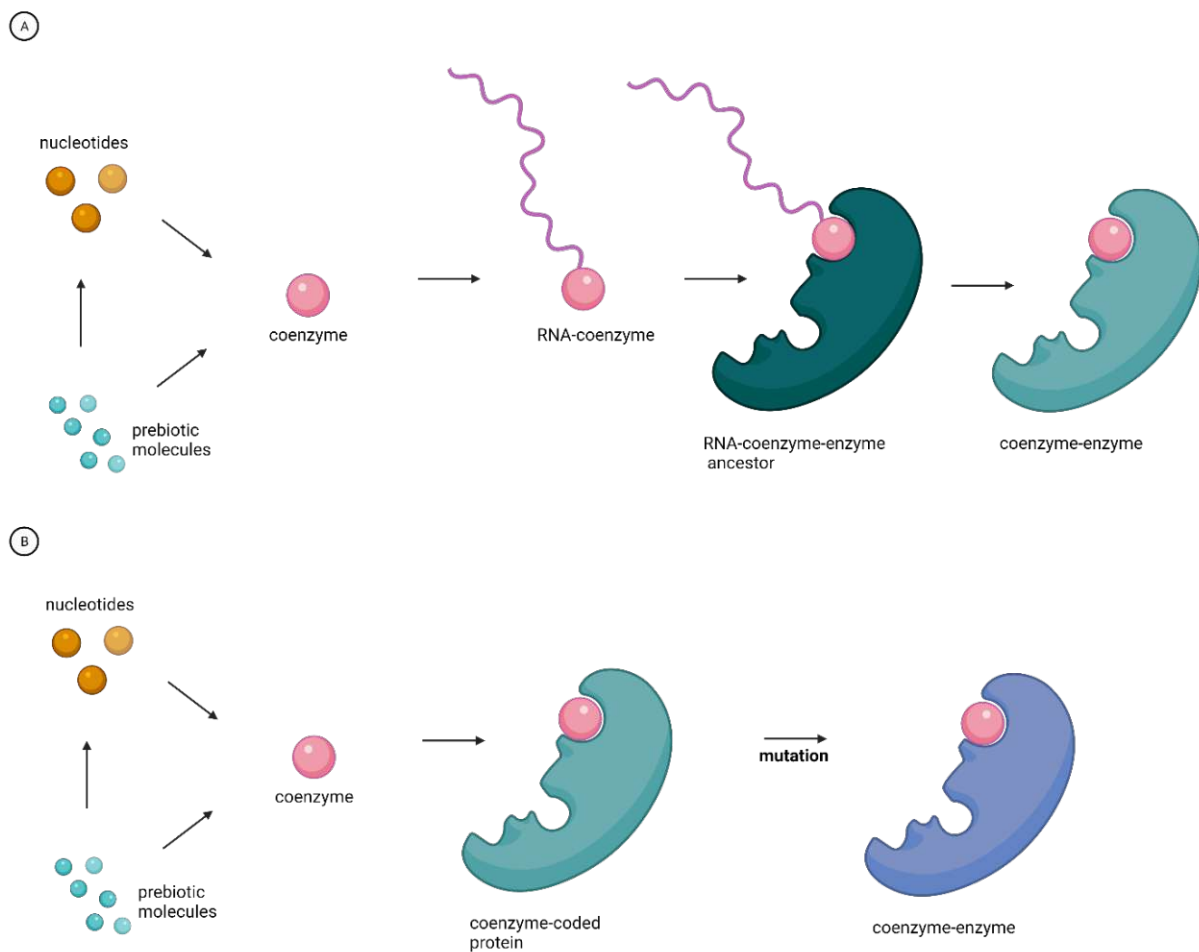


**Figure 7:** Theories on the evolution of coenzyme-dependent enzymes; A) RNA-world theory B) evolution in a coded protein world. The figure is adapted from reference.<sup>70</sup>

Therefore, coenzymes could have been developed at the same time RNA molecules emerged, binding to these RNA molecules. The first protein structures could have been formed by the condensation of single amino acids on these RNA templates, which would have been finally replaced by the protein structures, thus creating enzymes that were associated with a coenzyme (Figure 7 A).<sup>70</sup> This RNA-world theory is supported by experimental documentation of the tight binding of organic cofactor molecules to RNA.<sup>71</sup> Alternatively, coenzymes could

have directly broadened the catalytic toolbox of enzymes at a later stage in protein evolution (Figure 7 B).<sup>70</sup>

Since organic cofactors derive from a few building blocks of life, they often show similar chemical functional groups and thus can be categorized according to their substructures, as was done for all organic cofactors by Fischer *et al.*<sup>51</sup> (Figure 8).

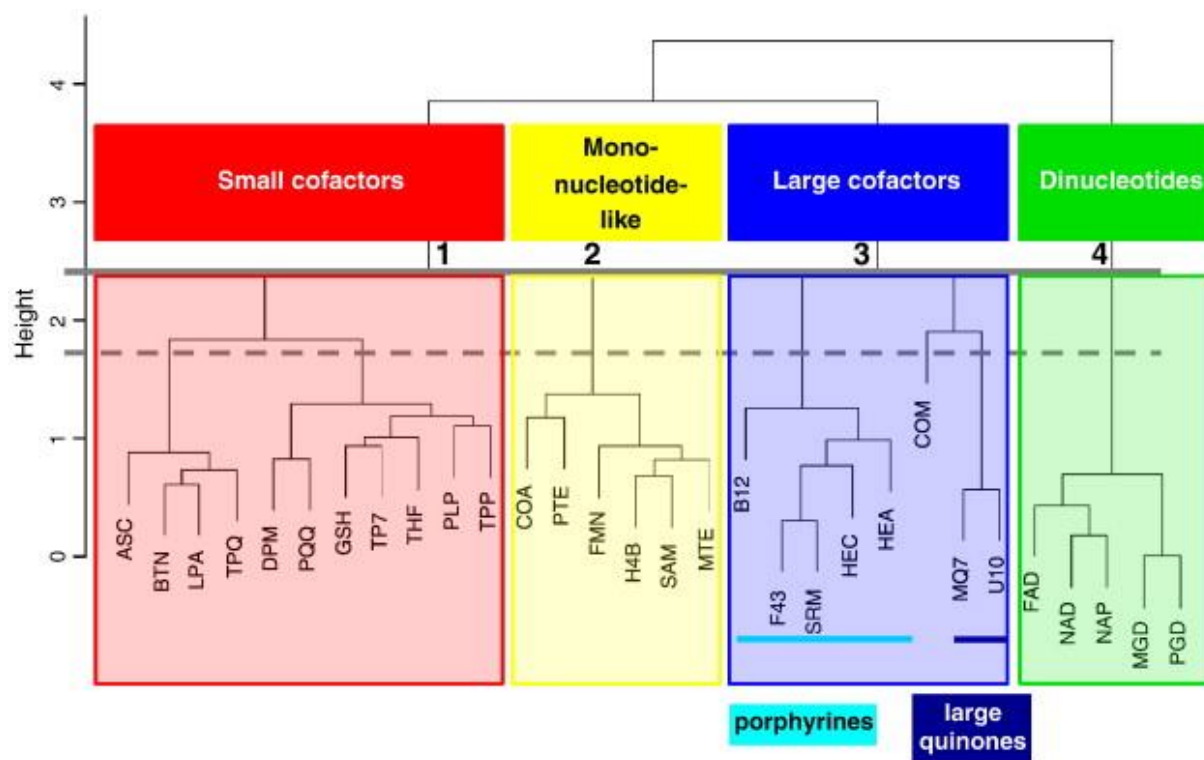


**Figure 8:** Hierarchical Ward's clustering of cofactor descriptors. The figure was taken from reference.<sup>51</sup>

However, the structure provides little information regarding the general catalytic functionality of cofactors, as similar moieties and classes of cofactors often catalyze different chemical reactions.<sup>51</sup> Therefore, categorizing their function in enzymatic reactions is more reasonable. According to Fischer *et al.*, organic molecule cofactors show seven chemical functions (see Figure 9) when directly involved in a biocatalytic reaction, which are as follows:<sup>51</sup>

- Transfer of chemical moieties
- Redox reactivity: transfer of hydrogen species and electrons
- Passing the substrate/intermediate between different active sites
- Photochemical activation of aromatic systems, which then act as initiators
- Cleavage or formation of a chemical bond
- Polymerization representing a particular case of bond formation

- Effecting intramolecular rearrangements of atoms in the substrate

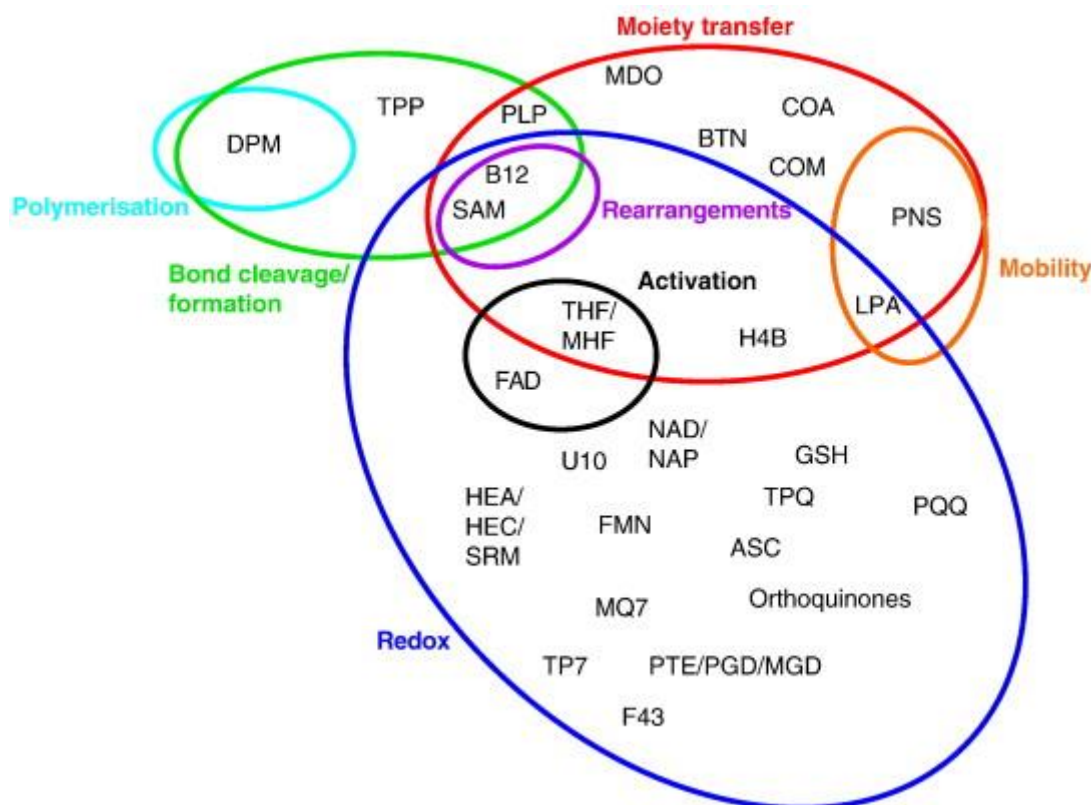


**Figure 9:** Functional classification of cofactors. The red ellipse shows cofactors participating in group transfer reactions. The blue ellipse shows cofactors that participate in redox reactions. The orange ellipse represents cofactors that pass substrates/intermediates between different active sites of the enzyme. The black ellipse shows cofactors acting as photosensitizers. The green ellipse shows cofactors involved in bond cleavage/formation. The cyan ellipse shows the only representative of polymerization (DPM). The purple ellipse demonstrates cofactors involved in intramolecular rearrangements. The PBD Het codes of the corresponding cofactors can be taken from Table 1. The figure was taken from reference.<sup>51</sup>

Further, organic cofactors can be categorized into the enzyme classes (EC number, see chapter B III) in which they participate. As shown in Figure 10, EC class 1 is most dependent on organic cofactors, while hydrolases (EC class 3) rarely employ these cofactors. The low number of organic cofactors in hydrolyses is likely due to the relative simplicity of the hydrolysis mechanism, in which many metal ions can act as Lewis acids and activate water for a nucleophilic attack. In contrast, the mechanisms in redox reactions are much more elaborate, and hydride ions and electrons must be shuttled. Thus, the structures of the involved cofactors are also more complex.

Table 1 summarizes the organic cofactors and their function in biotransformations.

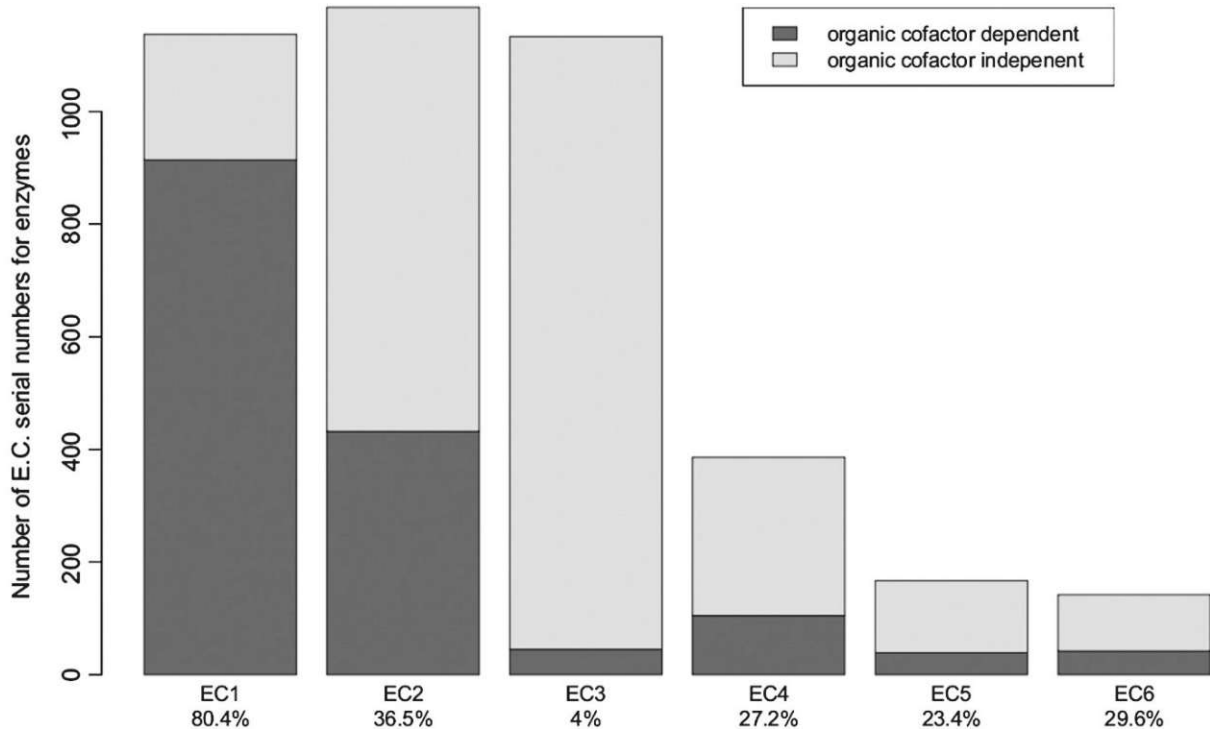


**Figure 10:** Dependence on organic cofactors in six EC classes. The figure was taken from reference.<sup>51</sup>

**Table 1:** Overview of all organic cofactors and their functions in biocatalytic transformations. The heterokaryon incompatibility (HET) code of the protein database (PDB) of the respective cofactor is also provided. An asterisk (\*) indicates that this cofactor may be covalently attached to the enzyme. The table was adapted from reference.<sup>51</sup>

Name(s)	Type of reaction	PDB HET
Ascorbate (ascorbic acid)	Redox	ASC
Adenosylcobalamin (vitamin B <sub>12</sub> )	Rearrangements, bond cleavage, group transfer (-CH <sub>3</sub> groups)	B12, COB
Biopterin	Group transfer (-OH groups), Redox	H4B, THB
Biotin*	Group transfer (-CO <sub>2</sub> groups)	BTN
Coenzyme A (CoA)	Group transfer (-CR groups)	COA
Coenzyme B (CoB)	Redox	TP7
Coenzyme M (CoM)	Group transfer (-CH <sub>3</sub> groups)	COM
Coenzyme Q (CoQ, ubiquinone)	Redox	U10
Dipyrromethane*	Polymerization	DPM
Cofactor 430 (factor F430)	Redox	F43
Flavin adenine dinucleotide* (FAD)	Redox	FAD
Flavin mononucleotide* (FMN)	Redox	FMN
Glutathione	Redox	GTT, GSH
Heme*	Redox	HEA, HEC, HEM
Lipoic acid*	Redox Group transfer [C(CH <sub>3</sub> )=O], mobility	LPA
MIO* (4-methyldieneimidazole-5-one)	Group transfer (NH <sub>2</sub> )	MDO
Molybdenum cofactor* (molybdopterin, MoCo), R = GMP or CMP	Redox	MGD, PTE
Menaquinone (vitamin K <sub>2</sub> )	Redox	MQ7
Nicotinamide adenosine dinucleotide (NAD, NADP)	Redox	NAD, NAP, NAI, NDP
Pyridoxal phosphate* (PLP)	Group transfer (-NH <sub>2</sub> and -CO <sub>2</sub> groups, Bond-cleavage/formation)	PLP
Phosphopantetheine*	Group transfer [-C(=O)R group], Mobility	PNS
Pyrroloquinoline quinone (PQQ)	Redox	PQQ
S-Adenosyl-methionine (SAM, AdoMet)	Group transfer (-CH <sub>3</sub> group), Redox	SAM
Siroheme	Redox	SRM
Thiamine diphosphate (ThDP, TDP)	Bond cleavage	TPP, TDP
Tetrahydrofolic acid (folic acid, folate)	Group transfer (-CH <sub>3</sub> ) activation	THF, MHF
Topaquinone* (TPQ)	Redox	TPQ
Orthoquinones* (TTQ, LTQ, CTQ)	Redox	-

## B IV.2 Flavin-dependent enzymes

Flavoproteins are a fundamental class of cofactor-dependent enzymes. They utilize flavin analogs derived from the yellow vitamin riboflavin (also known as vitamin B<sub>2</sub>) as cofactors to catalyze biochemical transformations.<sup>72</sup> Flavin-dependent enzymes play an essential role in many biological processes<sup>73</sup> and can catalyze a broad spectrum of catalytic reactions, including both redox and non-redox types. In most of these enzymes, a flavin is tightly but non-covalently bound.<sup>74</sup> However, in about 10% of flavoenzymes, the isoalloxazine ring of the flavin is covalently linked to a His, Cys, or Tyr residue of the polypeptide chain.<sup>75,76</sup> In a few cases, the flavin can also be anchored to the apoprotein via a bi-covalent linkage.<sup>77,78,79</sup> This covalent bond is formed via an autocatalytic process.<sup>80,81</sup>

Flavoenzymes are ubiquitous in nature. A total of 90 flavoproteins are encoded in the human genome and serve various biological functions.<sup>82</sup> The flavin analogs flavin adenine dinucleotide (FAD) and flavin mononucleotide (FMN) are the most common flavin cofactors bound to the apoprotein. The majority of flavoenzymes utilize FAD (75%) rather than FMN (25%) as the cofactor, while only a few use both.<sup>83</sup> Furthermore, most flavin-dependent enzymes belong to the class of oxidoreductases (91%), while transferases, lyases, isomerases, and ligases contribute only 9% (see Figure 11).

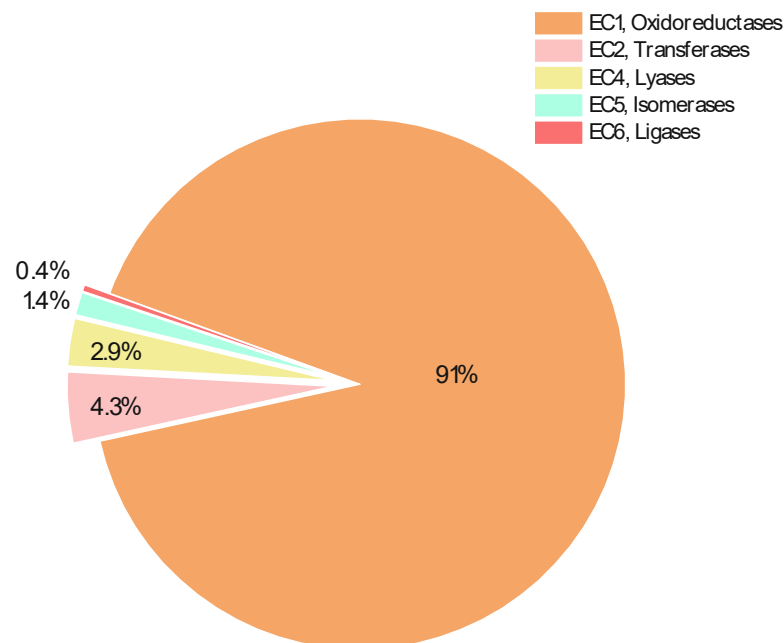


**Figure 11:** Pie chart of flavin-dependent enzymes in various enzyme classes.

Flavin-dependent enzymes play an essential role in humans' biological metabolism, including metabolic transformations, metabolic transportation, and control of metabolic

functions. Moreover, these enzymes have a crucial role in the biosynthesis of other cofactors, such as heme, coenzyme A, coenzyme Q, and pyridoxal 5'-phosphate, and they are also involved in the biosynthesis of hormones.<sup>72,82</sup> Hence, some illnesses and diseases of humans are linked to the malfunction of flavin-dependent enzymes.<sup>82</sup>

Flavoenzymes are among the most-studied families of enzymes and are thus heavily implemented in various applications, including the production of chemicals and pharmaceutical compounds by biotransformation. They are also involved in biodegradation and bioremediation, are used in biosensors, and are utilized as fluorescent reporters (see Figure 12).<sup>84-89</sup>

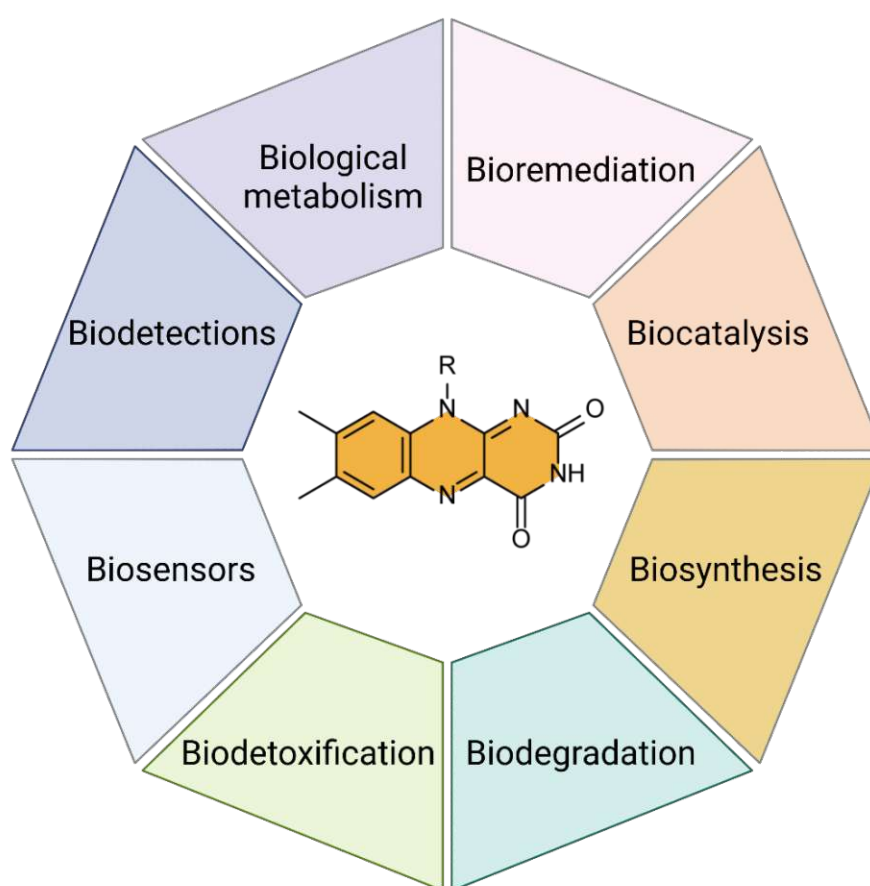


**Figure 12:** Some functions and applications of flavin-dependent enzymes in biological activities. The figure is adapted from reference.<sup>72</sup>

## B IV.2.1 Flavin derivatives and cofactors

As mentioned above, flavin derivatives are yellowish compounds originating from the vitamin riboflavin (7,8-dimethyl-10-ribityl-isoalloxazine), and they share the isoalloxazine core structure as their distinctive feature (Figure 13). Most bacteria, fungi, and plants contain



biosynthetic pathways to produce riboflavin, while other eukaryotes, such as humans, have lost the ability to produce it.<sup>90</sup> Consequently, humans must ingest riboflavin through food. The biosynthetic pathway of the most common cofactors FMN and FAD utilizes riboflavin as substrate, which is first converted to FMN by phosphorylation at the 5'-OH position of the ribityl side chain through *riboflavin kinase* (EC 2.7.1.26). Second, *FMN adenylyltransferase* (EC 2.7.7.2) adenylylates FMN to form FAD (see Figure 13).<sup>91</sup> Both steps require ATP. In archaea and eukaryotes, these two reactions are performed by two enzymes, while procaryotes utilize one bi-functional fusion protein (FAD synthetases).<sup>92,93</sup>

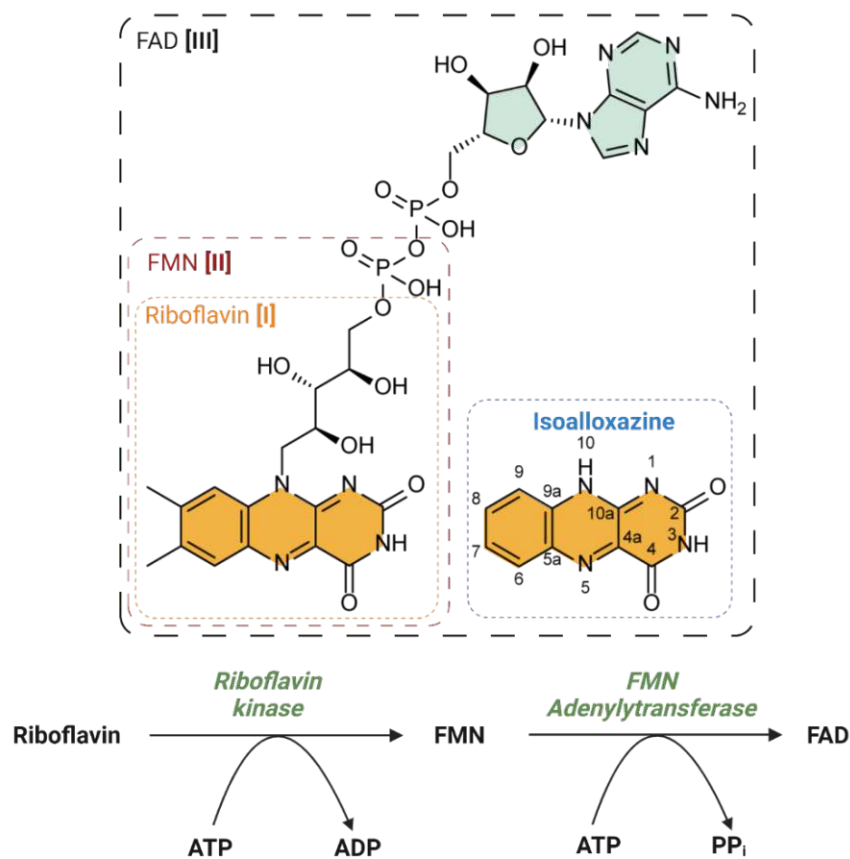


**Figure 13:** Structures of riboflavin, FMN, and FAD and their biosynthetic pathway.

Besides riboflavin [I], FMN [II], and FAD [III], structural analogs of riboflavin and its degradation products have been detected in nature in some organisms (see Figure 14).<sup>94</sup> For example, lumiflavin [IV] and lumichrome [V] are degradation products formed by photolysis reactions of flavins. Roseoflavin [VI] is the only known natural flavin analog that exhibits antibiotic activity.<sup>95</sup> The coenzyme F<sub>420</sub> [X] plays a key role in archaeal methanogenesis by donating electrons in the CO<sub>2</sub> reduction process.<sup>96,97</sup> It is derived from 5-deaza-7,8-didemethyl-8-hydroxy riboflavin (5-deazaflavin) [VIII].



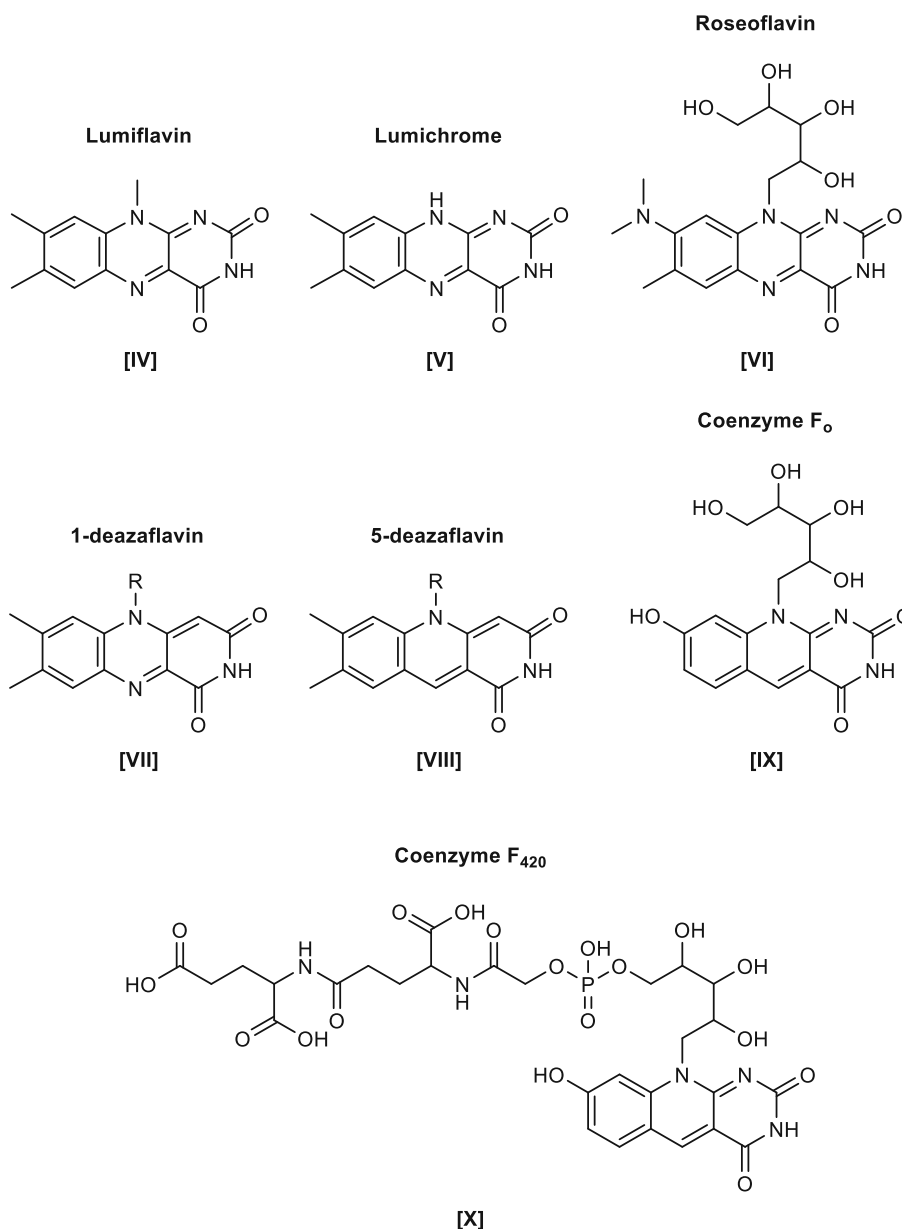


**Figure 14:** Flavin analogs are found in nature.

The chemically active portion of flavins is confined to the tricyclic dimethyl-isoalloxazine structure, which can be found in three oxidation states: the oxidized redox state, the flavin semiquinone (one-electron reduced), and the fully reduced form (two-electron reduced).<sup>98</sup> In the oxidized form (FL<sub>ox</sub>), which is primarily found in the resting state of enzymes, the isoalloxazine ring can accept one or two electrons. The N5 and C4a (see Figure 13) of the fully oxidized flavin are also susceptible to nucleophilic attack.

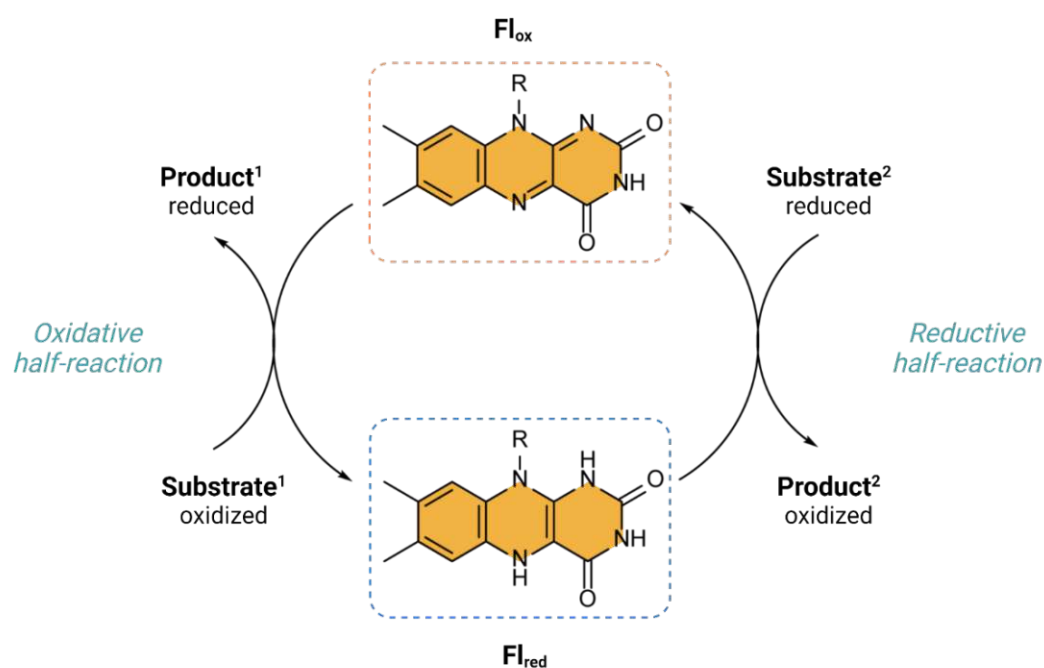
A one-electron transfer from a donor to the N5 of the isoalloxazine ring results in formation of the flavin semiquinone form (FL<sub>sq</sub>). Protonation of the N5 of the isoalloxazine ring results in the blue/neutral semiquinone, while deprotonation results in the red/anionic semiquinone. These single-electron-reduced forms are thermodynamically unstable in aqueous solutions;

however, they can be stabilized by protein interactions.<sup>99</sup> The two-electron reduced state, also known as hydroquinone, can be formed by a two-electron transfer from a reductant to the oxidized state. Hydroquinones can react as nucleophiles at the N5 and C4a positions of the isoalloxazine ring and can also act as single-electron donors or as hydride donors.<sup>72,98</sup>

A key factor for flavoenzymes is bound flavin's redox potential since it gives information on reactivity towards redox substrates and is also a measure of the electrophilicity or nucleophilicity of the isoalloxazine ring. At pH 7, the reduction potential of the two-electron reduction of free flavin in solution is -207 mV, while the single-electron potentials are -314 mV for the oxidized/semiquinone couple and -124 mV for the semiquinone/hydroquinone couple.<sup>98</sup> However, this value can greatly vary depending on the structure of the flavoprotein.<sup>100</sup>

## B IV.2.2 Reactions and the classification of flavin-dependent enzymes

The catalytic cycle of flavoenzymes generally consists of two half-reactions: reductive and oxidative (see Scheme 1).<sup>86,101,102</sup> In biotransformation processes, one half-reaction is used to convert a substrate to the corresponding product, while the other half-reaction is then used to regenerate the resting state of the enzyme.



**Scheme 1:** Representative catalytic cycle of flavin-dependent enzymes.

In the reductive half-reaction, the oxidized form of the flavin is typically reduced by a hydride transfer to form the reduced flavin  $\text{Fl}_{\text{red}}$  or by a single-electron transfer to produce the anionic semiquinone species (see Figure 15).<sup>103</sup> In many cases, the nicotinamide coenzymes nicotinamide adenine dinucleotide (NADH) and nicotinamide adenine dinucleotide phosphate (NADPH) are involved in the reduction of the flavin, though these compounds are expensive, unstable, and require stoichiometric amounts. Therefore, several NAD(P)H recycling systems have been developed. Using these systems, the reduced flavin species can engage molecular oxygen (see Figure 15) during the oxidative half-reaction to form a C4a-peroxyflavin, which protonation results in the formation of the C4a-hydroperoxyflavin.<sup>88</sup> C4a-peroxyflavin and C4a-hydroperoxyflavin are key intermediates in Baeyer-Villiger and hydroxylation reactions, respectively.<sup>103</sup>

The reduced flavin  $\text{Fl}_{\text{red}}$  in ene-reductases catalyzes the reduction of activated carbon-carbon double bonds (see Figure 15).<sup>104</sup>

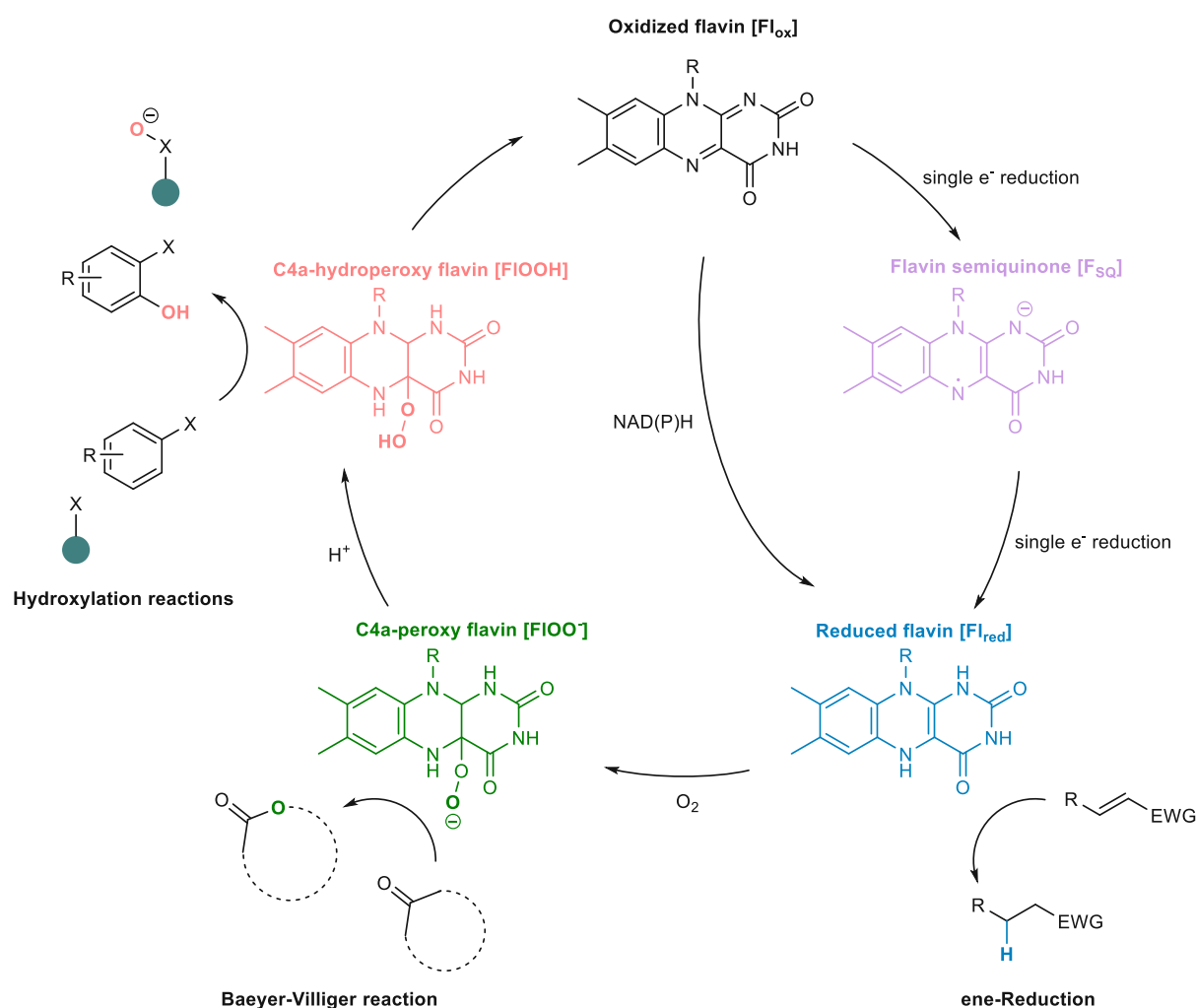


**Figure 15:** Overview of chemical transformations performed from flavin-dependent enzymes. The figure was adapted from reference.<sup>88</sup>

Due to the chemical versatility of flavins, flavin-dependent enzymes can catalyze a broad scope of chemical reactions (e.g., oxidation/reduction of carbon-heteroatom bonds,<sup>105-107</sup> oxidation/reduction of carbon-carbon bonds,<sup>108</sup> hydroxylation of aromatic and aliphatic structures,<sup>109</sup> Baeyer-Villiger reactions,<sup>110</sup> electron transfer, (de)halogenations<sup>111</sup> and (de)carboxylation). Based on their mechanisms, flavin-dependent enzymes can be divided into the following three main groups:

- (1) Oxidase/dehydrogenase
- (2) Monooxygenase
- (3) Reductase

## **B IV.2.3 Flavin-dependent oxidases and dehydrogenases**

Flavin-dependent oxidases oxidize a substrate with the concomitant reduction of molecular oxygen (electron acceptor) to hydrogen peroxide. In flavin-dependent dehydrogenases, in contrast, NAD(P)<sup>+</sup> or other organic molecules, such as benzoquinone derivatives, act as the electron acceptor.<sup>112</sup> Based on their sequence and structural similarity, flavin oxidases and dehydrogenases have been divided into six subclasses: vanillyl alcohol oxidase (VAO), amino acid oxidase (AAO), sulfhydryl oxidase (SOX), acyl-CoA oxidase (ACO), 2-hydroxyacid oxidase (HAO), and glucose-methanol-choline oxidoreductase (GMC).<sup>113</sup> Flavin-dependent oxidases and dehydrogenases have applications in various fields, ranging from utilization in biosensors<sup>114,115</sup> (e.g., to measure and monitor the sugar concentration in food or blood)<sup>116</sup> to applications as biocatalysts for the production of high-value compounds and for biomass-degradation.

## **B IV.2.4 Flavin-dependent monooxygenases**

Flavin-dependent monooxygenases can insert a single oxygen atom derived from molecular oxygen into an organic substrate while the other oxygen atom is reduced to water. Based on their structural features, protein sequences, electron donor, and type of oxygenation, flavin-dependent monooxygenases are categorized into eight subclasses (A–H).<sup>109</sup> Monooxygenases are further divided into two groups based on the number of polypeptide chains (one or two)

involved in the catalytic process; in single-component monooxygenases, the oxidative and reductive half-reactions are catalyzed by a single polypeptide chain, while in two-component enzymes, a reductase and an oxidase are required to catalyze each half-reaction.

Flavin-dependent monooxygenases catalyze a wide selection of chemical transformations, including hydroxylation, epoxidation, (de)halogenations, Baeyer-Villiger oxidations, and sulfoxidation.<sup>109</sup>

## **B IV.2.5 Flavin-dependent reductases**

Flavin-dependent reductases are two-component enzymes that consist of a flavin reductase and a flavin monooxygenase to oxidize various substrates. The flavin reductase plays a key role in supplying the reduced flavin to the monooxygenase, while the monooxygenase utilizes the reduced flavin in the oxidative half-reaction to activate molecular oxygen.<sup>117</sup> Compared to other flavoproteins with a tightly or even covalently bound flavin as a prosthetic group, this enzyme class relies on a diffusible flavin. Therefore, the reductive and oxidative half-reaction can occur on the two polypeptide chains. Examples of flavin-dependent reductases are nitro reductase and quinone reductase, which catalyze the reduction of nitroaromatics to hydroxylamine products<sup>118</sup> and benzoquinone to hydroquinone derivatives,<sup>119</sup> respectively. Nitro reductases and quinone reductases find application in the medicinal and environmental sectors.<sup>120-122</sup>

The most prominent examples of flavin-dependent reductases, however, are ene-reductases, which catalyze the reduction of carbon-carbon double bonds. Ene-reductases have been divided into five subclasses, with the FMN-dependent old yellow enzyme being the most famous example. Ene-reductases catalyze the reduction of  $\alpha,\beta$ -unsaturated alkenes (see Figure 15) containing activating groups such as aldehydes, ketones, nitro groups, nitriles, di-carboxylic acids, or di-esters.<sup>72</sup> Since ene-reductases depend on NAD(P)H, their utilization in industrial applications is limited.

## **B IV.3 The GMC-type oxidase family and Baeyer-Villiger monooxygenases**

In the previous chapters, general knowledge about flavin-dependent enzymes was provided. The following chapters examine flavin-dependent enzyme families and the enzymes relevant to this thesis.

## B IV.3.1 The GMC-type oxidase family

The glucose-methanol-choline oxidoreductase (GMC) family, which belongs to FAD-dependent oxidoreductases, was identified in the 1990s.<sup>123</sup> Members of the GMC family share a conserved N-terminal FAD-binding domain (GMC\_oxred\_N), which includes the Rossmann-fold motif (GxGxxG/A). In this family, the C-terminal domain is involved in the substrate binding and thus is less conserved. However, the C-terminal domain exhibits a highly conserved histidine at the active site, which is involved in the catalytic mechanism of the reductive half-reaction.<sup>124,125</sup> In GMCs, this conserved histidine residue acts as a catalytic base by abstracting the hydroxyl proton from the substrate.<sup>126</sup> Most enzymes of the GMC family utilize a tightly but non-covalently bound FAD cofactor, although some contain a covalently linked FAD (see Table 2). GMC enzymes catalyze the formation of aldehydes and ketones through the oxidation of a broad set of corresponding primary and secondary alcohols. Additionally, double oxidations have been reported in this family, in which a primary alcohol is converted first to the corresponding aldehyde and then to the carboxylic acid.<sup>127, 128</sup> Several members of the GMC family are compiled in Table 2.

**Table 2:** A list of members of the GMC family.

Enzyme	Name	Cofactor and attachment	Substrate	Reference
Alcohol oxidase	AO	FAD, xylo-FAD	Alcohol	129
Aryl-alcohol oxidase	AAO	FAD	Alcohol	130
Cellobiose dehydrogenase	CDH	FAD, 6-OH FAD, heme <i>b</i>	Carbohydrate	131
Cholesterol oxidase	CO	FAD	Sterol	132
Choline dehydrogenase	CHD	8 $\alpha$ -N <sup>3</sup> -hystidyl FAD*	Alcohol	133
Choline oxidase	CHO	8 $\alpha$ -N <sup>3</sup> -hystidyl FAD*	Alcohol	134
5-Hydroxymethylfurfural oxidase	HMFO	FAD	Alcohol	128
Glucose oxidase	GOx	FAD	Carbohydrate	135
Pyranose dehydrogenase	PDH	8 $\alpha$ -N <sup>3</sup> -hystidyl FAD*	Carbohydrate	136
Pyranose 2-oxidase	P2O	8 $\alpha$ -N <sup>3</sup> -hystidyl FAD*	Carbohydrate	137
Pyrodoxine 4-oxidase	PNOX	FAD	Alcohol	138

An asterisk (\*) indicates that this cofactor is covalently attached to the enzyme.

## B IV.3.1.1 Glucose oxidase

Likely the most-studied enzyme of the GMC flavoprotein family is glucose oxidase (EC 1.1.3.4), which catalyzes the oxidation of  $\beta$ -D-glucose to D-glucono- $\delta$ -lactone, thereby producing hydrogen peroxide.<sup>139</sup> The D-glucono- $\delta$ -lactone hydrolyzes spontaneously to the carboxylic acid. Some fungi and insects naturally produce glucose oxidase and experience its natural function to produce hydrogen peroxide, which has anti-bacterial and anti-fungal activity.<sup>140</sup> The enzyme was first isolated from *Aspergillus niger* extracts by Detlev Müller in 1928.<sup>141</sup> Glucose oxidase from *Aspergillus niger* is a homodimeric glycoprotein consisting of two identical polypeptide chains. Each subunit of the protein utilizes a non-covalently bound FAD as a cofactor.<sup>142</sup> In 1993, the crystal structure of glucose oxidase from *Aspergillus niger* was solved by Hecht *et al.*<sup>143</sup> Three amino acids, a glutamic acid (E412), and two conserved histidine residues (H516 and H559) have been identified as being located near the active site of the enzyme. Another well-studied glucose oxidase is derived from *Penicillium amagasakiense*, a homodimeric glycoprotein with each subunit containing FAD as a cofactor.<sup>144</sup> Similar to glucose oxidase from *Aspergillus niger*, glucose oxidase from *Penicillium amagasakiense* exhibits three amino acids in the active site, a glutamic acid (E416), and two histidines (H520 and H563).

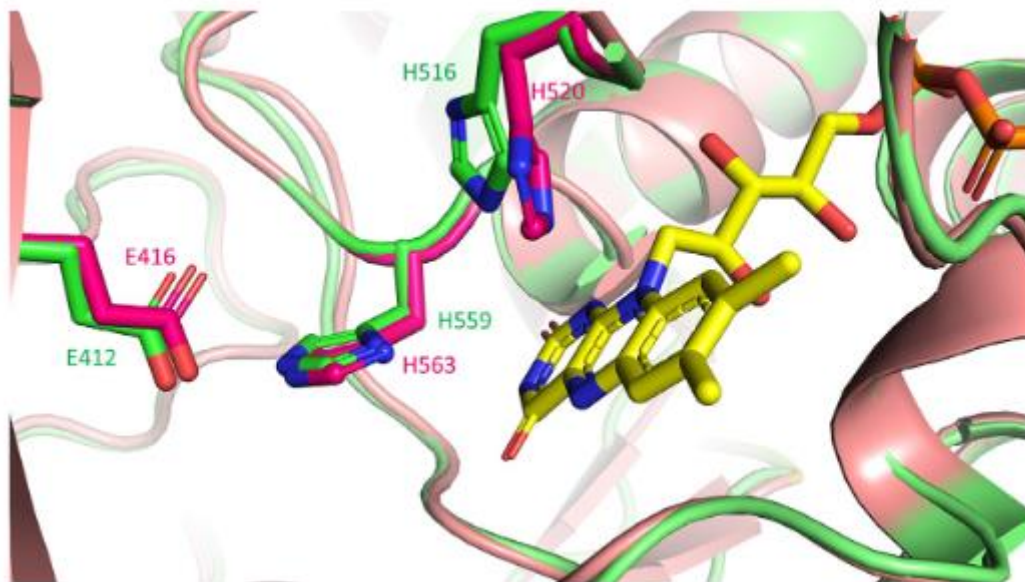
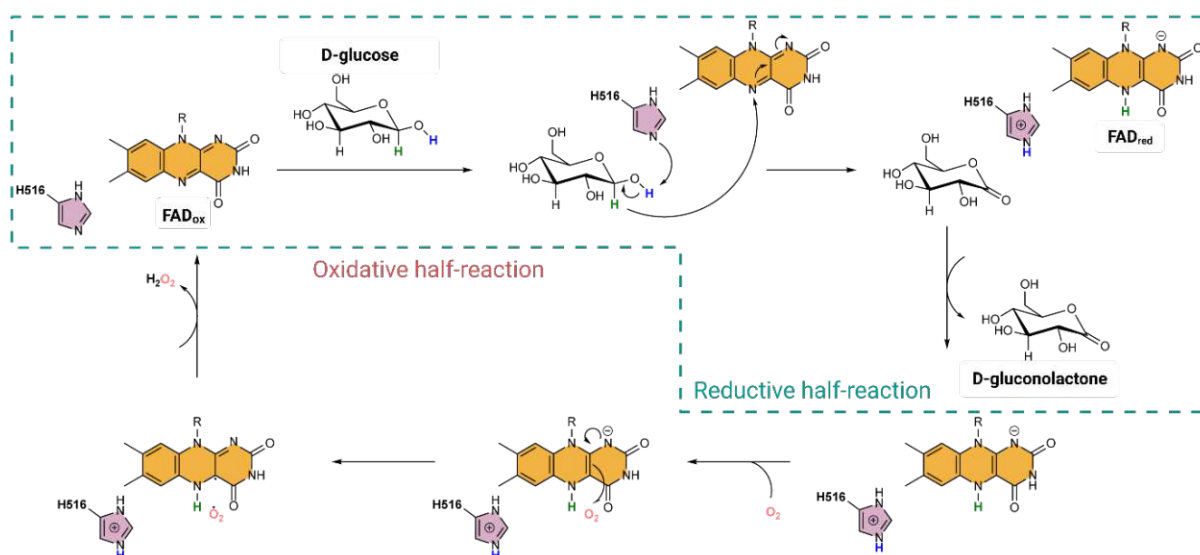


**Figure 16:** Comparison of the active sites of glucose oxidase from *Aspergillus niger* (PDB code: 1GAL; green color) and *Penicillium amagasakiense* (PDB: 1GPE; pink color). The figure was taken from reference.<sup>145</sup>



## B IV.3.1.2 Mechanistic aspects of glucose oxidase

In the resting state of glucose oxidase, a water molecule (W110) is located in the enzyme's active site, forming hydrogen bonds to the two conserved histidine residues, H516 and H559, and to the N1 position of the flavin. This water molecule is replaced by D-glucose, which then is deprotonated at the C1-hydroxyl group by the H516. This proton transfer from the C1-hydroxyl group of glucose to H516 coincides with the hydride transfer from the C1 of glucose to the N5 of FAD. Finally, the product is replaced by a water molecule.<sup>146</sup> Then, the reduced FAD cofactor is reoxidized by molecular oxygen via two single-electron transfer steps during the oxidative half-reaction, which forms hydrogen peroxide and regenerates the oxidized enzyme (see Scheme 2).<sup>145</sup>



**Scheme 2:** Overview of the catalytic cycle of glucose oxidase. The figure was adapted from reference.<sup>145</sup>

## B IV.3.1.3 Applications of glucose oxidase

Glucose oxidase has many industrial applications; for example, in the food industry, it is used to produce bread with better quality and extended loaf volume.<sup>147</sup> Another important application is the production of gluconic acid, which is often used in the food industry as a color stabilizer, antioxidant, and chelating operator in dough, feeds, and beverages.<sup>148</sup> Moreover, the salts of gluconic acid are important for the production and formulation of certain drugs.<sup>149</sup>

However, the most outstanding application of glucose oxidase is its utilization in biosensors for clinical applications<sup>150,151</sup> and in the food industry,<sup>152</sup> particularly the application as glucose biosensors for diabetic blood monitoring, which has enhanced treatment efficiency in patients with diabetes. In this context, continuous and long-term monitoring is of enormous



interest.<sup>151,153</sup> Although significant improvements regarding the stability of the enzyme have been made, today's glucose biosensors possess a lifetime of up to 14 days; the intrinsic instability of the enzyme and the loss of activity must be overcome for further developments.

## B IV.3.2 Cellobiose dehydrogenase

Cellobiose dehydrogenase (CDH) (EC 1.1.99.18) is another important enzyme belonging to the superfamily of GMC-oxidoreductase. This enzyme was first discovered by Westermark and Eriksson in 1974 in the secretomes of the ligninolytic fungi *Polyporus versicolor* and *Sporotrichum pulverulentum*, which were grown on cellulosic powder as a carbon source.<sup>154</sup> Cellobiose dehydrogenase is an extracellular flavocytochrome consisting of two distinct domains containing FAD and heme *b* as a prosthetic group. Both domains are connected by a protease-sensitive linker.<sup>131,155</sup> The enzyme catalyzes the oxidation of cellobiose to the corresponding lactone cellobiono-1,5-lactone, which hydrolyzes spontaneously to cellobionic acid. The biological function of cellobiose dehydrogenase has been highly debated; its proposed functions have ranged from removing substrate inhibition from cellulases by oxidation of cellobiose to detoxifying plant quinones.<sup>156-158</sup> Nevertheless, the activity of the isolated dehydrogenase domain was sufficient for all the proposed functions, but the requirement of the cytochrome domain was not explained. This changed with the discovery of lytic polysaccharide monooxygenases (LPMOs) in 2010.<sup>159</sup> LPMOs are metalloenzymes that catalyze the oxidative cleavage of 1,4-glycosidic polysaccharide bonds.<sup>160</sup> CDH acts as an electron donor for the initial reduction process of LPMO. While the isolated dehydrogenase domain of the CDH does not show any effect on LPMO activity, the cytochrome domain exhibits efficient electron shuttle properties between the FAD-containing dehydrogenase moiety and the copper ion in the active site of the LPMO.<sup>161,162</sup>

The mobility of the cytochrome domain, which is essential for the electron transfer between both enzymes, prevented initial attempts to crystallize the full-length CDH. Therefore, the first structures of the CDH were solved from individual domains after proteolytic cleavage of the linker. In 2000, the X-ray structure of the cytochrome domain was solved by Hallberg *et al.*,<sup>163</sup> who later clarified the structure of the flavin-containing dehydrogenase domain in 2002.<sup>164</sup>

The heme domain of CDH consists of 190 amino acids, which form five-stranded and six-stranded  $\beta$ -sheets designated as an inner and outer sheet.<sup>156</sup> The binding pocket of heme *b* is located in the inner sheet, and the iron center is hexacoordinated. M65 and H163 were assigned as the axial ligands in this center by site-directed mutagenesis studies.<sup>165</sup>

The dehydrogenase domain consists of 540 amino acids and features two distinct subdomains typically for GMC-oxidoreductases: the FAD-binding domain and the substrate-binding domain, which comprise 205 and 335 amino acids, respectively. The FAD-domain shows the specific consensus sequence of GxGxxG/A, which results in the characteristic  $\beta\alpha\beta$ -fold (Rossmann fold).

### **B IV.3.2.1 Mechanistic aspects of cellobiose dehydrogenase**

To obtain insights into CDH's mode of action, the enzyme was co-crystallized with the inhibitor cellobionolactam, which is the amid analog of cellobionic acid.<sup>166</sup> In these studies, a histidine residue H689 was proposed to act as a general base catalyst to deprotonate the equatorial 1-hydroxyl group of cellobiose. Another amino acid residue was found to be essential for catalytic activity. The N732 is believed to facilitate deprotonation through H689 by donating an H-bond to the C1 hydroxy group and supporting substrate binding and positioning relative to the cofactor and catalytic base.<sup>166</sup>

The identification of H689 as a catalytic base and the structural viewpoint regarding the relative orientation of substrate and cofactor provide a strong indication for a general base-catalyzed hydride transfer mechanism. This mechanism begins with the deprotonation of the C1 hydroxyl group of cellobiose catalyzed by H689 and subsequent hydride transfer from the C1 to the N5 atom of the flavin cofactor. This results in the two-electron reduction of FAD to FAD<sub>red</sub> with the concomitant oxidation of cellobiose to the corresponding lactone in the reductive half-reaction of CDH.

In the oxidative half-reaction, FAD is regenerated to complete the catalytic cycle. This can be accomplished via two routes. The CDH can directly reduce one- or two-electron acceptors at the site of FAD<sub>red</sub>, or, alternatively, can transfer single electrons from FAD<sub>red</sub> via the heme cofactor to external single-electron acceptors like LPMO or cytochrome c.<sup>167</sup>

### **B IV.3.2.2 Applications of cellobiose dehydrogenase**

CDH is widely used in diverse applications, including biomass hydrolysis,<sup>168,169</sup> bioremediation,<sup>170,171</sup> biocatalysis,<sup>172,173</sup> and bioelectrochemical applications.<sup>174,175</sup>

## B IV.4 Baeyer-Villiger monooxygenases

Baeyer-Villiger monooxygenases (BVMOs) belong to the superfamily of oxidoreductases. BVMOs are divided into two classes: type I BVMOs are NADPH-dependent, FAD-containing monooxygenases, while type II BVMOs are FMN-containing monooxygenases with strict NADH dependency.

Type I BVMOs are encoded in a single gene and thus belong to class B flavoprotein monooxygenases.<sup>176</sup> These BVMOs typically exhibit a highly conserved motif that can be either FxGxxxHxxxW[P/D]<sup>177</sup> or [A/G]GxWxxxx[F/Y]P[G/M]xxxD<sup>178</sup>. Although the role of these fingerprint motifs is not entirely understood, the long consensus sequence [AG]GxWxxxx[FY][GM]xxxD entails the conserved active-site aspartate. The short fingerprint FxGxxxHxxxW[P/D] is related to the linker connecting the NADP and FAD-binding domains.<sup>179,180</sup> These two fingerprint motifs are surrounded by two Rossmann fold domains (GxGxxG/A, also see chapters B IV.3.1 and B IV.3.2), which are essential for binding the cofactor FAD and the electron donor NADPH.

In contrast to type I BVMOs, type II BVMOs comprise two subunits and depend on FMN; hence, they are categorized as class C flavoprotein monooxygenases. A third class of BVMOs is called type O BVMOs, where O stands for odd or atypical. However, only a few representatives of type O BVMOs have been characterized, and this class is missing the consensus motif typical of type I BVMOs. Furthermore, this class does not show structural similarity with other types I or II BVMOs.<sup>181</sup> A list of characterized BVMOs is compiled in Table 3, and their relationships can be seen in Figure 17.

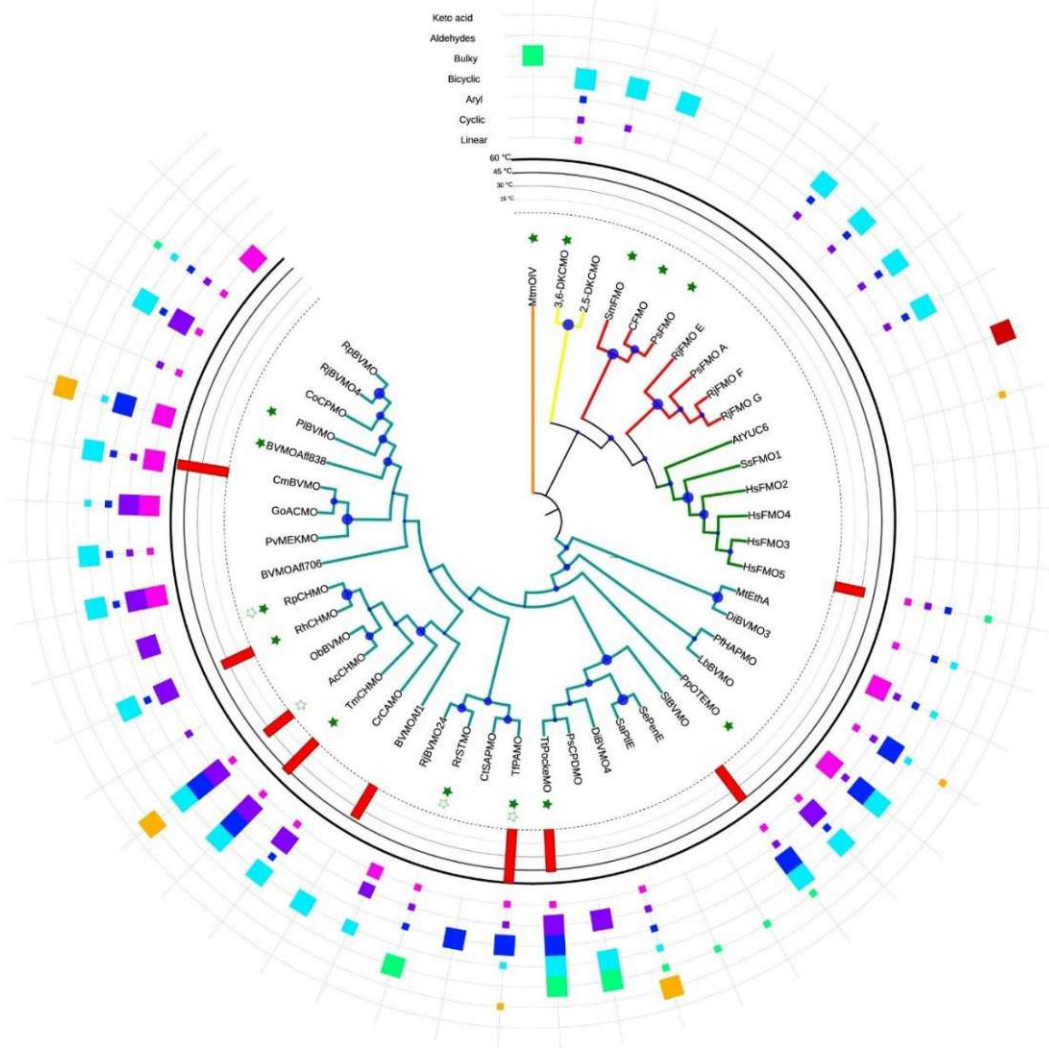


**Figure 17:** BVMOs phylogenetic tree. The figure was taken from reference.<sup>181</sup>

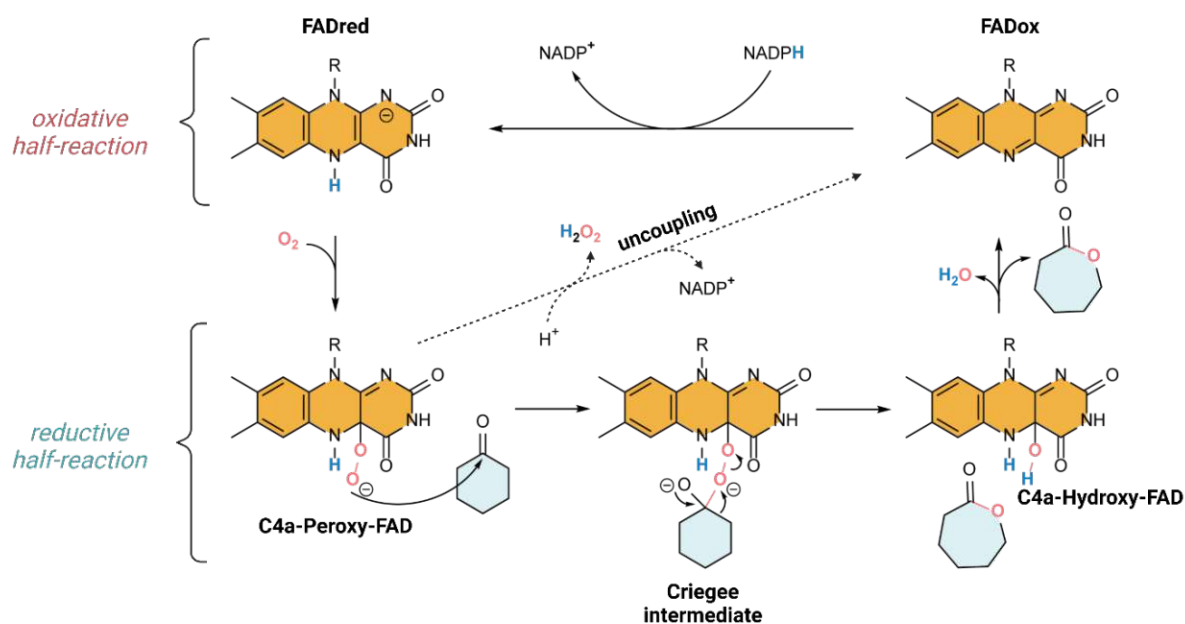
**Table 3:** A list of identified and characterized BVMOs.

Enzyme	Origin	Reference
CHMO <sub>Acineto</sub>	<i>Acinetobacter</i> NCIMB 9871	182
CHMO <sub>Coma</sub>	<i>Comamonas</i> NCIMB 9872	183
STMO	<i>Rhodococcus</i> <i>rhodochrous</i>	184
CHMO <sub>Brevi</sub>	<i>Brevibacterium</i> HCU	185
HAPMO	<i>Pseudomonas</i> <i>fluorescens</i> ACB	186
CDMO	<i>Rhodococcus</i> <i>ruber</i> SC1	187
BVMO <sub>P.putida</sub>	<i>Pseudomonas</i> <i>putida</i> KT2440	188
CHMO <sub>Xantho</sub>	<i>Xanthobacter</i> sp.strain ZL5	189
CHMO <sub>Arthro</sub>	<i>Arthrobacter</i> BP2	190
CHMO <sub>Brachy</sub>	<i>Brachymonas</i> <i>petroleovorans</i>	191
CHMO <sub>Rhodo 1&amp;2</sub>	<i>Rhodococcus</i> <i>Phi1</i> and <i>Phi2</i>	192
BVMO EtaA	<i>Mycobacterium</i> <i>tuberculosis</i>	193
PAMO	<i>Thermobifida</i> <i>fusca</i>	194
ACMO	<i>Gordonia</i> sp. strain TY-5	195
AKMO	<i>Pseudomonas</i> <i>fluorescens</i> DSM 50106	196
MEKMO	<i>Pseudomonas</i> <i>veronii</i> MEK700	197
HAPMO	<i>Pseudomonas</i> <i>putida</i> JD1	198
BVMO <sub>piiE</sub>	<i>Streptomyces</i> <i>avermitilis</i> MA4680	199
CHMOR.sp HI-31	<i>Rhodococcus</i> sp. strain HI-31	200
BVMO <sub>penE</sub>	<i>Streptomyces</i> <i>exfoliatus</i>	201
OTEMO	<i>Pseudomonas</i> <i>putida</i> ATCC 17453	202
SAPMO	<i>Comamonas</i> <i>testosteroni</i> KF-1	203
CAMO	<i>Cylindrocarpon</i> <i>radicicola</i> ATCC 11011	204
2,5-DKCMO, 3,6-DKCMO	<i>Pseudomonas</i> <i>putida</i> ATCC17453	205
SAFMO	<i>Staphylococcus</i> <i>aureus</i>	206
BVMO <sub>AFL</sub>	<i>Aspergillus</i> <i>Flavus</i>	207
TmCHMO	<i>Thermocrisum</i> <i>municipale</i>	208
PockeMO	<i>Thermothelomyces</i> <i>thermophila</i>	209
BVMO <sub>I:biflexa</sub>	<i>Leptospira</i> <i>biflexa</i>	210
MtmOIV	<i>Streptomyces</i> <i>argillaceus</i> ATCC 12956	211
BVMOSIe_13190 & SIe_62070	<i>Streptomyces</i> <i>leeuwenhoekii</i>	212
BoBVMO	<i>Bradyrhizobium</i> <i>oligotrophicum</i>	213
AmBVMO	<i>Aeromicrobium</i> <i>marinum</i>	213
BVMORp	<i>Rhodococcus</i> <i>pyridinivorans</i>	214

## B IV.4.1 The enzymatic mechanism of BVMOs

In the Baeyer-Villiger oxidation, BVMOs catalyze the enzymatic insertion of an oxygen atom next to a ketone-functionality of the substrate. In contrast to the chemically catalyzed reaction first reported by Baeyer and Villiger,<sup>215</sup> in which peracids are needed for oxidation, enzymatic Baeyer-Villiger oxidation uses molecular oxygen directly from the air. The mechanism of the catalytic cycle of BVMOs was solved by pre-steady-state kinetic studies on cyclohexanone monooxygenase (CHMO).<sup>216</sup> In the resting state of the enzyme, the FAD cofactor is in its oxidized form (FAD<sub>ox</sub>). The catalytic cycle (Scheme 3) is first initiated by the reduction of the flavin cofactor by NADPH, which produces the reduced form of the flavin (FAD<sub>red</sub>). Molecular oxygen then reacts with reduced FAD in the enzyme's active site, forming a flavin-C4a-peroxide intermediate, which is stabilized by the enzyme.<sup>217,218</sup> This C4a-peroxyflavin can be considered an activated form of oxygen that can incorporate a single oxygen into an organic substrate.<sup>218</sup> It attacks the carbonyl compound of the substrate (cyclohexanone) upon binding in the active site, leading to the formation of the Criegee intermediate. This tetrahedral intermediate rearranges in a fashion that allows the product ( $\epsilon$ -caprolactone) and a molecule of water to be released. The reduced FAD is finally regenerated by NADPH and ready for the next catalytic cycle<sup>219</sup> (see Scheme 3). A common side reaction is observed in BVMO-catalyzed reactions: the uncoupling reaction. In this reaction, the flavin-C4a-hydroperoxide intermediate decomposes into H<sub>2</sub>O<sub>2</sub> instead of the desired insertion of the oxygen atom into the substrate. Then, it returns to the resting state without substrate turnover.<sup>220</sup> Therefore, BVMOs show an NADPH oxidase activity, which can result in incorrect interpretations of results when the activity is measured using the NADPH consumption approach.<sup>221</sup>

Besides the classical reaction, BVMOs can oxygenate heteroatoms such as sulfur, nitrogen, phosphorus, boron, or selenium.<sup>222</sup> Due to the tremendous diversity of the catalytic properties of BVMOs, which provide access to many different classes of valuable compounds, enormous interest has been taken in their industrial applications. Nevertheless, the reported intrinsic instabilities of BVMOs limit their more comprehensive application.



**Scheme 3:** Catalytic cycle of cyclohexanone monooxygenase with cyclohexanone as substrate.

## B IV.4.2 Structures of BVMOs

The first crystal structure solved from a BVMO was phenylacetone monooxygenase (PAMO) from *Thermobifida fusca*, which was elucidated by Malito *et al.* in 2004.<sup>223</sup> The structure provided insight into a two-residue insertion displayed by PAMO, which was found in the active site and afterward called *the bulge*.<sup>181</sup> Subsequent structural studies on PAMO<sup>224</sup> and CHMO from *Rhodococcus* sp. HI-31<sup>225</sup> provided further details about the mechanism of these enzymes. In addition to *the bulge*, a highly conserved arginine residue in the active site was identified as playing a key role in the catalytic activity.<sup>224</sup> This residue was also found in the structures of several other BVMOs and subsequent mutants. Although the sequence identities of BVMOs are often less than 40%, their structures are remarkably similar. Except for PAMO, which shows high thermal stability, many other BVMOs are somewhat unstable.

Nevertheless, no apparent structural feature has been identified as responsible for PAMO's excellent stability. Instead, a possible explanation is PAMO's higher number of ionic bridges.<sup>226</sup> The identification of various structures of BVMOs has been essential for clarification of their catalytic mechanism, and comprehensive knowledge about key residues in these enzymes is crucial for their further development.



## B IV.4.3 Applications of BVMOs

Many BVMOs have been identified and studied thoroughly. These astonishing enzymes enable access to a wide variety of high-value compounds that can be used in various fields, such as polymer chemistry or the pharmaceutical industry. Moreover, their ability to catalyze a broad spectrum of reactions under mild conditions with high regio-, chemo-, and stereoselectivity has resulted in many biocatalytic applications. Nevertheless, due to their low stability and dependence on the expensive NAD(P)H cofactors, their industrial-scale application has typically not proceeded beyond the pilot scale, and only a few applications have been reported (Table 4).

**Table 4:** Examples of industrial applications of BVMOs. The table was adapted from reference.<sup>181</sup>

Product	Product concentration (g/L) + isolated yield	Enzyme	Biocatalyst yield (g <sub>product</sub> /g <sub>enzyme</sub> )	Ref.
<b>Esomeprazole</b>	50 (~151 mM) 87% yield (28.7 g)	AcCHMO (multiple mutant)	50	227
<b>Bicyclo[3.2.0]hept-2-en-6-one lactone</b>	4.5 (~41 mM) 55% yield (0.49 kg)	AcCHMO	3 <sup>a</sup>	228
<b>(Z)-11-(Heptanoyloxy)undec-9-enoic acid</b>	41 (132 mM) 68% yield (75 g)	<i>Pseudomonas putida</i> BVMO (E6-BVMO C302L)	1.6 <sup>a</sup>	229
<b>3,3,5-Trimethylcaprolactone</b>	24.4 (~156 mM) 76% yield (1.9 kg)	TmCHMO	0.6 <sup>a</sup>	230
<b>6-Hydroxyhexanoic acid</b>	20 (~151 mM) 81% yield (8.1 g)	AcCHMO C376L/M400I/T415C/A463C	0.7 <sup>a</sup>	231
<b>Lactone of (2R, 5R, 6R)-6-methyldihydrocarvone</b>	0.82 (4.5 mM) 90% yield (49 mg)	CHMO_Phi1	6.7	232
<b>Precursor of Nylon-9</b>	8 (70 mM) 70% yield (33 g)	CPDMO	2.3 <sup>a</sup>	233

<sup>a</sup> g<sub>product</sub>/g<sub>dcw</sub> = gram product per gram cell dry weight.

## B IV.4.4 Cyclohexanone monooxygenase

Since its isolation from *Acinetobacter calcoaceticus* NCIB 9871 (CHMO<sub>Acineto</sub>, EC 1.14.13.22) and identification by Trudgill *et al.* in 1976,<sup>183</sup> the bacterial flavoenzyme cyclohexanone monooxygenase (CHMO) has served as a role model for prokaryotic type I BVMOs. However, not until 2019 was the structure of CHMO, although a mutant with 10 substitutions in the active site, solved.<sup>234</sup> CHMO<sub>Acineto</sub> drew considerable attention because its product  $\epsilon$ -caprolactone was recognized as an important precursor for the production of polymers, including nylon 6. Moreover, CHMO<sub>Acineto</sub> shows an astoundingly broad substrate acceptance (more than 100 non-natural substrates).<sup>235</sup> Therefore, it can oxidize diverse



structural compounds with high regio-, chemo-, and enantioselectivity. Furthermore, like many other BVMOs, its oxidizing capability is not restricted to the Baeyer-Villiger reaction but can perform sulfoxidation, amine oxidation, and epoxidation.

Although its extraordinary versatility makes CHMO interesting for many purposes, its lack of stability remains a major hurdle for its industrial applications.

## **B V The stability of enzymes**

Although enzymes display many outstanding properties, their intrinsic instabilities often prevent their broader application in the industry; the stability of a biocatalyst is a vital factor that determines whether its industrial application will be successful.<sup>242</sup> Consequently, enormous interest lies in developing novel strategies to improve the stability of enzymes and, thus, their exploitation in industrial processes.

### **B V.1 Thermodynamic versus kinetic stability**

The term *protein stability* often has different meanings, making comparison of results in the literature ambiguous. The most used terms will be clarified in the following sections.

#### **B V.1.1 Thermodynamic stability**

Thermodynamic stability describes the tendency of a protein to unfold reversibly. The unfolding process is a measure of thermodynamic stability and can be described by the free energy of unfolding ( $dG_u$ ), the unfolding equilibrium constant ( $K_u$ ), or the melting temperature of the protein ( $T_m$ , the temperature at which 50% of the protein is unfolded).<sup>9,243</sup> Thermodynamic stability can be determined, for example, by differential scanning calorimetry and tryptophan fluorescence. This type of stability provides more information about the structural stability of the enzyme than about its stability under certain reaction conditions.

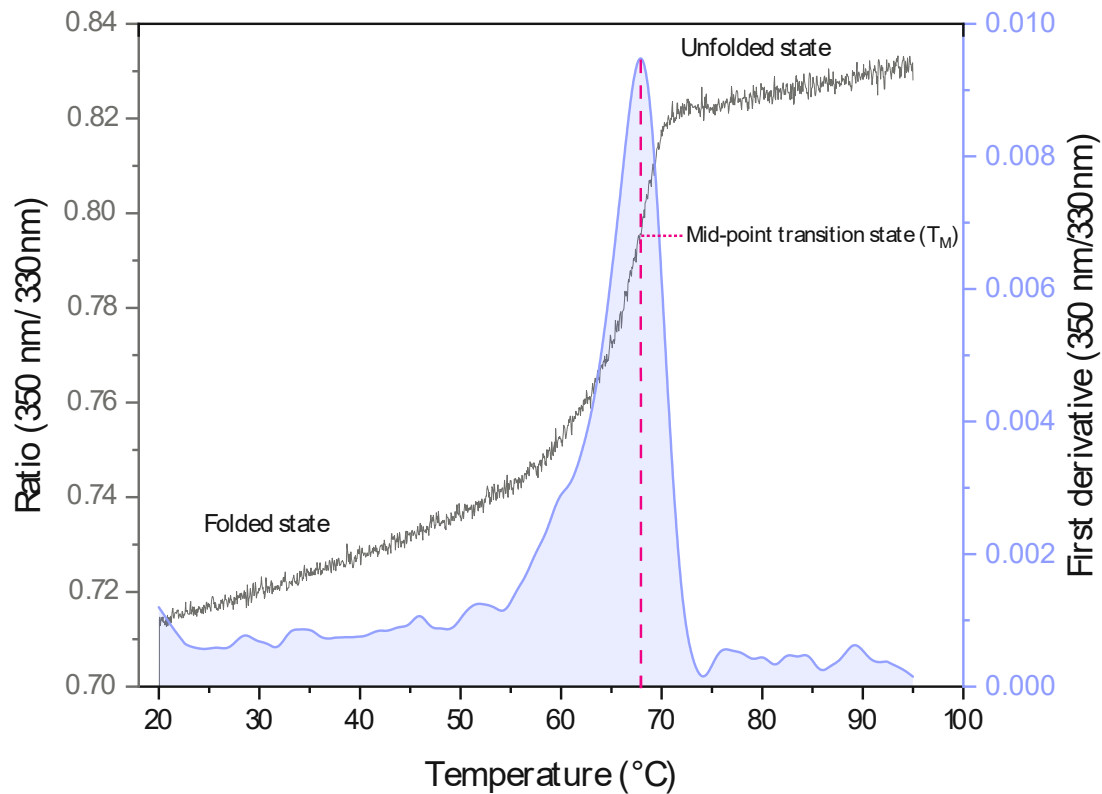


**Figure 18:** The thermodynamic stability is often represented by  $T_M$  or melting temperature and describes the unfolding of the enzyme.

## B V.1.2 Kinetic stability

Kinetic stability describes the length of time a protein remains in its functional form until it undergoes irreversible denaturation. In general, kinetic stability is expressed as the time required for the residual activity of the protein to be diminished by half under specific conditions, which is known as the half-life time  $t_{1/2}$ .<sup>9</sup>

Because kinetic stability provides valuable information about the enzyme's catalytic efficiency under specific reaction conditions, it is more beneficial than thermodynamic stability for determining the enzyme's applicability for industrial processes.

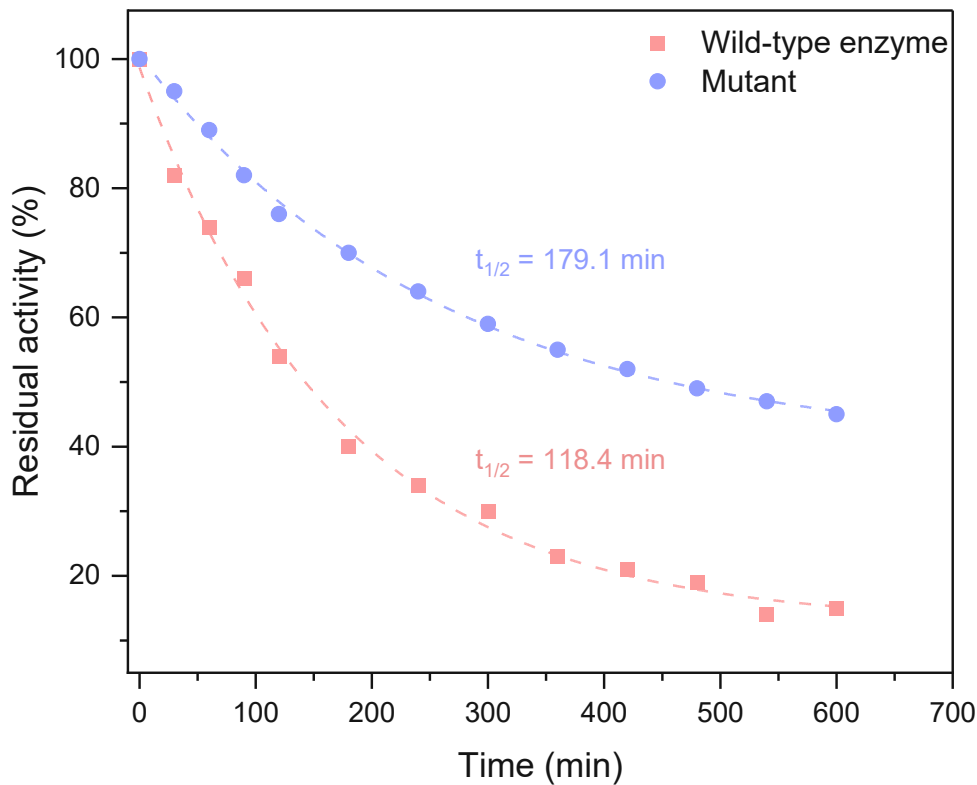


**Figure 19:** Typical representation of the kinetic stability as the half-life time  $t_{1/2}$ . The half-life time is calculated by measuring the enzyme's activity over time while it is incubated under certain conditions. The residual activity is draw versus time, and the half-life time can be measured by an exponential decay.

## B V.2 The role of the flavin cofactor on enzymes' stability and activity

As previously mentioned, flavin cofactors can be bound to the polypeptide chain either covalently or non-covalently. Thus, many studies have been conducted to elucidate the mechanism and the possible role of covalent flavin incorporation. These are explained in the following sections.

### B V.2.1 Types of covalent flavin-protein bonds

The first confirmation of a covalent bond between a flavin cofactor and the polypeptide chain was obtained by Kearney *et al.*, who isolated succinate dehydrogenase.<sup>244,245</sup> The flavin cofactor was covalently tethered via an  $8\alpha$ - $N^3$ -histidyl-bond to the polypeptide backbone.<sup>246</sup> Several other covalent flavoproteins have since been discovered, showing seven possibilities for covalent linkage:<sup>247</sup>  $8\alpha$ - $N^3$ -histidyl-FAD/FMN,  $8\alpha$ - $N^1$ -histidyl-FAD/FMN,  $8\alpha$ - $O$ -tyrosyl-

FAD, 8 $\alpha$ -S-cysteinyl-FAD, 6-S-cysteinyl-FMN, 8 $\alpha$ -N<sup>1</sup>-histidyl-6-S-cysteinyl-FAD/FMN, and phosphoester-threonyl-FMN.

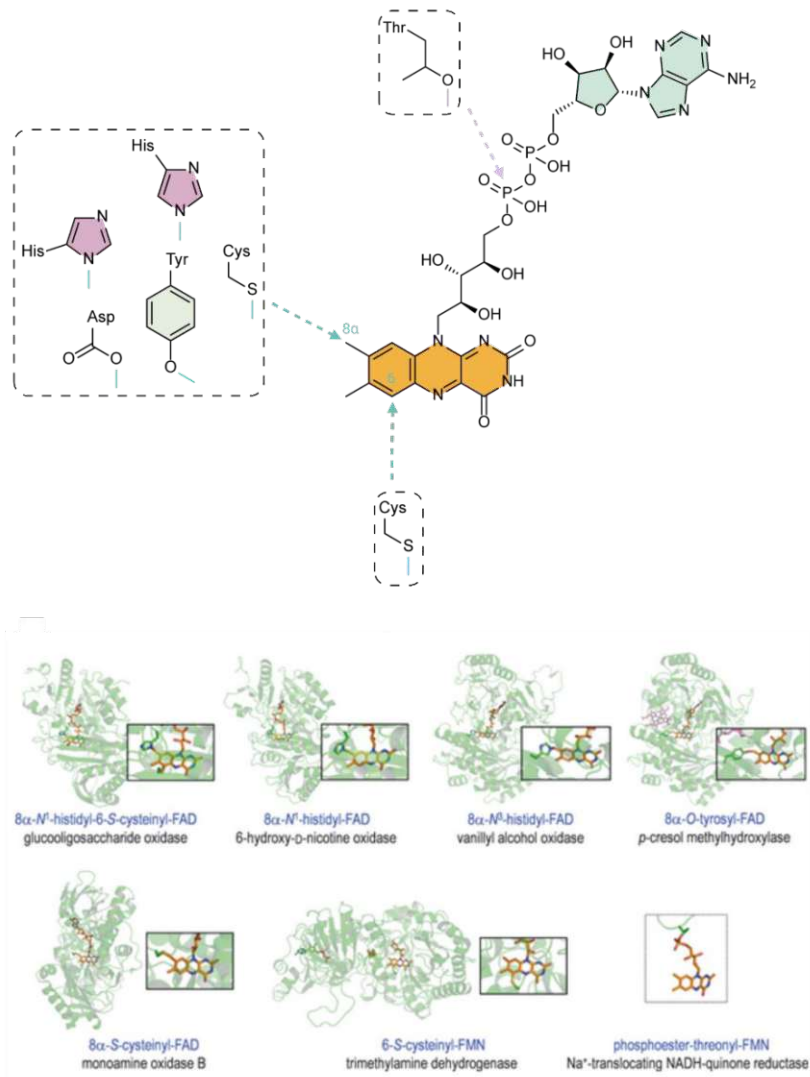


**Figure 20:** All known covalent bonds of flavoproteins. The figure was adapted from reference.<sup>247</sup>

**Table 5:** Flavoprotein containing a covalently linked flavin as a cofactor. The table was adapted from reference.<sup>247</sup><sup>a</sup>Sequence homology with BBE suggests an 8 $\alpha$ -histidyl-6-S-cysteinyI-FAD linkage.

Flavin– protein bond	Enzyme	N <sup>1</sup> -Histidyl or N <sup>3</sup> -histidyl	Origin	Family	Protein Data Bank ID
<i>Covalent FAD cofactor</i>					
8 $\alpha$ -Histidyl-6-S-cysteinyI	GOOX <sup>248</sup>	N <sup>1</sup>	Fungus	VAO	2AXR
	ChitO <sup>249</sup>	?	Fungus	VAO	–
	BBE <sup>250</sup>	N <sup>1</sup>	Plant	VAO	3D2D
	Hexose oxidase <sup>251</sup>	N <sup>1</sup>	Plant	VAO	–
	Aclacinomycin oxidoreductase <sup>252</sup>	N <sup>1</sup>	Bacteria	VAO	2IPI
	$\Delta$ -Tetrahydrocannabinolic acid synthase <sup>253</sup>	?	Plant	VAO	–
	Cannabidiolic acid synthase <sup>253</sup>	?	Plant	VAO	–
8 $\alpha$ -Histidyl	VAO <sup>254</sup>	N <sup>3</sup>	Fungus	VAO	1VAO
	CholO <sup>255</sup>	N <sup>1</sup>	Bacteria	VAO	1I19
	Alditol oxidase <sup>256</sup>	N <sup>1</sup>	Bacteria	VAO	2VFR
	6-HDNO <sup>80</sup>	N <sup>1</sup>	Bacteria	VAO	2BVG
	Cytokinin dehydrogenase <sup>257</sup>	N <sup>1</sup>	Plant	VAO	1W1O
	Eugenol oxidase <sup>258</sup>	N <sup>3</sup>	Bacteria	VAO	–
	I-Gulono- $\gamma$ -lactone oxidase <sup>259</sup>	N <sup>1</sup>	Animal	VAO	–
	I-Gluconolactone oxidase <sup>260</sup>	N <sup>3</sup>	Fungus	VAO	–
	I-Galactonolactone oxidase <sup>261</sup>	N <sup>1</sup>	Yeast	VAO	–
	d-Arabinono-1,4-lactone oxidase <sup>262</sup>		Yeast	VAO	–
	Sorbitol oxidase <sup>263</sup>	?	Bacteria	VAO	–
	Xylitol oxidase <sup>264</sup>	?	Bacteria	VAO	–
	Nectarin V <sup>265</sup>	?	Plant	VAO	–
	Choline oxidase <sup>266</sup>	N <sup>3</sup>	Bacteria	GMC	2JBV
	P2Ox <sup>267</sup>	N <sup>3</sup>	Fungus	GMC	2IGK
	Pyranose dehydrogenase <sup>268</sup>	?	Fungus	GMC	–
	Succinate dehydrogenase <sup>269</sup>	N <sup>3</sup>	All	Succinate dehydrogenase	1NEK
	Fumarate reductase <sup>266</sup>	N <sup>3</sup>	Bacteria	Succinate dehydrogenase	1QLB
	Sarcosine dehydrogenase <sup>266</sup>	N <sup>3</sup>	Animal	DAAO	–
	Dimethylglycine dehydrogenase <sup>266</sup>	N <sup>3</sup>	Animal	DAAO	–
	Dimethylglycine oxidase <sup>270</sup>	N <sup>3</sup>	Bacteria	DAAO	1PJ5
	$\gamma$ -N-methylaminobutyrate oxidase <sup>271</sup>	?	Bacteria	DAAO	–
	Thiamine oxidase <sup>266</sup>	N <sup>1</sup>	Bacteria	?	–
Cyclopiazonate oxidocyclase <sup>266,267</sup>	N <sup>1</sup>	Fungus	?	–	
8 $\alpha$ -O-Tyrosyl	PCMH <sup>272</sup>	–	Bacteria	VAO	1WVE
	MAO A <sup>273</sup>	–	Animal	AMO	2BXR
	MAO B <sup>274</sup>	–	Animal	AMO	1GOS
	Amadoriase I <sup>275</sup>	–	Fungus	DAAO	3DJD
	MSOX <sup>276</sup>	–	Bacteria	DAAO	2GB0
	Pipecolate oxidase <sup>276</sup>	–	Animal	DAAO	–
	N-methyltryptophan oxidase <sup>276,277</sup>	–	Bacteria	DAAO	2UZZ
	Sarcosine oxidase <sup>278</sup>	–	Plant	DAAO	–
	NikD <sup>279</sup>	–	Bacteria	DAAO	2OLN
	Flavocytochrome c552/c553 <sup>280,281</sup>	–	Bacteria	Pyridine nucleotide-disulfide oxidoreductase	1FCD
Unknown	Plant allergens BG60 <sup>a</sup> 282 and Phl P 4 <sup>a</sup> 283	–	Plant	VAO	–
	Tetrahydrofuran monooxygenase reductase component (ThmD) <sup>284</sup>	–	Bacteria	BDR	–

Flavin– protein bond	Enzyme	$N^1$ -Histidyl or $N^3$ -histidyl	Origin	Family	Protein Data Bank ID
<i>Covalent FMN cofactor</i>					
8 $\alpha$ -Histidyl-6-S-cysteinyll	Dbv29 <sup>a</sup> 285	$N^1$	Bacteria	VAO	–
8 $\alpha$ -Histidyl	Heterotetrameric sarcosine oxidase <sup>283</sup>	$N^3$	Bacteria	DAAO	1X31
	NADH dehydrogenase type II <sup>286</sup>	$N^1$	Archaea	Pyridine nucleotide-disulfide oxidoreductase	–
6-S-Cysteinyll	TMADH <sup>287</sup>	–	Bacteria	TMD	2TMD
	Dimethylamine dehydrogenase <sup>288</sup>	–	Bacteria	TMD	–
	Histamine dehydrogenase <sup>289</sup>	–	Bacteria	TMD	–
Phosphoester-threonyll	NqrB <sup>290</sup>		Bacteria	NQR	
	NqrC <sup>290</sup>		Bacteria	NQR	–

The covalent bond of FAD to a histidine has been discovered as the most common linkage, while the covalent attachment of FAD and FMN to a cysteine residue is less common, and the covalent flavinylation of FAD to a tyrosine has only been observed in *p*-cresol methylhydroxylase.<sup>247</sup> Besides the covalent attachment of a flavin cofactor to an enzyme via one covalent bond, FAD can also be bound to enzymes via two covalent linkages: an 8 $\alpha$ - $N^1$ -histidyl–FAD linkage and a 6-S-cysteinyll–FAD linkage.<sup>248,250-252,285,291</sup> In a study on the subunits NqrB and NqrC of the Na<sup>+</sup>-translocating NADH-quinone reductase from *Vibrio alginolyticus*,<sup>290</sup> FMN was found to be tethered covalently to a threonine residue via a phosphoester bond; thus, representing the only covalent flavinylation without a linkage via the flavin's tricyclic isoalloxazine moiety.<sup>247</sup>

Studies on the vanillyl-alcohol oxidase family, which includes a relatively large number of covalent flavoproteins,<sup>292</sup> have suggested a correlation between protein folding and the ability for covalent flavinylation.<sup>293</sup> However, no unique protein sequence motif has been identified that can predict whether a covalent flavin tethering will be formed.<sup>247</sup> Additionally, some examples show that a same reaction can be catalyzed with similar catalytic and kinetic properties by enzymes with a covalent or non-covalent flavin, which indicates that the role of the covalent flavinylation is more complex. Thus, possible reasons for the covalent flavinylation are discussed below.

## B V.2.2 The redox potential of covalent flavoenzymes

The role of the covalent bond between a flavin and the polypeptide chain has been fiercely debated, though the consensus in the field is that the most critical role of covalent tethering is the increased redox potential of the flavin cofactor. This increased potential allows for more thermodynamically demanding reactions and more efficient substrate turnovers. This effect has been observed in all covalent flavoenzymes, and numerous studies have investigated the redox potentials of several covalently and noncovalently bound flavins in mutant forms. The effect of covalent flavinylation on the midpoint potential was first studied on vanillyl-alcohol oxidase (VAO),<sup>294</sup> which typically contains an  $8\alpha$ - $N^3$ -His422 linkage. In this study, the H422 was substituted with alanine, serine, and cysteine, which resulted in tightly but noncovalently bound FAD. Structural analysis revealed that the structures of the mutants were similar to the wild-type enzyme, indicating that the covalent bond does not fundamentally change the enzyme's three-dimensional structure. Subsequent measurements of the redox potential revealed that the loss of the covalent bond is accompanied by a substantial decrease of the midpoint potential from +55 mV for wild-type VAO to -65 mV for the H422A mutant.<sup>294</sup> Additional kinetic measurement demonstrated a 10-fold decrease in  $k_{\text{cat}}$  for the H422A mutant. These findings clearly indicated that nature employs the covalent flavinylation to increase the oxidation power of the enzymes, thereby enabling more challenging reactions and more efficient catalysis.

The role of bicovalent flavoenzymes has also been investigated. A study by Fraaije *et al.*<sup>79</sup> on chito oligosaccharide oxidase (ChitO) from *Fusarium gaminearum* demonstrated that either covalent bond can be formed independently of the other and that each bond has an independent effect on the potential of FAD. Using site-specific mutagenesis, the residues H94 and C154, which are responsible for covalent tethering to FAD, were replaced by an alanine, and the redox potential of both mutants was measured. While the wild-type ChitO exhibited a redox potential of +131 mV, the C154A mutant showed a lower potential of +70 mV. However, the H94A mutant displayed an even higher redox potential of +164 mV. Further investigations revealed that both mutants exhibit a remarkable increase in the  $K_m$  for the substrate *N*-acetyl-D-glucosamine, indicating that covalent flavinylation is required not only for boosting the oxidation power but also for correct positioning of FAD relative to the substrate for efficient catalysis.<sup>79</sup> In this context, all bicovalent flavoproteins have been reported as having an astonishingly open active site due to the double anchoring of FAD, which allows them to bind relatively bulky substrates.

## B V.2.3 The structural integrity of flavoenzymes and retention of the flavin cofactor

In addition to increased oxidative power of enzymes through covalent flavinylation, enhanced stability of proteins and extended lifetimes for holo-enzymes could be further reasons for the covalent attachment.

The stabilization of the protein structure by the covalent bond was, for example, nicely demonstrated by a study on human monoamine oxidase A (MAO A), which contains covalent FAD via an  $8\alpha$ -S-cysteinyl bond.<sup>295</sup> The mutation C406A led to tightly but noncovalently bound FAD after reconstitution of the apoenzyme, and the activity was only 30% of that measured with the wild-type MAO A. However, when the mutant enzyme was solubilized from the outer mitochondrial membrane, it was found to be unstable, while the wild-type enzyme proved stable under the same conditions. These data suggest that the covalent bond of FAD in MAO A has a crucial role in maintaining the structural integrity of the enzyme.<sup>295</sup> Investigations on cholesterol oxidase (CholO) from *Brevibacterium sterolicum* have revealed that the urea-induced unfolding of the H69A mutant occurred at lower concentrations than for the wild-type CholO. In another study, the mutant enzyme showed a 10–15 °C lower melting temperature compared to the wild-type enzyme.<sup>296</sup>

Another example for the stabilizing effect of a covalently linked cofactor is quinol:fumarate reductase, which contains a covalent FAD. In facultative anaerobes, such as *E. coli*, which can switch between anaerobic and aerobic respiration, and obligate anaerobes, such as *Wolinella succinogenes*, which are only able to perform anaerobic respiration, this enzyme catalyzes the terminal step in anaerobic respiration with fumarate.<sup>297,298</sup> The enzyme quinol:fumarate reductase catalyzes the reduction of fumarate to succinate during anaerobic respiration. For this transformation, no increased redox potential of the FAD cofactor is required; however, in facultative anaerobes, the enzyme switches the direction of its reaction when the organism switches from anaerobic to aerobic respiration and performs succinate oxidation instead of fumarate reduction. Therefore, the covalent FAD is necessary for effective oxidation of the succinate. The FAD reduction potentials ( $E_m$ ) of quinol:fumarate reductases in *E. coli* were determined to be -30 to -55 mV at pH 7,<sup>299-301</sup> while in a variant containing a non-covalent FAD the  $E_{m,pH7}$  value was determined to be -134 mV and it lost succinate dehydrogenase activity but remained fumarate reductase activity.<sup>302</sup>

In contrast, obligate anaerobes never switch to aerobic respiration and thus would not require covalent FAD. However, while some obligate anaerobes contain quinol:fumarate reductase



homologs without covalently tethered FAD (e.g., fumarate reductase in *Shewanella frigidimarina*<sup>303</sup> has an  $E_{m,pH7}$  value of -152 mV and can only perform fumarate reduction), some enzymes have a covalent FAD, which is a strong indication for the dual role of covalent linkage *in vivo*. Tomasiak *et al.*<sup>304</sup> observed that quinol:fumarate reductase can change from a “closed” to an “open” form during catalysis that temporarily exposes FAD to solvent, which could cause loss of noncovalent FAD. Similarly, in an earlier study by Blaut *et al.*,<sup>305</sup> mutants of quinol:fumarate lacking in covalently linked FAD lost activity upon dialysis against KBr due to the loss of the cofactor.

Another rational reason for the covalent anchoring of the cofactor could be to enhance the *in vivo* lifetime of proteins by preventing cofactor dissociation through the covalent linkage. Generally, apo-flavoproteins are less stable than their holo forms. Additionally, the covalent bond may be required for flavoenzymes to function in a cell’s microenvironment that is flavin poor; thus, flavin reassociation would be difficult, and longer retention of the cofactor would be crucial for maintaining the enzyme’s function.<sup>247</sup>

## **B V.2.4 The formation of covalent flavin-protein bonds**

From a mechanistic point of view, the linkage of cysteine, tyrosine, or histidine to the 8 $\alpha$ -methyl group or the C6 atom of the isoalloxazine ring has been suggested as occurring posttranslationally in an autocatalytic process.<sup>247</sup> Alternatively, FMN is covalently attached to a threonine residue via a phosphoester bond in prokaryotes by flavin transferases (EC 2.7.1.180) of the ApbE family (PFAM ID: PF02424).<sup>306,307</sup>

## **B V.2.5 Artificial flavinylation**

The examples above demonstrate that some enzymes evolved with a covalently linked flavin to raise the redox potential of these enzymes to facilitate proper catalysis or enhance the enzymes’ stability and lifetime. Consequently, some studies investigated the artificial flavinylation of flavoproteins that do not typically contain a covalently tethered flavin. In one of these studies, the flavoproteins lipoamide dehydrogenase and lysine  $N^6$ -hydroxylase, which do not generally have a covalent FAD, slowly incorporated FAD covalently when the respective apo-proteins were incubated with 8-chloro-FAD as a result of a nucleophilic attack of a thiolate

on the 8-position of the FAD. After covalent incorporation, the enzymes did not show any residual activity due to the perturbed positioning of the cofactor in the active site.<sup>308-310</sup> In another artificial flavinylation approach, the native noncovalent FAD cofactor was replaced by a covalently attached flavin analog in recombinant human D-amino acid oxidase (DAAO).<sup>311,312</sup> The protein residue G281 was replaced with cysteine by site-directed mutagenesis, and the isolated G281C apo-DAAO was incubated with the thiol-reactive flavin analog 8-methylsulfonyl FAD. This FAD bound covalently to the C281 residue. The covalent DAAO variant showed an activity of 26% of the wild-type DAAO, and the covalent flavinylation affected the mobility of FAD, which was reflected in the 13-fold increased  $K_m$  value with D-alanine as substrate as compared to that of the native enzyme.<sup>312</sup> Another study of artificial covalent flavinylation was conducted on L-aspartate oxidase (LaspO),<sup>313</sup> which weakly binds noncovalent FAD. The apo-protein was incubated with the FAD analog *N*<sup>6</sup>-(6-carboxyhexyl)-FAD succinimidoester, which formed a covalent bond with the residue L38 of the polypeptide chain. The covalent tethering caused a dramatic change in the microenvironment around the isoalloxazine portion of the FAD analog, resulting in an activity of only 2% of the wild-type enzyme.<sup>313</sup>

These examples show that covalent flavinylation can benefit an enzyme's activity, stability, or lifetime, although no improved enzyme has been produced through artificial covalent flavinylation. Nevertheless, these data clearly demonstrate that a covalent bound flavin would constitute the ideal setting for a robust, long-lasting biocatalyst if the covalent attachment is done in a way that does not change the active site, the orientation of the isoalloxazine ring, or the structural conformation of the holoenzyme.

## **B VI Forming a new covalent bond (Photoaffinity labeling)**

To achieve stabilization of flavoenzymes through covalent bond formation of the cofactor to the apoenzyme, a binding method must be found that (1) does not interfere with catalysis by changing the active site of the enzyme, the orientation of the isoalloxazine ring, or the enzymes' redox potential; (2) changes the affinity of the modified FAD to the apoenzyme minimally; (3) is versatile enough to bind at different amino acid residues; (4) is small enough to avoid structural reorientations of the holoenzyme; and (5) can be initiated at will to allow the correct incorporation of the modified FADs.

All these criteria can be achieved with a technique known as photoaffinity labeling. Since its introduction by Frank Westheimer<sup>314</sup> in 1962, photoaffinity labeling has emerged as a powerful tool for target discovery in medicinal chemistry. Using this approach, a ligand is modified with a photolabile moiety and a purification or detection tag. The ligand, which shows a higher affinity to the target protein, binds to the protein's active site. Upon activation by ultraviolet light, the photolabile moiety forms a highly reactive species, forming a new covalent bond with residues of the target protein in the vicinity of its binding site.<sup>315</sup> The tagged proteins can be visualized by SDS-page and in-gel fluorescence or identified by MS/MS analysis after enrichment and sequence-specific proteolytic digestion (see Figure 21).<sup>316</sup>

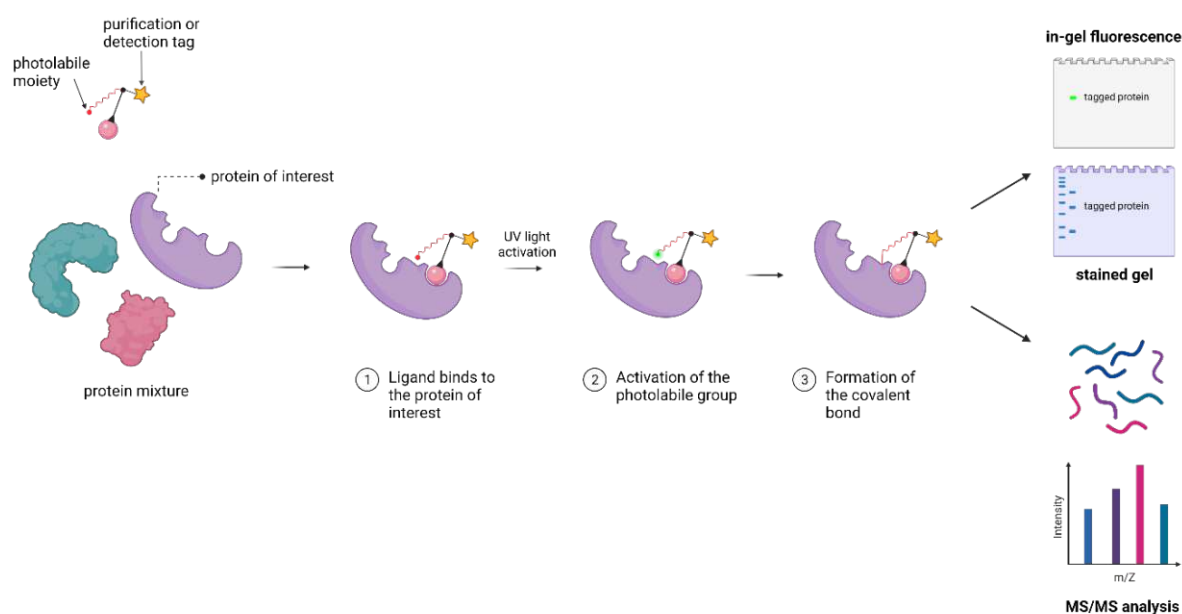


**Figure 21:** The principle of photoaffinity labeling. A cell lysate is incubated with a photoprobe. After binding the ligand to the protein of interest, irradiation forms a new covalent bond. Labeled proteins can be imaged on gel or enriched with a capture handle, digested, and identified through MS/MS analysis.

## B VI.1 Photoreactive groups used in photoaffinity labeling

Three types of photoreactive groups are commonly used in photoaffinity labeling: aryl azides, benzophenones, and diazirines (see Figure 22).<sup>317,318</sup> Of these, aryl azides (Figure 22 A) were the first photoaffinity reagents used. For example, Fleet *et al.*<sup>319</sup> chemically modified the bovine antibody gamma globulin and human serum albumin with a 4-azido-2-nitrophenyl group to trap interacting antibodies. Inspired by this approach, Kiefer *et al.*<sup>320</sup> applied the chemistry to map acetylcholine's binding site in red blood cell membranes and frog sartorius muscle cells

using an azide-functionalized analog. However, the widespread use of azides in photoaffinity labeling is hindered by the relatively short wavelength of light required for activation and the long lifetime of the nitrene intermediate.

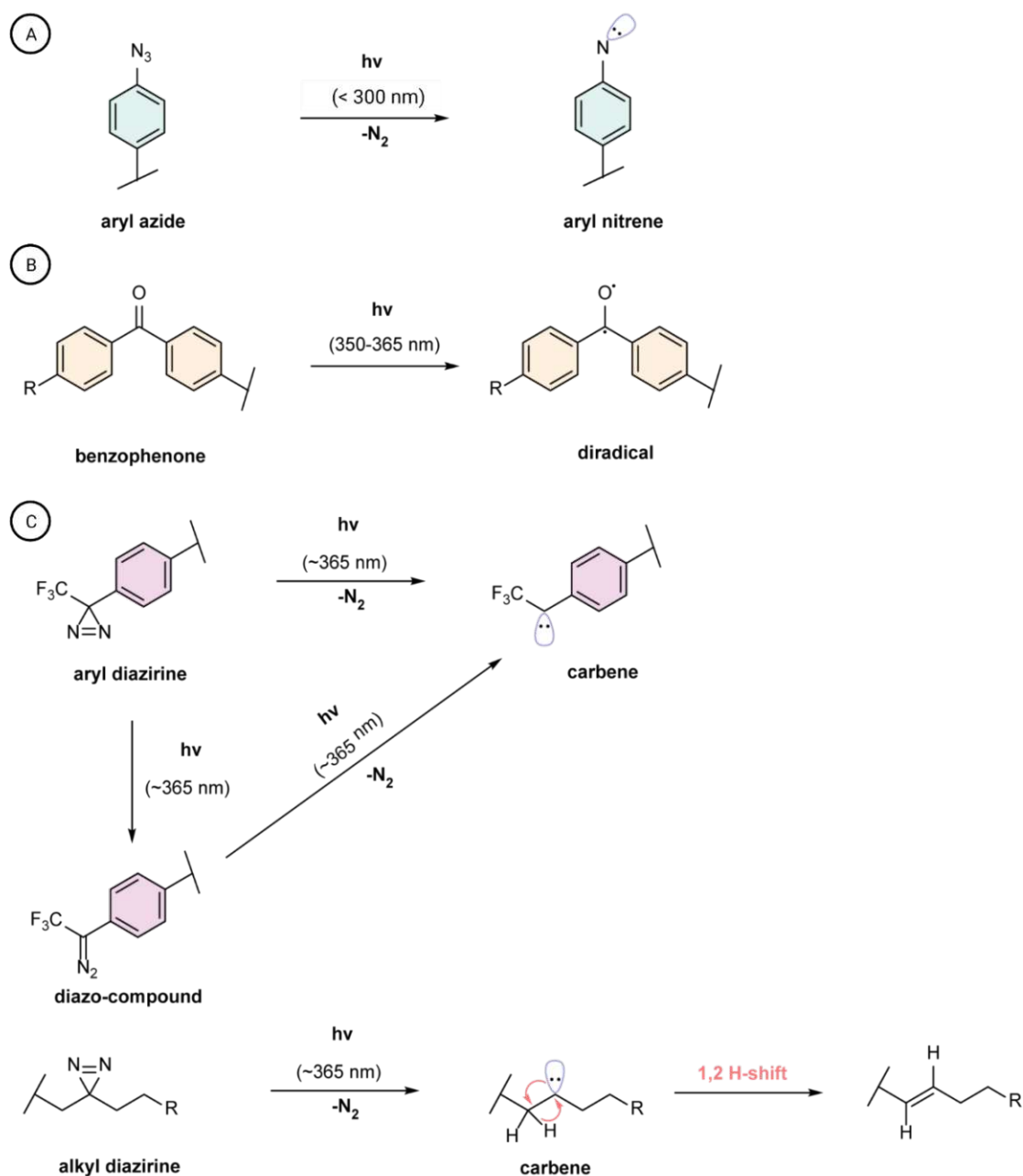


**Figure 22:** The three most common photoreactive groups used in photoaffinity labeling.

In contrast to aryl azides, the comparably long wavelength required for photoactivation of benzophenones (Figure 22 B) decreases protein damage.<sup>321</sup> Another advantage of benzophenones is that the formed diradical species can react with water, thus regenerating the benzophenone's ground state after subsequent dehydration. Consequently, benzophenones can be repeatedly excited over prolonged irradiation times, resulting in higher protein-labeling

efficiency. However, due to their intrinsically large size, benzophenone-based photo probes are not suitable for applications in which bulky substitutions would be an issue. Further, benzophenones require considerably longer irradiation times due to their reversible excitation.<sup>316</sup>

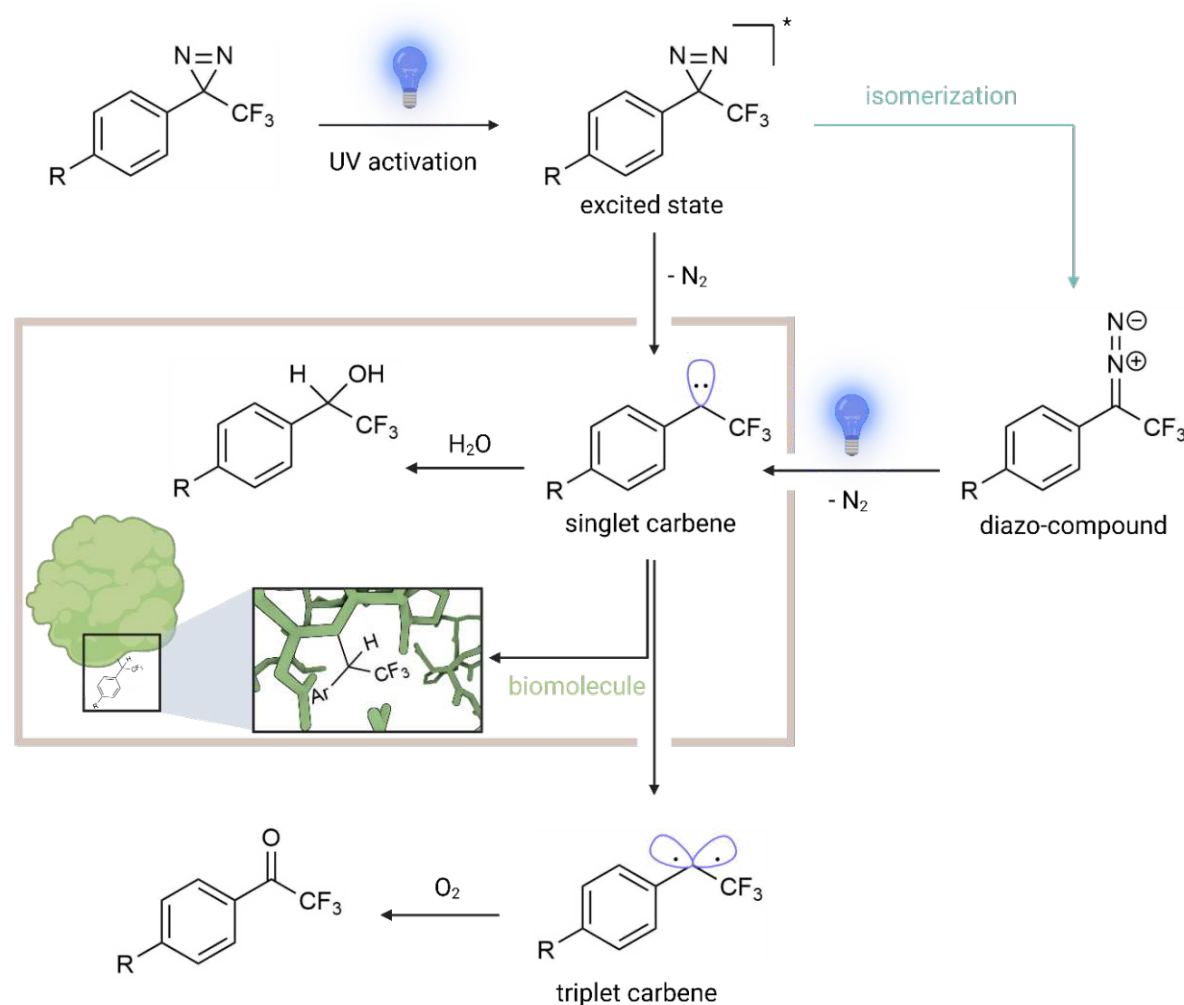
In many ways, aryl and alkyl diazirines are ideal alternatives to aryl azides and benzophenones and are nowadays ubiquitous in photoaffinity labeling studies due to their many beneficial characteristics.

## B VI.1.1 Diazirines as a photoreactive group

Diazirines (Figure 22 C) are three-membered, nitrogen-containing heterocycles that were first chemically synthesized in 1960.<sup>322</sup> Upon irradiation with light or elevated temperature, diazirines readily decompose into molecular nitrogen and a highly reactive singlet carbene. This species' notorious reactivity is responsible for forming a covalent bond with X-H (X = C, N, O, or S) or C-C bonds derived from a nearby molecule via insertion,<sup>323</sup> making the singlet carbene highly desirable for proximity-labeling applications. However, the singlet carbene's reactivity also enables insertion into water molecules, which forms hydrated products. As a result, the half-life times in solution are short ( $t_{1/2} < 1$  ns), leading to low cross-linking yields.<sup>324</sup> Besides the formation of carbenes, diazirines can undergo isomerization into linear diazo compounds (see Figure 23 and 25). The diazo species can either form the desired carbene through the loss of molecular nitrogen or, in acidic media, form the diazonium species by protonation. This species is known as alkylating reagents.<sup>316</sup> However, the diazo isomer displays a longer lifetime than the carbene, resulting in the dissociation of the photolabel from the target protein's binding site and, thus, unspecific labeling. Additionally, a proportion of the singlet carbenes can be transformed into triplet carbenes via intersystem crossing (see Figure 23).<sup>325,326</sup> Triplet carbenes display radical reactivity and thus require a two-step mechanism for the insertion reaction. Further complicating the matter, triplet carbenes react rapidly with adventitious oxygen, forming ketone side-products, whereas singlet carbenes do not undergo this undesirable reaction pathway.<sup>326</sup> Another limitation of alkyl diazirines is the carbene-concerted 1,2 hydride-shift, which forms undesirable alkene by-products.<sup>327</sup> Nevertheless, diazirines have increasingly been employed in photoaffinity labeling owing to their unique advantages, including their smaller size, longer excitation wavelengths (~360 nm), higher photocrosslinking efficiency, and improved chemical stability compared to other photoreactive groups.<sup>328-330</sup>

**Table 6:** Some characteristics of the most used photoaffinity tags.

Photoaffinity tag	Activation wavelength	Advantages	Disadvantages
Arylazide	< 300 nm	<ul style="list-style-type: none"> <li>• Easy synthesis</li> <li>• Small size</li> </ul>	<ul style="list-style-type: none"> <li>• Damaging activation wavelengths</li> <li>• Undesired side reactions</li> </ul>
Benzophenone	350-360 nm	<ul style="list-style-type: none"> <li>• Commercially available</li> <li>• Non-damaging activation wavelengths</li> </ul>	<ul style="list-style-type: none"> <li>• Bulky size</li> <li>• Prolonged irradiation times</li> </ul>
Diazirine	350-380 nm	<ul style="list-style-type: none"> <li>• Fast kinetics (<math>t_{1/2} &lt; 1</math> ns of the carbene intermediate)</li> <li>• Small size (alkyl diazirine)</li> <li>• Non-damaging activation wavelengths</li> </ul>	<ul style="list-style-type: none"> <li>• Elaborate synthesis</li> <li>• Formation of undesired diazo-isomer</li> <li>• Rearrangement reactions (alkyl diazirines)</li> </ul>

**Figure 23:** Reaction pathways of trifluoromethyl phenyl diazirines.

The diazirine's potential as a photolabile group was first revealed in 1973 by Jeremy Knowles, who prepared and conducted the photodecomposition of 3-aryl-3*H*-diazirines.<sup>331</sup> Aromatic diazirine derivatives, in which the diazirine group is directly connected to an aromatic moiety, have been developed to address some of the shortcomings associated with alkyl diazirines. Particularly, Brunner *et al.*<sup>332</sup> installed a trifluoromethyl group at the  $\alpha$ -position of

the diazirine moiety in 1980. The installation of the trifluoromethyl group not only prevents the carbene from undergoing the unfavorable rearrangement to the alkene (see Figure 24) but also leads to a more controllable reactivity by increasing the carbene formation and stabilizing the diazo isomer, thereby limiting undesirable background labeling.<sup>333-335</sup> Due to the superior characteristics of trifluoromethyl phenyl diazirines (TPDs) compared to other photoreactive groups, TPDs are considered the most promising photoreactive reagents. However, incorporation of TPDs into different chemical probes remains challenging due to their size and elaborate synthesis.<sup>330,333,335</sup> Consequently, an increasing number of researchers have used alkyl diazirines for photoaffinity studies despite their drawbacks, which include the generation of smaller amounts of carbenes upon UV light activation and moderate crosslinking efficiency due to rearrangement reactions. Nevertheless, these limitations can be compensated by the exceptionally compact size of alkyl diazirines, which makes them especially powerful in applications in which the biological activity of the original compound must be retained, or ligand-target interactions are sensitive to the size of the photoprobe.<sup>323</sup>

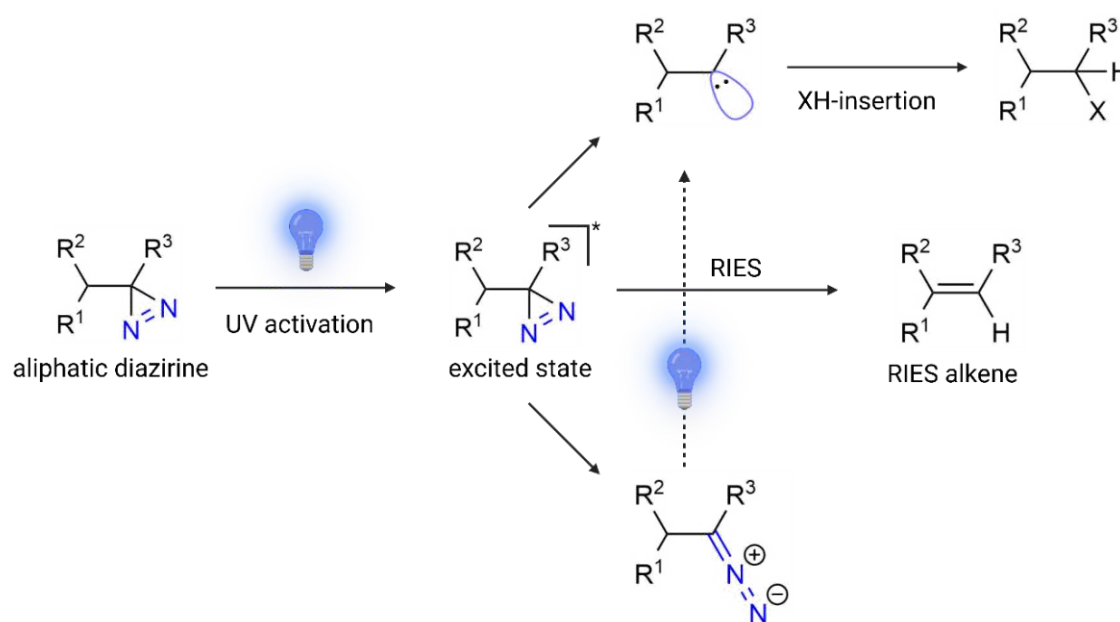


**Figure 24:** Reaction pathways of alkyl diazirines. (RIES = rearrangement in the excited state).

## B VI.1.2 Applications of diazirines in photoaffinity labeling studies

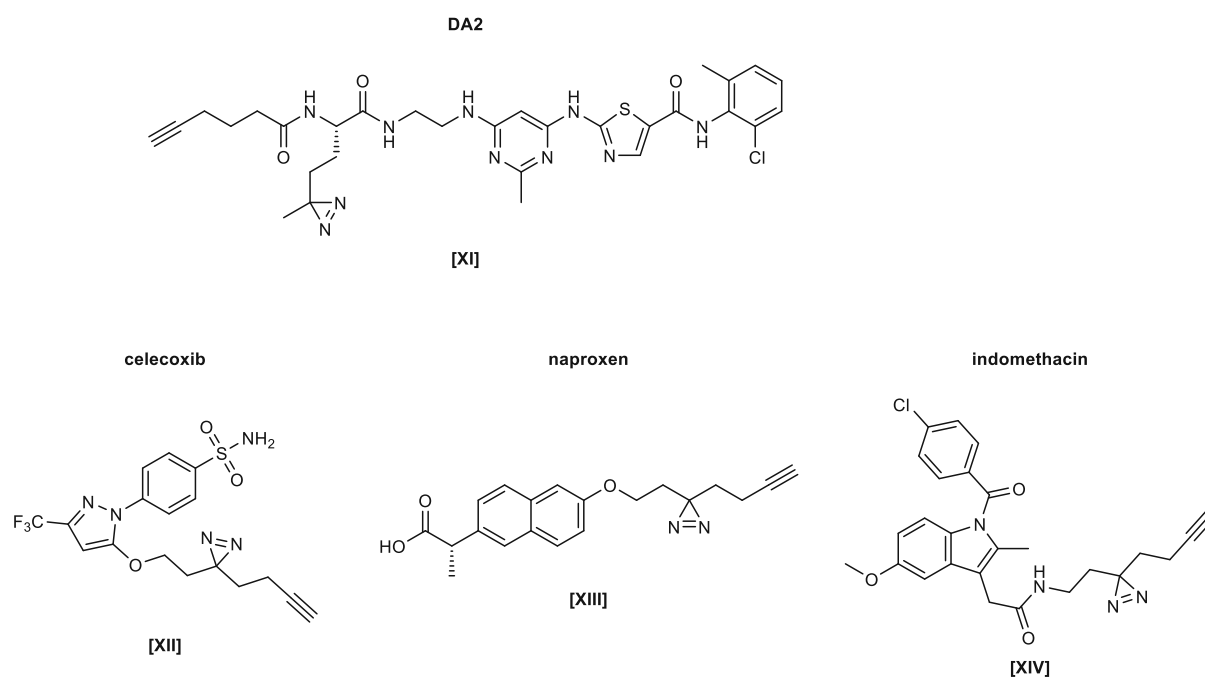
Target identification and mode-of-action studies are essential in the development of modern drugs to ensure the safety and efficacy of clinical candidates. In this context, photoaffinity



labeling has emerged as a powerful tool for small molecule interactome mapping studies, as it allows clinical candidates' on- and off-target activity to be identified.

Photoaffinity labeling coupled with a chemoproteomic readout aided in the study of Dasatinib (BMS-354825), a dual Src and Bcr-Abl family tyrosine kinase inhibitor and promising therapeutic agent for the treatment of imatinib-resistant chronic myelogenous leukemia.<sup>336</sup> Using a cell-permeable probe DA-2 [XI] bearing a diazirine group (see Figure 25), the study identified a number of previously unknown targets, including several serine/threonine kinases and off-targets of Dasatinib.<sup>337</sup>

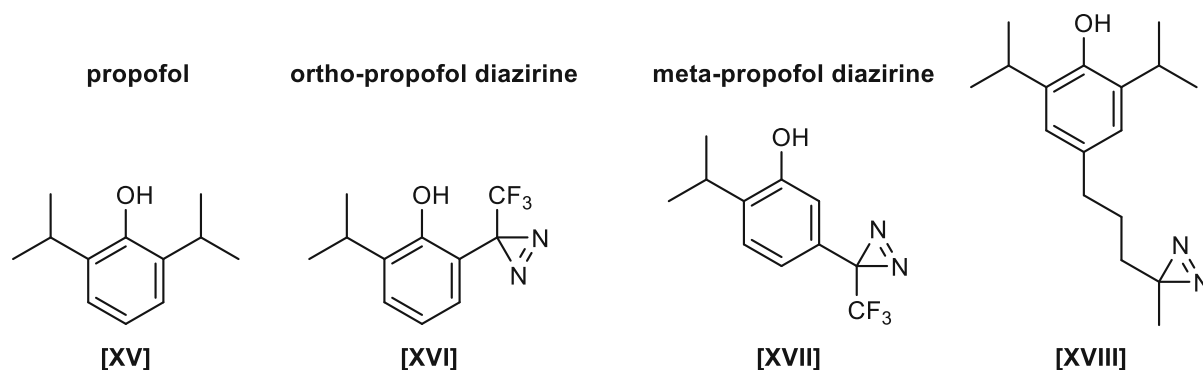
A similar study analyzed the interactomes of non-steroidal anti-inflammatory drugs (NSAIDs), including celecoxib, naproxen, and indomethacin (see Figure 25). In the study, the NSAID interactome was identified as comprising over 1000 proteins, and nearly 200 conjugated peptides were characterized as direct binding sites of the photo-NSAIDs.<sup>338</sup>



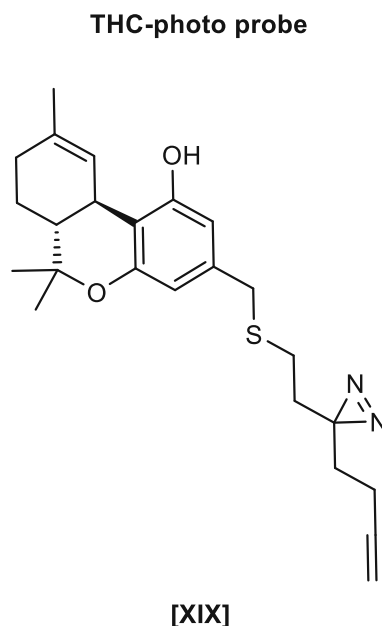
**Figure 25:** Chemical structures of photoaffinity probes [XI], [XII], [XIII], and [XIV].

Propofol is the world's most widely used intravenous general anesthetic. It acts by potentiating GABA type A receptors, but the binding sites are unknown. Over the past decade, a set of propofol-based photolabeling probes bearing diazirines groups (Figure 26) have been synthesized to identify propofol's potential binding sites and mechanisms.<sup>339-342</sup>



**p-4-AziC5-propofol****Figure 26:** Synthesized propofol analogs bearing a diazirine group.

Besides clinical drug candidates, photoaffinity-based protein profiling aids in identifying targets of traditional medicines and psychoactive natural products. Soethoudt *et al.*<sup>343</sup> synthesized a  $\Delta$ -8 tetrahydrocannabinol-diazirine probe **[XIX]** to identify unknown THC targets. The THC-photo probe captured not only the CB1 receptor but also four additional high-affinity interactors: Reep5, Mtch2, Gnb1, and Cox4il. These putative protein targets may help unravel some of the side effects of long-term THC usage.<sup>343</sup>

**Figure 27:** THC-photo probe **[XIX]**.

Despite the sophisticated installation of a diazirine moiety into a biological probe, the minimal changes in the original biological activity, as well as the native interactions, render diazirines a reliable tool besides the traditional small-molecule interactome mapping. Diazirines

can be used to study interactions, including lipid-protein interactions, steroid-protein interactions, carbohydrate-protein interactions, and nucleic acid-protein interactions.

Diazirine photoaffinity probes have also been utilized to discover cofactors' interactomes. For example, Horning *et al.* synthesized a series of biotinylated *S*-adenosyl-*L*-homocysteine photoaffinity probes to profile methyltransferases in three human cancer cell lysates. By doing so, they successfully enriched roughly 25% of the over 200 known and predicted human methyltransferases in cancer cell proteomes.<sup>344</sup>

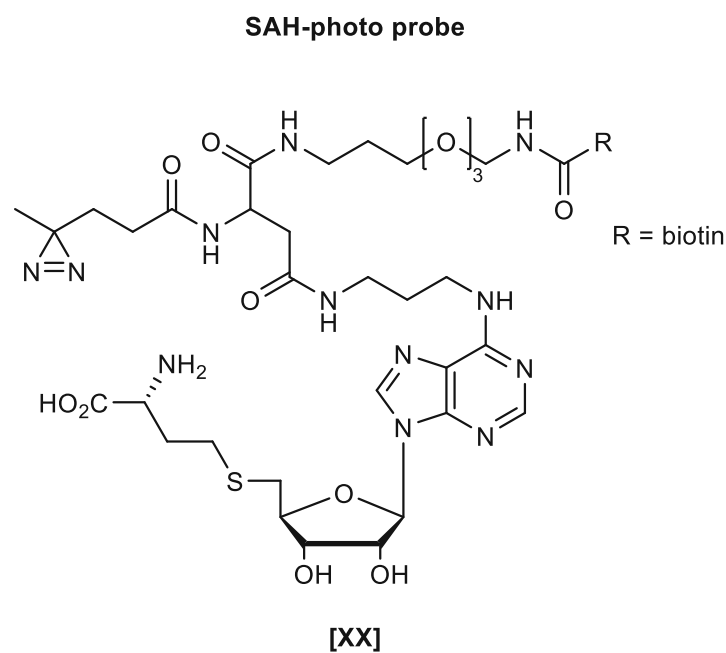


**Figure 28:** Structure of *S*-adenosyl-*L*-homocysteine photoaffinity probe **[XX]** to profile methyltransferases in human cancer cells.

In another study, photoaffinity probes derived from B vitamins, B<sub>1</sub> (thiamine), B<sub>2</sub> (riboflavin), and B<sub>7</sub> (biotin), were used for live cell labeling and subsequent identification of B vitamin transporters and intracellular binding proteins in live *Chloroflexus aurantiacus J-10-fl* using fluorescence and quantitative LC-MS based proteomic measurements.<sup>345</sup> The same research group developed a cobalamin (vitamin B<sub>12</sub>) cofactor mimic **[XXIV]** for the identification of B<sub>12</sub>-binding proteins in a nonphototrophic B<sub>12</sub>-producing bacterium.<sup>346</sup>

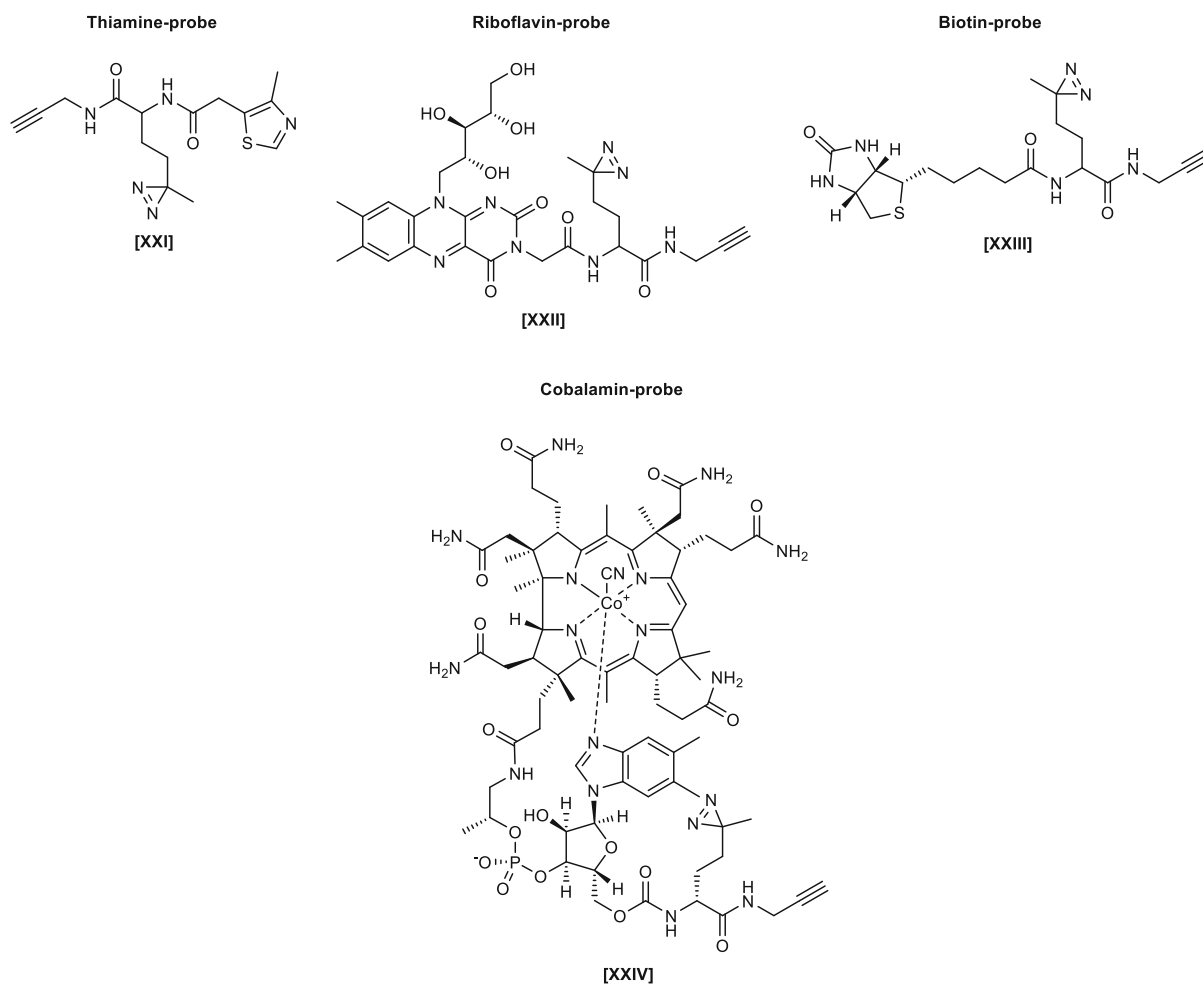
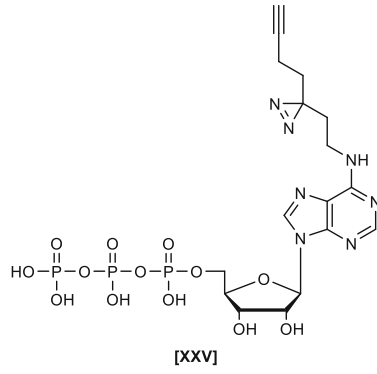


**Figure 29:** Chemical structures of photo probes of vitamins B<sub>1</sub>, B<sub>2</sub>, B<sub>7</sub>, and B<sub>12</sub>.

Jelcic *et al.*<sup>347</sup> developed a ATP-photoaffinity probe [XXV] for investigating ATP-interacting proteins. These proteins control inflammation, cell death, migration, and wound healing. However, the identification of allosteric ATP binding sites remained difficult. Using an ATP mimetic, the researchers enriched 59 known ATP-binding proteins in A549 cell membrane fractions and highly abundant cytosolic ATP binders from cell extracts.<sup>347</sup>

In two recently published studies, NAD cofactor mimetics with diazine moieties on different positions of the adenine were used to capture poly-ADP-ribose polymerases (PARPs) and other NAD<sup>+</sup>/NADH binding proteins.<sup>348,349</sup>

**ATP-photo probe**



**NAD-photo probes**

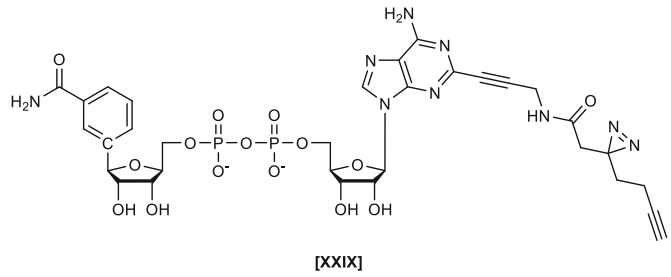
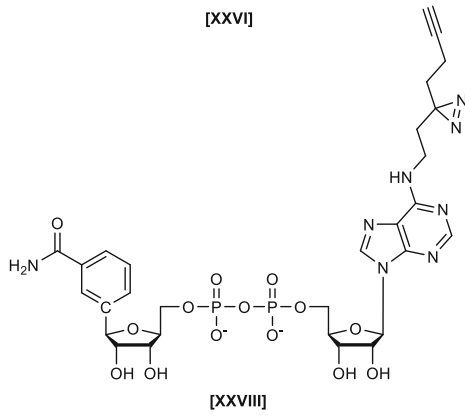
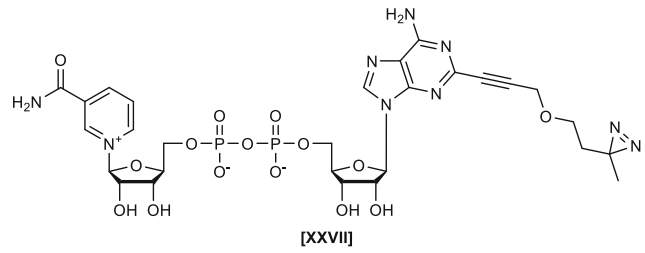
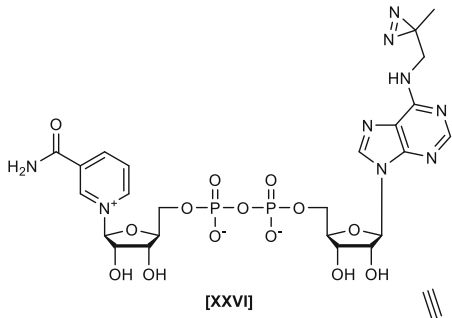


**Figure 30:** Chemical structures of ATP- and NAD-photo probes.

## B VII Objective

Flavoenzymes are extraordinary biocatalysts with a vast field of possible applications. However, their full potential cannot be exploited due to their intrinsic instabilities, so their utilization in industry is limited. Therefore, inspired by the photoaffinity-labeling technique, we aimed to develop a general approach to stabilize flavin-dependent enzymes by covalently attaching the cofactor FAD to flavoenzymes of interest (see Figure 31).

This goal was pursued using synthetic chemistry to create various FAD analogs bearing a diazirine moiety. Distinctive positions of the FAD cofactor were chosen as modification points, located far from the catalytical active isoalloxazine ring, to avoid detrimental effects on the enzymatic activity and redox potential. In addition, the diazirine-based modification allows the proper incorporation of modified FAD analogs due to the small size of the diazirine group, and thus, does not alter the orientation of the isoalloxazine ring.

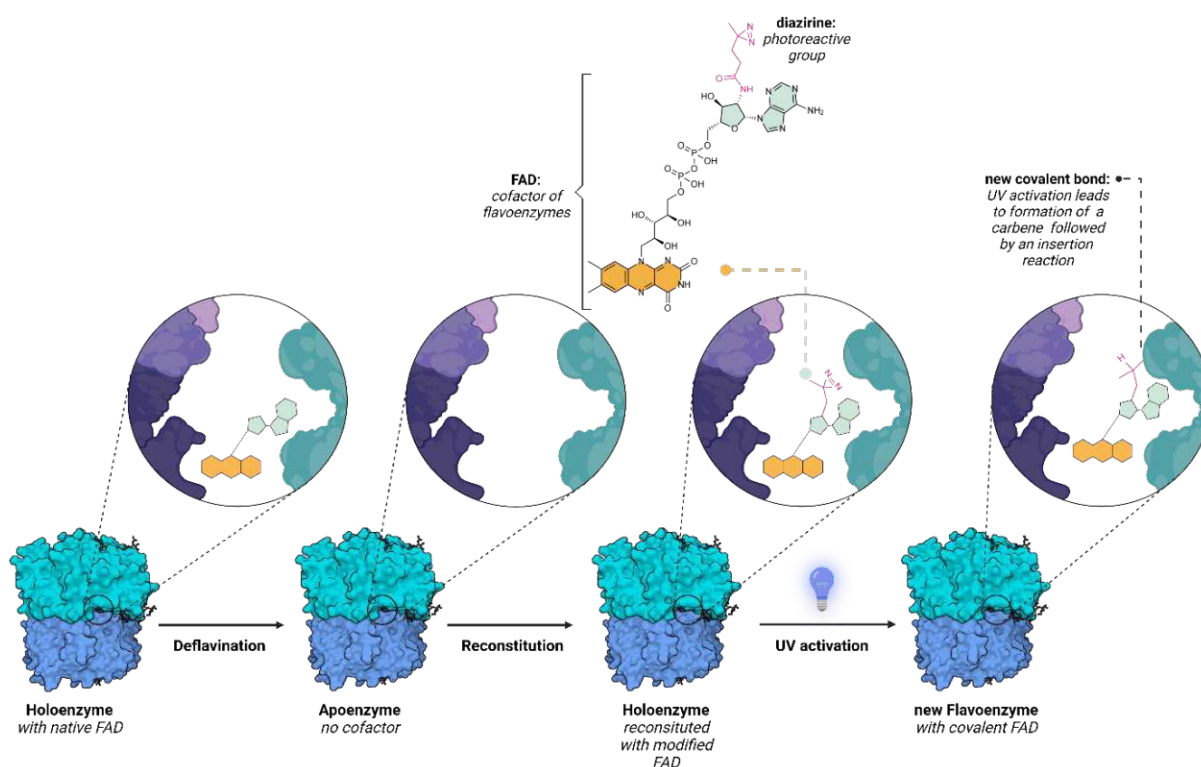


**Figure 31:** Schematic overview of the aim of this thesis. A modified diazirine-FAD can replace the native FAD by deflavination and reconstitution. The diazirine moiety (pink structure) forms a reactive carbene species that inserts into nearby amino acid residues by irradiation with light of a suitable wavelength. This diazirine-based FAD coupling method represents a minimally invasive enzyme modification by controlling the timing of the covalent bond formation and, hence, the correct positioning of the FAD cofactor.

The biological evaluation of these artificial cofactors was conducted with our collaborators by comparing the activities and the thermal- and kinetic stabilities of three different wild-type

and modified flavoenzymes (glucose oxidase, cellobiose dehydrogenase, and cyclohexanone monooxygenase).

This diazirine-based coupling method will open a genuinely novel route for increasing biocatalyst stability in biosensors and bioconversion processes and will enable the use of modified FADs as molecular probes for fluorescence detection of target proteins.

# C Results and Discussion

## C I Synthesis of flavin adenine dinucleotide derivatives

This chapter describes the possible functionalization of flavin adenine dinucleotide with diazine groups. Furthermore, the syntheses of all derivatives and intermediates of flavin adenine dinucleotide reported in this thesis are disclosed.

### C I.1 Retrosynthetic analysis and theoretical considerations of the synthesis of flavin adenine dinucleotide analogs bearing diazine groups

Analysis of FAD reveals two building blocks that occur from a retrosynthetic disconnection at the pyrophosphate group: an adenosine-5-monophosphate and a riboflavin-5-monophosphate building block. These two building blocks can be modified independently by introducing a diazine group at select positions, and then they can be coupled to produce the modified diazine-FAD derivative (see Figure 32).

From a chemist's perspective, the FAD scaffold offers plenty of possible locations for functionalization: at the isoalloxazine ring system, the ribityl side chain, the phosphate groups, the ribose ring, and the adenine base. However, the positions for modification must be considered carefully to ensure minimal detrimental effects on the binding and orientation of the catalytically relevant isoalloxazine core.

As previously mentioned, modifications of the isoalloxazine ring result in altered redox properties of enzymes; therefore, these modifications are not feasible. Additionally, the functionalization of the FAD phosphate groups will change the overall charge of the molecule, thus affecting the reconstitution of the involved proteins. Modifications of the adenine base at the N-6 position of FAD have been shown to be possible; nevertheless, they result in a

significant decrease in the oxidase activity by changing the microenvironment around the isoalloxazine core.<sup>313</sup> Furthermore, direct incorporation of a diazirine group at the adenine core is not possible in a nested<sup>330</sup> fashion.

However, the ribityl side chain and the ribose ring of adenosine, with their free hydroxyl groups, offer excellent synthetic access for the direct incorporation of a diazirine group as well as via an aliphatic or aromatic linker. Thus, they are considered the most promising modification sites (see Figure 32).

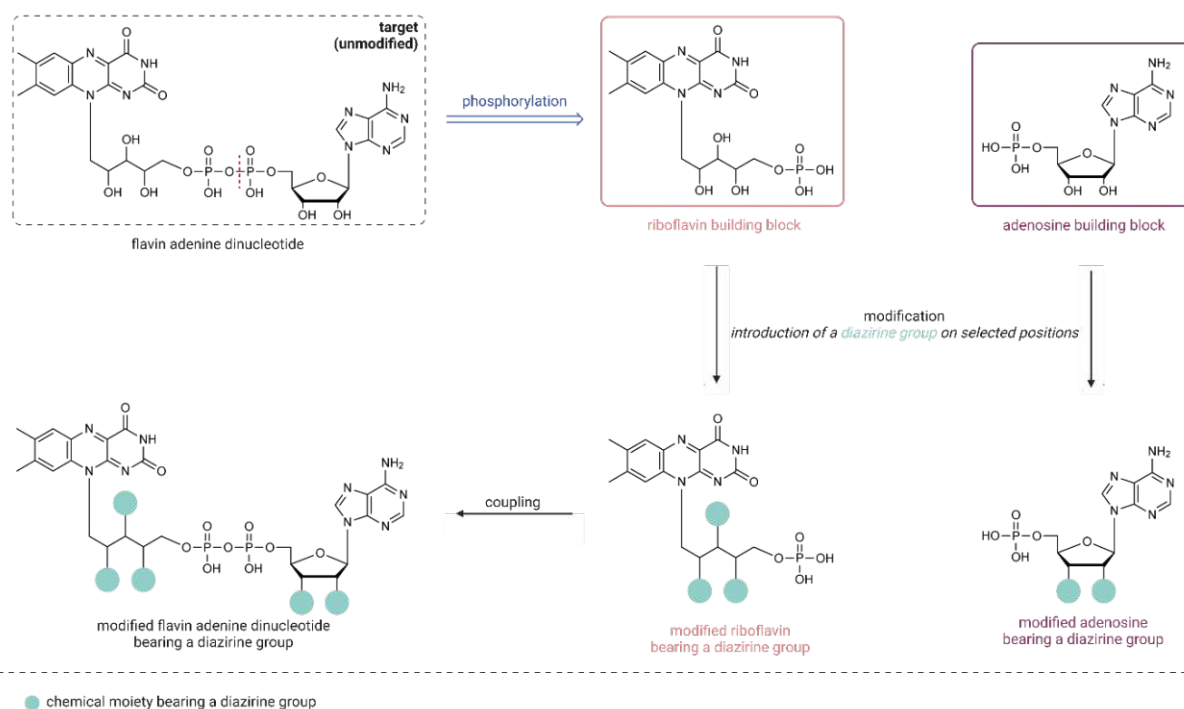


**Figure 32:** Retrosynthetic analysis of FAD (red retrosynthetic cut) and planned positions for diazirine incorporation (turquoise) towards diazirine-FAD molecules.

## C 1.2 Synthesis of FAD analogs

A critical step in the synthesis of FAD and its analogs is the coupling between the adenosine building block and the riboflavin building block. The first total synthesis of FAD was achieved by Todd *et al.* in 1952, who condensed salts of riboflavin-5'-phosphate with 2',3'-*O*-isopropylidene adenosine-5'-benzyl phosphorochloridate, followed by the removal of protective groups.<sup>350</sup> Only a few modifications in the preparation of FAD have since been reported.<sup>351,352</sup> All modifications have in common the low yield of FAD obtained via the chemical coupling step, which ranges from 6–14%.

Besides chemical coupling, an enzymatic reaction can achieve the conjugation of both building blocks to obtain FAD and its analogs. Enzymatic coupling that produces FAD and its



derivatives typically begins from riboflavin [II] and its analogs, which are first converted to the corresponding riboflavin-5-monophosphates [III] and then transformed to FAD [IV] (see Figure 33). These processes are performed through two enzymatic activities: the ATP:RF 5'-phosphotransferase (Riboflavin kinase [RFK]) and the ATP:FMN-adenylyltransferase (FMN adenylyltransferase).<sup>353</sup> The enzyme FAD synthetase from *Corynebacterium ammoniagenes* utilizes both the N-terminal adenylation domain and a C-terminal RFK domain.<sup>354,355</sup> Enzymatic FAD coupling is much more efficient than chemical routes to FAD, with yields ranging from 85–93%. However, as the literature has shown, the enzyme displays a broad substrate tolerance only for riboflavin derivatives but not for the adenosine moiety. Only successful couplings with ATP as a substrate have been reported.<sup>93</sup> Nevertheless, we sought to apply enzymatic coupling for FAD derivatives, which are modified on the ribityl group of riboflavin.

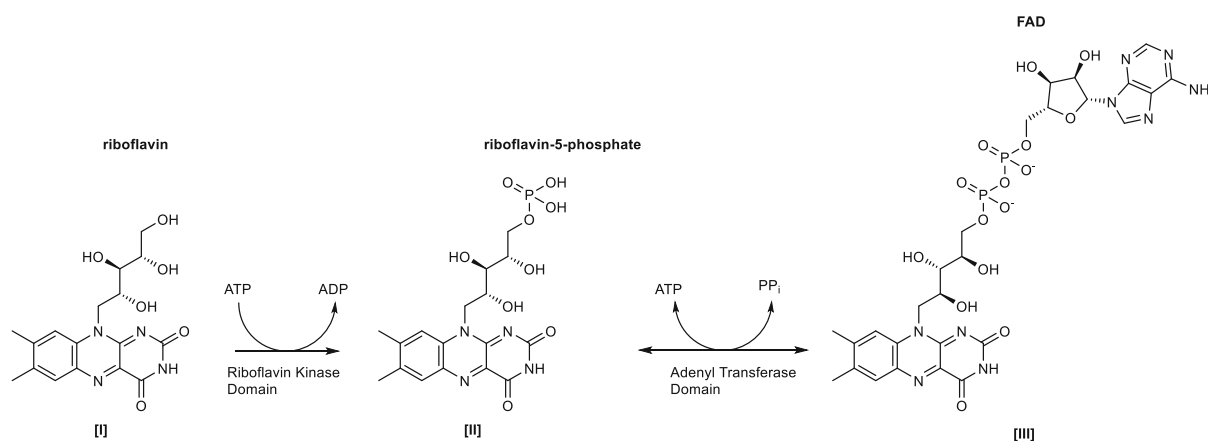
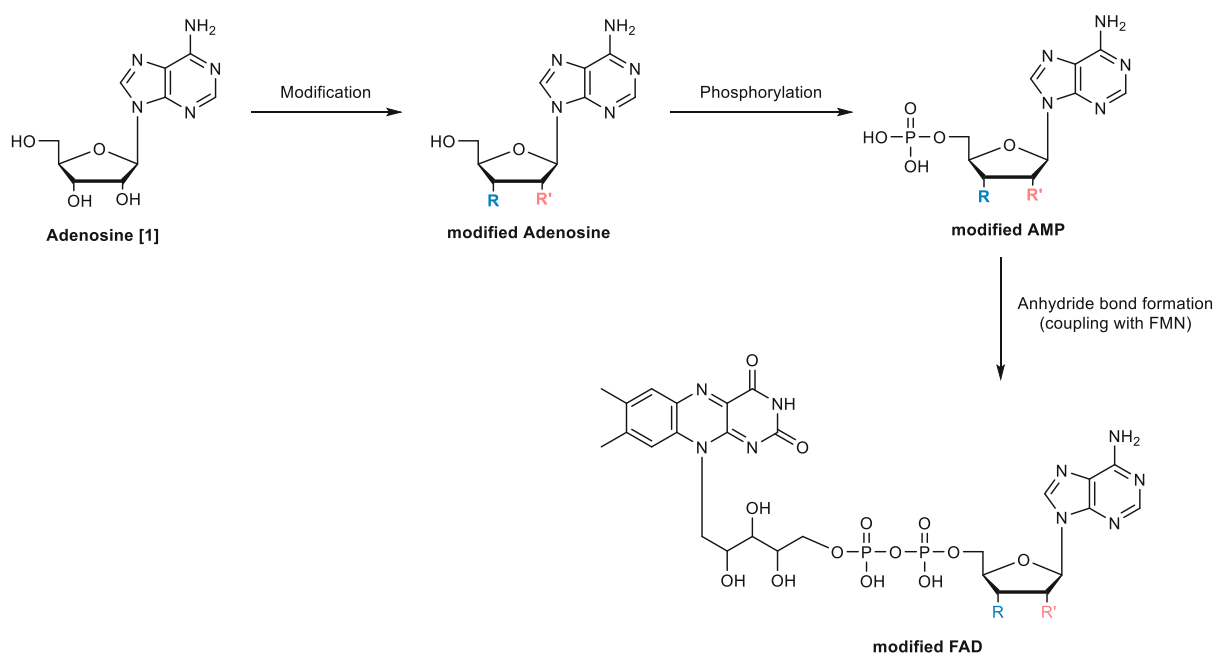


**Figure 33:** Enzymatic synthesis of FAD is catalyzed by two enzymatic activities: the riboflavin kinase (RFK), which catalyzes riboflavin's phosphorylation, and the FMN adenylyltransferase, which catalyzes the adenylyl transfer from ATP to the riboflavin-5-monophosphate.

Thorpe *et al.* utilized FAD synthetase of *Brevibacterium ammoniagenes* to synthesize eight FAD analogs from the respective riboflavin derivatives, thus demonstrating a broad specificity of flavin substrates.<sup>356</sup> More recently, Mishanina and colleagues used *Corynebacterium ammoniagenes* FAD synthetase to prepare isotopically labeled FAD analogs.<sup>354</sup>

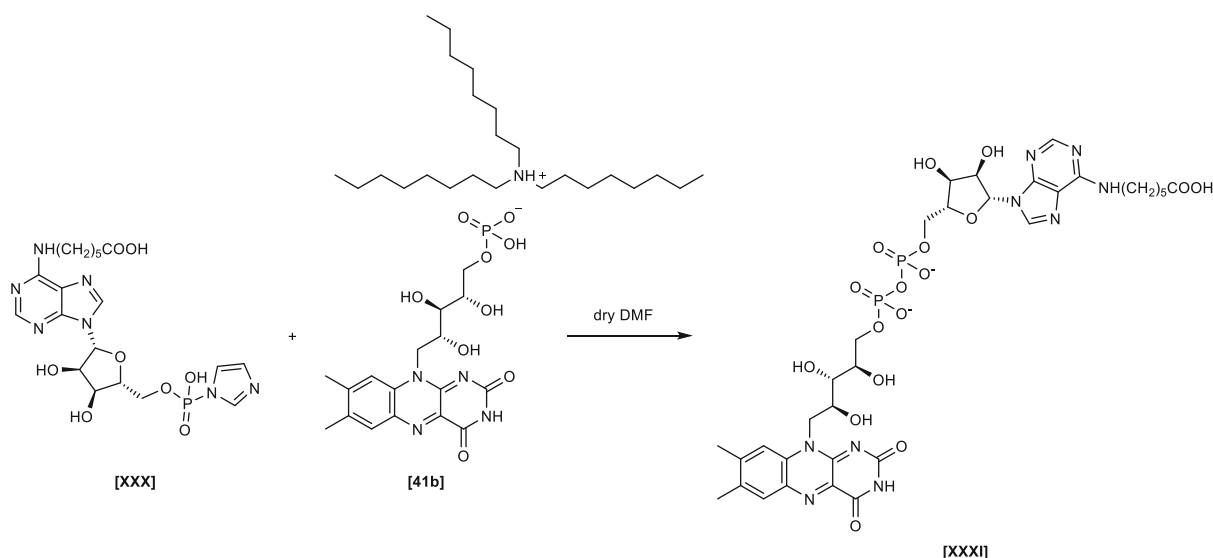
Since no successful literature precedent has been reported, we aimed to synthesize FAD analogs modified at the adenosine moiety via chemical coupling. Generally, FAD analogs modified at the adenosine moiety are synthesized according to the same synthetic principle (see Scheme 4). First, modifications are introduced at the level of the nucleosides. Then, the respective adenosine monophosphates are obtained using the phosphorylation method by Yoshikawa *et al.*<sup>357</sup> Subsequently, the obtained monophosphates are pre-activated (e.g., with CDI) and then coupled to FMN, thus producing modified FADs. However, due to the elaborate

synthesis, laborious purifications, and low overall yields, only a few FAD analogs modified at the adenosine moiety have been reported in the literature.

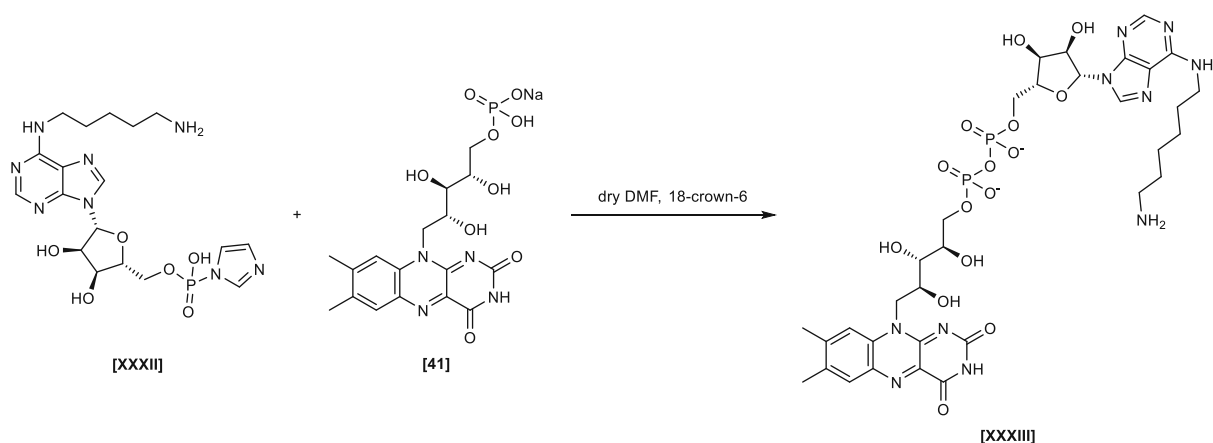


**Scheme 4:** General synthesis route for the preparation of modified FAD analogs.

Stocker *et al.* synthesized  $N^6$ -(6-carboxyhexyl)-FAD [XXXI] using the described synthetic pathway (Scheme 5) starting from 6-chloro-adenosine.<sup>358</sup> Saleh *et al.* prepared  $N^6$ -(6-aminoethyl)-FAD [XXXIII] using a similar method.<sup>359</sup> The strategies differed in how the FMN was solubilized. Since FMN is hardly soluble in organic solvents, it must first be converted to an ammonium salt, such as tri-*n*-octylammonium salt [41b], which was applied by Stocker *et al.* In contrast, Saleh *et al.* utilized 18-crown-6 ether to solubilize commercially available riboflavin-5-monophosphate sodium salt [41] in dry DMF.



**Scheme 5:** Coupling of activated adenosine-5-phosphate [XXX] with riboflavin-5-phosphate tri-*n*-octylammonium salt [41b].



**Scheme 6:** Coupling of activated adenosine-5-phosphate [XXXII] with riboflavin-5-phosphate sodium salt [41].

## C I.3 Possible modifications of the adenosine building block

Since we targeted the free hydroxyl groups at the C-2' and C-3' position of the ribose moiety as the primary modification sites of the adenosine building block, we sought to introduce the diazirine unit directly to the ribose core and via an aliphatic and an aromatic linker bearing the diazirine functionality (see Figure 34). The direct incorporation should result in minimal detrimental effects on the binding and orientation of the catalytically relevant isoalloxazine core compared to the native FAD. However, we also envisioned providing alternative structures that contain the diazirine unit. Furthermore, due to the aliphatic linker's small size and flexibility,

we expected only minor changes in the target proteins' side chains after its incorporation. However, we expected the aromatic phototag to result in a greater disturbance of the proteins.

To introduce a diazirine unit via an aliphatic or aromatic linker at the ribose's C-2' and C-3' position, the tethering can be achieved via an ether, ester, amine, or amide linkage. However, for the synthesis of amines or amides, the hydroxyl groups of the ribose moiety must first be converted to the corresponding amines. Although synthetic routes towards the amine functionality at the C-2' and C-3' position of adenosine have been reported in the literature,<sup>360-364</sup> their synthesis is significantly more elaborate compared to the synthesis of ethers or esters, in which the hydroxyl groups act as direct anchoring points. Furthermore, since ethers are less prone to hydrolysis than esters, and esters of ribonucleosides have been reported to undergo spontaneous acyl shifts,<sup>363</sup> we considered ethers the first choice.

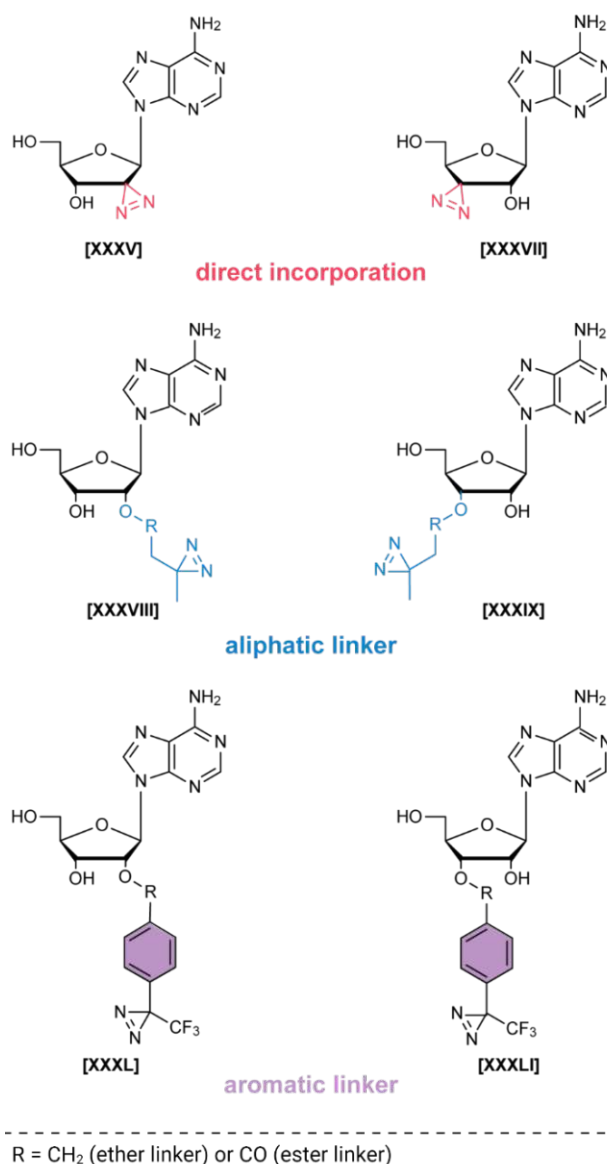
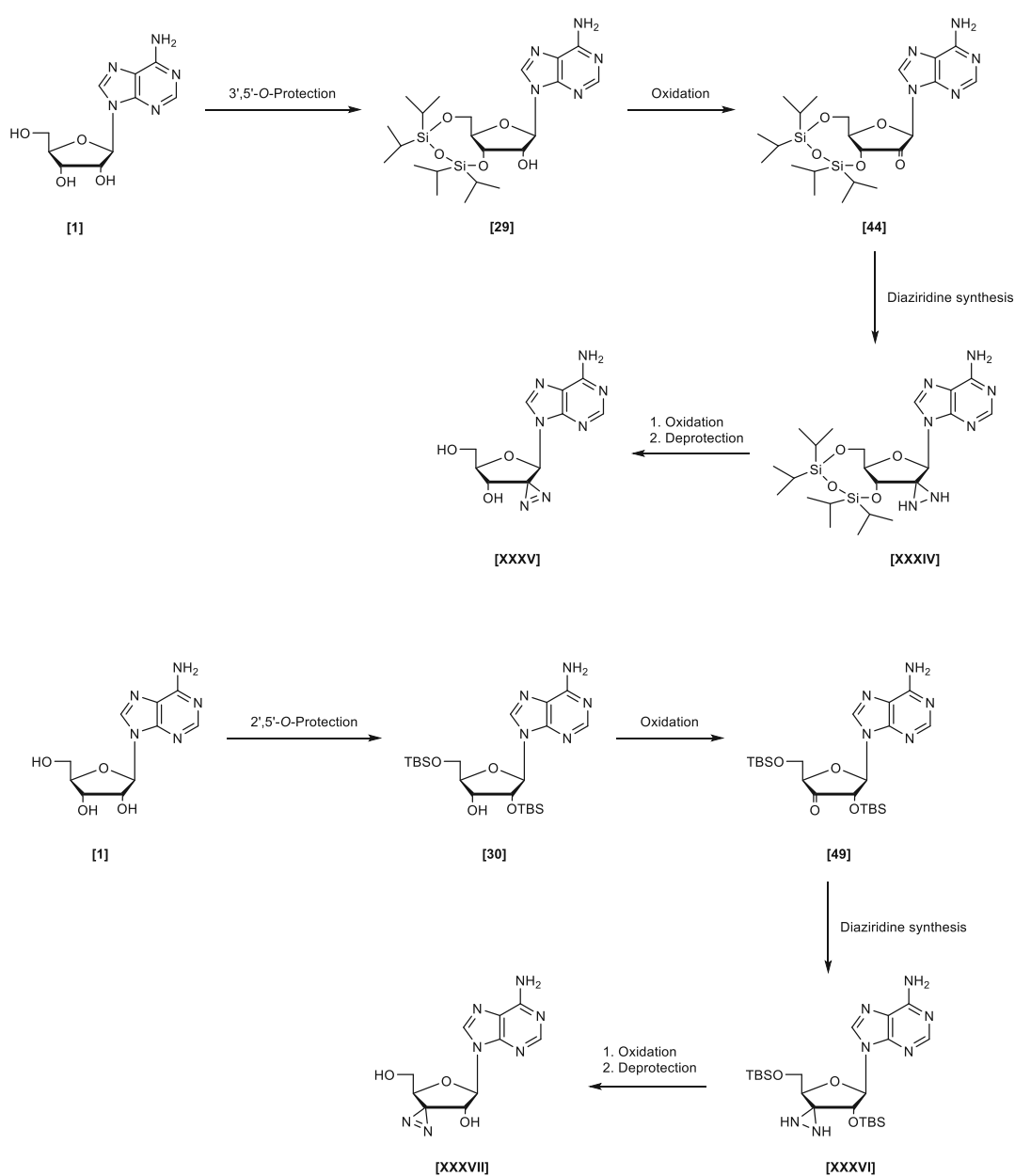


**Figure 34:** Selected building blocks for the modified adenosine-FAD derivatives.

## C I.3.1 Direct incorporation of the diazine unit at the adenosine moiety

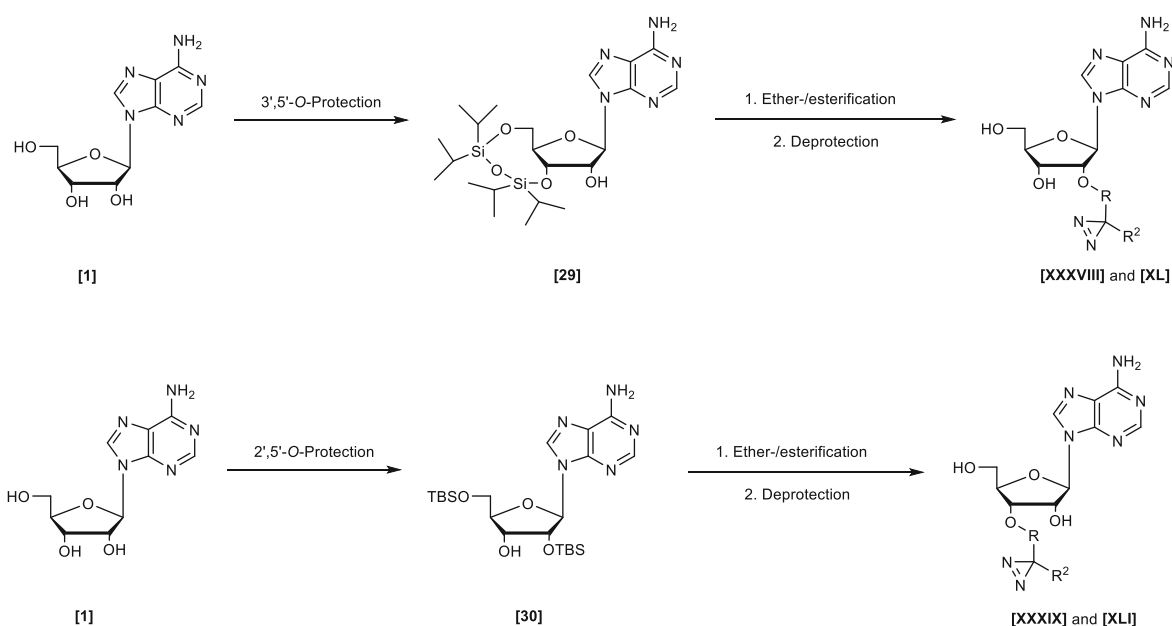
A possible synthetic route of compounds [XXXVI] and [XXXVII] is outlined in Scheme 7. The first step of direct incorporation of the diazine unit is the selective protection of the 2' and 5'-OH group and the 3' and 5'-OH group of adenosine [1], respectively. Next, the free hydroxyl group of compounds [29] and [30] could be oxidized to produce ketones [44] and [49]. The ketones would then be further converted to the corresponding diaziridines, and their oxidation would result in the formation of the diazirines.



**Scheme 7:** A proposed synthetic route towards compounds [XXXV] and [XXXVII].

## C I.3.2 Incorporation of the diazirine unit via an aliphatic and aromatic linker

The synthetic route for the adenosine derivatives containing the aliphatic and aromatic linker would also commence with the selective protection of adenosine [1] to leave one free hydroxyl group. The free hydroxyl groups of compounds [29] and [30] could then be coupled with an acid to produce an ester or react with an alkyl or aryl halide in the presence of a base to generate an ether via Williamson ether synthesis.



R = CH<sub>2</sub> (ether linker) or CO (ester linker)  
R<sup>2</sup> = CH<sub>3</sub> (aliphatic linker) or CF<sub>3</sub> (aromatic linker)

**Scheme 8:** A proposed synthetic route towards compounds [XXXVIII], [XXXIX], [XL], and [XLI].

## C I.4 Possible modifications of the riboflavin building block

Planning the modifications of the riboflavin building block, we also targeted integration of the diazirine moiety directly into the ribityl side chain of riboflavin and via an aliphatic and aromatic linker bearing the diazirine, in which the hydroxyl groups act as anchoring points (see Figure 35). Furthermore, since the hydroxyl group at the C-2' position of the ribityl side chain has been reported as being involved in the catalytic cycle in some flavoenzymes,<sup>365,366</sup> we sought to modify the hydroxyl groups only at the C-3' and C-4' position.

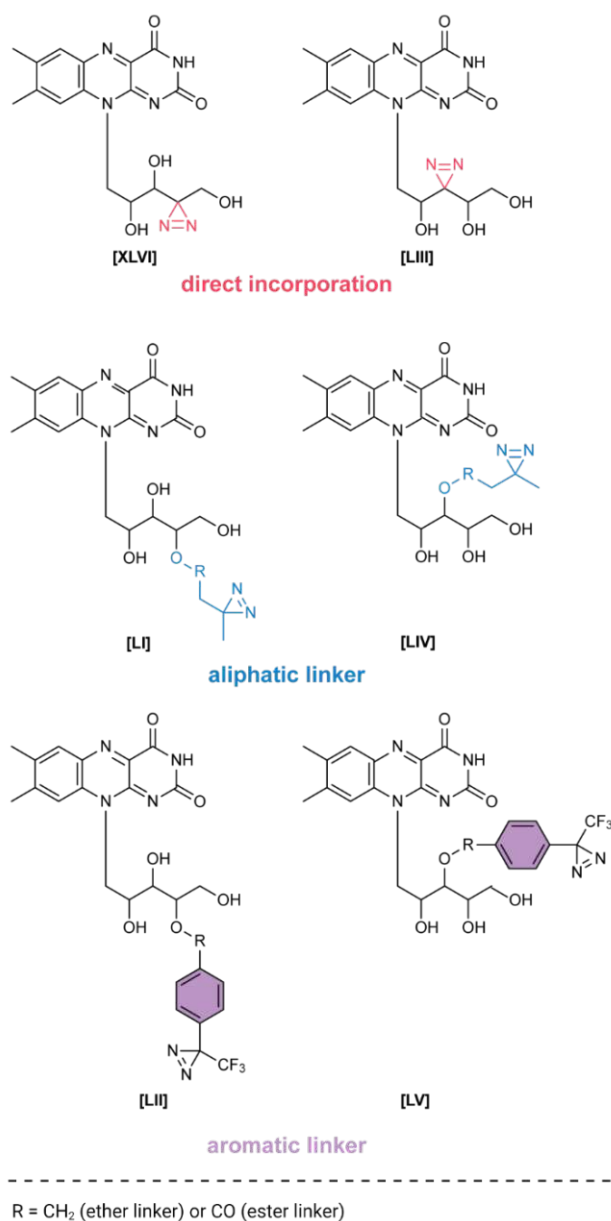


**Figure 35:** Selected building blocks for the modified riboflavin-FAD derivatives.

## C I.4.1 Synthesis of riboflavin building blocks

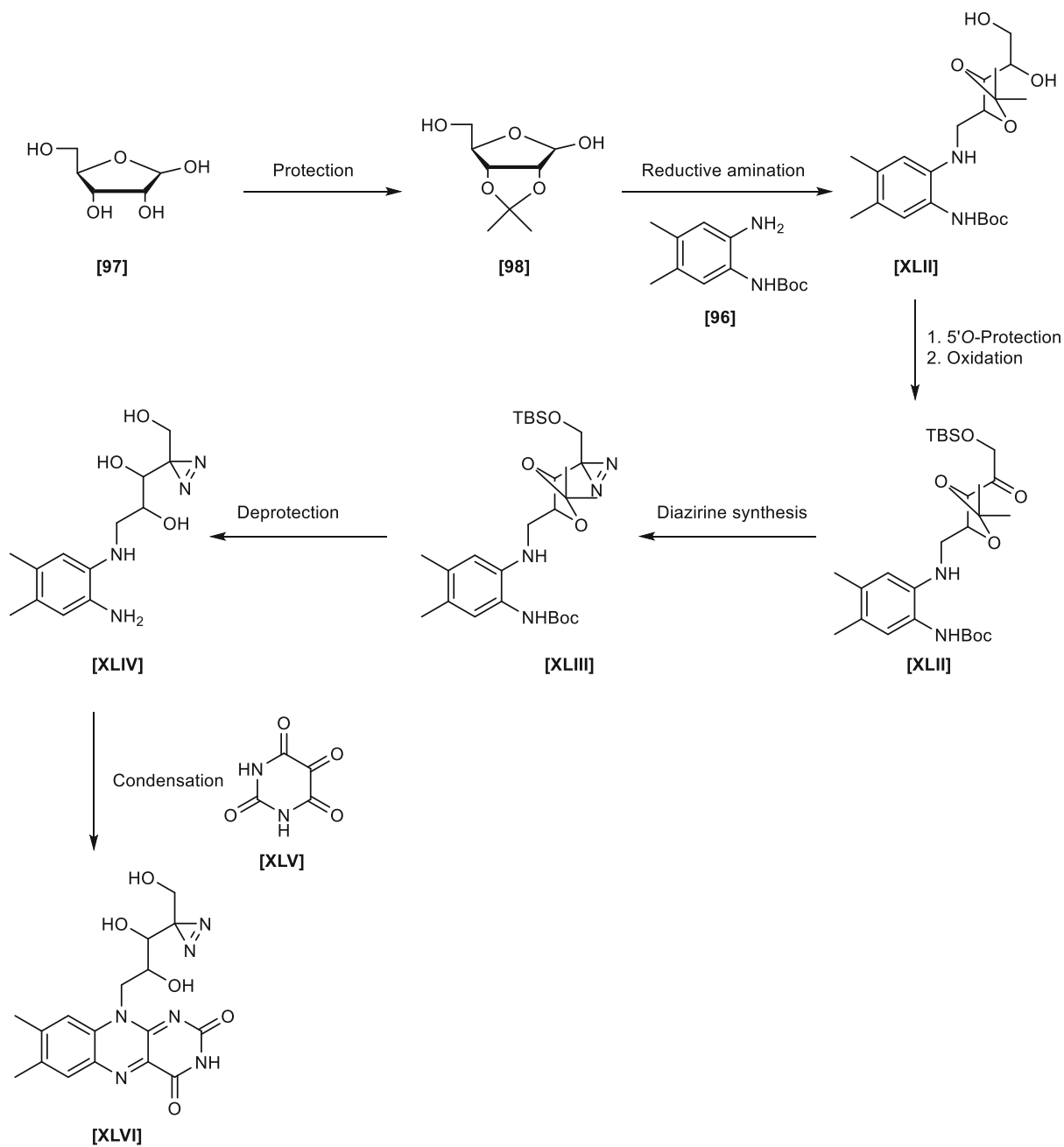
The first chemical synthesis of riboflavin was described by the research groups of Kuhn and Karrer in 1934 and 1935, respectively.<sup>367,368</sup> The synthetic route of Kuhn *et al.* commenced with a reductive condensation of 6-nitro-3,4-xylidine with D-ribose. The nitro compound was further reduced to phenylenediamine, followed by treatment with alloxan under acid conditions. Karrer *et al.* adopted this procedure, whereby the condensation of 3,4-xylidine with D-ribose furnished *N*-D-ribityl-3,4-xylidine, which was coupled with a diazonium salt. The reduction of the resulting compound and its treatment with alloxan provided riboflavin.<sup>369,370</sup> Since 1934, many modifications and refinements of these general syntheses have been developed,<sup>371-374</sup> and a

significant improvement in the synthesis of riboflavin resulted from the direct condensation of barbituric acid with an azo dye in acetic acid via the Tishler reaction.<sup>375</sup>

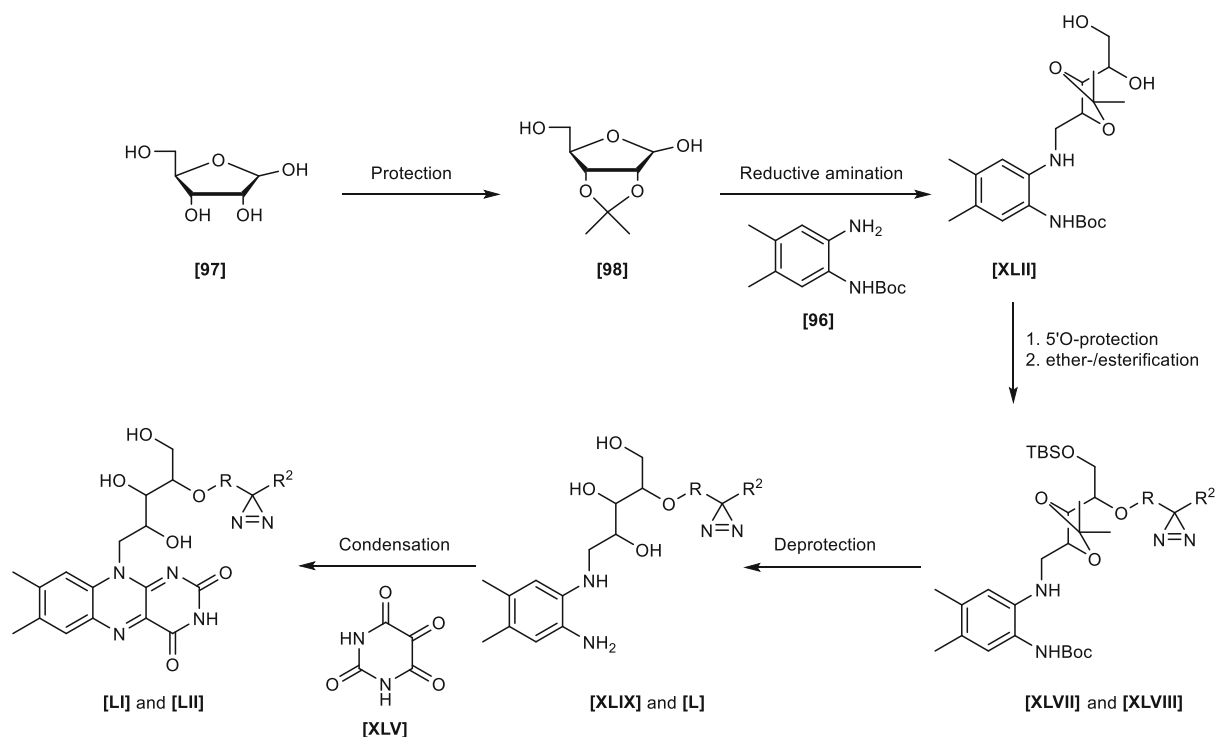
Generally, the chemical synthesis of riboflavin and its analogs begins with the desymmetrization of 4,5-dimethylbenzene-1,2-diamine [95] using Boc-protection, followed by reductive amination of the free amino group with D-ribose [97]. Deprotection of the Boc-group and condensation with alloxan results in riboflavin formation.<sup>374</sup>

Applying this strategy to our diazirine-based derivatives, we propose a possible synthetic route that would commence with the protection of the hydroxyl groups at the C-2' and C-3' position of D-ribose [95] as isopropylidene ketal [98], followed by reductive amination with the protected diamine [96]. The primary hydroxyl group could then be selectively protected with a suitable protecting group, such as the *tert*-butyldimethylsilyl (TBS) group. Next, oxidation of the remaining hydroxyl group to ketone [XLVIII] would result in the formation of the starting material for the direct incorporation of the diazirine unit at the ribityl chain. Alternatively, a suitable aliphatic or aromatic linker containing the diazirine unit could be attached to the free hydroxyl group through etherification or esterification. Then, deprotection of the Boc-group and the acetonide, followed by condensation with alloxan [XLV], would construct the modified riboflavin building block. The final step would be the enzymatic coupling of the modified riboflavin with ATP using the enzyme FAD synthetase (see chapter C V.1.4).





**Scheme 9:** A proposed synthetic route towards compound **[XLVI]**.



**Scheme 10:** A proposed synthetic route towards compounds [LI] and [LII].

## C II Chemical synthesis of building blocks and intermediates towards the synthesis of diazine-FADs

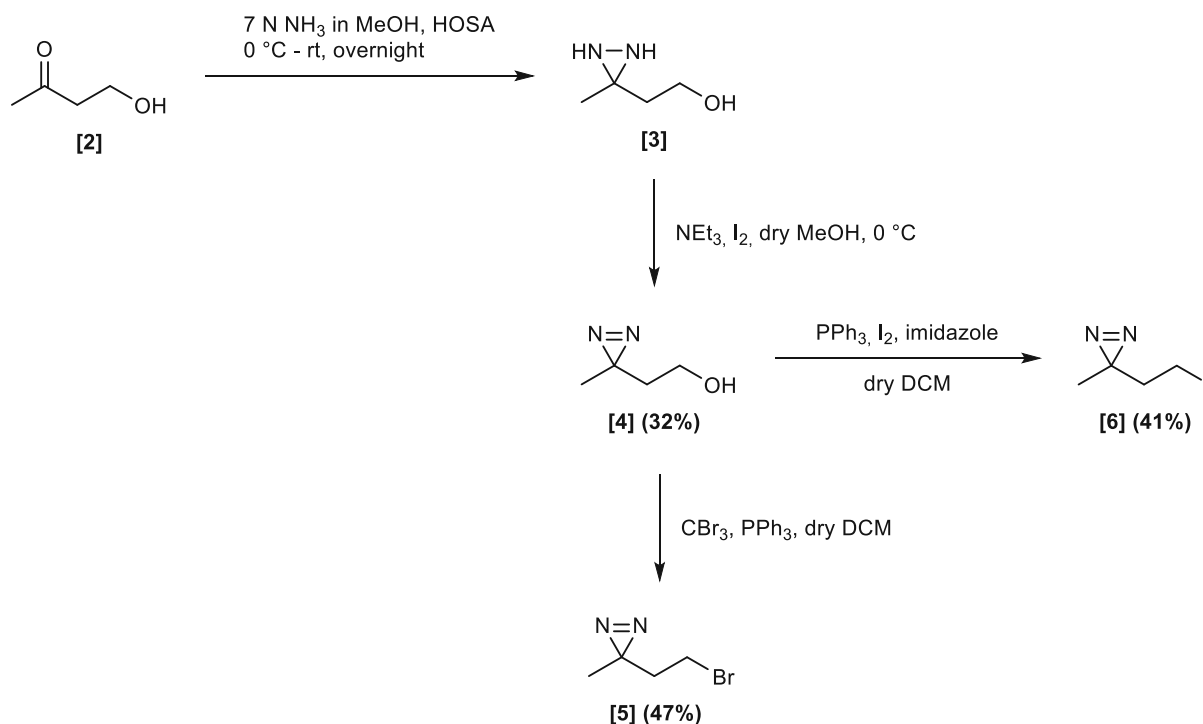
The following sections address the synthesis of important building blocks, intermediates, and diazine-FADs.

### C II.1 Synthesis of aliphatic diazine linkers

Considering the previously mentioned concepts of incorporating an aliphatic linker with a diazine unit into the FAD core (outlined in chapters C I.3 and C I.4), we first targeted synthesizing an alkyl halide, which would enable the subsequent etherification of the hydroxyl groups of the ribityl side chain of the flavin moiety and the ribose unit of adenosine.

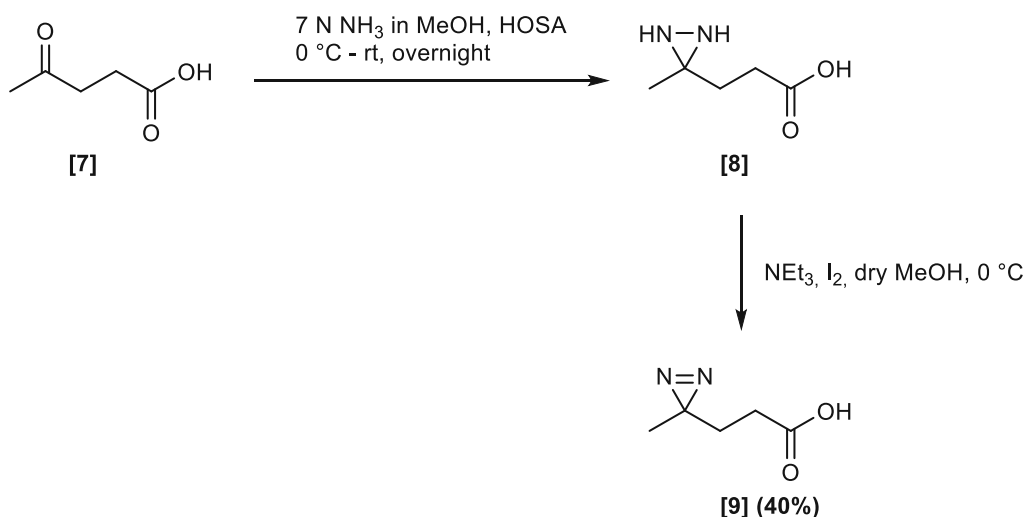
The synthesis of the aliphatic diazine linker began from 4-hydroxy-2-butanone [2] following a literature procedure.<sup>376</sup> The ketone was first converted to diaziridine [3] by

treatment with a 7 N  $\text{NH}_3$  solution in MeOH and hydroxylamine-*O*-sulfonic acid (HOSA). The obtained diaziridine alcohol **[3]** was subsequently oxidized using  $\text{I}_2$  in the presence of triethylamine in MeOH. The desired compound **[4]** was obtained in 32% yield over two steps and could be used in the following steps without further purification. The diazirine alcohol **[4]** was then converted to bromide **[5]** via the Appel reaction<sup>377</sup> using  $\text{CBr}_4$  and  $\text{PPh}_3$  in dry DCM and to iodide **[6]** through treatment with  $\text{PPh}_3$  and  $\text{I}_2$  in the presence of imidazole in dry DCM.<sup>378</sup>



**Scheme 11:** Synthetic routes towards aliphatic building blocks **[4]**, **[5]**, and **[6]**.

Since we also considered incorporating the aliphatic linker via an ester linkage, we sought to synthesize a carboxylic acid bearing a diazirine group. Similar to the previously described protocol, levulinic acid **[7]** was first converted to the diaziridine propionic acid **[8]**, which was subsequently oxidized using  $\text{I}_2$  in the presence of triethylamine in MeOH.<sup>379</sup> Compound **[9]** was obtained in 40% yield over two steps and could be used in the following steps without further purification.



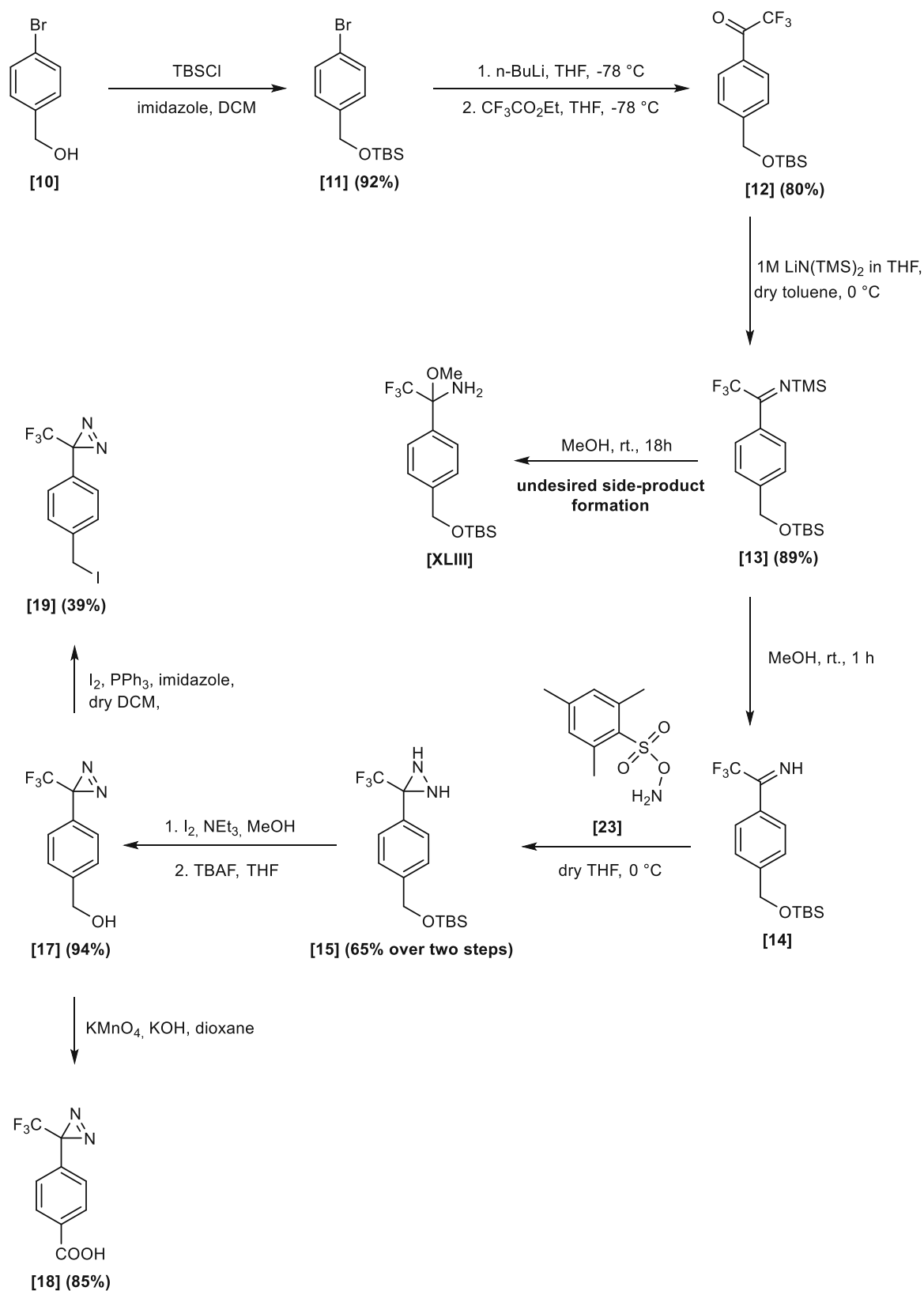
**Scheme 12:** Synthesis of diazirine acid [9].

## C II.2 Synthesis of aromatic diazirine linkers

For the synthesis of the aromatic diazirine linkers [18] and [19], we applied a novel ammonia-free synthesis method developed by Kumar *et al.*<sup>380</sup> (see Scheme 13). The synthetic route to aromatic diazirine [16] commenced from commercially available 4-bromobenzyl alcohol [10]. The hydroxyl group of the starting material [10] was first protected by the TBS group. Next, the metal halogen exchange reaction with *n*-BuLi and treatment with ethyl trifluoroacetate resulted in the formation of the trifluoromethyl phenyl ketone [12]. The crude material was purified via flash column chromatography to yield the desired compound [12] in 90% yield. The trifluoromethyl phenyl ketone [11] was then converted to *N*-TMS-ketimine [13] using treatment with bis(trimethylsilyl)amide as an ammonia equivalent. Next, solvolysis with MeOH provided the imine [14]. However, in contrast to the method described in the literature, in which solvolysis was conducted for 18 hours, we noticed that solvolysis was finished within one hour, and a prolonged reaction time resulted in the formation of the methanol adduct [XLIII] as the only product. Hence, the reaction progress was frequently monitored by <sup>1</sup>H-NMR and <sup>19</sup>F-NMR. Imine [14] was further converted to diaziridine [15] by a reaction with previously prepared *O*-mesitylenesulfonyl hydroxylamine [23]. Finally, oxidation of 3-trifluoromethyl-3-phenyldiaziridine [15] with I<sub>2</sub> in the presence of triethylamine in MeOH furnished diazirine [16] in 92% yield. Subsequent deprotection of the TBS group was achieved using tetra-*n*-butylammonium fluoride (TBAF) in tetrahydrofuran in 96%. The hydroxyl group

was further oxidized to the carboxylic acid using  $\text{KMnO}_4$  in the presence of potassium hydroxide in dioxane. The extractive workup provided acid **[18]** in 85% yield.

Alcohol **[17]** was additionally converted to iodide **[19]**, applying the same protocol used for aliphatic analog **[6]**.

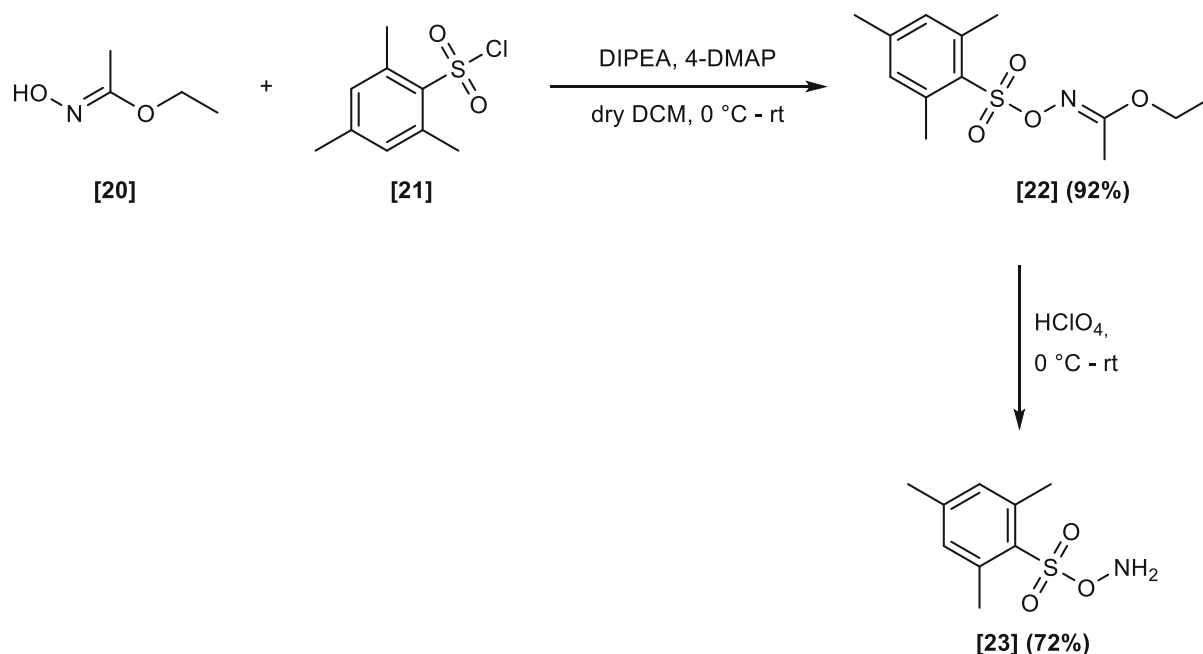


**Scheme 13:** Synthetic overview of aromatic diazirine building blocks.

Using this method, the important building block [17] was obtained in 40% overall yield. Compared to the conventional route, this novel synthetic protocol is significantly less time-

consuming and more convenient due to fewer overnight steps and the absence of liquid ammonia.

The required aminating reagent *O*-mesitylenesulfonyl hydroxylamine [**23**] was prepared in a two-step synthesis sequence, which is outlined in Scheme 14. Briefly, ethyl *N*-hydroxyacetimidate [**20**] was first reacted with 2-mesitylenesulfonyl chloride [**21**] to produce ethyl *O*-arylsulfonyl hydroxamate [**22**] in 92% after purification by flash column chromatography.<sup>381</sup> The subsequent treatment of [**22**] with 70% perchloric acid<sup>382</sup> furnished *O*-mesitylenesulfonyl hydroxylamine [**23**] in 72% yield after crystallization. Noteworthy, compound [**23**] readily decomposes and thus should be prepared immediately before usage.



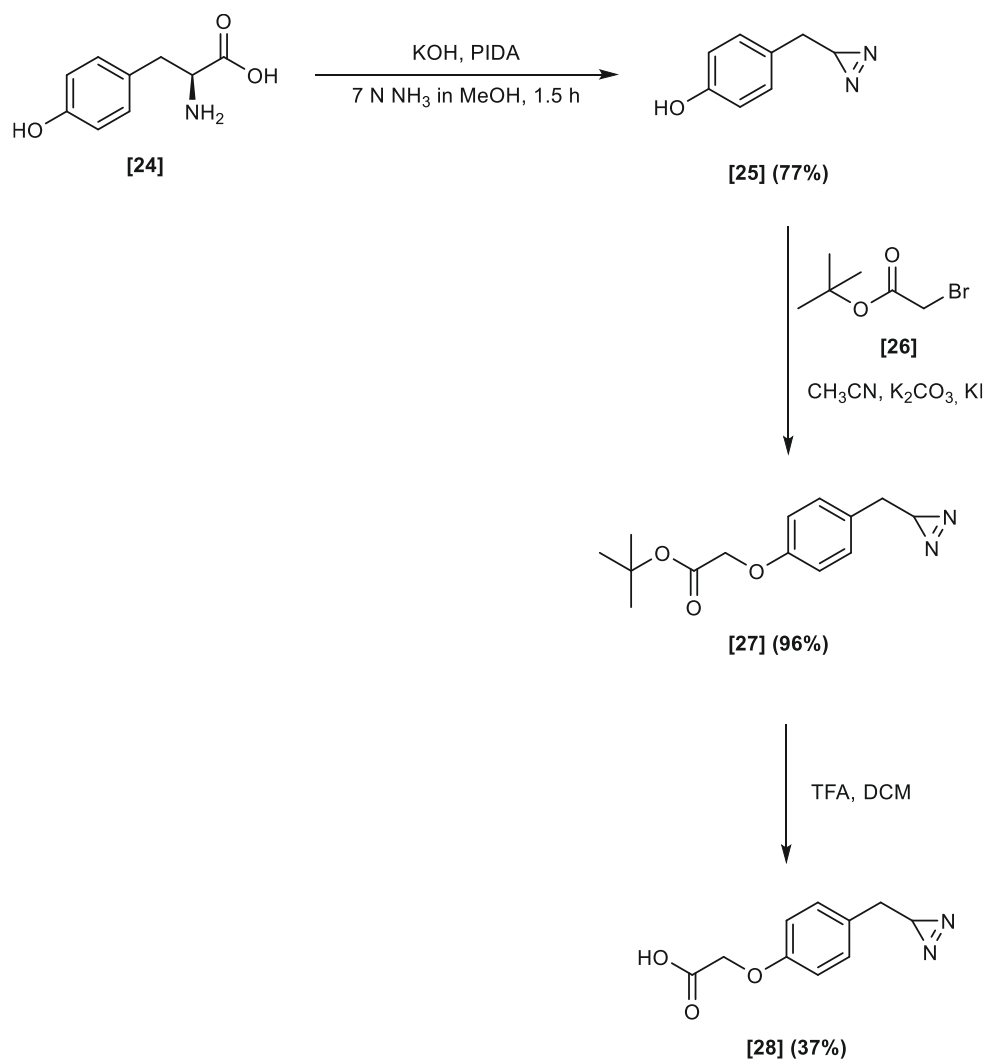
**Scheme 14:** Synthesis of the aminating reagent [**23**].

## C II.3 Synthesis of a terminal diazirine as an alternative building block

In 2019, Glachet *et al.*<sup>383</sup> reported the synthesis of terminal diazirines in a one-pot procedure beginning from cheap  $\alpha$ -amino acids. The synthesis used phenyl iodonium diacetate (PIDA) and ammonia. The authors reported high functional group tolerance and good yields. Therefore, based on this convenient protocol, we provided an alternative structure to the aromatic building block [17].

The synthetic route began from the cheap starting material *L*-tyrosine [**24**]. One portion of PIDA was added to a solution of *L*-tyrosine [**24**] in 7 M NH<sub>3</sub> in MeOH in the presence of KOH

under an argon atmosphere, and the resulting reaction mixture was stirred for 30 min at 0 °C. The batch was then allowed to warm up to room temperature and was stirred for an additional 90 min. Evaporation of the volatiles under reduced pressure and purification by flash column chromatography afforded the desired compound **[25]** in 77% yield. According to the protocol found in the literature,<sup>383</sup> the compound **[25]** was further transformed into carboxylic acid **[28]** through two-step synthesis via alkylation and subsequent deprotection of the *tert*-butyl group. The low yield of the deprotection step likely resulted from the condition of TFA.

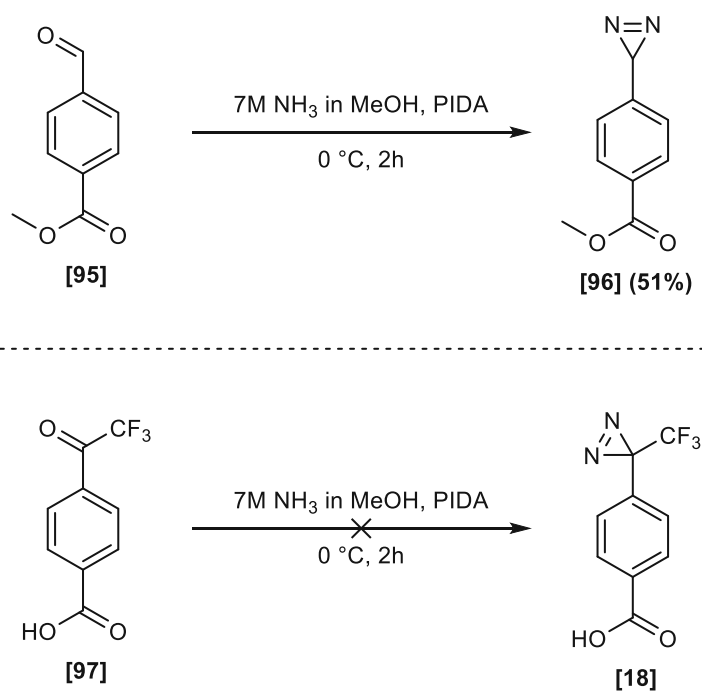


**Scheme 15:** Synthetic route towards aromatic diazirine **[28]**. Building block **[26]** represents an easily accessible alternative to aromatic diazirine **[18]**.



## C II.4 One-pot synthesis of diazirines from ketones and aldehydes

In the late stage of the project, we were inspired by a fairly recent publication from the Glachet group, in which they reported direct access to aromatic diazirines in the presence of the oxidizing agent (diacetoxyiodo)benzene (PIDA) starting from aldehydes and ketones.<sup>384</sup> These findings prompted us to investigate whether aromatic diazirine [18] can be directly synthesized in a one-step synthesis beginning from commercially available trifluoroketone [97]. While [95] (used as a reference reaction) was readily converted to the corresponding diazirine [96] when treated with eight equivalents of PIDA in a 7 N NH<sub>3</sub> in MeOH solution, no conversion of the trifluoroketone [97] was observed when treated under the same conditions. Nevertheless, this procedure offers convenient and efficient access to a wide range of diazirines.



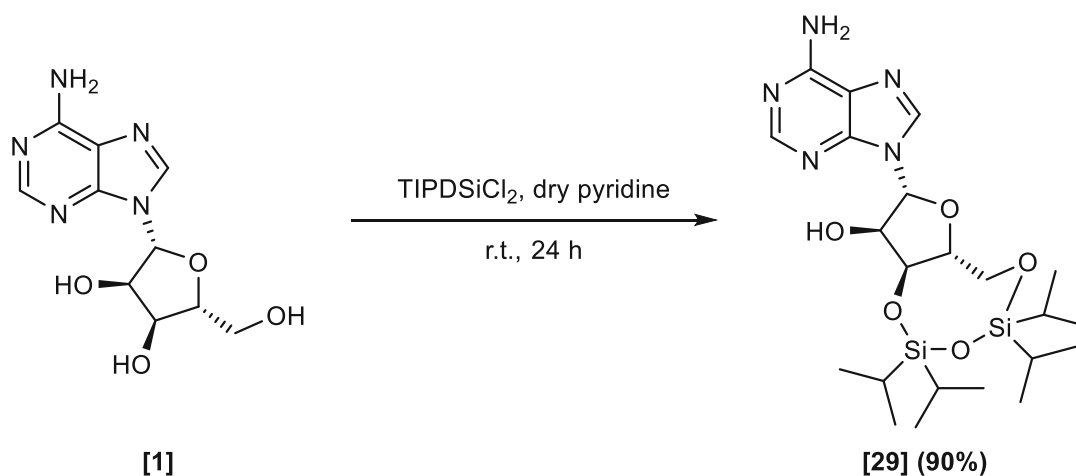
**Scheme 16:** One-pot synthesis of aromatic diazirines.

## C II.5 Derivatization of adenosine — Synthesis of FAD analogs modified at the adenosine moiety

Based on the synthetic analysis, the modifications of the adenine building block were prioritized due to the better accessibility of the target compounds. Furthermore, manipulations of the adenosine moiety would not have an overly strong deactivating effect on the enzyme activity, either by changing the orientation or by blocking the access of the substrate to the isoalloxazine system. Since we sought to manipulate the hydroxyl groups at the C-2' and the C-3', selective protection of the hydroxyl groups of the ribose unit of adenosine was the first step towards the synthesis of modified FAD analogs.

### C II.5.1 Protection of the hydroxyl groups at the C-3' and C-5' positions of adenosine

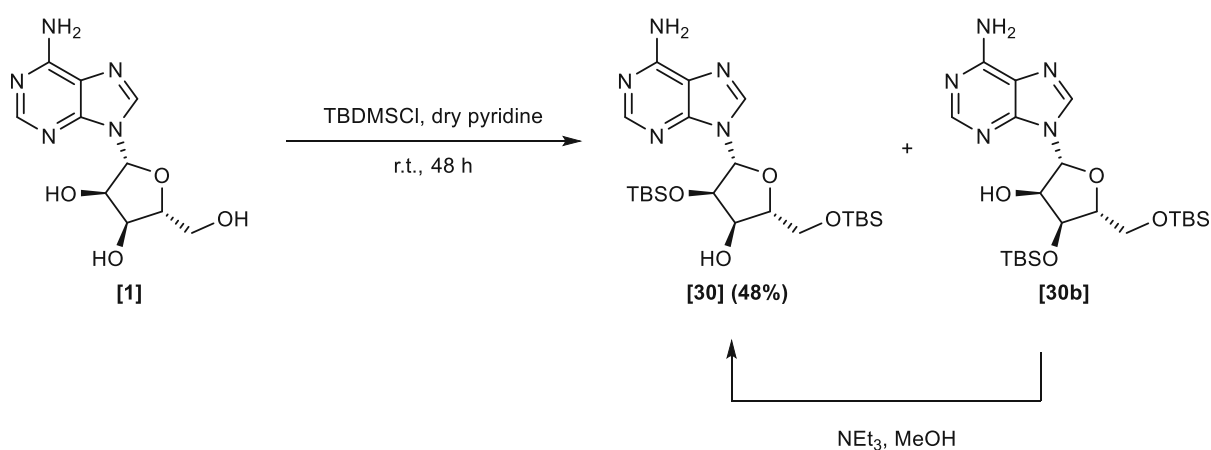
To allow for selective modification of the 2'-OH of adenosine [1], alcohols at the C-3' and C-5' were protected simultaneously<sup>385</sup> using the Markiewicz protecting group,<sup>385</sup> and this yielded cyclic siloxane [29]. Protection was achieved by treating adenosine with 1,3-dichloro-1,1,3,3-tetraisopropylidisiloxane (TIPDSiCl<sub>2</sub>) in dry pyridine.<sup>364</sup> Purification by flash column chromatography gave the silyl-protected adenosine derivative [2] in 90% yield.



**Scheme 17:** Protection of the hydroxyl groups at the C-3' and C-5' of adenosine [1].

## C II.5.2 Protection of the hydroxyl groups at the C-2' and C-5' positions of adenosine

For selective modification of the hydroxyl group at the C-3'-position of adenosine [1], adenosine [1] was partially protected at the alcohols at the C-2' and C-5' positions using *tert*-butyldimethylsilyl chloride (TBDMSCl). First, treatment of [1] with TBDMSCl in pyridine resulted in a mixture of the 2',5'- and 3',5'-bis-*O-tert*-butyldimethylsilyladenosines in a ratio of 4:3 according to NMR analysis. Subsequently, the two compounds were separated by flash column chromatography. Then, isomerization of 3',5'-bis-*O-tert*-butyldimethylsilyladenosine [30b] with triethylamine in MeOH and subsequent purification by flash column chromatography furnished 2',5'-bis-*O-tert*-butyldimethylsilyladenosine [30] in 48% overall yield.

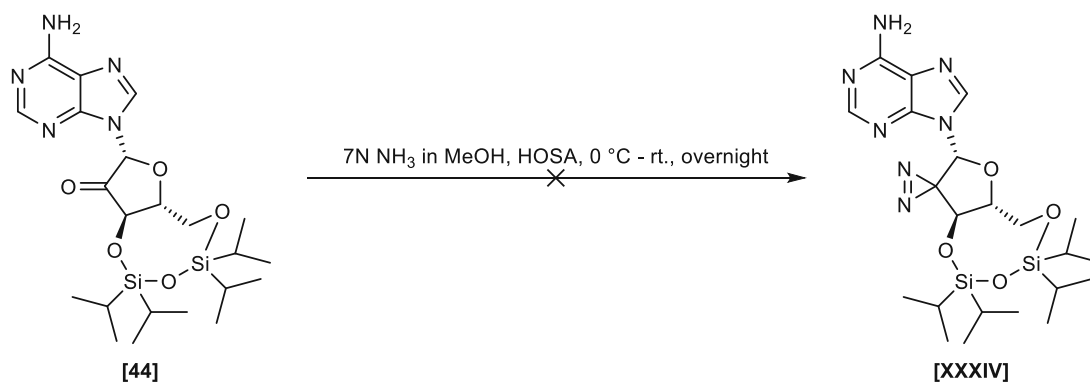


**Scheme 18:** Synthesis of protected adenosine building block [30]. Undesired isomer [30b] could further be isomerized by treatment with triethylamine in methanol.

## C II.5.3 Direct incorporation of a diazine unit at the ribose moiety of adenosine

As described in chapter C I.3.1, we intended to install the diazine group directly onto the ribose structure of adenosine. Hence, the first step was oxidation of the hydroxyl group of [27] to ketone [44] using Garegg reagent<sup>386</sup> (this oxidation is explained in more detail in chapter C II.6). Next, we attempted to transform the ketone functionality into the corresponding diaziridine [XXXIV] by applying the standard procedure for synthesizing aliphatic diazirines as described in chapter C II.1. However, under these conditions, many spots were detected on the thin layer chromatography (TLC) and attempts to lower the temperature failed.

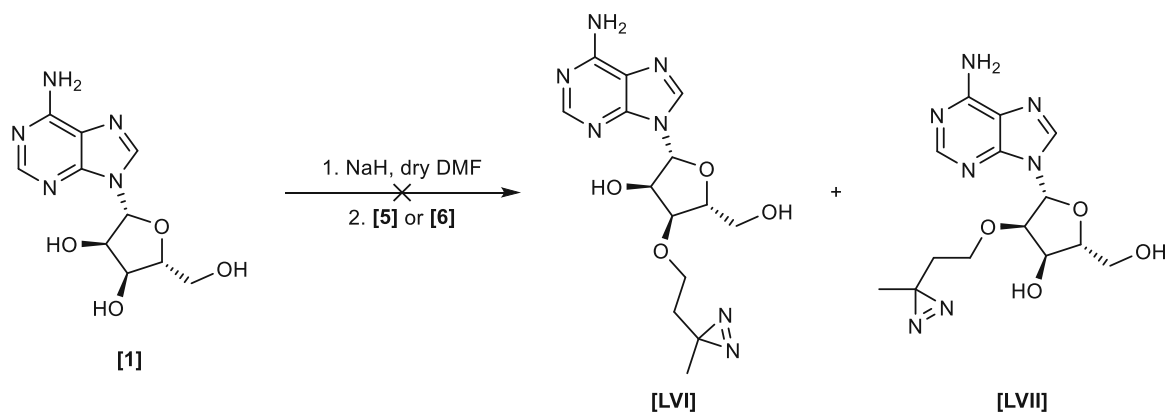
Since the concurrent elaboration of the ester derivatives proceeded smoothly at this stage, further investigations of the direct incorporation of diazirine functionality at the ribose moiety were halted.



**Scheme 19:** Attempted synthesis of diaziridine [XXXIV].

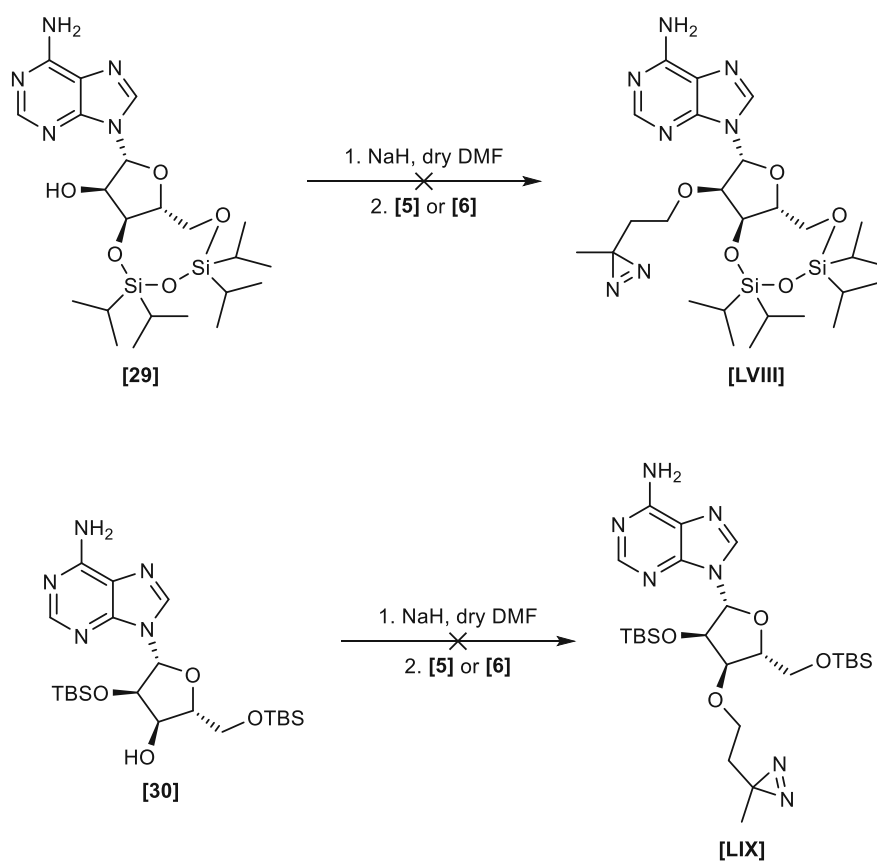
## C II.5.4 Etherification of adenosine on the protected adenosine derivatives

As outlined in chapter C I.1, we envisioned the synthesis of adenosine analogs bearing a diazirine unit via an aliphatic and aromatic linker. Since ethers should be more stable against hydrolysis than esters, we sought to synthesize ethers first. According to a literature procedure published by Sugihara *et al.*,<sup>387</sup> direct alkylation of adenosine [1] was achieved by treating unprotected adenosine [1] with 4-[3-(trifluoromethyl)-3*H*-diazirin-3-yl]benzyl bromide in the presence of NaH in DMF, yielding a mixture of 2'- and 3' alkylated isomers. The 2'-isomer was further purified using flash column chromatography and obtained in 31% yield. However, when we applied the literature conditions using the previously prepared diazirine bromide [5] and iodide [6], no conversion of [1] was observed, likely due to failed deprotonation of the hydroxyl groups of the ribose moiety. Further alkylation attempts with benzyl bromide remained unsuccessful.



**Scheme 20:** Failed synthesis of ether analogs [LVI] and [LVII].

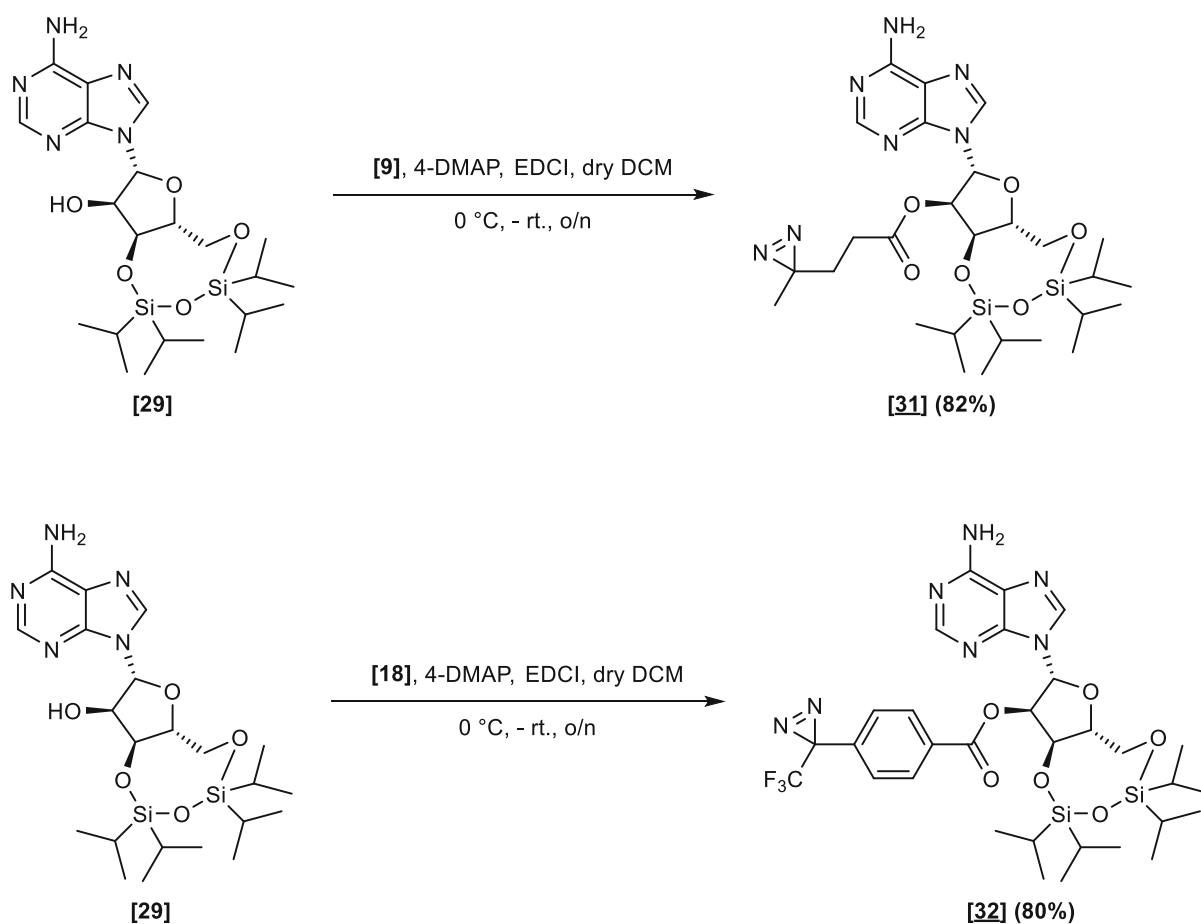
When the protected adenosine derivatives [29] and [30] were used, TLC and NMR analysis indicated heavy migration and decomposition of the starting materials. Therefore, etherification of the hydroxyl groups was abandoned.



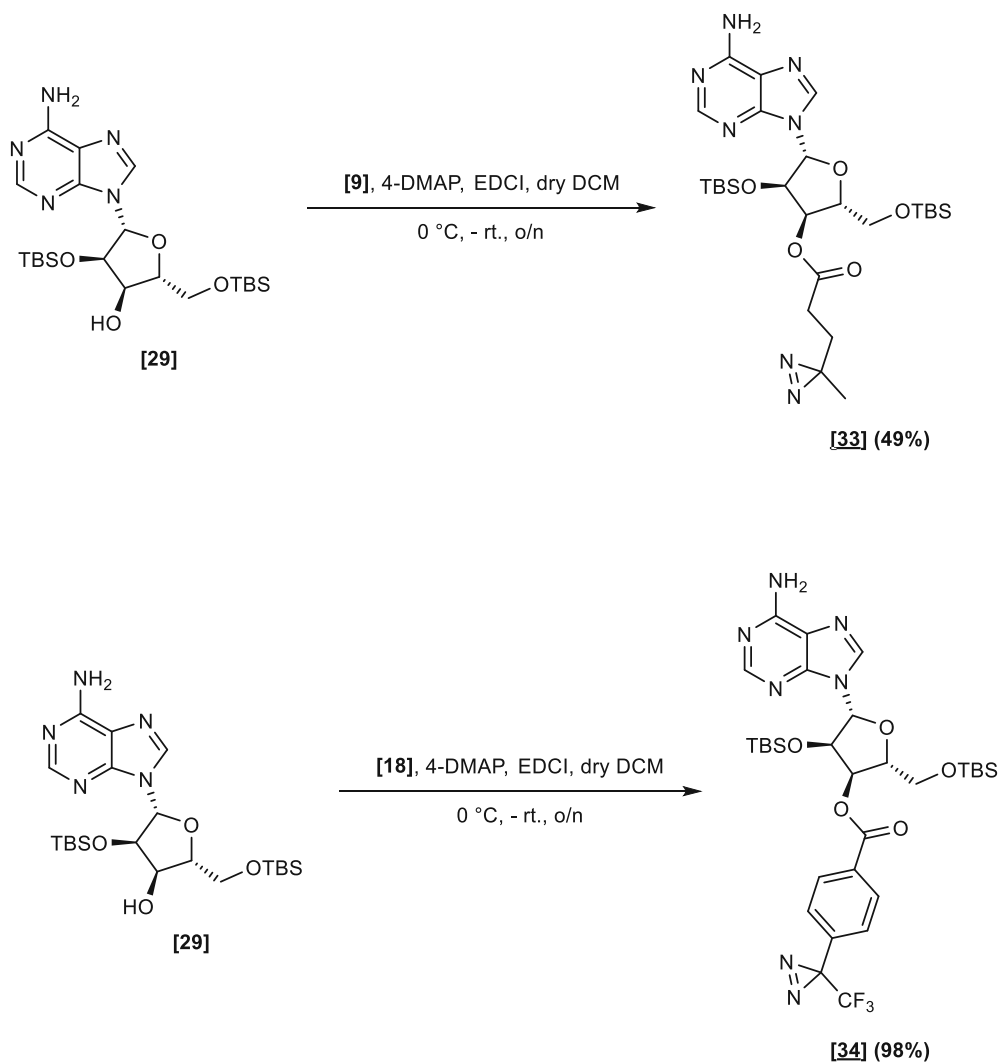
**Scheme 21:** Attempted synthesis of ether analogs [LVIII] and [LIX].

## C II.5.5 Esterification of protected adenosine

Since etherification was unsuccessful, we opted instead to synthesize ester analogs. To synthesize esters of adenosine [1], we chose Steglich conditions,<sup>388</sup> however, we decided to use 1-ethyl-3-(3-dimethylaminopropyl)carbodiimide (EDCI) as the coupling reagent since its urea by-product is water-soluble and thus can easily be removed by an aqueous workup. In contrast, the *N,N'*-dicyclohexylcarbodiimide (DCC) originally used by the authors can be troublesome to remove. Applying the modified literature procedure,<sup>388</sup> adenosine derivatives [29] and [30] were treated with EDCI·HCl in the presence of 4-DMAP in dry dichloromethane. This formed the activated esters, which reacted smoothly with previously prepared diazirine-comprising linkers [9] and [18] to the desired esters [31]-[34]. In all cases, good yields with excellent purity were achieved (see Table 7).



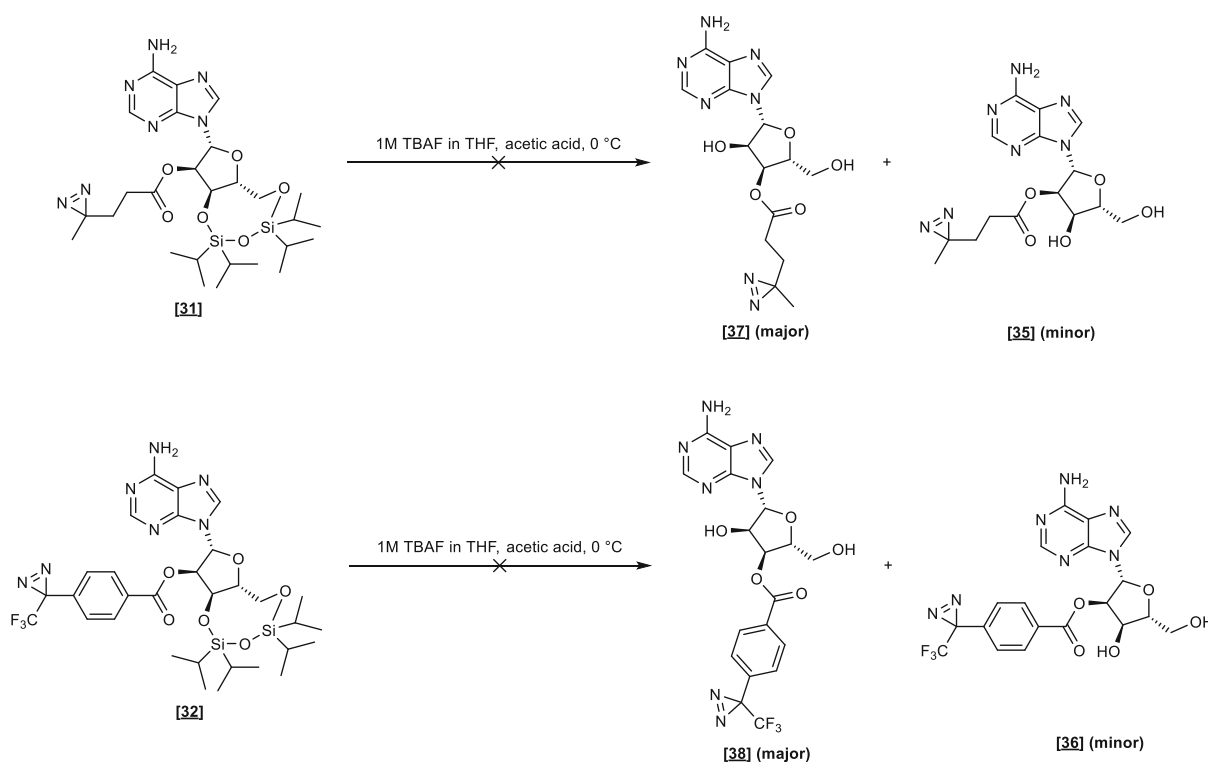
**Scheme 22:** Synthesis of ester analogs [31] and [32].

**Scheme 23:** Synthesis of ester analogs [33] and [34].**Table 7:** Overview of the obtained yields of synthesized ester analogs.

Compound	Yield [%]
[31]	82
[32]	80
[33]	49
[34]	98

## C II.5.6 Deprotection of protected adenosine ester analogs

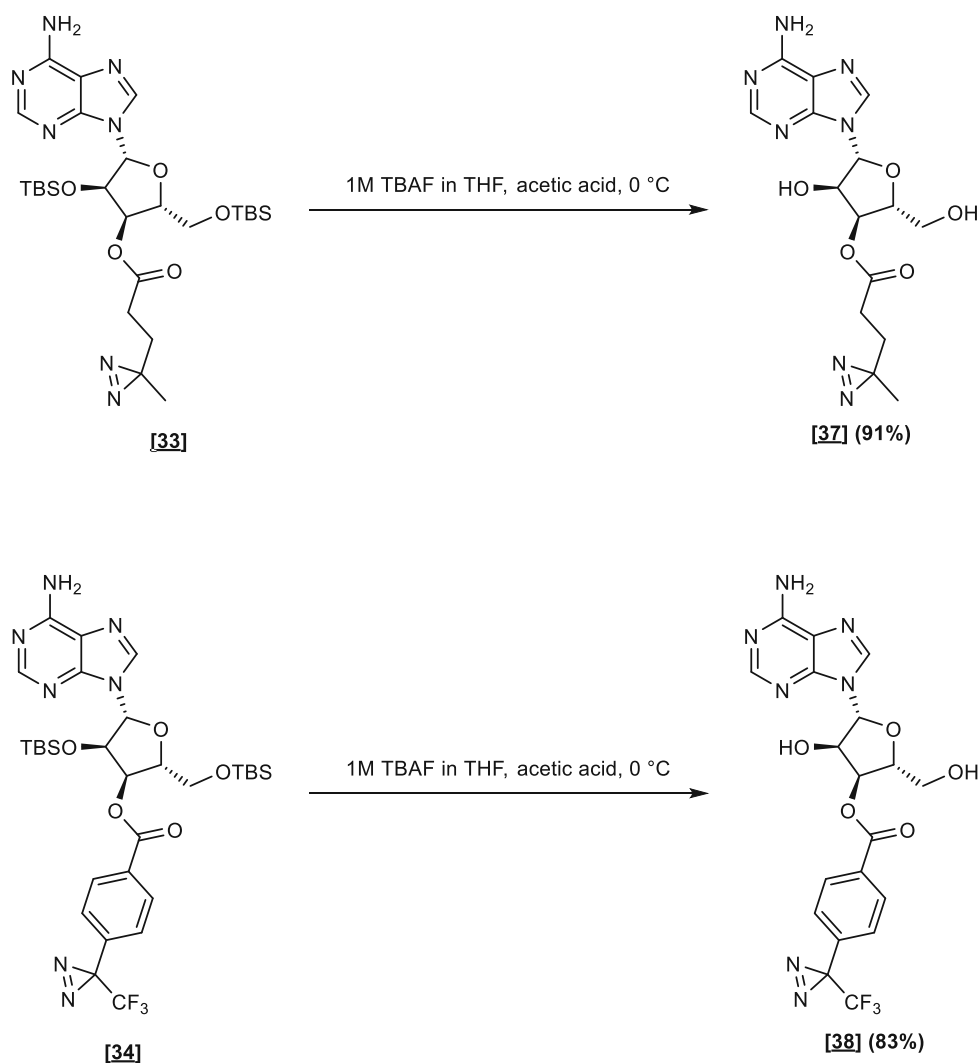
After protected esters **[31]**-**[34]** were produced, removal of the silyl protecting groups was the next step. However, when compound **[31]** was subjected to deprotection using a 1 M solution of TBAF in THF<sup>364</sup>, we could only isolate the 5'-*O*-acetylated compound, the structure of which was confirmed by <sup>1</sup>H - <sup>1</sup>H COSY, <sup>1</sup>H - <sup>1</sup>H NOESY, <sup>1</sup>H - <sup>13</sup>C HSQC, and <sup>1</sup>H - <sup>13</sup>C HMBC analysis. Interestingly, when compound **[32]** was treated under the same conditions, benzyl migration from the O-2' to the O-3' occurred. Due to the strong basicity of TBAF, we hoped that buffering TBAF with acetic acid<sup>389</sup> would suppress the migration tendency. However, deprotection of the 3',5'-*O*-protected derivatives **[31]** and **[32]** using the TBAF/AcOH system resulted in acyl/benzyl migration from the O-2' to the O-3' of the ribose moiety.



**Scheme 24:** Attempted deprotection of ester analogs **[31]** and **[32]**. Treatment with TBAF resulted in acyl migration.

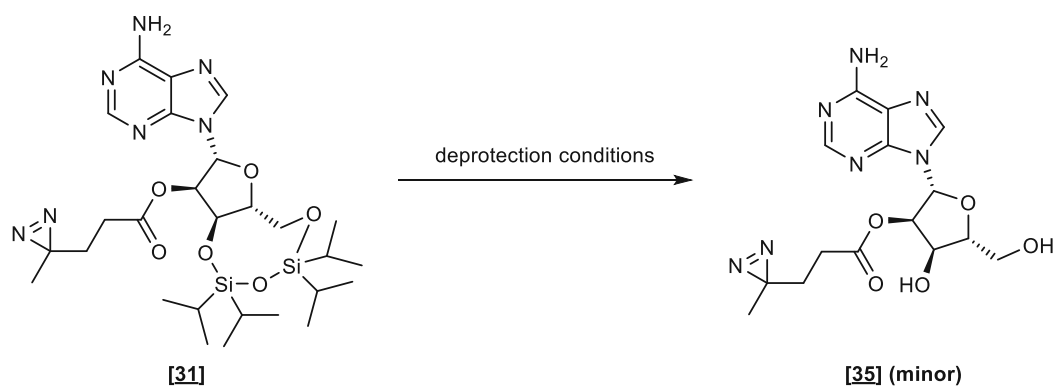
In contrast, deprotection of the protected derivatives **[33]** and **[34]** using a 1 M solution of TBAF in THF in the presence of acetic acid produced the unprotected building blocks **[37]** and **[38]** in 91% and 83% yield, respectively, after purification by flash column chromatography. In all deprotection steps, small amounts (12–18%) of the 2'-*O*-acylated compound co-existed with the 3'-*O*-acylated compound, indicating an equilibrium between these two isomers.<sup>390,391</sup>





**Scheme 25:** Deprotection of silyl protecting groups of compounds **[33]** and **[34]**.

To suppress or avoid acyl migration in compounds **[31]** and **[32]**, several deprotection conditions were screened on compound **[31]**. As shown in Table 8, the HF/pyridine complex produced the best results, with 60% of the desired 2'-*O*-acetylated compound as the major product and 40% of the 3'-*O*-acetylated compound as the minor product according to NMR analysis.



**Scheme 26:** Screening of deprotection conditions to obtain 2'-acylated compound **[35]**.

**Table 8:** Results of the deprotection of compound **[31]**. Given results were determined by NMR analysis.

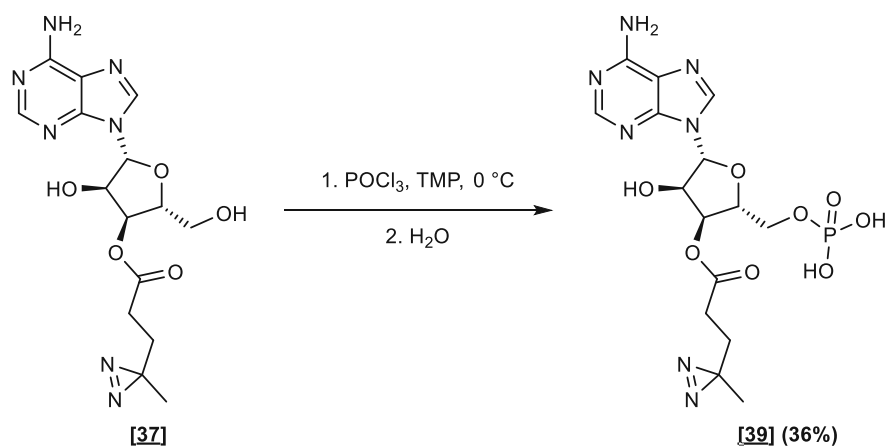
Reagent	Solvent	Time	Equiv.	Result
KF + 18-crown-6 <sup>392</sup>	THF	2 h	6	Acyl migration
H <sub>2</sub> SiF <sub>6</sub> <sup>393</sup>	THF	Overnight	10	No conversion
TBAF/pyridine HCl <sup>394</sup>	THF	2 h	1.2	Acyl migration
TBAF/acetic acid <sup>389</sup>	THF	2 h	1.2	Acyl migration
HF/pyridine <sup>395</sup>	CH <sub>3</sub> CN	2 h	14	60% 2'-O-isomer : 40% 3'-O-isomer

Despite the improvement of preventing the acyl migration by using HF/pyridine complex for the deprotection of 3'-*O*,5'-*O*-silylated compounds, we progressed only with the 3'-*O*-acylated compounds; further investigations and optimizations regarding the deprotection of the 2'-*O*-acylated compounds were abandoned.

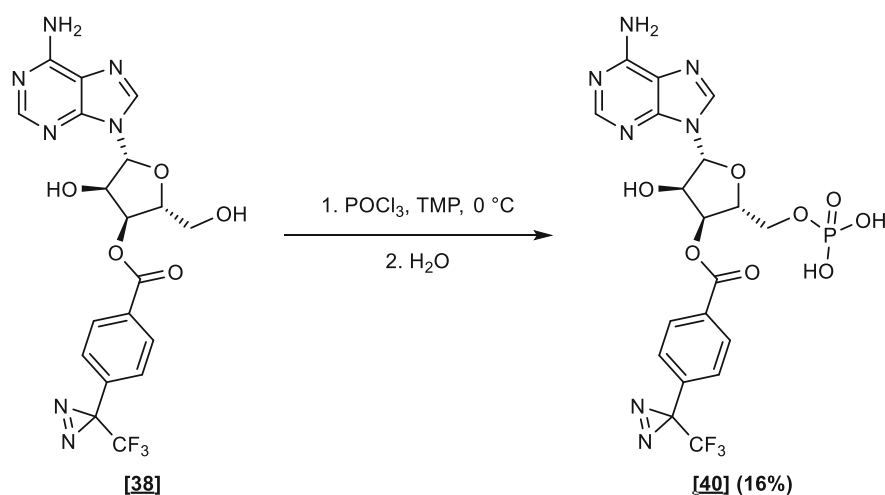
## C II.5.7 5'-*O*-Phosphorylation of ester analogs of adenosine

The next step towards the synthesis of FAD analogs bearing a diazirine unit was the phosphorylation of the hydroxyl group at the 5'-carbon of the ribose moiety. A frequently used method for preparing non-natural nucleoside 5'-monophosphates is Yoshikawa's procedure for selective phosphorylation of unprotected nucleosides at the 5'-position.<sup>357</sup> Based on Yoshikawa's method, we applied a modified literature procedure<sup>396</sup> on adenosine building blocks **[37]** and **[38]** using phosphorous oxychloride in trimethyl phosphate in the presence of the organic base 1,8-bis(dimethylamino)naphthalene (often also referred as proton sponge). The addition of the proton sponge resulted in shorter reaction times compared to that of reactions containing no proton sponge. Nevertheless, proton sponge was difficult to remove by extractive

workup and purification via preparative HPLC. Hence, we sought to omit it from the reaction mixture, which resulted in slower conversion of the starting materials. However, workup and purification were more accessible. Using this modified procedure, adenosine building blocks [37] and [38] were phosphorylated at the primary hydroxyl group using  $\text{POCl}_3$  in TMP, and monophosphates [39] and [40] were obtained after purification via reverse-phase HPLC and lyophilization in 36% and 16%, respectively.



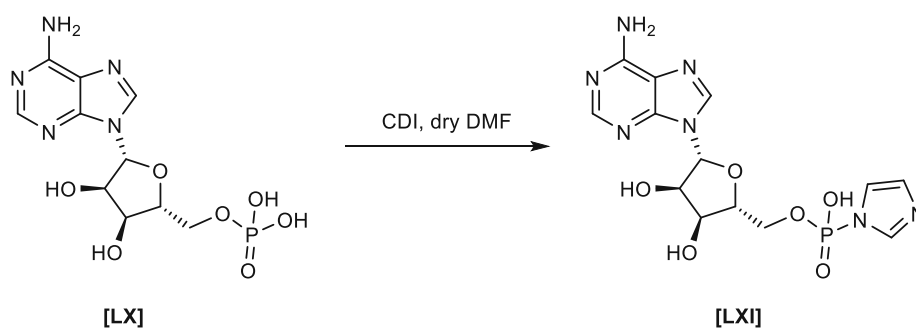
**Scheme 27:** Phosphorylation of the hydroxyl group at the C-5' of unprotected adenosine analog [37].



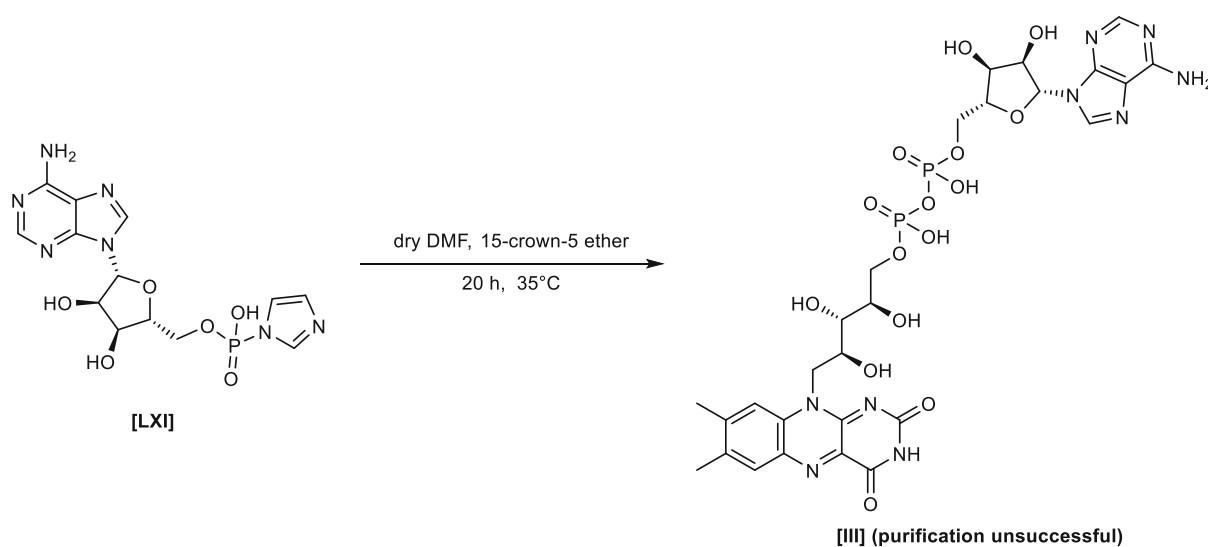
**Scheme 28:** Phosphorylation of the hydroxyl group at the C-5' of unprotected adenosine analog [38].

## C II.5.8 The final step—Chemical coupling of adenosine esters with flavin mononucleotide

The final and likely most critical step for synthesizing FAD derivatives was the coupling reaction of the synthesized adenosine building blocks [39] and [40] with flavin mononucleotide [41]. Hence, we first opted to gain experience in the chemical coupling reaction of commercially available adenosine monophosphate [LX] and flavin mononucleotide [41]. As mentioned previously, different chemical coupling strategies between these two building blocks have been developed. First, we applied a literature procedure in which Saleh and co-workers synthesized *N*<sup>6</sup>-(6-aminohexyl)FAD.<sup>359</sup> Using this procedure, the phosphate group of adenosine-5-monophosphate [LX] was first activated with CDI and then added to riboflavin-5-monophosphate sodium salt [41], which was solubilized in dry DMF through the addition of 18-crown-6 ether. After 24 hours, a new product with the characteristic UV/Vis spectra of flavins and the same retention time and mass spectrum as FAD [III] (commercially available FAD was injected as reference material) was found using UHPLC-MS analysis. However, even after three days, much of the activated adenosine-5-monophosphate remained unchanged. When we used 15-crown-5 ether instead of 18-crown-6 ether, nearly complete consumption of the activated adenosine 5-monophosphate was achieved after 20 hours. These findings suggested that the reaction was successful. However, the riboflavin-5-monophosphate was used in four-fold excess relative to the adenosine monophosphate, and purification via reverse-phase HPLC of the formed product thus was challenging.



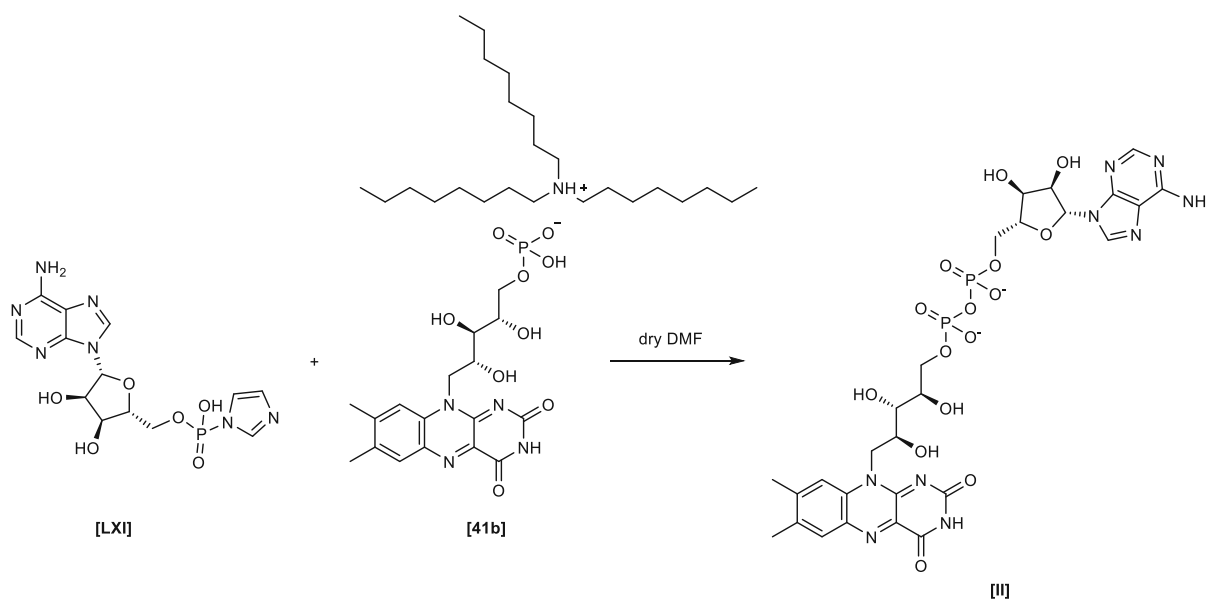
**Scheme 29:** Activation of adenosine-5-monophosphate [LX] with CDI.



**Scheme 30:** Coupling of activated adenosine-5-phosphate [LXI] with commercially available sodium salt in the presence of 15-crown-5 ether.

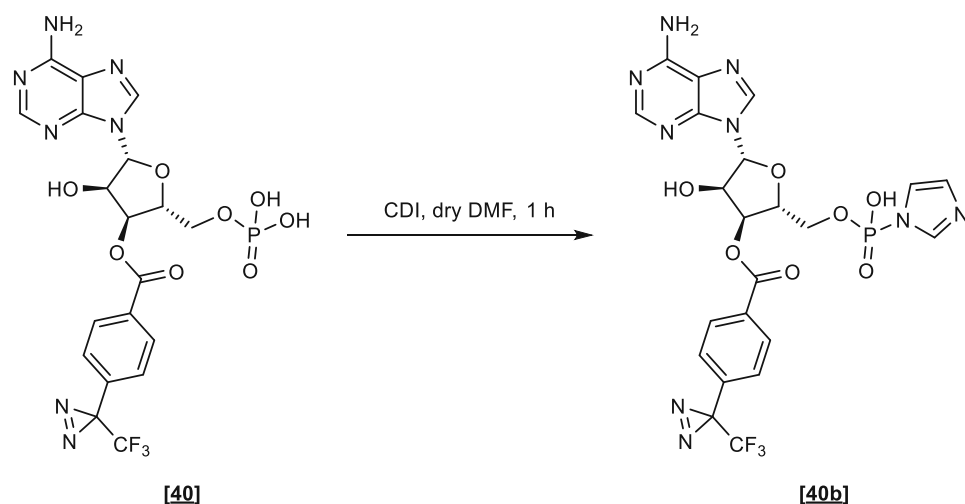
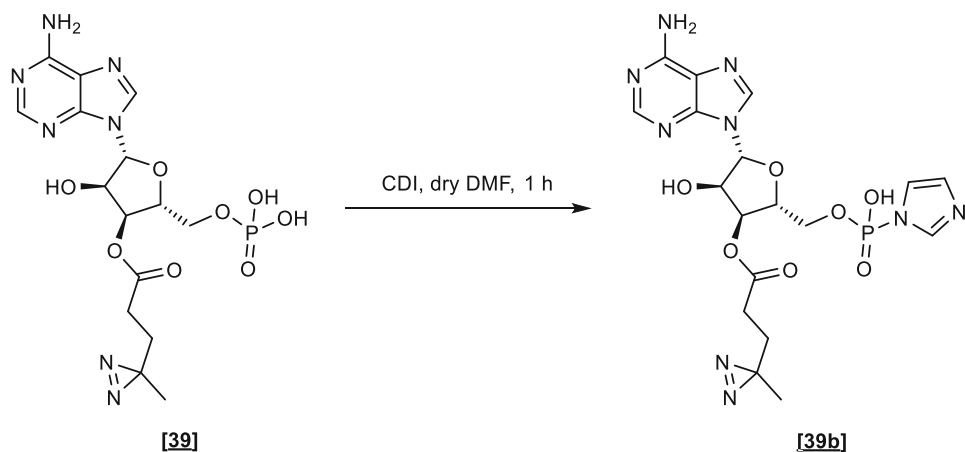
Consequently, we also applied another literature procedure reported by Cramer *et al.*,<sup>397</sup> in which they first converted commercially available riboflavin-5-monophosphate sodium salt into the trioctylammonium salt [41b]. This salt was then coupled with the activated adenosine-5-monophosphate [LXI].

However, when we converted the sodium salt into the free acid using DOWEX-(H<sup>+</sup> form), its addition to a solution of trioctylamine in EtOH resulted in decomposition according to UHPLC-MS/UV analysis. We reasoned that photodegradation under alkaline conditions caused this issue, as was reported previously.<sup>398,399</sup> Hence, the conversion was performed strictly in the dark, after which no decomposition was observed. Next, the trioctylammonium salt of riboflavin-5-monophosphate was dissolved in dry DMF and coupled with previously activated adenosine-5-phosphate. After 40 hours, nearly full consumption of both starting materials and the formation of a new product with retention time and mass spectrum related to FAD were observed using UHPLC-MS analysis, thus indicating successful coupling of both building blocks.

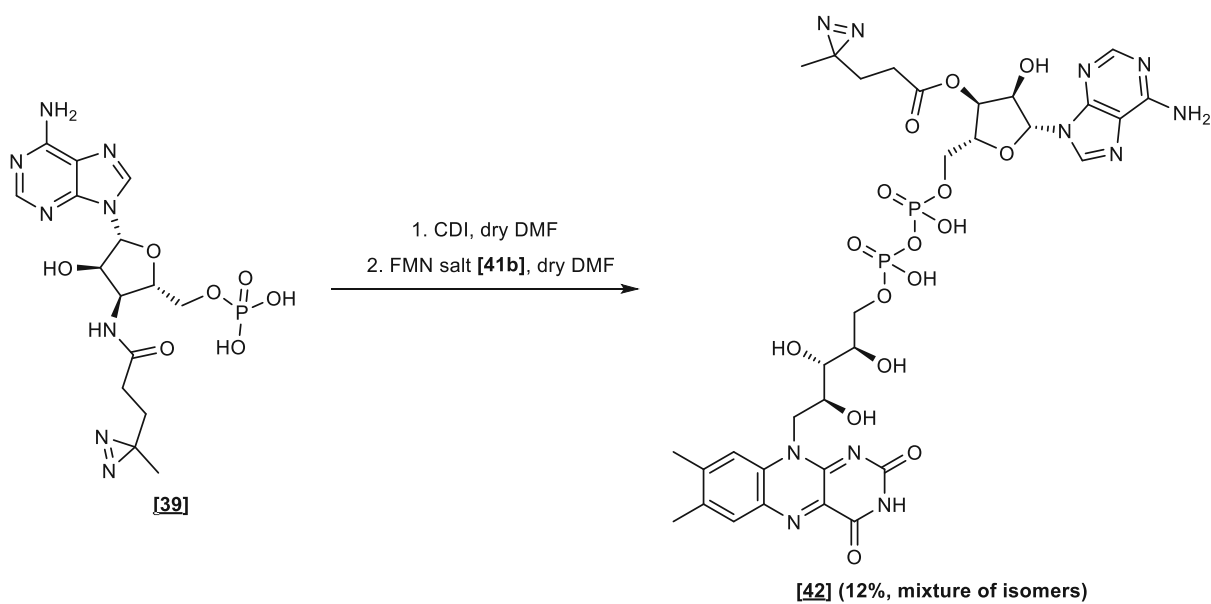


**Scheme 31:** Coupling of activated adenosine-5-phosphate [LXI] with riboflavin-5-phosphate trioctylammonium salt [41b].

Based on these encouraging results, we decided to apply chemical coupling with the trioctylammonium salt of FMN [41b] to our synthesized adenosine monophosphates [39] and [40]. The unprotected adenosine building blocks [39] and [40] were first activated with CDI and then further subjected to the coupling reaction with the previously prepared trioctylammonium salt of riboflavin monophosphate. According to the literature, phosphoimidazolides can be isolated and stored under anhydrous conditions, but an *in-situ* preparation is more feasible.<sup>400</sup> Hence, building blocks [39b] and [40b] were used without further purification in the coupling step. The coupling reaction was performed in dry DMF in the presence of molecular sieve to ensure strict anhydrous conditions, and the reaction progress was monitored using UHPLC-MS/UV analysis. Since the reaction did not show any further conversion of the starting materials, it was quenched with water, and after lyophilization, the crude material was purified via reverse-phase HPLC. However, UHPLC-MS/UV analysis of the purified product [42] indicated the presence of two compounds; the UV spectrum revealed a peak with a shoulder (see Figure 36). NMR studies supported these findings and suggested that acyl migration resulted in the formation of the 2'-*O*- and 3'-*O*-acylated compound. However, a proper signal assignment was impossible due to broad and overlapping peaks in the NMR spectrum.



**Scheme 32:** Activation of monophosphates with CDI. The intermediates **[39b]** and **[40b]** were directly used in the subsequent coupling step.



**Scheme 33:** Coupling reaction of FMN salt **[41b]** and monophosphate **[39]**.

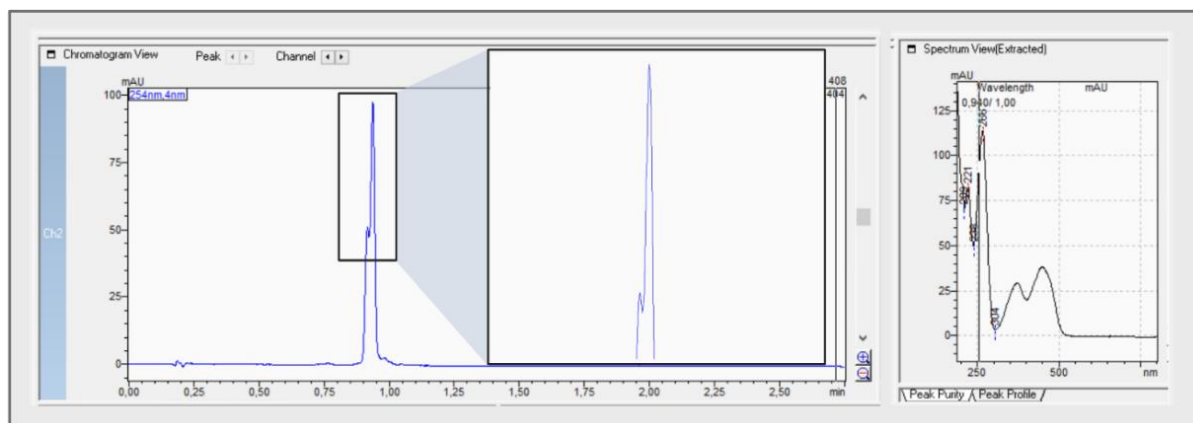
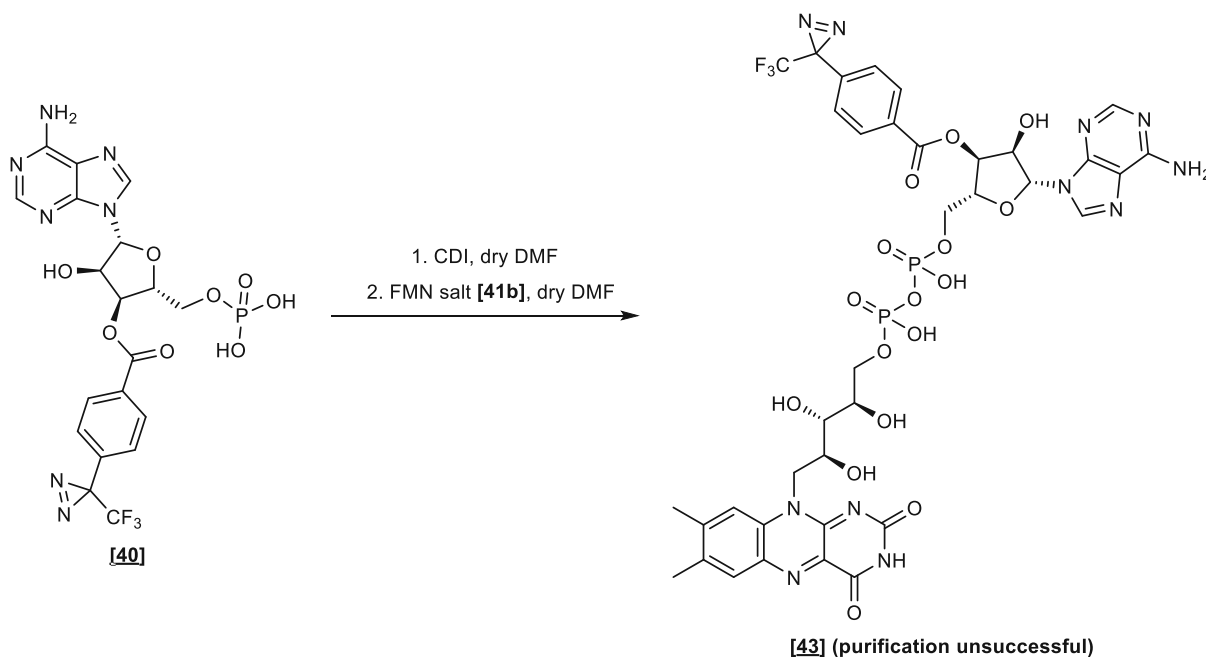


**Figure 36:** UV-spectrum of compound **[42]** after purification via preparative HPLC. The spectrum reveals a peak with a shoulder, indicating the presence of a second compound.

When we prepared a second batch of compound **[42]**, purification via reverse-phase HPLC led to partial cleavage of the ester bond, yielding native FAD. This finding indicated the potential risk of hydrolysis of the ester-linkage under aqueous conditions and prompted us to examine the sample of the first batch. The sample was dissolved in buffer and stored at 4 °C or -30 °C for several weeks. At 4 °C, about 10% of diazirine-FAD **[42]** hydrolyzed to native FAD, while about 2% hydrolyzed when stored at -30 °C. This hydrolysis posed a problem since native FAD will show a higher affinity to enzymes than modified FAD. Hence, the native FAD will occupy most of the enzymes' binding sites, which will falsify the results of the measured activity of the reconstituted holoenzyme and result in inefficient and unspecific labeling when the sample is subjected to irradiation with UV light.

The aromatic diazirine derivative **[43]** was prepared analogously; however, the purification proved unsuccessful because the riboflavin monophosphate could not be removed by preparative reverse-phase HPLC. Due to this fact, we planned to synthesize the corresponding amides since the first intended synthesis of ethers was unsuccessful and amides should be significantly less prone to hydrolysis than esters.

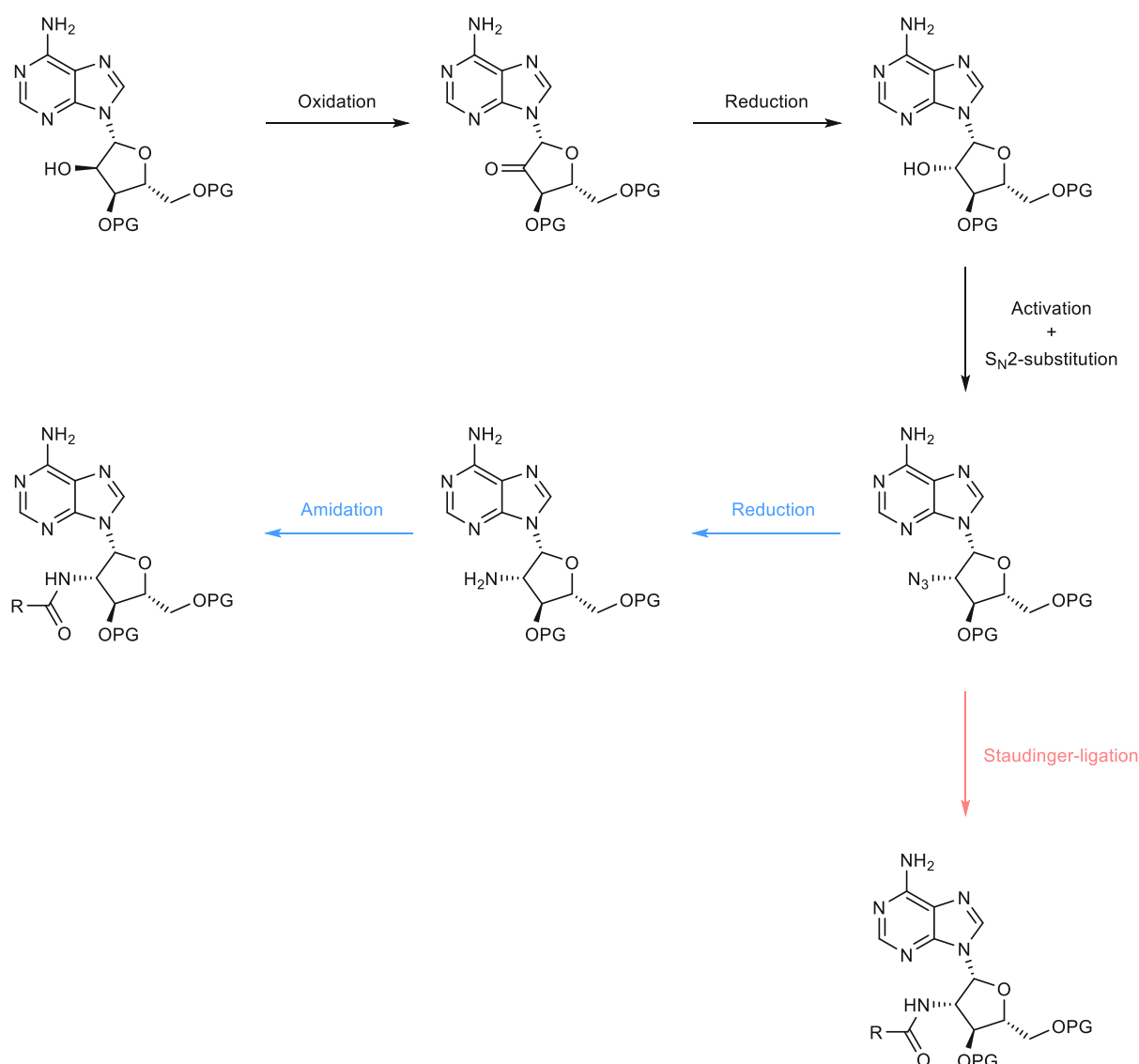




**Scheme 34:** Coupling reaction of FMN salt [41b] and monophosphate [40].

## C II.6 Synthesis of amides of adenosine

Although amides are less prone to hydrolysis than esters, we did not consider the synthesis of amides as first choice due to the considerably more elaborate synthesis required: one of the hydroxyl groups of adenosine [1] must first be converted to the corresponding amine functionality. Conversions of hydroxyl groups at the C-2' and C-3' of the ribose moiety of adenosine have been extensively reported in the literature.<sup>360,362-364</sup> A key step in the synthetic route is an oxidation/reduction/substitution reaction sequence (see Scheme 35), which ultimately results in the formation of the corresponding nitrogen functionality with retention of the stereochemistry. However, five additional steps must be performed to obtain the corresponding amines. Alternatively, the desired amides can be prepared directly from the corresponding azide analogs via the “traceless” Staudinger ligation (Scheme 35), which was developed by Bertozzi *et al.*<sup>401,402</sup> This strategy renders the reduction of the azide to the amine obsolete, although a Staudinger reagent must additionally be synthesized.



**Scheme 35:** Possible strategies for the synthetic route towards amide analogs demonstrated on adenosine analog protected on the hydroxyl groups at the C-3' and C-5'. Blue route: classical amidation approach. Red route: Staudinger ligation. PG = Protecting group.

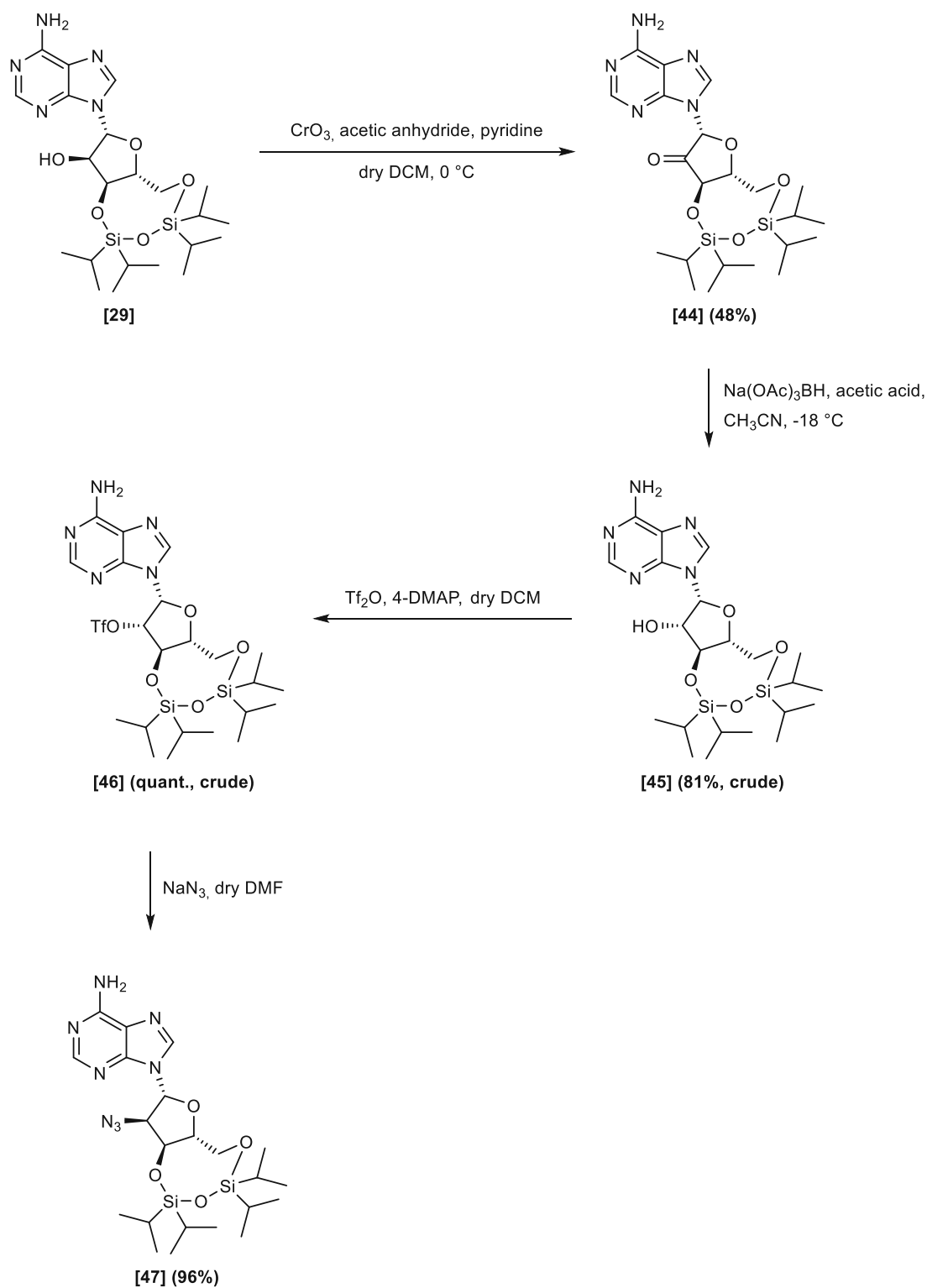
Based on the strategies and considerations discussed above, we approached the synthesis of our target compounds using two methodologies: 1) classical amide coupling and 2) the Staudinger ligation. Since both routes require the preparation of azides [47] and [52], the synthetic route commenced with oxidation of the hydroxyl group at the C-2' and the C-3' position of protected adenosines [29] and [30]. We originally planned to oxidize the free hydroxyl groups of protected adenosines under Dess-Martin periodinane<sup>363</sup> conditions, as has been previously reported. In our case, however, the reaction resulted in the formation of several side products according to TLC and NMR analysis. Therefore, as an alternative, we applied Swern-oxidation<sup>403</sup> conditions to compound [29]. This, however, resulted in the unsatisfying conversion of the starting material. Ultimately, the Garegg reagent (CrO<sub>3</sub> in Ac<sub>2</sub>O and pyridine) proved the most successful. Nevertheless, as reported previously,<sup>404</sup> purification via flash

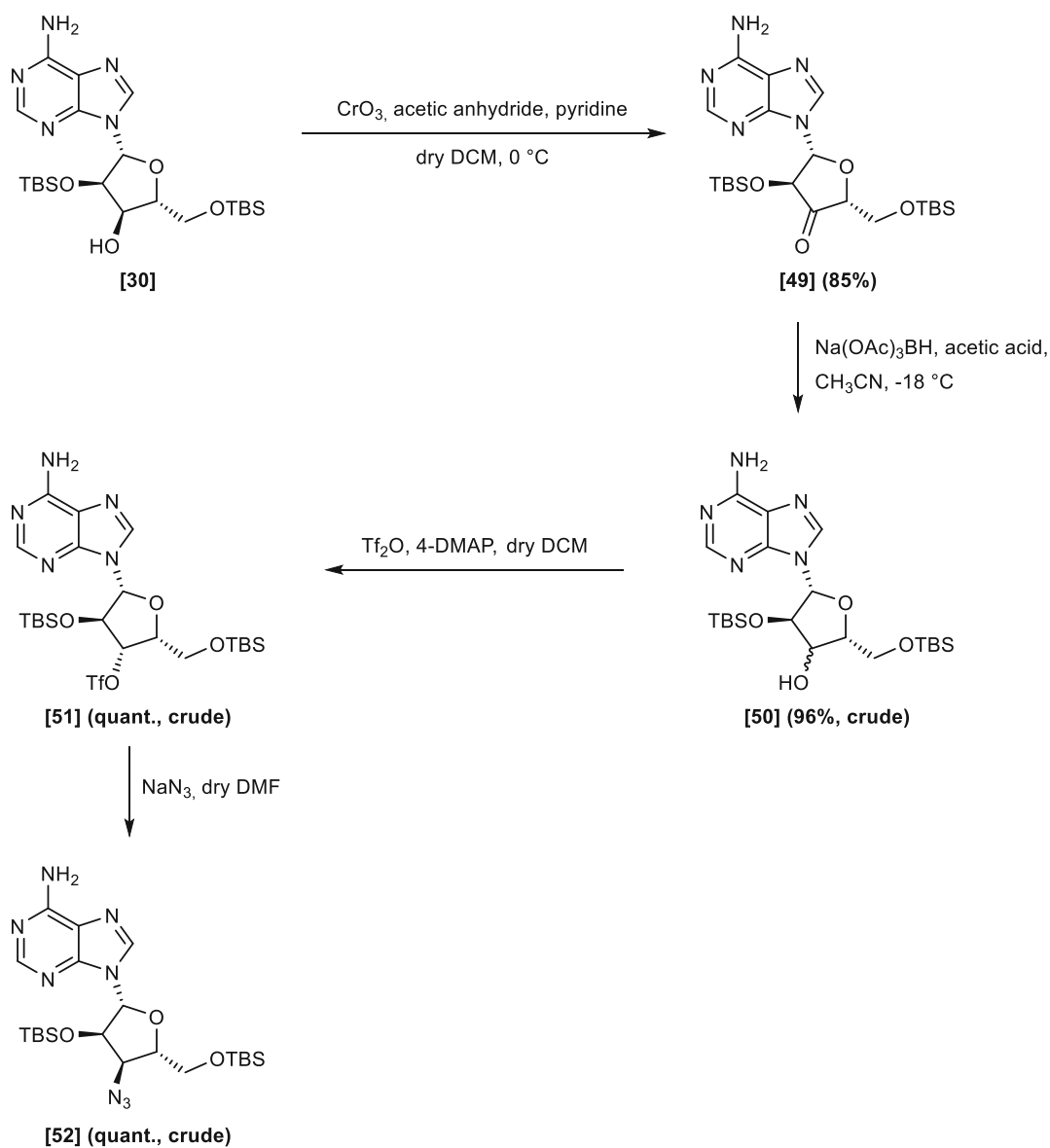
column chromatography proved troublesome, likely because the formed chromium–nucleoside complex became trapped on the silica gel. Therefore, we decided to filtrate the reaction mixture over a short pad of celite and used ketones [44] and [49] without further purification in the following step.

Next, ketones [44] and [49] were reduced to the corresponding hydroxyl functionality. First, we applied a literature procedure reported by Klinchan *et al.*,<sup>363</sup> in which they used an excess of sodium triacetoxyborohydride generated *in-situ* from NaBH<sub>4</sub> and acetic acid at 0 °C. However, this resulted in an unsatisfying yield of 48% for compound [45]. Hence, we opted for a different literature procedure, which utilized commercial sodium triacetoxyborohydride.<sup>362</sup> Applying this procedure, ketone [44] was cleanly reduced in 81% yield and could be used in the next step without the need for flash column chromatography after a simple workup procedure. Ketone [49] was reduced under the same reaction conditions and obtained in 96% yield.

Interestingly, the reduction of compound [44] resulted only in the formation of the desired *arabino* isomer, as the hydride preferentially attacked the sterically less hindered  $\alpha$  face. However, the same reaction conditions provided the *ribo* and *xylo* diastereomers of compound [50], as previously reported.<sup>363</sup> The small amount of the *ribo* isomer of [50] (~ 5% according to <sup>1</sup>H-NMR) could be removed during the purification in the next synthetic steps. In the case of compound [44], the stereoselectivity was likely induced by the steric hindrance of the adenine moiety, which directly flanked the reaction center.<sup>363</sup>

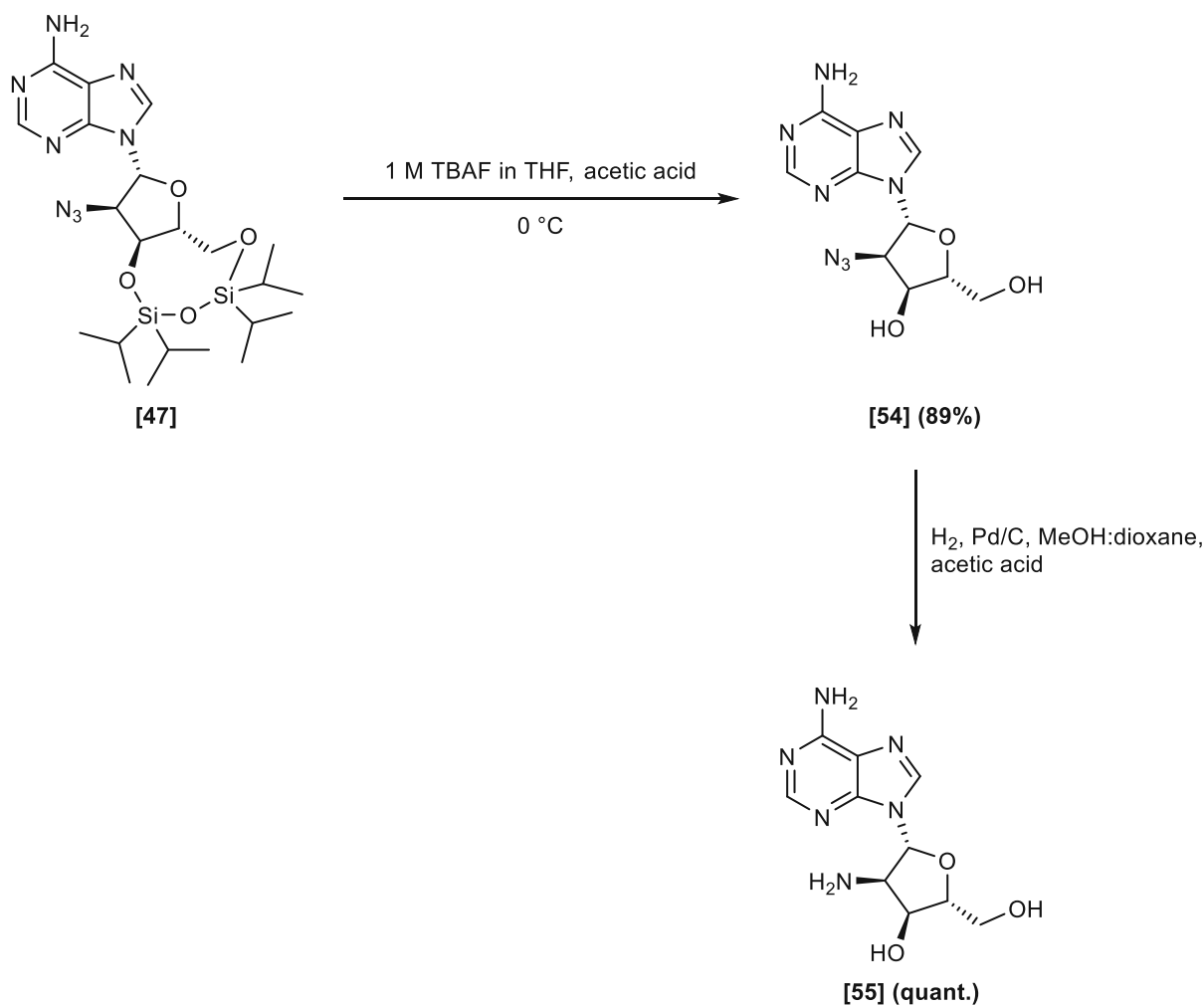
Next, the conversion of the C-2' and C-3' alcohols into the corresponding triflates [46] and [51] occurred smoothly using Tf<sub>2</sub>O in the presence of three equivalents of 4-DMAP in excellent yields without the need for further purification. Finally, S<sub>N</sub>2 displacement of the triflate by NaN<sub>3</sub> in DMF at room temperature proceeded with inversion of the configuration to provide azides [47] and [52] in 96% and quantitative yield, respectively.

**Scheme 36:** Synthetic route towards azide analog **[47]**.



**Scheme 37:** Synthetic route towards azide analog [52].

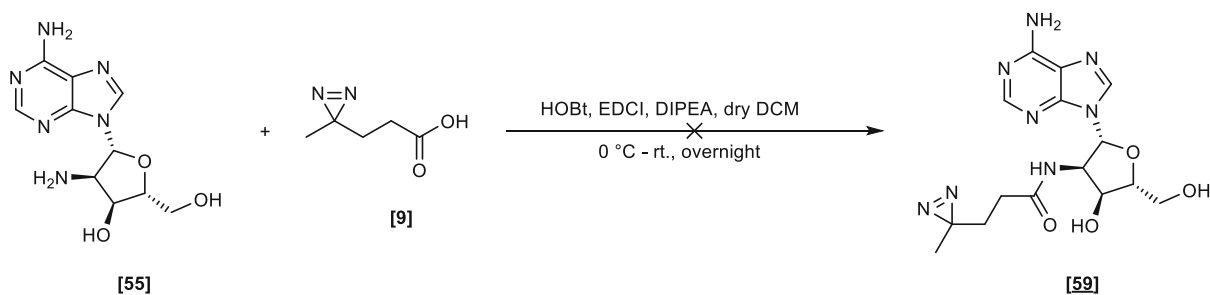
At this stage, the synthetic route towards the desired amides was further elaborated on compound [47]. Similar to the procedure by Klinchan *et al.*,<sup>363</sup> deprotection of the silyl protecting group of protected azido analog [47] was performed before azide reduction. Treatment of [47] with a 1 M solution of TBAF in THF in the presence of acetic acid furnished azido alcohol [54] in 89% yield after flash column chromatography. Then, the azide group was further reduced using Pd/C and hydrogen gas in a solvent mixture of MeOH:dioxane (1:1) in the presence of acetic acid to obtain amine [55] in quantitative yield. Noteworthy, removing the acetic acid, which seemed to interfere with the subsequent amide synthesis, was difficult. Hence, the hydrogenation was performed without acetic acid, and as the protected building blocks were readily soluble in methanol, dioxane was also omitted from the reaction mixture.



**Scheme 38:** Synthesis of amine analog [55].

To prepare amine [48], we attempted a Staudinger reduction<sup>364</sup> as an alternative synthetic route starting from azide [47]. However, TLC analysis indicated the formation of several side products, and separating the formed triphenylphosphine oxide proved challenging. Therefore, hydrogenation was the more feasible method for amine synthesis.

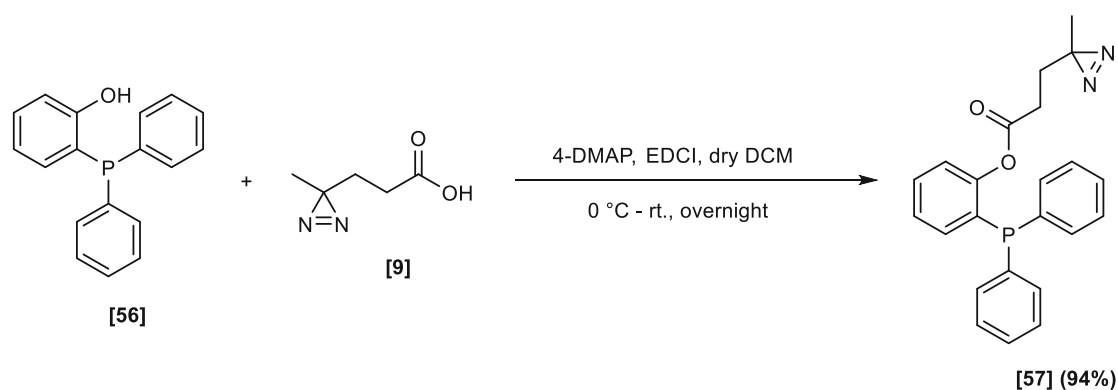
When amine [55] was subjected to the coupling reaction with diazirine acid [9] using standard amide coupling conditions, several spots were detected by TLC analysis, possibly due to the interference of the two free hydroxyl groups of the unprotected building block [55].



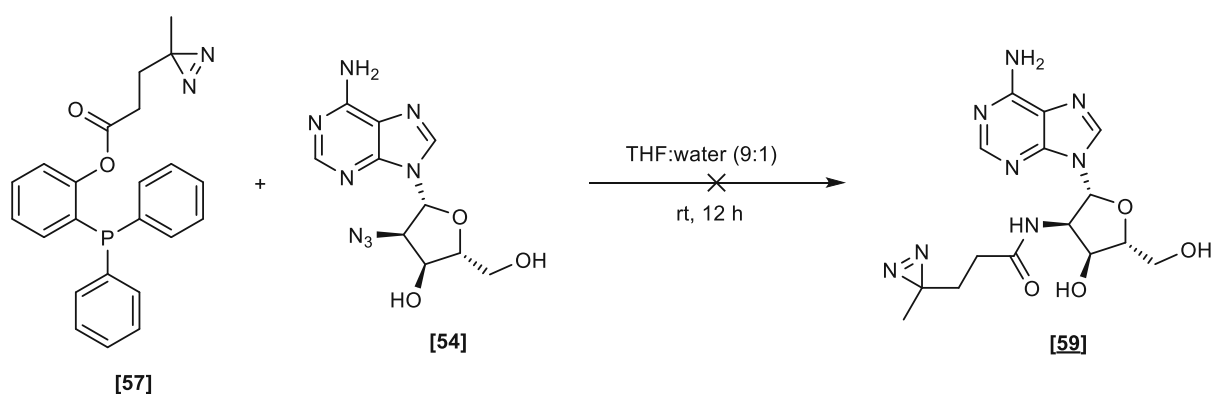
**Scheme 39:** Attempted synthesis of amide [59] starting from unprotected amine [55].

Since classical amidation on unprotected building block **[55]** was unsuccessful, we attempted the Staudinger ligation. This was inspired by a literature procedure, in which Ahad and coworkers accomplished a traceless Staudinger ligation to obtain amide-linked diazirines, beginning from complex organic azides.<sup>405</sup>

The first step was the synthesis of the Staudinger reagent **[57]**, which was achieved by coupling diazirine acid **[9]** with commercially available 2-hydroxydiphenylphosphinylbenzene **[56]** in 94% yield. Then, the Staudinger ligation was attempted with unprotected azide **[54]**. However, when we applied the exact literature conditions, many spots were detected on the TLC, although UHPLC-MS analysis indicated the formation of the desired product. Similar to the amidation approach, we reasoned that the free hydroxyl groups of **[54]** caused selectivity issues.



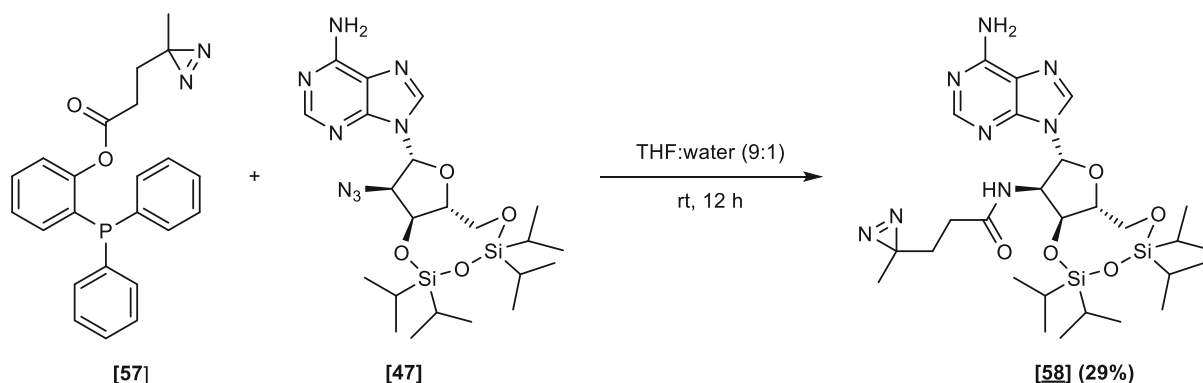
**Scheme 40:** Synthesis of Staudinger reagent **[57]**.



**Scheme 41:** Staudinger ligation of unprotected azide **[56]**.

Based on these findings, we examined the Staudinger ligation with the protected building block **[47]**. The Staudinger ligation seemed successful with protected azide **[47]** according to TLC and UHPLC-MS/UV analysis. However, only 29% of the amide **[58]** was obtained after

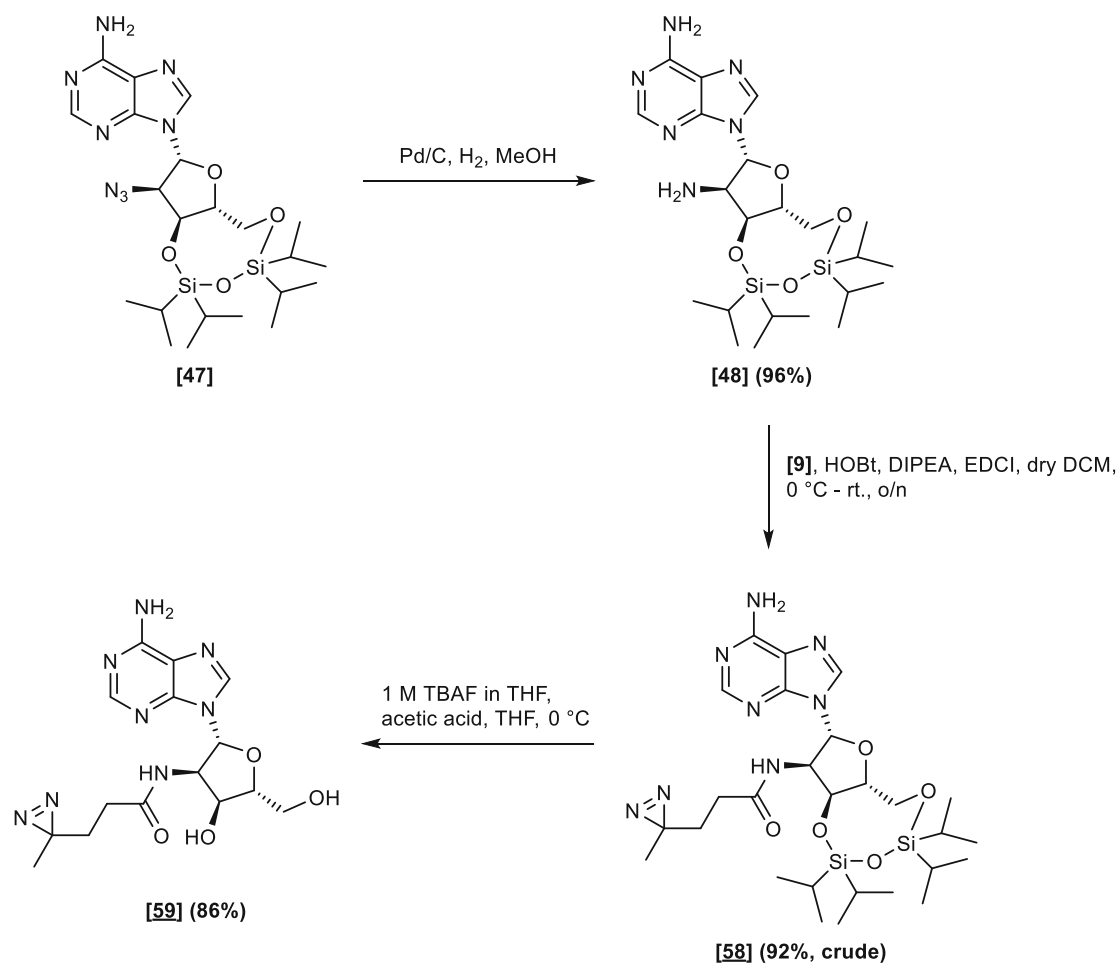
purification by flash column chromatography. Therefore, we focused on amide coupling instead of the Staudinger ligation.



**Scheme 42:** Staudinger ligation of protected azide [47].

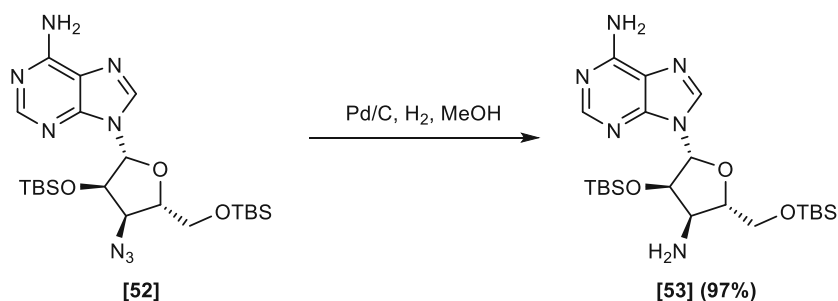
For amidation, azide [47] was first reduced to the amine [48], followed by a coupling reaction with the diazirine-linker [9]. As expected, protected amine [47] was smoothly converted to amide [58] in 87% yield. However, according to UHPLC-MS analysis, a small amount of the TIPDS group was partially cleaved.<sup>406</sup> Therefore, we decided to subject crude amide [58] directly to the subsequent deprotection step. Removal of the Markiewicz protecting group with TBAF and 1% AcOH afforded [59]. The crude product was purified via flash column chromatography with a yield of 86%. It is worth mentioning that the amino group on the C-6 of the adenine ring posed no threat to the coupling reaction.



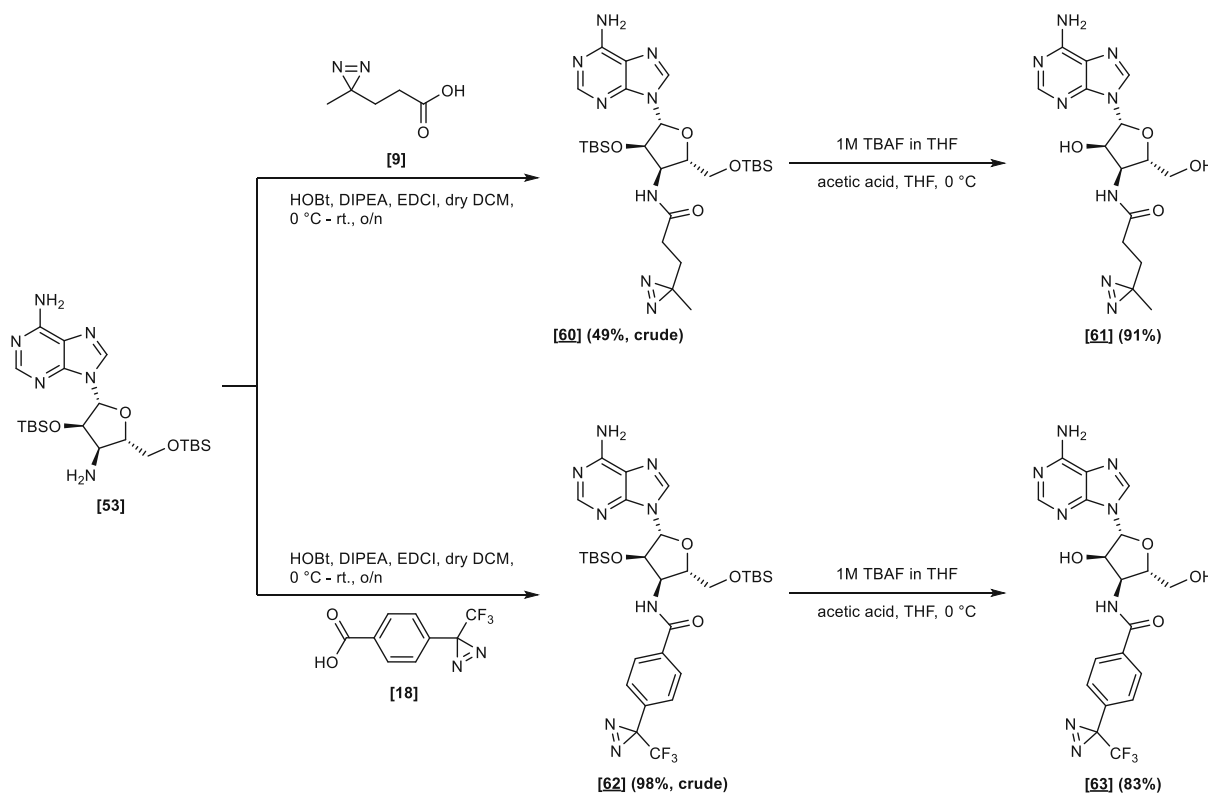


**Scheme 43:** Synthetic route towards amide analog **[59]**.

Based on the established synthetic route, azide **[52]** was reduced to the corresponding amine **[53]**, followed by a coupling reaction with the aliphatic diazirine acid **[9]** and the aromatic diazirine acid **[16]**. This produced protected amides **[60]** and **[62]**, which were then deprotected to yield amide analogs **[61]** and **[63]**. Finally, the crude products were purified via flash column chromatography with a yield of 45% and 81% over two steps, starting from amine **[53]**.



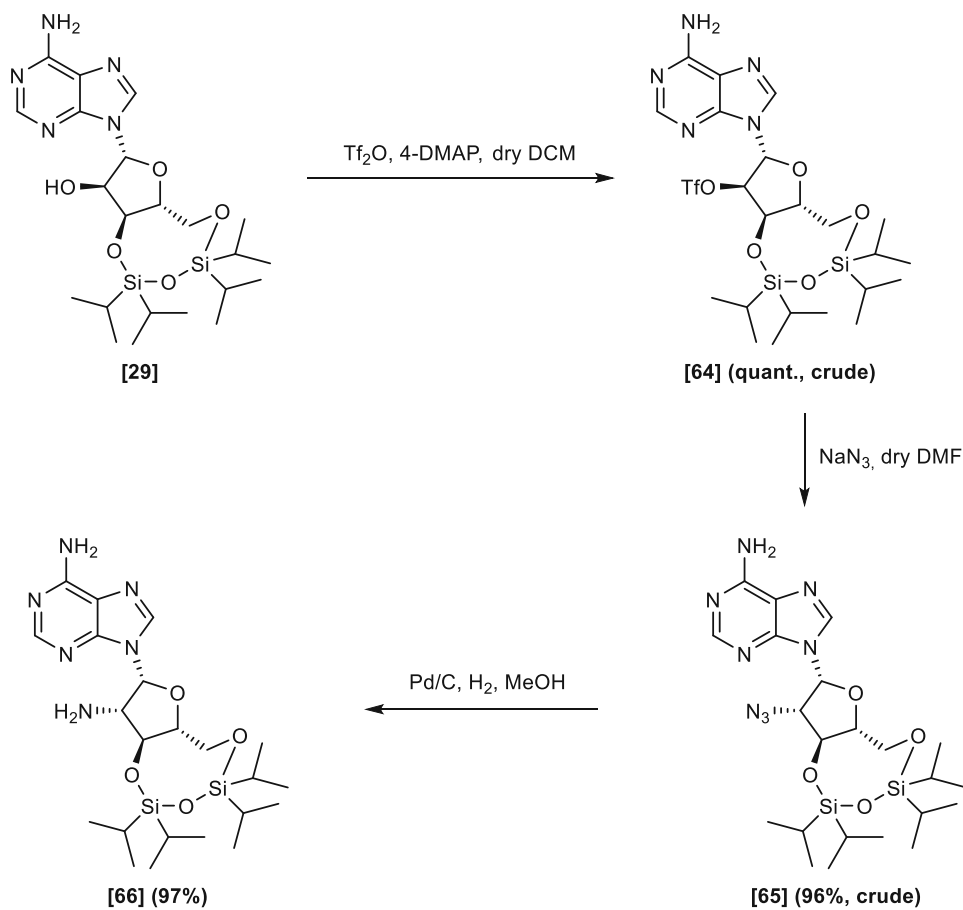
**Scheme 44:** Synthesis of amine **[53]**.



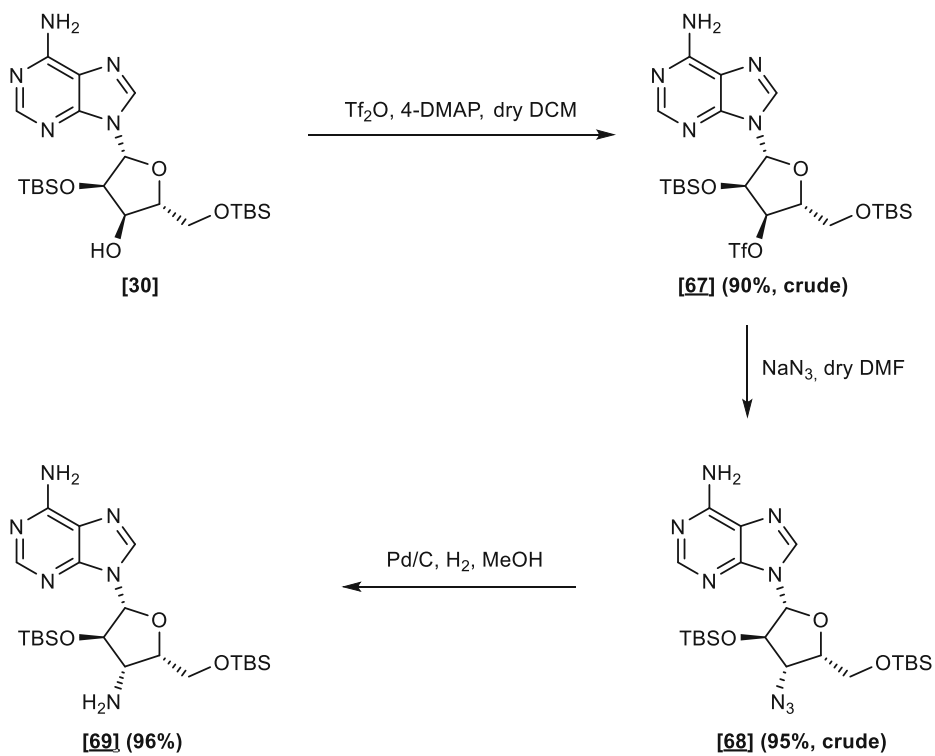
**Scheme 45:** Synthetic routes towards amide analogs [61] and [63].

Based on our experience and the elaborated synthetic route towards amides [59], [61], and [63], we considered preparing amides by inverting the configuration at the C-2' and C-3' positions, as doing so would render the oxidation/reduction steps redundant and further expand the substrate scope.

The synthetic route towards amide analogs with alteration of the stereocenter began by activating the alcohols at the C-2' and the C-3' positions from protected adenosines [29] and [30]. Next, nucleophilic substitution with NaN<sub>3</sub> furnished azides [65] and [68] in good yields after extractive workup and without further purification. Then, the reduction of azides [65] and [68] using the optimized hydrogenation procedure furnished amines [66] and [69].

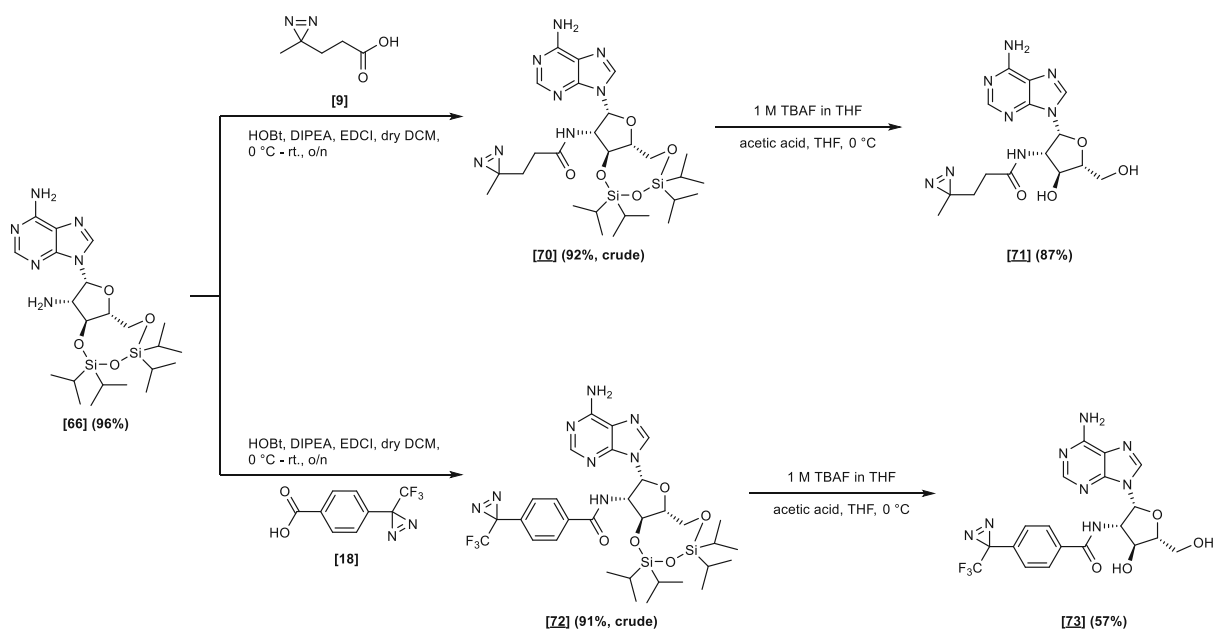


**Scheme 46:** Synthesis of amine analog **[66]**.

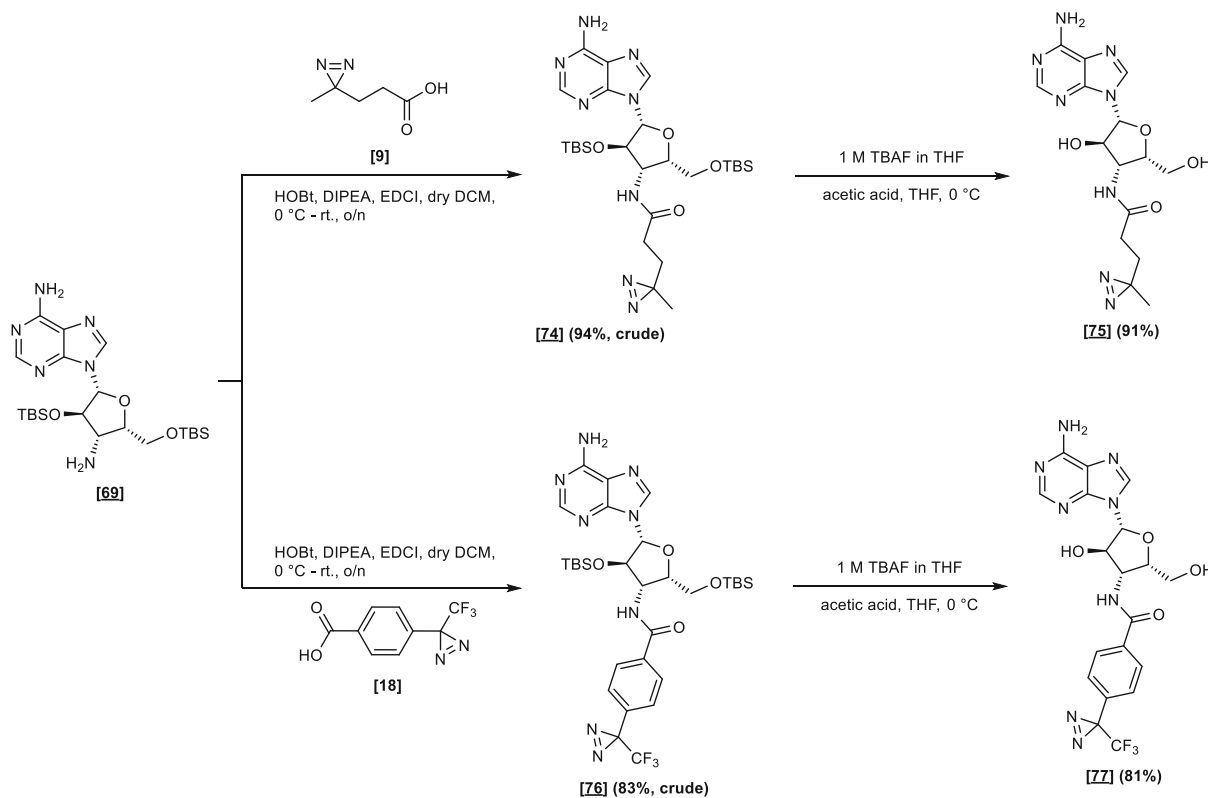


**Scheme 47:** Synthesis of amine analog **[69]**.

Amidation with diazirine acids **[9]** and **[18]** gave protected adenosines **[70]**, **[72]**, **[74]**, and **[76]** in good yields. Finally, crude amides were directly subjected to the removal of the silyl-protecting groups with TBAF in the presence of acetic acid to afford unprotected adenosine analogs **[71]**, **[73]**, **[75]**, and **[77]** in good yields after purification via flash column chromatography. In contrast to the ester analogs, no migration of the acyl and benzyl groups occurred.

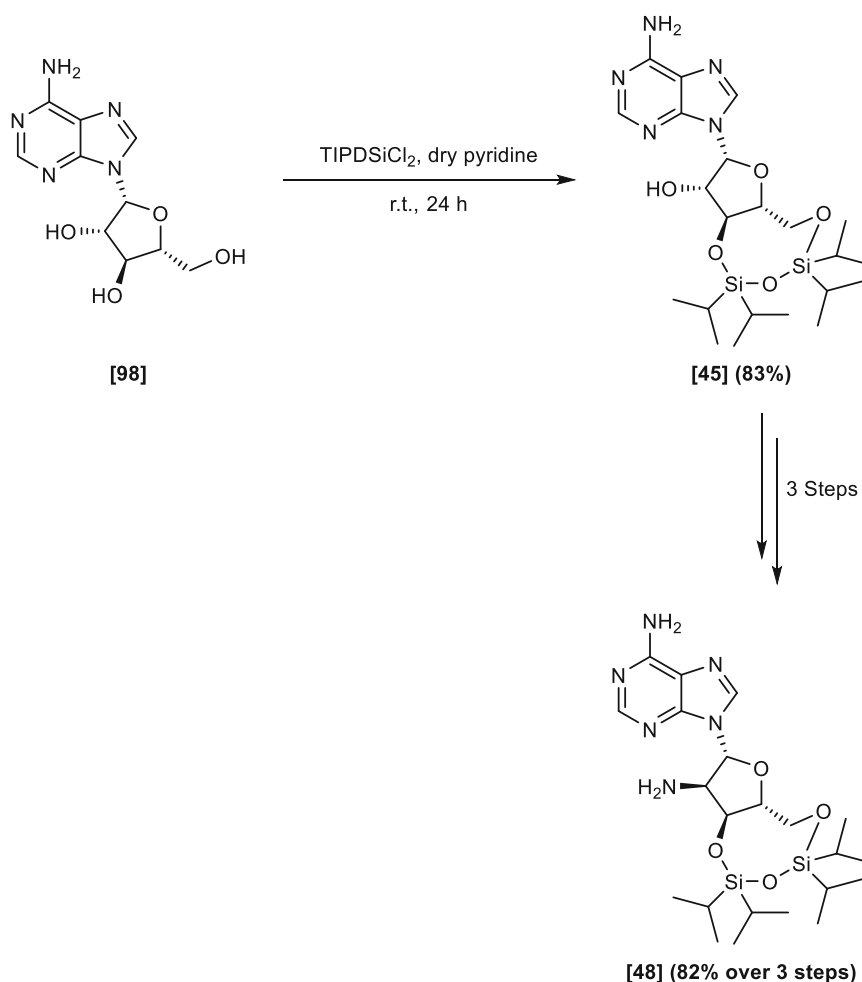


**Scheme 48:** Synthetic routes towards amide analogs **[71]** and **[73]**.



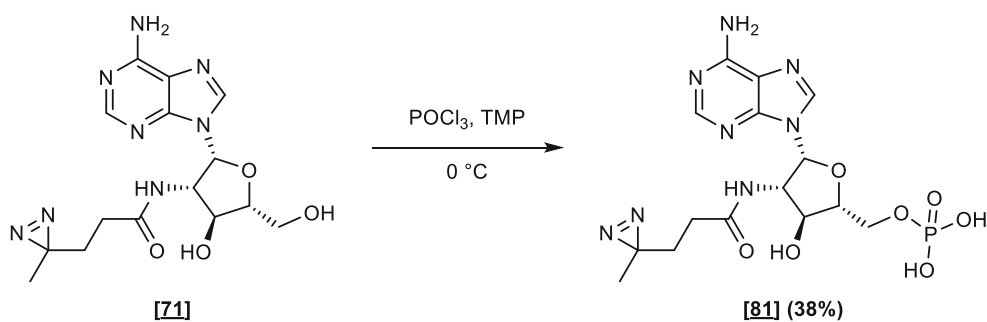
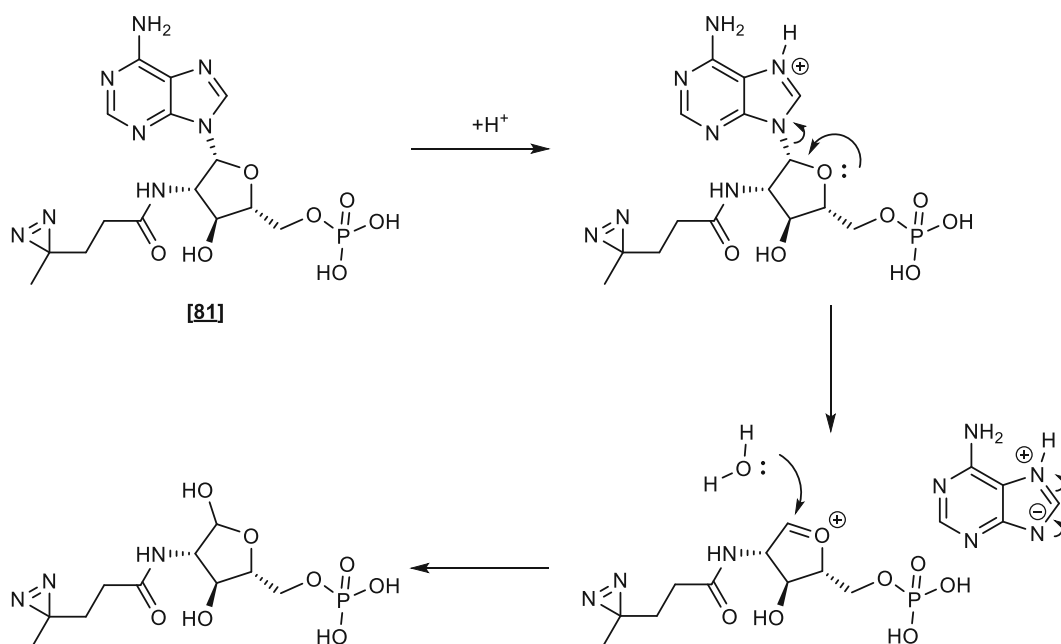
**Scheme 49:** Synthetic routes towards amide analogs [75] and [77].

Starting with commercially available vidarabine [98], amine [59] could also be synthesized without the oxidation/reduction sequence. However, since vidarabine is significantly more expensive than adenosine, we decided to start from adenosine. The following route was used in a later stage of the project when we sought to resynthesize amine [48]. Analogous to the above-described synthetic route, vidarabine [98] was simultaneously protected at the C-3' and C-5' alcohols using the Markiewicz protecting group. Activation of the free alcohol at the C-2' with  $\text{Tf}_2\text{O}$  and subsequent  $\text{S}_{\text{N}}2$  displacement with  $\text{NaN}_3$  furnished the corresponding azide [47], which was reduced to amine [48] via catalytic hydrogenation.

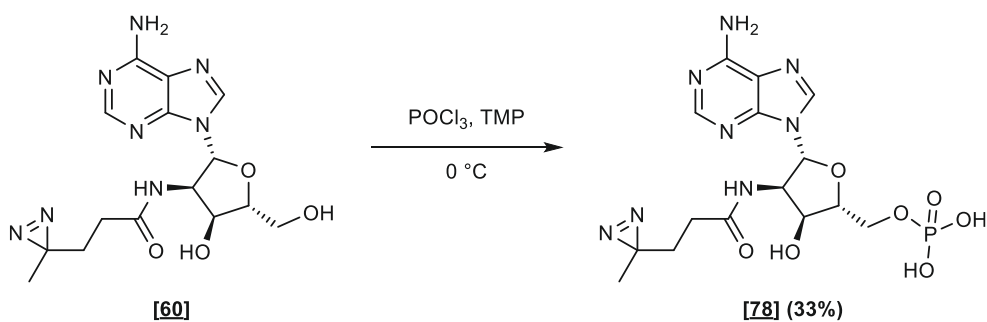


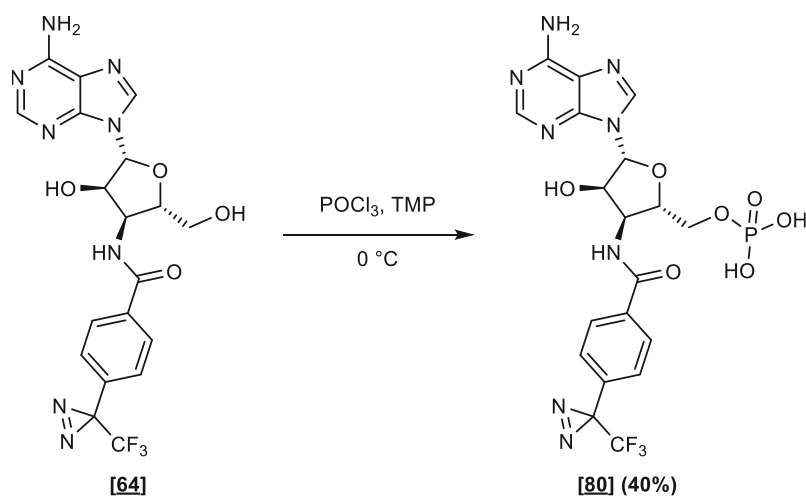
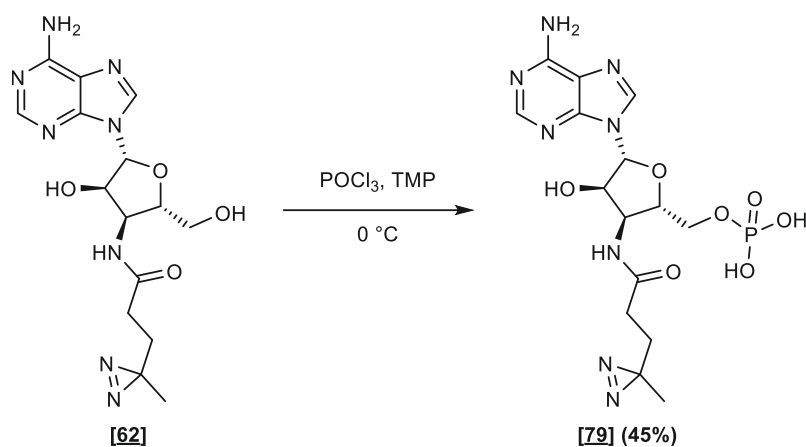
**Scheme 50:** Synthesis of amine **[48]** starting from vidarabine **[98]**.

With seven amides in hand, we investigated the selective phosphorylation of the primary alcohol at the C-5' position. To test the feasibility and compatibility of Yoshikawa's procedure on the synthesized amides, we first attempted phosphorylation of compound **[71]** in a small-scale experiment. Compound **[71]** was treated with POCl<sub>3</sub> in TMP at -5 °C, and a descent formation of the corresponding monophosphate **[81]** was achieved after 8 hours, although no complete conversion was accomplished. To our pleasant surprise, using a larger amount of the starting material, smooth conversion was achieved after 4 hours. However, the superb result had then been marred with depurination of compound **[81]** (see Scheme 52) due to acidic conditions after quenching the reaction through the slow addition of ice-cold water and concentration by lyophilization. Therefore, neutralization of the aqueous phase after extraction and before lyophilization was determined as the best method to utilize. Thus, the aqueous phase was neutralized using triethylammonium acetate (TEAA) buffer, and no depurination was observed after lyophilization. Finally, monophosphate **[81]** was purified via preparative reverse-phase HPLC and obtained in 38%.

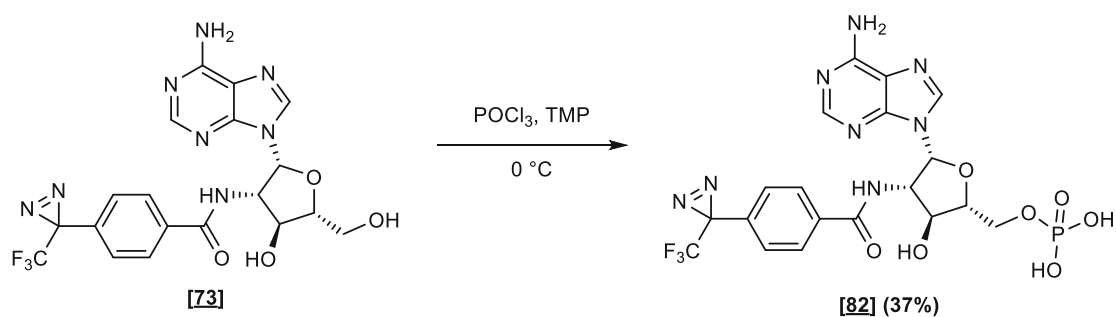
**Scheme 51:** Synthesis of monophosphate **[81]**.**Scheme 52:** Mechanism of the depurination of **[81]** under acidic conditions.

Based on the modified procedure, we attempted the phosphorylation of the remaining adenosine analogs **[60]**, **[62]**, **[64]**, **[73]**, **[75]** and **[77]**. The phosphorylation of compounds **[60]**, **[62]**, **[64]**, and **[73]** proceeded smoothly, and the corresponding monophosphates were obtained in 37–45% yield after purification via preparative reverse-phase HPLC.

**Scheme 53:** Synthesis of monophosphate **[78]**.



**Scheme 54:** Synthesis of monophosphates **[79]** and **[80]**.

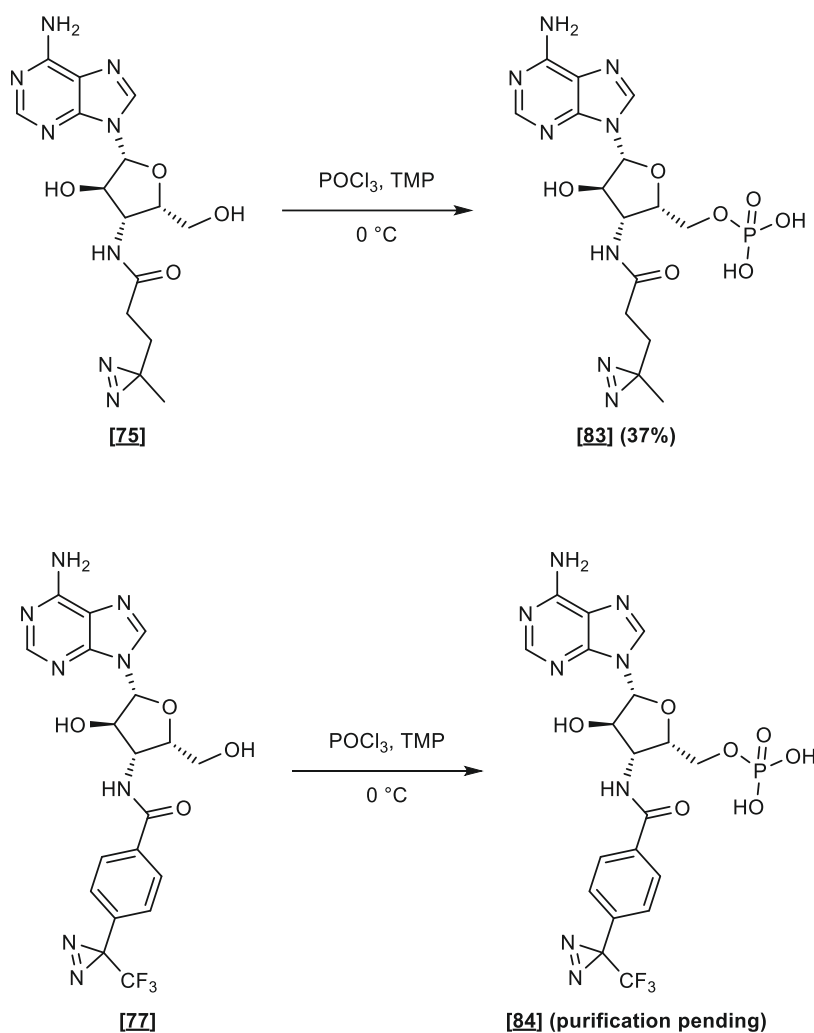


**Scheme 55:** Synthesis of monophosphate **[82]**.

However, phosphorylation of compounds **[75]** and **[77]** encountered challenges. According to UHPLC-MS/UV analysis, a decent formation of monophosphates **[83]** and **[84]** was observed after the complete addition of  $\text{POCl}_3$ . Nevertheless, over the course of the reaction, we observed new peaks with identical masses of the starting materials but different retention times. This indicated the formation of side products rather than hydrolysis of the phosphates. Since the desired reaction seemed successful, we assumed that a higher concentrated reaction mixture would result in faster conversion of the starting materials. Indeed, nearly complete conversion



of compounds **[75]** and **[77]** was achieved within 20 min, and monophosphate **[83]** was obtained in 37% yield after purification via preparative reverse-phase HPLC. However, the purification of monophosphate **[84]** was unsuccessful due to solubility issues. Additionally, the isolation of the side products was not accomplished. Thus, their nature remained unclear.



**Scheme 56:** Phosphorylation of compounds **[75]** and **[77]**.

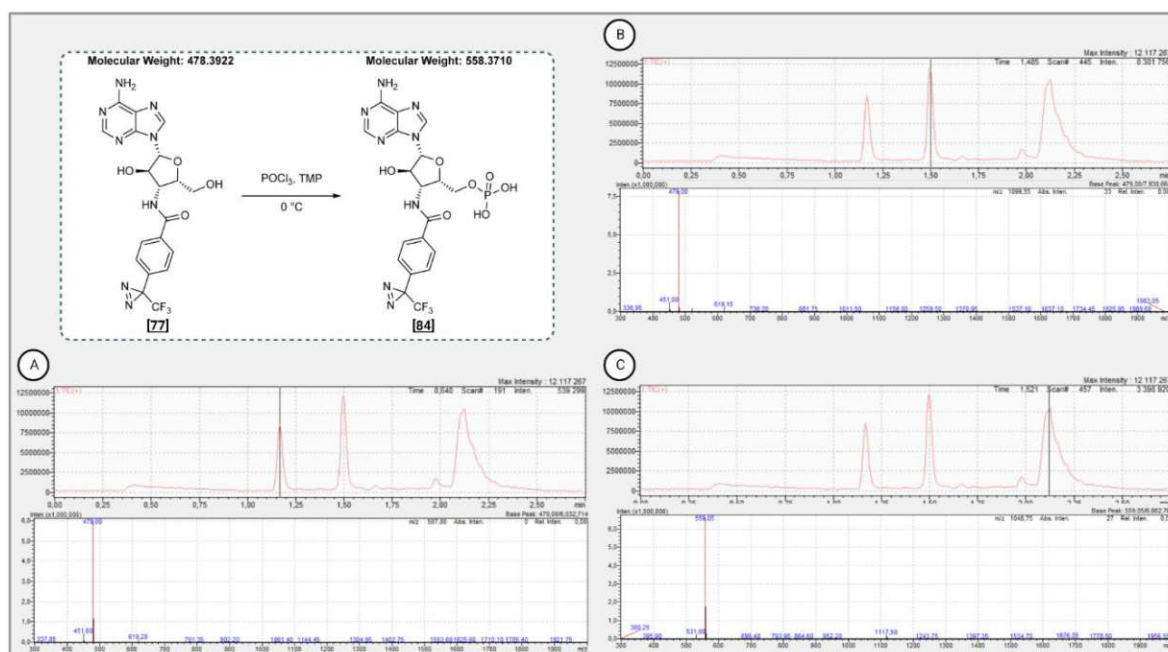
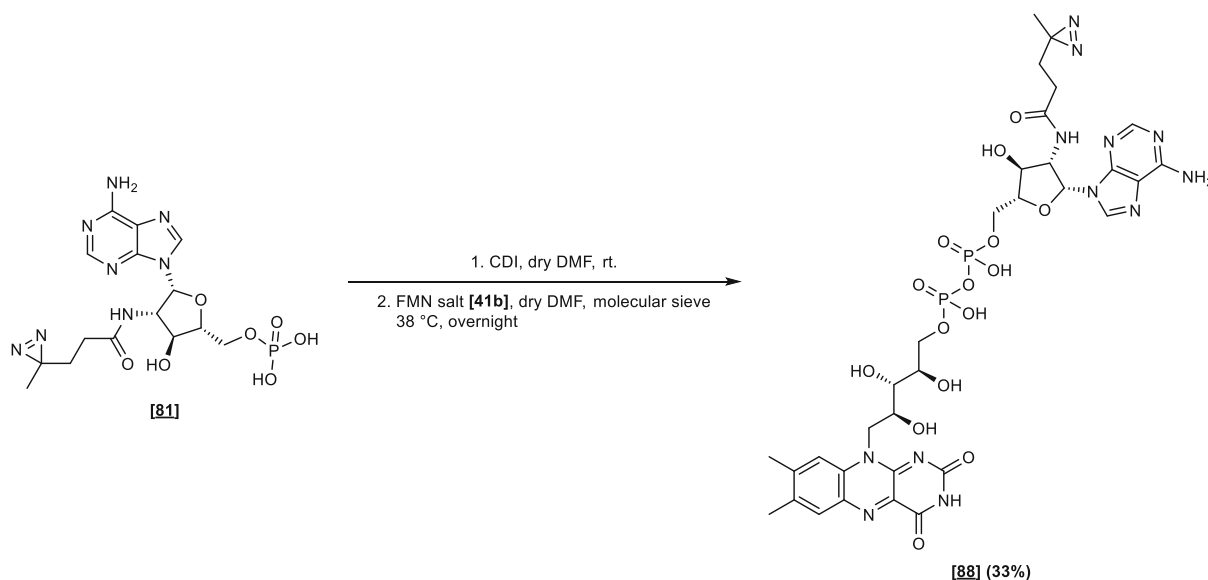


**Figure 37:** Possible side-product formation of compound **[84]**. **A**) The mass chromatogram shows the new peak (left) with the identical mass as the starting material (middle). **B**) The mass spectrum of the starting material. **C**) The mass spectrum of the product.

After achieving the successful synthesis of six monophosphate analogs bearing the diazirine moiety via an amide-linkage, the final step towards the elaboration of diazirine-FADs was the formation of the pyrophosphate group via chemical coupling of the respective adenosine building blocks with FMN. To test the feasibility of the chemical coupling on amide analogs, we again decided to perform the coupling reaction on compound **[81]**.

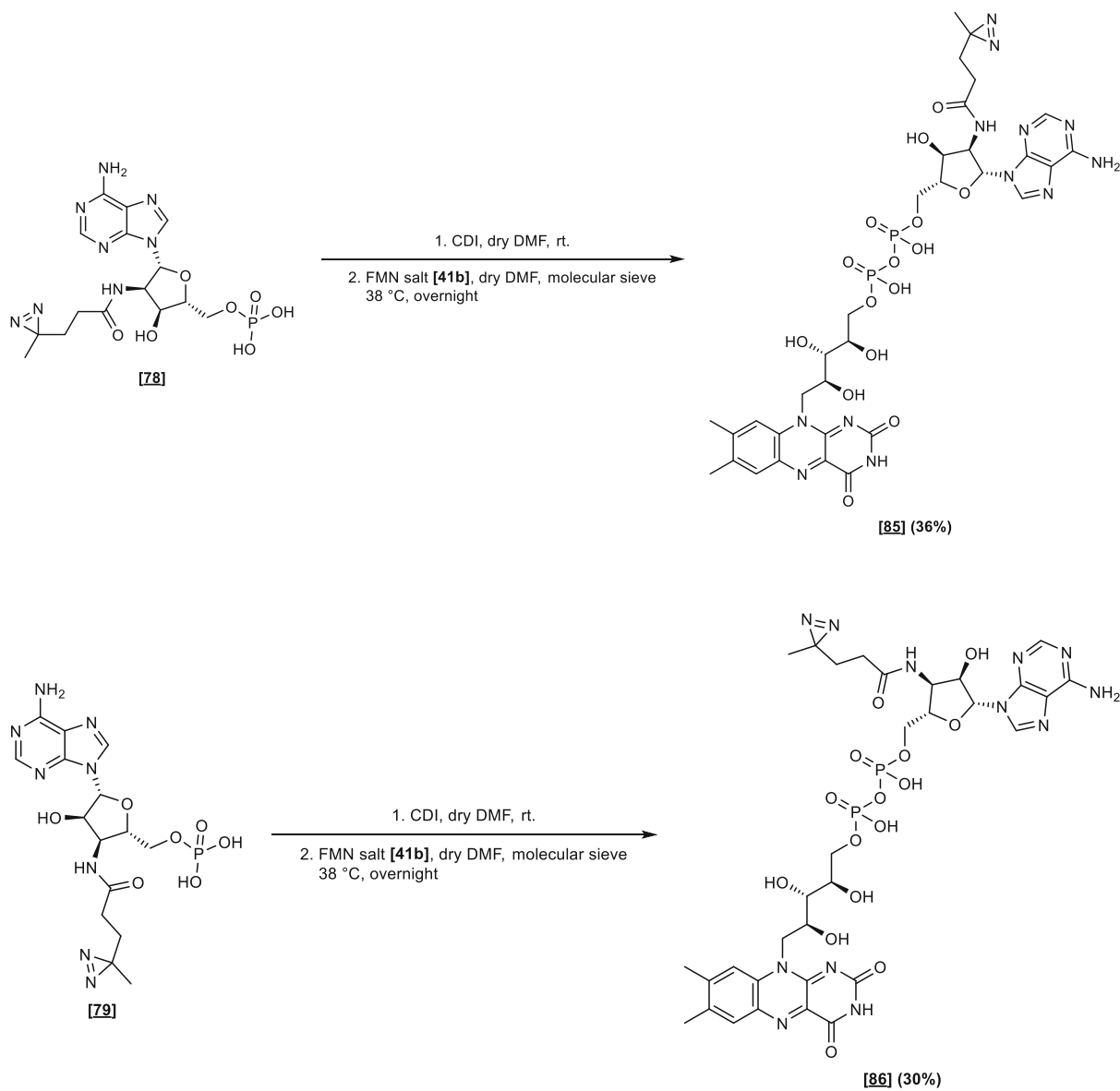
Based on the modified literature procedure<sup>397</sup> described in chapter C II.5.8, monophosphate **[81]** was first activated with CDI and then directly subjected to the coupling reaction with the previously prepared trioctylammonium salt of riboflavin monophosphate. The coupling reaction was again performed in dry DMF in the presence of molecular sieve to ensure strict anhydrous conditions. After UHPLC-MS/UV analysis did not show any further conversion of the starting materials, the reaction was quenched with water, and after lyophilization, the crude material was purified via preparative reverse-phase HPLC using water/acetonitrile + 0.1% formic acid as eluent. Due to the acidic conditions, we observed partial cleavage of the pyrophosphate group, as well as the formation of the corresponding monophosphate **[81]** using UHPLC-MS/UV analysis. Hence, we opted to optimize the purification conditions. First, since purification under neutral conditions was impossible because compound **[88]** stuck to the column under these conditions, we sought to prevent the cleavage of the pyrophosphate by neutralizing the fractions containing the desired compound before lyophilization. Neutralization using a TEAA buffer prevented the cleavage of the pyrophosphate group. However, since separating the FAD analog from FMN remained challenging, the purification

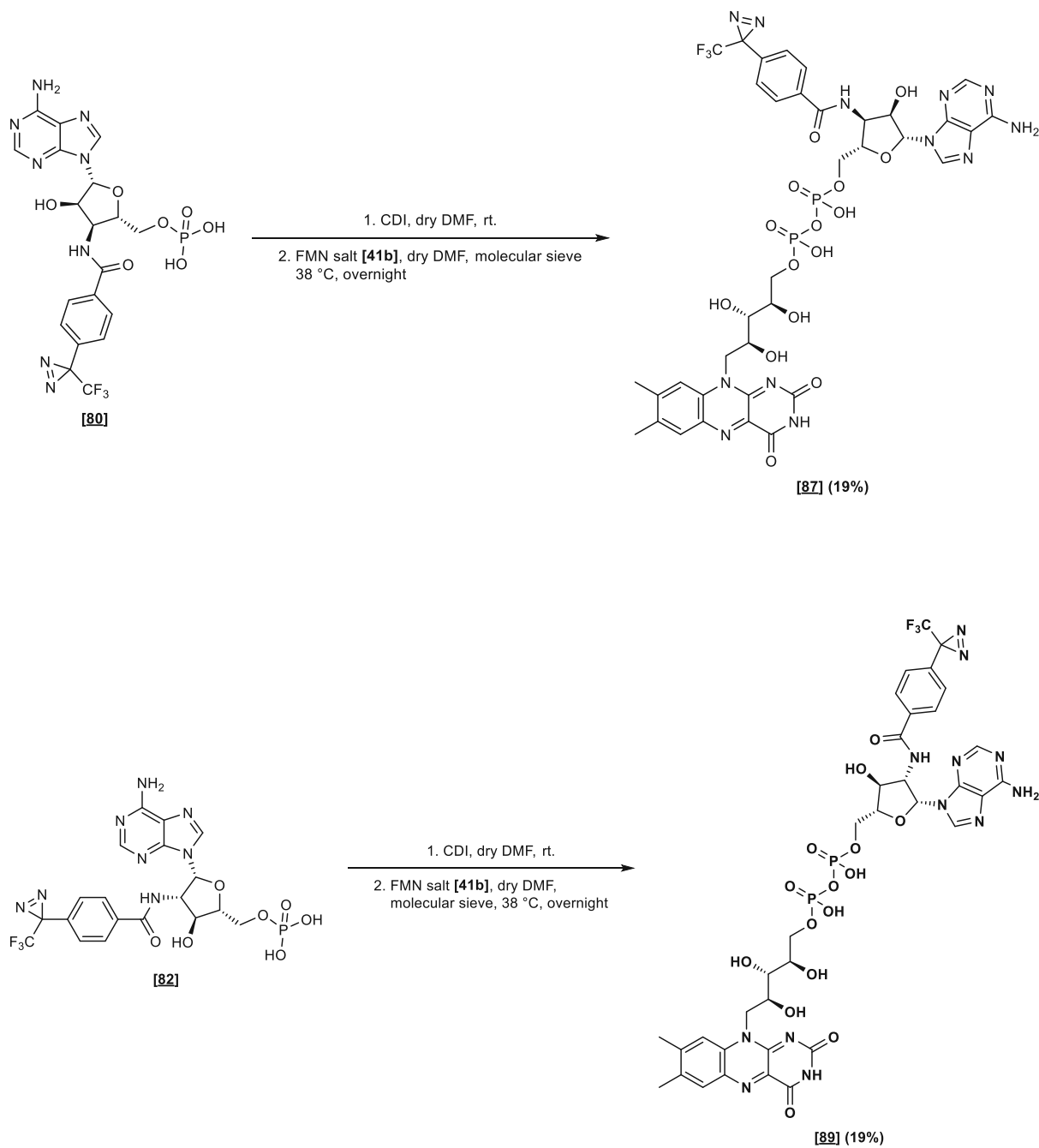
conditions were further optimized. Using alkaline conditions (2.5 mM ammonium formate pH 8.5) proved helpful for two reasons: 1) a better separation from unconverted FMN was achieved, and 2) the additional neutralization step was obsolete.

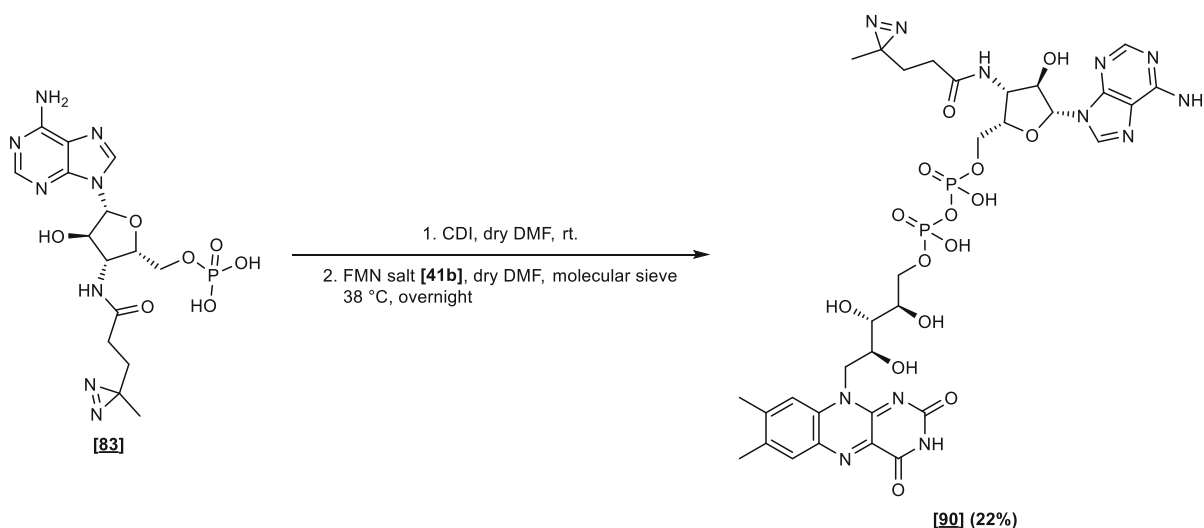


**Scheme 57:** Synthesis of FAD analog **[88]**.

Finally, FAD analog **[88]** was synthesized in 33% yield using this modified purification protocol. For synthesis of the desired FAD analogs **[85]**–**[90]**, monophosphates **[78]**, **[79]**, **[80]**, **[82]**, and **[83]** were analogously elaborated to the corresponding pyrophosphates by applying the described procedure and were obtained in 19–36% yield after purification via preparative reverse-phase HPLC and lyophilization. In contrast to the ester analogs of FAD, the amide linkers proved stable against hydrolysis.

**Scheme 58:** Synthesis of FAD analogs [85] and [86].

**Scheme 59:** Synthesis of FAD analogs **[87]** and **[89]**.

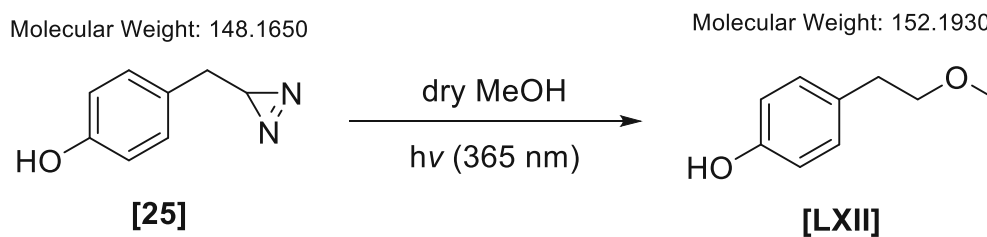


**Scheme 60:** Synthesis of FAD analog **[90]**.

In summary, we successfully designed and synthesized a set of six diazirine-FAD analogs by strategically installing amide linkers at two indicative positions of the ribose moiety of adenosine. While the series of aliphatic diazirine-FADs is complete, two compounds of the aromatic series are pending to complete the set. While synthesis of the compound with the aromatic linker attached to the C-2' and retention of the configuration was not attempted, the purification of monophosphate **[87]** failed. Nevertheless, we produced sufficient amounts of diazirine-FADs and could progress with the investigations regarding their compatibility with flavoenzymes of interest.

## C III Photolysis of diazirines—Obtaining first insights

Before evaluating the synthesized diazirine-FADs in biochemical assays, we sought to gain broad experience in the photolysis reaction of diazirines. Therefore, we used the easily accessible terminal diazirine **[25]** for photolysis experiments to obtain primary insights into the photolysis reaction of diazirines. According to a literature procedure,<sup>383</sup> diazirine **[25]** was irradiated with 360 nm (OmniCure® S2000 Spot UV curing system with a 365 nm bandpass filter) under argon in the presence of methanol. The reaction progress was monitored using GC-MS, and the formation of the corresponding methyl ether **[LXII]** was confirmed by mass as well as NMR analysis. In contrast to the literature, in which 70% of the methanol adduct was isolated after purification, we observed only 30% of the methyl ether after 8 hours of irradiation according to GC-MS analysis.



**Scheme 61:** Photolysis reaction of terminal diazine **[25]** in the presence of MeOH forming methyl ether **[LXII]**.

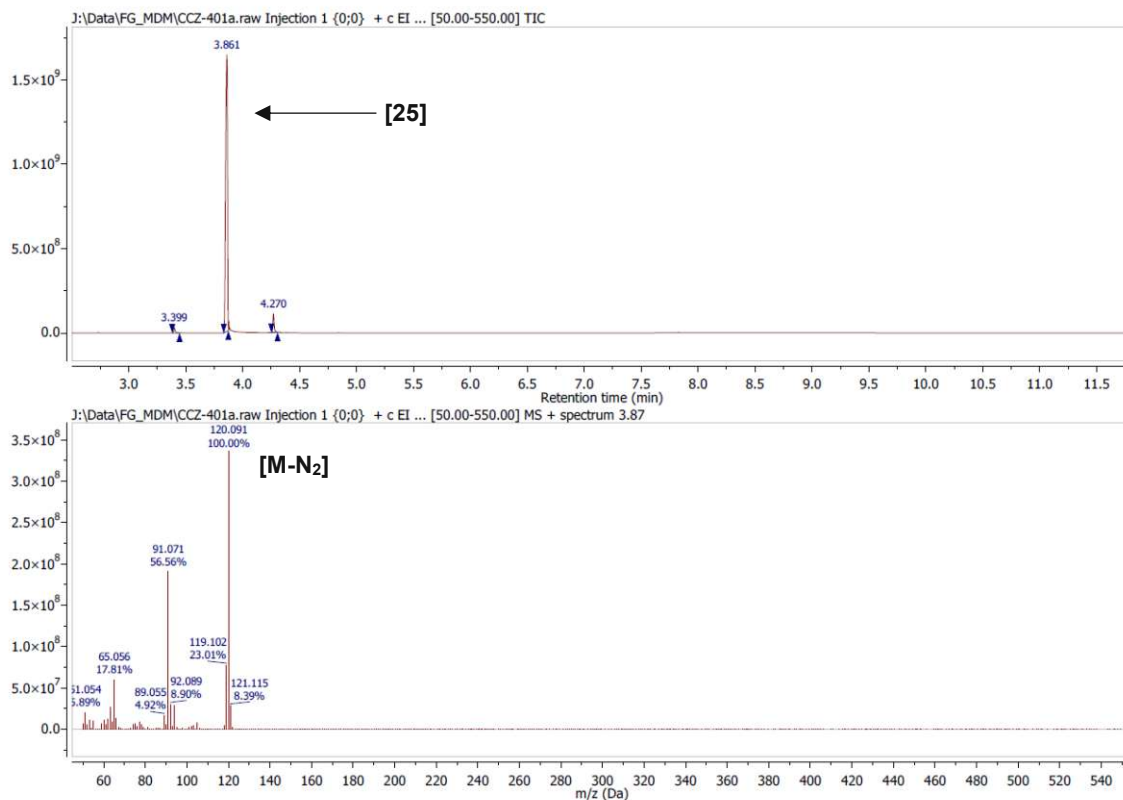


**Figure 38:** GC-MS spectra of compound **[25]**. The molecular mass was not determined due to the loss of molecular nitrogen.

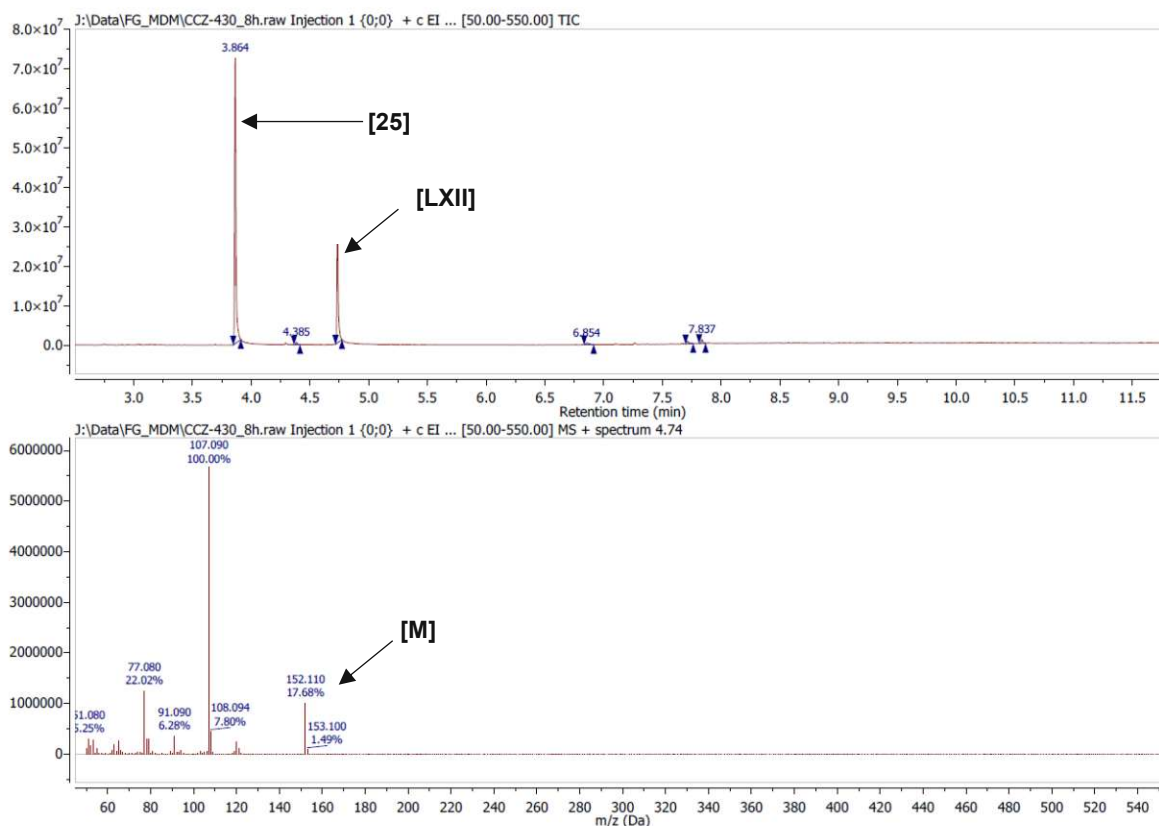


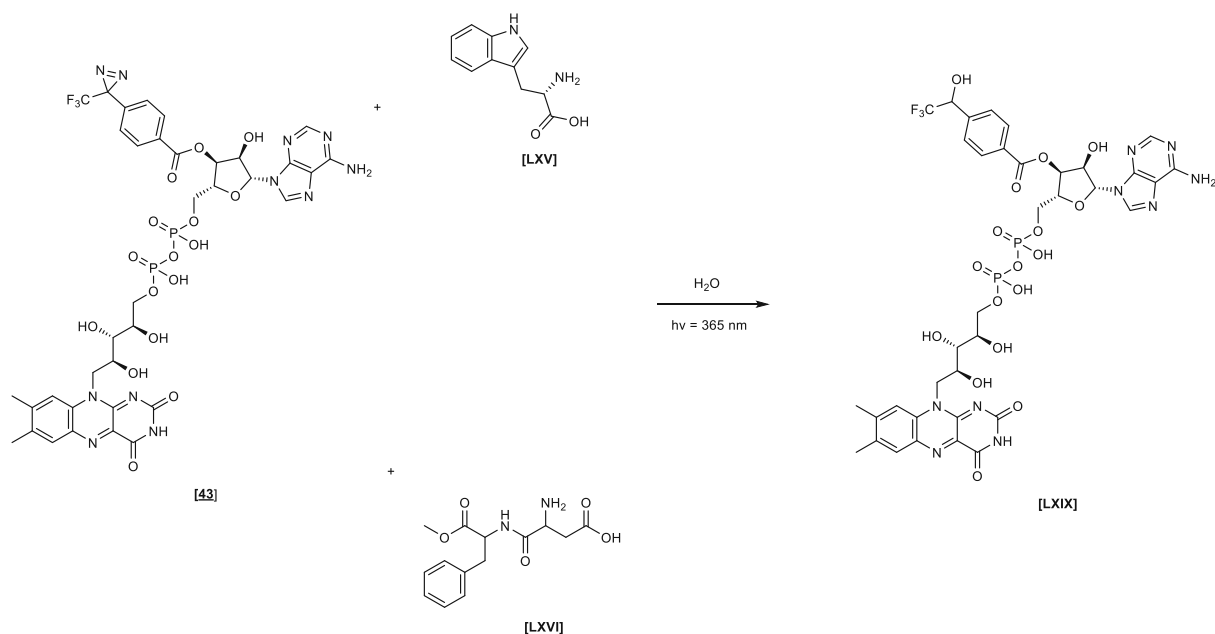
**Figure 39:** GC-MS spectra of compound [LXII] after irradiation for 480 min in dry MeOH.

However, since the photolysis reaction seemed successful, we sought to test the photolysis reaction of diazirine FADs [42] and [43] by capturing the formed carbene with a solvent molecule. The photolysis reactions were first tested on the synthesized ester derivatives of FAD to save precious FAD amide material. As described above, modified FAD [42] was dissolved in dry MeOH and irradiated with 365 nm. Samples were taken after 0 min, 15 min, 30 min, and 60 min and were analyzed using UHPLC-MS/UV. After 15 min of irradiation, the mass of the expected methanol adduct [LXIII] was detected. However, we observed a new product peak with a mass of 242, indicating the formation of lumichrome [V], a known degradation product of riboflavin. After 60 min of irradiation, most of the diazirine FAD [42] was consumed, and the intensity of the methyl ether [LXIII] signal had decreased. In contrast, the degradation product's mass signal increased, revealing that the pyrophosphate group was not stable under these irradiation conditions in MeOH.

Therefore, we changed the solvent from methanol to water while seeking to capture the formed carbene with individual amino acids to represent the closest possible binding interaction between the diazirine and a protein. For this purpose, we used capped amino acid phenylalanine ethyl ester [LXIV], unprotected amino acid *L*-tryptophan [LXV], and dipeptide aspartame [LXVI]. However, in all cases, we did not observe any of the amino acid adducts, although the







**Scheme 64:** Photolysis reaction of aromatic diazine FAD [51] in the presence of amino acids in water. No successful labeling was observed.

Due to the unsuccessful labeling of amino acids and peptides in the liquid phase, we were inspired by a publication<sup>407</sup> in which the authors performed photo-crosslinking reactions with diazirines in lyophilized powders to investigate protein-protein and peptide-matrix interactions in therapeutic formulations. The authors claimed better labeling efficiency when these reactions were performed in the solid state compared to the liquid state. Therefore, we dissolved diazine FAD [42] and dipeptide *DL*-leucyl-*DL*-phenylalanine [LXX] in MilliQ water, followed by thorough mixing and lyophilization. The obtained powder was then subjected to UV irradiation at 365 nm for over 1 hour, but the diazine-FAD remained unchanged, and no photo-labeled product was detected.

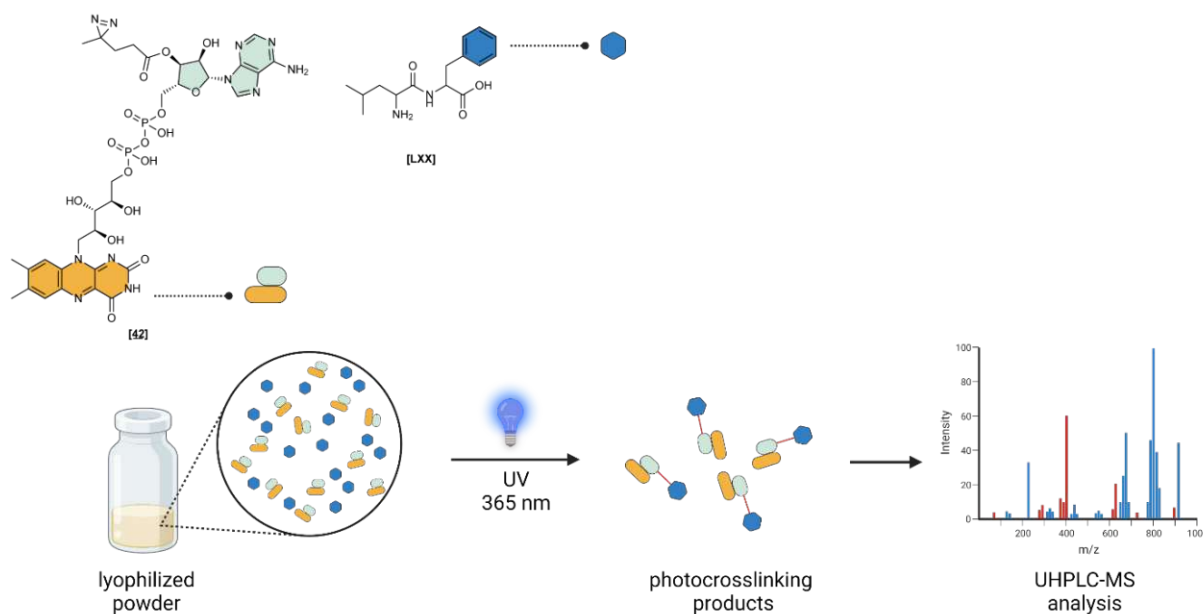


**Figure 40:** Attempted labeling of FAD analog [42] and dipeptide *DL*-Leucyl-*DL*-phenylalanine [LXX] as lyophilized powder.

Since labeling the amino acids and short peptides was unsuccessful, we investigated the photo-labeling of proteins. We were inspired by a publication<sup>405</sup> that described a method by which the authors detected successful labeling of the protein bovine serum albumin (BSA) using in-gel fluorescent measurement with the fluorescent dye rhodamine modified by a diazirine linker [LXXI].

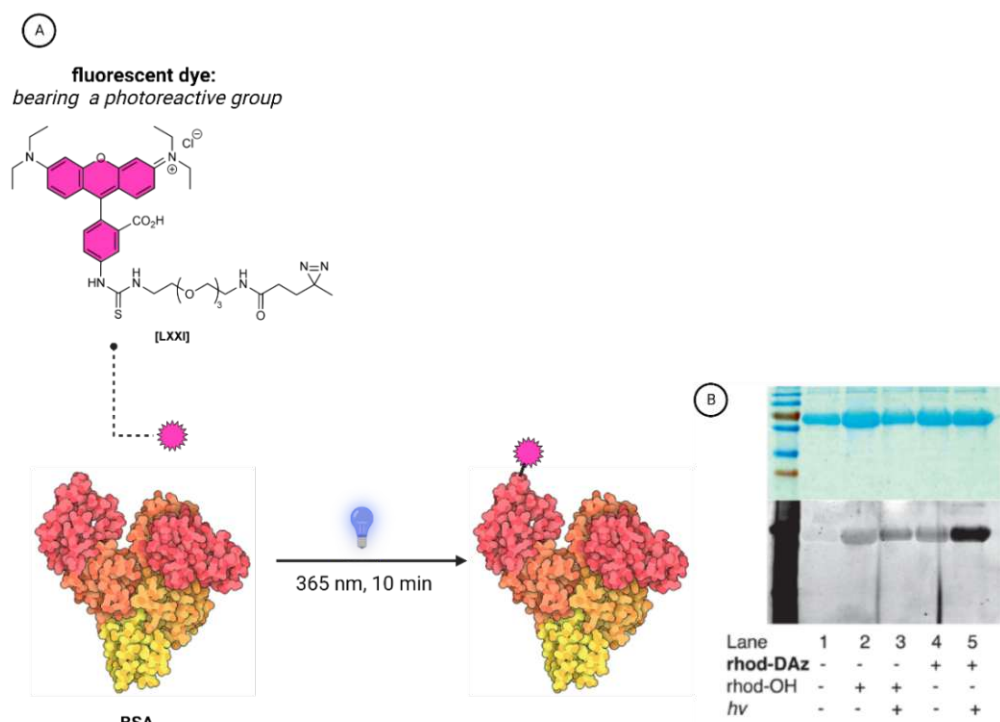
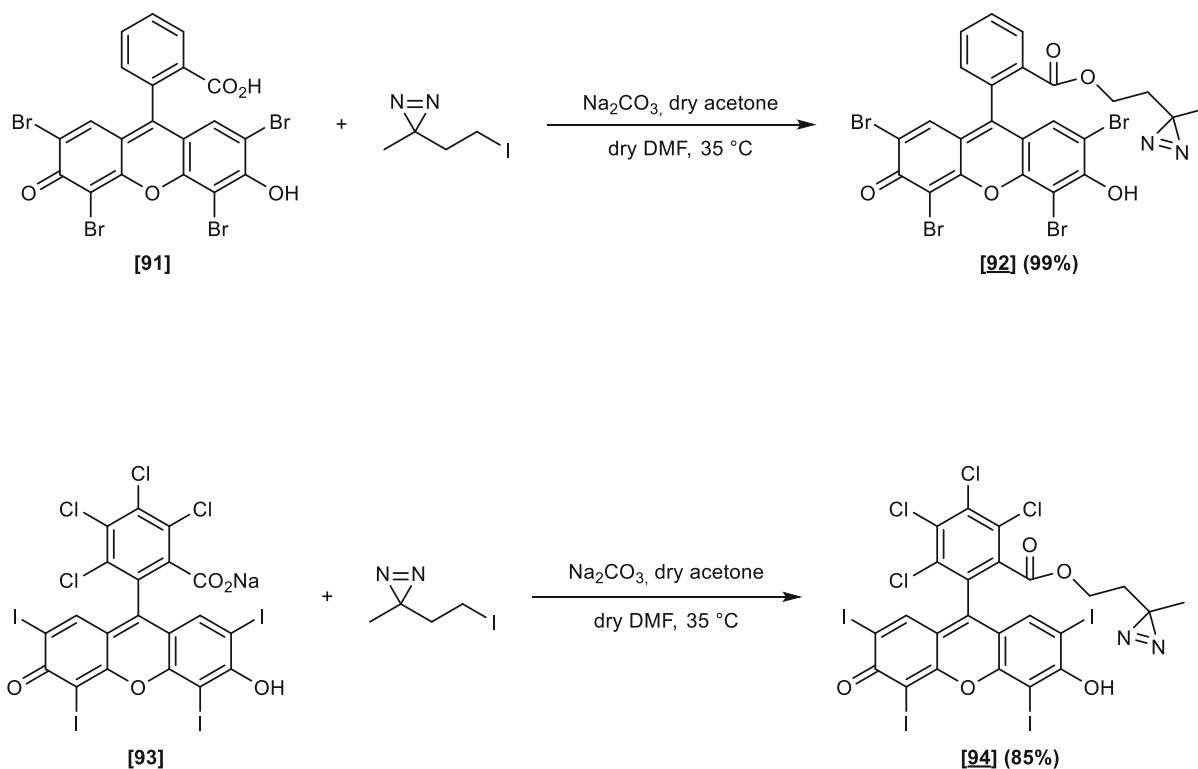


**Figure 41:** Photo-crosslinking reaction of modified rhodamine with BSA. **A)** Principle of the photo-labeling of the protein BSA with fluorescent dye [LXXI]. **B)** The successful labeling was confirmed by in-gel fluorescent measurement. The figure was adapted from reference.<sup>405</sup>

Based on this publication,<sup>405</sup> we synthesized a modified Eosin Y and a Rose bengal derivative containing a diazirine linker. Esterification<sup>408</sup> was achieved by using [6] in the presence of sodium carbonate in a solvent mixture of dry acetone and dry DMF at 35 °C in 99% and 85% of Eosin Y and Rose Bengal, respectively.



**Scheme 65:** Synthesis of modified fluorescent dyes [94] and [95].

After producing fluorescent dyes [92] and [94], we opted to examine the irradiation on BSA as reported in the literature. The Eosin Y derivative [92] was incubated with the protein BSA in the dark for 1 hour and then subjected to the photolysis reaction employing a Hg-UV lamp emitting at 365 nm as our light source (for more details, see E I.7.1). Light-dependent fluorescent labeling of BSA was confirmed using SDS-PAGE analysis (see Figure 42).

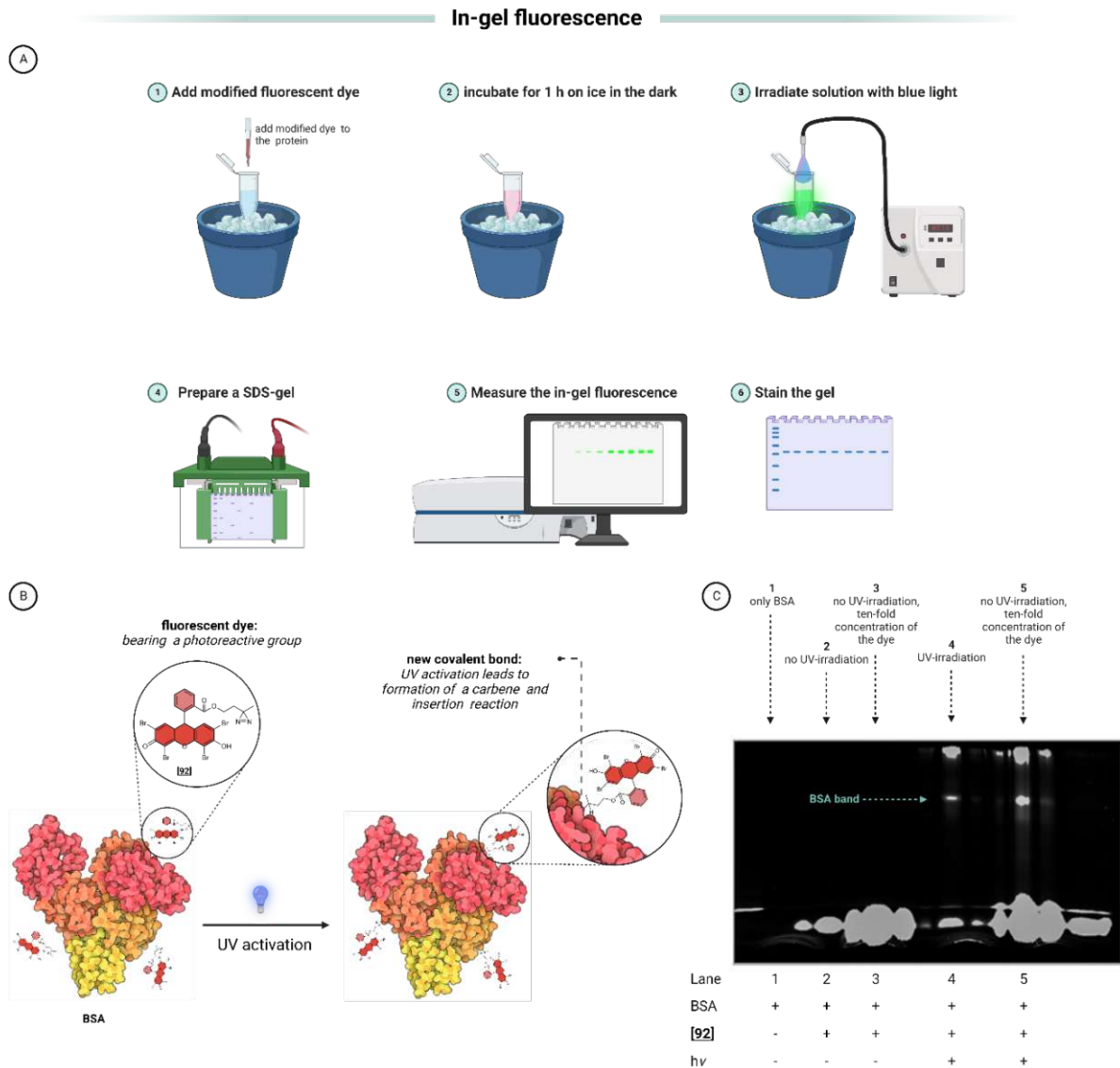


**Figure 42:** In-fluorescence analysis. **A)** Workflow of the in-gel fluorescence studies. **B)** Scheme of the photocrosslinking of the fluorescent dye [92] and the protein BSA. **C)** SDS-Gel analyzed by in-gel fluorescent measurement. The irradiated samples showed a fluorescent signal when the dye was present, indicating successful labeling.

The results of the in-gel fluorescence measurement shown in Figure 42 revealed successful dye labeling. Furthermore, higher dye concentrations led to a stronger fluorescent signal, indicating higher labeling. However, we also observed a strong fluorescent signal at the top of the SDS gel, implying protein crosslinking due to the formation of oxygen radicals. Thus, labeling conditions had to be optimized beforehand.

Based on these results, we pursued the labeling of the fluorescent dye [92] on the flavoprotein glucose oxidase (GOx). As described above, the dye [92] and GOx were well mixed and then incubated. Then, the prepared samples were irradiated with two different intensities, and samples were taken at specific time intervals. Finally, the samples were analyzed using SDS-PAGE and in-gel-fluorescence studies. As shown in Figure 43, the

crosslinking of the dye with GOx was successful, although, similar to BSA, longer irradiation times led to an increased crosslinking of proteins, indicating that the irradiation conditions must be optimized for each enzyme. Therefore, we conducted another experiment but took samples at earlier time points (Figure 44). As shown in Figure 44, irradiation of the enzyme GOx for 5 min resulted in sufficient labeling and low crosslinking of proteins.

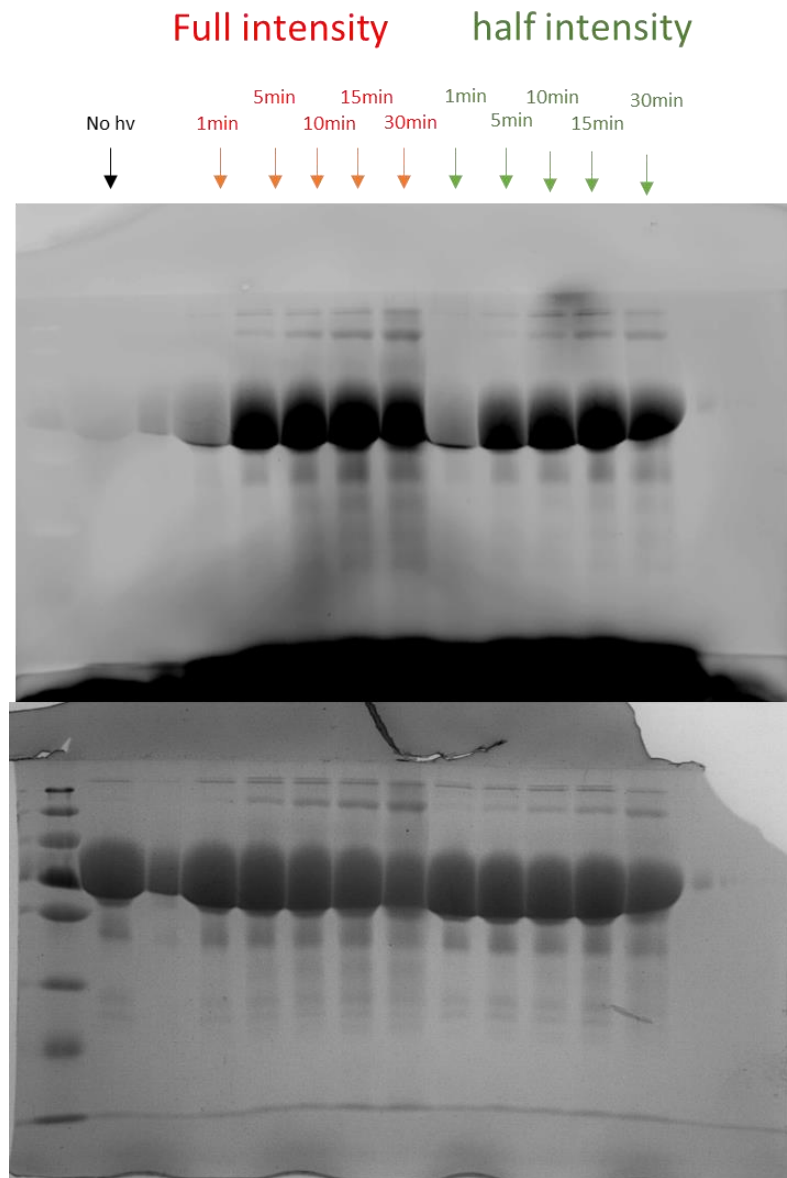


**Figure 43:** Optimization of the irradiation conditions for the enzyme GOx. The upper gel was analyzed by in-gel fluorescent measurement prior to staining (lower gel). Note: The 2<sup>nd</sup> pocket was left empty, but a small amount of the 3<sup>rd</sup> pocket's sample got into the 2<sup>nd</sup> pocket.

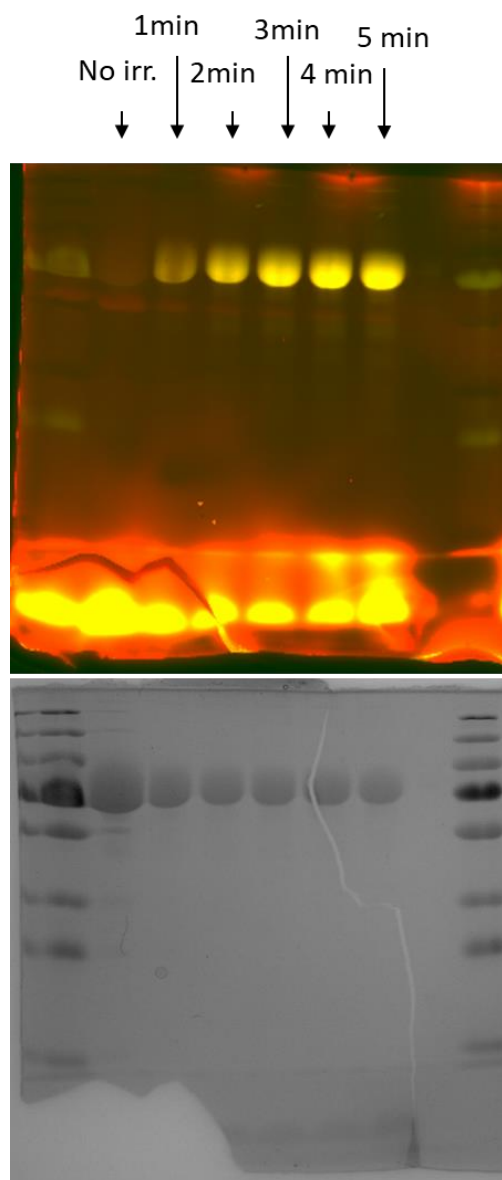


**Figure 44:** Optimization of the irradiation conditions for the enzyme GOx. The upper gel was analyzed by in-gel fluorescent measurement prior to staining (lower gel).

## C IV Biochemical evaluation of diazirine-FAD analogs on flavoenzymes

This section describes the biochemical assessment of the synthesized diazirine-FAD analogs on three model enzymes (GOx, CDH, and CHMO). The main aim of this thesis was the covalent tethering of FAD to various flavoenzymes to increase their stability and thus their applicability in biocatalysis and biosensing. Most of the following experiments were conducted at the University of Natural Resources and Life Sciences, Vienna, with the help of Dr. Su Ma, Dr. Erik Breselmayer, and Dr. Florian Csarman.

Since GOx and CDH are significantly more stable than CHMO, we sought to examine the characteristics of GOx and CDH with our synthesized diazirine-FAD derivatives to gain a better understanding of the deflavination, reconstitution, and photolysis conditions before working on unstable CHMO.

## C IV.1 Glucose oxidase and cellulose dehydrogenase

With six diazirine-FADs [85]-[90] in hand, we sought to test whether the photo-clickable FAD analogs could be incorporated correctly into the binding sites of GOx and CDH and whether the enzymes showed activity.

The first step was deflavination of the enzymes GOx and CDH. The deflavination procedure was established by our colleagues from the University of Natural Resources and Life Sciences, Vienna. To remove the native FAD, the enzyme was dissolved in distilled water, followed by the addition of solid potassium sulfate. Then, the mixture was shaken at 4 °C until all solids were dissolved. The resulting mixture was then centrifuged, and the precipitated enzyme was resuspended in an acidic K<sub>2</sub>SO<sub>4</sub> solution (pH 1.5). Centrifugation and washing were repeated until a nearly colorless pellet was obtained. In the case of the enzyme GOx, three washing steps were sufficient to obtain a colorless pellet, while eight washing steps were required for the enzyme CDH, indicating that CDH shows a higher binding affinity to FAD and FAD analogs. Next, the obtained apoenzyme was dissolved in reaction buffer, followed by the addition of native FAD or diazirine-FADs, which were dissolved in distilled water (20 mM stock solutions). Previous binding studies conducted by our collaborators regarding determination of the K<sub>A</sub>-values showed that a molar ratio of 1:100 is optimal for diazirine-FAD [88] for complete saturation of apo-GOx and apo-CDH. Therefore, the apoenzymes were incubated in a ratio of 1:100 of apoprotein:FAD overnight at 4 °C. Finally, the holoenzymes were washed for several rounds until a colorless filtrate was obtained to remove excess FAD.

Next, we evaluated our photo-clickable FAD analogs on GOx and CHD activity. The activity of GOx was determined via an ABTS assay (for detailed conditions, see E I.8.1), while CDH's



activity was assessed via a DCIP assay (for detailed conditions, see E I.8.2). The results of the activity measurements are shown in Figure 45 and 48.

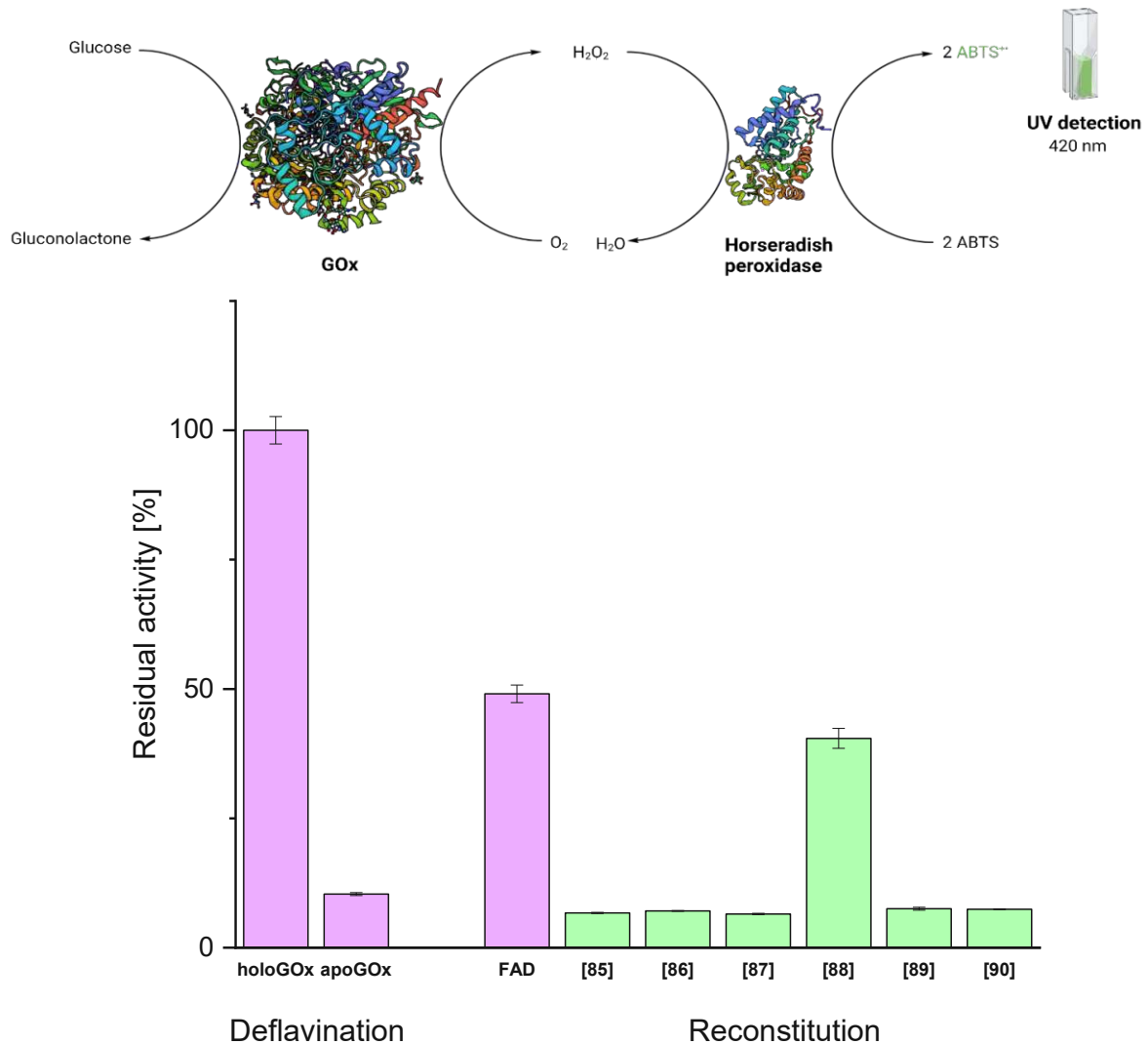


**Figure 45:** Activity measurement after reconstitution with synthesized FAD analogs.

Deflavination of the enzyme GOx did not result in the complete removal of native FAD, as indicated by the residual activity of ~15% compared to the holoenzyme. However, the refluination of GOx with native FAD restored about 49% of the enzyme's activity. Surprisingly, reconstitution with diazirine-functionalized FAD **[88]** restored 41% of the activity, implying the correct incorporation of the FAD analog **[88]** into the enzyme's binding site. None of the other FAD analogs could restore the activity of GOx. While we expected that incorporation of the aromatic diazirine-FADs **[87]** and **[90]** would be more challenging due to their sterical demand, the unsuccessful incorporation of the other aliphatic FAD analogs was unexpected. Not only the position of the linker (2'-position versus 3'-position) but also the configuration at the 2'-position seem to be crucial for restoring the enzyme's activity. While

the alteration of the configuration at the C-2' position (FAD analog [88]) provided an active biocatalyst, the retention of the stereochemistry at the C-2' (FAD analog [85]) resulted in an inactive enzyme. To obtain reasonable conclusions, in-silico studies must be performed in further studies.

The deflavination and reconstitution of the CDH were similar, although removing the native FAD was not as efficient as for the GOx, presumably due to the higher binding affinity observed previously in binding studies. Replavination with native FAD restored about 53% of the holoenzyme's activity, and reconstitution of diazirine-FAD [88] restored about 49% of the enzyme's activity. Remarkably, aromatic diazirine-FAD [89] seemed to be incorporated adequately into the enzyme's binding site, providing a fully active enzyme with about 38% residual activity compared to the holoenzyme. Besides FAD analogs [88] and [89], none of the other diazirine-FADs provided an active enzyme.

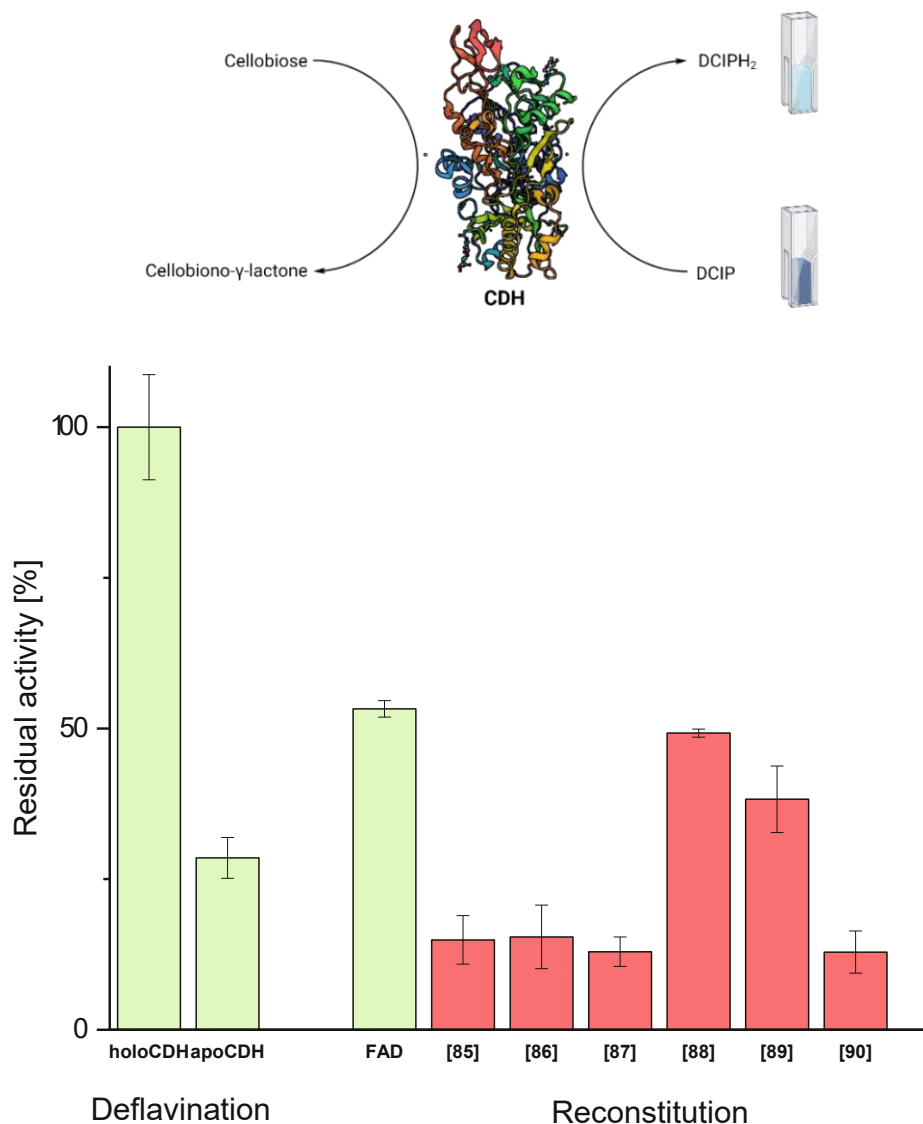


**Figure 46:** Activity measurement after reconstitution with synthesized FAD analogs.

Based on these results, we investigated whether the modified FADs could be covalently linked to the enzymes GOx and CDH via a photocrosslinking reaction. However, before we performed the photocrosslinking with our precious reconstituted enzymes, we investigated the enzymes' stability upon UV light irradiation. Although we expected that UV light irradiation at 365 nm should not overly harm the protein structure, literature precedence has indicated that UV irradiation under air could result in increased degradation due to the formation of oxygen radicals.<sup>409-412</sup> Therefore, we subjected native GOx and CDH to UV light irradiation in the presence and absence of oxygen. The results can be seen in Figure 47 and Figure 48.

In agreement with the literature, UV light irradiation resulted in drastic degradation of GOx's activity when oxygen was not excluded from the reaction mixture. In contrast, the exclusion of oxygen did not have such a dramatic effect on the CDH. However, irradiation had, in general, a more negative effect on CDH than on GOx. These results indicated that the irradiation times had to be thoroughly considered to avoid harming the enzymes and to achieve sufficient crosslinking. Considering the preliminary results of the photocrosslinking of fluorescence dyes (see chapter C III), we reasoned that 5 min of irradiation would result in sufficient crosslinking and tolerable enzyme degradation.

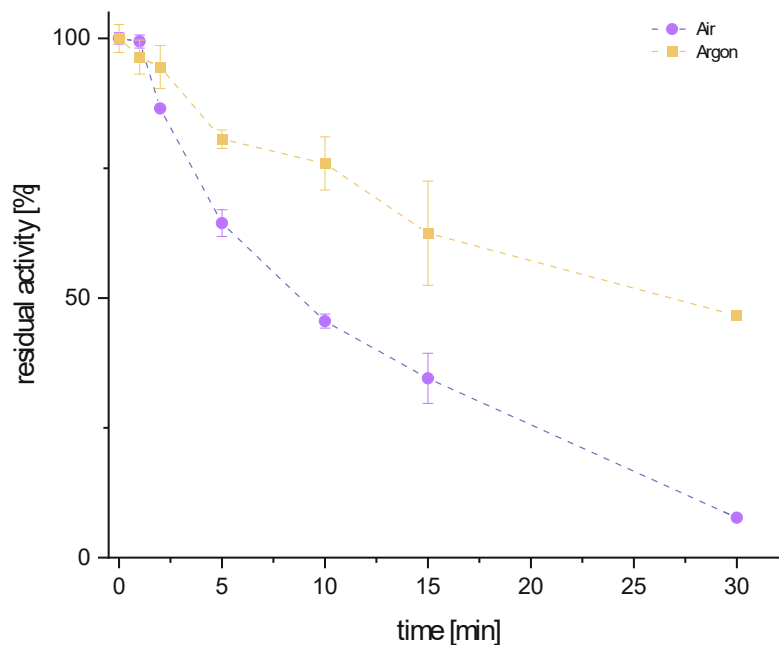


**Figure 47:** Influence of the presence of oxygen during irradiation of the enzyme GOx.

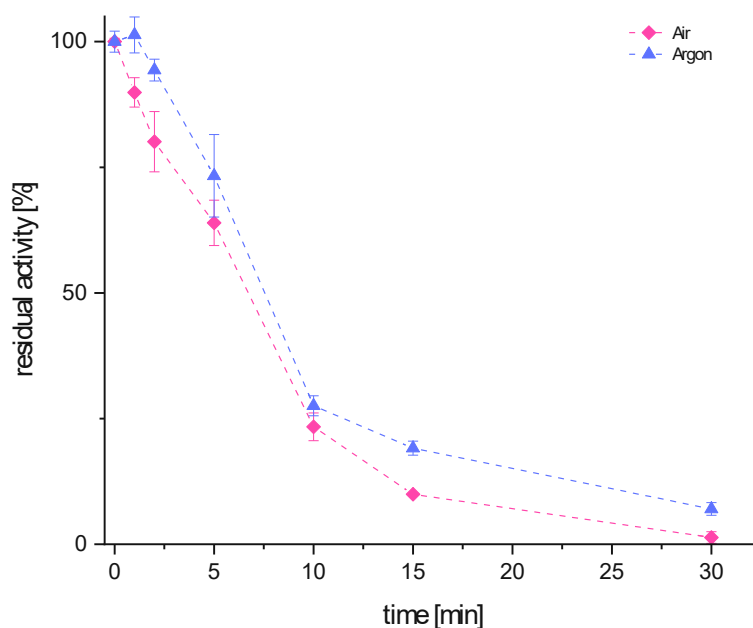


**Figure 48:** Influence of the presence of oxygen during irradiation of the enzyme CDH.

Based on these considerations, we progressed with the photocrosslinking reaction of the reconstituted enzymes. First, oxygen was removed by repeated evacuation and purging with nitrogen (for more details, see E I.7.2), and the samples were subsequently exposed to 365 nm light on ice under an argon atmosphere to initiate covalent labeling. Next, to assess whether the irradiated samples were still active, we measured the activity of the probes analogously, as previously described. Control experiments with native FAD were again conducted.

As expected, irradiation caused a decrease in the activity of the enzymes of roughly 10% compared to the non-irradiated samples. Comparison with the control experiments (native FAD) did not show any significant differences in activity loss; only the irradiation of CDH reconstituted with the aromatic diazirine-FAD [89] resulted in a severe drop in activity of over 20%. This may have been because the covalent bond formation caused a change in the orientation of the isoalloxazine ring, thus preventing efficient catalysis.

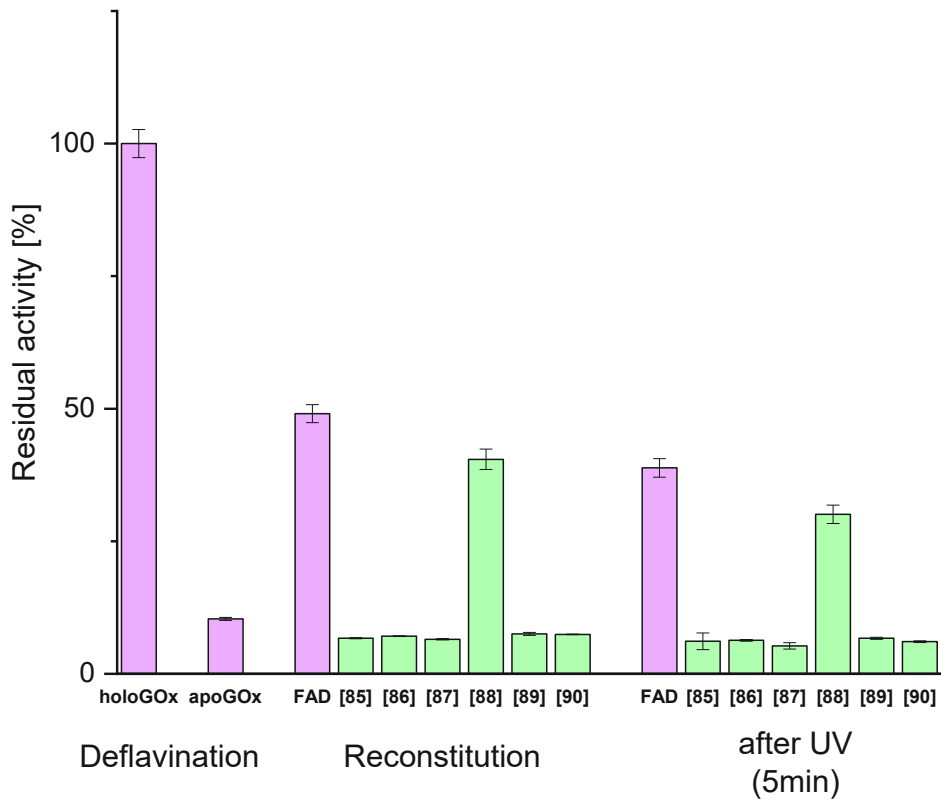


**Figure 49:** Activities of reconstituted and irradiated samples of the enzyme GOx.

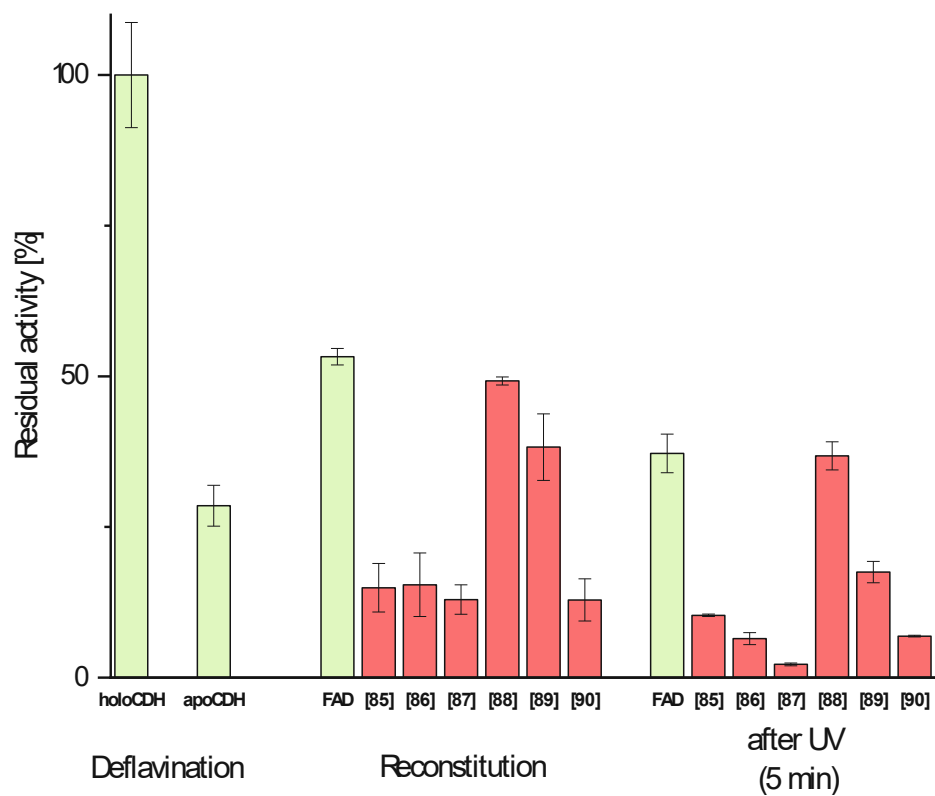


**Figure 50:** Activities of reconstituted and irradiated samples of the enzyme CDH.

To assess whether the covalent attachment had a beneficial effect on the stability of the enzymes reconstituted with FAD analog **[88]**, we measured thermodynamic stability through

nano differential scanning fluorimetry using  $2 \text{ mg}\cdot\text{mL}^{-1}$  enzyme in 100-mM citrate-phosphate buffer at various pHs and compared the samples with the native holoenzymes. However, no improvement in the melting temperature  $T_m$  was observed for GOx or CDH.

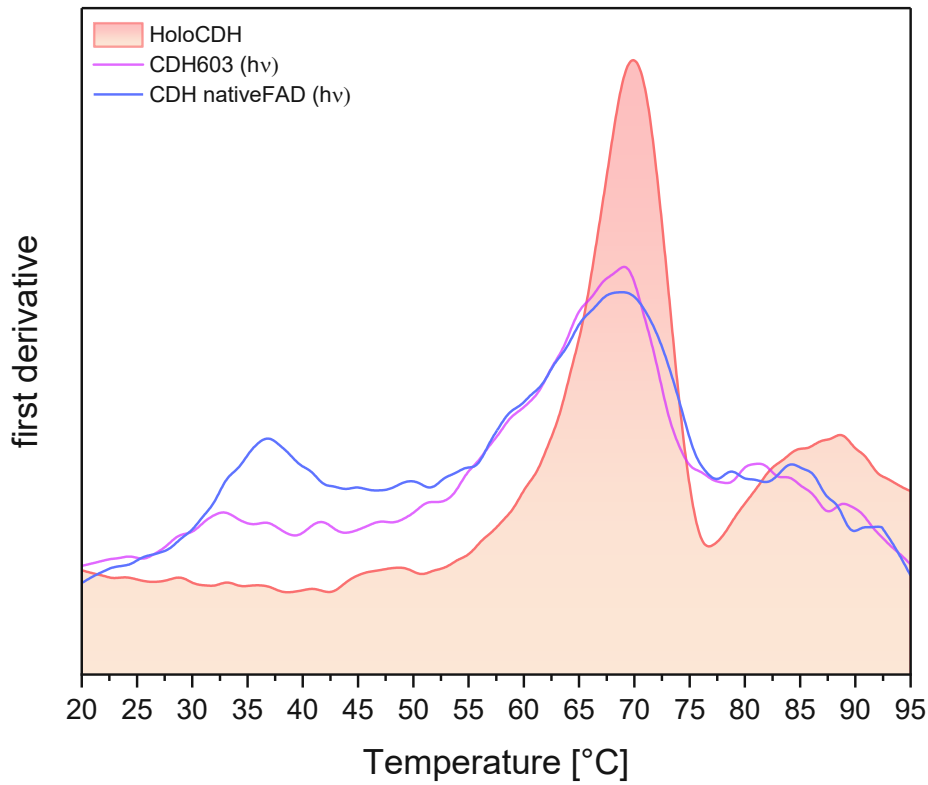


**Figure 51:** Measurement of the thermodynamic stability ( $T_m$ ) of the enzyme GOx by nano differential scanning fluorimetry (nanoDSF).

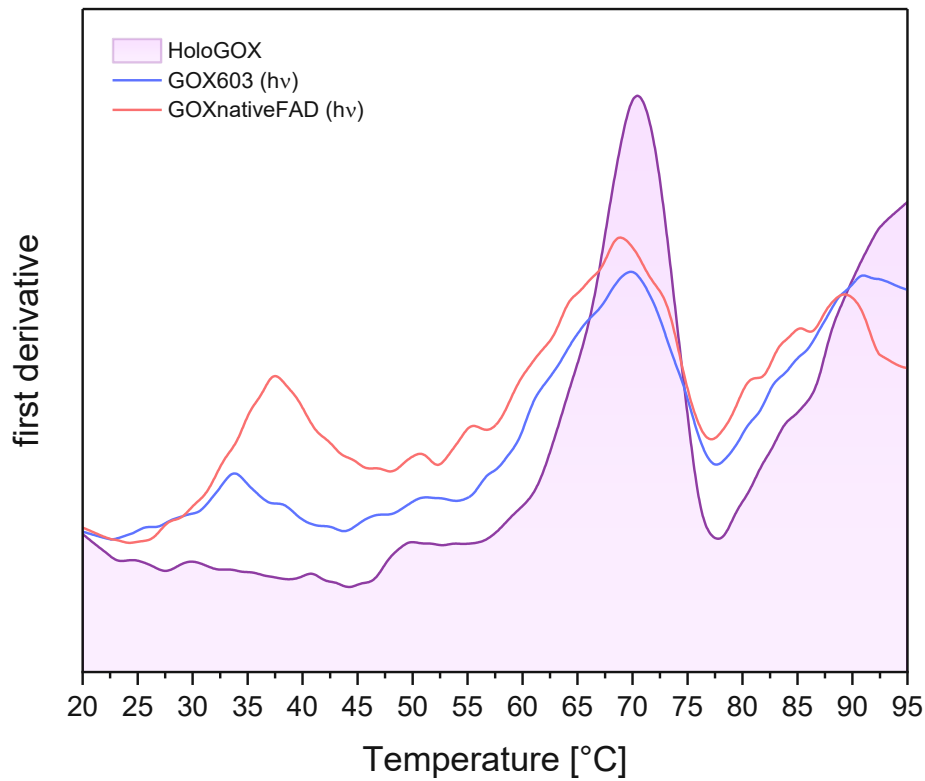


**Figure 52:** Measurement of the thermodynamic stability ( $T_m$ ) of the enzyme CDH by nano differential scanning fluorimetry (nanoDSF).

At this stage, we still lacked evidence of covalent bond formation between the enzymes GOx and CDH and the diazirine-FAD analogs. Therefore, we conducted chemical proteomic studies. To identify possible residues for covalent bond formations, our collaborators first performed molecular modeling studies in MOE2019. Based on the position of the diazirine group of FAD analog [88], the possible peptides for covalent tethering were estimated for subsequent MS/MS analysis.

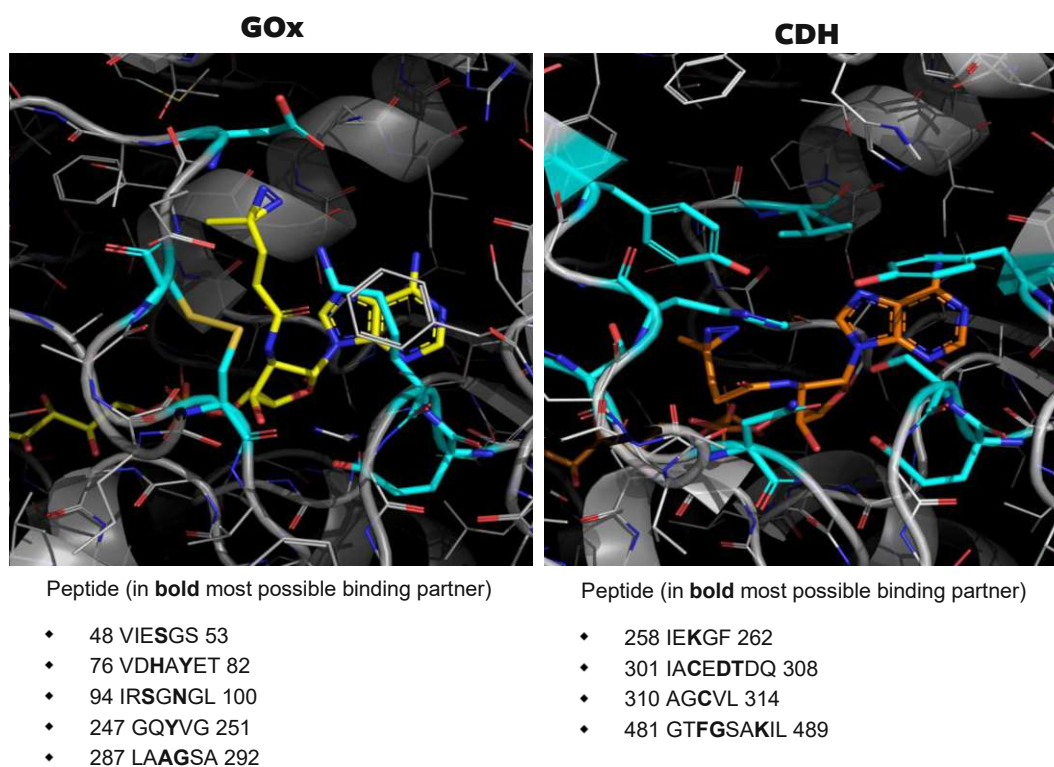


**Figure 53:** Modeling studies to elucidate possible binding partners.

For GOx, five peptides were discovered as possible binding partners, while the molecular modeling identified four peptides as possible binding partners for CDH (Figure 53). Next, we investigated the fragmentation pattern of the aliphatic diazirine-FADs and the aromatic-diazirine FADs. For all compounds, the same fragment with a mass of 439.10 was detected (see Figure 54), which enabled a specific search for this fragment. Finally, the irradiated samples were analyzed using LC-MS/MS-studies. However, assessment of the protein's total molecular weight through intact mass analysis was unsuccessful since only unresolved masses were obtained for both enzymes. While glycosylations of the enzymes may have caused this issue, the enzymes' degradation due to UV light irradiation cannot be excluded.

The samples were further analyzed by mass spectroscopy after enzymatic digestion of the proteins into peptides, and five peptides with a possible covalent bond were detected for the sample irradiated with aromatic diazirine-FAD analog [89]. These findings were further confirmed by the detection of the fragment with a mass of 439.10 (Figure 54). However, the labeling pattern implied rather random crosslinking of the protein structure than specific labeling in the enzyme's binding pocket. In addition, no reliable results were observed for the other samples.



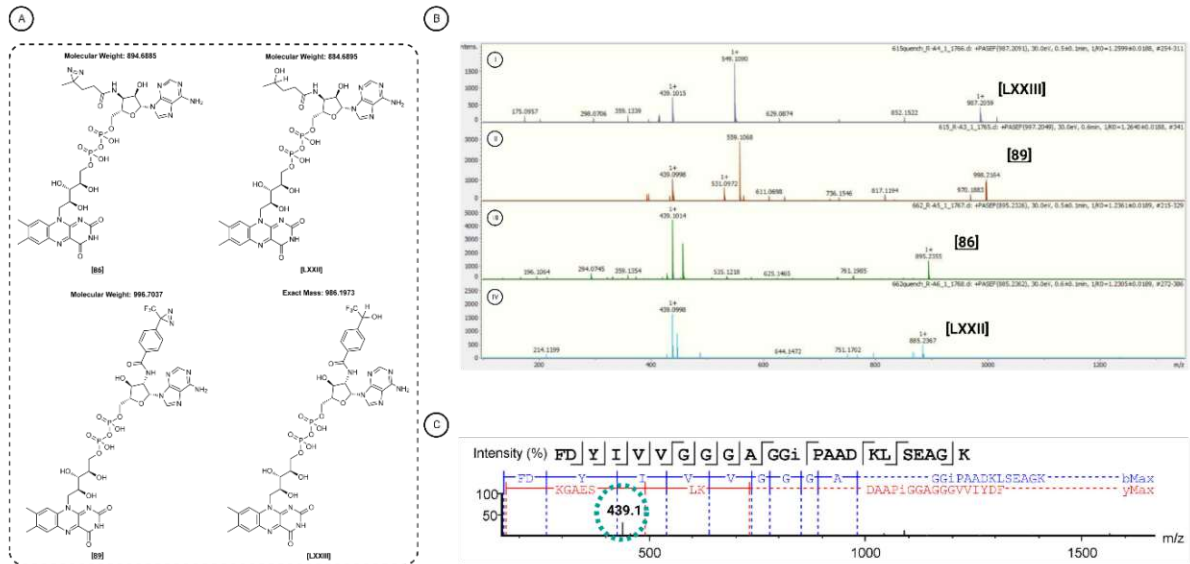


**Figure 54:** MS/MS studies. **A)** Structures and molecular masses of compounds [86], [89], [LXXII], and [LXXIII]. **B)** Mass spectra of compounds [86], [89], [LXXII], and [LXXIII]. All compounds show a mass fragment with a mass of 439.10. **C)** Some peptides of CDH showed a mass fragment with a mass of 439.10 when CDH was irradiated in the presence of compound [89].

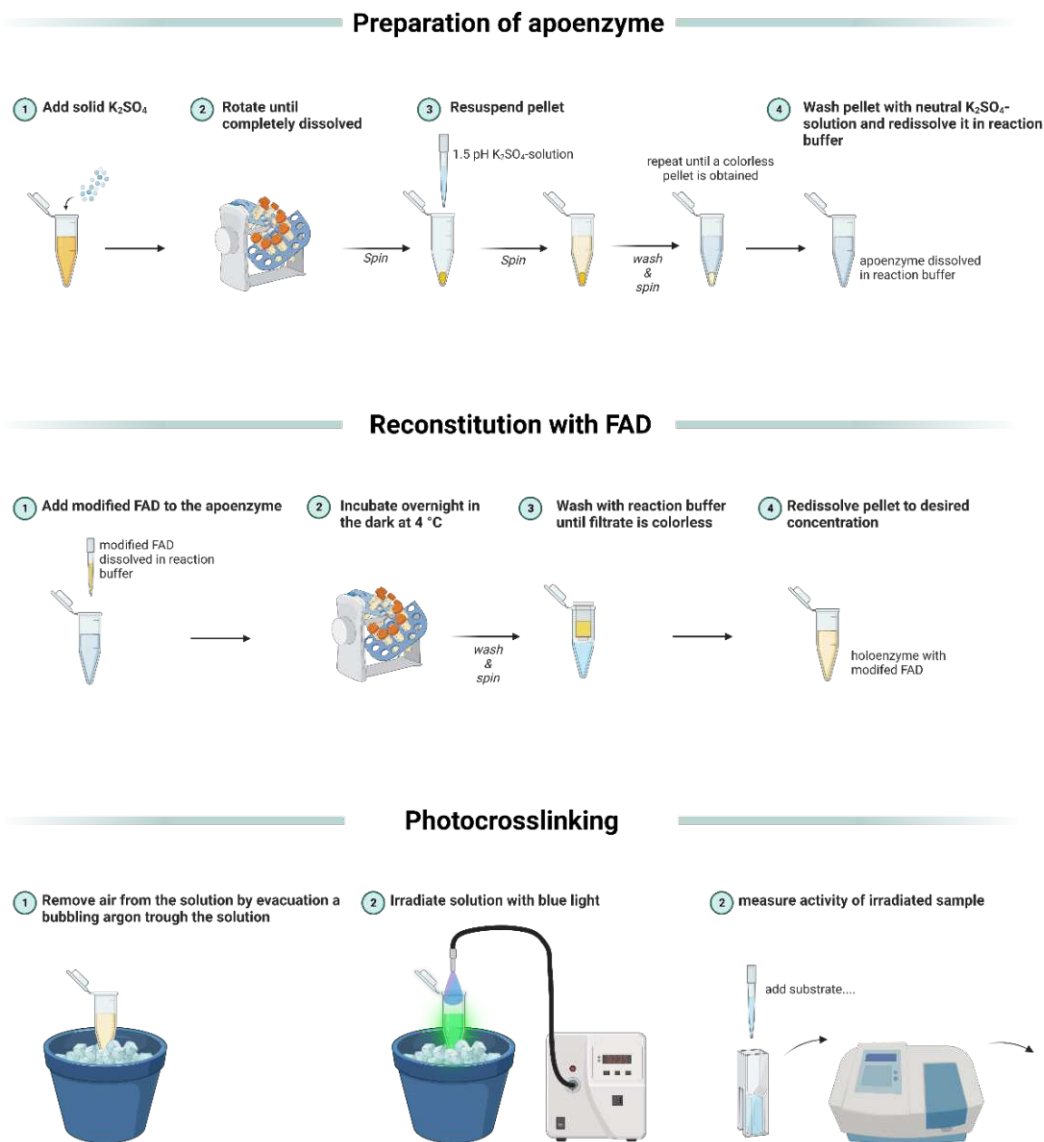


**Figure 55:** Workflow of the deflavination, reconstitution with diazirine-FAD derivatives, and photocrosslinking with the flavoenzymes GOx and CHD.

In summary, we deflavinated and reconstituted two enzymes with modified FADs. Two probes ([88] and [89]) were accepted as a cofactor, as they provided fully active semi-synthetic enzymes that were still active after UV-light irradiation. Furthermore, the formation of a new covalent bond was confirmed for CDH reconstituted with diazirine-FAD [89] using LC-MS/MS analysis. This confirms the principal validity of this genuinely novel approach for artificial cofactor incorporation into biocatalysts.

## C IV.2 Cyclohexanone monooxygenase

We next conducted further studies on the BVMO CHMO<sub>Acineto</sub>. Since CHMO<sub>Acineto</sub> is highly unstable, we postulated that, of the investigated enzymes, a covalently bound FAD would have the most significant effect on the stability.<sup>239,413</sup> Numerous studies have used protein engineering to boost thermodynamic stability; however, these variants showed lower activity than the wild-type enzyme.<sup>236-238</sup> In a recent study of our group, this trade-off was solved by the introduction of mutations in CHMO<sub>Acineto</sub> using a combination of rational and structure-guided consensus approaches.<sup>239</sup>

In the first step, the low binding affinity for the FAD cofactor was addressed by replacing a glycine residue with an alanine at position 14 (second position of the Rossmann fold), which was found in thermostable BVMOs (e.g., TmCHMO, PAMO). This G14A mutant showed an increase in activity (13%), thermodynamic stability (1.4 °C), and kinetic stability (30%) over the wild-type. Other mutations (library 1) at this position resulted in low or undetectable activities and lowered thermodynamic stabilities than the wild-type. In the second step, further optimization of the stability and activity was achieved by applying a structure-guided consensus approach. Seven mutants were selected and created using this methodology, whereby the best improvement in activity was found with substitution N336E (40% higher activity than the wild-type). Next, a second-generation library of mutants was designed by the combination of the best variants from the first generation, which resulted in further improvement of the activity (40% increase over wild-type) and thermodynamic and kinetic stability (up to 3 °C higher  $T_m$  and 3-fold half-life of the wild-type). Finally, a third library was created by combining the mutations of the second generation with three literature-known mutations that increase stability: a pair of mutations (T415C/A463C) that demonstrated to have a positive effect on kinetic stability (3-fold half-life);<sup>240</sup> and a replacement of oxygen-sensitive methionine by isoleucine (M400I), which showed to reduce the rate of unfolding.<sup>241</sup> The best variants from the third-generation library showed an increase in thermodynamic stability (+4 °C) and half-life time (5–8-fold that of the wild-type) and were 51–55% more active than the wild-type enzyme. These results clearly show that the stability and activity of CHMO<sub>Acineto</sub> can be enhanced by increasing the binding affinity of the FAD cofactor.

To assess the potential utility of our synthesized FAD analogs for improving the stability of CHMO<sub>Acineto</sub> through covalent bond formation, CHMO<sub>Acineto</sub> was first overexpressed in *Escherichia Coli* (for a detailed explanation, see E I.4), and the expression was confirmed by SDS-PAGE analysis (Figure 56). Next, the harvested cell pellets were re-suspended in disruption buffer (for more details, see E I.5.1), placed on ice, and sonicated. Finally, the cell

debris was removed by centrifugation, and the polyhistidine-tagged CHMO<sub>Acineto</sub> was purified on a Ni<sup>2+</sup>-Sepharose HP affinity column (Figure 57; for more details, see E I.5.1) to obtain purified holoenzyme.



**Figure 56:** SDS-Page result for the expression of CHMO<sub>Acineto</sub>.

To determine whether the diazirine-FAD probes would be accepted as a cofactor by CHMO<sub>Acineto</sub>, we had to remove the native FAD first. Since the native FAD is only weakly bound to CHMO<sub>Acineto</sub>, we opted to use a milder deflavination procedure.<sup>413</sup> To this end, the holoenzyme was again loaded on a Ni<sup>2+</sup>-Sepharose HP affinity column, and the native FAD was removed using a KBr-buffer (Figure 57), which weakens the interactions between FAD and the protein backbone. The apoprotein was then eluted by increasing the imidazole concentration (see E I.6.2 for further details).

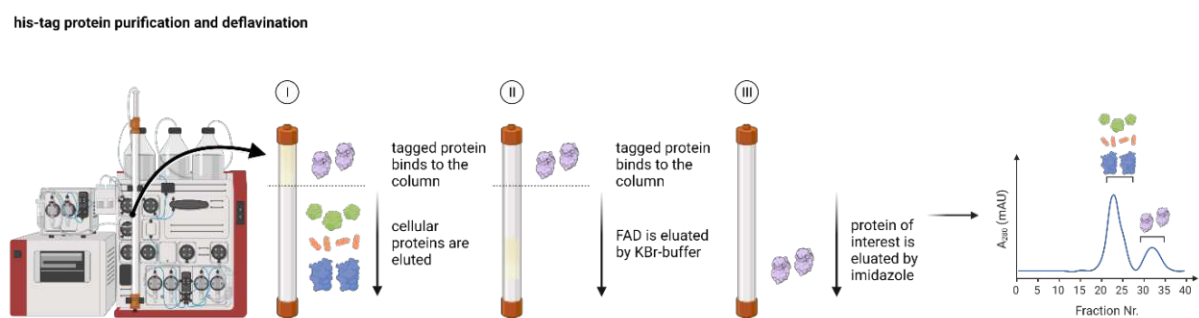


**Figure 57:** Workflow of the CHMO-purification and deflavination.

With the apoprotein in hand, we performed reconstitution with the modified FAD analogs and again with native FAD as a control experiment. We used a molar ratio of 1:100 of FAD:enzyme. Since CHMO<sub>Acineto</sub> is significantly more unstable than GOx and CDH, an aliquot of each sample was immediately removed, and the activity was measured (see Figure 58). The

rest of the samples were incubated overnight at 4 °C, after which rebuffering was performed to remove excess FAD, and the activity was measured.

As shown in Figure 58, the deflavination of CHMO<sub>Acineto</sub> was efficient since no activity of the apoenzyme was observed. The reconstitution of three of our FAD analogs ([85], [88], and [89]) provided fully active CHMOs<sub>Acineto</sub> with comparable activity to the control sample with the native FAD. These results implied that FAD analogs [85], [88], and [89] were correctly incorporated into the binding pocket of the enzyme. Additionally, since the reconstitution with diazirine-FADs [88] and [89] provided active GOx and CDH, the C-2' position of the ribose with altering the configuration is likely a suitable position for modifications for other flavoenzymes. The comparable low activity of the holoenzyme (first bar) could be explained by the excess FAD used for reconstitution of the other samples, which is known to enhance CHMO<sub>Acineto</sub> activity.<sup>413</sup> The prolonged incubation (22 hours) and rebuffering resulted in a severe decline in activity, conforming to the low stability of CHMO<sub>Acineto</sub>. Therefore, all subsequent experiments we conducted immediately after reconstitution.

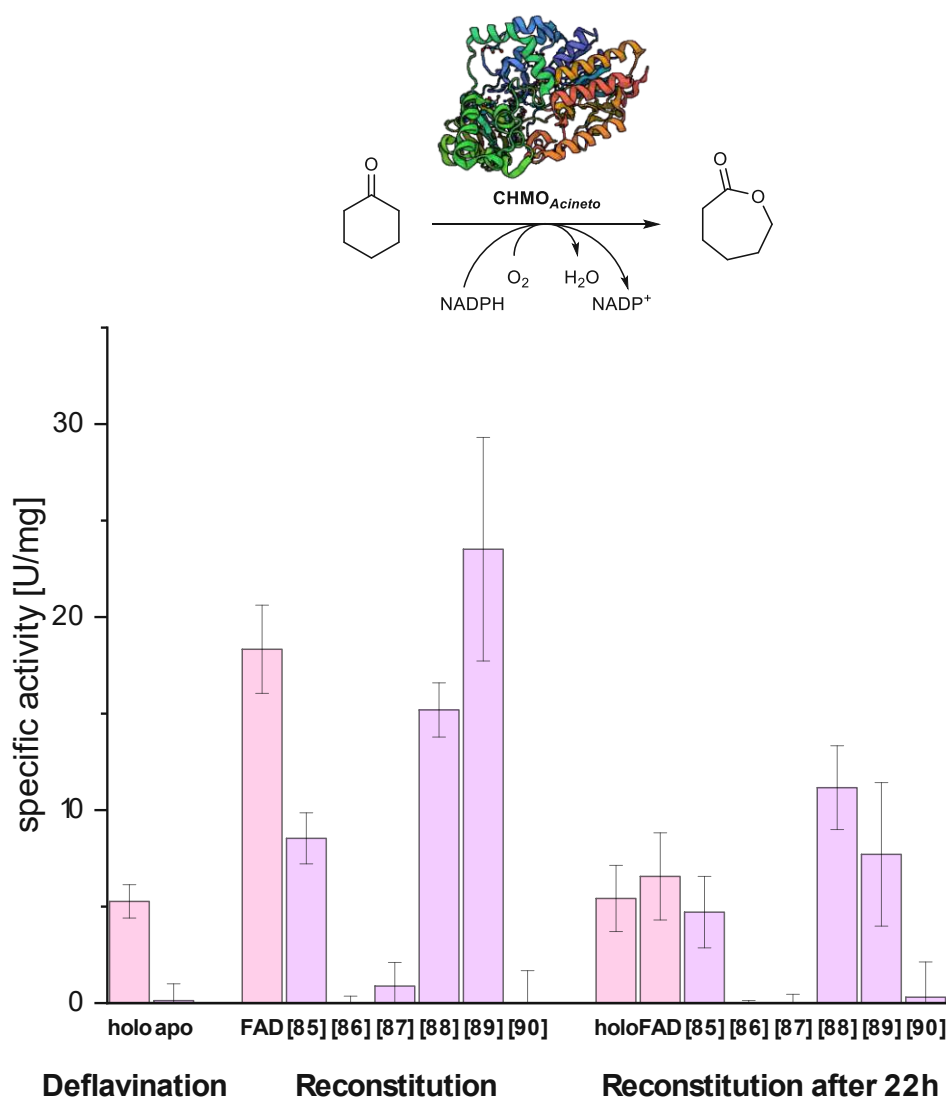


**Figure 58:** Activity of the enzyme CHMO after reconstitution with synthesized FAD analogs.

To demonstrate further that we could covalently link the diazirine-FADs to CHMO<sub>Acineto</sub>, we performed photoaffinity labeling on the reconstituted samples as previously described. However, we used 100 mM MOPS buffer since this has been reported as preventing excessive ROS formation and, thus, the degradation of the enzyme.<sup>412</sup> As shown in Figure 59, with the exception of FAD analog **[88]**, the irradiation did not seem to have the negative effect on the enzyme's activity previously observed.

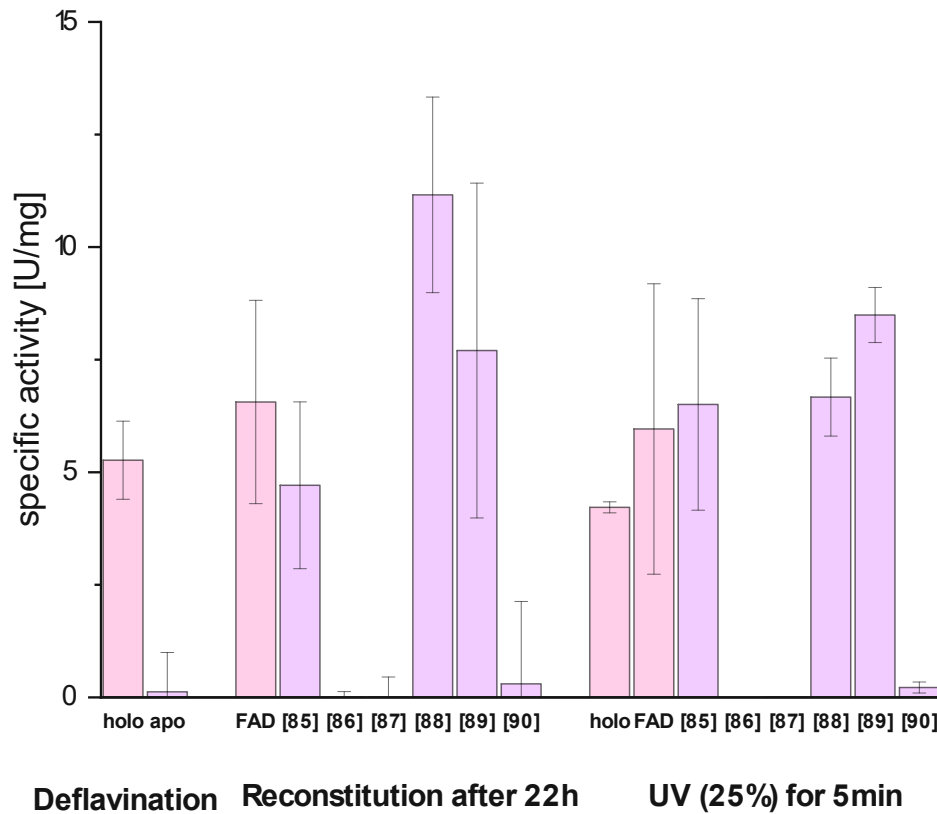


**Figure 59:** Activity of the enzyme CHMO after reconstitution with synthesized FAD analogs and irradiation.

Based on these results, we performed a second deflavination step on the enzyme reconstituted with the diazirine-FAD analog **[88]** to remove excess unbound FAD. To achieve this, we conducted deflavination as described above. Furthermore, to determine whether the enzyme was still active with a covalently bound FAD, we again measured the activity. We observed a significant drop in the enzyme activity compared to the sample that was not deflaminated a second time (see Figure 60), which implied that the covalent bond formation was inefficient and requires further optimization. Nevertheless, these findings demonstrated that the covalently attached cofactor was incorporated correctly into the binding site of CHMO<sub>Acineto</sub>.

To show further that the covalent bond formation was successful, we sought to analyze the photo-labeling by SDS-PAGE and in-gel fluorescence measurement. To this end, CHMO<sub>Acineto</sub> reconstituted with FAD analog **[88]** was subjected to various labeling conditions (Figure 61) of which one was also deflaminated a second time. All samples that were not deflaminated twice displayed efficient labeling, whereas the deflaminated sample did not show any fluorescence. We reasoned that the deflavination conditions may have caused degradation of the FAD, or a handling failure may have occurred during the experiment. Nevertheless, these findings revealed the successful crosslinking of FAD analog **[88]** to CHMO<sub>Acineto</sub>.

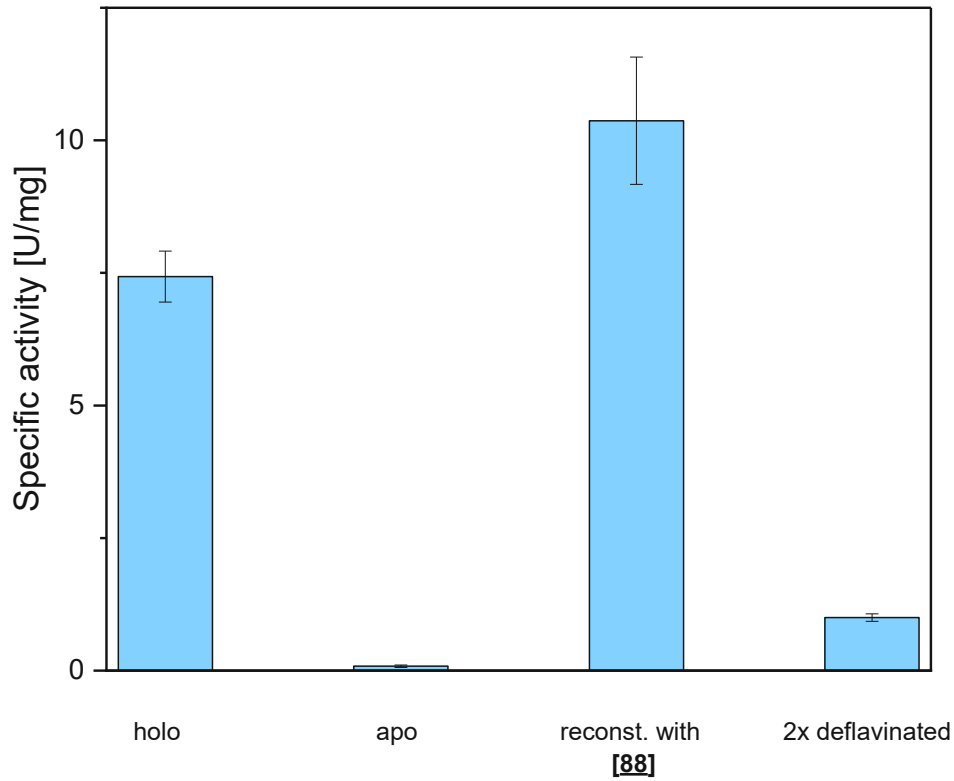


**Figure 60:** Activity of the enzyme CHMO after a second deflavination step.

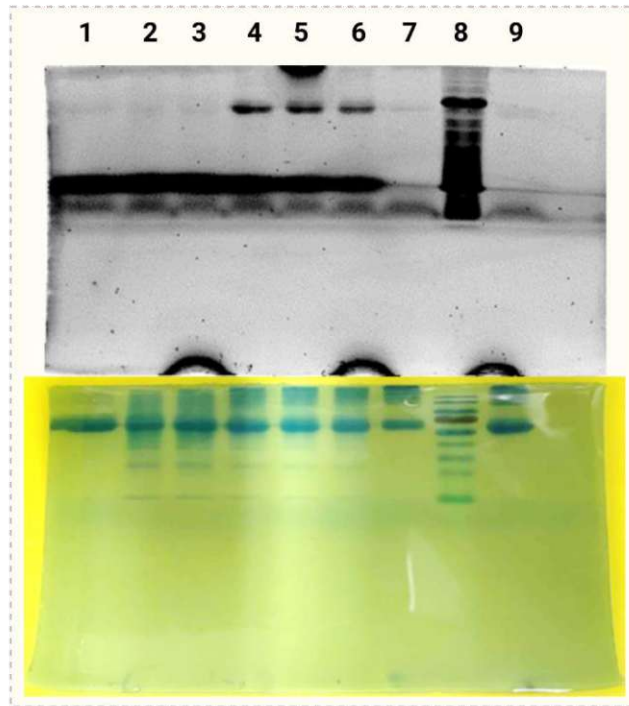


**Figure 61:** In-gel fluorescence analysis of the enzyme CHMO. **Line 1:** native holoenzyme; **Line 2:** CHMO reconstituted with native FAD and irradiated for 5 min (lamp intensity 25%); **Line 3:** CHMO reconstituted with native FAD and irradiated for 5 min (lamp intensity 100%); **Line 4:** CHMO reconstituted with [88] and irradiated for 5 min (lamp intensity 25%); **Line 5:** CHMO reconstituted with [88] and irradiated for 20 min (lamp intensity 25%); **Line 6:** CHMO reconstituted with [88] and irradiated for 5 min (lamp intensity 100%); **Line 7:** CHMO reconstituted with [88] and irradiated for 5 min (lamp intensity 25%) and deflavinated a second time after photocrosslinking; **Line 8:** Marker; **Line 9:** apoenzyme.



Finally, to assess whether covalent anchoring of the cofactor has the potential to improve the stability of cofactor-dependent enzymes, we analyzed the thermodynamic and kinetic stability of CHMO<sub>Acineto</sub> reconstituted with FAD probe [88]. First, the thermodynamic stability was determined using nano differential scanning fluorimetry as described in chapter C IV.1. However, no improvement in the  $T_m$ -value was observed (Figure 62).

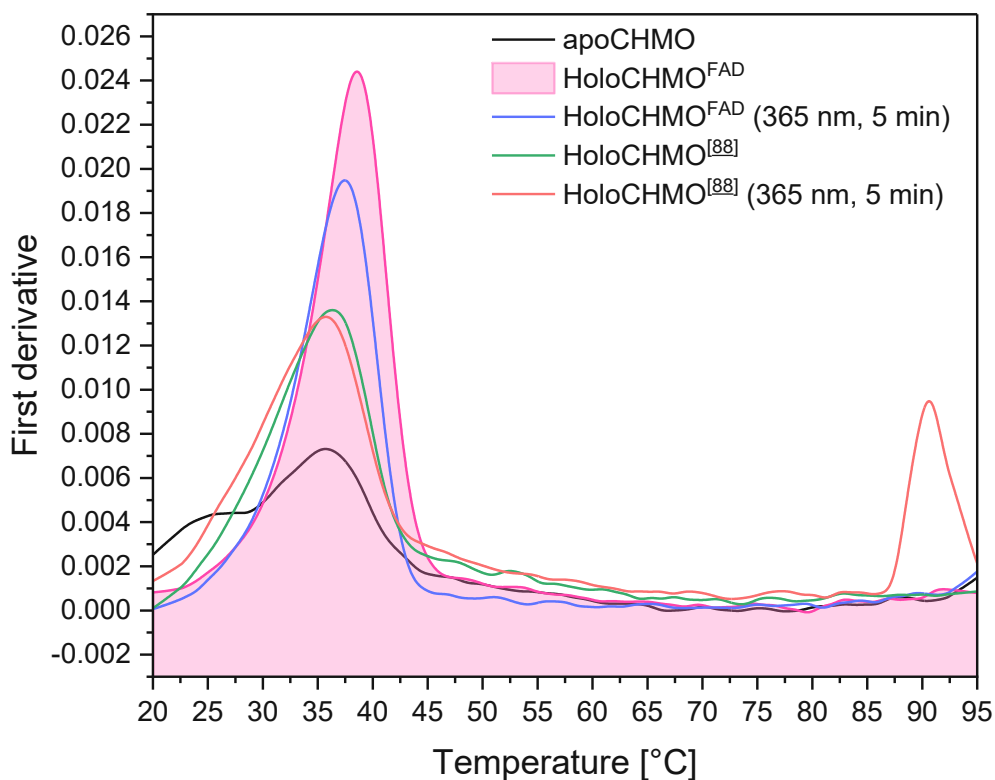


**Figure 62:** Measurement of the thermodynamic stability ( $T_m$ ) of the enzyme CHMO by nano differential scanning fluorimetry (nanoDSF). Note: The peak at  $\sim 90$  °C resulted from a device error and not from the enzyme.

Next, we investigated the kinetic stability of the semi-synthetic enzyme and compared it with that of the native CHMO<sub>Acineto</sub> by measuring the conversion of 4-phenylcyclohexanone [96] (for detailed reaction conditions, see E I.9).<sup>413</sup> Since it is converted at a low rate, 4-phenylcyclohexanone is suitable as a substrate;<sup>414</sup> it allows the measurement of kinetic stability over more than one period of  $t_{1/2}$ , while there is still substrate available.

As shown in Figure 63, the semi-synthetic CHMO showed a slower conversion than the native FAD, and according to these results, no increased kinetic stability was observed. However, the obtained data points fluctuated, so this experiment must be repeated to draw a reasonable conclusion. Furthermore, the experiment was conducted on a sample that was not deflavinated twice, implying that a large amount of unbound FAD is present, misrepresenting the results. Therefore, to obtain convincing results, the same experiment should be performed

with a sample in which only covalently bound FAD is present. However, the amounts of the sample obtained after the second deflavination step were too small to determine kinetic stability.

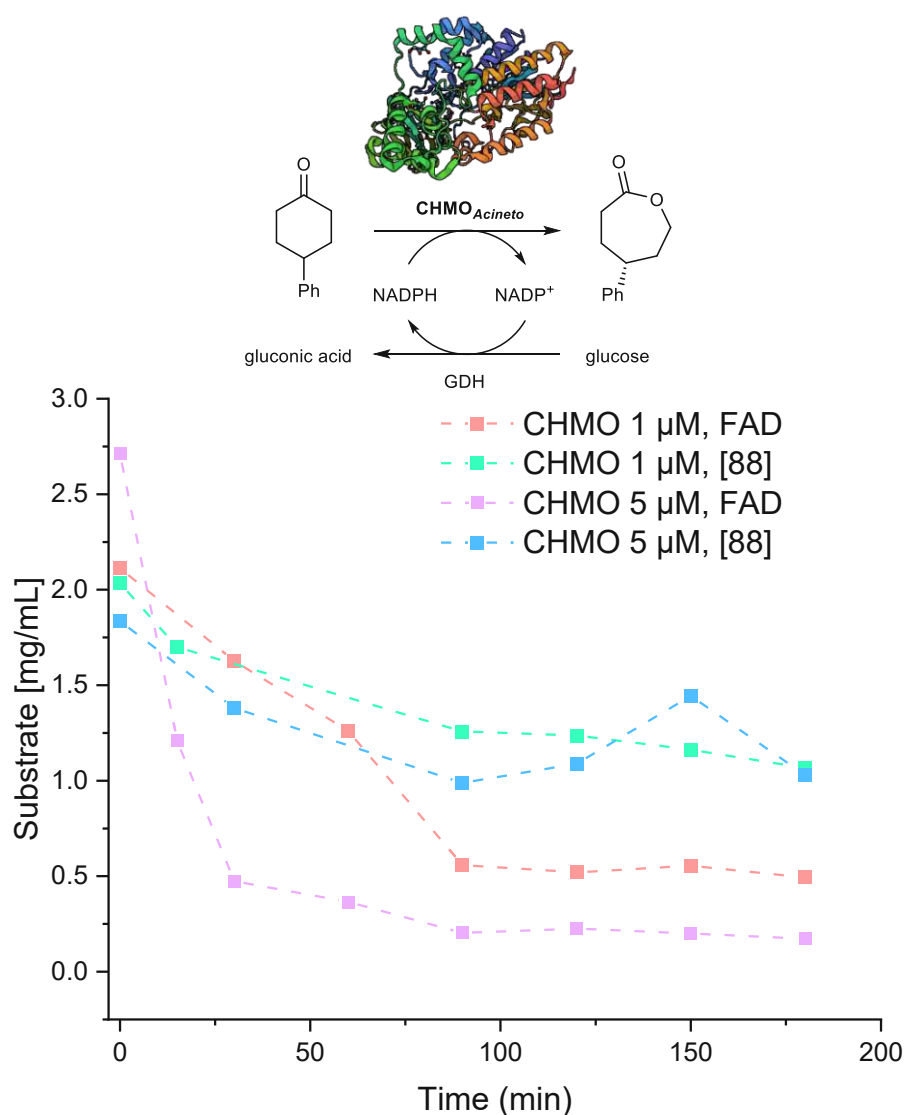


**Figure 63:** Measurement of the kinetic stability of the enzyme CHMO.

## C V Modifications of the riboflavin building block

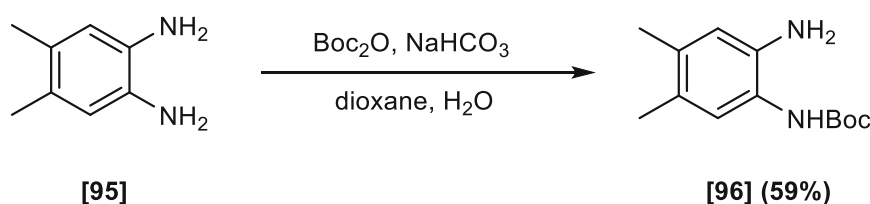
Since synthesis of FAD analogs modified at the adenosine moiety was prioritized, elaboration of FAD analogs adapted at the flavin moiety was in early stages at the time of writing this thesis. Nevertheless, this chapter describes the first steps taken towards the synthesis of modified riboflavin building blocks and the enzymatic coupling reaction.

## C V.1 Chemical synthesis of the riboflavin building block—First steps

The following sections deal with the synthesis of the first building blocks for synthesizing FAD analogs modified at the flavin moiety.

### C V.1.1 Protection of 4,5-dimethyl-1,2-phenylenediamine

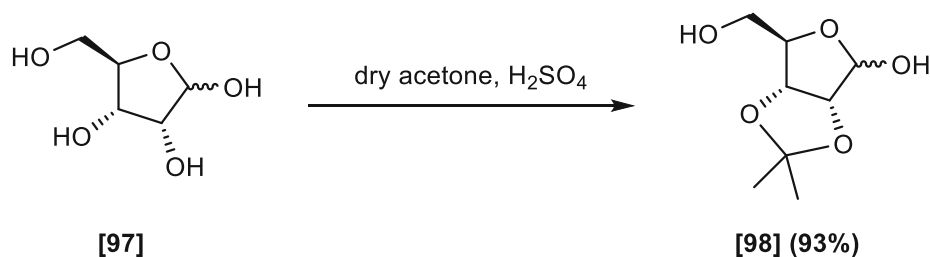
As outlined in chapter C I.4, the synthesis of modified riboflavin building blocks commenced with 4,5-dimethyl-1,2-phenylenediamine [95], which was mono-protected using the Boc-group. Then, [95] was treated with di-*tert*-butyl dicarbonate in the presence of NaHCO<sub>3</sub> in a solvent mixture of water and dioxane furnished crude [96]. Purification of the crude material via flash column chromatography afforded mono-protected diamine [96] in 59% yield.



**Scheme 66:** Mono-protection of diamine [95].

### C V.1.2 Protection of D-ribose

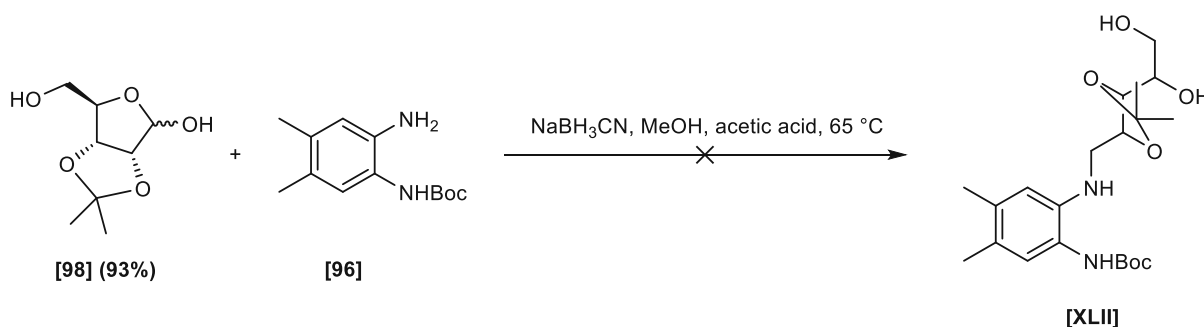
Using dry acetone as solvent and reagent and sulfuric acid as catalyst, the hydroxyl groups at the C-2 and C-3 positions of D-ribose [97] were protected as isopropylidene ketal. The protected D-ribose [98] was obtained in 93% yield and could be used without further purification.



**Scheme 67:** Synthesis of protected D-ribose [98].

## C V.1.3 Reductive amination

After achieving building blocks [96] and [98], we performed reductive amination to provide protected compound [XLII]. Similar to the procedure described in the literature,<sup>374,415</sup> unprotected [97], [96], and [98] and sodium cyanoborohydride were reacted in dry methanol under an argon atmosphere at 65 °C. We observed a new spot on the TLC after stirring the reaction overnight. However, when we isolated the new spot by flash column chromatography, we obtained a mixture of two compounds according to UHPLC-MS/UV and NMR analysis. We assumed the mixture to consist of the desired compound [XLII] and a side-product due to the migration of the protecting group. Hence, we tested other direct reductive amination conditions, but these resulted only in imine formation. Since the synthesis of the adenosine building block was prioritized, further work towards the modified riboflavin building block was halted. Nevertheless, the reductive amination may be successfully conducted by optimizing the conditions (e.g., reductive amination via catalytic hydrogenation) or changing the protecting groups.



**Scheme 68:** Attempted synthesis of compound [XLII].

**Table 9:** Screening of reductive amination conditions.

Reagent	Solvent	Result
NaBH <sub>3</sub> CN, acetic acid <sup>416</sup>	THF	isomers
NaBH <sub>3</sub> CN <sup>374</sup>	THF	isomers
Na(CH <sub>3</sub> COO) <sub>3</sub> BH <sup>417</sup>	CH <sub>3</sub> CN	Imine formation
Na(CH <sub>3</sub> COO) <sub>3</sub> BH <sup>417</sup>	THF	Imine formation
Na(CH <sub>3</sub> COO) <sub>3</sub> BH, acetic acid <sup>417</sup>	THF	Imine formation

## C V.1.4 Enzymatic conversion of riboflavin analogs to FAD

Since we targeted synthesizing FAD analogs amended at the flavin moiety by enzymatic pyrophosphate formation that starts from the corresponding riboflavin derivatives, we first sought to establish the enzymatic coupling reaction on native riboflavin [I].

### C V.1.4.1 Transformation of FAD synthetase gene into *E. coli*.

The FAD synthetase gene from *Corynebacterium ammoniagenes* was inserted to pET22b+ using the NdeI and NotI restriction sites (Figure 64).

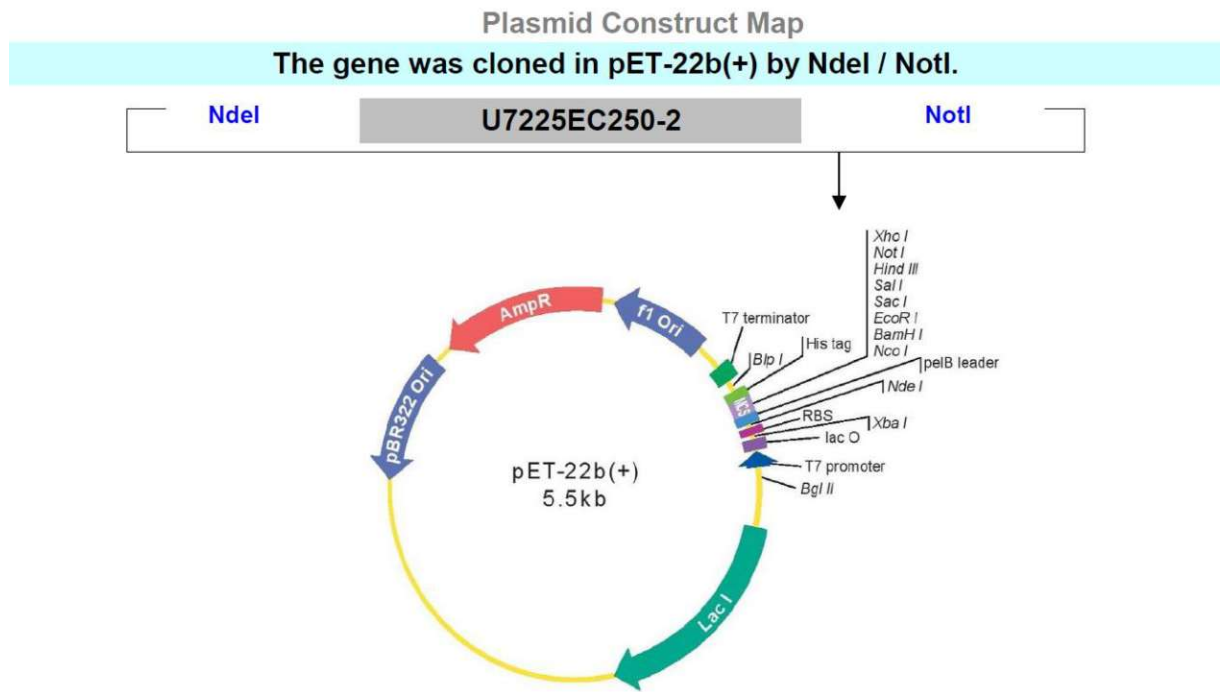


**Figure 64:** Plasmid construct map.

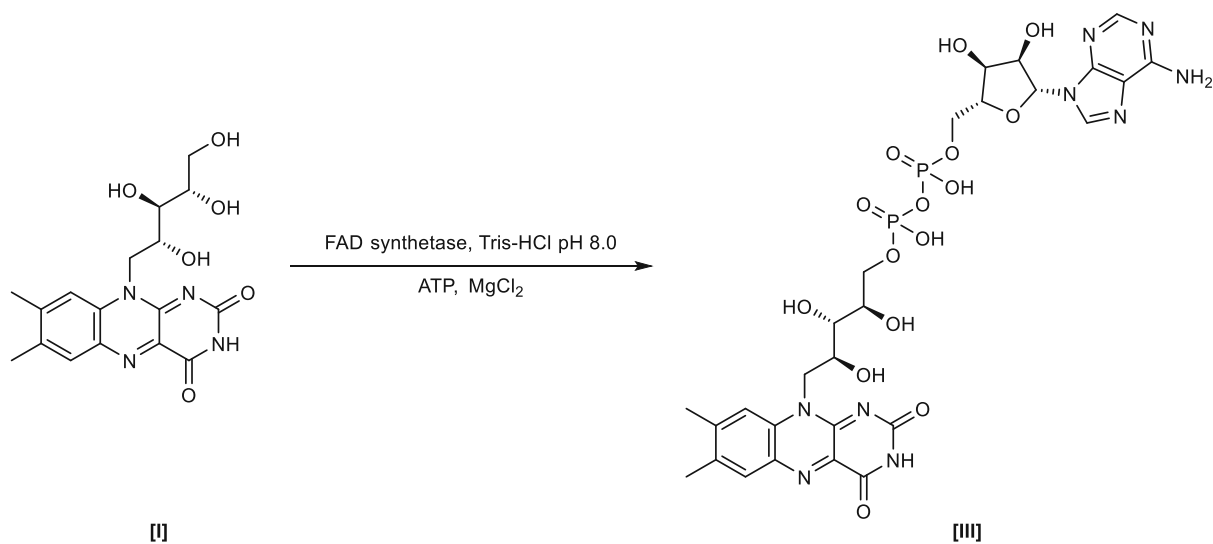
### C V.1.4.2 Enzyme expression and purification

*E. coli* BL21 DE(3) was used as the expression host and was transformed using a heat shock protocol. Furthermore, isopropyl- $\beta$ -D-thiogalactopyranoside (IPTG, 50  $\mu$ M) was used as the inducing agent for protein expression. This expression was conducted by adding IPTG at 20  $^{\circ}$ C for 20–22 hours (for more details, see E I.3).

Purification was performed using a standard His-Trap affinity column (explained in more detail in E I.5.2).

### C V.1.4.3 The enzymatic reaction using purified FAD synthetase

To assess the feasibility of the enzymatic FAD coupling reaction, we tested the coupling on commercially available riboflavin [I] and ATP. Following a literature protocol,<sup>92</sup> 1 or 5  $\mu$ M enzyme were added to a mixture of 50  $\mu$ M riboflavin and 1 mM ATP, and the reaction progressed at 37  $^{\circ}$ C. Aliquots were removed from the reaction mixture after selected time points and were analyzed by UHPLC-MS/UV.



**Scheme 69:** Enzymatic synthesis of FAD using FAD synthetase as catalyst and riboflavin and ATP as substrates.

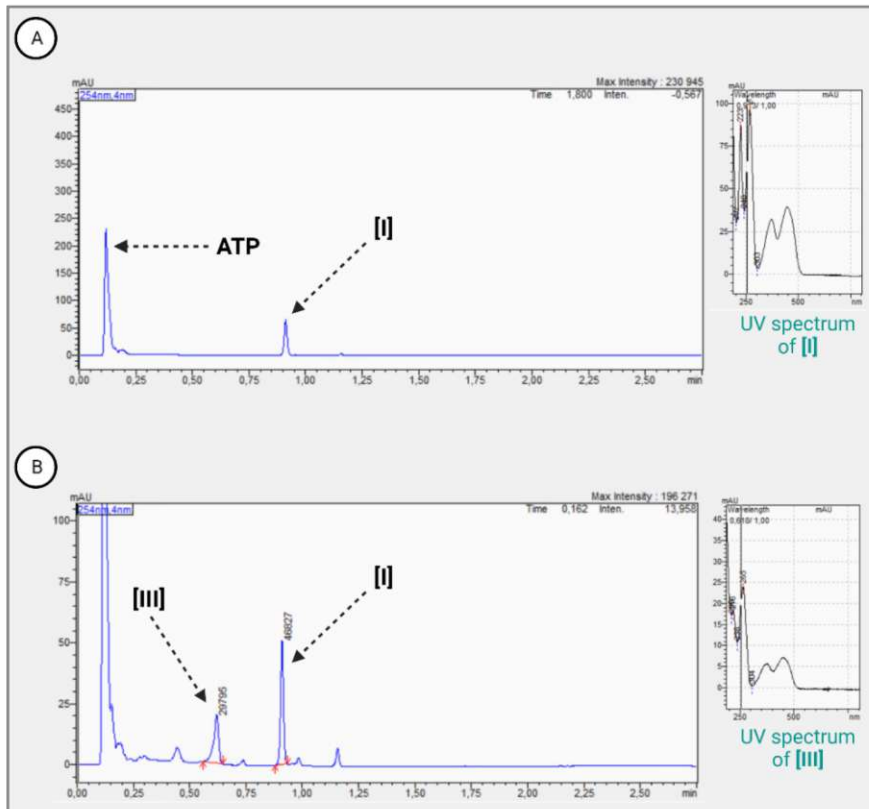


**Figure 65:** UV spectrum of the enzymatic synthesis of FAD. **A)** This spectrum shows the starting point of the reaction. **B)** This spectrum shows the reaction after 20 hours. After 20 hours of reaction time, the formation of FAD **[III]** could be confirmed by UPHLC-MS/UV analysis.

When 1  $\mu\text{M}$  of the enzyme was applied, we could only detect the formation of FAD **[III]** after 20 hours of reaction time, and much of the riboflavin **[I]** was still present (Figure 65). We then used 5  $\mu\text{M}$  of the enzyme, and the formation of FAD was confirmed after 1 hour. After 6 hours, all the riboflavin **[I]** was consumed (Figure 66).



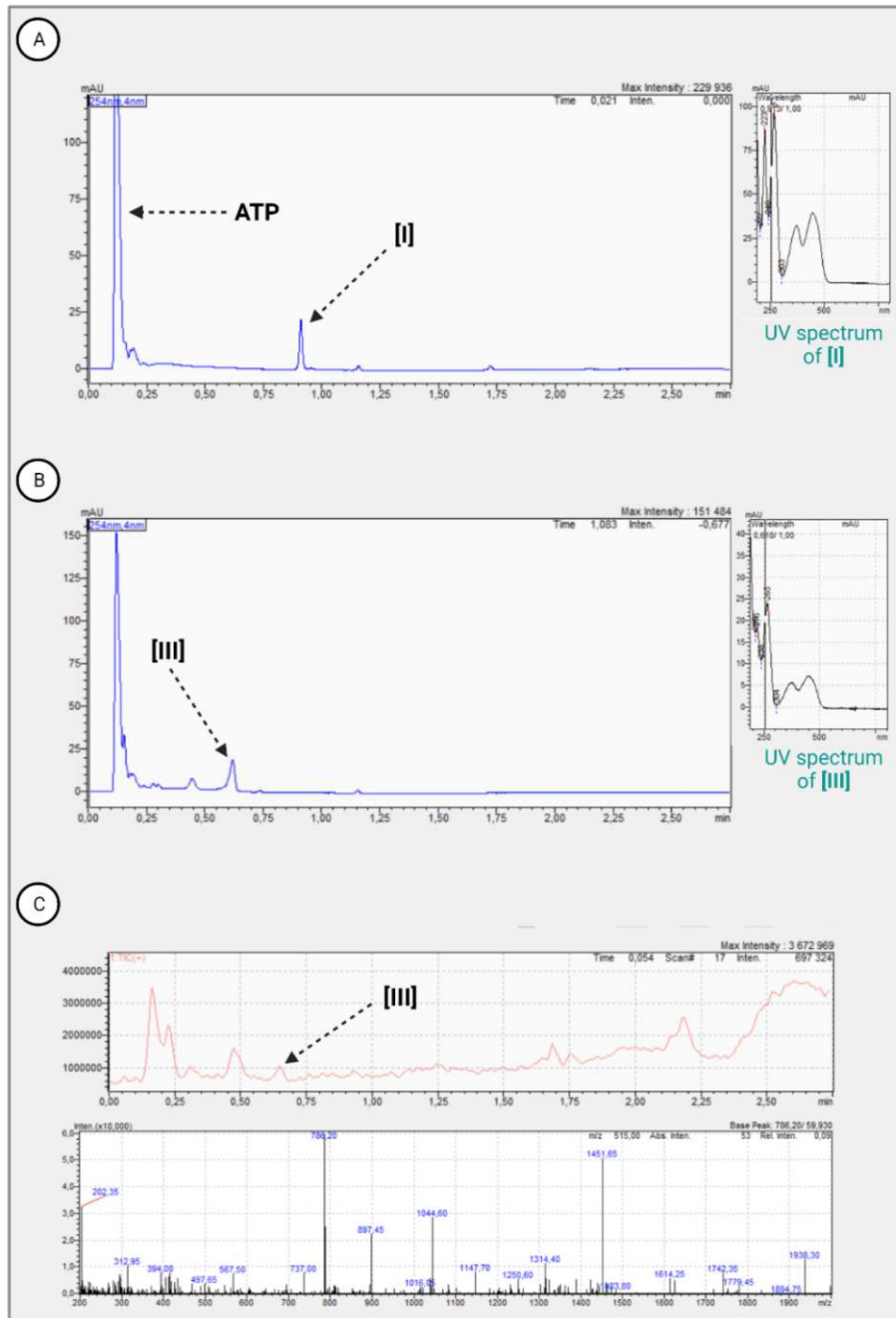


**Figure 66:** UV spectrum of the enzymatic synthesis of FAD. **A)** This spectrum shows the starting point of the reaction with a higher amount of the enzyme FAD synthetase (5  $\mu$ M). **B)** This spectrum shows the reaction after 6 hours. Using a five-fold concentration of the enzyme FAD-synthetase resulted in faster conversion of the riboflavin [I], which was consumed after 6 hours. **C)** Mass spectrum of the reaction after 6 hours with the fragmentation pattern of FAD [III].

## D Conclusion

Flavin-dependent enzymes represent an extraordinary class of biocatalysts that is important to industry and life. However, although the flavin cofactors enable their remarkable transformations, their cofactor dependency is a limitation. Typically, the cofactors are non-covalently bound to the enzymes, and their dissociation results in the loss of the enzymes' activities and stabilities. This drawback of flavoenzymes prevents their broad industrial application.

In this project, we aimed to develop a general approach for improving the stability of flavoenzymes by covalently binding the cofactor FAD to proteins of interest to prevent the cofactor's dissociation. Based on the photoaffinity labeling technique, covalent anchoring of the cofactor should occur only using a light stimulus, which allows tethering at will and thus enables the correct incorporation of the cofactor.

Therefore, we designed and synthesized FAD analogs bearing a diazirine moiety to allow covalent attachment. In a first approach (see chapter C II.5.5), we prepared esters of FAD by installing aliphatic and aromatic linkers bearing the diazirine group at the ribose unit of adenosine. However, the ester linkage was prone to hydrolysis, which prompted us to synthesize the corresponding amide derivatives. Their elaborate synthesis is described in chapter C II.6. Within this Ph.D. project, a set of six FAD analogs ([85]–[90]) was successfully synthesized. These compounds were modified at two positions of the ribose moiety of adenosine with varying stereochemistries on the modification sites. Before we further assessed the biological function of these new synthetic cofactors, we first gained broad experience of the photolysis reaction of the diazirine group by synthesizing various probes bearing a diazirine unit. Their photophysical behavior was further studied by capturing the formed carbene with solvent molecules or measuring the in-gel fluorescence with prepared fluorescent dyes (see chapter C III).

As described in chapter C IV, we assessed the feasibility of our novel stabilization approach by first removing the native FAD from three enzymes (GOx, CDH, and CHMO) and replacing it with our synthesized diazirine-FAD analogs [85]–[90]. Then, we evaluated whether the enzymes accepted the synthetic cofactors by measuring their activities. While GOx only accepted analog [88] as a cofactor by showing similar activity as the native FAD, CDH additionally allowed the incorporation of the bulky modification in [89], delivering an active enzyme for both compounds. The elucidation of the activity of the enzyme CHMO indicated that, along with analogs [88] and [89], FAD analog [85] was compatible and appropriately

incorporated into the binding site of FAD. Since all accepted FAD analogs exhibited modifications at the C-2' position of the ribose moiety of adenosine, C-2' adjustments on FAD would likely be an excellent choice for providing active enzymes in other flavoproteins. However, for clarification on why analogs [85], [88], and [89] provided active enzymes while all others did not, further studies using *in-silico* modeling are necessary.

We next performed an extensive assessment of the covalent anchoring of our synthesized analogs and the characteristics of the obtained semi-synthetic enzymes. UV-irradiation was used to initiate the covalent attachment and resulted in a drop in activity. The formation of oxygen radical species likely caused this drop; by excluding oxygen and switching the buffer system from Tris-HCl to MOPS, which proved beneficial in a previous study,<sup>413</sup> we minimized the loss in activity. However, loss of activity remained the limitation for longer irradiation times and, therefore, better cross-linking efficiency. The measurement of thermal stability did not reveal any improvement for the three enzymes, and preliminary results of kinetic stability also indicated no development. However, further studies are needed to draw reasonable conclusions.

In chapter C IV.2, we described a second deflavination procedure used on the enzyme CHMO<sub>Acineto</sub>, which was reconstituted with analog [88] to remove all unbound FAD after the covalent bond formation. Measurement of the activity showed an active enzyme with about one-tenth of the activity of the holoenzyme, which indicated the correct incorporation of the covalent bound FAD analog [88]. However, the vast drop in activity compared to the enzyme deflavinated once further reinforces the supposition of inefficient labeling.

As detailed in chapter C V, we synthesized the first building blocks for FAD analogs modified on the flavin moiety. Additionally, we established the enzymatic coupling of native riboflavin and ATP by using the enzyme FAD synthetase. Based on this result, we aimed to synthesize FAD analogs modified at the flavin moiety. Nevertheless, the elaboration of modifications of the riboflavin building blocks is still in early stages and their synthesis and enzymatic coupling can be realized in a future project.

Although the central aim of this project—stabilizing flavoproteins by covalently attaching the cofactor FAD to the protein structure—has not yet been accomplished, we are convinced that further optimization of the photolysis conditions will result in better crosslinking efficiency and delivery of thermostable flavoenzymes. When further improved, this methodology will represent a unique and novel approach for stabilization of flavoenzymes and will enhance their applicability in biocatalysis and biosensing.

# E Experimental part

## E I Materials and methods—standard microbiological techniques

Unless otherwise notified, all chemicals, reagents, and enzymes were purchased from commercial suppliers and used without further purification. All the glass equipment and plastic consumables were either sterilized before use by autoclaving (121 °C, 20 min, > 15 psi) or were sterile upon purchase.

### E I.1 Standard buffer solutions and media

#### E I.1.1 Buffers

Photochemical experiments were carried out in one of the following solutions, which were prepared in MillW water and the pH set with 1 M NaOH or 1 M HCl:

- A) 100 mM MOPS buffer (3-(*N*-Morpholino)propanesulfonic acid, > 99.5%);
- B) 100 mM Tris-HCl buffer (Tris base, > 99.0%);

#### E I.1.2 Media

##### E I.1.2.1 Standard media

**Table 10:** Composition of standard media for bacterial cell growth.

LB Medium (400 mL)	TB Medium (400 mL)
4 g bacto-peptone	4.8 g bacto-tryptone
2 g yeast extract	9.6 g yeast extract
4 g NaCl	0.9 g KH <sub>2</sub> PO <sub>4</sub>
-	5 g K <sub>2</sub> HPO <sub>4</sub>

Standard media were sterilized by autoclaving and stored at room temperature.

## E I.1.2.2 Autoinduction media

**Table 11:** Composition of the autoinduction media.

LB-08G (400 mL)	LB-5052
4 g bacto-peptone	4 g bacto-peptone
2 g yeast extract	2 g yeast extract
4 g NaCl	4 g NaCl
0.4 mL 1 M MgSO <sub>4</sub>	0.4 mL 1 M MgSO <sub>4</sub>
8 mL 40% (w/v) glucose	8 mL 50 x 5052
20 mL 20 x NPS	20 mL 20 x NPS

Glucose and glucose-containing solutions were added at last and sterilized by filtration. All other components were dissolved in water and sterilized by autoclavation.

## E I.2 SDS-PAGE

**Table 12:** Reagents for SDS-PAGE

30% (w/v) Acrylamide (100 mL)	10% (w/v) APS (10 mL)
29.2 g acrylamide	1 g APS
0.8 g <i>N,N</i> -bis-methylene acrylamide	-

Reagents were sterilized by filtration. 30% (w/v) acrylamide was stored in an amber bottle. Reagents were stored at 4 °C.

**Table 13:** Buffers used for SDS-Page.

10 x SDS running buffer (1000 mL)	Resolving gel buffer (250 mL, pH 8.8)	Stacking gel buffer (50 mL, pH 6.8)	Sample buffer
30.3 g trizma base	46.2 g Tris (1.5 M)	15.1 g Tris (0.5 M)	7.3 mL MilliQ water
144 g glycine	10 mL 10% (w/v) SDS	10 mL 10% (w/v) SDS	2.3 mL stacking gel buffer
10 g SDS	2 M HCl for pH adjustment	2 M HCl for pH adjustment	4 mL 10% (w/v) SDS
-	-	-	0.2 mL 1% (w/v) bromphenol blue
-	-	-	5 mL glycerol
-	-	-	1 mL β-mercapto ethanol

Buffers were autoclaved/filtered for sterilization and stored at room temperature.

## **E I.2.1 Gel staining**

The gel was removed from the cassette after electrophoresis, and the stacking gel was removed carefully. The resolving gel was placed in the staining box and covered with distilled water, and microwaved at 750 W for 1 min. Subsequently, the gel was shaken for 2 min at room temperature (PSU-10i, Grant-bio). The distilled water was removed and replaced with fresh distilled water. Then, the mixture was microwaved at 500 W for 1 min and shaken for 2 min. The water was removed, the dyeing solution (SimplyBlue™ SafeStain; LC6065, Novex®) was added, and microwaved at 350 W for 1 min. Next, the gel was shaken at room temperature for 10 min. The dyeing solution was removed, and the gel was placed in distilled water and shaken for 10 min. Finally, the water was removed, and the gel was scanned for documentation.

## **E I.3 Transformation of *E. coli* competent cell**

### **E I.3.1 Heat shock transformation**

The NEB transformation protocol for *E. coli* BL21 (DE3) was used for the plasmid transformation. First, 50 µL of the chemically competent *E. coli* BL21 (DE3) cells stored at -80 °C were thawed for 5 min on ice. Subsequently, plasmid DNA (1-5 µL, 1 pg - 100 ng) was added to the cell suspension and incubated for 30 min on ice. Next, the cells were heat-shocked at 42 °C for 1 min and then immediately placed on ice for 2 min. SOC-Medium (950 µl), warmed to 37 °C, was then added, and the cells were incubated at 37 °C, 200 rpm for 1 hour. The cell suspension was then diluted ten-fold in LB medium, and 50-100 µL were stroke-plated on an LB-Agar plate (warmed to 37 °C) supplemented with the appropriate antibiotic and incubated upside down at 37 °C for 17 hours.

## **E I.4 Growth of bacterial cells for enzyme expression and isolation**

### **E I.4.1 CHMO**

CHMO<sub>Acineto</sub> (cyclohexanone monooxygenase from *Acinetobacter calcoaceticus* NCIMB 9871) was expressed in *E. coli* strain BL21(DE3). Lysogeny broth (LB) 0.8G medium (12 mL) supplemented with ampicillin (100 µg mL<sup>-1</sup>) was inoculated with *E. coli* BL21(DE3) pET22b(+)\_CHMO<sub>Acineto</sub><sup>418</sup> and incubated in an orbital shaker at 37 °C, 150 rpm overnight. The cultures (0.2% v/v) were transferred to a 1 L baffled Erlenmeyer flask containing 200 mL LB autoinduction (LB-5052) medium supplemented with ampicillin (100 µg mL<sup>-1</sup>) and shaken at 150 rpm and 37 °C for 4 h. The flask was transferred to 20 °C and incubated for 20 h. Cells were harvested by centrifugation (4000 x g, 4 °C, 15 min).

### **E I.4.2 FAD synthetase**

Lysogeny broth (LB) medium (10 mL) supplemented with ampicillin (100 µg mL<sup>-1</sup>) was inoculated with a single colony containing the DNA coding regions for FAD synthetase (FAD synthetase expressed in *E. coli* strain BL21 (DE3)). The culture was grown overnight at 37 °C in an orbital shaker at 200 rpm. The next day, the ON-culture was transferred to a 1 L Erlenmeyer flask containing 250 mL of a TB/ampicillin medium, which was shaken at 200 rpm and 37 °C for approximately 2.5 hours to a final optical cell density at 600 nm of 0.6-0.8. Isopropyl-β-D-thiogalactopyranoside (IPTG, 50 µM) was used as an inducer for the expression of FAD synthetase. The culture was incubated for 18–22 hours at 20 °C. Finally, cells were harvested by centrifugation (15 min, 6000 rpm).

## **E I.5 Enzyme purification**

### **E I.5.1 CHMO**

Cell pellets were re-suspended in 50 mM Tris-HCl buffer, pH 7.5, containing 0.1 mM phenylmethylsulfonyl fluoride (PMSF) and 0.1 mM FAD. Cells were placed on ice and sonicated using a Bandelin KE76 sonotrode connected to a Bandelin Sonoplus HD 3200 in 9



cycles (5 s pulse, 55 s break, amplitude 50%). Cell debris was removed by centrifugation (15000 × g, 4 °C, 45 min), and the clarified supernatants containing the polyhistidine-tagged CHMO<sub>Acineto</sub> was loaded on a Ni<sup>2+</sup>-Sepharose HP affinity column (5 mL, GE Healthcare bioscience) equilibrated with 50 mM Tris-HCl buffer, pH 8.0, containing 0.5 M NaCl. Enzymes were eluted in 4 column volumes within a linear gradient from 25 to 250 mM imidazole in 50 mM Tris-HCl buffer, pH 8.0, containing 0.5 M NaCl. Fractions containing the enzymes (identified by measuring the UV-absorbance of the eluting fractions) were pooled, desalted, washed with 50 mM Tris-HCl, pH 8.5, and concentrated by ultrafiltration by using ultracentrifugal tubes with a cut-off of 10 kDa.<sup>413</sup> Protein concentrations were determined by measuring the UV-absorbance at 280 nm (NanoDrop 2000, Thermo Scientific).

## **E I.5.2 FAD synthetase**

Cell pellets were resuspended in 50 mM Tris-HCl buffer, pH 8.0, containing 0.1 mM phenylmethylsulfonyl fluoride (PMSF). Cells were placed on ice and sonicated in 12 cycles (5 s pulse, 55 s break, amplitude 50%). Precipitates were removed by centrifugation (45 min, 12000 rpm), and the clear supernatant containing the polyhistidine-tagged FAD synthetase was loaded on a 5 mL Ni<sup>2+</sup>-sepharose HP affinity column (chromatographic equipment and materials from GE Healthcare bioscience) equilibrated with 50 mM Tris-HCl buffer, pH 8.0. The enzyme was eluted within a linear gradient from 25 to 250 mM imidazole in 4 column volumes. Fractions containing the enzyme were identified by SDS-PAGE analysis, pooled, desalted, washed with 50 mM Tris-HCl pH 8.5, and concentrated by ultrafiltration using ultracentrifugal tubes with a cut-off of 10 kDa. Protein concentration was determined by the dye-binding method of Bradford using a prefabricated assay (BioRad) and bovine serum albumin as the calibration standard.

## **E I.6 Deflavination and Reconstitution**

### **E I.6.1 Deflavination of GOx and CDH**

FAD-free apo-GOx and apo-CDH were generated by an acidic ammonium sulfate precipitation procedure,<sup>419</sup> further optimized by our collaborators. All steps were conducted on ice. To a solution of the respective holoenzyme (450 μL, protein concentration 5 mg/mL) and 2 M KBr (50 μL) was added solid ammonium sulfate (NH<sub>4</sub>SO<sub>4</sub>) to obtain a 90% solution (~0.33



g  $\text{NH}_4\text{SO}_4/0.5$  mL). Next, 500  $\mu\text{L}$  saturated acidic  $\text{NH}_4\text{SO}_4$  solution (pH 1.4) was added, and the solution was centrifuged at 16.000 rpm and 4 °C for 3 min. The pellet was washed with saturated acidic  $\text{NH}_4\text{SO}_4$  solution and centrifuged again. This procedure was repeated until a colorless pellet was obtained (~3 washing steps for GOx and 8 for CDH). Finally, the pellet was washed once with saturated  $\text{NH}_4\text{SO}_4$  solution (pH 6) and centrifuged. The apoprotein was redissolved in 50 mM potassium phosphate buffer (KPB) (pH 7.0). Denatured protein was removed by centrifugation (10 min, 16.000 rpm, 4 °C).

## E I.6.2 Deflavination of CHMO

FAD-free apo-CHMO was generated by column chromatography.<sup>413</sup> Therefore, cleared cell-free extracts were re-suspended in 50 mM Tris-HCl buffer, pH 8.0, containing 0.5 M NaCl and 25 mM imidazole, and loaded onto a  $\text{Ni}^{2+}$ -Sephacrose HP resin (5 mL, GE Healthcare) equilibrated with the same buffer. After loading the extract at a flow rate of  $0.5 \text{ mL min}^{-1}$ , the protein-bound FAD was removed by washing the column with 250 mM phosphate buffer, pH 8.0, containing 3 M KBr. This resulted in a column-bound apo-form of the protein, which was eluted with 50 mM Tris-HCl buffer, pH 8.0, containing 0.5 M NaCl and 250 mM imidazole at a flow rate of  $5 \text{ mL min}^{-1}$ . The apoenzyme was desalted, washed with 50 mM Tris-HCl, pH 8.5, and concentrated by ultrafiltration using ultracentrifugal tubes with a 10 kDa cut-off.

## E I.6.3 Reconstitution

Apoproteins were reconstituted according to the following procedure. First, to 30  $\mu\text{M}$  apoenzyme in an Eppendorfer tube was added 10  $\mu\text{L}$  native FAD or its analogs (dissolved in MilliQ water, 30 mM stock solution) to obtain a concentration of 3 mM (100-fold excess). The solution was incubated in the dark at 4 °C on a rotary shaker for 1 hour (CHMO) or overnight (GOx and CDH). After reconstitution, unbound FAD was removed by buffer exchange using ultracentrifugal tubes with 30 kDa cut off to 50 mM KPB. Activities of reconstituted enzymes were assessed before and after UV light irradiation.

## **E 1.7 Photolysis experiments**

### **E 1.7.1 Photolabeling of proteins with diazirine-comprising dyes**

To a solution of 10  $\mu\text{M}$  protein (BSA, GOx, or CDH) in HPLC-grade water (1 mL) was added dye [92] to a final concentration of 33  $\mu\text{M}$  (or 330  $\mu\text{M}$ ). The mixtures were incubated at 4 °C in the dark for 1 hour. Samples were taken and split into equal volumes and either left non-irradiated or exposed to UV light. UV light irradiation was performed on ice using OmniCure® S2000 Spot UV curing system with a 365 nm bandpass filter. The lamp was placed at a 2 cm distance from the test tube. Samples were taken at specific time points and analyzed by 12% SDS-polyacrylamide gel electrophoresis (SDS-PAGE), followed by fluorescence scanning (Typhoon™ FLA9500 biomolecular imager, GE Healthcare; or ChemiDoc XRS+, Biorad) with excitation at 532 nm, and 555 nm emission filter.

### **E 1.7.2 Photolabeling of enzymes with diazirine-FADs**

Protein solutions were kept on ice during the photolabeling procedure, and exposure to light was minimized to prevent unintended crosslinking. Solutions (100  $\mu\text{L}$ ) of reconstituted enzymes (30  $\mu\text{M}$ ) in Eppendorfer tubes were degassed by repeatedly evacuating and purging the solutions with  $\text{N}_2$  over 15 min. The degassed samples were then subjected to UV light irradiation for 5 min using OmniCure® S2000 Spot UV curing system with a 365 nm bandpass filter. The lamp was placed at a 2 cm distance from the test tube. The Eppendorfer tube was purged with argon during the UV irradiation to impede ROS formation. Irradiated samples were further subjected to activity assays, LC-MS/MS analysis, or in-gel fluorescence studies.

## **E 1.8 Activity measurement**

### **E 1.8.1 ABTS-Assay**

Glucose oxidase activity was measured via an ABTS assay.<sup>420</sup>

**Table 14:** Assay composition.

Stock solution	Volume [ $\mu\text{L}$ ]	Final concentrations
KPB (60 mM, pH 6.5)	840	-
Horseradish peroxidase (HRP) ~285.6 U/mL)	20	~6 U/mL
ABTS (50 mM)	20	1 mM
Glucose (1 M)	100	100 mM
Enzyme (GOx)	20	0.02 $\mu\text{M}$
Assay total volume	1000	-

All solutions were prewarmed to 30 °C and the reaction was started by the addition of 20  $\mu\text{L}$  enzyme (properly diluted in KPB). The absorbance was measured at 420 nm for 180 s.

## E I.8.2 DCIP-Assay

Cellobiose dehydrogenase activity was measured via a DCIP assay.<sup>421,422</sup>

**Table 15:** Assay composition.

Stock solution	Volume [ $\mu\text{L}$ ]	Final concentrations
NaOAc (65 mM, pH 5.5)	780	-
DCIP (3 mM)	100	300 $\mu\text{M}$
Glucose (1 M)	100	100 mM
Enzyme (CDH)	20	0.02 $\mu\text{M}$
Assay total volume	1000	-

All solutions were prewarmed to 30 °C and the reaction was started by the addition of 20  $\mu\text{L}$  enzyme (properly diluted in NaOAc pH 5.5). The absorbance was measured at 520 nm for 180 s.

## E I.8.3 NADPH-Assay

CHMO activity was measured via a NADPH assay.<sup>413</sup>

**Table 16:** Assay composition.

Stock solution	Volume [ $\mu$ L]	Final concentrations
Tris-HCl (50 mM, pH 8.0)	876	-
Cyclohexanone (5 mM, dissolved in EtOH)	100	0.5 mM
NADPH (25 mM)	4	100 $\mu$ M
Enzyme (CHMO)	20	0.02 $\mu$ M
Assay total volume	1000	-

The buffer solution was prewarmed to 30 °C and cyclohexanone and the enzyme were added. The reaction started immediately with the addition of NADPH. The absorbance was measured at 340 nm for 120 s.

## E I.9 Conversion reactions – Kinetic stability of CHMO

The stability of CHMO under turn over conditions was determined by running a reaction set-up as reported previously.<sup>413</sup>

**Table 17:** Assay composition.

Stock solution	Volume [ $\mu$ L]	Final concentrations
Tris-HCl (50 mM, pH 8.5)	705 or 480	-
4-Phenylcyclohexanone (20 mM, dissolved in EtOH)	150	2 mM
NADPH (10 mM)	15	100 $\mu$ M
Glucose (200 mM)	150	20 mM
GDH (NAD <sup>+</sup> /NADP <sup>+</sup> -dependent glucose dehydrogenase from <i>Bacillus sp.</i> , 100 U/mL)	300	20 U/mL
SOD (superoxide dismutase, recombinantly expressed in <i>E. coli</i> , Sigma Aldrich, ~4120 U/mL)	7	~20 U/mL
CAT (catalase from bovine liver, Sigma Aldrich, ~10000 U/mL)	23	~150 U/mL
Enzyme (CHMO, 20 $\mu$ M)	150 or 375	2 or 5 $\mu$ M
Assay total volume	1500	-

All solutions were prewarmed to 30 °C under constant shaking. The reaction was started by the addition of the enzyme. Samples were taken regularly, and the extraction of the substrate/product was performed immediately in EtOAc. The reaction progress was monitored via quantification of the remaining substrate of the EtOAc extracts by calibrated GC.

## **E I.10 Enzymatic FAD synthesis (FAD synthetase)**

To assess the FAD synthetase activity, the following literature protocol was used.<sup>92</sup> For activity assays, 1 or 5  $\mu\text{M}$  enzyme was added to a 2 mL reaction mixture containing 50  $\mu\text{M}$  riboflavin, 1 mM ATP, and 10 mM  $\text{MgCl}_2$  in 50 mM Tris-HCl pH 8.0, and the biotransformation was incubated at 37 °C. Aliquots (200  $\mu\text{L}$ ) were removed from the reaction mixture after specific time points (0 hours, 1 hour, 6 hours, 12 hours, 20 hours) and added to an Eppendorfer vial containing 200  $\mu\text{L}$  of a 1:1 mixture of MilliQ water and MeOH (HPLC-grade). The mixture was mixed and filtrated over a syringe filter (0.2  $\mu\text{L}$ ) into an HPLC vial. This solution was used for UHPLC-MS/UV analysis.

## **E I.11 Protein concentration**

### **E I.11.1 Bradford-Assay**

In order to determine the protein concentration, standard Bradford assay was used. The protein solution was diluted 1:30 in (MilliQ  $\text{H}_2\text{O}$ ), and 5  $\mu\text{L}$  of diluted protein solution was transferred to the 96 well plates and mixed with 200  $\mu\text{L}$  of 1:5 diluted Bradford reagent (Protein Assay Dye Reagent Concentrate; 500- 0006, Bio-Rad) and mixed for 30 s (1350 rpm; Heidolph Titramax 1000). The plate was incubated at room temperature for 15 min. Finally, the absorbance was determined using a plate reader (Anthos Zenyth 3100) at 590 nm. The protein concentration was determined by using the bovine serum albumin (BSA) calibration curve.

## E II Materials and methods—chemical synthesis

Unless otherwise noted, chemicals were purchased from commercial suppliers and used without further purification. The purity of the compounds reported is > 95% according to NMR.

### E II.1 NMR spectroscopy

NMR spectra were recorded on a Bruker *AC 200* ( $^1\text{H}$ : 200MHz,  $^{13}\text{C}$ : 50 MHz), Bruker *Avance Ultrashield 400* ( $^1\text{H}$ : 400 MHz,  $^{13}\text{C}$ : 101 MHz) and Bruker *Avance IIIHD 600* spectrometer equipped with a Prodigy BBO cryo probe ( $^1\text{H}$ : 600 MHz,  $^{13}\text{C}$ : 151MHz). Chemical shifts are given in parts per million (ppm) and were calibrated with internal standards of deuterium labeled solvents  $\text{CDCl}_3$  ( $^1\text{H}$  7.26 ppm,  $^{13}\text{C}$  77.16 ppm) and  $\text{DMSO-}d_6$  ( $^1\text{H}$  2.50 ppm,  $^{13}\text{C}$  39.52 ppm). NMR assignments of unknown compounds were confirmed by  $^1\text{H}$  -  $^1\text{H}$  COSY,  $^1\text{H}$  -  $^1\text{H}$ ,  $^1\text{H}$  -  $^{13}\text{C}$ , HSQC and  $^1\text{H}$  -  $^{13}\text{C}$ , HMBC and by comparison to predicted spectra. Proton multiplicities are denoted by the following abbreviations: s (singlet), br s (broad singlet), d (doublet), dd (doublet of a doublet), ddd (doublet of a doublet of a doublet), t (triplet), dt (doublet of a triplet), dtd (doublet of a triplet of a doublet), q (quartet), dq (doublet of a quartet), p (quintet), h (hextet) m (multiplet). Coupling constants ( $J$ ) are presented in Hz (Hertz). Carbon multiplicities (suppressed CH coupling) are denoted by the following abbreviations: s (singlet), d (doublet), t (triplet) and q (quartet). In the case of fluoro structures, the coupling constant is generally denoted as “x/y,  $^zJ_{CF} = \dots\text{Hz}$ ”, whereby x represents the multiplicity of the CH coupling, y the multiplicity of the CF coupling, and z the order of spin-spin coupling. In the case of phosphorus structures, the coupling constant is generally denoted as “x/y,  $^zJ_{CP} = \dots\text{Hz}$ ”, whereby x represents the multiplicity of the CH coupling, y the multiplicity of the CP coupling, and z the order of spin-spin coupling.

### E II.2 Chromatographic methods

TLC was performed using silica gel 60 aluminum plates containing fluorescent indicator from Merck and detected either with UV light at 254 nm or by charring in ninhydrin solution (300 mg ninhydrin, 3 mL acetic acid, 100 mL butanol), potassium permanganate (1 g  $\text{KMnO}_4$ ,

6.6 g NaOH, 100 mL H<sub>2</sub>O in 1M NaOH), or *p*-anisaldehyde (3.7 mL *p*-anisaldehyde, 5 mL conc. H<sub>2</sub>SO<sub>4</sub>, 1.5 mL glacial acetic acid) with heating.

HPLC chromatography was carried out with an Autopurification system of Waters using an ACQUITY QDa Detector in combination with a 2998 Photodiode Array Detector. Analytical separation was conducted using XSELECT CSH Fluorophenyl 5 μm 4.6 x 150 mm and XSELECT CSH C18 5 μm 4.6 x 150 mm columns. Preparative separation was performed using XSELECT CSH Prep Fluoro-Phenyl 5 μm 30 x 150 mm and XSELECT CSH Prep C18 5 μm OBD 30 x 150 mm columns. Milli-Q water containing 0.1% formic acid or 2.5 mM ammonium formate (NH<sub>4</sub><sup>+</sup>HCOO<sup>-</sup>) buffer was used as Solvent A, and HPLC grade acetonitrile was used as Solvent B.

Flash column chromatography was carried out at Büchi Sepacore<sup>TM</sup> MPLC system using silica gel 60 M (particle size 40-63 μm, 230-400 mesh ASTM, Macherey Nagel, Düren). Unless otherwise noted, all compounds were purified with a ratio of 1/80 (weight (compound)/ weight (silica)).

GC/MS spectra were measured on a Thermo Trace 1300 / ISQ LT (single quadrupole MS (EI)) using a standard capillary column BGB 5 (30 m x 0.25 mm ID); Carrier gas: helium, column flow: 2.0 mL/min; Method: 2 minutes at 100 °C, 35 °C/min until 300 °C, 4 minutes at 300 °C – run time 12 minutes.

GC analysis for reaction control of biotransformations was performed on a Thermo Scientific Trace 1300 Dual GC, equipped with a TR-5MS column (15 m, 0.25 mm ID, film thickness 1.0 μm) and an FID detector using the following temperature program: Carrier gas: helium, column flow: 1.5 mL/min, 1 minute at 80 °C, 60°C/min until 280 °C, 5 minutes at 280 °C – run time 10 minutes.

UHPLC-MS/UV analysis was performed on a Nexera X2 UHPLC system (Shimadzu) comprised of LC-30AD pumps, SIL-30AC autosampler, CTO-20AC column oven, and DGU-20A5/3degasser module. Detection was done using an SPD-M20A photo diode array and an LCMS-2020 mass spectrometer (ESI/APCI). If not stated otherwise, all separations were performed using a Waters XSelect CSH C18 2,5 μm (3.0 x 50 mm) column XP at 40 °C, and a flowrate of 1.7 mL/min. Gradient elution was performed using mixtures of HPLC grade MeCN and HPLC grade water with either 0.1 vol% formic acid (acidic separation) or as 50 mM pH NH<sub>4</sub>HCO<sub>2</sub> solution (basic separation).

## **E II.3 Melting point**

Melting points were determined by a Leica Galen III Kofler and a Büchi Melting Point B-545 and are uncorrected.

## **E II.4 HR-MS**

An Agilent 6230 LC TOFMS mass spectrometer equipped with an Agilent Dual AJS ESI-Source was used for the analysis. The mass spectrometer was connected to a liquid chromatography system of the 1100/1200 series from Agilent Technologies, Palo Alto, CA, USA. The system consisted of a 1200SL binary gradient pump, a degasser, a column thermostat, and an HTC PAL autosampler (CTC Analytics AG, Zwingen, Switzerland). A silica-based Phenomenex C-18 Security Guard Cartridge was used as the stationary phase.

Data evaluation was performed using Agilent MassHunter Qualitative Analysis B.07.00. Identification was based on peaks obtained from extracted ion chromatograms (extraction width  $\pm 20$  ppm).

## **E II.5 Specific rotation**

Specific rotation  $[\alpha]_D^{20}$  was determined using an MCP 500 polarimeter from Anton Paar by the following equation:  $[\alpha]_D^{20} = 100 \cdot \alpha / [c] \cdot l$ ; c in [g/100 mL], l in [dm]

## **E III General operating proceducer (E°II)**

### **E III.1 General procedure A: Synthesis of esters of modified adenosines**

Esters of protected adenosine [29] and [30] were prepared using the following literature procedure.<sup>423</sup> An oven-dried 25 mL three-neck round bottom flask was charged with protected adenosine (1.96 mmol, 1.00 equiv.) and 4-DMAP (0.024 g, 0.20 mmol, 0.10 equiv.). The flask was closed with a septum and evacuated and flushed with argon three times. Dry DCM (15 mL) and diazine acids [9] or [18] (2.35 mmol, 1.20 equiv.) were added, and the solution was cooled



to 0 °C using an ice bath with stirring for 10 min. To this solution was then added EDCI·HCl (0.450 g, 2.35 mmol, 1.20 equiv.) in one portion, and the reaction mixture was stirred for 10 min at the same temperature. Subsequently, the reaction mixture was allowed to warm up to room temperature. After completion of the reaction (monitored by TLC), the mixture was diluted with DCM and washed once with satd. aqu. NaHCO<sub>3</sub>-solution (10 mL), water (2 times, 15 mL) and brine (10 mL). The organic layer was then dried over MgSO<sub>4</sub>. Filtration and evaporation of the volatiles under vacuum afforded the crude product, which was purified by flash column chromatography.

## **E III.2 General procedure B: Synthesis of amides of modified adenosines**

Amides of modified adenosines were prepared using the following modified literature procedure.<sup>424</sup> An oven-dried 25 mL three-neck round bottom flask equipped with a stirring bar and closed with a septum was evacuated and flushed with argon three times. Diazirine acids [9] (12.12 mmol, 3.00 equiv.) or [18] (4.44 mmol, 1.10 equiv.) and HOBt (1.24 g, 8.08 mmol, 2.00 equiv.) were added under an inert atmosphere, followed by the addition of dry DMF (5 mL), protected adenosines [48], [53], [66], or [69] (4.04 mmol, 1.00 equiv.), and DIPEA (1.41 mL, 8.08 mmol, 2.00 equiv.). The mixture was cooled to 0 °C using an ice bath, and EDCI·HCl (1.55 mg, 8.08 mmol, 2.00 equiv.) was added in one portion at the same temperature. The reaction mixture was stirred for 10 min at 0 °C and then allowed to warm up to room temperature. The reaction was stirred overnight and after TLC analysis indicated full conversion, was quenched with H<sub>2</sub>O. The aqueous phase was further extracted with DCM (2 times, 20 mL), and the combined organic phases were washed with water (2 times, 20 mL), satd. aqu. NaHCO<sub>3</sub>-solution (2 times, 20 mL) and brine (20 mL). The organic phase was then dried over MgSO<sub>4</sub>. Filtration and evaporation under reduced pressure afforded the crude product, which was purified by flash column chromatography.

### **E III.3 General procedure C: Deprotection of TIPDS group**

The TIPDS group was removed according to following modified literature procedures.<sup>389,425</sup> A solution of the corresponding protected adenosine (1.00 equiv.) in anhydrous THF (5 mL/0.300 mmol) was cooled with an ice bath and was then treated with a solution TBAF/AcOH (1:1, 1 M in THF, 2.00 equiv.). The reaction was stirred for 30 min, and after TLC analysis indicated complete conversion of the starting material, the solvent was removed, and the crude product was subjected to flash column chromatography.

### **E III.4 General procedure D: Deprotection of TBDMS group**

The TBDMS group was removed according to the following modified literature procedure.<sup>426</sup> A solution of the corresponding protected adenosine in anhydrous THF (5 mL/0.300 mmol) was cooled with an ice bath and was then treated with a solution TBAF/AcOH (1:1, 1 M in THF, 2.00 equiv.). The reaction was stirred for 30 min, and the ice bath was subsequently removed. Next, the reaction was allowed to warm up to room temperature and stirred for 1.5 hours. After TLC analysis indicated complete conversion of the starting material, the solvent was removed, and the crude product was subjected to flash column chromatography.

### **E III.5 General procedure E: Monophosphate synthesis—Selective phosphorylation of the 5'OH-group.**

Unprotected adenosine building blocks were converted to their corresponding monophosphates based on modified literature procedures.<sup>396,427</sup> In a typical reaction, the respective modified nucleoside (1.00 equiv.) was weighted into an oven-dried Schlenk-tube, which was previously flushed with argon using standard Schlenk-technique. Next, dry acetonitrile (8 mL) was added via syringe under an inert atmosphere, and the solvent was removed under high vacuum. This procedure was repeated once, and the nucleoside was dried

under high vacuum for one hour. The dried nucleoside was then redissolved in dry PO(OMe)<sub>3</sub> (15 mL/1.00 mmol nucleoside), and the resulting mixture was stirred for 10 min at room temperature and was then cooled with an ice/water bath to 0 °C (external temperature). Freshly distilled POCl<sub>3</sub> (3.00 equiv.) was added dropwise, and the reaction progress was frequently monitored by UHPLC-MS analysis. After complete conversion of the starting material, the reaction was quenched by carefully adding ice-cold water (20 mL) and was left to stir for 30 min at 0 °C. Subsequently, the mixture was extracted with DCM (3 times, 10 mL), and the aqueous phase was neutralized by the dropwise addition of TEAA-buffer (pH 8.5) and freeze-dried to obtain the crude product. Finally, the crude product was purified by preparative reverse-phase HPLC (Milli-Q H<sub>2</sub>O + 0.1% formic acid [Solvent A], acetonitrile [Solvent B]).

## **E III.6 General procedure F: Chemical coupling reaction—Modified flavin adenine dinucleotide synthesis**

Modified monophosphates were converted to their corresponding modified flavin adenine dinucleotides using modified literature procedures.<sup>400,427</sup> In a typical reaction, the respective modified monophosphate (1.00 equiv.) was weighed into an oven-dried Schlenk-tube, which was previously flushed with argon using standard Schlenk-technique. Next, dry acetonitrile was added (8 mL) via syringe under an inert atmosphere, and the solvent was removed under high vacuum. This procedure was repeated once, CDI (1.25 equiv.) was subsequently added under an argon atmosphere, and the solids were dried under high vacuum for one hour. The dried solids were then redissolved in dry DMF (0.1 M), and the resulting solution was stirred at room temperature until UHPLC-MS/UV analysis indicated complete conversion of the starting material (~1.5 h). Then, the reaction was quenched by adding dry MeOH (1 mL), and volatiles were carefully removed under high vacuum at 35 °C and dried for 1 hour.

In a second oven-dried Schlenk-tube, which was flushed with argon using standard Schlenk-technique, FMN salt [**41b**] (1.20 equiv.) was weighed in, followed by the addition of dry DMF (8 mL). The solvent was then carefully removed under high vacuum at 35 °C, and the solid was dried for 1 hour.

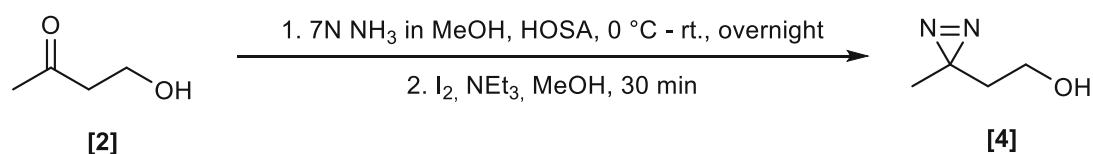
The previously prepared activated monophosphate was then redissolved in dry DMF (to obtain a 0.1 M solution) and added to the flask containing the dried FMN salt [**41b**] via syringe. The reaction mixture was then stirred at 35 °C, and the reaction progress was frequently

monitored by UHPLC-MS/UV analysis. After all activated monophosphate was converted to the corresponding pyrophosphate, the reaction was cooled to room temperature and quenched by adding distilled H<sub>2</sub>O. Next, volatiles were carefully removed under reduced pressure using a rotary evaporator, and the obtained crude material was redissolved in distilled H<sub>2</sub>O and freeze-dried. Finally, the crude product was purified by preparative reverse-phase HPLC (2.5 mM NH<sub>4</sub><sup>+</sup>HCOO<sup>-</sup> buffer [Solvent A]/acetonitrile [Solvent B]).

## E IV Chemical synthesis

### E IV.1 Synthesis of aliphatic diazidine building blocks

#### E IV.1.1 2-(3-Methyl-3*H*-diazirin-3-yl)ethan-1-ol [3]



Molecular Weight: 88.11

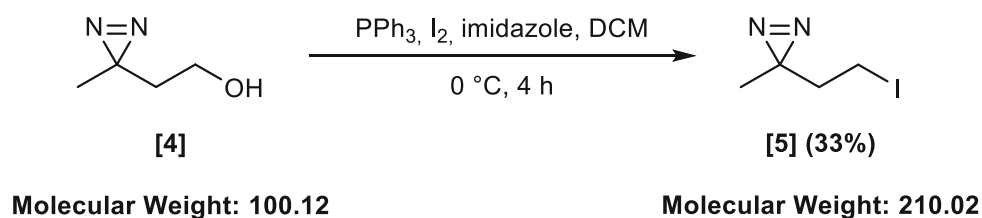
Molecular Weight: 100.12

2-(3-Methyl-3*H*-diazirin-3-yl)ethan-1-ol [4] was prepared from 4-hydroxybutan-2-one [2] following a literature procedure.<sup>428</sup> An oven-dried 250 mL three-neck flask was flushed with argon using standard Schlenk-technique. 4-hydroxy-2-butanone [2] (6.20 g, 70.37 mmol, 1.00 equiv.) was added, and the flask was further cooled with an ice/water bath. A 7 N solution of NH<sub>3</sub> in MeOH (70 mL) was added dropwise via syringe, and the resulting colorless solution was stirred for 3 hours at 0 °C. Then, hydroxylamine-*O*-sulfonic acid (9.15 g, 80.93 mmol, 1.15 equiv.) dissolved in dry MeOH (70 mL) was added via syringe (precipitation of ammonium salt), and the reaction was left stirring overnight at room temperature. The reaction mixture was filtered, and the remaining ammonia was removed by bubbling argon through the solution for 30 min. Subsequently, the solvent was removed by rotary evaporation (water bath at 30 °C). Diaziridine alcohol [3] was obtained as a yellow oil. The reaction flask was covered with aluminum foil to minimize exposure to light. MeOH (25 mL) was added to dissolve the diaziridine alcohol [3], and the solution was stirred for 5 min at 0 °C in an ice/water bath and was then treated with Et<sub>3</sub>N (7.5 mL). The mixture was stirred for additional 5 min, followed by

slow addition of I<sub>2</sub>. I<sub>2</sub> addition was stopped when the dark red-brown color persisted for more than 10 min. The reaction mixture was diluted with EtOAc (25 mL) and washed with 2M aq. HCl (25 mL). The organic layer was separated and washed with 10% aq. Na<sub>2</sub>S<sub>2</sub>O<sub>3</sub> solution until the organic phase became colorless. The organic phase was further washed with saturated aq. NaCl (25 mL). The organic phase was dried over anhydrous MgSO<sub>4</sub>, filtered, and concentrated by rotary evaporation (water bath 30 °C). The product was used directly for the next step without further purification (2.87 g, yield 41 %).

<b>Yield</b>	41% (2.87 g, 28.65 mmol)
<b>Appearance</b>	yellowish oil
<b>TLC</b>	R <sub>f</sub> (PE/EtOAc = 1/1) = 0.5
<b>Sum formula</b>	C <sub>4</sub> H <sub>8</sub> N <sub>2</sub> O
<b><sup>1</sup>H-NMR (400 MHz, CDCl<sub>3</sub>)</b>	δ = 1.07 (s, 3H, CH <sub>3</sub> ), 1.64 (t, <i>J</i> = 6.3 Hz, 2H, CH <sub>2</sub> -CH <sub>2</sub> -OH), 3.53 (t, <i>J</i> = 6.3 Hz, 2H, CH <sub>2</sub> -CH <sub>2</sub> -OH) ppm.
<b><sup>13</sup>C-NMR (101 MHz, CDCl<sub>3</sub>)</b>	δ = 20.4 (q, CH <sub>3</sub> ), 24.4 (s, diazirine), 37.1 (t, -CH <sub>2</sub> -CH <sub>2</sub> -OH), 57.9 (t, -CH <sub>2</sub> -CH <sub>2</sub> -OH) ppm.
<b>Comment</b>	Spectral data are in accordance with the literature.

## E IV.1.2 3-(2-Iodoethyl)-3-methyl-3*H*-diazirine [5]

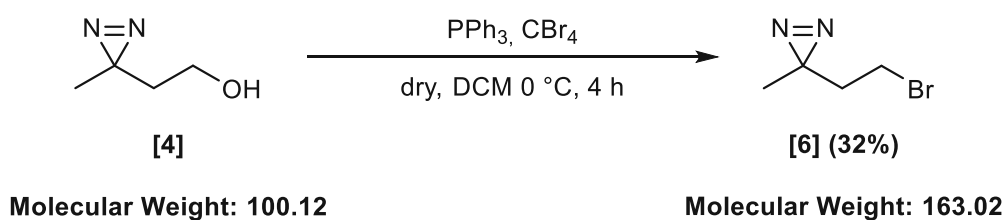


3-(2-Iodoethyl)-3-methyl-3*H*-diazirine [5] was prepared from 2-(3-methyl-3*H*-diazirin-3-yl)ethan-1-ol [4] following a literature procedure.<sup>429</sup> To a solution of triphenylphosphine (2.88 g, 10.99 mmol, 1.10 equiv.) and imidazole (2.04 g, 29.96 mmol, 3.00 equiv.) in DCM (150 mL) iodine (913.7 mg, 3.60 mmol) was added slowly at 0 °C. After stirring for 15 min, a solution of 2-(3-methyl-3*H*-diazirin-3-yl)ethan-1-ol [4] (1.00 g, 9.99 mmol, 1.00 equiv.) in DCM (30 mL) was added dropwise, and the solution was stirred for additional 4 hours at this temperature. After warming to room temperature, a saturated solution of Na<sub>2</sub>S<sub>2</sub>O<sub>3</sub> (90 mL) was added, and the mixture was extracted with EtOAc (3 times, 75 mL). The combined organic layers were washed with brine (2 times, 75 mL), dried over MgSO<sub>4</sub>, and the solvent was evaporated. After

flash chromatographic purification (EtOAc in PE, 2-10% 30min), 3-(2-iodoethyl)-3-methyl-3*H*-diazirine [5] was obtained as a slightly yellow oil (700 mg, 3.33 mmol, 33%).

<b>Yield</b>	33% (700 mg, 3.33 mmol)
<b>Appearance</b>	pale yellowish oil
<b>TLC</b>	R <sub>f</sub> (PE/EtOAc = 95/5) = 0.5
<b>Sum formula</b>	C <sub>4</sub> H <sub>7</sub> IN <sub>2</sub>
<b><sup>1</sup>H-NMR (400 MHz, CDCl<sub>3</sub>)</b>	δ = 1.07 (s, 3H, CH <sub>3</sub> ), 2.02 (t, <i>J</i> = 7.6 Hz, 2H, CH <sub>2</sub> -CH <sub>2</sub> -I), 2.95 (t, <i>J</i> = 7.6 Hz, 2H, CH <sub>2</sub> -CH <sub>2</sub> -I) ppm.
<b><sup>13</sup>C-NMR (101 MHz, CDCl<sub>3</sub>)</b>	δ = -3.5 (t, -CH <sub>2</sub> -CH <sub>2</sub> -I), 19.5 (q, CH <sub>3</sub> ), 26.3 (s, diazirine), 39.1 (t, -CH <sub>2</sub> -CH <sub>2</sub> -I) ppm.
<b>Comment</b>	Spectral data are in accordance with the literature.

### E IV.1.3 3-(2-Bromoethyl)-3-methyl-3*H*-diazirine [6]



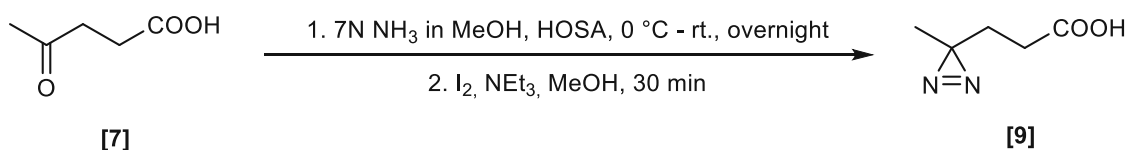
3-(2-Bromoethyl)-3-methyl-3*H*-diazirine [6] was synthesized from 2-(3-methyl-3*H*-diazirin-3-yl)ethan-1-ol [4] following a literature procedure.<sup>430</sup> 2-(3-Methyl-3*H*-diazirin-3-yl)ethan-1-ol [4] (200 mg, 2.00 mmol, 1.00 equiv.) and carbon tetrabromide (729 mg, 2.20 mmol, 1.10 equiv.) were dissolved in DCM (1 mL), and the resulting solution was cooled with an ice/water bath. Triphenyl phosphine (576 mg, 2.20 mmol, 1.00 equiv.) was added in small portions over 30 min with vigorous stirring, and upon complete addition, the reaction mixture was allowed to warm up to room temperature slowly and stirred for 2 hours at this temperature. The reaction mixture was then concentrated to a brown oil and taken up in hexane. The white precipitate was filtered, and the filtrate was subjected to purification via flash column chromatography with a gradient of EtOAc in PE (2-15% in 30 min) to afford 3-(2-bromoethyl)-3-methyl-3*H*-diazirine [6] as a brown oil.

<b>Yield</b>	33% (700 mg, 3.33 mmol)
<b>Appearance</b>	brown oil
<b>TLC</b>	R <sub>f</sub> (PE/EtOAc = 95/5) = 0.4
<b>Sum formula</b>	C <sub>4</sub> H <sub>7</sub> BrN <sub>2</sub>

$^1\text{H-NMR}$  (400 MHz,  $\text{CDCl}_3$ )  $\delta$  = 1.09 (s, 3H,  $\text{CH}_3$ ), 1.95 (t,  $J$  = 7.2 Hz, 2H,  $-\text{CH}_2-\text{CH}_2-\text{Br}$ ), 3.22 (t,  $J$  = 7.1 Hz, 2H,  $-\text{CH}_2-\text{CH}_2-\text{Br}$ ) ppm.

$^{13}\text{C-NMR}$  (101 MHz,  $\text{CDCl}_3$ )  $\delta$  = 19.8 (q,  $\text{CH}_3$ ), 25.1 (s, diazirine), 26.1 (t,  $-\text{CH}_2-\text{CH}_2-\text{Br}$ ), 38.0 (t,  $-\text{CH}_2-\text{CH}_2-\text{Br}$ ) ppm.

## E IV.1.4 3-(3-Methyl-3*H*-diazirin-3-yl)propanoic acid [9]



Molecular Weight: 116.12

Molecular Weight: 128.13

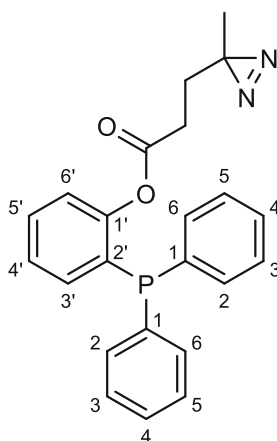
3-(3-Methyl-3*H*-diazirin-3-yl)propanoic acid [9] was synthesized from Levulinic acid [7] according to the following literature procedure.<sup>428</sup> An oven-dried 250 mL three-neck flask was flushed with argon using Schlenk-technique. Levulinic acid [7] (7.14 g, 61.51 mmol, 1.00 equiv.) was added, and the flask was further cooled with an ice-water bath. A 7 N solution of  $\text{NH}_3$  in MeOH (70 mL) was added dropwise via syringe, and the resulting colorless solution was stirred for 3 hours at 0 °C. Then, HOSA (8.0 g, 70.74 mmol, 1.15 equiv.) dissolved in dry MeOH (70 mL) was added via syringe (precipitation of ammonium salt), and the reaction was left stirring overnight at room temperature. The reaction mixture was filtered, and  $\text{NH}_3$  was removed by bubbling argon through the solution for 30 min. Next, the solvent was removed by rotary evaporation (water bath at 30 °C). Diaziridine acid [8] was obtained as a yellow oil. The reaction flask was covered with aluminum foil to minimize exposure to light. MeOH (25 mL) was added to dissolve the diaziridine acid [8], and the solution was stirred for 5 min at 0 °C in an ice/water bath and was then treated with  $\text{Et}_3\text{N}$  (7.5 mL). The mixture was stirred for additional 5 min, followed by slow addition of  $\text{I}_2$ .  $\text{I}_2$  addition was stopped when the dark red-brown color persisted for more than 10 min. The reaction mixture was diluted with EtOAc (25 mL) and washed with 2M aq. HCl (25 mL). The organic layer was separated and washed with 10% aq.  $\text{Na}_2\text{S}_2\text{O}_3$  solution until the organic phase became colorless. The organic phase was further washed with saturated aq. NaCl (25 mL). The organic phase was dried over anhydrous  $\text{MgSO}_4$ , filtered, and concentrated by rotary evaporation (water bath 30 °C). The product was used directly for the next step without further purification (3.75 g, yield 48 %).



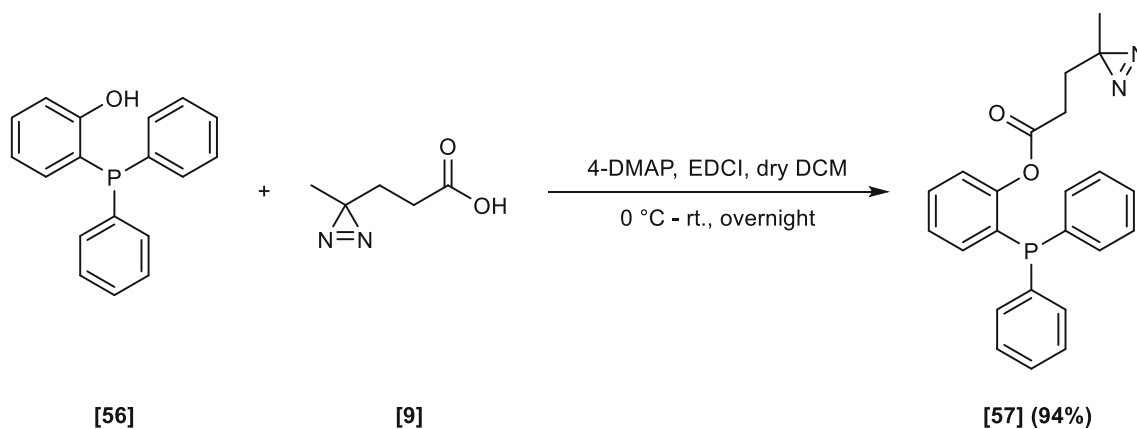
<b>Yield</b>	48% (3.75 g, 0.71 mmol)
<b>Appearance</b>	pale yellow oil
<b>Sum formula</b>	C <sub>5</sub> H <sub>8</sub> N <sub>2</sub> O <sub>2</sub>
<b><sup>1</sup>H-NMR (400 MHz, CDCl<sub>3</sub>)</b>	$\delta = 1.05$ (s, 3H, CH <sub>3</sub> ), 1.72 (t, $J = 7.7$ Hz, 2H, -CH <sub>2</sub> -CH <sub>2</sub> -COOH), 2.24 (t, $J = 7.7$ Hz, 2H, -CH <sub>2</sub> -CH <sub>2</sub> -COOH) ppm.
<b><sup>13</sup>C-NMR (101 MHz, CDCl<sub>3</sub>)</b>	$\delta = 19.8$ (q, CH <sub>3</sub> ), 25.2 (s, diazirine), 28.6 (t, CH <sub>2</sub> -CH <sub>2</sub> -COOH), 29.5 (t, CH <sub>2</sub> -CH <sub>2</sub> -COOH), 178.3 (COOH) ppm.
<b>Comment</b>	Spectral data are in accordance with the literature.

## E IV.2 Synthesis of Staudinger reagent [57]

The assignments of protons and carbon atoms in the NMR codes of compound [57] were carried out as follows:



### E IV.2.1 2-(Diphenylphosphaneyl)phenyl 3-(3-methyl-3*H*-diazirin-3-yl)propanoate [57]



Molecular Weight: 278.29    Molecular Weight: 128.13

Molecular Weight: 388.41

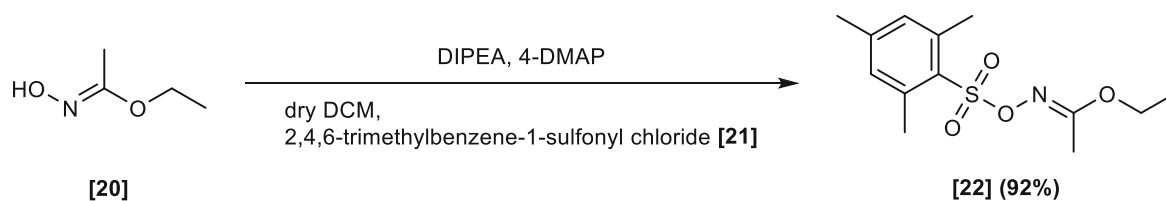


2-(Diphenylphosphaneyl)phenyl 3-(3-methyl-3*H*-diazirin-3-yl)propanoate [57] was synthesized from 2-hydroxydiphenylphosphinylbenzene [56] and 3-(3-methyl-3*H*-diazirin-3-yl)propanoic acid [9] according to a modified literature procedure.<sup>405</sup> An oven-dried 25 mL three-neck round bottom flask closed with a septum was evacuated and flushed with argon three times using standard Schlenk-technique. Diazirine acid [9] (276 mg, 2.16 mmol, 1.20 equiv.) and 4-DMAP (240 mg, 0.20 mmol, 0.10 equiv.) were added under an inert atmosphere, followed by the addition of dry DCM (15 mL) and 2-hydroxydiphenylphosphinylbenzene [56] (500 mg, 1.80 mmol, 1.00 equiv.). The obtained mixture was cooled to 0 °C using an ice bath with stirring for 10 min. To this solution was then added EDCI·HCl (0.450 g, 2.35 mmol, 1.20 equiv.) in one portion, and the reaction mixture was stirred for 10 min at the same temperature. Subsequently, the reaction mixture was allowed to warm up to room temperature. After completion of the reaction (monitored by TLC), the mixture was diluted with DCM and washed once with saturated. aq. NaHCO<sub>3</sub>-solution (10 mL), water (2 times, 15 mL) and brine (10 mL). The organic layer was then dried over MgSO<sub>4</sub>. Filtration and evaporation of the volatiles under vacuum afforded the crude product. After purification by flash column chromatography (silica gel/crude material = 100/1, 1-10% EtOAc in PE), the pure product was obtained as a colorless oil.

<b>Yield</b>	94% (654 mg, 1.68 mmol)
<b>Appearance</b>	colorless oil
<b>TLC</b>	R <sub>f</sub> (PE/EtOAc = 95/5) = 0.2
<b>Sum formula</b>	C <sub>23</sub> H <sub>21</sub> N <sub>2</sub> O <sub>2</sub> P
<b><sup>1</sup>H-NMR (400 MHz, CDCl<sub>3</sub>)</b>	δ = 0.97 (s, 3H, CH <sub>3</sub> (aliphatic linker)), 1.50 – 1.54 (m, 2H, -CH <sub>2</sub> -CH <sub>2</sub> -COOR), 2.09 – 2.12 (m, 2H, -CH <sub>2</sub> -CH <sub>2</sub> -COOR), 6.81 (ddd, <i>J</i> = 7.7, 4.4, 1.6 Hz, 1H, H-3'), 7.10 – 7.19 (m, 2H, H-4' & H-6'), 7.28 – 7.40 (m, 11H, 2x H-2 & 2x H-3 & 2x H-4 & 2x H-5 & 2x H-6 & H-5') ppm.
<b><sup>13</sup>C-NMR (101 MHz, CDCl<sub>3</sub>)</b>	δ = 19.6 (q, CH <sub>3</sub> (aliphatic linker)), 25.0 (s, diazirine), 28.6 (t, -CH <sub>2</sub> -CH <sub>2</sub> -COOR), 29.4 (t, -CH <sub>2</sub> -CH <sub>2</sub> -COOR), 122.5 (d, <i>J</i> = 1.6 Hz, C-6'), 126.3 (d, C-4'), 128.7 (d, <i>J</i> = 7.4 Hz, 2x C-3 & 2x C-5), 129.1 (d, 2x C-4), 130.0 (d, C-5'), 130.2 (d, <i>J</i> = 14.7 Hz, C-2'), 133.7 (d, <i>J</i> = 2.0 Hz, C-3'), 134.0 (d, <i>J</i> = 20.6 Hz, 2x C-2 & 2x C-6), 135.4 (s, <i>J</i> = 9.9 Hz, 2x C-1), 152.5 (s, <i>J</i> = 16.8 Hz, C-1'), 170.2 (s, carbonyl (ester)) ppm.
<b><sup>31</sup>P NMR (162 MHz, CDCl<sub>3</sub>)</b>	δ = -15.88 ppm.
<b>Comment</b>	Spectral data are in accordance with the literature.

## E IV.3 Synthesis of aminating reagent [23]

### E IV.3.1 Ethyl *(E)*-*N*-**((mesitylsulfonyl)oxy)acetimidate [22]**



Molecular Weight: 103.12

Molecular Weight: 285.36

Ethyl *(E)*-*N*-((mesitylsulfonyl)oxy)acetimidate [22] was prepared from ethyl *(E)*-*N*-hydroxyacetimidate [20] and 2,4,6-trimethylbenzene-1-sulfonyl chloride [21] following a literature procedure.<sup>380</sup> A solution of ethyl *N*-hydroxyacetimidate (10 g, 96.97 mmol, 1.00 equiv.), *N,N*-diisopropylethylamine (20.3 mL, 116.37 mmol, 1.20 equiv.) and 4-dimethylaminopyridine (1.18 g, 9.70 mmol, 0.10 equiv.) in anhydrous DCM (35 mL) was cooled to 0 °C. To this cold solution 2,4,6-trimethylbenzene-1-sulfonyl chloride [21] (23.33 g, 106.67 mmol, 1.10 equiv.) was added slowly, warmed to room temperature and stirred for 1 hour (orange suspension). The reaction was quenched with the addition of water (100 mL), and this mixture was extracted with DCM (3 times, 50 mL). The combined DCM layers were dried with magnesium sulfate and concentrated under reduced pressure to obtain the crude product as orange oil, which crystallized on standing (29.88 g, 108 %). The crude material obtained was purified by silica flash column chromatography with a two-step gradient of EtOAc in PE (1%, 5 min; 1-10% 25 min) as the eluent to obtain [22] as a colorless oil, which crystallized on standing (25.43 g, 92 %).

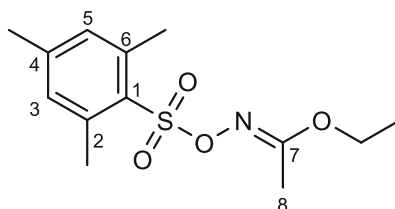
<b>Yield</b>	92% (25.43 g, 89.11 mmol)
<b>Appearance</b>	colorless crystals
<b>Melting point</b>	55.0 – 56.0 °C (Lit. <sup>431</sup> : 56.0 – 58.0 °C)
<b>TLC</b>	R <sub>f</sub> (PE/EtOAc = 4/1) = 0.8
<b>Sum formula</b>	C <sub>13</sub> H <sub>19</sub> NO <sub>4</sub> S
<b><sup>1</sup>H-NMR (400 MHz, CDCl<sub>3</sub>)</b>	δ = 1.19 (t, <i>J</i> = 7.1 Hz, 3H, -O-CH <sub>2</sub> -CH <sub>3</sub> ), 2.04 (s, 3H, CH <sub>3</sub> ), 2.31 (s, 3H, CH <sub>3</sub> ), 2.64 (s, 6H, 2x CH <sub>3</sub> ), 3.91 (q, <i>J</i> = 7.1 Hz, 2H, -O-CH <sub>2</sub> -CH <sub>3</sub> ), 6.96 (s, 2H, aromatic) ppm.
<b><sup>13</sup>C-NMR (101 MHz, CDCl<sub>3</sub>)</b>	δ = 14.1 (q, CH <sub>3</sub> -CH <sub>2</sub> -O-), 15.0 (q, CH <sub>3</sub> -C8), 21.2 (q, CH <sub>3</sub> -C4), 23.0 (q, CH <sub>3</sub> -C2 & CH <sub>3</sub> -C6), 63.7 (t, CH <sub>3</sub> -CH <sub>2</sub> -O-), 130.6 (s, C2

& C6), 131.6 (d, C3 & C5), 140.9 (s, C4), 143.42 (s, C1), 169.4 (s, C7) ppm.

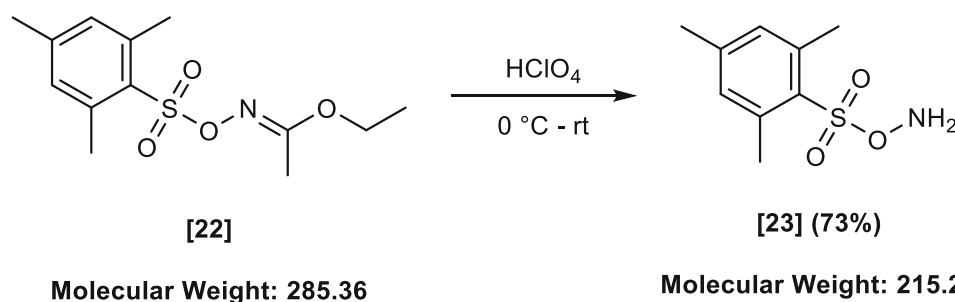
### Comment

Spectral data are in accordance with the literature.

The assignments of protons and carbon atoms in the NMR codes of compound [22] were carried out as follows:



## E IV.3.2 *O*-(Mesitylsulfonyl)hydroxylamine [23]

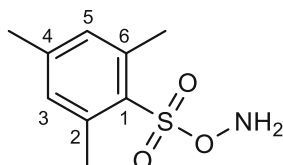


*O*-(mesitylsulfonyl)hydroxylamine [23] was prepared from ethyl (*E*)-*N*-((mesitylsulfonyl)oxy)acetimidate [22] according to the following literature procedure.<sup>382</sup> A 50 mL round bottom flask, equipped with a big magnetic stirring bar, was charged with ethyl (*E*)-*N*-((mesitylsulfonyl)oxy)acetimidate [22] (10.00 g, 35.04 mmol, 1.00 equiv.) and dioxane (17 mL) was added. The solution was cooled with an ice bath, and perchloric acid (6.5 mL) was added dropwise. The reaction was stirred vigorously at 0 °C and thickened and solidified over the course of 5 min. The reaction was incubated for additional 5 min to ensure complete hydrolysis. The reaction mixture was then portioned between ice water (100 mL) and diethyl ether (100 mL), and upon isolation of the organic phase, the aqueous phase was extracted with ether one more time (30 mL). The combined organic layer was further dried/neutralized with K<sub>2</sub>CO<sub>3</sub> for 2 min. The filtrate was concentrated carefully under reduced pressure to about 50 mL total volume and then poured into a beaker containing 150 mL of petrol ether (-20 °C), and crystals were formed immediately. The beaker was stored for 1 hour at -20 °C to complete the crystallization, and the formed crystals were isolated by vacuum filtration and dried under high

vacuum for 15 min. The crystals were stored in a plastic container sealed with parafilm at -20 °C (5.52 g, 73 %).

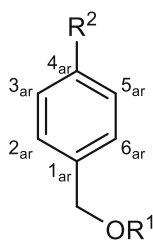
<b>Yield</b>	73% (5.52 g, 25.64 mmol)
<b>Appearance</b>	colorless crystals
<b>Melting point</b>	92.0 – 94.0 °C (Lit. <sup>432</sup> : 90.0 – 91.0 °C)
<b>TLC</b>	R <sub>f</sub> (PE/EtOAc = 80/20) = 0.3
<b>Sum formula</b>	C <sub>9</sub> H <sub>13</sub> NO <sub>3</sub> S
<b><sup>1</sup>H-NMR (400 MHz, CDCl<sub>3</sub>)</b>	δ = 2.32 (s, 1H, CH <sub>3</sub> ), 2.64 (s, 2H, 2 x CH <sub>3</sub> ), 5.76 (s, 1H, NH <sub>2</sub> ), 6.99 (s, 1H, 2x CH (aromatic) ppm.
<b><sup>13</sup>C-NMR (101 MHz, CDCl<sub>3</sub>)</b>	δ = 21.2 (q, CH <sub>3</sub> -C <sub>4</sub> ), 22.8 (q, CH <sub>3</sub> -C <sub>2</sub> & CH <sub>3</sub> -C <sub>6</sub> ), 129.1 (s, C <sub>2</sub> & C <sub>6</sub> ), 131.9 (d, C <sub>3</sub> & C <sub>5</sub> ), 141.1 (s, C <sub>4</sub> ), 144.0 (s, C <sub>1</sub> ) ppm.
<b>Comment</b>	Spectral data are in accordance with the literature.

The assignments of protons and carbon atoms in the NMR codes of compound [23] were carried out as follows:

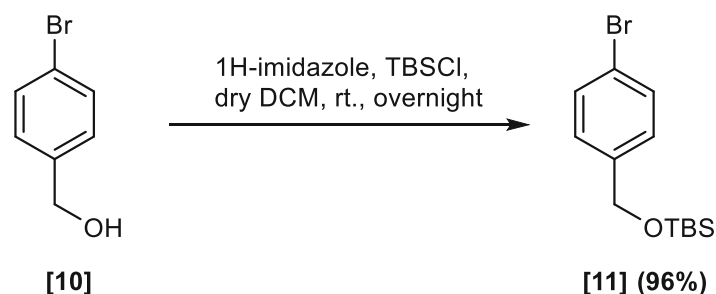


## E IV.4 Synthesis of aromatic diazine building blocks

The assignments of protons and carbon atoms in the NMR codes of compounds [11]-[17] were carried out as follows:



## E IV.4.1 ((4-Bromobenzyl)oxy)(*tert*-butyl)dimethylsilane [11]



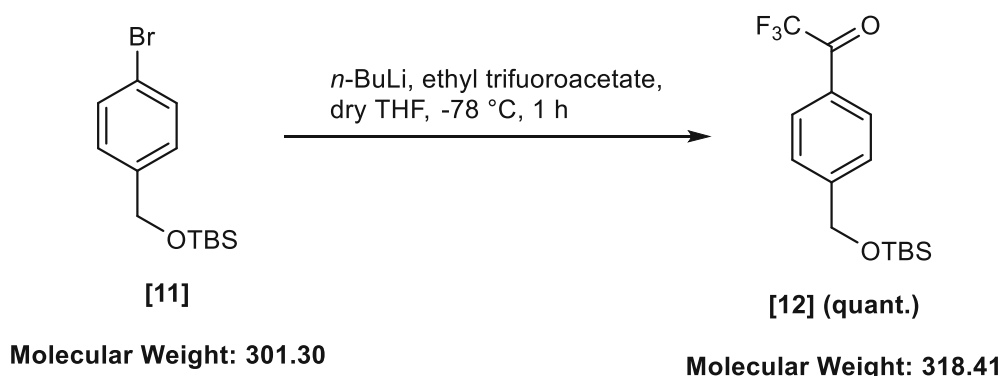
**Molecular Weight: 187.04**

**Molecular Weight: 301.30**

((4-Bromobenzyl)oxy)(*tert*-butyl)dimethylsilane [11] was prepared from (4-bromophenyl) methanol [10] in analogy to a literature procedure.<sup>380</sup> An oven-dried 100 mL three-neck round bottom flask was flushed with argon three times using standard Schlenk-technique. (4-Bromophenyl) methanol (10.00 g, 26.73 mmol, 1.00 equiv.) and 1*H*-imidazole (7.28 g, 106.9 mmol, 2.0 equiv.) were dissolved in 100 mL of dry DCM. TBDMSCl (16.12 g, 106.9 mmol, 2.00 equiv) was further added, at which point a colorless precipitate formed. The mixture was stirred at room temperature overnight, then poured into water (50 mL) and extracted with DCM (50 mL, three times). The combined organic layers were dried over anhydrous MgSO<sub>4</sub>, filtered, and concentrated under reduced pressure. After removal of the solvent in vacuum, the crude material (22.24 g, 138 %) was purified by flash column chromatography (2-step gradient EtAOc in PE: 0-1% 4 min; 1-5% 30 min) on silica gel (180 g) to afford the ((4-bromobenzyl)oxy)(*tert*-butyl)dimethylsilane [11] as a colorless liquid in 96% yield.

<b>Yield</b>	96% (15.53 g, 51.54 mmol)
<b>Appearance</b>	colorless liquid
<b>TLC</b>	R <sub>f</sub> (PE/EtOAc = 99/1) = 0.37
<b>Sum formula</b>	C <sub>13</sub> H <sub>31</sub> BrOSi
<b><sup>1</sup>H-NMR (400 MHz, CDCl<sub>3</sub>)</b>	δ = 0.09 (s, 6H, Si-(CH <sub>3</sub> ) <sub>2</sub> ), 0.94 (s, 9H, <i>tert</i> -butyl), 4.68 (s, 2H, CH <sub>2</sub> -OTBS), 7.20 (dt, <i>J</i> = 8.5, 0.8 Hz, 2H, H-3ar & H-5ar), 7.40 – 7.50 (m, 2H, H-2ar & H-6ar) ppm.
<b><sup>13</sup>C-NMR (101 MHz, CDCl<sub>3</sub>)</b>	δ = -5.1 (q, 2x Si-CH <sub>3</sub> ), 18.5 (s, Si-C(CH <sub>3</sub> ) <sub>3</sub> ), 26.1 (q, Si-C(CH <sub>3</sub> ) <sub>3</sub> ), 64.5 (t, CH <sub>2</sub> -OTBS), 120.7 (s, C-1ar), 127.9 (d, C-3ar & C-5ar), 131.4 (d, C-2ar & C-6ar), 140.6 (s, C-4ar) ppm.
<b>Comment</b>	Spectral data are in accordance with the literature.

## E IV.4.2 1-(4-(((*tert*-Butyldimethylsilyl)oxy)methyl)phenyl)-2,2,2-trifluoroethan-1-one [12]



1-(4-(((*tert*-Butyldimethylsilyl)oxy)methyl)phenyl)-2,2,2-trifluoroethan-1-one [12] was prepared from ((4-bromobenzyl)oxy)(*tert*-butyl)dimethylsilane [11] in analogy to a literature procedure.<sup>380</sup> An oven-dried 500 mL three-neck flask was flushed with argon three times using Schlenk-technique. ((4-Bromobenzyl)oxy)(*tert*-butyl)dimethylsilane [11] (15.0 g, 49.78 mmol) and dry THF (300 ml) were added under an inert atmosphere. *n*-BuLi (2.5 M in hexane, 33.6 mL, 41.82 mmol, 2.10 equiv.) was added dropwise at  $-78\text{ }^{\circ}\text{C}$  over 30 min. The solution was stirred for 15 min, and then ethyl trifluoroacetate (14.85 g, 41.82 mmol, 2.10 equiv.) was added over 15 min via syringe. The resulting mixture was stirred at  $-78\text{ }^{\circ}\text{C}$  for 1 hour and quenched at  $-78\text{ }^{\circ}\text{C}$  using saturated aq.  $\text{NaHCO}_3$  (50 mL) and then extracted with  $\text{Et}_2\text{O}$  (3 times, 50 mL). The combined organic layer was washed with saturated aq.  $\text{NaHCO}_3$  (50 mL) and brine (50 mL), dried over  $\text{MgSO}_4$ , and concentrated under reduced pressure to obtain 1-(4-(((*tert*-butyldimethylsilyl)oxy)methyl)phenyl)-2,2,2-trifluoroethan-1-one [12] as slightly yellow liquid (15.91 g, quant.). The product could be used in the following step without further purification.

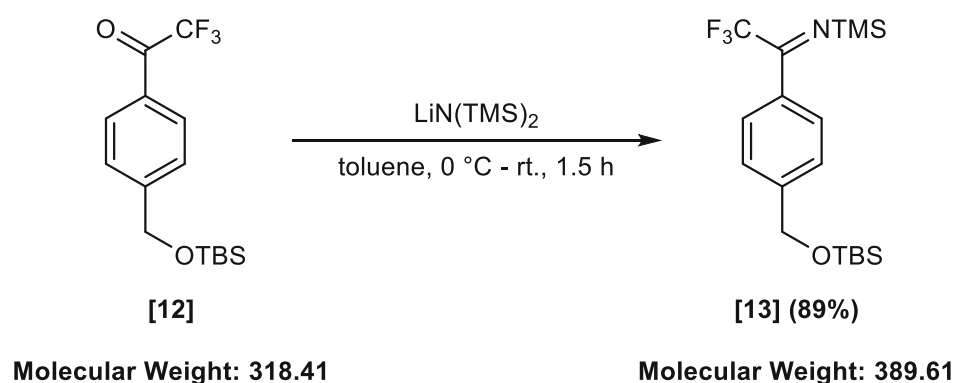
<b>Yield</b>	quant. (15.91 g, 49.78 mmol)
<b>Appearance</b>	pale yellow liquid
<b>TLC</b>	$R_f$ (PE/EtOAc = 95/5) = 0.68
<b>Sum formula</b>	$\text{C}_{15}\text{H}_{21}\text{F}_3\text{O}_2\text{Si}$
<b><math>^1\text{H-NMR}</math> (400 MHz, <math>\text{CDCl}_3</math>)</b>	$\delta = 0.13$ (s, 6H, Si-( $\text{CH}_3$ ) <sub>2</sub> ), 0.96 (s, 9H, <i>tert</i> butyl), 4.83 (d, $J = 1.0$ Hz, 2H, Ar- $\text{CH}_2$ -OTBS), 7.51 (d, $J = 8.8$ Hz, 2H, H-3ar & H-5ar), 8.05 (d, $J = 7.6$ Hz, 2H, H-2ar & H-6ar) ppm.

$^{13}\text{C-NMR}$  (101 MHz,  $\text{CDCl}_3$ )  $\delta = -5.2$  (q, 2x Si- $\text{CH}_3$ ), 18.5 (s, Si- $\text{C}(\text{CH}_3)_3$ ), 26.0 (q, Si- $\text{C}(\text{CH}_3)_3$ ), 64.4 (t, Ar- $\text{CH}_2\text{-OTBS}$ ), 116.9 (s/q,  $^1J_{\text{CF}} = 291.4$  Hz,  $\text{CF}_3$ ), 126.3 (d, C-2ar & C-6ar), 128.7 (s, C-1ar), 130.4 (d/q,  $^3J_{\text{CF}} = 2.1$  Hz, C-3ar & C-5ar), 150.2 (s, C-4ar), 180.3 (s/q,  $^2J_{\text{CF}} = 34.9$  Hz, carbonyl) ppm.

$^{19}\text{F NMR}$  (376 MHz,  $\text{CDCl}_3$ )  $\delta = -71.34$  ppm.

**Comment** Spectral data are in accordance with the literature.

### E IV.4.3 (Z)-1-(4-(((*tert*-Butyldimethylsilyl)oxy)methyl)phenyl)-2,2,2-trifluoro-*N*-(trimethylsilyl)ethan-1-imine [13]

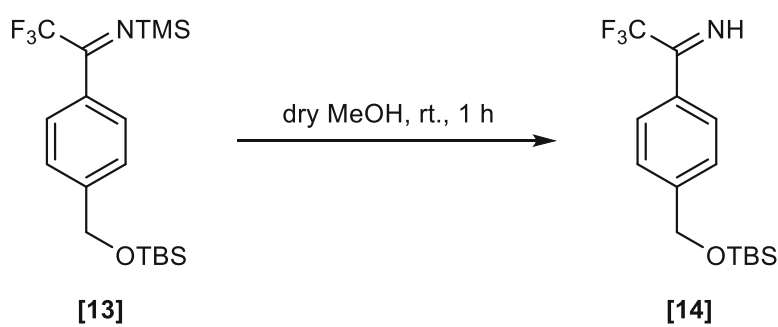


(*Z*)-1-(4-(((*tert*-Butyldimethylsilyl)oxy)methyl)phenyl)-2,2,2-trifluoro-*N*-(trimethylsilyl)ethan-1 imine [13] was prepared from 1-(4-(((*tert*-butyldimethylsilyl)oxy)methyl)phenyl)-2,2,2-trifluoroethan-1-one [12] according to a literature procedure.<sup>380</sup> To a solution of 1-(4-(((*tert*-butyldimethylsilyl)oxy)methyl)phenyl)-2,2,2-trifluoroethanone [12] (3.00 g, 1.57 mmol, 1.00 equiv.) in anhydrous toluene (7.2 mL) at 0 °C, a 1 M solution of lithium bis(trimethylsilyl)amide in THF (10.4 mL, 6.80 mmol, 1.10 equiv.) was added and warmed to room temperature (color change from colorless to bright yellow). After stirring for 1 hour, the reaction was extracted between water (20 mL, with 10% brine) and ether (30 mL). Upon isolation of the ether layer, the water layer was further extracted with fresh portions of  $\text{Et}_2\text{O}$  (30 mL) two more times. The combined ether layer from the extraction was washed with a fresh portion of water. The resultant organic layer was dried with anhydrous  $\text{MgSO}_4$  and concentrated under reduced pressure to obtain (*Z*)-1-(4-(((*tert*-butyldimethylsilyl)oxy)methyl)phenyl)-2,2,2-trifluoro-*N*-(trimethylsilyl)ethan-1-imine [13] as

a yellow liquid (3.27 g, 89 %), which was immediately used in the following step without further purification.

<b>Yield</b>	89% (3.27 g, 8.39 mmol)
<b>Appearance</b>	yellow liquid
<b>TLC</b>	R <sub>f</sub> (PE/EtOAc = 9/1) = 0.76
<b>Sum formula</b>	C <sub>18</sub> H <sub>30</sub> F <sub>3</sub> NOSi <sub>2</sub>
<b><sup>1</sup>H-NMR (400 MHz, CDCl<sub>3</sub>)</b>	δ = 0.11 (s, 6H, Si-(CH <sub>3</sub> ) <sub>2</sub> ), 0.18 (s, 9H, trimethylsilyl), 0.95 (s, 9H, tertbutyl), 4.78 (s, 2H, Ar-CH <sub>2</sub> -OTBS), 7.33 – 7.39 (m, 2H, H-3ar & H-5ar), 7.50 – 7.58 (m, 2H, H-2ar & H-6ar) ppm.
<b><sup>13</sup>C-NMR (101 MHz, CDCl<sub>3</sub>)</b>	δ = -5.1 (q, Si-(CH <sub>3</sub> ) <sub>2</sub> ), 0.5 (q, Si-(CH <sub>3</sub> ) <sub>3</sub> (TMS)), 18.5 (s, Si-C-(CH <sub>3</sub> ) <sub>3</sub> ), 26.1 (q, Si-C-(CH <sub>3</sub> ) <sub>3</sub> ), 64.6 (t, Ar-CH <sub>2</sub> -OTBS), 118.1 (s/q, <sup>1</sup> J <sub>CF</sub> = 285.7 Hz, CF <sub>3</sub> ), 125.8 (d, C-2ar & C-6ar), 127.9 (d/q, <sup>3</sup> J <sub>CF</sub> = 1.7 Hz, C-3ar & C-5ar), 134.4 (s, C-4ar), 144.5 (s, C-1ar), 158.6 (d/q, <sup>2</sup> J <sub>CF</sub> = 34.0 Hz, -C=NTMS) ppm.
<b><sup>19</sup>F NMR (376 MHz, CDCl<sub>3</sub>)</b>	δ = -69.16 ppm.
<b>Comment</b>	The compound was described in the literature as an intermediate, but no analytical data was available.

## E IV.4.4 1-(4-(((*tert*-Butyldimethylsilyl)oxy)methyl)phenyl)-2,2,2-trifluoroethan-1-imine [14]



**Molecular Weight: 389.61**

**Molecular Weight: 389.61**

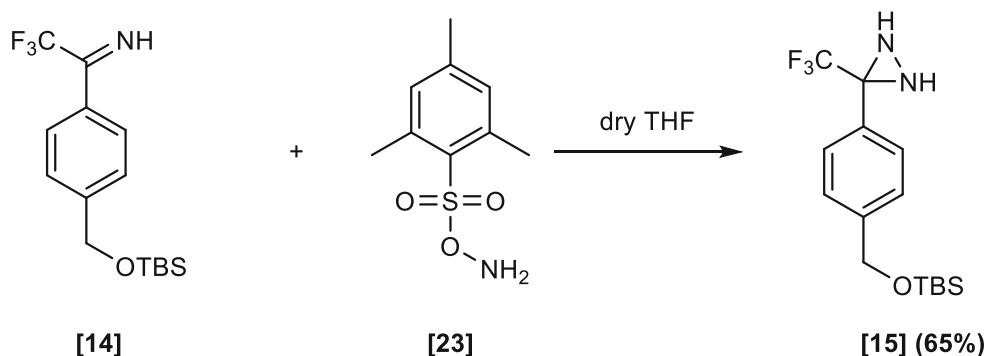
1-(4-(((*tert*-Butyldimethylsilyl)oxy)methyl)phenyl)-2,2,2-trifluoroethan-1-imine [14] was prepared from (*Z*)-1-(4-(((*tert*-butyldimethylsilyl)oxy)methyl)phenyl)-2,2,2-trifluoro-*N*-(trimethylsilyl)ethan-1-imine [13] according to a literature procedure.<sup>380</sup> An oven-dried Schlenk-tube was flushed with argon using standard Schlenk-technique. (*Z*)-1-(4-(((*tert*-butyldimethylsilyl)oxy)methyl)phenyl)-2,2,2-trifluoro-*N*-(trimethylsilyl)ethan-1-imine [13]



(3.27 g, 8.39 mmol, 1.00 equiv.) and dry methanol (6 mL) were added, and the resulting reaction mixture was stirred at room temperature, and the reaction progress was frequently monitored by  $^{19}\text{F}$ -NMR analysis. The resultant solution was then again concentrated under reduced pressure and further dried with a high vacuum pump for 15 min to obtain 1-(4-(((*tert*-butyldimethylsilyl)oxy)methyl)phenyl)-2,2,2-trifluoroethan-1-imine [14] as a yellow liquid (2.66 g, quant.), which was used in the following step without further purification.

<b>Yield</b>	quant. (2.66 g, 8.39 mmol)
<b>Appearance</b>	yellow liquid
<b>Sum formula</b>	$\text{C}_{15}\text{H}_{22}\text{F}_3\text{NOSi}$
<b><math>^1\text{H}</math>-NMR (400 MHz, <math>\text{CDCl}_3</math>)</b>	$\delta = 0.11$ (s, 6H, Si-( $\text{CH}_3$ ) <sub>2</sub> (major)), 0.12 (s, 6H, Si-( $\text{CH}_3$ ) <sub>2</sub> (minor)), 0.95 (s, 18H, <i>tert</i> butyl (major & minor)), 4.79 (s, 2H, Ar- $\text{CH}_2$ -OTBS (minor)), 4.80 (s, 2H, Ar- $\text{CH}_2$ -OTBS (major)), 7.37 – 7.47 (m, 4H, H-3ar & H-5-ar (major & minor)), 7.55 (d, $J = 8.2$ Hz, 2H, H-2ar & H-6-ar (minor)), 7.91 – 7.99 (m, 2H, H-2ar & H-6-ar (major)), 10.60 (s, 1H, NH-imine (major)), 10.73 (d, $J = 3.2$ Hz, 1H, NH-imine (minor)) ppm.
<b><math>^{13}\text{C}</math>-NMR</b>	not determined
<b><math>^{19}\text{F}</math> NMR (376 MHz, <math>\text{CDCl}_3</math>)</b>	$\delta = -68.61$ (minor), $-69.56$ (major), $-82.99$ (methanol adduct) ppm.
<b>Comment</b>	The compound was described in the literature as an intermediate, but no analytical data was available.

## E IV.4.5 3-(4-(((*tert*-Butyldimethylsilyl)oxy)methyl)phenyl)-3-(trifluoromethyl)diaziridine [15]



Molecular Weight: 317.43

Molecular Weight: 215.27

Molecular Weight: 332.44

3-(4-(((*tert*-Butyldimethylsilyl)oxy)methyl)phenyl)-3-(trifluoromethyl)diaziridine [**15**] was prepared from 1-(4-(((*tert*-butyldimethylsilyl)oxy)methyl)phenyl)-2,2,2-trifluoroethan-1-imine [**14**] in analogy to a literature procedure.<sup>380</sup> An oven-dried 25 mL three-neck flask equipped with a thermometer was flushed with argon using standard Schlenk-technique and 1-(4-(((*tert*-butyldimethylsilyl)oxy)methyl)phenyl)-2,2,2-trifluoroethan-1-imine [**14**] (2.21 g, 6.97 mmol, 1.00 equiv.) was added via syringe. Next, dry THF (5 mL) was added, and the mixture was cooled to -5 °C using an ice/NaCl bath. The aminating reagent MHS [**23**] (1.50 g, 6.97 mmol, 1.00 equiv.) dissolved in 5 mL dry THF was added dropwise to keep the temperature below 0 °C. The reaction mixture was then stirred for 1 hour at 0 °C, and after TLC indicated full conversion, piperidine (4 mL) was added dropwise to quench possible excess of the aminating reagent (precipitation of a colorless solid). The reaction was allowed to warm to room temperature and was stirred for 1 hour at this temperature. The reaction mixture was then extracted between water (30 mL) and ether (30 mL), and the aqueous phase was further extracted with ether (30 mL) two more times. The combined organic layers were dried over MgSO<sub>4</sub> and concentrated under reduced pressure to obtain the crude material as a yellowish oil (2.243 g, 96 %). The crude material was purified via flash column chromatography using a gradient of EtOAc in PE (1-7%, 30 min) to obtain 3-(4-(((*tert*-butyldimethylsilyl)oxy)methyl)phenyl)-3-(trifluoromethyl)diaziridine [**15**] as a colorless oil (1.51 g, 65%)

**Yield** 65% (1.51 g, 4.54 mmol)

**Appearance** colorless oil

**TLC** R<sub>f</sub> (PE/EtOAc = 95/5) = 0.35

**Sum formula** C<sub>15</sub>H<sub>23</sub>F<sub>3</sub>N<sub>2</sub>OSi

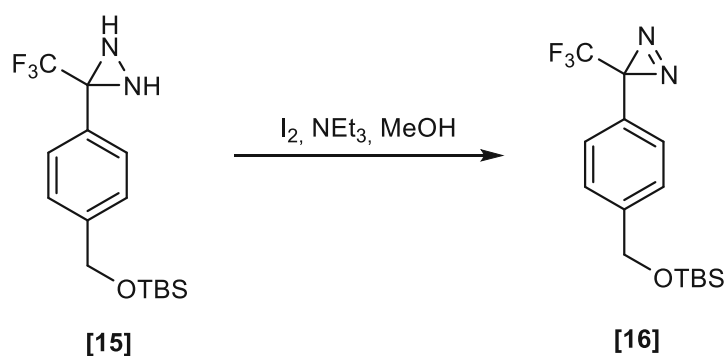
**<sup>1</sup>H-NMR (400 MHz, CDCl<sub>3</sub>)** δ = 0.11 (s, 6H, Si-(CH<sub>3</sub>)<sub>2</sub>), 0.95 (s, 9H, *tert*butyl), 2.20 (d, *J* = 8.0 Hz, 1H, NH (diaziridine)), 2.78 (d, *J* = 9.3 Hz, 1H, NH (diaziridine)), 4.76 (s, 2H, Ar-CH<sub>2</sub>-OTBS), 7.34 – 7.42 (m, 2H, C-3ar & C-5ar), 7.58 (d, *J* = 8.1 Hz, 2H, C-2ar & C-6ar) ppm.

**<sup>13</sup>C-NMR (101 MHz, CDCl<sub>3</sub>)** δ = -5.2 (q, Si-(CH<sub>3</sub>)<sub>2</sub>), 18.6 (s, Si-C-(CH<sub>3</sub>)<sub>3</sub>), 26.1 (q, Si-C-(CH<sub>3</sub>)<sub>3</sub>), 58.1 (s/q, <sup>2</sup>*J*<sub>CF</sub> = 36.1 Hz, diaziridine), 64.5 (t, Ar-CH<sub>2</sub>-OTBS), 123.7 (s/q, <sup>1</sup>*J*<sub>CF</sub> = 287.2 Hz, CF<sub>3</sub>), 126.3 (d, C-2ar & C-6ar), 128.2 (d, C-3ar & C-5ar), 130.4 (s, C-1ar), 143.9 (s, C-4ar) ppm.

**<sup>19</sup>F NMR (376 MHz, CDCl<sub>3</sub>)** δ = -75.60 ppm.

**Comment** The spectral data are in accordance with the literature.<sup>380</sup>

## E IV.4.6 3-(4-(((*tert*-Butyldimethylsilyl)oxy)methyl)phenyl)-3-(trifluoromethyl)-3*H*-diazirine [16]



Molecular Weight: 332.44

Molecular Weight: 330.43

3-(4-(((*tert*-Butyldimethylsilyl)oxy)methyl)phenyl)-3-(trifluoromethyl)-3*H*-diazirine [16] was prepared from 3-(4-(((*tert*-butyldimethylsilyl)oxy)methyl)phenyl)-3-(trifluoromethyl)diaziridine [15] in analogy to a literature procedure.<sup>380</sup> 3-(4-(((*tert*-Butyldimethylsilyl)oxy)methyl)phenyl)-3-(trifluoromethyl)diaziridine [15] (1.25 g, 3.76 mmol, 1.00 equiv.) was placed in a 25 mL round bottom flask, which was wrapped in aluminum foil to prevent exposure to light. Dry MeOH (7 mL) was added, and the solution was cooled with an ice/water bath. NEt<sub>3</sub> (0.8 mL) was added, and the mixture was stirred for 5 min. I<sub>2</sub> was added in small portions until a dark red-brown color persisted for more than 10 min. The reaction was then diluted with EtOAc (20 mL), and the organic phase was washed with 10% aq. Na<sub>2</sub>S<sub>2</sub>O<sub>3</sub> (20 mL), water (20 mL), and brine (20 mL). The organic phase was dried over MgSO<sub>4</sub>, filtrated, and evaporated to obtain the crude material as a yellow liquid (1.18 g, 95 %), which was used in the following deprotection step without further purification.

**Yield** 95% (1.18 g, 3.56 mmol)

**Appearance** yellow liquid

**TLC** R<sub>f</sub> (PE/EtOAc = 9/1) = 0.48

**Sum formula** C<sub>15</sub>H<sub>21</sub>F<sub>3</sub>N<sub>2</sub>OSi

**<sup>1</sup>H-NMR (400 MHz, CDCl<sub>3</sub>)** δ = 0.11 (s, 6H, Si-(CH<sub>3</sub>)<sub>2</sub>), 0.96 (s, 9H, tertbutyl), 4.76 (s, 2H, Ar-CH<sub>2</sub>-OTBS), 7.18 (d, *J* = 7.6 Hz, 2H, H-3ar & H-5ar), 7.37 (d, *J* = 8.8 Hz, 2H, H-2ar & H-6ar) ppm.

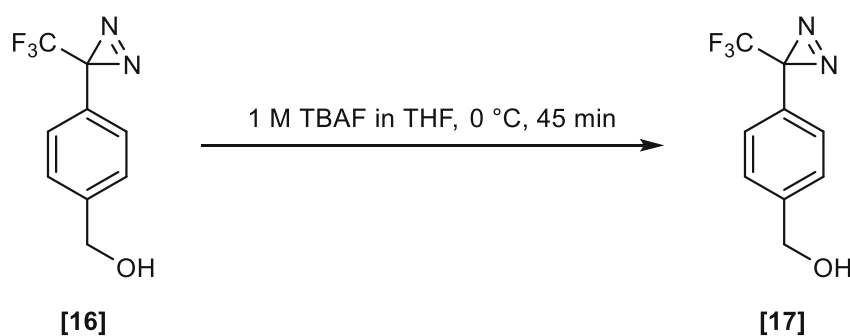
**<sup>13</sup>C-NMR (101 MHz, CDCl<sub>3</sub>)** δ = -5.2 (q, Si-(CH<sub>3</sub>)<sub>2</sub>), 18.5 (s, Si-C-(CH<sub>3</sub>)<sub>3</sub>), 26.0 (q, Si-C-(CH<sub>3</sub>)<sub>3</sub>), 28.6 (s/q, <sup>2</sup>*J*<sub>CF</sub> = 40.5 Hz, diazirine), 64.4 (t, Ar-CH<sub>2</sub>-OTBS), 122.4 (s/q, <sup>1</sup>*J*<sub>CF</sub> = 274.7 Hz, CF<sub>3</sub>), 126.4 (d, C-2ar & C-

6ar), 126.6 (d, C-3ar & C-5ar), 127.7 (s, C-1ar), 143.5 (s, C-4ar) ppm.

$^{19}\text{F}$  NMR (376 MHz,  $\text{CDCl}_3$ )  $\delta = -65.34$  ppm.

**Comment** The spectral data are in accordance with the literature.<sup>380</sup>

## E IV.4.7 (4-(3-(Trifluoromethyl)-3*H*-diazirin-3-yl)phenyl)methanol [17]



**Molecular Weight: 330.43**

**Molecular Weight: 216.16**

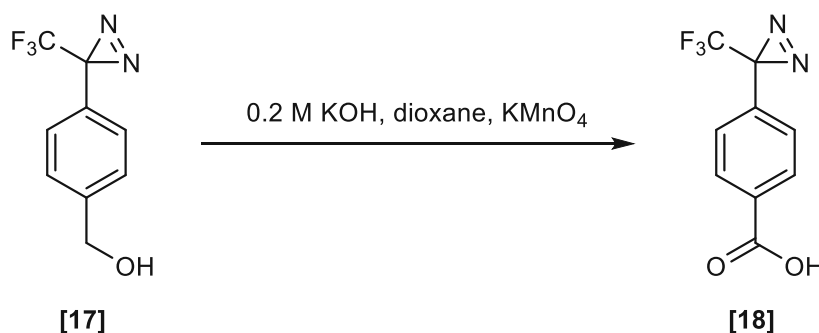
(4-(3-(Trifluoromethyl)-3*H*-diazirin-3-yl)phenyl)methanol [17] was prepared from 3-(4-(((*tert*-butyldimethylsilyloxy)methyl)phenyl)-3-(trifluoromethyl)-3*H*-diazirine [16] in analogy to a literature procedure.<sup>380</sup> 3-(4-(((*tert*-Butyldimethylsilyloxy)methyl)phenyl)-3-(trifluoromethyl)-3*H*-diazirine [16] (1.10 g, 0.48 mmol, 1.00 equiv.) was placed in a 25 mL round bottom flask, which was wrapped in aluminum foil to prevent exposure to light. THF (15 mL) was added, and the solution was cooled with an ice/water bath. A 1 M solution of TBAF in THF (3.66 mL, 3.66 mmol, 1.10 equiv.) was added and stirred at 0 °C until TLC analysis indicated full conversion of the starting material (45 min). The reaction was further diluted with EtOAc (50 mL), and the organic phase was washed with brine. Upon isolation of the organic phase, the aqueous phase was further extracted with EtOAc (50 mL) one more time. The combined organic layers were then dried over  $\text{MgSO}_4$ , filtrated, and evaporated under reduced pressure (water bath ambient temperature) to obtain the crude material as orange oil. Purification by flash column chromatography using a gradient of EtOAc in PE (5-20% 30 min) afforded (4-(3-(trifluoromethyl)-3*H*-diazirin-3-yl)phenyl)methanol [17] as colorless oil (692 mg, 96%).

**Yield** 96% (692 mg, 3.20 mmol)

**Appearance** colorless oil

<b>TLC</b>	$R_f$ (PE/EtOAc = 4/1) = 0.36
<b>Sum formula</b>	$C_9H_7F_3N_2O$
<b><math>^1H</math>-NMR (400 MHz, <math>CDCl_3</math>)</b>	$\delta$ = 1.71 (t, $J$ = 5.9 Hz, 1H, Ar-CH <sub>2</sub> -OH), 4.72 (d, $J$ = 5.8 Hz, 2H, Ar-CH <sub>2</sub> -OH), 7.20 (d, $J$ = 8.6 Hz, 2H, C-3ar & C-5ar), 7.40 (d, $J$ = 8.0 Hz, 2H, C-2ar & C-6ar) ppm.
<b><math>^{13}C</math>-NMR (101 MHz, <math>CDCl_3</math>)</b>	$\delta$ = 28.2 (s/q, $^2J_{CF}$ = 41.0 Hz, diazirine), 64.5 (Ar-CH <sub>2</sub> -OH), 122.1 (s/q, $^1J_{CF}$ = 274.7 Hz, CF <sub>3</sub> ), 126.7 (d/q, $^3J_{CF}$ = 1.5 Hz, C-3ar & C-5ar), 127.1 (d, C-2ar & C-6ar), 128.4 (s, C-1ar), 142.6 (d, C-4ar) ppm.
<b><math>^{19}F</math> NMR (376 MHz, <math>CDCl_3</math>)</b>	$\delta$ = -65.30
<b>Comment</b>	The spectral data are in accordance with the literature. <sup>380</sup>

## E IV.4.8 4-(3-(Trifluoromethyl)-3H-diazirin-3-yl)benzoic acid [18]



[17]

[18]

Molecular Weight: 216.16

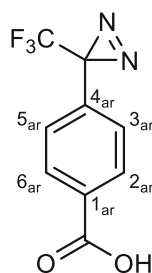
Molecular Weight: 230.15

4-(3-(Trifluoromethyl)-3H-diazirin-3-yl)benzoic acid [18] was prepared from 3-(4-(((tert-butylideneamino)oxy)phenyl)methanol [19] in analogy to a literature procedure.<sup>433</sup> A solution of 4-(3-(trifluoromethyl)-3H-diazirin-3-yl)phenyl)methanol [17] (1.33 g, 6.15 mmol, 1.00 equiv.) in 0.2 N KOH (36 mL) and dioxane (4.8 mL) was treated with  $KMnO_4$  (1.10 g, 9.23 mmol, 1.5 equiv.). The biphasic mixture was vigorously stirred at rt. in the dark until TLC analysis indicated full conversion of the starting material and was then filtered. To the filtrate, 24 mL of 1 N HCl was added, and the resulting solid was dissolved in 100 mL  $Et_2O$ . The organic solution was washed with water (3 times, 30 mL), dried with anhydrous  $MgSO_4$ , and the solvents were evaporated under vacuum to give 1.30 g (92% yield) of 4-(3-(trifluoromethyl)-3H-diazirin-3-yl)benzoic acid [18] as a colorless solid.

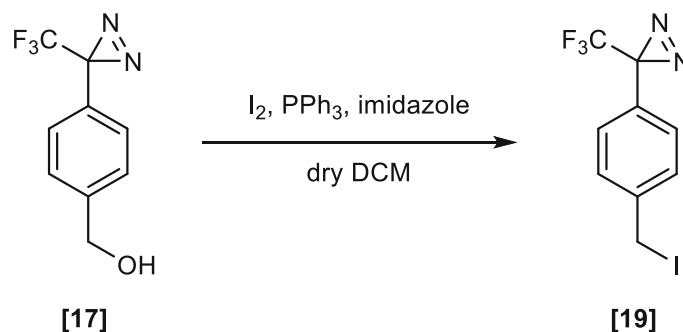
**Yield** 92% (1.30 mg, 5.63 mmol)

<b>Appearance</b>	colorless solid
<b>TLC</b>	$R_f$ (CHCl <sub>3</sub> /MeOH = 80/20) = 0.56
<b>Melting point</b>	122.0 °C – 123.0 °C [decomposition] (Lit. <sup>434</sup> : 123.0 °C – 125.0 °C [decomposition])
<b>Sum formula</b>	C <sub>9</sub> H <sub>5</sub> F <sub>3</sub> N <sub>2</sub> O <sub>2</sub>
<b><sup>1</sup>H-NMR (400 MHz, CDCl<sub>3</sub>)</b>	$\delta$ = 7.29 (d, $J$ = 8.1 Hz, 2H, H-3 & H-5), 8.10 – 8.18 (m, 2H, H-2 & H-6), 12.08 (s, 1H, COOH) ppm.
<b><sup>13</sup>C-NMR (101 MHz, CDCl<sub>3</sub>)</b>	$\delta$ = 28.6 (s/q, $^2J_{CF}$ , $J$ = 40.9 Hz, diazirine), 122.0 (s/q, $^1J_{CF}$ = 274.8 Hz, CF <sub>3</sub> ), 126.6 (d/q, $^3J_{CF}$ = 1.7 Hz, C-3ar & C-5ar), 130.4 (s, C-1ar), 130.7 (d, C-2ar & C-6ar), 135.0 (s, C-4ar), 171.4 (s, COOH) ppm.
<b><sup>19</sup>F NMR (376 MHz, CDCl<sub>3</sub>)</b>	$\delta$ = -64.87 ppm.
<b>Comment</b>	Spectral data are in accordance with the literature.

The assignments of protons and carbon atoms in the NMR codes of compound [18] were carried out as follows:



## E IV.4.9 3-(4-(Iodomethyl)phenyl)-3-(trifluoromethyl)-3H-diazirine [19]



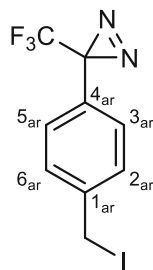
Molecular Weight: 216.16

Molecular Weight: 326.06

3-(4-(Iodomethyl)phenyl)-3-(trifluoromethyl)-3*H*-diazirine [19] was synthesized from (4-(3-(trifluoromethyl)-3*H*-diazirin-3-yl)phenyl)methanol [17] according to the following protocol. PPh<sub>3</sub> (2.13 g, 8.12 mmol, 1.8 eq.) and imidazole (0.95 g, 13.93 mmol, 3.0 eq.) were dissolved in DCM (20 mL). Iodine (2.38 g, 18.73 mmol, 4.10 equiv.) was added slowly to the solution, and the mixture was stirred at rt. for 25 min. (4-(3-(Trifluoromethyl)-3*H*-diazirin-3-yl)phenyl)methanol [17] (1.00 g, 4.62 mmol, 1.0 eq.) was dissolved in DCM (10 mL) and added to the reaction, which was stirred for another 2 hours at room temperature, and the reaction progress was monitored by TLC. After completion, saturated aq. Na<sub>2</sub>S<sub>2</sub>O<sub>3</sub> solution (30 mL) was added to the reaction mixture until the brownish color disappeared. The solution was extracted with EtOAc (2 times, 25 mL), and the combined organic phases were washed with brine and dried over Na<sub>2</sub>SO<sub>4</sub>. Finally, the solvent was removed at reduced pressure to obtain the crude product as a yellow oil, which solidified in the cold. Purification via flash column chromatography (silica:crude = 100:1, petrol ether, 2% EtOAc) furnished 3-(4-(iodomethyl)phenyl)-3-(trifluoromethyl)-3*H*-diazirine [19] as a pale yellow solid (0.58 g, 1.78 mmol, 39%).

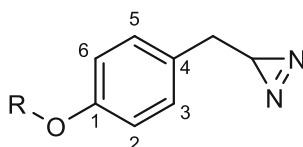
<b>Yield</b>	39% (0.58 g, 1.78 mmol)
<b>Appearance</b>	pale yellow solid
<b>TLC</b>	R <sub>f</sub> (PE/EtOAc = 98/2) = 0.73
<b>Sum formula</b>	C <sub>9</sub> H <sub>6</sub> F <sub>3</sub> IN <sub>2</sub>
<b><sup>1</sup>H-NMR (400 MHz, CDCl<sub>3</sub>)</b>	δ = 4.42 (s, 2H, CH <sub>2</sub> -I), 7.08 – 7.15 (d, <i>J</i> = 7.7 Hz, 2H, H-2 & H-6), 7.36 – 7.44 (d, <i>J</i> = 8.4 Hz, 2H, H-3 & H-5) ppm.
<b><sup>13</sup>C-NMR (101 MHz, CDCl<sub>3</sub>)</b>	δ = 3.7 (t, Ar-CH <sub>2</sub> -I), 28.7 (s, diazirine), 122.2 (s/q, <sup>1</sup> <i>J</i> <sub>CF</sub> = 274.8 Hz, CF <sub>3</sub> ), 127.1 (d, C-2 & C-6), 128.8 (s, C-4), 129.3 (d, C-3 & C-5), 141.3 (s, C-1) ppm.
<b><sup>19</sup>F-NMR (376 MHz, CDCl<sub>3</sub>)</b>	δ = -64.87 ppm.

The assignments of protons and carbon atoms in the NMR codes of compound [19] were carried out as follows:

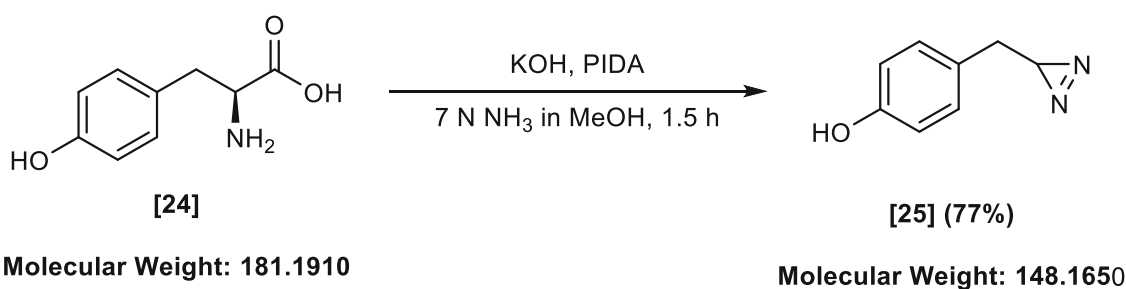


## E IV.5 Synthesis of alternative aromatic diazirine building blocks

The assignments of protons and carbon atoms in the NMR codes of compounds [25], [27], and [28] were carried out as follows:



### E IV.5.1 4-((3*H*-Diazirin-3-yl)methyl)phenol [25]



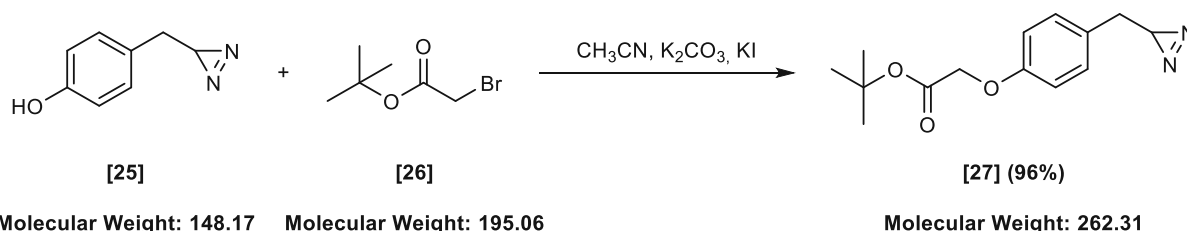
4-((3*H*-Diazirin-3-yl)methyl)phenol [25] was prepared from *L*-tyrosine [24] according to the following literature procedure.<sup>383</sup> An oven-dried Schlenk-flask was flushed with argon using standard Schlenk-technique. *L*-tyrosine [24] (2.00 g, 11.04 mmol, 1.00 equiv.) and KOH (1.24 g, 22.08 mmol, 2.00 equiv.) were added under an inert atmosphere. 7 NH<sub>3</sub> in MeOH (27.60 mL) was added via syringe, and the resulting mixture was cooled with an ice/water bath to 0 °C (external temperature). (Diacetoxyiodo)benzene (9.08 g, 33.11 mmol, 3.00 equiv.) was added in one portion, and the reaction was stirred for 30 min at 0 °C and then allowed to slowly warm up to room temperature and stirred for an additional 90 minutes. After TLC analysis indicated full conversion of the starting material, the volatiles were removed under reduced pressure using a rotary evaporator. The crude material was purified via flash column chromatography (SiO<sub>2</sub>, 100:1, EtOAc in PE (10% 4 min; 10-25% 20 min) to obtain 4-((3*H*-diazirin-3-yl)methyl)phenol [25] as a brown oil.

**Yield** 77% (1.26 g, 11.04 mmol)  
**Appearance** brown oil



<b>TLC</b>	$R_f$ (PE/EtOAc = 80/20) = 0.4
<b>Sum formula</b>	$C_8H_8N_2O$
<b><math>^1H</math>-NMR (400 MHz, <math>CDCl_3</math>)</b>	$\delta$ = 1.09 (t, $J$ = 4.4 Hz, 3H, CH (terminal diazirine)), 2.48 (d, $J$ = 4.4 Hz, 2H, Ar- $CH_2$ -), 6.76 – 6.84 (m, 1H, H-3 & H-5 (aromatic)), 7.08 – 7.16 (m, 2H, H-2 & H-6 (aromatic)) ppm.
<b><math>^{13}C</math>-NMR (101 MHz, <math>CDCl_3</math>)</b>	$\delta$ = 22.2 (d, CH (terminal diazirine)), 35.8 (t, -Ar- $CH_2$ -), 115.7 (d, C-2 & C-6), 128.4 (s, C-4), 130.3 (d, C-3 & C-5), 154.6 (s, C-1) ppm.
<b>Comment</b>	Spectral data are in accordance with the literature. <sup>383</sup>

## E IV.5.2 *tert*-Butyl 2-(4-((3*H*-diazirin-3-yl)methyl)phenoxy)acetate [27]



*tert*-Butyl 2-(4-((3*H*-diazirin-3-yl)methyl)phenoxy)acetate [27] was synthesized from 4-((3*H*-diazirin-3-yl)methyl)phenol [25] following a literature procedure.<sup>383</sup> An oven-dried Schlenk-tube was flushed with argon using standard Schlenk-technique. 4-((3*H*-diazirin-3-yl)methyl)phenol [25] (300 mg, 2.02 mmol, 1.00 equiv.) was added under an inert atmosphere followed by the addition of dry acetonitrile (10 mL).  $K_2CO_3$  (420 mg, 3.04 mmol, 1.50 equiv.) and KI (50 mg, 0.30 mmol, 0.15 equiv.) were further added, followed by the dropwise addition of *tert*-butyl bromoacetate [26] (494 mg, 2.53 mmol, 1.25 equiv.). The resulting colorless suspension was left to stir overnight at room temperature. After full conversion (monitored by TLC), the reaction was quenched with water (20 mL) and extracted with EtOAc (3 times, 20 mL). The combined organic layers were dried over anhydrous magnesium sulfate and filtered. Organic volatiles were removed under reduced pressure to obtain *tert*-butyl 2-(4-((3*H*-diazirin-3-yl)methyl)phenoxy)acetate [27] as a yellow oil, which crystallized on standing.

<b>Yield</b>	96% (510 mg, 1.95 mmol)
<b>Appearance</b>	yellow solid
<b>Melting point</b>	45.0 – 47.0 °C (Lit. <sup>383</sup> : 45.5 – 47.8 °C)
<b>TLC</b>	$R_f$ (PE/EtOAc = 80/20) = 0.65

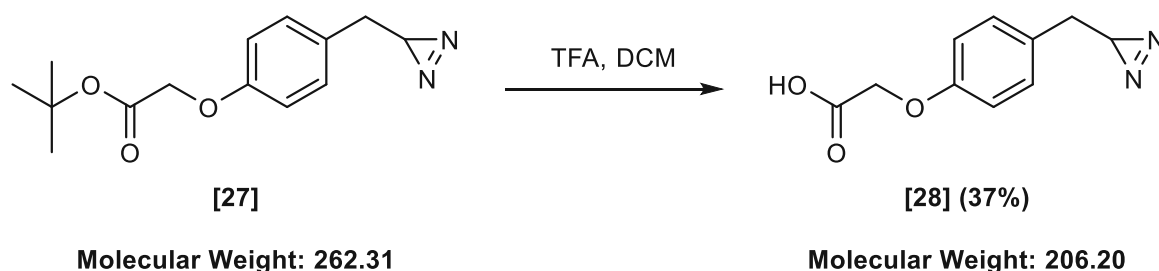
**Sum formula**  $C_{14}H_{18}N_2O_3$

**$^1H$ -NMR (400 MHz,  $CDCl_3$ )**  $\delta$  = 1.09 (t,  $J$  = 4.4 Hz, 1H,  $\underline{C}H$  (terminal diazirine)), 1.49 (s, 9H, tertbutyl), 2.48 (d,  $J$  = 4.4 Hz, 2H, Ar- $\underline{C}H_2$ -CH), 4.50 (s, 1H, Ar-O- $\underline{C}H_2$ -COOtertbutyl), 6.86 (d,  $J$  = 8.7 Hz, 2H, H-3 & H-5), 7.10 – 7.26 (m, 2H, H-2 & H-6) ppm.

**$^{13}C$ -NMR (101 MHz,  $CDCl_3$ )**  $\delta$  = 22.2 (d,  $\underline{C}H$  (terminal diazirine)), 28.2 (q,  $-C(\underline{C}H_3)_3$ ), 35.9 (t, Ar- $\underline{C}H_2$ -CH), 65.9 (t, Ar-O- $\underline{C}H_2$ -COOC(CH<sub>3</sub>)<sub>3</sub>), 82.5 (s,  $\underline{C}(\underline{C}H_3)_3$ ), 115.0 (d, C-2 & C-6), 129.1 (s, C-4), 130.1 (d, C-3 & C-5), 157.1 (s, C-1), 168.2 (s,  $\underline{C}OOC(\underline{C}H_3)_3$ ) ppm.

**Comment** Spectral data are in accordance with the literature.<sup>383</sup>

### E IV.5.3 2-(4-((3*H*-Diazirin-3-yl)methyl)phenoxy)acetic acid [28]



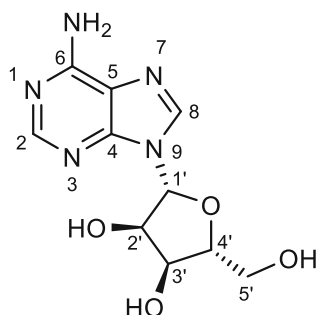
2-(4-((3*H*-Diazirin-3-yl)methyl)phenoxy)acetic acid [28] was synthesized from *tert*-butyl 2-(4-((3*H*-diazirin-3-yl)methyl)phenoxy)acetate [27] according to a modified literature procedure.<sup>383</sup> A 25 mL round bottom flask was charged with *tert*-butyl 2-(4-((3*H*-diazirin-3-yl)methyl)phenoxy)acetate [27] (400 mg, 1.52 mmol, 1.00 equiv.) and DCM (15 mL) was added. Next, TFA (15 mL) was added dropwise. The reaction progress was monitored by TLC analysis, and after full conversion of the starting material, the reaction mixture was then concentrated under reduced pressure. The remaining crude was dissolved in EtOAc (20 mL), and the organic layer was washed with water (20 mL) and brine (20 mL), dried over anhydrous  $MgSO_4$ , filtered, and then removed under reduced pressure. 2-(4-((3*H*-Diazirin-3-yl)methyl)phenoxy)acetic acid [28] was obtained as grey oil, which crystallized on standing.

**Yield** 37% (116 mg, 1.52 mmol)  
**Appearance** off-white solid  
**Melting point** 101.0 – 103.0 °C (Lit.<sup>383</sup>: 103.6 °C)  
**TLC**  $R_f$  (EtOAc) = 0.68

<b>Sum formula</b>	C <sub>10</sub> H <sub>10</sub> N <sub>2</sub> O <sub>3</sub>
<b><sup>1</sup>H-NMR (400 MHz, CDCl<sub>3</sub>)</b>	$\delta = 1.09$ (t, $J = 4.4$ Hz, 1H, CH (terminal diazirine)), $2.50$ (d, $J = 4.4$ Hz, 1H, Ar-CH <sub>2</sub> -CH), $4.67$ (s, 2H, Ar-O-CH <sub>2</sub> -COOH), $6.89$ (d, $J = 8.7$ Hz, 1H, H-2 & H-6), $7.19$ (d, $J = 8.6$ Hz, 2H, H-3 & H-5) ppm.
<b><sup>13</sup>C-NMR (101 MHz, CDCl<sub>3</sub>)</b>	$\delta = 22.1$ (d, CH (terminal diazirine)), $35.8$ (t, Ar-CH <sub>2</sub> -CH), $65.1$ (t, Ar-O-CH <sub>2</sub> -COOH), $115.1$ (d, C-2 & C-6), $129.7$ (s, C-4), $130.3$ (d, C-3 & C-5), $156.6$ (s, C-1), $173.95$ (s, COOH) ppm.
<b>Comment</b>	Spectral data are in accordance with the literature.

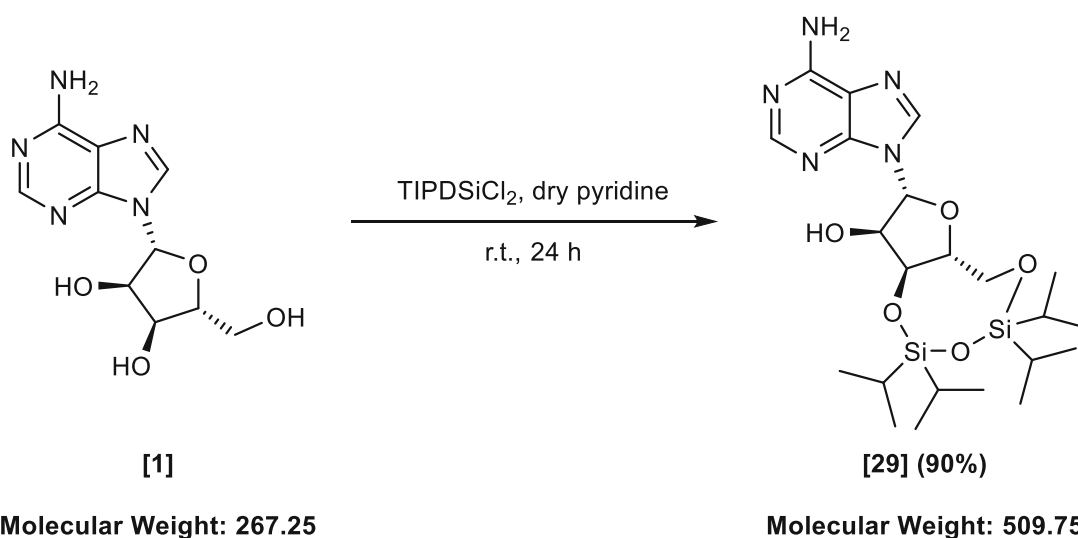
## E IV.6 Synthesis of modified adenylyl building blocks

The assignments of protons and carbon atoms in the NMR codes of derivatives of compound [1] were carried out as follows:



## E IV.7 Synthesis of protected adenosine building blocks

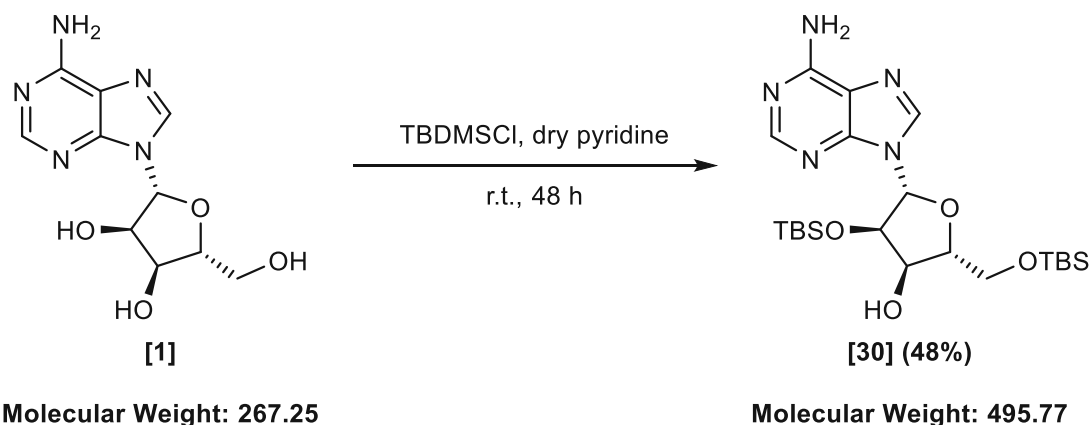
### E IV.7.1 (6*aR*,8*R*,9*R*,9*aS*)-8-(6-Amino-9*H*-purin-9-yl)-2,2,4,4-tetraisopropyltetrahydro-6*H*-furo[3,2-*f*][1,3,5,2,4]trioxadisilocin-9-ol [1]



(6*aR*,8*R*,9*R*,9*aS*)-8-(6-Amino-9*H*-purin-9-yl)-2,2,4,4-tetraisopropyltetrahydro-6*H*-furo[3,2-*f*][1,3,5,2,4]trioxadisilocin-9-ol [29] was prepared from adenosine [1] according to a literature procedure.<sup>364</sup> An oven-dried 250 mL three-necked round bottom flask was flushed with argon using Schlenk-technique. Adenosine [1] (10 g, 37.42 mmol, 1.00 equiv.) and anhydrous pyridine (120 mL) were added. To the resulting suspension was further added 4-DMAP (2.29 g, 18.71 mmol, 0.5 equiv.) and dichloro-1,1,3,3-tetraisopropylidisiloxane (14.4 mL, 44.90 mmol, 1.20 equiv.) under an inert atmosphere and the reaction was stirred at room temperature over night. After TLC analysis indicated full conversion of the starting material, pyridine was removed under reduced pressure to obtain the crude material as a colorless solid. The residue was re-dissolved in MeOH, silica was added, and the mixture was again concentrated to obtain a free-flowing mixture. The crude product was then subjected to flash column chromatography using a gradient of MeOH in DCM (3%, 4 min; 3-10% 26 min, dry load) as eluent to obtain (6*aR*,8*R*,9*R*,9*aS*)-8-(6-amino-9*H*-purin-9-yl)-2,2,4,4-tetraisopropyltetrahydro-6*H*-furo[3,2-*f*][1,3,5,2,4]trioxadisilocin-9-ol [29] as colorless solid (17.16 g, 90% yield).

<b>Yield</b>	90% (17.16 g, 33.66 mmol)
<b>Appearance</b>	colorless solid
<b>Melting point</b>	94.0 – 95.0 °C (Lit. <sup>435</sup> : 98.0 – 99.5 °C)
<b>TLC</b>	R <sub>f</sub> (CHCl <sub>3</sub> /MeOH = 19/1) = 0.25
<b>Sum formula</b>	C <sub>22</sub> H <sub>39</sub> N <sub>5</sub> O <sub>5</sub> Si <sub>2</sub>
<b><sup>1</sup>H-NMR (400 MHz, CDCl<sub>3</sub>)</b>	δ = 1.03 (s, 28H, 4x isopropyl), 3.92 (dd, <i>J</i> = 12.6, 2.7 Hz, 1H, H-5'b), 4.00 (dt, <i>J</i> = 8.6, 3.0 Hz, 1H, H-4'), 4.05 (dd, <i>J</i> = 12.6, 3.4 Hz, 1H, H-5'a), 4.51 (t, <i>J</i> = 4.8 Hz, 1H, H-2'), 4.79 (dd, <i>J</i> = 8.5, 5.1 Hz, 1H, H-3'), 5.61 (d, <i>J</i> = 4.6 Hz, 1H, OH-2'), 5.87 (d, <i>J</i> = 1.2 Hz, 1H, H-1'), 7.32 (s, 2H, NH <sub>2</sub> ), 8.07 (s, 1H, H-2), 8.20 (s, 1H, H-8) ppm.
<b><sup>13</sup>C-NMR (101 MHz, CDCl<sub>3</sub>)</b>	δ = 12.1 (d, Si-CH-CH <sub>3</sub> ), 12.2 (d, Si-CH-CH <sub>3</sub> ), 12.4 (d, Si-CH-CH <sub>3</sub> ), 12.7 (d, Si-CH-CH <sub>3</sub> ), 16.8 (q, Si-CH-CH <sub>3</sub> ), 16.9 (q, Si-CH-CH <sub>3</sub> ), 16.9 (q, Si-CH-CH <sub>3</sub> ), 17.0 (q, Si-CH-CH <sub>3</sub> ), 17.2 (q, Si-CH-CH <sub>3</sub> ), 17.2 (q, 2x Si-CH-CH <sub>3</sub> ), 17.4 (q, Si-CH-CH <sub>3</sub> ), 60.8 (t, C-5'), 69.8 (d, C-3'), 73.6 (d, C-2'), 80.8 (d, C-4'), 89.3 (d, C-1'), 119.3 (s, C-5), 139.2 (d, C-8), 148.6 (s, C-4), 152.5 (d, C-2), 156.1 (s, C-6) ppm.
<b>Optical rotation</b>	[α] <sub>D</sub> <sup>20</sup> = -45.2 (c = 1.0, CHCl <sub>3</sub> )
<b>Comment</b>	Spectral data are in accordance with the literature. <sup>436,437</sup>

## E IV.7.2 (2*R*,3*R*,4*R*,5*R*)-5-(6-Amino-9*H*-purin-9-yl)-4-((*tert*-butyldimethylsilyl)oxy)-2-(((*tert*-butyldimethylsilyl)oxy)methyl)tetrahydrofuran-3-ol [30]

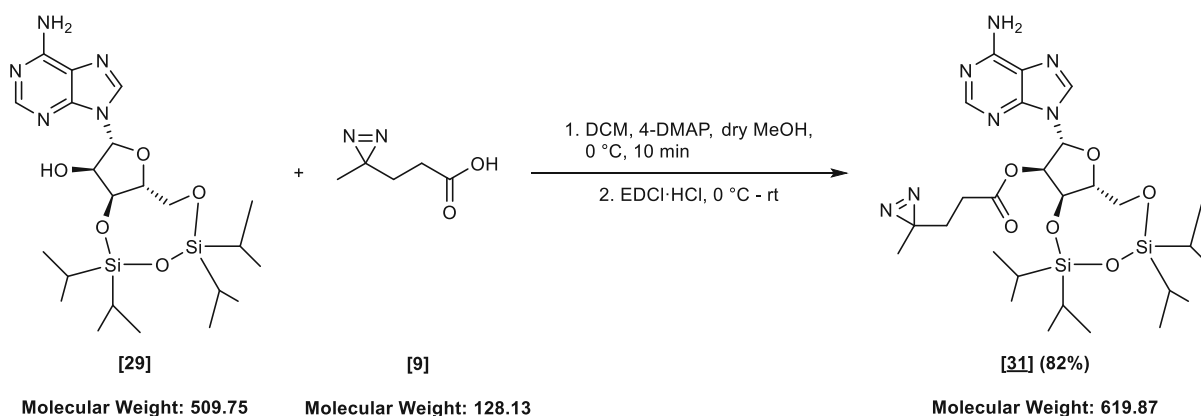


(2*R*,3*R*,4*R*,5*R*)-5-(6-Amino-9*H*-purin-9-yl)-4-((*tert*-butyldimethylsilyl)oxy)-2-(((*tert*-butyldimethylsilyl)oxy)methyl)tetrahydrofuran-3-ol [**30**] was prepared from adenosine [**1**] according to a literature procedure.<sup>363</sup> A 10 mL oven-dried three-necked flask was flushed with argon using standard Schlenk-technique. Adenosine [**1**] (4.00g, 14.97 mmol, 1.00 equiv., scaled up to 10.00 g) was suspended in dry pyridine (40 mL), and TBDMSCl (6.77 g, 44.90 mmol, 3.00 equiv.) was added. The reaction was stirred for 48 h (monitored by TLC) and was then diluted with CH<sub>2</sub>Cl<sub>2</sub>. The organic phase was further washed with 2 N HCl solution, sat. aq. NaHCO<sub>3</sub>, and brine. The organic phase was dried with MgSO<sub>4</sub> and concentrated under reduced pressure to yield a crude mixture of 2',5'-and 3',5'-isomers. The crude material was then subjected to flash column chromatography using a three-step gradient of EtOAc in PE (dry load, 20-30% 10 min; 30-50% 30 min; 50-70% 20min) to obtain (2*R*,3*R*,4*R*,5*R*)-5-(6-amino-9*H*-purin-9-yl)-4-((*tert*-butyldimethylsilyl)oxy)-2-(((*tert*-butyldimethylsilyl)oxy)methyl)tetrahydrofuran-3-ol [**30**] as colorless solid (2.89 g, 39%). The isolated 3',5'-*O*-isomer [**30b**] was further isomerized by dissolving it in MeOH (20 mL) and NEt<sub>3</sub> (1 mL), and the resulting solution was stirred until TLC analysis did not show any further conversion of the starting material. Next, volatiles were removed, and the crude material was subjected to flash column chromatography to obtain 0.67 g of pure [**30**].

<b>Yield</b>	48% (3.56 g, 14.97 mmol)
<b>Appearance</b>	colorless solid
<b>Melting point</b>	174 °C – 175 °C (Lit. <sup>363</sup> : 172 °C – 175 °C)
<b>TLC</b>	R <sub>f</sub> (PE/EtOAc = 1:1) = 0.23
<b>Sum formula</b>	C <sub>22</sub> H <sub>41</sub> N <sub>5</sub> O <sub>3</sub> Si <sub>2</sub>
<b><sup>1</sup>H-NMR (400 MHz, DMSO-<i>d</i><sub>6</sub>)</b>	δ = -0.16 (s, 3H, Si-CH <sub>3</sub> ), -0.07 (s, 3H, Si-CH <sub>3</sub> ), 0.07 (s, 3H, Si-CH <sub>3</sub> ), 0.08 (s, 3H, Si-CH <sub>3</sub> ), 0.74 (s, 9H, <i>tert</i> butyl), 0.90 (s, 9H, <i>tert</i> butyl), 3.79 (dd, <i>J</i> = 11.4, 3.8 Hz, 1H, H-5' <i>b</i> ), 3.92 (dd, <i>J</i> = 11.4, 3.8 Hz, 1H, H-5' <i>a</i> ), 4.01 (q, <i>J</i> = 3.7 Hz, 1H, H-4'), 4.10 – 4.19 (m, 1H, H-3'), 4.63 (t, <i>J</i> = 5.1 Hz, 1H, H-2'), 5.12 (d, <i>J</i> = 5.6 Hz, 1H, OH-3'), 5.94 (d, <i>J</i> = 5.3 Hz, 1H, H-1'), 7.29 (s, 2H, NH <sub>2</sub> -aromatic), 8.13 (s, 1H, H-2), 8.28 (s, 1H, H-8) ppm.
<b><sup>13</sup>C-NMR (101 MHz, DMSO-<i>d</i><sub>6</sub>)</b>	δ = -5.5 (q, Si-CH <sub>3</sub> ), -5.5 (q, Si-CH <sub>3</sub> ), -5.3 (q, Si-CH <sub>3</sub> ), -5.0 (q, Si-CH <sub>3</sub> ), 17.8 (s, Si-C(CH <sub>3</sub> ) <sub>3</sub> ) 18.1 (s, Si-C(CH <sub>3</sub> ) <sub>3</sub> ), 25.5 (q, Si-C(CH <sub>3</sub> ) <sub>3</sub> ), 25.8 (s, Si-C(CH <sub>3</sub> ) <sub>3</sub> ), 62.9 (t, C-5'), 70.0 (d, (C-3')), 76.0 (d, C-2'), 84.9 (d, C-4'), 87.3 (d, C-1'), 118.9 (s, C-5), 138.7 (d, C-8), 149.4 (s, C-4), 152.7 (d, C-2), 156.0 (s, C-6) ppm.
<b>Optical rotation</b>	[α] <sub>D</sub> <sup>20</sup> = -41.6 (c = 1.0, CHCl <sub>3</sub> )
<b>Comment</b>	Spectral data are in accordance with the literature.

## E IV.8 Synthesis of ester derivatives of adenosine and FAD

### E IV.8.1 (6*R*,8*R*,9*R*,9*aR*)-8-(6-Amino-9*H*-purin-9-yl)-2,2,4,4-tetraisopropyltetrahydro-6*H*-furo[3,2-*f*][1,3,5,2,4]trioxadisilocin-9-yl 3-(3-methyl-3*H*-diazirin-3-yl)propanoate [31]



(6*R*,8*R*,9*R*,9*aR*)-8-(6-Amino-9*H*-purin-9-yl)-2,2,4,4-tetraisopropyltetrahydro-6*H*-furo[3,2-*f*][1,3,5,2,4]trioxadisilocin-9-yl 3-(3-methyl-3*H*-diazirin-3-yl)propanoate [31] was synthesized according to general procedure A using protected adenosine [29] (1.00 g, 1.96 mmol, 1.00 equiv.) and aliphatic diazirine building block [9] (302 mg, 2.35 mmol, 1.20 equiv.). The pure product was obtained after purification by flash column chromatography (silica gel/crude material = 100/1, PE/EtOAc = 98/2) using a gradient of MeOH in DCM (1 % 6 min; 1-5 % 24 min) as eluent.

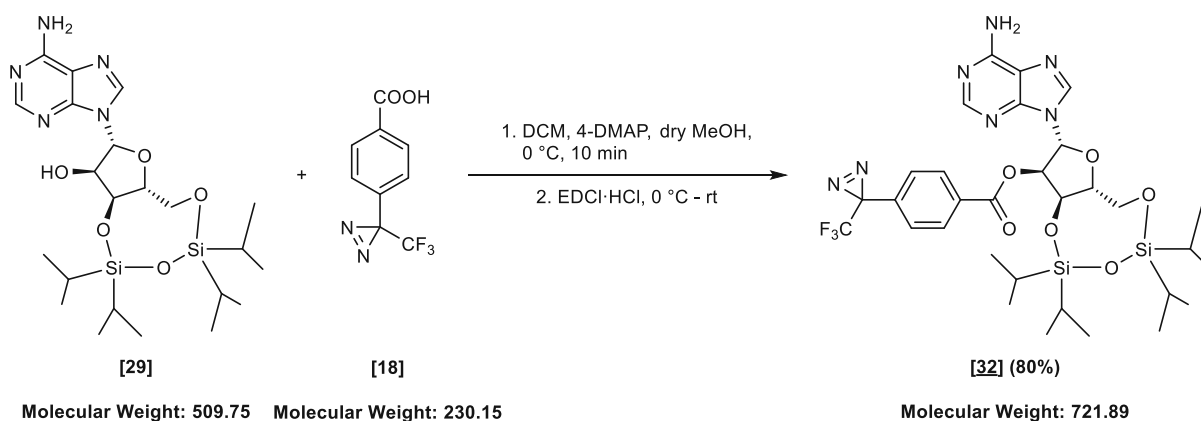
<b>Yield</b>	82% (1.00 g, 1.61 mmol)
<b>Appearance</b>	colorless crystals
<b>Melting point</b>	> 167.5 °C (decomposition; formation of bubbles)
<b>TLC</b>	R <sub>f</sub> (CHCl <sub>3</sub> /MeOH = 9/1) = 0.72
<b>Sum formula</b>	C <sub>27</sub> H <sub>45</sub> N <sub>7</sub> O <sub>6</sub> Si <sub>2</sub>
<b>HR-MS</b>	[M+Na] <sup>+</sup> : calculated: 642.2862 Da, found: 642.2862 Da, difference: 0.0 ppm
<b><sup>1</sup>H-NMR (400 MHz, DMSO-<i>d</i><sub>6</sub>)</b>	δ = 0.91 – 1.09 (m, 28H, 4x isopropyl), 1.54 – 1.71 (m, 2H, -CH <sub>2</sub> -CH <sub>2</sub> -COOR), 2.26 – 2.45 (m, 2H, -CH <sub>2</sub> -CH <sub>2</sub> -COOR), 3.72

– 4.15 (m, 3H, H-4' & H-5'a & H-5'b), 5.26 (dd,  $J = 8.5, 5.7$  Hz, 2H, H-3'), 5.91 (dd,  $J = 5.6, 1.4$  Hz, 1H, H-2'), 6.08 (d,  $J = 1.4$  Hz, 1H, H-1'), 7.37 (s, 2H, NH<sub>2</sub>-aromatic), 8.04 (s, 1H, H-2), 8.24 (s, 1H, H-8) ppm.

<sup>13</sup>C-NMR (101 MHz, DMSO-*d*<sub>6</sub>)  $\delta = 12.1$  (d, 2x Si-CH(CH<sub>3</sub>)<sub>3</sub>), 12.4 (d, Si-CH(CH<sub>3</sub>)<sub>3</sub>), 12.7 (d, 2x Si-CH(CH<sub>3</sub>)<sub>3</sub>), 16.7 (q, 2x Si-CH(CH<sub>3</sub>)<sub>3</sub>), 16.8 (q, Si-CH(CH<sub>3</sub>)<sub>3</sub>), 16.8 (q, Si-CH(CH<sub>3</sub>)<sub>3</sub>), 17.1 (q, Si-CH(CH<sub>3</sub>)<sub>3</sub>), 17.1 (q, Si-CH(CH<sub>3</sub>)<sub>3</sub>), 17.3 (q, 2x Si-CH(CH<sub>3</sub>)<sub>3</sub>), 19.1 (q, Si-CH(CH<sub>3</sub>)<sub>3</sub>), 25.4 (s, diazirine), 28.2 (t, -CH<sub>2</sub>-CH<sub>2</sub>-COOR), 29.2 (t, -CH<sub>2</sub>-CH<sub>2</sub>-COOR), 60.7 (t, C-5'), 69.2 (d, C-3'), 74.9 (d, C-2'), 81.1 (d, C-4'), 86.5 (d, C-1'), 119.3 (s, C-5), 140.4 (d, C-8), 148.5 (s, C-4), 152.5 (d, C-2), 156.2 (s, C-6), 170.6 (s, carbonyl (ester)) ppm.

**Optical rotation**  $[\alpha]_D^{20} = -38.2$  ( $c = 0.5$ , MeOH)

## E IV.8.2 (6*R*,8*R*,9*R*,9*aR*)-8-(6-Amino-9*H*-purin-9-yl)-2,2,4,4-tetraisopropyltetrahydro-6*H*-furo[3,2-*f*][1,3,5,2,4]trioxadisilocin-9-yl 4-(3-(trifluoromethyl)-3*H*-diazirin-3-yl)benzoate [32]



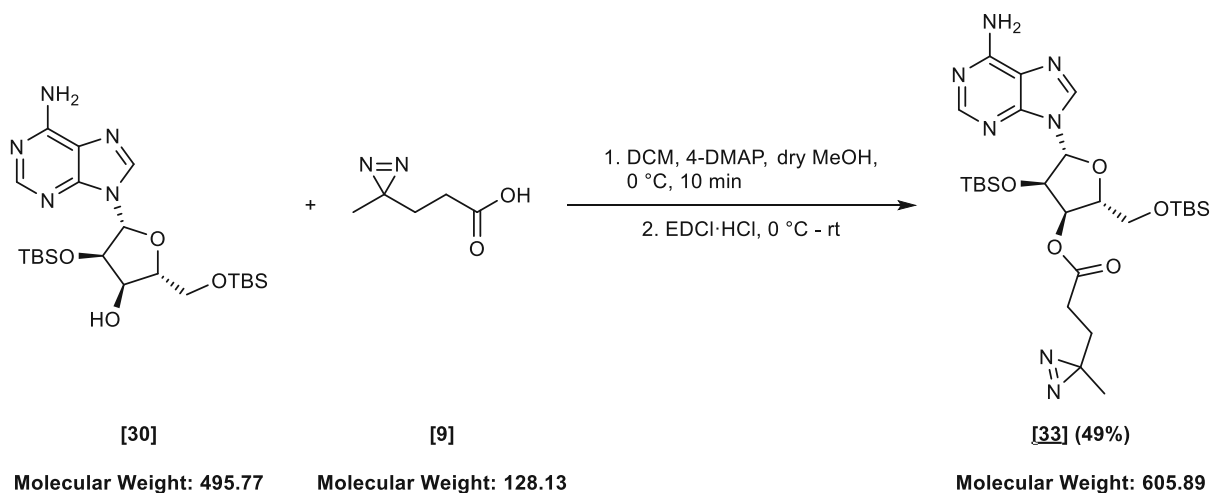
(6*R*,8*R*,9*R*,9*aR*)-8-(6-amino-9*H*-purin-9-yl)-2,2,4,4-tetraisopropyltetrahydro-6*H*-furo[3,2-*f*][1,3,5,2,4]trioxadisilocin-9-yl 4-(3-(trifluoromethyl)-3*H*-diazirin-3-yl)benzoate [32] was synthesized according to general procedure A using protected adenosine [29] (1.00 g, 1.96 mmol, 1.00 equiv.) and aromatic diazirine building block [18] (542 mg, 2.35 mmol, 1.20 equiv.). The pure product was obtained after purification by flash column chromatography



(silica gel/crude material = 100/1, PE/EtOAc = 98/2) using a gradient of MeOH in DCM (1% 6 min; 1-5 % 24 min) as eluent.

<b>Yield</b>	93% (1.32 g, 1.83 mmol)
<b>Appearance</b>	colorless crystals
<b>Melting point</b>	> 139.0 °C (decomposition; formation of bubbles/foam, color change to yellow)
<b>TLC</b>	R <sub>f</sub> (CHCl <sub>3</sub> /MeOH = 9/1) = 0.68
<b>Sum formula</b>	C <sub>31</sub> H <sub>42</sub> F <sub>3</sub> N <sub>7</sub> O <sub>6</sub> Si <sub>2</sub>
<b>HR-MS</b>	[M+H] <sup>+</sup> : calculated: 722.2760 Da, found: 722.2779 Da, difference: 2.6 ppm
<b><sup>1</sup>H-NMR (400 MHz, DMSO-<i>d</i><sub>6</sub>)</b>	$\delta = 0.74 - 0.85$ (m, 7H, 4 x Si-CH-(CH <sub>3</sub> ) <sub>2</sub> & 1x Si-CH-CH <sub>3</sub> ), 0.96 – 1.10 (m, 21H, 7x Si-CH-CH <sub>3</sub> ), 3.90 – 4.16 (m, 3H, H-4' & H-5'a & H-5'b), 5.41 (dd, $J = 8.4, 5.6$ Hz, 1H, H-3'), 6.13 (dd, $J = 5.6, 1.3$ Hz, 1H, H-2'), 6.29 (d, $J = 1.3$ Hz, 1H, H-1'), 7.36 (s, 2H, NH <sub>2</sub> -aromatic), 7.46 (d, $J = 8.1$ Hz, 2H, H-3ar & H-5ar), 8.06 (s, 1H, H-2), 8.14 (d, $J = 8.8$ Hz, 2H, H-2ar & H-6ar), 8.25 (s, 1H, H-8) ppm.
<b><sup>13</sup>C-NMR (101 MHz, DMSO-<i>d</i><sub>6</sub>)</b>	$\delta = 12.2$ (d, 2x Si-CH-(CH <sub>3</sub> ) <sub>2</sub> ), 12.5 (d, Si-CH-(CH <sub>3</sub> ) <sub>2</sub> ), 12.7 (d, Si-CH-(CH <sub>3</sub> ) <sub>2</sub> ), 16.6 (q, 2x Si-CH-CH <sub>3</sub> ), 16.8 (q, Si-CH-CH <sub>3</sub> ), 16.9 (q, Si-CH-CH <sub>3</sub> ), 17.2 (q, 2x Si-CH-CH <sub>3</sub> ), 17.3 (q, Si-CH-CH <sub>3</sub> ), 17.4 (q, Si-CH-CH <sub>3</sub> ), 25.5 (s, diazirine), 61.1 (t, C-5'), 70.0 (d, C-3'), 76.2 (d, C-2'), 81.3 (d, C-2'), 86.6 (d, C-1'), 118.6 (s/q, $^1J_{CF} = 304.1$ Hz, CF <sub>3</sub> ) 119.4 (s, C-5), 127.0 (d, C-3ar & C-5ar), 130.3 (d, C-2ar & C-6ar), 130.9 (s, C-1ar), 132.8 (s, C-4ar), 140.7 (d, C-8), 148.7 (s, C-4), 152.6 (d, C-2), 156.3 (s, C-6), 163.9 (s, carbonyl (ester)) ppm.
<b><sup>19</sup>F NMR (376 MHz, DMSO-<i>d</i><sub>6</sub>)</b>	$\delta = -64.38$ ppm.
<b>Optical rotation</b>	$[\alpha]_D^{20} = -48.6$ (c = 0.54, MeOH)

### E IV.8.3 (2*R*,3*R*,4*R*,5*R*)-5-(6-amino-9*H*-purin-9-yl)-4-((*tert*-butyldimethylsilyl)oxy)-2-(((*tert*-butyldimethylsilyl)oxy)methyl)tetrahydrofuran-3-yl 3-(3-methyl-3*H*-diazirin-3-yl)propanoate [33]



(2*R*,3*R*,4*R*,5*R*)-5-(6-Amino-9*H*-purin-9-yl)-4-((*tert*-butyldimethylsilyl)oxy)-2-(((*tert*-butyldimethylsilyl)oxy)methyl)tetrahydrofuran-3-yl 3-(3-methyl-3*H*-diazirin-3-yl)propanoate [33] was synthesized according to general procedure A using protected adenosine [30] (1.00 g, 2.02 mmol, 1.00 equiv.) and aliphatic diazirine building block [9] (310 mg, 2.42 mmol, 1.20 equiv.). The pure product was obtained after purification by flash column chromatography (silica gel/crude material = 100/1) using a gradient of MeOH in DCM (1% 6 min; 1-5% 24 min) as eluent.

<b>Yield</b>	49% (598 mg, 0.99 mmol)
<b>Appearance</b>	colorless solid
<b>Melting point</b>	51.5 – 54.0 °C
<b>TLC</b>	R <sub>f</sub> (CHCl <sub>3</sub> /MeOH = 9/1) = 0.76
<b>Sum formula</b>	C <sub>27</sub> H <sub>47</sub> N <sub>7</sub> O <sub>5</sub> Si <sub>2</sub>
<b>HR-MS</b>	[M+Na] <sup>+</sup> : calculated: 628.3069 Da, found: 628.3061 Da, difference: -1.3 ppm

<sup>1</sup>H-NMR (400 MHz, DMSO-*d*<sub>6</sub>) δ = -0.36 (s, 3H, Si-CH<sub>3</sub>), -0.14 (s, 3H, Si-CH<sub>3</sub>), 0.09 (s, 3H, Si-CH<sub>3</sub>), 0.11 (s, 3H, Si-CH<sub>3</sub>), 0.63 (s, 9H, *tert*butyl), 0.91 (s, 9H, *tert*butyl), 1.03 (s, 3H, CH<sub>3</sub> (aliphatic linker)), 1.54 – 1.77 (m, 2H, -CH<sub>2</sub>-CH<sub>2</sub>-COOR), 2.23 – 2.46 (m, 2H, -CH<sub>2</sub>-CH<sub>2</sub>-COOR), 3.85

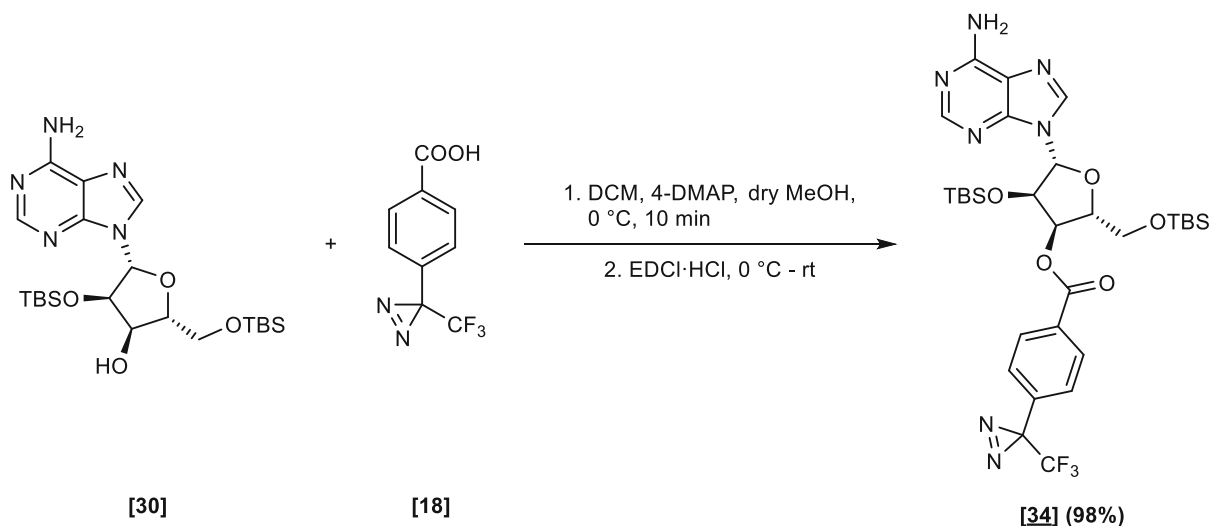
(dd,  $J = 11.3, 4.0$  Hz, 1H, H-5'b), 3.96 (dd,  $J = 11.3, 4.5$  Hz, 1H, H-5'a), 4.21 (td,  $J = 4.3, 4.2, 1.9$  Hz, 1H, H-4'), 4.99 (dd,  $J = 7.0, 5.2$  Hz, 1H, H-2'), 5.35 (dd,  $J = 5.2, 2.0$  Hz, 1H, H-3'), 5.94 (d,  $J = 6.9$  Hz, 1H, H-1'), 7.35 (s, 2H, NH<sub>2</sub>-aromatic), 8.14 (s, 1H, H-2), 8.30 (s, 1H, H-8) ppm.

<sup>13</sup>C-NMR (101 MHz, DMSO-*d*<sub>6</sub>)  $\delta = -5.9$  (q, Si-CH<sub>3</sub>), -5.5 (q, 2x Si-CH<sub>3</sub>), -5.5 (q, Si-CH<sub>3</sub>), 17.4 (s, Si-C-(CH<sub>3</sub>)<sub>3</sub>), 18.0 (s, Si-C-(CH<sub>3</sub>)<sub>3</sub>), 19.1 (q, CH<sub>3</sub> (aliphatic linker)), 25.1 (q, Si-C-(CH<sub>3</sub>)<sub>3</sub>), 25.4 (s, diazirine), 25.8 (q, Si-C-(CH<sub>3</sub>)<sub>3</sub>), 28.1 (t, -CH<sub>2</sub>-CH<sub>2</sub>-COOR), 29.0 (t, -CH<sub>2</sub>-CH<sub>2</sub>-COOR), 62.9 (t, C-5'), 72.7 (d, C-3'), 73.6 (d, C-2'), 82.6 (d, C-4'), 86.7 (d, C-1'), 119.0 (s, C-5), 138.7 (d, C-8), 149.5 (s, C-4), 152.8 (d, C-2), 156.1 (s, C-6), 170.8 (s, carbonyl (acid)) ppm.

**Optical rotation**

$[\alpha]_D^{20} = -34.5$  (c = 0.52, MeOH)

## E IV.8.4 (2*R*,3*R*,4*R*,5*R*)-5-(6-Amino-9*H*-purin-9-yl)-4-((*tert*-butyldimethylsilyl)oxy)-2-(((*tert*-butyldimethylsilyl)oxy)methyl)tetrahydrofuran-3-yl 4-(3-(trifluoromethyl)-3*H*-diazirin-3-yl)benzoate [34]



Molecular Weight: 495.77    Molecular Weight: 230.15

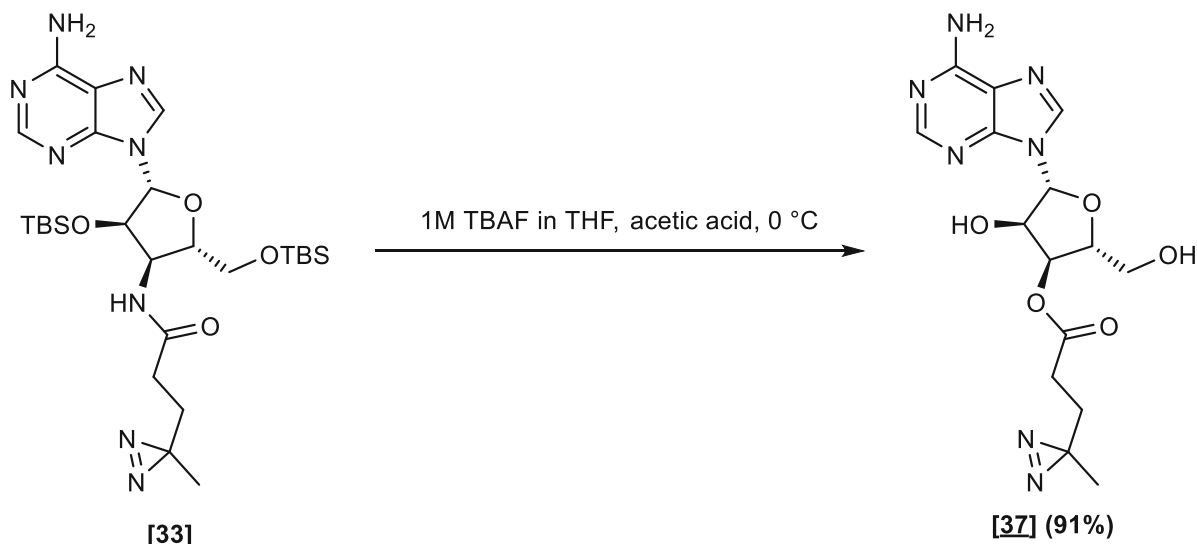
Molecular Weight: 707.90

(2*R*,3*R*,4*R*,5*R*)-5-(6-Amino-9*H*-purin-9-yl)-4-((*tert*-butyldimethylsilyl)oxy)-2-(((*tert*-butyldimethylsilyl)oxy)methyl)tetrahydrofuran-3-yl 4-(3-(trifluoromethyl)-3*H*-diazirin-3-yl)benzoate [34] was synthesized according to general procedure A using protected adenosine

[**30**] (972 mg, 1.96 mmol, 1.00 equiv.) and aromatic diazirine building block [**18**] (542 mg, 2.35 mmol, 1.20 equiv.). The pure product was obtained after purification by flash column chromatography (silica gel/crude material = 100/1) using a gradient of MeOH in DCM (1% 6 min; 1-5 % 24 min) as eluent.

<b>Yield</b>	98% (1.36 g, 1.92 mmol)
<b>Appearance</b>	colorless solid
<b>Melting point</b>	69.5 – 71.5 °C
<b>TLC</b>	R <sub>f</sub> (CHCl <sub>3</sub> /MeOH = 9/1) = 0.74
<b>Sum formula</b>	C <sub>31</sub> H <sub>44</sub> F <sub>3</sub> N <sub>7</sub> O <sub>5</sub> Si <sub>2</sub>
<b>HR-MS</b>	[M+Na] <sup>+</sup> : calculated: 730.2787 Da, found: 730.2788 Da, difference: 0.2 ppm
<b><sup>1</sup>H-NMR (400 MHz, DMSO-<i>d</i><sub>6</sub>)</b>	δ = -0.41 (s, 2H, Si-CH <sub>3</sub> ), -0.18 (s, 3H, Si-CH <sub>3</sub> ), 0.10 (s, 3H, Si-CH <sub>3</sub> ), 0.13 (s, 3H, Si-CH <sub>3</sub> ), 0.49 (s, 9H, tertbutyl), 0.91 (s, 9H, tertbutyl), 3.85 – 4.08 (m, 2H, H-5'a & H-5'b), 4.42 (td, <i>J</i> = 4.3, 4.1, 1.8 Hz, 1H, H-4'), 5.08 (dd, <i>J</i> = 7.0, 5.2 Hz, 1H, H-2'), 5.62 (dd, <i>J</i> = 5.2, 1.9 Hz, 1H, H-3'), 6.06 (d, <i>J</i> = 7.0 Hz, 1H, H-1'), 7.38 (s, 2H, NH <sub>2</sub> -aromatic), 7.50 (d, <i>J</i> = 8.1 Hz, 2H, H-3ar & H-5ar), 8.15 (s, 1H, H-2), 8.17 (d, <i>J</i> = 8.8 Hz, 2H, H-2ar & H-6ar), 8.34 (s, 1H, H-8) ppm.
<b><sup>13</sup>C-NMR (101 MHz, DMSO-<i>d</i><sub>6</sub>)</b>	δ = -6.0 (q, Si-CH <sub>3</sub> ), -5.5 (q, Si-CH <sub>3</sub> ), -5.5 (q, Si-CH <sub>3</sub> ), -5.5 (q, Si-CH <sub>3</sub> ), 17.2 (s, Si-C-(CH <sub>3</sub> ) <sub>3</sub> ), 18.0 (s, Si-C-(CH <sub>3</sub> ) <sub>3</sub> ), 25.0 (q, Si-C-(CH <sub>3</sub> ) <sub>3</sub> ), 25.7 (q, Si-C-(CH <sub>3</sub> ) <sub>3</sub> ), 28.1 (s/q, <sup>2</sup> <i>J</i> <sub>CF</sub> = 40.2 Hz, diazirine), 63.0 (t, C-5'), 73.8 (d, C-3'), 74.0 (d, C-2'), 82.4 (d, C-4'), 86.8 (d, C-1'), 118.9 (s, C-5), 121.6 (s/q, <sup>1</sup> <i>J</i> <sub>CF</sub> = 274.8 Hz, CF <sub>3</sub> ), 126.9 (d, C-3ar & C-5ar), 130.2 (d, C-2ar & C-6ar), 130.8 (s, C-1ar), 132.7 (s, C-4ar), 138.6 (d, C-8), 149.5 (s, C-4), 152.8 (d, C-2), 156.1 (s, C-6), 163.9 (s, carbonyl (acid)) ppm.
<b><sup>19</sup>F NMR (376 MHz, DMSO-<i>d</i><sub>6</sub>)</b>	δ = -64.34 ppm.
<b>Optical rotation</b>	[α] <sub>D</sub> <sup>20</sup> = -71.2 (c = 0.5, MeOH)

**E IV.8.5 (2*R*,3*S*,4*R*,5*R*)-5-(6-Amino-9*H*-purin-9-yl)-4-hydroxy-2-(hydroxymethyl)tetrahydrofuran-3-yl 3-(3-methyl-3*H*-diazirin-3-yl)propanoate [37]**



**Molecular Weight: 604.90**

**Molecular Weight: 377.36**

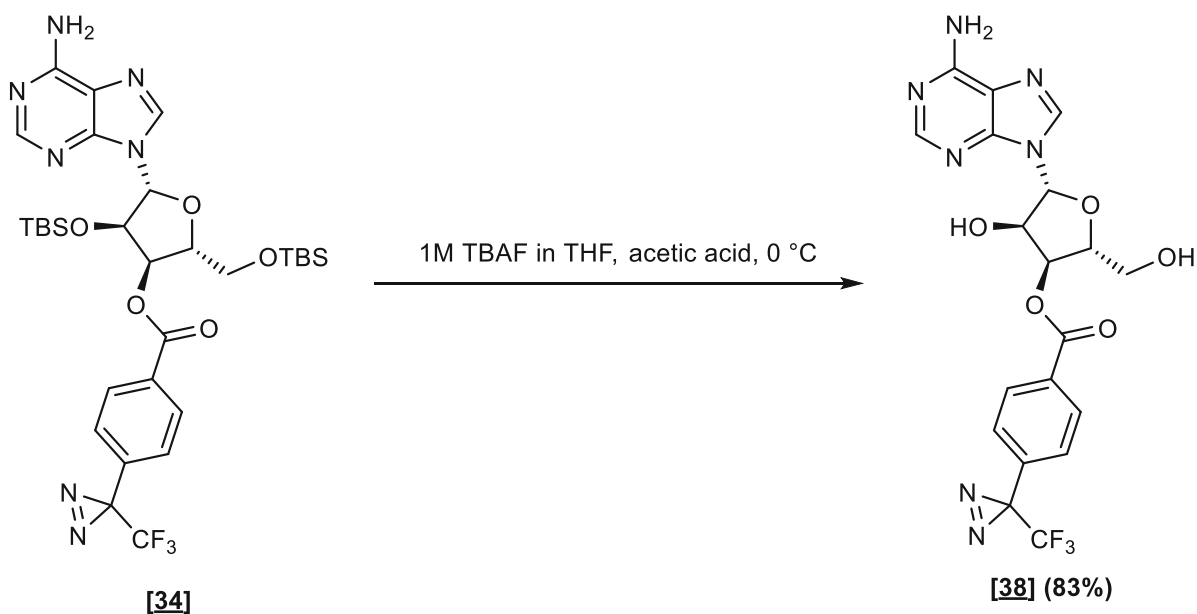
(2*R*,3*S*,4*R*,5*R*)-5-(6-Amino-9*H*-purin-9-yl)-4-hydroxy-2-(hydroxymethyl)tetrahydrofuran-3-yl 3-(3-methyl-3*H*-diazirin-3-yl)propanoate [37] was synthesized according to general procedure D using protected adenosine (2*R*,3*R*,4*R*,5*R*)-5-(6-amino-9*H*-purin-9-yl)-4-((*tert*-butyldimethylsilyloxy)-2-(((*tert*-butyldimethylsilyloxy)methyl)tetrahydrofuran-3-yl 3-(3-methyl-3*H*-diazirin-3-yl)propanoate [33] (1.30 g, 2.15 mmol, 1.00 equiv.). The crude material was subjected to flash column chromatography using a gradient of MeOH in DCM (5% 6 min; 5-10% 24 min) as eluent to obtain (2*R*,3*S*,4*R*,5*R*)-5-(6-amino-9*H*-purin-9-yl)-4-hydroxy-2-(hydroxymethyl)tetrahydrofuran-3-yl 3-(3-methyl-3*H*-diazirin-3-yl)propanoate [37] as colorless solid (738 mg, 91%).

<b>Yield</b>	91% (738 mg, 1.96 mmol)
<b>Appearance</b>	colorless solid
<b>Melting point</b>	79 – 92 °C
<b>TLC</b>	R <sub>f</sub> (CHCl <sub>3</sub> /MeOH = 9/1) = 0.48
<b>Sum formula</b>	C <sub>15</sub> H <sub>19</sub> N <sub>7</sub> O <sub>5</sub>
<b>HR-MS</b>	[M+Na] <sup>+</sup> : calculated: 400.1340 Da, found: 400.1334 Da, difference: -1.6 ppm

**<sup>1</sup>H-NMR (400 MHz, DMSO-*d*<sub>6</sub>)**  $\delta$  = 1.04 (s, 3H, CH<sub>3</sub> (aliphatic linker)), 1.66 (t, *J* = 7.6 Hz, 2H, -CH<sub>2</sub>-CH<sub>2</sub>-COOR), 2.36 (t, *J* = 7.6 Hz, 2H, -CH<sub>2</sub>-CH<sub>2</sub>-COOR), 3.54 – 3.74 (m, 2H, H-5'a & H-5'b), 4.14 (td, *J* = 3.4, 3.4, 1.9 Hz, 1H, H-4'), 4.89 (s, 1H, H-2'), 5.30 (dd, *J* = 5.3, 2.0 Hz, 1H, H-3'), 5.65 (t, *J* = 5.7 Hz, 1H, OH-5'), 5.78 (s, 1H, OH-2'), 5.89 (d, *J* = 7.2 Hz, 1H, H-1'), 7.39 (s, 2H, NH<sub>2</sub>-aromatic), 8.15 (s, 1H, H-2), 8.37 (s, 1H, H-8) ppm.

**<sup>13</sup>C-NMR (101 MHz, DMSO-*d*<sub>6</sub>)**  $\delta$  = 19.6 (q, CH<sub>3</sub> (aliphatic linker)), 26.0 (s, diazirine), 28.8 (t, -CH<sub>2</sub>-CH<sub>2</sub>-COOR), 29.6 (t, -CH<sub>2</sub>-CH<sub>2</sub>-COOR), 62.0 (t, C-5'), 72.2 (d, C-2'), 74.1 (d, C-3'), 84.0 (d, C-4'), 88.1 (d, C-1'), 119.8 (s, C-5), 140.3 (d, C-8), 149.5 (s, C-4), 153.0 (d, C-2), 156.7 (s, C-6), 171.7 (s, carbonyl (ester)) ppm.

**E IV.8.6 (2*R*,3*S*,4*R*,5*R*)-5-(6-Amino-9*H*-purin-9-yl)-4-hydroxy-2-(hydroxymethyl)tetrahydrofuran-3-yl 4-(3-(trifluoromethyl)-3*H*-diazirin-3-yl)benzoate [38]**



Molecular Weight: 707.90

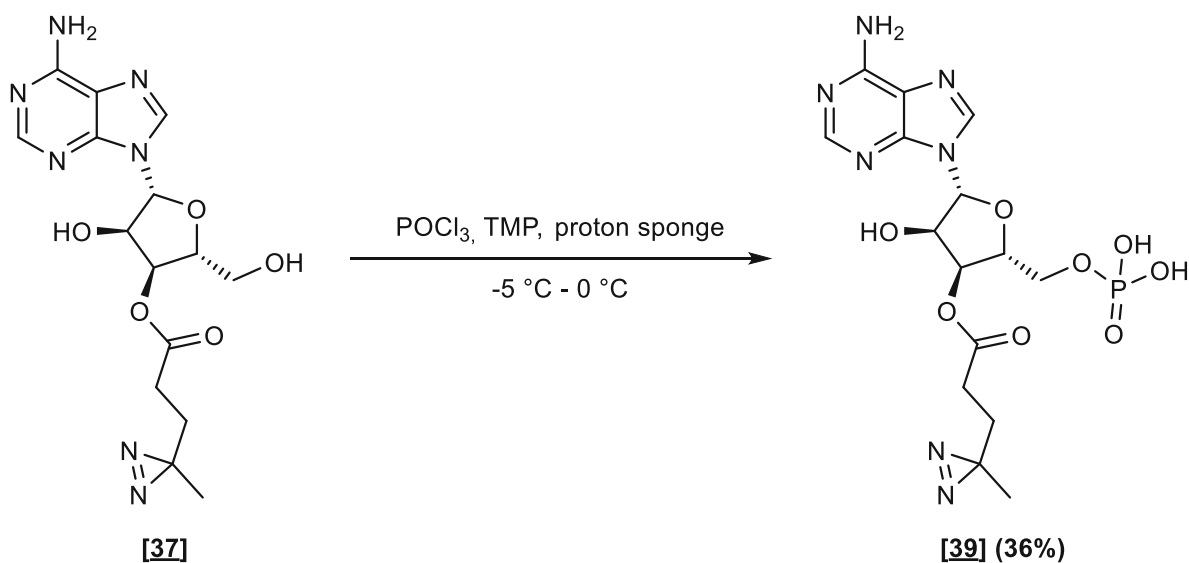
Molecular Weight: 479.38

(2*R*,3*S*,4*R*,5*R*)-5-(6-amino-9*H*-purin-9-yl)-4-hydroxy-2-(hydroxymethyl)tetrahydrofuran-3-yl 4-(3-(trifluoromethyl)-3*H*-diazirin-3-yl)benzoate [38] was synthesized according to

general procedure D using protected adenosine (2*R*,3*R*,4*R*,5*R*)-5-(6-amino-9*H*-purin-9-yl)-4-(((tert-butylidimethylsilyl)oxy)-2-(((tert-butylidimethylsilyl)oxy)methyl)tetrahydrofuran-3-yl 4-(3-(trifluoromethyl)-3*H*-diazirin-3-yl)benzoate [34] (950 mg, 1.34 mmol, 1.00 equiv.) The crude material was subjected to flash column chromatography using a gradient of MeOH in DCM (5% 6 min; 5-10% 24 min) as eluent to obtain (2*R*,3*S*,4*R*,5*R*)-5-(6-amino-9*H*-purin-9-yl)-4-hydroxy-2-(hydroxymethyl)tetrahydrofuran-3-yl 4-(3-(trifluoromethyl)-3*H*-diazirin-3-yl)benzoate [38] as colorless solid (534 mg, 83%).

<b>Yield</b>	83% (534 mg, 1.11 mmol)
<b>Appearance</b>	colorless solid
<b>Melting point</b>	> 203 °C (decomposition; bubbles formation and color change to yellow)
<b>TLC</b>	R <sub>f</sub> (CHCl <sub>3</sub> /MeOH = 9/1) = 0.69
<b>Sum formula</b>	C <sub>19</sub> H <sub>16</sub> F <sub>3</sub> N <sub>7</sub> O <sub>5</sub>
<b>HR-MS</b>	[M+Na] <sup>+</sup> : calculated: 502.1057 Da, found: 502.1049 Da, difference: -1.7 ppm
<b><sup>1</sup>H-NMR (400 MHz, DMSO-<i>d</i><sub>6</sub>)</b>	δ = 3.57 – 3.83 (m, 2H, H-5'a & H-5'b), 4.33 (d, <i>J</i> = 2.1 Hz, 1H, H-4'), 4.95 – 5.12 (m, 1H, H-2'), 5.56 (dd, <i>J</i> = 5.3, 2.0 Hz, 1H, H-3'), 5.71 (dd, <i>J</i> = 7.4, 4.6 Hz, 1H, OH-5'), 5.93 (d, <i>J</i> = 6.3 Hz, 1H, OH-2'), 6.01 (d, <i>J</i> = 7.3 Hz, 1H, H-1'), 7.40 (s, 2H, NH <sub>2</sub> -aromatic), 7.50 (d, <i>J</i> = 7.8 Hz, 2H, H-3ar & H-5ar), 8.16 (s, 1H, H-2), 8.19 (d, <i>J</i> = 8.6 Hz, 2H, H-2ar & H-6ar), 8.40 (s, 1H, H-8) ppm.
<b><sup>13</sup>C-NMR (101 MHz, DMSO-<i>d</i><sub>6</sub>)</b>	δ = 28.1 (s/q, <sup>2</sup> <i>J</i> <sub>CF</sub> = 40.4 Hz, diazirine), 62.1 (t, C-5'), 72.4 (d, C-2'), 75.2 (d, C-3'), 83.9 (d, C-4'), 88.1 (d, C-1'), 119.8 (s, C-5), 121.7 (s/q, <sup>2</sup> <i>J</i> <sub>CF</sub> <i>J</i> = 259.2, CF <sub>3</sub> ) 127.3 (d, C-3ar & C-5ar), 130.8 (d, C-2ar & C-6ar), 131.1 (s, C-1ar), 133.0 (s, C-4ar), 140.3 (d, C-8), 149.6 (d C-4), 153.0 (d, C-2), 156.7 (s, C-6), 164.6 (s, carbonyl (ester)) ppm.
<b><sup>19</sup>F NMR (376 MHz, DMSO-<i>d</i><sub>6</sub>)</b>	δ = -64.36 ppm.

**E IV.8.7 (2*R*,3*S*,4*R*,5*R*)-5-(6-Amino-9*H*-purin-9-yl)-4-hydroxy-2-((phosphonoxy)methyl)tetrahydrofuran-3-yl 3-(3-methyl-3*H*-diazirin-3-yl)propanoate [39]**



**Molecular Weight: 377.36**

**Molecular Weight: 457.34**

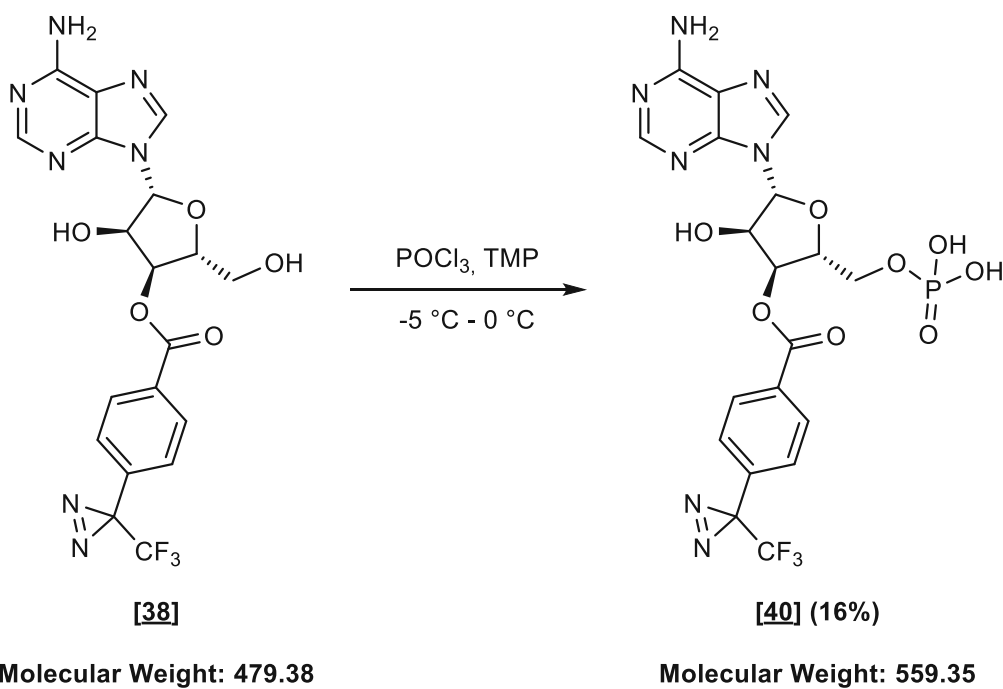
(2*R*,3*S*,4*R*,5*R*)-5-(6-Amino-9*H*-purin-9-yl)-4-hydroxy-2-((phosphonoxy)methyl)tetrahydrofuran-3-yl 3-(3-methyl-3*H*-diazirin-3-yl)propanoate [39] was synthesized according to following literature procedure.<sup>427</sup> An oven-dried 50 mL three-necked round bottom flask, equipped with a thermometer, was flushed with argon using Schlenk-technique. Dry TMP (15 mL) was added via syringe followed by the addition of (2*R*,3*S*,4*R*,5*R*)-5-(6-amino-9*H*-purin-9-yl)-4-hydroxy-2-(hydroxymethyl)tetrahydrofuran-3-yl 3-(3-methyl-3*H*-diazirin-3-yl)propanoate [37] (300 mg, 0.80 mmol, 1.00 equiv.) and proton sponge (256 mg, 1.19 mmol, 1.50 equiv.). The mixture was stirred for 25 min at room temperature and was then cooled to -5 °C using an ice/NaCl bath. At this temperature, POCl<sub>3</sub> (223 μL, 2.38 mmol, 3.00 equiv.) was added dropwise and the reaction was stirred at -5 °C. UHPLC-MS/UV analysis indicated nearly full conversion of the starting material right after the complete addition of POCl<sub>3</sub>. Hence, water (2 mL) was added dropwise, and the mixture was stirred for 30 min at 0 °C. The reaction mixture was then extracted with DCM (3 times, 10 mL), and the aqueous phase was lyophilized. The crude compound was purified by preparative reverse-phase HPLC (HPLC-grade H<sub>2</sub>O + 0.1% formic acid [Solvent A], MeOH [Solvent B])



and lyophilized to obtain (2*R*,3*S*,4*R*,5*R*)-5-(6-amino-9*H*-purin-9-yl)-4-hydroxy-2-((phosphonoxy)methyl)tetrahydrofuran-3-yl 3-(3-methyl-3*H*-diazirin-3-yl)propanoate **[39]** (contaminated with proton sponge) as slightly pink powder that was used in the next step without further purification.

<b>Yield</b>	36% (130 mg, 0.284 mmol)
<b>Appearance</b>	slightly pink powder
<b>Melting point</b>	> 140 °C (decomposition; bubbles formation)
<b>Sum formula</b>	C <sub>15</sub> H <sub>20</sub> N <sub>7</sub> O <sub>8</sub> P
<b>HR-MS</b>	[M+H] <sup>+</sup> : calculated: 458.1184 Da, found: 458.1180 Da, difference: -0.8 ppm
<b><sup>1</sup>H NMR (400 MHz, D<sub>2</sub>O)</b>	δ = 1.06 (s, 3H, CH <sub>3</sub> (aliphatic linker)), 1.78 (t, <i>J</i> = 7.3 Hz, 2H, -CH <sub>2</sub> -CH <sub>2</sub> -COOR-), 2.48 (t, <i>J</i> = 7.3 Hz, 2H, -CH <sub>2</sub> -CH <sub>2</sub> -COOR-), 4.10 – 4.23 (m, 2H, H-5'a & H-5'b), 4.56 (t, <i>J</i> = 2.6 Hz, 1H, H-4'), 4.96 (dd, <i>J</i> = 6.9, 5.4 Hz, 1H, H-2'), 5.47 (dd, <i>J</i> = 5.4, 2.5 Hz, 1H, H-3'), 6.12 (d, <i>J</i> = 6.9 Hz, 1H, H-1'), 8.25 (s, 1H, H-2), 8.53 (s, 1H, H-8) ppm.
<b><sup>13</sup>C-NMR (101 MHz, D<sub>2</sub>O)</b>	δ = 18.5 (q, CH <sub>3</sub> (aliphatic linker)), 26.1 (s, diazirine), 28.4 (-CH <sub>2</sub> -CH <sub>2</sub> -COOR-), 28.8 (-CH <sub>2</sub> -CH <sub>2</sub> -COOR-), 64.5 (t, C-5'), 73.2 (d, C-2'), 73.6 (d, C-3'), 82.4 (d, C-4'), 86.7 (d, C-1'), 118.6 (s, C-5), 140.9 (d, C-8), 148.6 (d, C-2), 148.7 (s, C-4), 152.3 (s, C-6), 174.1 (s, carbonyl (ester)) ppm.
<b><sup>31</sup>P NMR (162 MHz, D<sub>2</sub>O)</b>	δ = 0.21 ppm.

**E IV.8.8 (2*R*,3*S*,4*R*,5*R*)-5-(6-Amino-9*H*-purin-9-yl)-4-hydroxy-2-((phosphonoxy)methyl)tetrahydrofuran-3-yl 3-(3-methyl-3*H*-diazirin-3-yl)propanoate [43]**

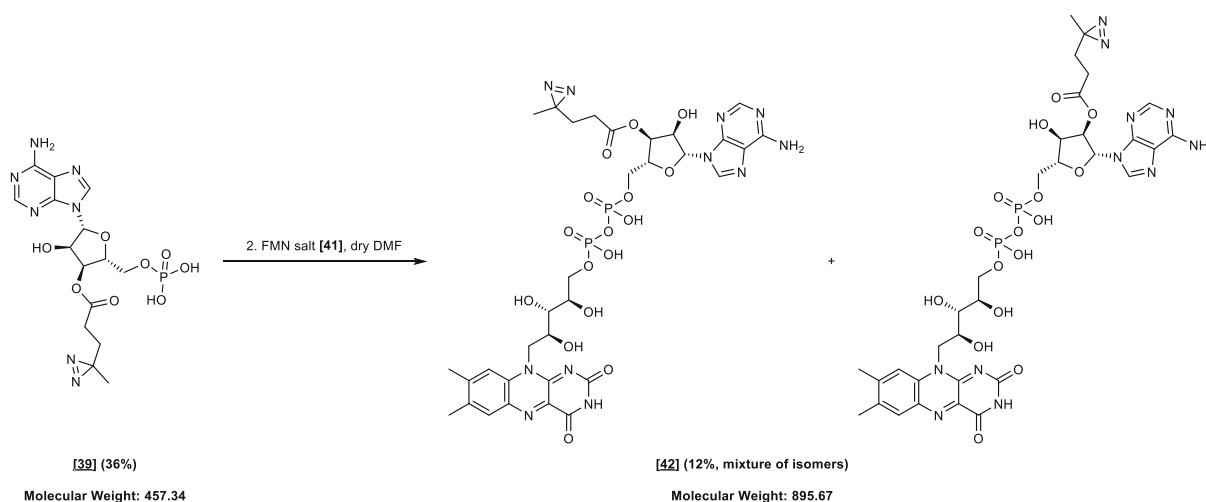


(2*R*,3*S*,4*R*,5*R*)-5-(6-Amino-9*H*-purin-9-yl)-4-hydroxy-2-((phosphonoxy)methyl)tetrahydrofuran-3-yl 4-(3-(trifluoromethyl)-3*H*-diazirin-3-yl)benzoate **[40]** was synthesized according to general procedure E using (2*R*,3*S*,4*R*,5*R*)-5-(6-amino-9*H*-purin-9-yl)-4-hydroxy-2-(hydroxymethyl)tetrahydrofuran-3-yl 4-(3-(trifluoromethyl)-3*H*-diazirin-3-yl)benzoate **[38]** (300 mg, 0.626 mmol, 1.00 equiv.). The crude compound was purified by preparative reverse-phase HPLC (HPLC-grade H<sub>2</sub>O + 0.1% formic acid [Solvent A], MeOH [Solvent B]) and lyophilized to obtain (2*R*,3*S*,4*R*,5*R*)-5-(6-amino-9*H*-purin-9-yl)-4-hydroxy-2-((phosphonoxy)methyl)tetrahydrofuran-3-yl 4-(3-(trifluoromethyl)-3*H*-diazirin-3-yl)benzoate **[40]** as slightly beige powder.

<b>Yield</b>	16% (57 mg, 0.101 mmol)
<b>Appearance</b>	slightly beige powder
<b>Melting point</b>	> 235 °C (decomposition; bubbles formations and color change to brown)

<b>Sum formula</b>	$C_{19}H_{17}F_3N_7O_8P$
<b>HR-MS</b>	$[M-H]^-$ : calculated: 558.0756 Da, found: 558.0748 Da, difference: -1.3 ppm
<b><math>^1H</math> NMR (600 MHz, <math>D_2O</math>)</b>	$\delta = 4.14$ (s, 1H, H-5'), 5.05 (t, $J = 6.0$ Hz, 1H, H-2'), 5.66 – 5.70 (m, 1H, H-3'), 6.28 (d, $J = 6.6$ Hz, 1H, H-1'), 8.05 (t, $J = 7.9$ Hz, 2H, H-3ar & H-5ar), 8.12 (d, $J = 8.4$ Hz, 2H, H-2ar & H-6ar), 8.39 (s, 1H, H-2), 8.62 (s, 1H, H-8) ppm.
<b><math>^{13}C</math>-NMR (101 MHz, <math>D_2O</math>)</b>	not determined
<b>Comment</b>	The H-4' peak is below the $D_2O$ peak. A proper $^{13}C$ -NMR could not be measured due to the precipitation of the compound in the course of time.

**E IV.8.9 (2*R*,3*S*,4*R*,5*R*)-5-(6-Amino-9*H*-purin-9-yl)-2-((((((((2*R*,3*S*,4*S*)-5-(7,8-dimethyl-2,4-dioxo-3,4-dihydrobenzo[*g*]pteridin-10(2*H*)-yl)-2,3,4-trihydroxypentyl)oxy)(hydroxy)phosphoryl)oxy)(hydroxy)phosphoryl)oxy)methyl)-4-hydroxytetrahydrofuran-3-yl 3-(3-methyl-3*H*-diazirin-3-yl)propanoate**



(2*R*,3*S*,4*R*,5*R*)-5-(6-Amino-9*H*-purin-9-yl)-2-((((((((2*R*,3*S*,4*S*)-5-(7,8-dimethyl-2,4-dioxo-3,4-dihydrobenzo[*g*]pteridin-10(2*H*)-yl)-2,3,4-trihydroxypentyl)oxy)(hydroxy)phosphoryl)oxy)(hydroxy)phosphoryl)oxy)methyl)-4-hydroxytetrahydrofuran-3-yl 3-(3-methyl-3*H*-diazirin-3-yl)propanoate **[42]** was synthesized according to general procedure F using adenosine monophosphate **[39]** (50 mg, 109  $\mu\text{mol}$ , 1.00 equiv.). The product was obtained as a mixture of 2' and 3' acylated isomers after purification by preparative reverse-phase HPLC (HPLC-grate water [Solvent A]/methanol [Solvent B]) and lyophilization as a yellow-orange powder.

<b>Yield</b>	12% (12 mg, 13 $\mu\text{mol}$ )
<b>Appearance</b>	yellow-orange powder
<b>Melting point</b>	not determined
<b>Sum formula</b>	$\text{C}_{32}\text{H}_{39}\text{N}_{11}\text{O}_{16}\text{P}_2$

**HR-MS** [M-H]<sup>-</sup>: calculated: 894.1978 Da, found: 894.1964 Da, difference: -1.69 ppm

**<sup>1</sup>H-NMR (600 MHz, D<sub>2</sub>O)**  $\delta$  = 0.71 (s, 3H, CH<sub>3</sub> (aliphatic linker, 2' acyl)), 0.96 (s, 3H, CH<sub>3</sub> (aliphatic linker, 3' acyl)), 1.46 (t,  $J$  = 7.3 Hz, 2H, -CH<sub>2</sub>-CH<sub>2</sub>-COOR- (3' acyl)), 1.62 – 1.72 (m, 2H, -CH<sub>2</sub>-CH<sub>2</sub>-COOR- (2' acyl)), 2.15 – 2.34 (m, 14H, -CH<sub>2</sub>-CH<sub>2</sub>-COOR- (2' acyl) & CH<sub>3</sub>-F7 (2' acyl & 3' acyl) & CH<sub>3</sub>-C8 (2' acyl & 3' acyl)), 2.35 – 2.40 (m, 2H, -CH<sub>2</sub>-CH<sub>2</sub>-COOR- (3' acyl)), 3.84 (m, 2H, H-F3' (2' acyl & 3' acyl)), 3.91 – 4.06 (m, 4H, H-A5'b (2' acyl & 3' acyl) & H-F4' (2' acyl & 3' acyl)), 4.15 – 4.45 (m, 6H, H-A4' (2' acyl & 3' acyl) & H-5'a (2' acyl & 3' acyl) & H-F2' (2' acyl & 3' acyl)), 4.56 (t,  $J$  = 5.1 Hz, 1H, H-3' (2' acyl)), 5.29 (t,  $J$  = 5.4 Hz, 1H, H-2' (2' acyl)), 5.35 (dd,  $J$  = 5.4, 2.5 Hz, 1H, H-3' (3-acyl isomer)), 5.77 (d,  $J$  = 7.0 Hz, 1H, H-1' (3-acyl isomer)), 5.86 (d,  $J$  = 4.9 Hz, 1H, H-1' (2-acyl isomer)), 7.28 (s, 4H, H-F9 & H-F6 (2' acyl & 3' acyl)), 7.76 (s, 2H, H-2 (2' acyl & 3' acyl)), 8.24 (s, 2H, H8 (2' acyl & 3' acyl)) ppm.

**<sup>13</sup>C-NMR (151 MHz, D<sub>2</sub>O)**  $\delta$  = 18.2 (q, CH<sub>3</sub> (aliphatic linker, 2' acyl)), 18.5 (q, CH<sub>3</sub> (aliphatic linker, 3' acyl)), 18.5 (q, CH<sub>3</sub>-F7 (2' acyl & 3' acyl)), 20.7 (q, CH<sub>3</sub>-F8 (2' acyl & 3' acyl)), 25.7 (s, diazirine (2' acyl)), 26.1 (s, diazirine (3' acyl)), 28.1 (-CH<sub>2</sub>-CH<sub>2</sub>-COOR- (2' acyl)), 28.4 (-CH<sub>2</sub>-CH<sub>2</sub>-COOR- (3' acyl)), 28.6 (-CH<sub>2</sub>-CH<sub>2</sub>-COOR- (3' acyl)), 28.7 (-CH<sub>2</sub>-CH<sub>2</sub>-COOR- (2' acyl)), 47.5 (t, C-F1' (2' acyl & 3' acyl)), 65.3 (t/d,  $^2J_{CP}$  = 5.0 Hz, C-A5' (3' acyl)), 67.5 (t, C-F5' (2' acyl & 3' acyl)), 69.3 (d, C-F2' (2' acyl & 3' acyl)), 71.1 (d, C-F4' (2' acyl & 3' acyl)), 72.6 (d, C-F3' (2' acyl & 3' acyl)), 73.4 (d, C-A3' (2' acyl)), 73.6 (d, C-A3' (3' acyl)), 76.4 (d, C-A2' (2' acyl)), 82.0 (d/d,  $^3J_{CP}$  = 8.9 Hz, C-A4' (3' acyl)), 83.8 (d, C-A4' (2' acyl)), 85.1 (d, C-A1' (2' acyl)), 86.1 (d, C-A1' (3' acyl)), 116.5 (d, C-F9 (2' acyl & 3' acyl)), 117.7 (s, C-A5 (2' acyl & 3' acyl)), 130.3 (d, C-F6 (2' acyl & 3' acyl)), 131.4 (s, C-F7 (2' acyl & 3' acyl)), 134.2 (s, C-F4a & C-F5a (2' acyl & 3' acyl)), 139.0 (C-A8 (2' acyl) or C-A8 (3' acyl) or C-F9a (2' acyl) or C-F9a (3' acyl)), 139.2 (C-A8 (2' acyl) or C-A8 (3' acyl) or C-F9a (2' acyl) or C-F9a (3' acyl)), 139.3 (C-A8 (2' acyl) or C-A8 (3' acyl) or C-F9a (2' acyl) or C-F9a (3' acyl)), 147.8 (s, C-A4 (2' acyl) or C-A4 (3' acyl)), 148.5 (d, C-A4 (2' acyl) or C-A4 (3' acyl)), 149.9 (s, C-F10a (2' acyl & 3' acyl)), 150.4 (s, C-F8 (2' acyl & 3' acyl)), 152.4 (d, C-A2 (2' acyl & 3' acyl)), 154.8 (s, C-A6 (2' acyl & 3' acyl)), 157.6 (s, C-F2 (2' acyl & 3' acyl)), 161.1 (s, C-F4 (2' acyl & 3' acyl)), 173.5 (carbonyl (2' acyl)), 174.05 (carbonyl (3' acyl)).

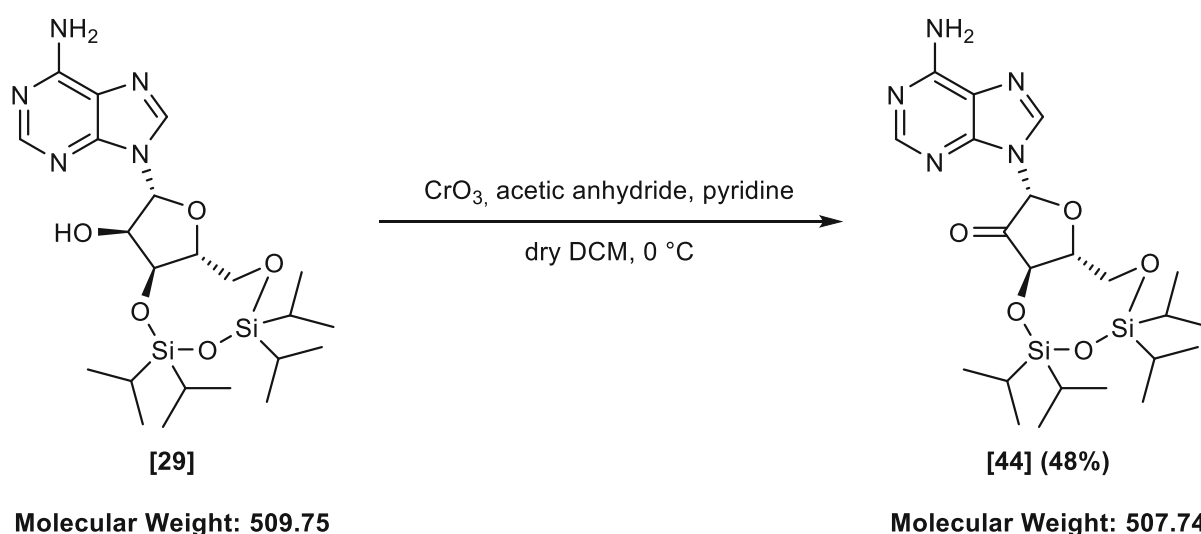
$^{31}\text{P}$ -NMR (243 MHz,  $\text{D}_2\text{O}$ )  $\delta = -11.27$  (d,  $J_{PP} = 21.9$  Hz,  $\text{R}^{\text{flavin}}\text{-}\underline{\text{P}}\text{O}_3\text{-O-PO}_3\text{-R}^{\text{adenosine}}$ ),  $-10.50$  ( $\text{PO}_3\text{-O-}\underline{\text{P}}\text{O}_3\text{-R}^{\text{adenosine}}$ ) ppm.

**Comment**

The  $^1\text{H}$ -NMR and the  $^{13}\text{C}$ -NMR spectra show broad peaks; consequently, the proper assignments of protons and carbons were complex. Nevertheless, selected signals were listed to confirm the formation of [42].

## E IV.9 Synthesis of amide derivatives of adenosine

### E IV.9.1 (6*R*,8*R*,9*aR*)-8-(6-Amino-9*H*-purin-9-yl)-2,2,4,4-tetraisopropylidihydro-6*H*-furo[3,2-*f*][1,3,5,2,4]trioxadisilocin-9(8*H*)-one [44]

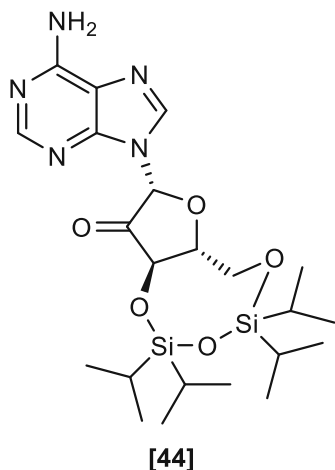


(6*R*,8*R*,9*aR*)-8-(6-amino-9*H*-purin-9-yl)-2,2,4,4-tetraisopropylidihydro-6*H*-furo[3,2-*f*][1,3,5,2,4]trioxadisilocin-9(8*H*)-one [44] was synthesized from (6*R*,8*R*,9*aS*)-8-(6-amino-9*H*-purin-9-yl)-2,2,4,4-tetraisopropyltetrahydro-6*H*-furo[3,2-*f*][1,3,5,2,4]trioxadisilocin-9-ol [29] following a literature procedure.<sup>438</sup> An oven-dried 500 mL three-necked round bottom flask was flushed with argon using standard Schlenk-technique.  $\text{CrO}_3$  (8.25 g, 82.54 mmol, 2.55 equiv.) and dry DCM (250 mL) were added under an inert atmosphere, and the resulting mixture was cooled with an ice/water bath. Dry pyridine (13.30 mL, 165.08 mmol, 5.10 equiv.) and acetic anhydride (7.80 mL, 82.54 mmol, 2.55 equiv.) were added, and the resulting black mixture was stirred at  $0\text{ }^\circ\text{C}$  for 30 min. (6*R*,8*R*,9*aS*)-8-(6-Amino-9*H*-purin-9-yl)-2,2,4,4-

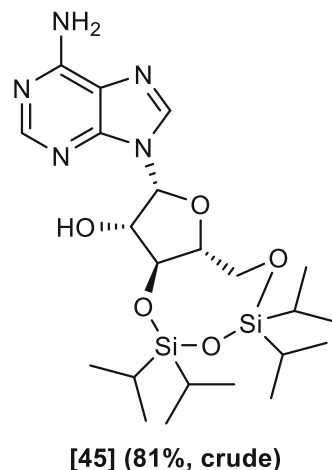
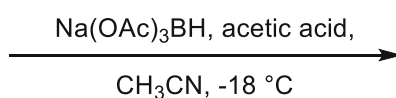
tetraisopropyltetrahydro-6*H*-furo[3,2-*f*][1,3,5,2,4]trioxadisilocin-9-ol [29] (16.50 g, 32.37 mmol, 1.00 equiv.) was added in one portion and the reaction was stirred at 0 °C until TLC analysis indicated full conversion of the starting material. The mixture was diluted with EtOAc (500 mL) and filtrated through a short pad of silica. The filtrate was further washed with saturated aq. NaHCO<sub>3</sub> solution (300 mL) was dried over MgSO<sub>4</sub> and evaporated to obtain the crude material as a yellow solid, which was used in the following step without further purification. If necessary, the crude material can be purified by flash column chromatography (MeOH in DCM, 3% 4min; 3-10% 24 min).

<b>Yield</b>	48% (7.86 g, 15.48 mmol)
<b>Appearance</b>	colorless to yellow solid
<b>Melting point</b>	88.0 – 90.0 °C [Lit.: not reported]
<b>TLC</b>	R <sub>f</sub> (DCM/MeOH = 9/1) = 0.71
<b>Sum formula</b>	C <sub>22</sub> H <sub>37</sub> N <sub>5</sub> O <sub>5</sub> Si <sub>2</sub>
<b><sup>1</sup>H-NMR (400 MHz, DMSO-<i>d</i><sub>6</sub>)</b>	$\delta$ = 0.68 – 1.36 (m, 28H, 4x isopropyl), 4.01 – 4.09 (m, 1H, H-4'), 4.11 – 4.25 (m, 2H, H-5'a & H-5'b), 5.59 (d, <i>J</i> = 9.8 Hz, 1H, H-3'), 5.71 (s, 1H, H-1'), 5.74 (s, 2H, NH <sub>2</sub> ), 7.83 (s, 1H, H-8), 8.17 (s, 1H, H-2) ppm.
<b><sup>13</sup>C-NMR (101 MHz, DMSO-<i>d</i><sub>6</sub>)</b>	$\delta$ = 12.6 (d, Si- <u>CH</u> -CH <sub>3</sub> ), 12.7 (d, Si- <u>CH</u> -CH <sub>3</sub> ), 13.1 (d, Si- <u>CH</u> -CH <sub>3</sub> ), 13.6 (d, Si- <u>CH</u> -CH <sub>3</sub> ), 16.9 (q, Si-CH- <u>CH</u> <sub>3</sub> ), 16.9 (q, Si-CH- <u>CH</u> <sub>3</sub> ), 17.0(q, Si-CH- <u>CH</u> <sub>3</sub> ), 17.1 (q, Si-CH- <u>CH</u> <sub>3</sub> ), 17.4 (q, Si-CH- <u>CH</u> <sub>3</sub> ), 17.4 (q, Si-CH- <u>CH</u> <sub>3</sub> ), 17.5 (q, Si-CH- <u>CH</u> <sub>3</sub> ), 61.3 (d, C-5'), 72.9 (d, C-3'), 79.1 (d, C-4'), 80.7 (d, C-1'), 119.9 (s, C-5), 140.4 (d, C-8), 149.5 (s, C-4), 153.1 (d, C-2), 155.5(s, C-6), 205.8 (s, C-2' (ketone)) ppm.
<b>Optical rotation</b>	$[\alpha]_D^{20}$ = -52.2 (c = 0.5, CHCl <sub>3</sub> )
<b>Comment</b>	Spectral data are in accordance with the literature.

## **E IV.9.2 (6*R*,8*R*,9*S*,9*aS*)-8-(6-Amino-9*H*-purin-9-yl)-2,2,4,4-tetraisopropyltetrahydro-6*H*-furo[3,2-*f*][1,3,5,2,4]trioxadisilocin-9-ol [45]**



Molecular Weight: 507.74



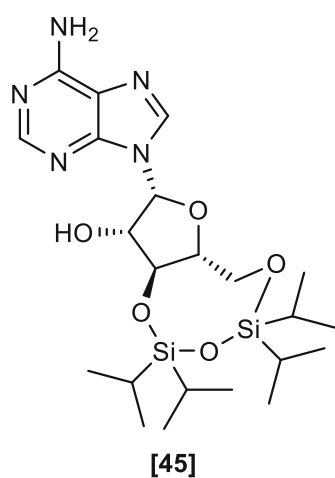
Molecular Weight: 509.75

(6*R*,8*R*,9*S*,9*aS*)-8-(6-Amino-9*H*-purin-9-yl)-2,2,4,4-tetraisopropyltetrahydro-6*H*-furo[3,2-*f*][1,3,5,2,4]trioxadisilocin-9-ol [45] was synthesized from (6*R*,8*R*,9*aR*)-8-(6-amino-9*H*-purin-9-yl)-2,2,4,4-tetraisopropyl-dihydro-6*H*-furo[3,2-*f*][1,3,5,2,4]trioxadisilocin-9(8*H*)-one [44] following a literature procedure.<sup>362</sup> A 500 mL round bottom flask was charged with sodium triacetoxyborohydride (29.22 g, 137.87 mmol, 10.00 equiv.), and THF (200 mL) was added. The resulting suspension was cooled with an ice/water bath and stirred for 10 min. ((6*R*,8*R*,9*aR*)-8-(6-Amino-9*H*-purin-9-yl)-2,2,4,4-tetraisopropyl-dihydro-6*H*-furo[3,2-*f*][1,3,5,2,4]trioxadisilocin-9(8*H*)-one [44] (7.00 g, 13.79 mmol, 1.00 equiv.) was added in one portion and the reaction mixture was stirred for 4 hours (reaction progress was monitored by TLC) with cooling. The residue was partitioned between EtOAc (400 mL) and saturated aq. NaHCO<sub>3</sub> (400 mL) and the aqueous layer was extracted with EtOAc (3 times, 200 mL). The combined organic extracts were washed with water (200 mL) and brine (200 mL) and dried over MgSO<sub>4</sub>. The mixture was then filtered and evaporated under reduced pressure. The crude material was subjected to flash column chromatography (MeOH in DCM, 3% 4min; 3-10% 24min) to give (6*R*,8*R*,9*S*,9*aS*)-8-(6-amino-9*H*-purin-9-yl)-2,2,4,4-tetraisopropyltetrahydro-6*H*-furo[3,2-*f*][1,3,5,2,4]trioxadisilocin-9-ol [45] (5.67 g, 81%) as a pale yellow powder.

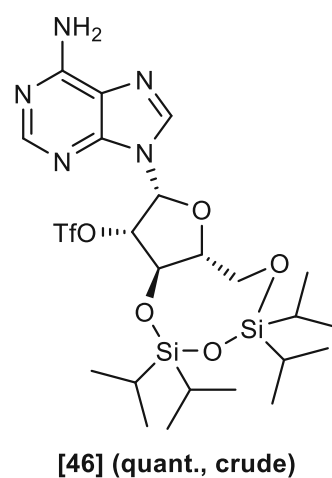


<b>Yield</b>	81% (5.67 g, 11.12 mmol)
<b>Appearance</b>	colorless to pale yellow solid
<b>Melting point</b>	101 – 103 °C [Lit. <sup>439</sup> : 97.0 – 98.6 °C]
<b>TLC</b>	R <sub>f</sub> (CHCl <sub>3</sub> /MeOH = 10/1) = 0.53
<b>Sum formula</b>	C <sub>22</sub> H <sub>39</sub> N <sub>5</sub> O <sub>5</sub> Si <sub>2</sub>
<b><sup>1</sup>H-NMR (400 MHz, DMSO-<i>d</i><sub>6</sub>)</b>	δ = 0.99 – 1.16 (m, 28H, 4x isopropyl), 3.80 (ddd, <i>J</i> = 7.7, 4.4, 3.0 Hz, 1H, H-3'), 3.93 (dd, <i>J</i> = 12.6, 3.1 Hz, 1H, H-5'b), 4.11 (dd, <i>J</i> = 12.6, 4.4 Hz, 1H, H-5'a), 4.51 (dt, <i>J</i> = 7.9, 6.2 Hz, 1H, H-2'), 4.58 (t, <i>J</i> = 8.0 Hz, 1H, H-4'), 5.78 (d, <i>J</i> = 5.8 Hz, 1H, OH-2'), 6.21 (d, <i>J</i> = 6.6 Hz, 1H, H-1'), 7.27 (s, 2H, NH <sub>2</sub> ), 8.04 (s, 1H, H-8), 8.11 (s, 1H, H-2).
<b><sup>13</sup>C-NMR (101 MHz, DMSO-<i>d</i><sub>6</sub>)</b>	δ = 12.0 (d, Si-CH-CH <sub>3</sub> ), 12.2 (d, Si-CH-CH <sub>3</sub> ), 12.5 (d, Si-CH-CH <sub>3</sub> ), 12.8 (d, Si-CH-CH <sub>3</sub> ), 16.8 (q, Si-CH-CH <sub>3</sub> ), 16.8 (q, Si-CH-CH <sub>3</sub> ), 16.9 (q, Si-CH-CH <sub>3</sub> ), 17.0 (q, Si-CH-CH <sub>3</sub> ), 17.2 (q, 3x Si-CH-CH <sub>3</sub> ), 17.4 (q, Si-CH-CH <sub>3</sub> ), 61.5 (t, C-5'), 74.8 (d, C-2'), 75.1 (d, C-4'), 79.5 (d, C-3'), 81.8 (d, C-1'), 118.5 (s, C-5), 139.6 (d, C-8), 149.5 (s, C-4), 152.4 (d, C-2), 156.0 (s, C-6) ppm.
<b>Optical rotation</b>	[α] <sub>D</sub> <sup>20</sup> = -54.2 (c = 0.5, CHCl <sub>3</sub> )
<b>Comment</b>	Spectral data are in accordance with the literature.

### E IV.9.3 (6*R*,8*R*,9*S*,9*aR*)-8-(6-Amino-9*H*-purin-9-yl)-2,2,4,4-tetraisopropyltetrahydro-6*H*-furo[3,2-*f*][1,3,5,2,4]trioxadisilocin-9-yl trifluoromethanesulfonate [46]



Molecular Weight: 509.75



Molecular Weight: 641.81

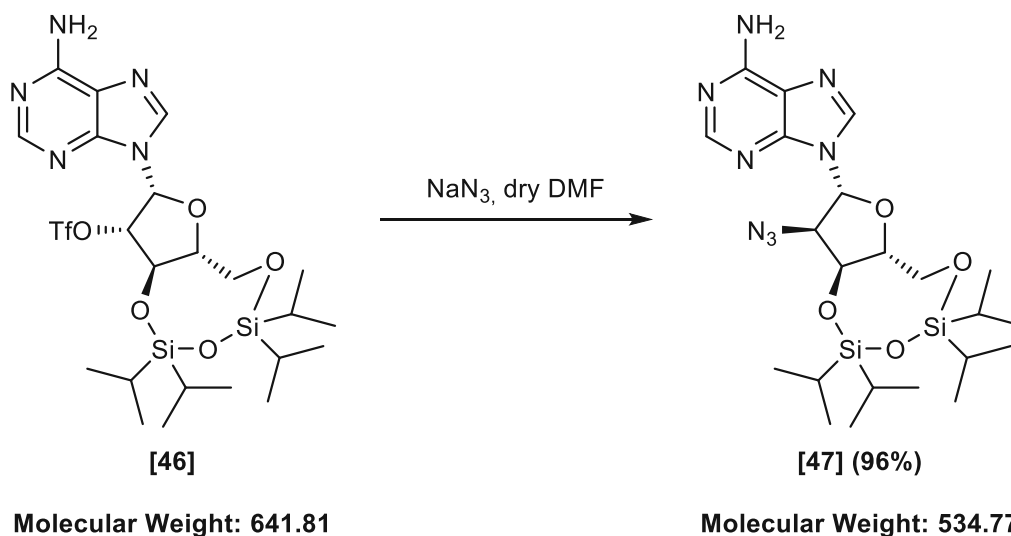
(6*aR*,8*R*,9*S*,9*aR*)-8-(6-Amino-9*H*-purin-9-yl)-2,2,4,4-tetraisopropyltetrahydro-6*H*-furo[3,2-*f*][1,3,5,2,4]trioxadisilocin-9-yl trifluoromethanesulfonate [46] was synthesized from (6*aR*,8*R*,9*S*,9*aS*)-8-(6-amino-9*H*-purin-9-yl)-2,2,4,4-tetraisopropyltetrahydro-6*H*-furo[3,2-*f*][1,3,5,2,4]trioxadisilocin-9-ol [45] following a modified literature procedure.<sup>364</sup> An oven-dried 100 mL Schlenk-flask was flushed with argon using standard Schlenk-technique. (6*aR*,8*R*,9*S*,9*aS*)-8-(6-amino-9*H*-purin-9-yl)-2,2,4,4-tetraisopropyltetrahydro-6*H*-furo[3,2-*f*][1,3,5,2,4]trioxadisilocin-9-ol [45] (1.20 g, 2.35 mmol, 1.00 equiv., scaled up in some instances), 4-DMAP (1.44 g, 11.77 mmol, 5.00 equiv.) and dry DCM (34 mL) were added under an inert atmosphere, and the resulting colorless suspension was cooled with an ice/water bath with stirring. TfO<sub>2</sub> (791 μL, 4.71 mmol, 2.00 equiv.) was added via syringe in two portions, whereby the color changed to an intense yellow, and the reaction mixture was stirred at 0 °C. The reaction was allowed to proceed at this temperature with continuous stirring and frequently monitored by TLC, and upon completion (30 min), the reaction mixture (yellow suspension) was portioned between ice-cold 1% aq. AcOH solution (100 mL) and DCM (80 mL), and the aqueous phase was extracted with DCM (3 times, 30 mL). The combined organic layers were further washed with saturated aq. NaHCO<sub>3</sub> (50 mL) and brine (50 mL), dried over MgSO<sub>4</sub>, filtrated, and evaporated under reduced pressure to obtain the crude compound as a slightly yellow solid (1.51 g, quant.), which was used in the following step without further purification.

<b>Yield</b>	quant. (1.51 g, 2.35 mmol)
<b>Appearance</b>	colorless to pale yellow solid
<b>Melting point</b>	82.0 – 84.0 °C [Lit.: not reported]
<b>TLC</b>	R <sub>f</sub> (CHCl <sub>3</sub> /MeOH = 10/1) = 0.75
<b>Sum formula</b>	C <sub>23</sub> H <sub>38</sub> F <sub>3</sub> N <sub>5</sub> O <sub>7</sub> SSi <sub>2</sub>
<b><sup>1</sup>H-NMR (400 MHz, DMSO-<i>d</i><sub>6</sub>)</b>	δ = 1.00 – 1.15 (m, 28H, 4x isopropyl), 3.87 – 4.04 (m, 2H, H-4' & H-5'b), 4.14 – 4.26 (m, 1H, H-5'a), 5.67 (t, <i>J</i> = 8.1 Hz, 1H, H-3'), 6.05 (t, <i>J</i> = 7.5 Hz, 1H, H-2'), 6.49 (d, <i>J</i> = 7.1 Hz, 1H, H-1'), 7.39 (s, 2H, NH <sub>2</sub> (aromatic)), 8.07 (s, 1H, H-2), 8.28 (s, 1H, H-8) ppm.
<b><sup>13</sup>C-NMR (101 MHz, DMSO-<i>d</i><sub>6</sub>)</b>	δ = 12.2 (d, Si-CH-CH <sub>3</sub> ), 12.2 (d, Si-CH-CH <sub>3</sub> ), 12.4 (d, Si-CH-CH <sub>3</sub> ), 12.5 (d, Si-CH-CH <sub>3</sub> ), 16.7 (q, 2x Si-CH-CH <sub>3</sub> ), 16.7 (q, Si-CH-CH <sub>3</sub> ), 16.7 (q, Si-CH-CH <sub>3</sub> ), 17.1 (q, Si-CH-CH <sub>3</sub> ), 17.1 q, Si-CH-CH <sub>3</sub> ), 17.1 (q, Si-CH-CH <sub>3</sub> ), 17.3 (q, Si-CH-CH <sub>3</sub> ), 62.0 (t, C-5'), 74.1 (d, C-3'), 78.5 (d, C-4'), 78.9 (d, C-1'), 89.2 (d, C-2'), 119.1 (s, C-5), 119.3 (q, CF <sub>3</sub> ), 140.4 (d, C-8), 149.1 (s, C-4), 152.5 (d, C-2), 156.2 (s, C-6) ppm.
<b><sup>19</sup>F NMR (376 MHz, DMSO-<i>d</i><sub>6</sub>)</b>	δ -77.75 ppm.
<b>Optical rotation</b>	[α] <sub>D</sub> <sup>20</sup> = -27.0 (c = 0.25, CHCl <sub>3</sub> )

Comment

Spectral data are in accordance with the literature.

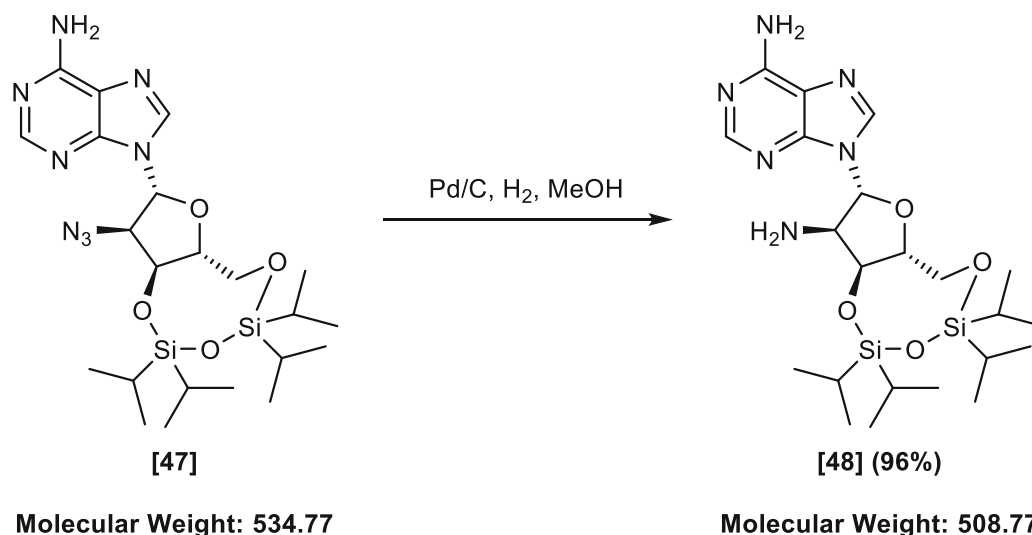
## E IV.9.4 9-((6*R*,8*R*,9*R*,9*aS*)-9-Azido-2,2,4,4-tetraisopropyltetrahydro-6*H*-furo[3,2-*f*][1,3,5,2,4]trioxadisilocin-8-yl)-9*H*-purin-6-amine [47]



9-((6*R*,8*R*,9*R*,9*aS*)-9-Azido-2,2,4,4-tetraisopropyltetrahydro-6*H*-furo[3,2-*f*][1,3,5,2,4]trioxadisilocin-8-yl)-9*H*-purin-6-amine [47] was synthesized from (6*aR*,8*R*,9*S*,9*aR*)-8-(6-Amino-9*H*-purin-9-yl)-2,2,4,4-tetraisopropyltetrahydro-6*H*-furo[3,2-*f*][1,3,5,2,4]trioxadisilocin-9-yl trifluoromethanesulfonate [46] using following modified literature procedure.<sup>364</sup> An oven-dried 25 mL Schlenk flask was flushed with argon using standard Schlenk-technique. (6*aR*,8*R*,9*S*,9*aR*)-8-(6-amino-9*H*-purin-9-yl)-2,2,4,4-tetraisopropyltetrahydro-6*H*-furo[3,2-*f*][1,3,5,2,4]trioxadisilocin-9-yl trifluoromethanesulfonate [46] (910 mg, 1.42 mmol, 1.00 equiv., scaled up in some instances) and dry DMF (15 mL) were added under an inert atmosphere followed by the addition of  $\text{NaN}_3$  (461 mg, 7.09 mmol, 5.00 equiv.). The resulting slightly yellow reaction mixture was stirred at room temperature until TLC analysis indicated full conversion of the starting material (5 hours). Subsequently, the mixture was diluted with EtOAc (60 mL), and the organic layer was washed with water (3 times, 40 mL) and brine (40 mL). The organic phase was further dried over  $\text{MgSO}_4$ , filtrated, and evaporated to obtain the crude material as a slightly yellow solid (725 mg, 96%), which was used in the following step without further purification.

<b>Yield</b>	96% (725 mg, 1.36 mmol)
<b>Appearance</b>	yellow solid
<b>Melting point</b>	161.0 – 163.0 °C [Lit. <sup>440</sup> : 168.0 – 170.0 °C]
<b>TLC</b>	R <sub>f</sub> (CHCl <sub>3</sub> /MeOH = 9/1) = 0.58
<b>Sum formula</b>	C <sub>22</sub> H <sub>38</sub> N <sub>8</sub> O <sub>4</sub> Si <sub>2</sub>
<b><sup>1</sup>H-NMR (400 MHz, DMSO-<i>d</i><sub>6</sub>)</b>	δ = 1.00 – 1.12 (m, 28H, 4x isopropyl), 3.89 – 4.06 (m, 3H, H-4' & H-5'a & H-5'b), 5.01 (dd, <i>J</i> = 5.8, 1.5 Hz, 1H, H-2'), 5.44 (dd, <i>J</i> = 8.2, 6.0 Hz, 1H, H-3'), 5.83 (d, <i>J</i> = 1.5 Hz, 1H, H-1'), 7.35 (s, 2H, NH <sub>2</sub> ), 8.06 (s, 1H, H-2), 8.22 (s, 1H, H-8) ppm.
<b><sup>13</sup>C-NMR (101 MHz, DMSO-<i>d</i><sub>6</sub>)</b>	δ = 12.6 (d, (Si-CH-CH <sub>3</sub> )), 12.7 (d, (Si-CH-CH <sub>3</sub> )), 12.9 (d, (Si-CH-CH <sub>3</sub> )), 13.2 (d, (Si-CH-CH <sub>3</sub> )), 17.2 (q, Si-CH-CH <sub>3</sub> ), 17.3 (q, Si-CH-CH <sub>3</sub> ), 17.4 (q, Si-CH-CH <sub>3</sub> ), 17.5 (q, Si-CH-CH <sub>3</sub> ), 17.6 (q, Si-CH-CH <sub>3</sub> ), 17.6 (q, 2x Si-CH-CH <sub>3</sub> ), 17.8 (q, Si-CH-CH <sub>3</sub> ), 61.3 (t, C-5'), 65.1 (d, C-2'), 72.4 (d, C-3'), 81.5 (d, C-4'), 86.6 (d, C-1'), 119.8 (s, C-5), 140.4 (d, C-8), 149.0 (s, C-4), 152.9 (d, C-2), 156.6 (s, C-6) ppm.
<b>Optical rotation</b>	[α] <sub>D</sub> <sup>20</sup> = -33.9 (c = 0.37, CHCl <sub>3</sub> ) [Lit. <sup>364</sup> : [α] <sub>D</sub> <sup>21</sup> = -33.8 (c = 0.06, CHCl <sub>3</sub> )
<b>Comment</b>	Spectral data are in accordance with the literature.

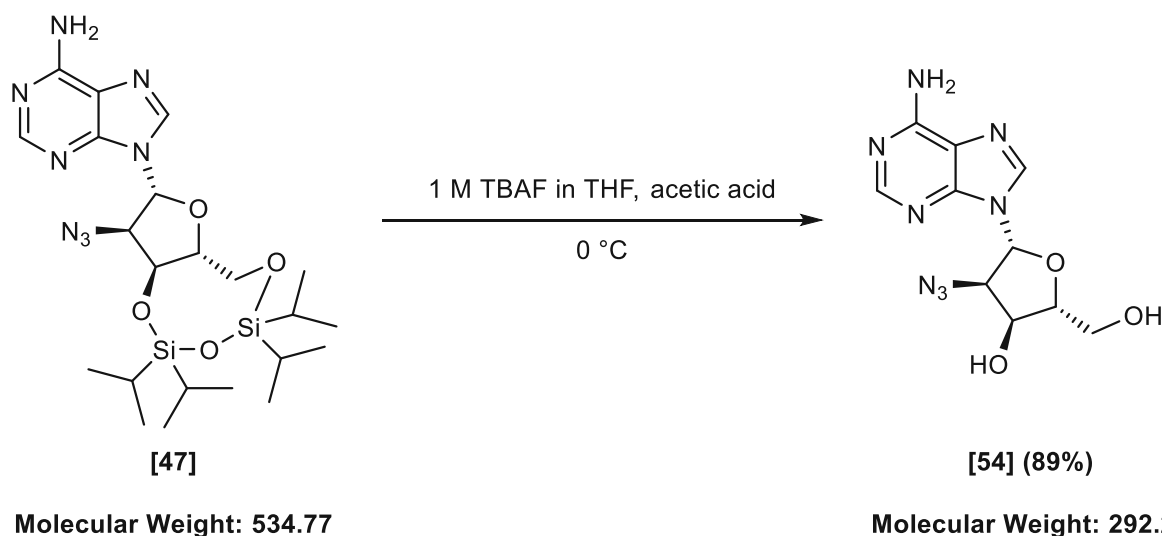
### E IV.9.5 9-((6*aR*,8*R*,9*R*,9*aS*)-9-Amino-2,2,4,4-tetraisopropyltetrahydro-6*H*-furo[3,2-*f*][1,3,5,2,4]trioxadisilocin-8-yl)-9*H*-purin-6-amine [48]



9-((6*aR*,8*R*,9*R*,9*aS*)-9-Amino-2,2,4,4-tetraisopropyltetrahydro-6*H*-furo[3,2-*f*][1,3,5,2,4]trioxadisilocin-8-yl)-9*H*-purin-6-amine [48] was synthesized from 9-((6*aR*,8*R*,9*R*,9*aS*)-9-azido-2,2,4,4-tetraisopropyltetrahydro-6*H*-furo[3,2-*f*][1,3,5,2,4]trioxadisilocin-8-yl)-9*H*-purin-6-amine [47] according to following modified literature procedure.<sup>441</sup> A 500 mL three-necked flask equipped with an H<sub>2</sub>-balloon and argon inlet was charged with 9-((6*aR*,8*R*,9*R*,9*aS*)-9-azido-2,2,4,4-tetraisopropyltetrahydro-6*H*-furo[3,2-*f*][1,3,5,2,4]trioxadisilocin-8-yl)-9*H*-purin-6-amine [47] (2.49 g, 4.66 mmol, 1.00 equiv., scaled up in some instances) and MeOH (170 mL) was further added, and the resulting colorless suspension was stirred until the solid dissolved (5 min). Subsequently, the flask was carefully evacuated and flushed with argon using standard Schlenk-technique, followed by the addition of Pd/C (250 mg). The flask was then shortly evacuated and flushed with hydrogen four times to provide a hydrogen atmosphere, and the reaction mixture was stirred at room temperature under a hydrogen atmosphere overnight. The reaction progress was monitored by TLC and HPLC-MS analysis, and at complete consumption of the starting material, the reaction mixture was filtrated through a short pad of celite. The filtrate was evaporated to obtain the crude material as a colorless to off-white solid, which could be used in the following step without further purification.

<b>Yield</b>	quant. (2.37 g, 4.79 mmol)
<b>Appearance</b>	off-white solid
<b>Melting point</b>	75.0 – 77.0 °C [Lit.: not reported]
<b>TLC</b>	R <sub>f</sub> (CHCl <sub>3</sub> /MeOH = 19/1) = 0.22
<b>Sum formula</b>	C <sub>22</sub> H <sub>40</sub> N <sub>6</sub> O <sub>4</sub> Si <sub>2</sub>
<b><sup>1</sup>H-NMR (400 MHz, DMSO-<i>d</i><sub>6</sub>)</b>	δ = 1.00 – 1.08 (m, 28H, 4x isopropyl), 3.89 – 4.05 (m, 4H, H-2' & H-4' & H-5'a & H-5'b), 4.82 (t, <i>J</i> = 6.4 Hz, 1H, H-3'), 5.72 (d, <i>J</i> = 3.7 Hz, 1H, H-1'), 7.29 (s, 2H, NH <sub>2</sub> (aromatic), ), 8.08 (s, 1H, H-2), 8.25 (s, 1H, H-8) ppm.
<b><sup>13</sup>C-NMR (101 MHz, DMSO-<i>d</i><sub>6</sub>)</b>	δ = 12.7 (d, Si- <u>CH</u> -CH <sub>3</sub> ), 12.9 (d, Si- <u>CH</u> -CH <sub>3</sub> ), 13.2 (d, Si- <u>CH</u> -CH <sub>3</sub> ), 13.3 (d, Si- <u>CH</u> -CH <sub>3</sub> ), 17.5 (q, Si-CH- <u>CH</u> <sub>3</sub> ), 17.5 (q, Si-CH- <u>CH</u> <sub>3</sub> ), 17.6 (q, Si-CH- <u>CH</u> <sub>3</sub> ), 17.7 (q, Si-CH- <u>CH</u> <sub>3</sub> ), 17.8 (q, Si-CH- <u>CH</u> <sub>3</sub> ), 17.8 (q, 2x Si-CH- <u>CH</u> <sub>3</sub> ), 18.0 (q, Si-CH- <u>CH</u> <sub>3</sub> ), 57.5 (t, C-5'), 63.0 (d, C-4'), 71.9 (d, C-3'), 83.0 (d, C-2'), 89.6 (d, C-1'), 119.8 (s, C-5), 140.3 (d, C-8), 149.6 (s, C-4), 153.1 (d, C-2), 156.7 (s, C-6) ppm.
<b>Optical rotation</b>	[α] <sub>D</sub> <sup>20</sup> = -32.5 (c = 0.1, CHCl <sub>3</sub> )
<b>Comment</b>	The <sup>1</sup> H-NMR is in accordance with the literature, <sup>442</sup> but the <sup>13</sup> C-NMR is not reported.

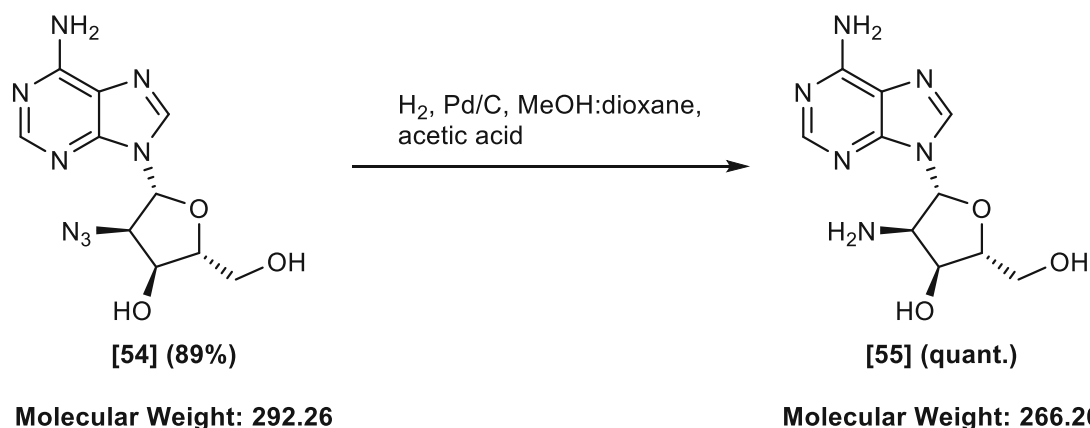
## E IV.9.6 (2*R*,3*S*,4*R*,5*R*)-5-(6-amino-9*H*-purin-9-yl)-4-azido-2-(hydroxymethyl)tetrahydrofuran-3-ol



(2*R*,3*S*,4*R*,5*R*)-5-(6-amino-9*H*-purin-9-yl)-4-azido-2-(hydroxymethyl)tetrahydrofuran-3-ol **[54]** was synthesized according to general procedure C using protected adenosine **[47]** (700 mg, 1.31 mmol, 1.00 equiv.). The pure product was obtained after purification by flash column chromatography (silica gel/crude material = 100/1, solid load) using MeOH in DCM (5% 10 min; 5-10% 20 min) as eluent.

<b>Yield</b>	85% (341 mg, 1.17 mmol)
<b>Appearance</b>	colorless solid
<b>Melting point</b>	211 – 212 °C [Lit. <sup>363</sup> : 213 – 214 °C]
<b>TLC</b>	R <sub>f</sub> (CHCl <sub>3</sub> /MeOH = 8/2) = 0.38
<b>Sum formula</b>	C <sub>10</sub> H <sub>12</sub> N <sub>8</sub> O <sub>3</sub>
<b><sup>1</sup>H NMR (600 MHz, DMSO-<i>d</i><sub>6</sub>)</b>	δ = 3.57 (ddd, <i>J</i> = 12.1, 6.5, 4.0 Hz, 1H, H-5'b), 3.68 (ddd, <i>J</i> = 12.1, 5.0, 3.7 Hz, 1H, H-5'a), 3.99 (q, <i>J</i> = 3.8 Hz, 1H, H-4'), 4.54 (td, <i>J</i> = 5.2, 5.2, 3.7 Hz, 1H, H-3'), 4.64 (dd, <i>J</i> = 6.2, 5.2 Hz, 1H, H-2'), 5.29 (dd, <i>J</i> = 6.5, 4.9 Hz, 1H, OH-5), 5.92 – 6.07 (m, 2H, H-1' & OH-3'), 7.38 (s, 2H, NH <sub>2</sub> -aromatic), 8.15 (s, 1H, H-2), 8.39 (s, 1H, H-8) ppm.
<b><sup>13</sup>C NMR (151 MHz, DMSO-<i>d</i><sub>6</sub>)</b>	δ = 61.1 (t, C-5'), 64.2 (d, C-2'), 71.1 (d, C-3'), 85.2 (d, C-1'), 86.1 (d, C-4'), 119.2 (s, C-5), 139.5 (d, C-8), 149.0 (s, C-4), 152.7 (d, C-2), 156.2 (s, C-6) ppm.

## E IV.9.7 (2*R*,3*S*,4*R*,5*R*)-4-amino-5-(6-Amino-9*H*- purin-9-yl)-2- (hydroxymethyl)tetrahydrofuran-3-ol



(2*R*,3*S*,4*R*,5*R*)-4-amino-5-(6-Amino-9*H*-purin-9-yl)-2-(hydroxymethyl)tetrahydrofuran-3-ol **[55]** was synthesized from (2*R*,3*S*,4*R*,5*R*)-5-(6-amino-9*H*-purin-9-yl)-4-azido-2-(hydroxymethyl)tetrahydrofuran-3-ol **[54]** according to following modified literature procedure.<sup>363</sup> A 25 mL three-necked round bottom flask equipped with an H<sub>2</sub>-balloon and argon inlet was charged with (2*R*,3*S*,4*R*,5*R*)-5-(6-amino-9*H*-purin-9-yl)-4-azido-2-(hydroxymethyl)tetrahydrofuran-3-ol **[54]** (250 mg, 0.85 mmol, 1.00 equiv.) and MeOH (7 mL), dioxane (7 mL) and acetic acid (1.4 mL) were further added, and the resulting colorless suspension was stirred until the solid dissolved (5 min). Subsequently, the flask was carefully evacuated and flushed with argon using standard Schlenk-technique, followed by the addition of Pd/C (80 mg). The flask was then shortly evacuated and flushed with hydrogen four times to provide a hydrogen atmosphere, and the reaction mixture was stirred at room temperature overnight. As TLC analysis indicated full conversion of the starting material, the reaction mixture was filtrated through a short pad of celite, and the filtrate was further evaporated to obtain the crude material as a colorless solid, which could be used in the following step without further purification.

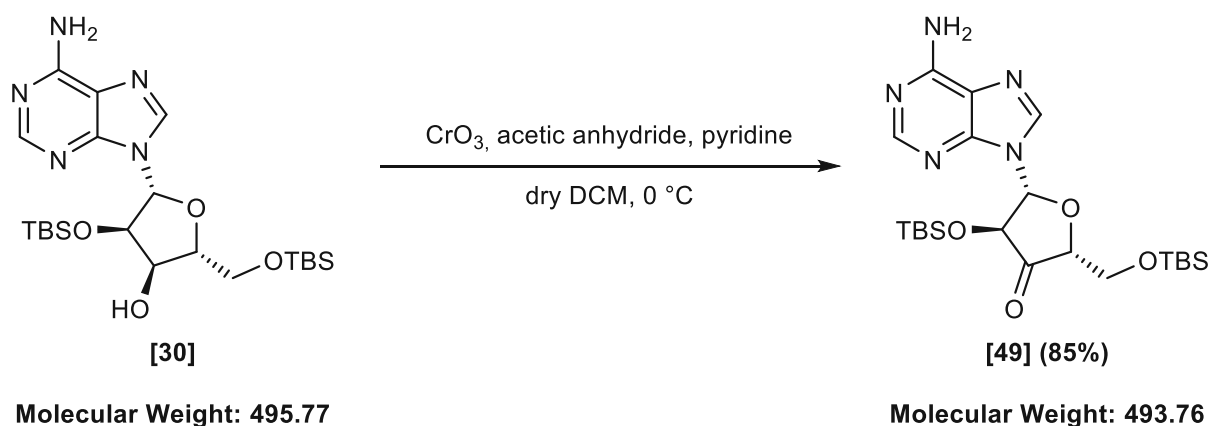
<b>Yield</b>	quant. (228 mg, 0.85 mmol)
<b>Appearance</b>	colorless solid
<b>Melting point</b>	197.0 – 198.0 °C [Lit. <sup>443</sup> : 194.0 – 198.0 °C]
<b>Sum formula</b>	C <sub>10</sub> H <sub>14</sub> N <sub>6</sub> O <sub>3</sub>
<b><sup>1</sup>H NMR (600 MHz, DMSO-<i>d</i><sub>6</sub>)</b>	$\delta = 3.54$ (dd, $J = 12.1, 3.6$ Hz, 1H, H-5'b), 3.65 (dd, $J = 12.0, 4.1$ Hz, 1H, H-5'a), 3.93 – 4.00 (m, 2H, H-2' & H-4'), 4.04 (dd, $J$



= 5.2, 1.5 Hz, 1H, H-3'), 5.68 (d,  $J = 8.1$  Hz, 1H, H-1'), 7.33 (s, 2H, NH<sub>2</sub>-aromatic), 8.12 (s, 1H, H-2), 8.29 (s, 1H, H-8) ppm.

<sup>13</sup>C NMR (151 MHz, DMSO-*d*<sub>6</sub>)  $\delta = 57.8$  (d, C-2'), 62.7 (t, C-5'), 72.4 (d, C-3'), 87.6 (d, C-4'), 89.6 (d, C-1'), 120.1 (s, C-5), 140.9 (d, C-8), 149.7 (s, C-4), 152.8 (d, C-2), 156.8 (s, C-6) ppm.

## E IV.9.8 (2*R*,4*S*,5*R*)-5-(6-Amino-9*H*-purin-9-yl)-4-((*tert*-butyldimethylsilyl)oxy)-2-(((*tert*-butyldimethylsilyl)oxy)methyl)dihydrofuran-3(2*H*)-one [49]



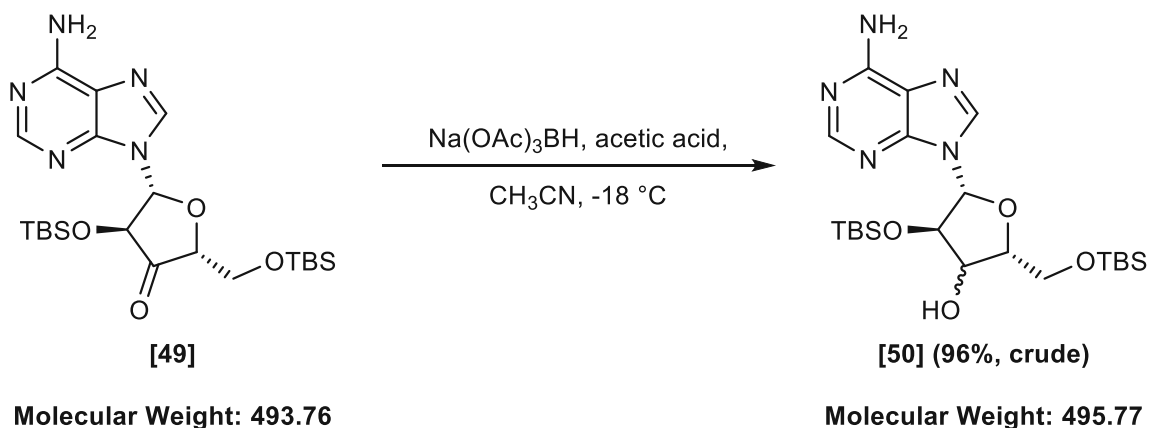
(2*R*,4*S*,5*R*)-5-(6-Amino-9*H*-purin-9-yl)-4-((*tert*-butyldimethylsilyl)oxy)-2-(((*tert*-butyldimethylsilyl)oxy)methyl)dihydrofuran-3(2*H*)-one [49] was synthesized from (2*R*,3*R*,4*R*,5*R*)-5-(6-amino-9*H*-purin-9-yl)-4-((*tert*-butyldimethylsilyl)oxy)-2-(((*tert*-butyldimethylsilyl)oxy)methyl)tetrahydrofuran-3-ol [30] following a literature procedure.<sup>438</sup> An oven-dried 500 mL three-necked round bottom flask was flushed with argon using standard Schlenk-technique. CrO<sub>3</sub> (8.14 g, 70.16 mmol, 2.55 equiv.) and dry DCM (200 mL) were added under an inert atmosphere, and the resulting mixture was cooled with an ice/water bath. Dry pyridine (11.40 mL, 140.93 mmol, 5.10 equiv.) and acetic anhydride (6.63 mL, 70.16 mmol, 2.55 equiv.) were added, and the resulting black mixture was stirred at 0 °C for 30 min. (2*R*,3*R*,4*R*,5*R*)-5-(6-Amino-9*H*-purin-9-yl)-4-((*tert*-butyldimethylsilyl)oxy)-2-(((*tert*-butyldimethylsilyl)oxy)methyl)tetrahydrofuran-3-ol [30] (13.64 g, 27.51 mmol, 1.00 equiv.) was added in one portion, and the reaction was stirred at 0 °C until TLC analysis indicated full conversion of the starting material. The mixture was diluted with EtOAc (500 mL) and filtrated through a short pad of silica. The filtrate was further washed with saturated aq. NaHCO<sub>3</sub>



solution (300 mL), was dried over  $\text{MgSO}_4$  and evaporated to obtain the crude material as a colorless solid, which could be used in the following step without further purification.

<b>Yield</b>	85% (11.52 g, 23.33 mmol)
<b>Appearance</b>	colorless solid
<b>Melting point</b>	> 174 °C (decomposition) [Lit. <sup>363</sup> : 177– 178 °C]
<b>TLC</b>	$R_f$ (EtOAc) = 0.61
<b>Sum formula</b>	$\text{C}_{22}\text{H}_{39}\text{N}_5\text{O}_4\text{Si}_2$
<b><math>^1\text{H-NMR}</math> (400 MHz, <math>\text{CDCl}_3</math>)</b>	$\delta$ = -0.20 (s, 3H, Si- $\text{CH}_3$ ), -0.02 (s, 3H, Si- $\text{CH}_3$ ), 0.07 (s, 3H, Si- $\text{CH}_3$ ), 0.10 (s, 3H, Si- $\text{CH}_3$ ), 0.72 (s, 9H, tertbutyl), 0.92 (s, 9H, tertbutyl), 3.97 (t, $J$ = 2.4 Hz, 2H, H-5'a & H-5'b), 4.30 (q, $J$ = 1.6 Hz, 1H, H-4'), 4.94 (dd, $J$ = 8.3, 0.8 Hz, 1H, H-2'), 5.80 (s, 2H, $\text{NH}_2$ ), 6.13 (d, $J$ = 8.3 Hz, 1H, H-1'), 8.14 (s, 1H, H-8), 8.36 (s, 1H, H-2) ppm.
<b><math>^{13}\text{C-NMR}</math> (101 MHz, <math>\text{CDCl}_3</math>)</b>	$\delta$ = -5.7 (q, Si- $\text{CH}_3$ ), -5.6 (q, Si- $\text{CH}_3$ ), -5.4 (q, Si- $\text{CH}_3$ ), -4.8 (q, Si- $\text{CH}_3$ ), 18.0 (s, Si- $\text{C}(\text{CH}_3)_3$ ), 18.3 (s, Si- $\text{C}(\text{CH}_3)_3$ ), 25.3 (q, Si- $\text{C}(\text{CH}_3)$ ), 25.9 (q, Si- $\text{C}(\text{CH}_3)$ ), 62.5 (t, C-5'), 77.9 (d, C-2'), 82.4 (d, C-4'), 85.0 (d, C-1'), 119.8 (s, C-5), 138.6 (d, C-8), 150.4 (s, C-4), 153.5 (d, C-2), 155.5 (s, C-6), 208.6 (s, C-3' (ketone)) ppm.
<b>Optical rotation</b>	$[\alpha]_D^{20}$ = +10.1 (c = 0.25, MeOH)
<b>Comment</b>	The spectral data are in accordance with the literature.

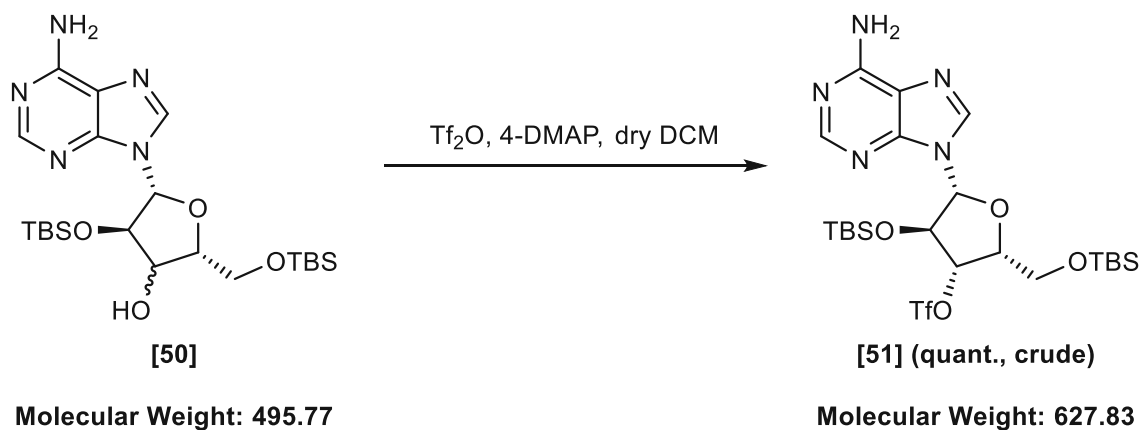
## E IV.9.9 (2*R*,3*S*,4*R*,5*R*)-5-(6-Amino-9*H*-purin-9-yl)-4-((*tert*-butyldimethylsilyl)oxy)-2-(((*tert*-butyldimethylsilyl)oxy)methyl)tetrahydrofuran-3-ol [50]



(2*R*,3*S*,4*R*,5*R*)-5-(6-Amino-9*H*-purin-9-yl)-4-((*tert*-butyldimethylsilyl)oxy)-2-(((*tert*-butyldimethylsilyl)oxy)methyl)tetrahydrofuran-3-ol [**50**] was synthesized from (2*R*,4*S*,5*R*)-5-(6-amino-9*H*-purin-9-yl)-4-((*tert*-butyldimethylsilyl)oxy)-2-(((*tert*-butyldimethylsilyl)oxy)methyl)dihydrofuran-3(2*H*)-one [**49**] following a literature procedure.<sup>362</sup> An oven-dried 500 mL three-necked round bottom flask was charged with (2*R*,4*S*,5*R*)-5-(6-amino-9*H*-purin-9-yl)-4-((*tert*-butyldimethylsilyl)oxy)-2-(((*tert*-butyldimethylsilyl)oxy)methyl)dihydrofuran-3(2*H*)-one [**49**] (6.00 g, 12.15 mmol, 1.00 equiv.) and dry acetonitrile (200 mL) was added via syringe. Acetic acid (12 mL) was added to dissolve the solid. The mixture was cooled to -18 °C, and NaHB(OAc)<sub>3</sub> (25.75 g, 121.5 mmol, 10.00 equiv.) was added. Since only slow conversion was detected by TLC and HPLC analysis, the reaction mixture was allowed to warm up slowly to room temperature and stirred overnight. TLC analysis indicated nearly full conversion of the starting material the following day, and the obtained solution was taken up in saturated aq. NaHCO<sub>3</sub> (100 mL) and DCM (200 mL) and extracted. The combined organic layers were washed with saturated aq. NaHCO<sub>3</sub> (100 mL) and water (100 mL). The resulting organic layer was dried over MgSO<sub>4</sub> and evaporated to dryness under reduced pressure to obtain crude (2*R*,3*S*,4*R*,5*R*)-5-(6-amino-9*H*-purin-9-yl)-4-((*tert*-butyldimethylsilyl)oxy)-2-(((*tert*-butyldimethylsilyl)oxy)methyl)tetrahydrofuran-3-ol [**50**] as a pale yellow powder (5.80 g, 96%), which was used in the next step without further purification.

<b>Yield</b>	96% (5.80 g, 11.70 mmol)
<b>Appearance</b>	colorless to pale yellow solid
<b>Melting point</b>	170.0 – 172.0 °C [Lit. <sup>363</sup> : 172.0 – 175.0 °C]
<b>TLC</b>	R <sub>f</sub> (EtOAc) = 0.54
<b>Sum formula</b>	C <sub>22</sub> H <sub>41</sub> N <sub>5</sub> O <sub>4</sub> Si <sub>2</sub>
<b><sup>1</sup>H-NMR (400 MHz, DMSO-<i>d</i><sub>6</sub>)</b>	δ = -0.01 (s, 3H, Si-CH <sub>3</sub> ), 0.03 (s, 3H, Si-CH <sub>3</sub> ), 0.05 (s, 3H, Si-CH <sub>3</sub> ), 0.06 (s, 3H, Si-CH <sub>3</sub> ), 0.83 (s, 9H, <i>tert</i> butyl), 0.87 (s, 9H, <i>tert</i> butyl), 3.88 (dd, <i>J</i> = 11.0, 6.1 Hz, 1H, H-5'b), 3.98 (dd, <i>J</i> = 11.0, 4.4 Hz, 1H, H-5'a), 4.05 (td, <i>J</i> = 4.6, 4.6, 2.4 Hz, 1H, H-3'), 4.17 (dt, <i>J</i> = 6.1, 4.3 Hz, 1H, H-4'), 4.44 (t, <i>J</i> = 2.3 Hz, 1H, H-2'), 5.87 (s, 1H, OH-3'), 5.88 (s, 1H, H-1'), 7.32 (s, 2H, NH <sub>2</sub> ), 8.15 (s, 1H, H-2), 8.24 (s, 1H, H-8) ppm.
<b><sup>13</sup>C-NMR (101 MHz, DMSO-<i>d</i><sub>6</sub>)</b>	δ = -4.9 (q, Si-CH <sub>3</sub> ), -4.8 (q, Si-CH <sub>3</sub> ), -4.6 (q, Si-CH <sub>3</sub> ), -4.5 (q, Si-CH <sub>3</sub> ), 18.1 (s, Si-C(CH <sub>3</sub> ) <sub>3</sub> ), 18.5 (s, Si-C(CH <sub>3</sub> ) <sub>3</sub> ), 26.0 (q, Si-C(CH <sub>3</sub> ) <sub>3</sub> ), 26.3 (Si-C(CH <sub>3</sub> ) <sub>3</sub> ), 62.1 (t, C-5'), 75.5 (d, C-3'), 82.2 (d, C-2'), 83.5 (d, C-4'), 89.7 (d, C-1'), 119.2 (s, C-5), 139.6 (d, C-8), 149.4 (s, C-4), 153.0 (d, C-2), 156.5 (s, C-6) ppm.
<b>Optical rotation</b>	[α] <sub>D</sub> <sup>20</sup> = -28.2 (c = 1.0, CHCl <sub>3</sub> )
<b>Comment</b>	Spectral data are in accordance with the literature.

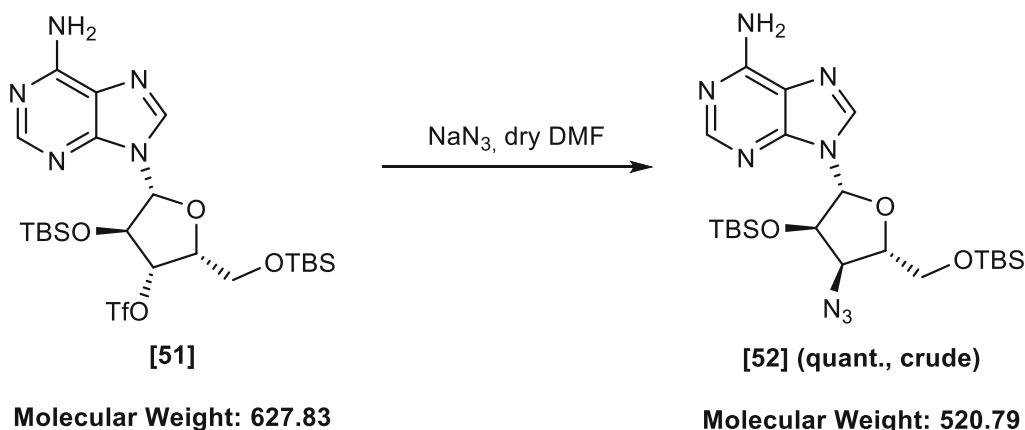
## E IV.9.10 (2*R*,3*S*,4*R*,5*R*)-5-(6-Amino-9*H*-purin-9-yl)-4-((*tert*-butyldimethylsilyl)oxy)-2-(((*tert*-butyldimethylsilyl)oxy)methyl)tetrahydrofuran-3-yl trifluoromethanesulfonate [51]



(2*R*,3*S*,4*R*,5*R*)-5-(6-Amino-9*H*-purin-9-yl)-4-((*tert*-butyldimethylsilyl)oxy)-2-(((*tert*-butyldimethylsilyl)oxy)methyl)tetrahydrofuran-3-yl trifluoromethanesulfonate [51] was synthesized from (2*R*,3*S*,4*R*,5*R*)-5-(6-amino-9*H*-purin-9-yl)-4-((*tert*-butyldimethylsilyl)oxy)-2-(((*tert*-butyldimethylsilyl)oxy)methyl)tetrahydrofuran-3-ol [50] following a modified literature procedure.<sup>363</sup> An oven-dried 100 mL Schlenk-flask was flushed with argon using standard Schlenk-technique. (2*R*,3*S*,4*R*,5*R*)-5-(6-Amino-9*H*-purin-9-yl)-4-((*tert*-butyldimethylsilyl)oxy)-2-(((*tert*-butyldimethylsilyl)oxy)methyl)tetrahydrofuran-3-ol [50] (1.20 g, 2.35 mmol, 1.00 equiv., scaled up in some instances), 4-DMAP (1.44 g, 11.77 mmol, 5.00 equiv.) and dry DCM (34 mL) were added under an inert atmosphere, and the resulting colorless suspension was cooled with an ice/water bath with stirring. Tf<sub>2</sub>O (813 μL, 4.84 mmol, 2.00 equiv.) was added via syringe in two portions, and the reaction mixture was stirred at 0 °C. The reaction was allowed to proceed at this temperature with continuous stirring and frequently monitored by TLC, and upon completion (~1.5 h), the reaction mixture was portioned between ice-cold 1% aq. AcOH solution (100 mL) and DCM (150 mL), and the aqueous phase was extracted with DCM (3 times, 100 mL). The combined organic layers were further washed with saturated aq. NaHCO<sub>3</sub> (100 mL) and brine (100 mL), dried over MgSO<sub>4</sub>, filtrated, and evaporated under reduced pressure to obtain the crude compound as a slightly yellow solid (1.52 g, quant.), which was used in the following step without further purification.

<b>Yield</b>	quant. (1.52 g, 2.42 mmol)
<b>Appearance</b>	pale yellow solid
<b>Melting point</b>	131.0 – 133.0 °C [Lit. <sup>363</sup> : 48 – 52 °C]
<b>TLC</b>	R <sub>f</sub> (CHCl <sub>3</sub> /MeOH = 9/1) = 0.78
<b>Sum formula</b>	C <sub>23</sub> H <sub>40</sub> F <sub>3</sub> N <sub>5</sub> O <sub>6</sub> SSi <sub>2</sub>
<b><sup>1</sup>H-NMR (400 MHz, CDCl<sub>3</sub>)</b>	δ = -0.00 (s, 3H, Si-CH <sub>3</sub> ), 0.04 (s, 3H, Si-CH <sub>3</sub> ), 0.12 (s, 3H, Si-CH <sub>3</sub> ), 0.14 (s, 6H, 2x Si-CH <sub>3</sub> ), 0.89 (s, 9H, tertbutyl), 0.94 (s, 9H, tertbutyl), 3.90 – 4.15 (m, 2H, H-5'a & H-5'b), 4.56 (ddd, <i>J</i> = 6.4, 4.9, 3.9 Hz, 1H, H-4'), 4.97 (s, 1H, H-2'), 5.20 (dd, <i>J</i> = 4.0, 2.4 Hz, 1H, H-3'), 5.65 (s, 2H, NH <sub>2</sub> ), 6.07 (d, <i>J</i> = 2.2 Hz, 1H, H-1'), 8.03 (s, 1H, H-8), 8.35 (s, 1H, H-2) ppm.
<b><sup>13</sup>C-NMR (101 MHz, CDCl<sub>3</sub>)</b>	δ = -5.4 (q, Si-CH <sub>3</sub> ), -5.4 (q, Si-CH <sub>3</sub> ), -5.1 (q, Si-CH <sub>3</sub> ), -4.9 (q, Si-CH <sub>3</sub> ), 17.9 (s, Si-C(CH <sub>3</sub> ) <sub>3</sub> ), 18.5 (s, Si-C(CH <sub>3</sub> ) <sub>3</sub> ), 25.6 (q, Si-C(CH <sub>3</sub> ) <sub>3</sub> ), 26.0 (q, Si-C(CH <sub>3</sub> ) <sub>3</sub> ), 60.3 (t, C-5'), 79.3 (d, C-2'), 80.7 (d, C-4'), 88.6 (d, C-3'), 90.0 (d, C-1'), 118.4 (s/q, <sup>1</sup> <i>J</i> <sub>CF</sub> = 319.7 Hz, CF <sub>3</sub> ) 119.9 (s, C-5), 138.6 (d, C-8), 149.8 (s, C-4), 153.4 (d, C-2), 155.5 (s, C-6) ppm.
<b><sup>19</sup>F NMR (376 MHz, CDCl<sub>3</sub>)</b>	δ = -74.82 ppm
<b>Optical rotation</b>	[α] <sub>D</sub> <sup>20</sup> = -22.4 (c = 1.0, CHCl <sub>3</sub> )
<b>Comment</b>	Spectral data are in accordance with the literature, but the melting point is not.

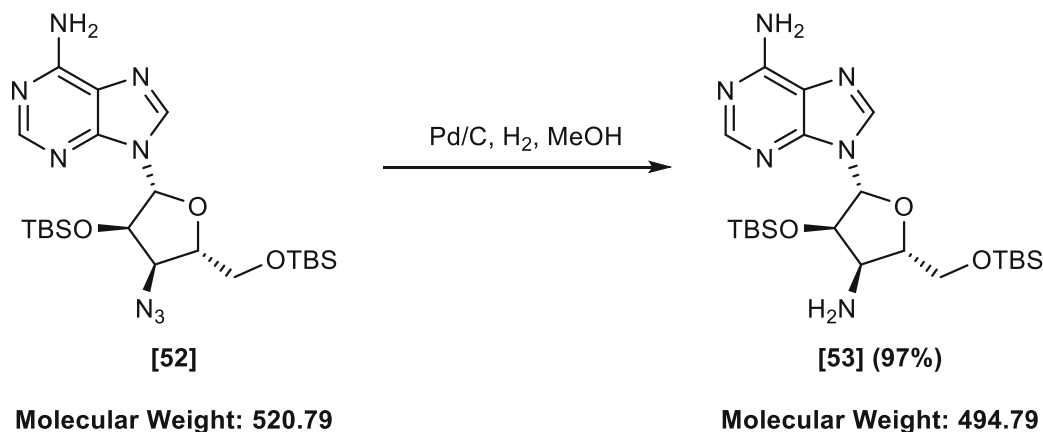
## E IV.9.119-((2*R*,3*R*,4*R*,5*S*)-4-Azido-3-((*tert*-butyldimethylsilyl)oxy)-5-(((*tert*-butyldimethylsilyl)oxy)methyl)tetrahydrofuran-2-yl)-9*H*-purin-6-amine [52]



9-((2*R*,3*R*,4*R*,5*S*)-4-Azido-3-((*tert*-butyldimethylsilyl)oxy)-5-(((*tert*-butyldimethylsilyl)oxy)methyl)tetrahydrofuran-2-yl)-9*H*-purin-6-amine [52] was synthesized from (2*R*,3*S*,4*R*,5*R*)-5-(6-amino-9*H*-purin-9-yl)-4-((*tert*-butyldimethylsilyl)oxy)-2-(((*tert*-butyldimethylsilyl)oxy)methyl)tetrahydrofuran-3-yl trifluoromethanesulfonate [51] in analogy to following literature procedure.<sup>364</sup> An oven-dried 100 mL Schlenk-flask was flushed with argon using standard Schlenk-technique. (2*R*,3*S*,4*R*,5*R*)-5-(6-Amino-9*H*-purin-9-yl)-4-((*tert*-butyldimethylsilyl)oxy)-2-(((*tert*-butyldimethylsilyl)oxy)methyl)tetrahydrofuran-3-yl trifluoromethanesulfonate [51] (3.00 g, 4.78 mmol, 1.00 equiv., scaled up in some instances) and dry DMF (40 mL) were added under an inert atmosphere followed by the addition of NaN<sub>3</sub> (1.55 g, 23.89 mmol, 5.00 equiv.). The resulting slightly yellow reaction mixture was stirred at room temperature until TLC analysis indicated full conversion of the starting material (~5 hours). Subsequently, the mixture was diluted with EtOAc (60 mL), and the organic layer was washed with water (3 times, 40 mL) and brine (40 mL). The organic phase was further dried over MgSO<sub>4</sub>, filtrated, and evaporated to obtain the crude material as a slightly yellow solid (2.48 g, quant.), which was used in the next step without further purification.

<b>Yield</b>	quant. (2.48 g, 4.78 mmol)
<b>Appearance</b>	yellow solid
<b>Melting point</b>	115.0 – 117.0 °C [Lit. <sup>363</sup> : 106– 109 °C]
<b>TLC</b>	R <sub>f</sub> (DCM/MeOH = 9/1) = 0.76
<b>Sum formula</b>	C <sub>22</sub> H <sub>38</sub> N <sub>8</sub> O <sub>4</sub> Si <sub>2</sub>
<b><sup>1</sup>H-NMR (400 MHz, CDCl<sub>3</sub>)</b>	δ = -0.04 (s, 3H, Si-CH <sub>3</sub> ), 0.06 (s, 3H, Si-CH <sub>3</sub> ), 0.14 (s, 3H, Si-CH <sub>3</sub> ), 0.15 (s, 3H, Si-CH <sub>3</sub> ), 0.87 (s, 9H, <i>tert</i> butyl), 0.95 (s, 9H, <i>tert</i> butyl), 3.84 (dd, <i>J</i> = 11.6, 2.7 Hz, 1H, H-5'b), 4.03 – 4.12 (m, 2H, H-3' & H-5'a), 4.22 (dt, <i>J</i> = 5.7, 2.8 Hz, 1H, H-4'), 4.87 (dd, <i>J</i> = 4.9, 3.9 Hz, 1H, H-2'), 5.75 (s, 2H, NH <sub>2</sub> ), 6.02 (d, <i>J</i> = 4.0 Hz, 1H, H-1'), 8.16 (s, 1H, H-8), 8.33 (s, 1H, H-2) ppm.
<b><sup>13</sup>C-NMR (101 MHz, CDCl<sub>3</sub>)</b>	δ = -5.3 (q, Si-CH <sub>3</sub> ), -5.2 (q, Si-CH <sub>3</sub> ), -5.0 (q, Si-CH <sub>3</sub> ), -4.9 (q, Si-CH <sub>3</sub> ), 18.1 (s, Si-C(CH <sub>3</sub> ) <sub>3</sub> ), 18.6 (s, Si-C(CH <sub>3</sub> ) <sub>3</sub> ), 25.7 (q, Si-C(CH <sub>3</sub> ) <sub>3</sub> ), 26.1 (q, Si-C(CH <sub>3</sub> ) <sub>3</sub> ), 61.1 (d, C-3'), 62.6 (t, C-5'), 77.1 (d, C-2'), 82.2 (d, C-4'), 89.1 (d, C-1'), 120.2 (s, C-5), 139.1 (d, C-8), 149.9 (s, C-4), 153.2 (d, C-2), 155.5 (s, C-6) ppm.
<b>Optical rotation</b>	[α] <sub>D</sub> <sup>20</sup> = -3.8 (c = 1.0, CHCl <sub>3</sub> )
<b>Comment</b>	The spectral data are in accordance with the literature.

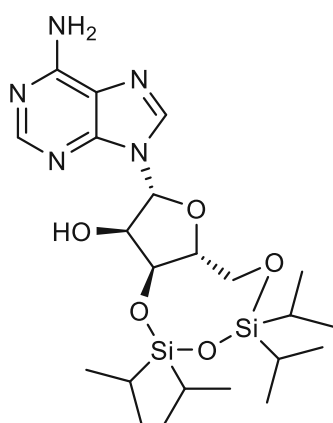
## E IV.9.129-((6*R*,8*R*,9*R*,9*aS*)-9-Amino-2,2,4,4-tetraisopropyltetrahydro-6*H*-furo[3,2-*f*][1,3,5,2,4]trioxadisilocin-8-yl)-9*H*-purin-6-amine [53]



9-((6*R*,8*R*,9*R*,9*aS*)-9-Amino-2,2,4,4-tetraisopropyltetrahydro-6*H*-furo[3,2-*f*][1,3,5,2,4]trioxadisilocin-8-yl)-9*H*-purin-6-amine [53] was synthesized from 9-((2*R*,3*R*,4*R*,5*S*)-4-azido-3-((*tert*-butyldimethylsilyl)oxy)-5-(((*tert*-butyldimethylsilyl)oxy)methyl)tetrahydrofuran-2-yl)-9*H*-purin-6-amine [52] according to following modified literature procedure.<sup>441</sup> A 500 mL three-necked flask equipped with an H<sub>2</sub>-balloon and argon inlet was charged with 9-((2*R*,3*R*,4*R*,5*S*)-4-azido-3-((*tert*-butyldimethylsilyl)oxy)-5-(((*tert*-butyldimethylsilyl)oxy)methyl)tetrahydrofuran-2-yl)-9*H*-purin-6-amine [52] (3.40 g, 6.53 mmol, 1.00 equiv.) and MeOH (150 mL) was further added, and the resulting colorless suspension was stirred until the solid dissolved (5 min). Subsequently, the flask was carefully evacuated and flushed with argon using standard Schlenk-technique, followed by the addition of Pd/C (340 mg). The flask was then shortly evacuated and flushed with hydrogen four times to provide a hydrogen atmosphere, and the reaction mixture was stirred at room temperature overnight. As TLC and UHPLC-MS analysis indicated full conversion of the starting, the reaction mixture was filtrated through a short pad of celite, and the filtrate was further evaporated to obtain the crude material as colorless to off-white solid, which could be used in the following step without further purification. If necessary, the crude product can be purified by flash column chromatography (MeOH in DCM, 2% 5min; 2-5% 15 min; 5-10% 20 min).

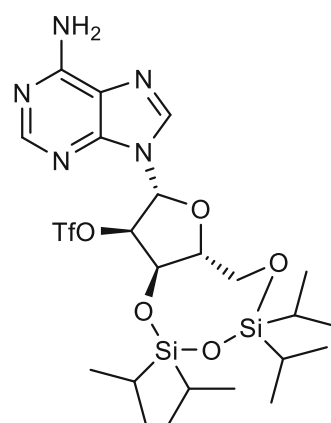
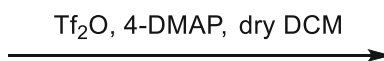
<b>Yield</b>	97% (3.13 g, 12.39 mmol)
<b>Appearance</b>	off-white solid
<b>Melting point</b>	161.0 – 163.0 °C [Lit.: not reported]
<b>TLC</b>	R <sub>f</sub> (CHCl <sub>3</sub> /MeOH = 19/1) = 0.35
<b>Sum formula</b>	C <sub>22</sub> H <sub>42</sub> N <sub>6</sub> O <sub>3</sub> Si <sub>2</sub>
<b><sup>1</sup>H-NMR (400 MHz, DMSO-<i>d</i><sub>6</sub>)</b>	δ = 0.02 (s, 3H, Si-CH <sub>3</sub> ), 0.03 (s, 3H, Si-CH <sub>3</sub> ), 0.07 (s, 6H, 2x Si-CH <sub>3</sub> ), 0.85 (s, 9H, tertbutyl), 0.89 (s, 9H, tertbutyl), 3.51 (t, <i>J</i> = 6.4 Hz, 1H, H-3'), 3.72 – 3.85 (m, 2H, H-4' & H-5'b), 3.92 – 4.02 (m, 1H, H-5'a), 4.40 (dd, <i>J</i> = 5.0, 2.6 Hz, 1H, H-2'), 5.94 (d, <i>J</i> = 2.5 Hz, 1H, H-1'), 7.29 (s, 2H, NH <sub>2</sub> -aromatic), 8.13 (s, 1H, H-2), 8.31 (s, 1H, H-8) ppm.
<b><sup>13</sup>C-NMR (101 MHz, CDCl<sub>3</sub>)</b>	δ = -5.4 (q, 2x Si-CH <sub>3</sub> ), -5.1 (q, Si-CH <sub>3</sub> ), -5.0 (q, Si-CH <sub>3</sub> ), 17.7 (s, Si-C(CH <sub>3</sub> ) <sub>3</sub> ), 18.1 (s, Si-C(CH <sub>3</sub> ) <sub>3</sub> ), 25.6 (q, Si-C(CH <sub>3</sub> ) <sub>3</sub> ), 25.9 (q, Si-C(CH <sub>3</sub> ) <sub>3</sub> ), 52.3 (d, C-3'), 62.5 (t, C-5'), 76.6 (d, C-2'), 84.3 (d, C-4'), 88.3 (d, C-1'), 118.9 (s, C-5), 138.5 (d, C-8), 149.0 (s, C-4), 152.7 (d, C-2), 156.0 (s, C-6) ppm.
<b>Optical rotation</b>	[α] <sub>D</sub> <sup>20</sup> = -24.8 (c = 0.4, MeOH)
<b>Comment</b>	The spectral data are in accordance with the literature.

**E IV.9.13 (6*aR*,8*R*,9*R*,9*aR*)-8-(6-Amino-9*H*-purin-9-yl)-2,2,4,4-tetraisopropyltetrahydro-6*H*-furo[3,2-*f*][1,3,5,2,4]trioxadisilocin-9-yl trifluoromethanesulfonate [64]**



[29]

Molecular Weight: 509.75



[64] (quant., crude)

Molecular Weight: 641.81



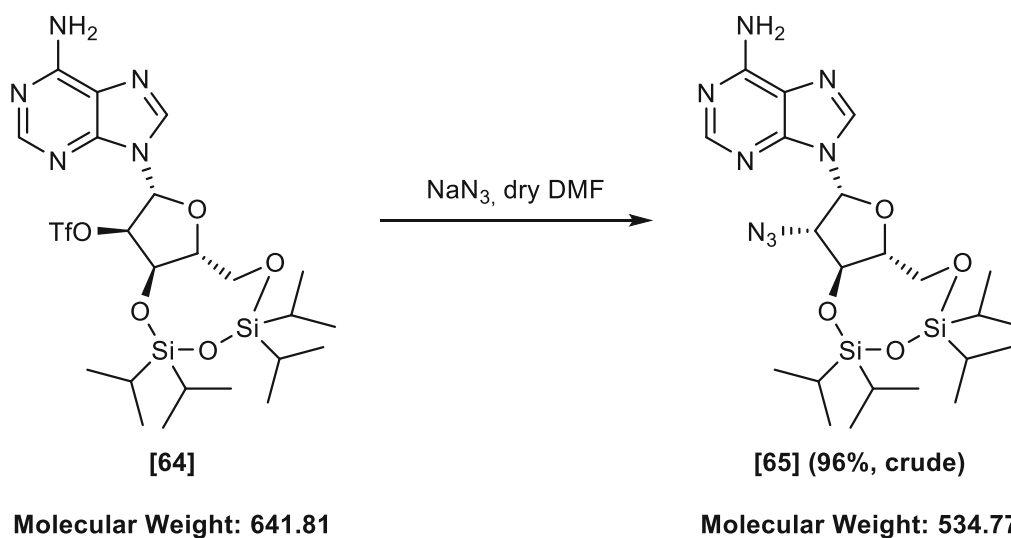
(6*R*,8*R*,9*R*,9*aR*)-8-(6-Amino-9*H*-purin-9-yl)-2,2,4,4-tetraisopropyltetrahydro-6*H*-furo[3,2-*f*][1,3,5,2,4]trioxadisilocin-9-yl trifluoromethanesulfonate [64] was synthesized from (6*R*,8*R*,9*R*,9*aS*)-8-(6-amino-9*H*-purin-9-yl)-2,2,4,4-tetraisopropyltetrahydro-6*H*-furo[3,2-*f*][1,3,5,2,4]trioxadisilocin-9-ol [29] in analogy to following literature procedure.<sup>364</sup> An oven-dried 500 mL three-necked round bottom flask was flushed with argon using standard Schlenk-technique. (6*R*,8*R*,9*R*,9*aS*)-8-(6-Amino-9*H*-purin-9-yl)-2,2,4,4-tetraisopropyltetrahydro-6*H*-furo[3,2-*f*][1,3,5,2,4]trioxadisilocin-9-ol [29] (11.52 g, 22.60 mmol, 1.00 equiv., scaled up in some instances), 4-DMAP (13.80 g, 113.00 mmol, 5.00 equiv.) and dry DCM (350 mL) were added under an inert atmosphere, and the resulting colorless suspension was cooled with an ice/water bath with stirring. Tf<sub>2</sub>O (7.60 mL, 45.20 mmol, 2.00 equiv.) was added via syringe in two portions, whereby the color changed to an intense yellow, and the reaction mixture was stirred at 0 °C. The reaction was allowed to proceed at this temperature with continuous stirring and frequently monitored by TLC, and upon completion (30 min), the reaction mixture (yellow suspension) was portioned between ice-cold 1% aq. AcOH solution (200 mL) and DCM (300 mL), and the aqueous phase was extracted with DCM (3 times, 200 mL). The combined organic layers were further washed with saturated aq. NaHCO<sub>3</sub> (250 mL) and brine (250 mL), dried over MgSO<sub>4</sub>, filtrated, and evaporated under reduced pressure to obtain the crude compound as a slightly yellow solid (14.50 g, quant.), which was used in the following step without further purification.

<b>Yield</b>	quant. (14.50 g, 22.60 mmol)
<b>Appearance</b>	colorless to pale yellow solid
<b>Melting point</b>	144.0 – 146.0 °C [Lit.: not reported]
<b>TLC</b>	R <sub>f</sub> (CHCl <sub>3</sub> /MeOH = 97/3) = 0.40
<b>Sum formula</b>	C <sub>23</sub> H <sub>38</sub> F <sub>3</sub> N <sub>5</sub> O <sub>7</sub> SSi <sub>2</sub>
<b><sup>1</sup>H-NMR (400 MHz, DMSO-<i>d</i><sub>6</sub>)</b>	δ = 0.97 – 1.38 (m, 28H, 4x isopropyl), 3.83 – 4.20 (m, 3H, H-4' & H-5'a & H-5'b), 5.35 (dd, <i>J</i> = 9.0, 5.0 Hz, 1H, H-3'), 6.05 (d, <i>J</i> = 4.9 Hz, 1H, H-2'), 6.45 (s, 1H, H-1'), 7.51 (s, 2H, NH <sub>2</sub> ), 8.04 (s, 1H, H-8), 8.26 (s, 1H, H-2) ppm.
<b><sup>13</sup>C-NMR (101 MHz, DMSO-<i>d</i><sub>6</sub>)</b>	δ = 12.1 (d, Si-CH(CH <sub>3</sub> ) <sub>2</sub> ), 12.3 (d, Si-CH(CH <sub>3</sub> ) <sub>2</sub> ), 12.3 (d, Si-CH(CH <sub>3</sub> ) <sub>2</sub> ), 12.6 (d, Si-CH(CH <sub>3</sub> ) <sub>2</sub> ), 16.6 (q, Si-CH(CH <sub>3</sub> ) <sub>2</sub> ), 16.6 (q, Si-CH(CH <sub>3</sub> ) <sub>2</sub> ), 16.6 (q, 2x Si-CH(CH <sub>3</sub> ) <sub>2</sub> ), 17.0 (q, Si-CH(CH <sub>3</sub> ) <sub>2</sub> ), 17.0 (q, Si-CH(CH <sub>3</sub> ) <sub>2</sub> ), 17.1 (q, Si-CH(CH <sub>3</sub> ) <sub>2</sub> ), 17.2 (q, Si-CH(CH <sub>3</sub> ) <sub>2</sub> ), 60.4 (t, C-5'), 69.0 (d, C-3'), 80.9 (d, C-4'), 86.1 (d, C-1'), 90.0 (d, C-2'), 118.6 (d, <i>J</i> = 319.4 Hz, CF <sub>3</sub> ), 118.0 (s/q, <sup>1</sup> <i>J</i> <sub>CF</sub> = 319.1 Hz, CF <sub>3</sub> ), 119.7 (s, C-5), 140.0 (d, C-8), 149.0 (s, C-4), 152.9 (d, C-2), 156.5 (s, C-6) ppm.
<b><sup>19</sup>F NMR (376 MHz, DMSO-<i>d</i><sub>6</sub>)</b>	δ = -75.13



Optical rotation	$[\alpha]_{\text{D}}^{20} = -25.4$ ( $c = 1.0$ , $\text{CHCl}_3$ )
Comment	The spectral data are in accordance with the literature.

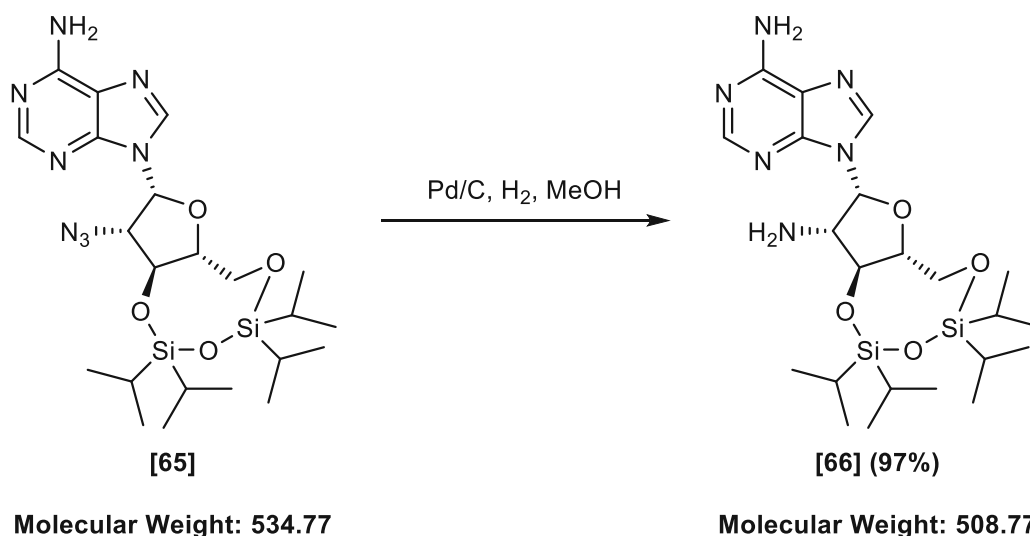
## E IV.9.149-((6*aR*,8*R*,9*S*,9*aS*)-9-Azido-2,2,4,4-tetraisopropyltetrahydro-6*H*-furo[3,2-*f*][1,3,5,2,4]trioxadisilocin-8-yl)-9*H*-purin-6-amine [65]



9-((6*aR*,8*R*,9*S*,9*aS*)-9-Azido-2,2,4,4-tetraisopropyltetrahydro-6*H*-furo[3,2-*f*][1,3,5,2,4]trioxadisilocin-8-yl)-9*H*-purin-6-amine [65] was synthesized from (6*aR*,8*R*,9*R*,9*aR*)-8-(6-amino-9*H*-purin-9-yl)-2,2,4,4-tetraisopropyltetrahydro-6*H*-furo[3,2-*f*][1,3,5,2,4]trioxadisilocin-9-yl trifluoromethanesulfonate [64] in analogy to following literature procedure.<sup>364</sup> An oven-dried 250 mL Schlenk-flask was flushed with argon using standard Schlenk-technique. (6*aR*,8*R*,9*R*,9*aR*)-8-(6-Amino-9*H*-purin-9-yl)-2,2,4,4-tetraisopropyltetrahydro-6*H*-furo[3,2-*f*][1,3,5,2,4]trioxadisilocin-9-yl trifluoromethanesulfonate [64] (12.00 g, 18.70 mmol, 1.00 equiv.) and dry DMF (150 mL) were added under an inert atmosphere followed by the addition of  $\text{NaN}_3$  (6.08 mg, 94.49 mmol, 5.00 equiv.). The resulting slightly yellow reaction mixture was stirred overnight at room temperature. Subsequently, the mixture was diluted with EtOAc (600 mL), and the organic layer was washed with water (3 times, 400 mL) and brine (400 mL). The organic phase was further dried over  $\text{MgSO}_4$ , filtrated, and evaporated to obtain the crude material as a yellow solid (9.63 g, 96%), which was used in the following step without further purification.

<b>Yield</b>	96% (9.63 g, 18.01 mmol)
<b>Appearance</b>	yellow solid
<b>Melting point</b>	120 – 121 °C [Lit.: not reported]
<b>TLC</b>	R <sub>f</sub> (CDCl <sub>3</sub> /MeOH = 95/5) = 0.41
<b>Sum formula</b>	C <sub>22</sub> H <sub>38</sub> N <sub>8</sub> O <sub>4</sub> Si <sub>2</sub>
<b><sup>1</sup>H-NMR (400 MHz, DMSO-<i>d</i><sub>6</sub>)</b>	δ = 0.95 – 1.19 (m, 28H, 4x isopropyl), 3.86 – 4.00 (m, 2H, H-3' & H-5'b), 4.23 (dd, <i>J</i> = 13.0, 5.3 Hz, 1H, H-5'a), 4.88 (s, 2H, H-2' & H-4'), 6.40 (d, <i>J</i> = 6.6 Hz, 1H, H-1'), 7.36 (s, 1H, NH <sub>2</sub> -aromatic), 8.10 (s, 2H, H-2 & H-8) ppm.
<b><sup>13</sup>C-NMR (101 MHz, DMSO-<i>d</i><sub>6</sub>)</b>	δ = 12.5 (d, Si-CH(CH <sub>3</sub> ) <sub>2</sub> ), 12.7 (d, Si-CH(CH <sub>3</sub> ) <sub>2</sub> ), 12.9 (d, Si-CH(CH <sub>3</sub> ) <sub>2</sub> ), 13.3 (d, Si-CH(CH <sub>3</sub> ) <sub>2</sub> ), 17.1 (q, Si-CH(CH <sub>3</sub> ) <sub>2</sub> ), 17.2 (q, Si-CH(CH <sub>3</sub> ) <sub>2</sub> ), 17.2 (q, Si-CH(CH <sub>3</sub> ) <sub>2</sub> ), 17.3 (q, Si-CH(CH <sub>3</sub> ) <sub>2</sub> ), 17.6 (q, 2x Si-CH(CH <sub>3</sub> ) <sub>2</sub> ), 17.6 (q, Si-CH(CH <sub>3</sub> ) <sub>2</sub> ), 17.8 (q, Si-CH(CH <sub>3</sub> ) <sub>2</sub> ), 61.9 (d, C-2'), 67.6 (t, C-5'), 74.4 (d, C-4'), 81.2 (d, C-3'), 81.6 (d, C-1'), 119.5 (s, C-5), 139.4 (d, C-8), 149.6 (s, C-4), 153.0 (d, C-2), 156.6 (s, C-6) ppm.
<b>Optical rotation</b>	[α] <sub>D</sub> <sup>20</sup> = -43.2 (c = 0.45, MeOH)
<b>Comment</b>	The spectral data are in accordance with the literature.

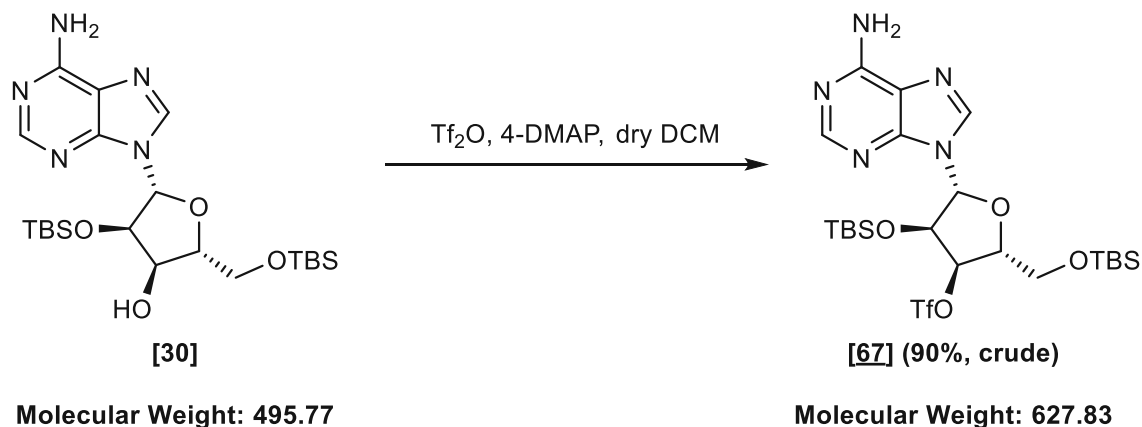
## E IV.9.159-((6aR,8R,9S,9aS)-9-Amino-2,2,4,4-tetraisopropyltetrahydro-6H-furo[3,2-f][1,3,5,2,4]trioxadisilocin-8-yl)-9H-purin-6-amine [66]



9-(((6*R*,8*R*,9*S*,9*aS*)-9-Amino-2,2,4,4-tetraisopropyltetrahydro-6*H*-furo[3,2-*f*][1,3,5,2,4]trioxadisilocin-8-yl)-9*H*-purin-6-amine [66] was synthesized from 9-(((6*R*,8*R*,9*S*,9*aS*)-9-azido-2,2,4,4-tetraisopropyltetrahydro-6*H*-furo[3,2-*f*][1,3,5,2,4]trioxadisilocin-8-yl)-9*H*-purin-6-amine [65] according to following modified literature procedure. A 500 mL three-necked round bottom flask equipped with an H<sub>2</sub>-balloon and argon inlet was charged with 9-(((6*R*,8*R*,9*S*,9*aS*)-9-azido-2,2,4,4-tetraisopropyltetrahydro-6*H*-furo[3,2-*f*][1,3,5,2,4]trioxadisilocin-8-yl)-9*H*-purin-6-amine [65] (7.00 g, 13.09, 1.00 equiv.) and MeOH (300 mL) was further added, and the resulting suspension was stirred until the solid dissolved (5 min). Subsequently, the flask was carefully evacuated and flushed with argon using standard Schlenk-technique, followed by the addition of Pd/C (700 mg). The flask was then shortly evacuated and flushed with hydrogen four times to provide a hydrogen atmosphere, and the reaction mixture was stirred at room temperature overnight. The reaction mixture was filtrated through a short pad of celite, and the filtrate was further evaporated to obtain the crude material as a off-white solid, which could be used in the following step without further purification.

<b>Yield</b>	97% (6.44 g, 12.66 mmol)
<b>Appearance</b>	off-white solid
<b>Melting point</b>	81.0 – 84.0 °C [Lit.: not reported]
<b>TLC</b>	R <sub>f</sub> (CHCl <sub>3</sub> /MeOH = 95/5) = 0.23
<b>Sum formula</b>	C <sub>22</sub> H <sub>40</sub> N <sub>6</sub> O <sub>4</sub> Si <sub>2</sub>
<b><sup>1</sup>H-NMR (400 MHz, DMSO-<i>d</i><sub>6</sub>)</b>	δ = 0.87 – 1.23 (m, 28H, 4x isopropyl), 1.56 (s, 2H, NH <sub>2</sub> -C2'), 3.77 (dd, <i>J</i> = 9.4, 6.8 Hz, 2H, H-2' & H4'), 3.88 (dd, <i>J</i> = 12.3, 3.1 Hz, 1H, H-5'b), 4.06 (dd, <i>J</i> = 12.4, 5.4 Hz, 1H, H-5'a), 4.68 (t, <i>J</i> = 8.3 Hz, 1H, H-3'), 6.12 (d, <i>J</i> = 7.4 Hz, 1H, H-1'), 7.29 (s, 2H, NH <sub>2</sub> (aromatic)), 8.07 (s, 1H, H-2), 8.13 (s, 1H, H-8) ppm.
<b><sup>13</sup>C-NMR (101 MHz, DMSO-<i>d</i><sub>6</sub>)</b>	δ = 12.0 (d, Si-CH(CH <sub>3</sub> ) <sub>2</sub> ), 12.3 (d, Si-CH(CH <sub>3</sub> ) <sub>2</sub> ), 12.5 (d, Si-CH(CH <sub>3</sub> ) <sub>2</sub> ), 12.8 (d, Si-CH(CH <sub>3</sub> ) <sub>2</sub> ), 17.0 (q, Si-CH(CH <sub>3</sub> ) <sub>2</sub> ), 17.0 (q, Si-CH(CH <sub>3</sub> ) <sub>2</sub> ), 17.0 (q, Si-CH(CH <sub>3</sub> ) <sub>2</sub> ), 17.0 (q, Si-CH(CH <sub>3</sub> ) <sub>2</sub> ), 17.3 (q, 2x Si-CH(CH <sub>3</sub> ) <sub>2</sub> ), 17.3 (q, Si-CH(CH <sub>3</sub> ) <sub>2</sub> ), 17.4 (q, Si-CH(CH <sub>3</sub> ) <sub>2</sub> ), 60.3 (d, C-2'), 62.1 (t, C-5'), 76.2 (d, C-3'), 81.4 (d, C-4'), 84.1 (d, C-1'), 119.2 (s, C-5), 140.4 (d, C-8), 149.1 (s, C-4), 152.3 (d, C-2), 156.1 (s, C-6) ppm.
<b>Optical rotation</b>	[α] <sub>D</sub> <sup>20</sup> = -59.2 (c = 0.1, MeOH)
<b>Comment</b>	Spectral data are in accordance with the literature. <sup>444</sup>

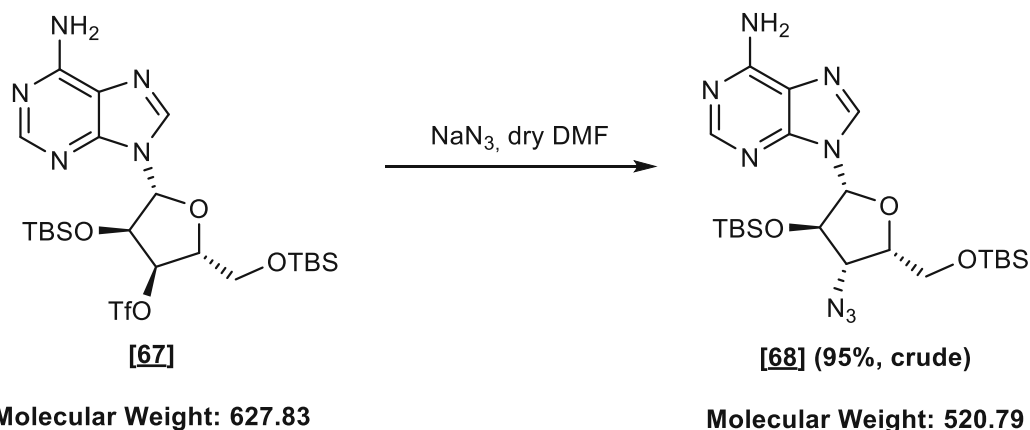
**E IV.9.16 (2*R*,3*R*,4*R*,5*R*)-5-(6-Amino-9*H*-purin-9-yl)-4-((*tert*-butyldimethylsilyl)oxy)-2-(((*tert*-butyldimethylsilyl)oxy)methyl)tetrahydrofuran-3-yl trifluoromethanesulfonate [67]**



(2*R*,3*R*,4*R*,5*R*)-5-(6-Amino-9*H*-purin-9-yl)-4-((*tert*-butyldimethylsilyl)oxy)-2-(((*tert*-butyldimethylsilyl)oxy)methyl)tetrahydrofuran-3-yl trifluoromethanesulfonate [67] was synthesized from (2*R*,3*R*,4*R*,5*R*)-5-(6-amino-9*H*-purin-9-yl)-4-((*tert*-butyldimethylsilyl)oxy)-2-(((*tert*-butyldimethylsilyl)oxy)methyl)tetrahydrofuran-3-ol [30] following a modified literature procedure.<sup>363</sup> An oven-dried 500 mL three-necked round bottom flask was flushed with argon using standard Schlenk-technique. (2*R*,3*R*,4*R*,5*R*)-5-(6-Amino-9*H*-purin-9-yl)-4-((*tert*-butyldimethylsilyl)oxy)-2-(((*tert*-butyldimethylsilyl)oxy)methyl)tetrahydrofuran-3-ol [30] (6.76 g, 13.64 mmol, 1.00 equiv., scaled up in some instances), 4-DMAP (5.00 g, 40.91 mmol, 3.00 equiv.) and dry DCM (200 mL) were added under an inert atmosphere, and the resulting colorless suspension was cooled with an ice/water bath with stirring. Tf<sub>2</sub>O (2.98 mL, 17.73 mmol, 1.30 equiv.) was added via syringe in two portions, whereby the color changed to an intense yellow, and the reaction mixture was stirred at 0 °C. The reaction was allowed to proceed at this temperature with continuous stirring and frequently monitored by TLC, and upon completion (1.5 hours), the reaction mixture (yellow suspension) was portioned between ice-cold 1% aq. AcOH solution (150 mL) and DCM (200 mL), and the aqueous phase was extracted with DCM (3 times, 100 mL). The combined organic layers were further washed with saturated aq. NaHCO<sub>3</sub> (200 mL) and brine (200 mL), dried over MgSO<sub>4</sub>, filtrated, and evaporated under reduced pressure to obtain the crude compound as a slightly yellow solid (7.70 g, 90%), which was used in the following step without further purification.

<b>Yield</b>	90% (7.70 g, 12.26 mmol)
<b>Appearance</b>	colorless to pale yellow solid
<b>Melting point</b>	103 – 104 °C
<b>TLC</b>	R <sub>f</sub> (PE/EE = 1/1) = 0.33
<b>Sum formula</b>	C <sub>23</sub> H <sub>40</sub> F <sub>3</sub> N <sub>5</sub> O <sub>6</sub> SSi <sub>2</sub>
<b>HR-MS</b>	[M+H] <sup>+</sup> : calculated: 628.2263 Da, found: 628.2279 Da, difference: 2.7 ppm
<b><sup>1</sup>H NMR (400 MHz, CDCl<sub>3</sub>)</b>	δ = -0.40 (s, 3H, Si-CH <sub>3</sub> ), -0.02 (s, 3H, Si-CH <sub>3</sub> ), 0.14 (s, 3H, Si-CH <sub>3</sub> ), 0.16 (s, 3H, Si-CH <sub>3</sub> ), 0.75 (s, 9H, tertbutyl), 0.96 (s, 9H, tertbutyl), 3.83 (dd, <i>J</i> = 11.4, 3.3 Hz, 1H, H-5'b), 4.06 (dd, <i>J</i> = 11.3, 4.7 Hz, 1H, H-5'a), 4.44 (ddd, <i>J</i> = 4.7, 3.3, 1.5 Hz, 1H, H-4'), 5.17 (dd, <i>J</i> = 7.0, 4.7 Hz, 1H, H-2'), 5.32 (dd, <i>J</i> = 4.8, 1.4 Hz, 1H, H-3'), 5.86 (s, 2H, NH <sub>2</sub> -aromatic), 6.04 (d, <i>J</i> = 7.1 Hz, 1H, H-1'), 8.02 (s, 1H, H-8), 8.35 (s, 1H, H-2) ppm.
<b><sup>13</sup>C-NMR (101 MHz, CDCl<sub>3</sub>)</b>	δ = -5.6 (q, Si-CH <sub>3</sub> ), -5.6 (q, Si-CH <sub>3</sub> ), -5.5 (q, Si-CH <sub>3</sub> ), -5.1 (q, Si-CH <sub>3</sub> ), 17.7 (s, Si-C-(CH <sub>3</sub> ) <sub>3</sub> ), 18.3 (s, Si-C-(CH <sub>3</sub> ) <sub>3</sub> ), 25.3 (q, Si-C-(CH <sub>3</sub> ) <sub>3</sub> ), 25.9 (q, Si-C-(CH <sub>3</sub> ) <sub>3</sub> ), 62.4 (t, C-5'), 73.4 (d, C-2'), 82.5 (d, C-4'), 87.0 (d, C-3'), 87.4 (d, C-1'), 117.0 (q, CF <sub>3</sub> ), 120.1 (s, C-5), 139.3 (d, C-8), 150.1 (s, C-4), 153.1 (d, C-2), 155.5 (s, C-6) ppm.
<b><sup>19</sup>F NMR (376 MHz, CDCl<sub>3</sub>)</b>	δ = -75.45 ppm.
<b>Optical rotation</b>	[α] <sub>D</sub> <sup>20</sup> = -34.2 (c = 0.5, MeOH)

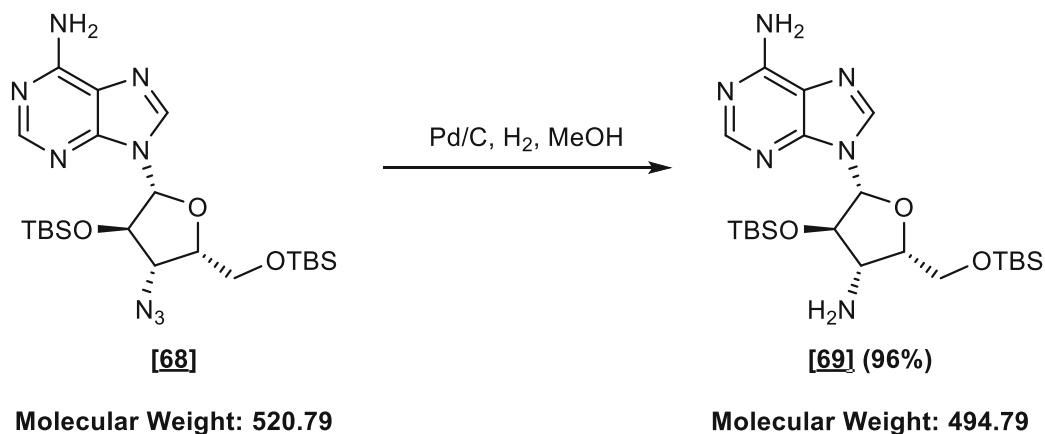
## E IV.9.179-((2*R*,3*R*,4*S*,5*S*)-4-Azido-3-((*tert*-butyldimethylsilyl)oxy)-5-(((*tert*-butyldimethylsilyl)oxy)methyl)tetrahydrofuran-2-yl)-9*H*-purin-6-amine [68]



9-((2*R*,3*R*,4*S*,5*S*)-4-Azido-3-((*tert*-butyldimethylsilyl)oxy)-5-(((*tert*-butyldimethylsilyl)oxy)methyl)tetrahydrofuran-2-yl)-9*H*-purin-6-amine [68] was synthesized from (2*R*,3*R*,4*R*,5*R*)-5-(6-amino-9*H*-purin-9-yl)-4-((*tert*-butyldimethylsilyl)oxy)-2-(((*tert*-butyldimethylsilyl)oxy)methyl)tetrahydrofuran-3-yl trifluoromethanesulfonate [67] in analogy to following literature procedure. An oven-dried 250 mL Schlenk-flask was flushed with argon using standard Schlenk-technique. (2*R*,3*R*,4*R*,5*R*)-5-(6-Amino-9*H*-purin-9-yl)-4-((*tert*-butyldimethylsilyl)oxy)-2-(((*tert*-butyldimethylsilyl)oxy)methyl)tetrahydrofuran-3-yl trifluoromethanesulfonate [67] (7.50 g, 11.95 mmol, 1.00 equiv., scaled up in some instances) and dry DMF (150 mL) were added under an inert atmosphere followed by the addition of NaN<sub>3</sub> (3.88 g, 59.73 mmol, 5.00 equiv.). The resulting slightly yellow reaction mixture was stirred at room temperature overnight. Subsequently, the mixture was diluted with EtOAc (400 mL), and the organic layer was washed with water (3 times, 300 mL) and brine (300 mL). The organic phase was further dried over MgSO<sub>4</sub>, filtrated, and evaporated to obtain the crude material as a beige solid (5.90 g, 95%), which was used in the following step without further purification.

<b>Yield</b>	95% (5.90 g, 11.33 mmol)
<b>Appearance</b>	beige solid
<b>Melting point</b>	117.0 – 118.0 °C
<b>TLC</b>	R <sub>f</sub> (CHCl <sub>3</sub> /MeOH = 19/1) = 0.86
<b>Sum formula</b>	C <sub>22</sub> H <sub>40</sub> N <sub>8</sub> O <sub>3</sub> Si <sub>2</sub>
<b>HR-MS</b>	[M+H] <sup>+</sup> : calculated: 521.2835 Da, found: 521.2853 Da, difference: 3.5 ppm
<b><sup>1</sup>H NMR (400 MHz, CDCl<sub>3</sub>)</b>	δ = -0.04 (s, 3H, Si-CH <sub>3</sub> ), 0.08 (s, 3H, Si-CH <sub>3</sub> ), 0.14 (s, 3H, Si-CH <sub>3</sub> ), 0.15 (s, 3H, Si-CH <sub>3</sub> ), 0.86 (s, 9H, tertbutyl), 0.94 (s, 9H, tertbutyl), 3.96 (d, <i>J</i> = 5.4 Hz, 2H, H-5'), 4.09 (dd, <i>J</i> = 5.3, 3.5 Hz, 1H, H-3'), 4.45 (q, <i>J</i> = 5.3 Hz, 1H, H-4'), 4.63 (t, <i>J</i> = 3.3 Hz, 1H, H-2'), 5.95 (s, 2H, NH <sub>2</sub> -aromatic), 6.02 (d, <i>J</i> = 3.0 Hz, 1H, H-1'), 8.16 (s, 1H, H-8), 8.33 (s, 1H, H-2) ppm.
<b><sup>13</sup>C-NMR (101 MHz, CDCl<sub>3</sub>)</b>	δ = -5.3 (q, Si-CH <sub>3</sub> ), -5.2 (q, Si-CH <sub>3</sub> ), -5.0 (q, Si-CH <sub>3</sub> ), -4.8 (q, Si-CH <sub>3</sub> ), 18.0 (s, Si-C(CH <sub>3</sub> ) <sub>3</sub> ), 18.5 (s, Si-C(CH <sub>3</sub> ) <sub>3</sub> ), 25.7 (q, Si-C(CH <sub>3</sub> ) <sub>3</sub> ), 26.1 (q, Si-C(CH <sub>3</sub> ) <sub>3</sub> ), 61.7 (t, C-5'), 67.9 (d, C-3'), 80.4 (d, C-2'), 80.9 (d, C-4'), 89.6 (d, C-1'), 119.7 (s, C-5), 139.1 (d, C-8), 145.0 (s, C-4), 153.1 (d, C-2), 155.4 (s, C-6) ppm.
<b>Optical rotation</b>	[α] <sub>D</sub> <sup>20</sup> = -51.8 (c = 1.0, MeOH)

**E IV.9.189-((2*R*,3*R*,4*S*,5*S*)-4-Amino-3-((*tert*-butyldimethylsilyl)oxy)-5-(((*tert*-butyldimethylsilyl)oxy)methyl)tetrahydrofuran-2-yl)-9*H*-purin-6-amine [69]**



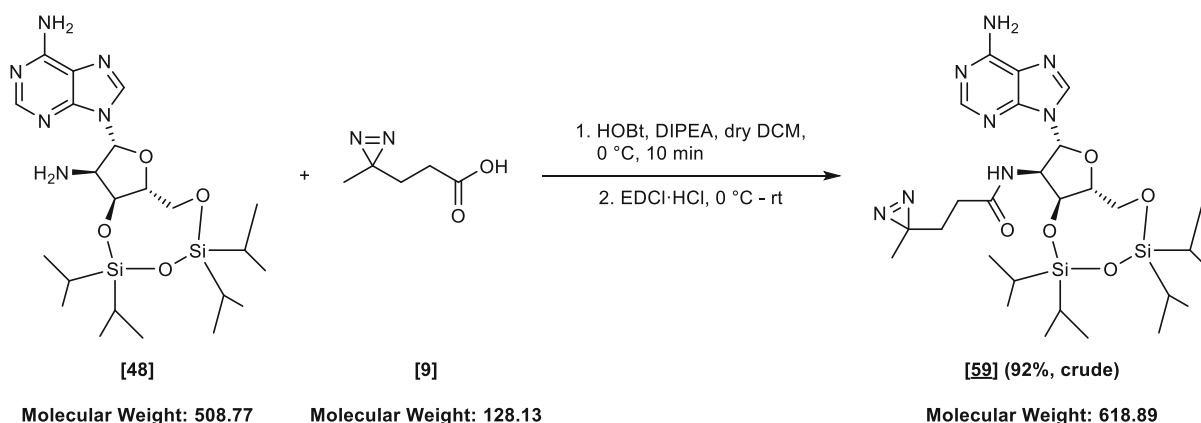
9-((2*R*,3*R*,4*S*,5*S*)-4-Amino-3-((*tert*-butyldimethylsilyl)oxy)-5-(((*tert*-butyldimethylsilyl)oxy)methyl)tetrahydrofuran-2-yl)-9*H*-purin-6-amine [69] was synthesized from 9-((2*R*,3*R*,4*S*,5*S*)-4-azido-3-((*tert*-butyldimethylsilyl)oxy)-5-(((*tert*-butyldimethylsilyl)oxy)methyl)tetrahydrofuran-2-yl)-9*H*-purin-6-amine [68] according to following modified literature procedure.<sup>441</sup> A 500 mL three-necked round bottom flask equipped with an H<sub>2</sub>-balloon and argon inlet was charged with 9-((2*R*,3*R*,4*S*,5*S*)-4-azido-3-((*tert*-butyldimethylsilyl)oxy)-5-(((*tert*-butyldimethylsilyl)oxy)methyl)tetrahydrofuran-2-yl)-9*H*-purin-6-amine [68] (5.50 g, 10.56 mmol, 1.00 equiv.) and MeOH (250 mL) was further added, and the resulting suspension was stirred until the solid dissolved (5 min). Subsequently, the flask was carefully evacuated and flushed with argon using standard Schlenk-technique, followed by the addition of Pd/C (550 mg). The flask was then shortly evacuated and flushed with hydrogen four times to provide a hydrogen atmosphere, and the reaction mixture was stirred at room temperature. The reaction progress was monitored by TLC and UHPLC-MS analysis, and at complete consumption of the starting material, the reaction mixture was filtrated through a short pad of celite. The filtrate was evaporated to obtain the crude material as an off-white solid, which could be used in the following step without further purification.

<b>Yield</b>	96% (5.01 g, 10.13 mmol)
<b>Appearance</b>	off-white solid
<b>Melting point</b>	178 – 180.0 °C



<b>TLC</b>	$R_f$ (CHCl <sub>3</sub> /MeOH = 19/1) = 0.23
<b>Sum formula</b>	C <sub>22</sub> H <sub>42</sub> N <sub>6</sub> O <sub>3</sub> Si <sub>2</sub>
<b>HR-MS</b>	[M+H] <sup>+</sup> : calculated: 495.2930 Da, found: 495.2943 Da, difference: 2.7 ppm
<b><sup>1</sup>H-NMR (400 MHz, DMSO-<i>d</i><sub>6</sub>)</b>	$\delta$ = -0.24 (s, 3H, Si-CH <sub>3</sub> ), -0.04 (s, 3H, Si-CH <sub>3</sub> ), 0.08 (s, 3H, Si-CH <sub>3</sub> ), 0.09 (s, 3H, Si-CH <sub>3</sub> ), 0.74 (s, 9H, tertbutyl), 0.90 (s, 9H, tertbutyl), 3.45 (t, $J$ = 6.0 Hz, 1H, H-3'), 3.90 (d, $J$ = 4.1 Hz, 2H, H-5'a & H-5'b), 4.16 (dt, $J$ = 6.7, 4.2, Hz, 1H, H-4'), 4.38 (t, $J$ = 5.1 Hz, 1H, H-2'), 5.82 (d, $J$ = 4.7 Hz, 1H, H-1'), 7.29 (s, 2H, NH <sub>2</sub> -aromatic), 8.14 (s, 1H, H-2), 8.37 (s, 1H, H-8) ppm.
<b><sup>13</sup>C-NMR (101 MHz, DMSO-<i>d</i><sub>6</sub>)</b>	$\delta$ = -4.8 (q, Si-CH <sub>3</sub> ), -4.8 (q, Si-CH <sub>3</sub> ), -4.7 (q, Si-CH <sub>3</sub> ), -4.1 (q, Si-CH <sub>3</sub> ), 18.1 (s, Si-C(CH <sub>3</sub> ) <sub>3</sub> ), 18.5 (s, Si-C(CH <sub>3</sub> ) <sub>3</sub> ), 26.1 (q, Si-C(CH <sub>3</sub> ) <sub>3</sub> ), 26.4 (q, Si-C(CH <sub>3</sub> ) <sub>3</sub> ), 59.4 (d, C-3'), 63.3 (t, C-5'), 81.8 (d, C-4'), 82.8 (d, C-2'), 88.0 (d, C-1'), 119.2 (s, C-5'), 139.5 (d, C-8'), 150.1 (s, C-4'), 153.3 (d, C-2'), 156.6 (s, C-6) ppm.
<b>Optical rotation</b>	$[\alpha]_D^{20}$ = -11.2 (c = 1.0, CHCl <sub>3</sub> )

### E IV.9.19 *N*-((6*aR*,8*R*,9*R*,9*aR*)-8-(6-Amino-9*H*-purin-9-yl)-2,2,4,4-tetraisopropyltetrahydro-6*H*-furo[3,2-*f*][1,3,5,2,4]trioxadisilocin-9-yl 3-(3-methyl-3*H*-diazirin-3-yl)propanoate [59]



*N*-((6*aR*,8*R*,9*R*,9*aR*)-8-(6-Amino-9*H*-purin-9-yl)-2,2,4,4-tetraisopropyltetrahydro-6*H*-furo[3,2-*f*][1,3,5,2,4]trioxadisilocin-9-yl 3-(3-methyl-3*H*-diazirin-3-yl)propanoate [59] was synthesized according to general procedure B using protected adenosine [48] (1.40 g, 2.75 mmol, 1.00 equiv.) and diazirine [9] (881 mg, 6.88 mmol, 2.50 equiv.). The crude product was used in the next step directly without purification.



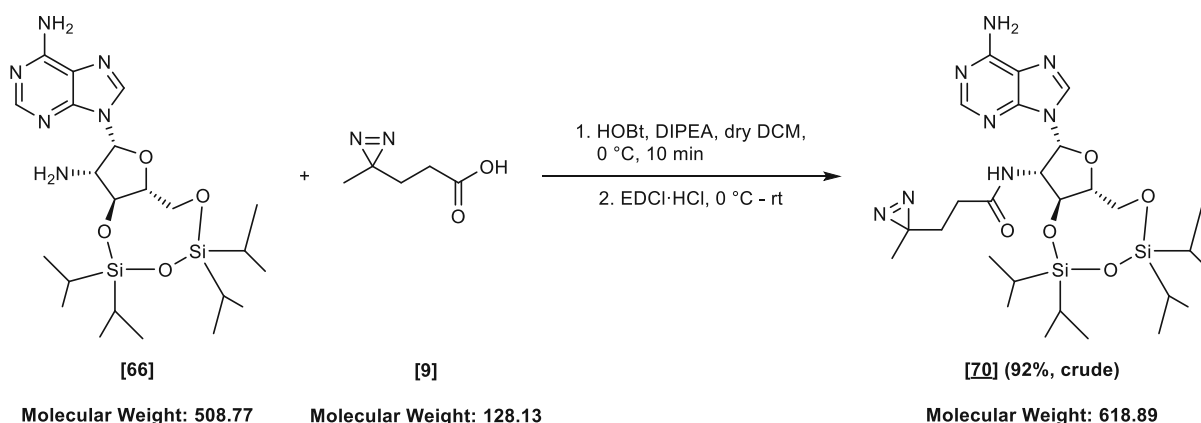


(m, 2H, CH<sub>2</sub>-CH<sub>2</sub>-CONH-), 3.90 – 4.03 (m, 3H, H-4' & H-5'a & H-5'b), 4.98 (dd,  $J = 7.7, 5.7$  Hz, 1H, H-3'), 5.10 (ddd,  $J = 8.9, 7.6, 4.4$  Hz, 1H, H-2'), 5.86 (d,  $J = 4.4$  Hz, 1H, H-1'), 7.32 (s, 2H, NH<sub>2</sub>-C6), 8.07 (s, 1H, H-2), 8.29 (d,  $J = 9.1$  Hz, 1H, NH (amide)), 8.30 (s, 1H, H-8) ppm.

<sup>13</sup>C-NMR (101 MHz, DMSO-*d*<sub>6</sub>)  $\delta = 12.2$  (d, Si-CH(CH<sub>3</sub>)<sub>3</sub>), 12.2 (d, Si-CH(CH<sub>3</sub>)<sub>3</sub>), 12.5 (d, Si-CH(CH<sub>3</sub>)<sub>3</sub>), 12.7 (d, Si-CH(CH<sub>3</sub>)<sub>3</sub>), 16.8 (q, Si-CH(CH<sub>3</sub>)<sub>3</sub>), 16.8 (q, Si-CH(CH<sub>3</sub>)<sub>3</sub>), 17.2 (q, Si-CH(CH<sub>3</sub>)<sub>3</sub>), 17.2 (q, Si-CH(CH<sub>3</sub>)<sub>3</sub>), 17.4 (q, Si-CH(CH<sub>3</sub>)<sub>3</sub>), 19.1 (q, CH<sub>3</sub> (aliphatic linker)), 25.7 (s, diazirine), 29.6 (t, -CH<sub>2</sub>-CH<sub>2</sub>-CONH-), 29.9 (t, -CH<sub>2</sub>-CH<sub>2</sub>-CONH-), 54.2 (d, C-2'), 62.4 (t, C-5'), 70.0 (d, C-3'), 82.9 (d, C-4'), 86.8 (d, C-1'), 119.1 (s, C-5), 140.0 (d, C-8), 148.9 (s, C-4), 152.5 (d, C-2), 156.1 (s, C-6), 171.1 (s, carbonyl (amide)) ppm.

**Optical rotation**  $[\alpha]_D^{20} = -39.5$  ( $c = 0.5$ , MeOH)

## E IV.9.20 *N*-((6*aR*,8*R*,9*S*,9*aS*)-8-(6-Amino-9*H*-purin-9-yl)-2,2,4,4-tetraisopropyltetrahydro-6*H*-furo[3,2-*f*][1,3,5,2,4]trioxadisilocin-9-yl)-3-(3-methyl-3*H*-diazirin-3-yl)propanamide [70]



*N*-((6*aR*,8*R*,9*S*,9*aS*)-8-(6-Amino-9*H*-purin-9-yl)-2,2,4,4-tetraisopropyltetrahydro-6*H*-furo[3,2-*f*][1,3,5,2,4]trioxadisilocin-9-yl)-3-(3-methyl-3*H*-diazirin-3-yl)propanamide [70] was synthesized according to general procedure B using protected adenosine [66] (1.03 g, 2.02

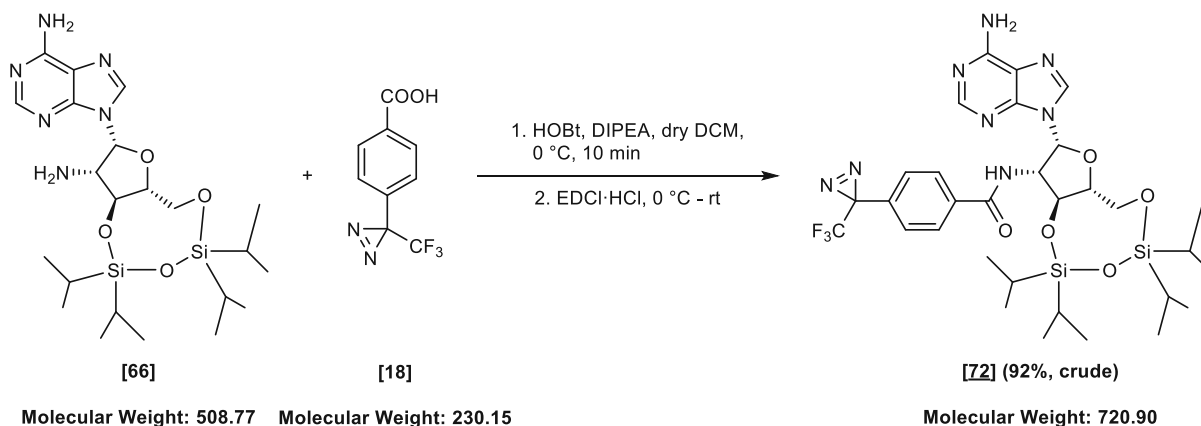
mmol, 1.00 equiv.) and diazirine [9] (649 mg, 5.06 mmol, 2.50 equiv.). The crude product was used in the next step directly without further purification.

<b>Yield</b>	82% (1.00 g, 1.61 mmol)
<b>Appearance</b>	light brown solid
<b>Melting point</b>	not determined
<b>TLC</b>	$R_f$ (CHCl <sub>3</sub> /MeOH = 9/1) = 0.36
<b>Sum formula</b>	C <sub>27</sub> H <sub>46</sub> N <sub>8</sub> O <sub>4</sub> Si <sub>2</sub>
<b>HR-MS</b>	[M+Na] <sup>+</sup> : calculated: 641.3022 Da, found: 641.3018 Da, difference: -0.5 ppm

**<sup>1</sup>H-NMR (400 MHz, DMSO-*d*<sub>6</sub>)**  $\delta$  = 0.81 (s, 3H, CH<sub>3</sub> (aliphatic linker)), 0.98 – 1.03 (m, 12H, isopropyl), 1.07 (s, 8H, isopropyl), 1.15 (dd,  $J$  = 6.7, 3.3 Hz, 8H, isopropyl), 1.24 – 1.36 (m, 1H, -CH<sub>2</sub>-CH<sub>2</sub>-CONH-), 1.53 – 1.71 (m, 2H, -CH<sub>2</sub>-CH<sub>2</sub>-CONH-), 3.90 – 4.00 (m, 2H, H-4' & H-5'b), 4.13 – 4.20 (m, 1H, H-5'a), 4.54 (dd,  $J$  = 9.9, 8.3 Hz, 1H, H-3'), 4.89 (td,  $J$  = 9.5, 9.4, 7.0 Hz, 1H, H-2'), 6.20 (d,  $J$  = 7.0 Hz, 1H, H-1'), 7.28 (s, 2H, NH<sub>2</sub>-C6), 7.84 (d,  $J$  = 9.2 Hz, 1H, NH (amide)), 8.05 (s, 2H, H-2 & H-8) ppm.

**<sup>13</sup>C-NMR (101 MHz, DMSO-*d*<sub>6</sub>)**  $\delta$  = 11.7 (d, Si-CH(CH<sub>3</sub>)<sub>3</sub>), 12.4 (d, 2x Si-CH(CH<sub>3</sub>)<sub>3</sub>), 12.6 (d, Si-CH(CH<sub>3</sub>)<sub>3</sub>), 16.8 (q, Si-CH(CH<sub>3</sub>)<sub>3</sub>), 16.9 (q, Si-CH(CH<sub>3</sub>)<sub>3</sub>), 16.9 (q, Si-CH(CH<sub>3</sub>)<sub>3</sub>), 17.0 (q, Si-CH(CH<sub>3</sub>)<sub>3</sub>), 17.2 (q, Si-CH(CH<sub>3</sub>)<sub>3</sub>), 17.3 (q, Si-CH(CH<sub>3</sub>)<sub>3</sub>), 17.4 (q, Si-CH(CH<sub>3</sub>)<sub>3</sub>), 17.4 (q, Si-CH(CH<sub>3</sub>)<sub>3</sub>), 19.0 (q, CH<sub>3</sub> (aliphatic linker)), 25.5 (s, diazirine), 29.4 (t, -CH<sub>2</sub>-CH<sub>2</sub>-CONH-), 29.5 (t, -CH<sub>2</sub>-CH<sub>2</sub>-CONH-), 56.4 (d, C-2'), 60.6 (t, C-5'), 70.4 (d, C-3'), 80.9 (d, C-4'), 81.5 (d, C-1'), 118.8 (s, C-5), 138.6 (d, C-8) 149.3 (s, C-4), 152.4 (d, C-2), 156.0 (s, C-6), 171.1 (s, carbonyl (amide)) ppm.

## E IV.9.21 *N*-((6*aR*,8*R*,9*S*,9*aS*)-8-(6-Amino-9*H*-purin-9-yl)-2,2,4,4-tetraisopropyltetrahydro-6*H*-furo[3,2-*f*][1,3,5,2,4]trioxadisilocin-9-yl)-4-(3-(trifluoromethyl)-3*H*-diazirin-3-yl)benzamide [72]



*N*-((6*aR*,8*R*,9*S*,9*aS*)-8-(6-Amino-9*H*-purin-9-yl)-2,2,4,4-tetraisopropyltetrahydro-6*H*-furo[3,2-*f*][1,3,5,2,4]trioxadisilocin-9-yl)-4-(3-(trifluoromethyl)-3*H*-diazirin-3-yl)benzamide [72] was synthesized according to general procedure B using protected adenosine [66] (1.41 g, 2.77 mmol, 1.00 equiv.) and diazirine [18] (700 mg, 3.04 mmol, 1.10 equiv.). The crude product was used in the next step directly without purification.

<b>Yield</b>	92% (1.83 g, 2.55 mmol)
<b>Appearance</b>	light brown solid
<b>Melting point</b>	not determined
<b>TLC</b>	$R_f$ (CHCl <sub>3</sub> /MeOH = 9/1) = 0.46
<b>Sum formula</b>	C <sub>31</sub> H <sub>43</sub> F <sub>3</sub> N <sub>8</sub> O <sub>5</sub> Si <sub>2</sub>
<b>HR-MS</b>	[M+Na] <sup>+</sup> : calculated: 743.2739 Da, found: 743.2734 Da, difference: -0.7 ppm

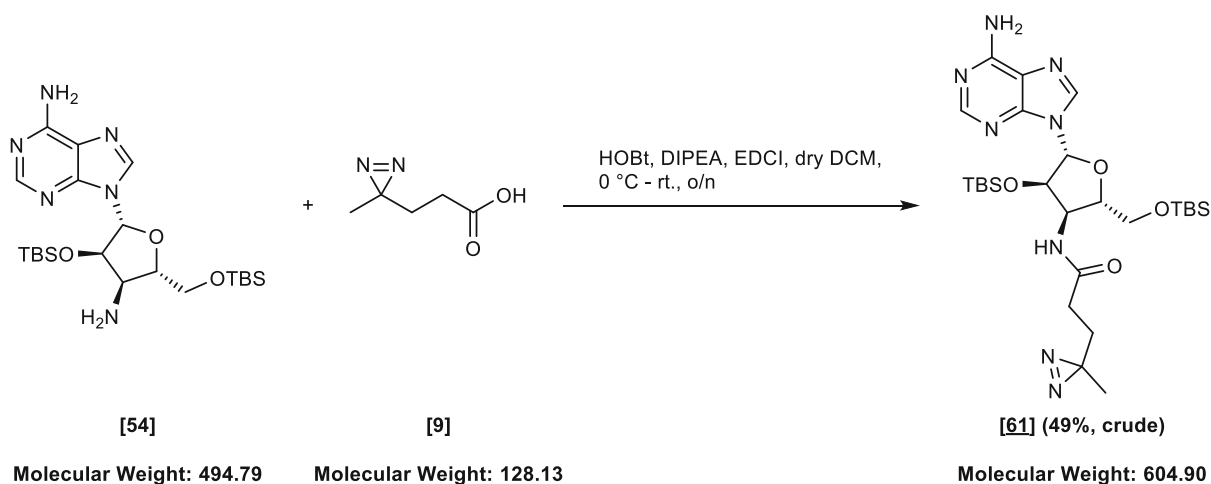
<sup>1</sup>H-NMR (400 MHz, DMSO-*d*<sub>6</sub>)  $\delta$  = 0.95 – 1.17 (m, 28H, 4x isopropyl), 3.98 – 4.10 (m, 2H, H-4' & H-5'b), 4.16 (dd,  $J$  = 13.9, 3.5 Hz, 1H, H-5'a), 4.69 (dd,  $J$  = 9.9, 8.2 Hz, 1H, H-3'), 5.13 (td,  $J$  = 9.5, 9.5, 6.9 Hz, 1H, H-2'), 6.33 (d,  $J$  = 6.9 Hz, 1H, H-1'), 7.26 (d,  $J$  = 8.2 Hz, 4H, NH<sub>2</sub>-C6 & H-3ar & H-5ar), 7.42 (d,  $J$  = 8.5 Hz, 2H, H-2ar & H-6ar), 8.00 (s, 1H, H-2), 8.12 (s, 1H, H-8), 8.52 (d,  $J$  = 9.1 Hz, 1H, NH (amide)) ppm.

$^{13}\text{C-NMR}$  (101 MHz,  $\text{DMSO-}d_6$ )  $\delta$  = 12.3 (d, Si- $\underline{\text{C}}\text{H}(\text{CH}_3)_3$ ), 13.0 (d, Si- $\underline{\text{C}}\text{H}(\text{CH}_3)_3$ ), 13.1 (d, Si- $\underline{\text{C}}\text{H}(\text{CH}_3)_3$ ), 13.2 (d, Si- $\underline{\text{C}}\text{H}(\text{CH}_3)_3$ ), 17.4 (q, Si- $\underline{\text{C}}\text{H}(\text{CH}_3)_3$ ), 17.4 (q, Si- $\underline{\text{C}}\text{H}(\text{CH}_3)_3$ ), 17.6 (q, Si- $\underline{\text{C}}\text{H}(\text{CH}_3)_3$ ), 17.6 (q, Si- $\underline{\text{C}}\text{H}(\text{CH}_3)_3$ ), 17.9 (q, Si- $\underline{\text{C}}\text{H}(\text{CH}_3)_3$ ), 17.9 (q, Si- $\underline{\text{C}}\text{H}(\text{CH}_3)_3$ ), 18.1 (q, Si- $\underline{\text{C}}\text{H}(\text{CH}_3)_3$ ), 18.1 (q, Si- $\underline{\text{C}}\text{H}(\text{CH}_3)_3$ ), 28.4 (s, diazirine), 57.8 (d, C-2'), 61.2 (t, C-5'), 70.6 (d, C-3'), 81.7 (d, C-4'), 82.2 (d, C-1'), 119.3 (s, C-5), 126.8 (d, C-3ar & C-5ar), 128.5 (d, C-2ar & C-6ar), 130.7 (d, C-8), 136.8 (s, C-1ar), 139.4 (s, C-4ar), 149.8 (s, C-4), 153.1 (d, C-2), 156.5 (s, C-6), 167.2 (s, carbonyl (amide)) ppm.

$^{19}\text{F}$  NMR (376 MHz,  $\text{DMSO-}d_6$ )  $\delta$  = -64.52 ppm.

**Comment** The  $\text{CF}_3$  signal was not detected in the  $^{13}\text{C-NMR}$  spectrum.

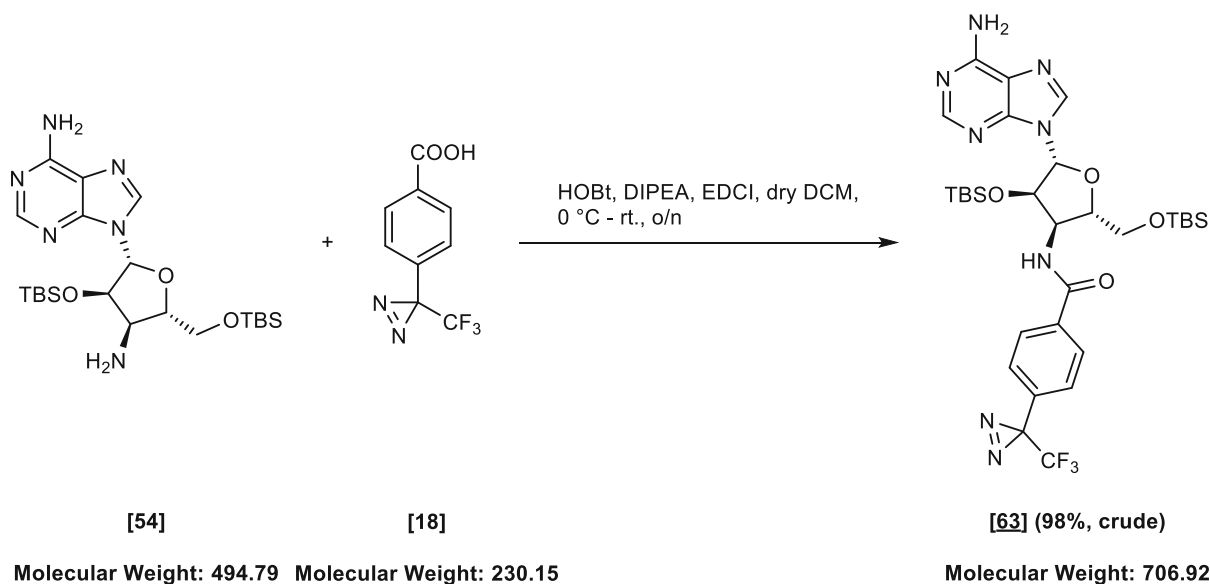
## E IV.9.22 *N*-((2*S*,3*R*,4*R*,5*R*)-5-(6-Amino-9*H*-purin-9-yl)-4-((*tert*-butyldimethylsilyl)oxy)-2-(((*tert*-butyldimethylsilyl)oxy)methyl)tetrahydrofuran-3-yl)-3-(3-methyl-3*H*-diazirin-3-yl)propanamide [61]



*N*-((2*S*,3*R*,4*R*,5*R*)-5-(6-Amino-9*H*-purin-9-yl)-4-((*tert*-butyldimethylsilyl)oxy)-2-(((*tert*-butyldimethylsilyl)oxy)methyl)tetrahydrofuran-3-yl)-3-(3-methyl-3*H*-diazirin-3-yl)propanamide [61] was synthesized according to general procedure B using protected adenosine [54] (2.00 g, 4.04 mmol, 1.00 equiv.) and diazirine [9] (1.55 g, 12.13 mmol, 3.00 equiv.). The crude product was used in the next step directly without further purification.

<b>Yield</b>	49% (1.20 g, 1-98 mmol)
<b>Appearance</b>	dark brown sticky solid
<b>Melting point</b>	not determined
<b>TLC</b>	$R_f$ (CHCl <sub>3</sub> /MeOH = 9/1) = 0.64
<b>Sum formula</b>	C <sub>27</sub> H <sub>48</sub> N <sub>8</sub> O <sub>4</sub> Si <sub>2</sub>
<b>HR-MS</b>	[M+Na] <sup>+</sup> : calculated: 627.3229 Da, found: 627.3221 Da, difference: -1.4 ppm
<b><sup>1</sup>H-NMR (400 MHz, DMSO-<i>d</i><sub>6</sub>)</b>	$\delta = \delta$ -0.07 (s, 3H, Si-CH <sub>3</sub> ), -0.05 (s, 3H, Si-CH <sub>3</sub> ), 0.06 (s, 3H, Si-CH <sub>3</sub> ), 0.07 (s, 3H, Si-CH <sub>3</sub> ), 0.76 (s, 9H, tertbutyl), 0.88 (s, 9H, tertbutyl), 0.99 (s, 3H, CH <sub>3</sub> (aliphatic linker)), 1.52 – 1.65 (m, 2H, -CH <sub>2</sub> -CH <sub>2</sub> -CONH-), 2.04 – 2.13 (m, 2H, -CH <sub>2</sub> -CH <sub>2</sub> -CONH-), 3.76 (dd, $J = 11.7, 3.4$ Hz, 1H, H-5'b), 3.96 (dd, $J = 11.7, 2.4$ Hz, 1H, H-5'a), 4.09 (dt, $J = 6.5, 3.0$ Hz, 1H, H-4'), 4.42 – 4.48 (m, 1H, H-3'), 4.54 (dd, $J = 5.8, 3.5$ Hz, 1H, H-2'), 5.99 (d, $J = 3.5$ Hz, 1H, H-1'), 7.33 (s, 2H, NH <sub>2</sub> -C6), 8.15 (s, 1H, H-2), 8.32 (s, 1H, H-8) ppm.
<b><sup>13</sup>C-NMR (101 MHz, DMSO-<i>d</i><sub>6</sub>)</b>	$\delta =$ 5.6 (q, Si-CH <sub>3</sub> ), -5.6 (q, Si-CH <sub>3</sub> ), -5.3 (q, Si-CH <sub>3</sub> ), -5.3 (q, Si-CH <sub>3</sub> ), 17.7 (q, Si-C(CH <sub>3</sub> ) <sub>3</sub> ), 18.1 (q, Si-C(CH <sub>3</sub> ) <sub>3</sub> ), 19.3 (q, CH <sub>3</sub> (aliphatic linker)), 25.4 (s, Si-C(CH <sub>3</sub> ) <sub>3</sub> ), 25.7 (s, diazirine), 25.879 (s, Si-C(CH <sub>3</sub> ) <sub>3</sub> ), 29.6 (t, -CH <sub>2</sub> -CH <sub>2</sub> -CONH-), 29.8 (t, -CH <sub>2</sub> -CH <sub>2</sub> -CONH-), 50.1 (d, C-3'), 62.5 (t, C-5'), 75.1 (d, C-2'), 82.4 (d, C-4'), 88.5 (d, C-1'), 118.9 (s, C-5), 137.9 (d, C-8), 149.1 (s, C-4), 152.7 (d, C-2), 156.1 (s, C-6), 170.7 (s, carbonyl (amide)) ppm.

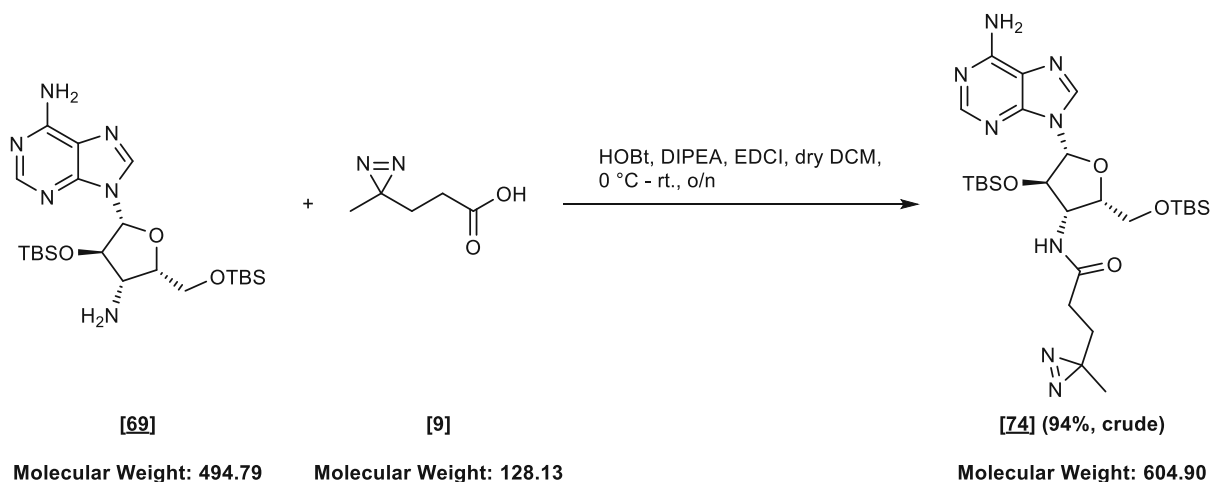
**E IV.9.23 *N*-((2*S*,3*R*,4*R*,5*R*)-5-(6-Amino-9*H*-purin-9-yl)-4-((*tert*-butyldimethylsilyl)oxy)-2-(((*tert*-butyldimethylsilyl)oxy)methyl)tetrahydrofuran-3-yl)-4-(3-(trifluoromethyl)-3*H*-diazirin-3-yl)benzamide [63]**



*N*-((2*S*,3*R*,4*R*,5*R*)-5-(6-Amino-9*H*-purin-9-yl)-4-((*tert*-butyldimethylsilyl)oxy)-2-(((*tert*-butyldimethylsilyl)oxy)methyl)tetrahydrofuran-3-yl)-4-(3-(trifluoromethyl)-3*H*-diazirin-3-yl)benzamide [63] was synthesized according to general procedure B using protected adenosine [54] (1.50 g, 3.03 mmol, 1.00 equiv.) and diazirine [18] (767 mg, 3.33 mmol, 1.10 equiv.). The crude product was used in the next step directly without purification. Since UHPLC-MS/UV analysis indicated distinct cleavage of the protection groups, crude [63] was directly subjected to the subsequent deprotection step without further analysis.

<b>Yield</b>	98% (2.10 g, 2.97 mmol)
<b>Appearance</b>	dark brown oil
<b>Melting point</b>	not determined
<b>TLC</b>	not determined
<b>Sum formula</b>	C <sub>31</sub> H <sub>44</sub> F <sub>3</sub> N <sub>7</sub> O <sub>5</sub> Si <sub>2</sub>
<b><sup>1</sup>H-NMR (400 MHz, DMSO-<i>d</i><sub>6</sub>)</b>	not determined
<b><sup>13</sup>C-NMR (101 MHz, DMSO-<i>d</i><sub>6</sub>)</b>	not determined

## E IV.9.24 *N*-((2*S*,3*S*,4*R*,5*R*)-5-(6-Amino-9*H*-purin-9-yl)-4-((*tert*-butyldimethylsilyl)oxy)-2-(((*tert*-butyldimethylsilyl)oxy)methyl)tetrahydrofuran-3-yl)-3-(3-methyl-3*H*-diazirin-3-yl)propanamide [74]



*N*-((2*S*,3*S*,4*R*,5*R*)-5-(6-Amino-9*H*-purin-9-yl)-4-((*tert*-butyldimethylsilyl)oxy)-2-(((*tert*-butyldimethylsilyl)oxy)methyl)tetrahydrofuran-3-yl)-3-(3-methyl-3*H*-diazirin-3-yl)propanamide [74] was synthesized according to general procedure B using protected adenosine [69] (1.72 g, 3.48 mmol, 1.00 equiv.) and diazirine [9] (1.34 g, 10.43 mmol, 3.00 equiv.). The crude product was used in the next step directly without further purification.

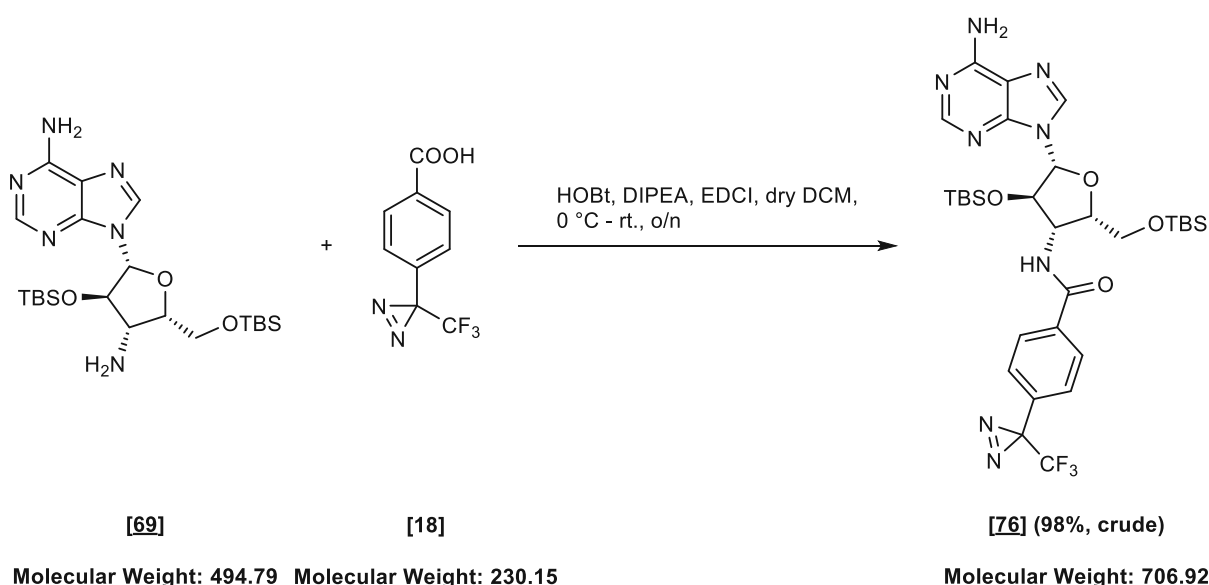
<b>Yield</b>	82% (1.97 g, 3.26 mmol)
<b>Appearance</b>	brown semisolid
<b>Melting point</b>	not determined
<b>TLC</b>	R <sub>f</sub> (CHCl <sub>3</sub> /MeOH = 9/1) = 0.76
<b>Sum formula</b>	C <sub>27</sub> H <sub>48</sub> N <sub>8</sub> O <sub>4</sub> Si <sub>2</sub>
<b>HR-MS</b>	[M+Na] <sup>+</sup> : calculated: 627. 3229 Da, found: 627.3224 Da, difference: -0.8 ppm
<b><sup>1</sup>H-NMR (600 MHz, DMSO-<i>d</i><sub>6</sub>)</b>	δ = -0.27 (s, 3H, Si-CH <sub>3</sub> ), -0.08 (s, 3H, Si-CH <sub>3</sub> ), -0.03 (s, 3H, Si-CH <sub>3</sub> ), -0.00 (s, 3H, Si-CH <sub>3</sub> ), 0.72 (s, 9H, tertbutyl), 0.82 (s, 9H, tertbutyl), 0.98 (s, 3H, CH <sub>3</sub> (aliphatic linker)), 1.60 (t, <i>J</i> = 7.7 Hz, 2H, -CH <sub>2</sub> -CH <sub>2</sub> -CONH-), 2.03 – 2.09 (m, 2H, -CH <sub>2</sub> -CH <sub>2</sub> -CONH-), 3.80 (dd, <i>J</i> = 11.3, 3.9 Hz, 1H, H-5'b), 3.88 (dd, <i>J</i> = 11.4, 7.1 Hz, 1H, H-5'a), 4.22 (tt, <i>J</i> = 7.5, 3.7 Hz, 1H, H-4'), 4.44 (ddd, <i>J</i> =



8.7, 6.6, 4.9 Hz, 1H, H-3'), 4.81 (t,  $J = 5.0$  Hz, 1H, H-2'), 5.81 (d,  $J = 5.0$  Hz, 1H, H-1'), 7.39 (s, 2H, NH<sub>2</sub>-C6), 8.18 (s, 1H, H-2), 8.35 (s, 1H, H-8), 8.61 (d,  $J = 8.6$  Hz, 1H, NH (amide)) ppm.

<sup>13</sup>C-NMR (151 MHz, DMSO-*d*<sub>6</sub>)  $\delta = -5.4$  (q, 2x Si-CH<sub>3</sub>),  $-5.3$  (q, Si-CH<sub>3</sub>),  $-5.0$  (q, Si-CH<sub>3</sub>), 17.5 (q, Si-C(CH<sub>3</sub>)<sub>3</sub>), 18.0 (q, Si-C(CH<sub>3</sub>)<sub>3</sub>), 25.4 (s, Si-C(CH<sub>3</sub>)<sub>3</sub>), 19.4 (q, CH<sub>3</sub> (aliphatic linker)) 25.8 (s, Si-C(CH<sub>3</sub>)<sub>3</sub>), 25.8 (s, diazirine), 29.7 (t, -CH<sub>2</sub>-CH<sub>2</sub>-CONH-), 29.8 (t, -CH<sub>2</sub>-CH<sub>2</sub>-CONH-), 56.1 (d, C-3'), 62.4 (t, C-5'), 78.8 (d, C-2'), 79.3 (d, C-4'), 88.6 (d, C-1'), 119.3 (s, C-5), 140.0 (d, C-8), 148.9 (s, C-4), 152.5 (d, C-2), 156.2 (s, C-6), 170.8 (s, carbonyl (amide)) ppm.

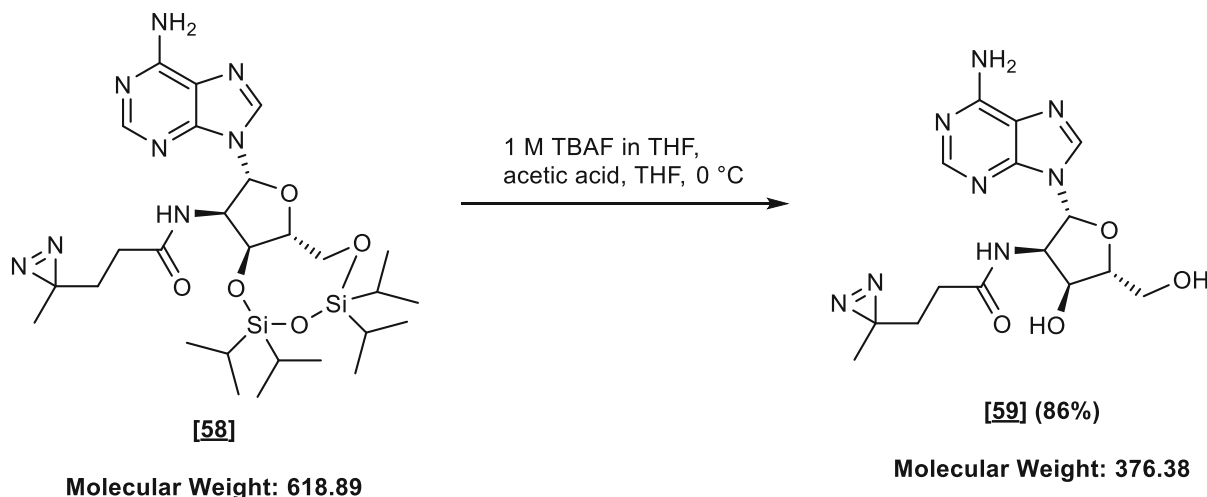
## E IV.9.25 *N*-((2*S*,3*S*,4*R*,5*R*)-5-(6-Amino-9*H*-purin-9-yl)-4-((*tert*-butyldimethylsilyl)oxy)-2-(((*tert*-butyldimethylsilyl)oxy)methyl)tetrahydrofuran-3-yl)-4-(3-(trifluoromethyl)-3*H*-diazirin-3-yl)benzamide [76]



*N*-((2*S*,3*S*,4*R*,5*R*)-5-(6-Amino-9*H*-purin-9-yl)-4-((*tert*-butyldimethylsilyl)oxy)-2-(((*tert*-butyldimethylsilyl)oxy)methyl)tetrahydrofuran-3-yl)-4-(3-(trifluoromethyl)-3*H*-diazirin-3-yl)benzamide [76] was synthesized according to general procedure B using protected adenosine [69] (1.84 g, 3.72 mmol, 1.00 equiv.) and diazirine [18] (941 mg, 4.09 mmol, 1.10 equiv.). The crude product was used in the next step directly without further purification.

<b>Yield</b>	98% (2.57 g, 3.64 mmol)
<b>Appearance</b>	light brown solid
<b>Melting point</b>	not determined
<b>TLC</b>	$R_f$ (CHCl <sub>3</sub> /MeOH = 9/1) = 0.64
<b>Sum formula</b>	C <sub>31</sub> H <sub>45</sub> F <sub>3</sub> N <sub>8</sub> O <sub>4</sub> Si <sub>2</sub>
<b>HR-MS</b>	[M+Na] <sup>+</sup> : calculated: 729.2947 Da, found: 729.2939 Da, difference: -1.1 ppm
<b><sup>1</sup>H-NMR (400 MHz, DMSO-<i>d</i><sub>6</sub>)</b>	$\delta$ = -0.25 (s, 3H, Si-CH <sub>3</sub> ), -0.10 (s, 3H, Si-CH <sub>3</sub> ), -0.07 (s, 3H, Si-CH <sub>3</sub> ), -0.06 (s, 3H, Si-CH <sub>3</sub> ), 0.72 (s, 9H, tertbutyl), 0.75 (s, 9H, tertbutyl), 3.84 – 3.90 (m, 2H, H-5'a & H-5'b), 4.25 – 4.37 (m, 1H, H-4'), 4.75 (ddd, $J$ = 9.1, 6.4, 4.6 Hz, 1H, H-3'), 4.93 (t, $J$ = 4.7 Hz, 1H, H-2'), 5.88 (d, $J$ = 4.8 Hz, 1H, H-1'), 7.39 – 7.52 (m, 4H, NH <sub>2</sub> -C6 & H-3ar & H-5ar), 7.96 (d, $J$ = 8.6 Hz, 2H, H-2ar & H-6ar), 8.07 (s, 1H, H-2), 8.34 (s, 1H, H-8), 9.29 (d, $J$ = 9.0 Hz, 1H, NH (amide)) ppm.
<b><sup>13</sup>C-NMR (101 MHz, DMSO-<i>d</i><sub>6</sub>)</b>	$\delta$ = -5.0 (q, Si-CH <sub>3</sub> ), -5.0 (q, Si-CH <sub>3</sub> ), -4.9 (q, Si-CH <sub>3</sub> ), -4.6 (q, Si-CH <sub>3</sub> ), 18.0 (q, Si-C(CH <sub>3</sub> ) <sub>3</sub> ), 18.4 (q, Si-C(CH <sub>3</sub> ) <sub>3</sub> ), 25.8 (s, Si-C(CH <sub>3</sub> ) <sub>3</sub> ), 26.1 (s, Si-C(CH <sub>3</sub> ) <sub>3</sub> ), 26.3 (s, diazirine), 57.4 (d, C-3'), 62.7 (t, C-5'), 79.5 (d, C-2'), 79.7 (d, C-4'), 89.7 (d, C-1'), 121.0 (s/q, $^1J_{CF}$ = 275.1 Hz, CF <sub>3</sub> ), 120.0 (s, C-5), 127.2 (d, C-3ar & C-5ar), 128.6 (d, C-2ar & C-6ar), 131.1 (s, C-1ar), 136.4 (d, C-8), 140.8 (s, C-4ar), 149.2 (s, C-4), 153.0 (d, C-2), 156.8 (s, C-6), 166.0 (s, carbonyl (amide)) ppm.
<b><sup>19</sup>F NMR (376 MHz, DMSO-<i>d</i><sub>6</sub>)</b>	$\delta$ = -64.48 ppm.

**E IV.9.26 *N*-((2*R*,3*R*,4*S*,5*R*)-2-(6-Amino-9*H*-purin-9-yl)-4-hydroxy-5-(hydroxymethyl)tetrahydrofuran-3-yl)-3-(3-methyl-3*H*-diazirin-3-yl)propanamide [59]**



*N*-((2*R*,3*R*,4*S*,5*R*)-2-(6-Amino-9*H*-purin-9-yl)-4-hydroxy-5-(hydroxymethyl)tetrahydrofuran-3-yl)-3-(3-methyl-3*H*-diazirin-3-yl)propanamide [59] was synthesized according to general procedure C using protected adenosine [58] (1.70 g, 2.75 mmol, 1.00 equiv.). The pure product was obtained after purification by flash column chromatography (silica gel/crude material = 100/1, solid load) using a gradient of MeOH in DCM (4% 5 min; 4-10% 10 min; 10% 10 min) as eluent.

<b>Yield</b>	86% (886 mg, 2.37 mmol)
<b>Appearance</b>	tan solid
<b>Melting point</b>	> 179.0 °C (decomposition; formation of bubbles)
<b>TLC</b>	R <sub>f</sub> (CHCl <sub>3</sub> /MeOH = 9/1) = 0.18
<b>Sum formula</b>	C <sub>15</sub> H <sub>20</sub> N <sub>8</sub> O <sub>4</sub>
<b>HR-MS</b>	[M+H] <sup>+</sup> : calculated: 377.1681 Da, found: 377.1696 Da, difference: 4.3 ppm

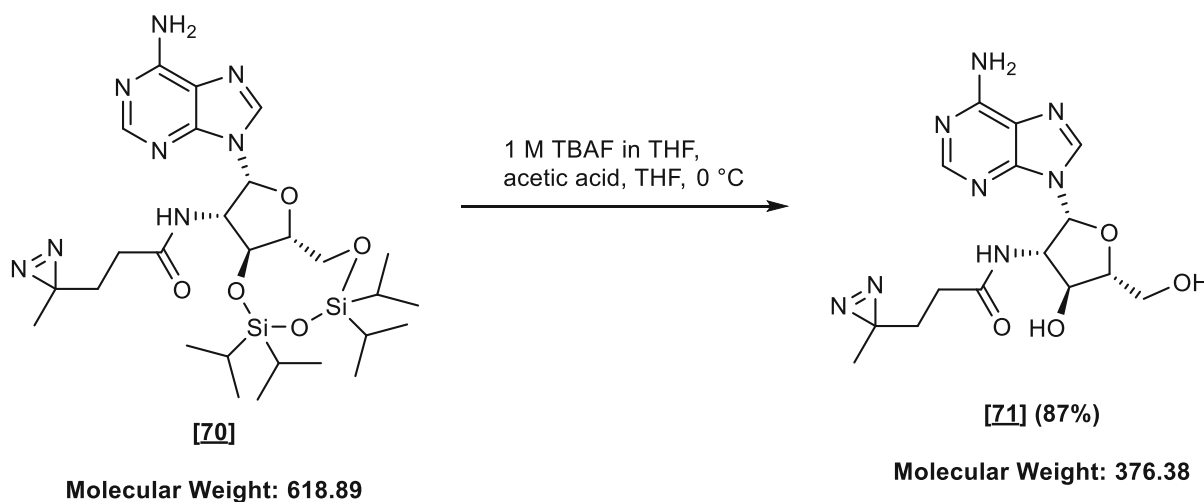
**<sup>1</sup>H-NMR (400 MHz, DMSO-*d*<sub>6</sub>)** δ = 0.83 (s, 3H, CH<sub>3</sub> (aliphatic linker)), 1.33 – 1.47 (m, 2H, -CH<sub>2</sub>-CH<sub>2</sub>-CONH-), 1.95 – 2.03 (m, 2H, -CH<sub>2</sub>-CH<sub>2</sub>-CONH-), 3.54 – 3.60 (m, 1H, H-5'b), 3.67 (dt, *J* = 12.2, 3.8 Hz, 1H, H-5'a), 4.03 (td, *J* = 3.7, 3.6, 1.4 Hz, 1H, H-4'), 4.20 – 4.22 (m, 1H, H-3'), 5.07 (td, *J* = 8.6, 8.6, 5.2 Hz, 1H, H-2'), 5.57 (dd, *J* = 7.5, 4.3 Hz, 1H, OH-5'), 5.69 (s, 1H, OH-3'), 5.93 (d, *J* = 8.5 Hz, 1H, H-1'), 7.32

(s, 2H, NH<sub>2</sub>-C6), 8.03 (d, *J* = 8.6 Hz, 1H, NH (amide)), 8.11 (s, 1H, H-2), 8.24 (s, 1H, H-8) ppm.

<sup>13</sup>C-NMR (101 MHz, DMSO-*d*<sub>6</sub>)  $\delta$  = 19.0 (q, CH<sub>3</sub> (aliphatic linker)), 25.6 (s, diazirine), 29.5 (t, -CH<sub>2</sub>-CH<sub>2</sub>-CONH-), 29.8 (t, -CH<sub>2</sub>-CH<sub>2</sub>-CONH-), 54.9 (d, C-2'), 62.0 (t, C-5'), 70.6 (d, C-3'), 86.0 (d, C-1'), 87.5 (d, C-4'), 119.3 (s, C-5), 139.7 (d, C-8), 149.3 (s, C-4), 152.3 (d, C-2), 156.1 (s, C-6), 171.3 (s, carbonyl (amide)) ppm.

Optical rotation  $[\alpha]_D^{20}$  = -69.5 (c = 0.5, MeOH)

## E IV.9.27 *N*-((2*R*,3*S*,4*S*,5*R*)-2-(6-Amino-9*H*-purin-9-yl)-4-hydroxy-5-(hydroxymethyl)tetrahydrofuran-3-yl)-3-(3-methyl-3*H*-diazirin-3-yl)propanamide [71]

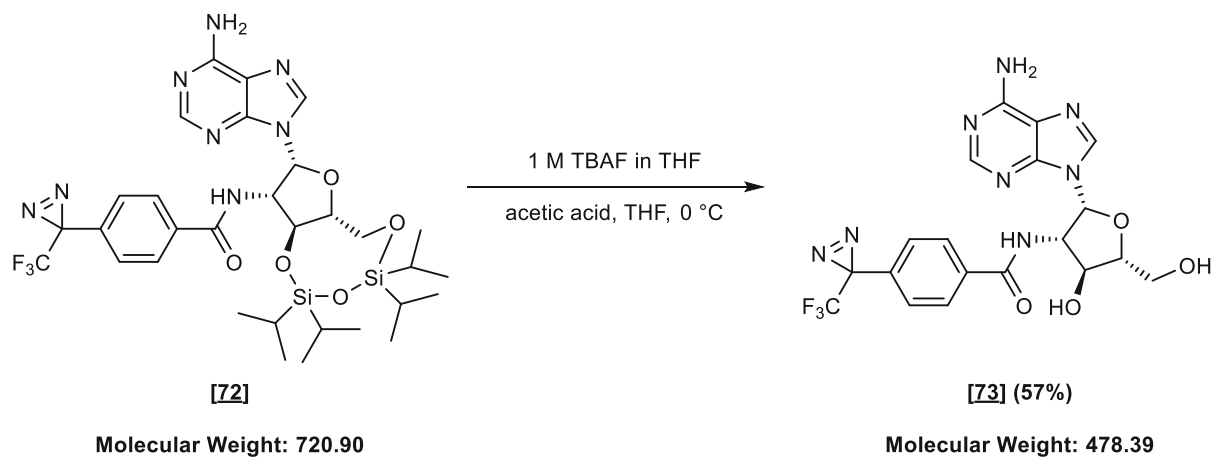


*N*-((2*R*,3*S*,4*S*,5*R*)-2-(6-Amino-9*H*-purin-9-yl)-4-hydroxy-5-(hydroxymethyl)tetrahydrofuran-3-yl)-3-(3-methyl-3*H*-diazirin-3-yl)propanamide [71] was synthesized according to general procedure C using protected adenosine [70] (1.90 g, 3.07 mmol, 1.00 equiv.). The pure product was obtained after purification by flash column chromatography (silica gel/crude material = 100/1, dry load) using MeOH in DCM (4% 5 min; 4-10 % 10 min; 10% 10 min) as eluent.

<b>Yield</b>	87% (1.00 g, 2.66 mmol)
<b>Appearance</b>	colorless crystals
<b>Melting point</b>	> 139.0 °C (decomposition; formation of bubbles)

<b>TLC</b>	$R_f$ (CHCl <sub>3</sub> /MeOH = 19/1) = 0.13
<b>Sum formula</b>	C <sub>15</sub> H <sub>20</sub> N <sub>8</sub> O <sub>4</sub>
<b>HR-MS</b>	[M+Na] <sup>+</sup> : calculated: 399.1500 Da, found: 399.1497 Da, difference: -0.6 ppm
<b><sup>1</sup>H-NMR (400 MHz, DMSO-<i>d</i><sub>6</sub>)</b>	$\delta$ = 0.78 (s, 3H, CH <sub>3</sub> (aliphatic linker)), 1.08 (ddd, $J$ = 14.7, 9.7, 6.4 Hz, 1H, -CH <sub>2</sub> -CH <sub>2</sub> -CONH-), 1.22 (ddd, $J$ = 14.7, 9.5, 6.3 Hz, 1H, -CH <sub>2</sub> -CH <sub>2</sub> -CONH-), 1.58 (ddd, $J$ = 14.5, 9.4, 6.4 Hz, 1H, -CH <sub>2</sub> -CH <sub>2</sub> -CONH-), 1.72 (ddd, $J$ = 14.5, 9.7, 6.3 Hz, 1H, -CH <sub>2</sub> -CH <sub>2</sub> -CONH-), 3.59 – 3.71 (m, 1H, H-5'a), 3.72 – 3.82 (m, 2H, H-4' & H-5'a), 4.38 (t, $J$ = 8.3 Hz, 1H, H-3'), 4.49 – 4.58 (m, 1H, H-2'), 6.29 (d, $J$ = 6.8 Hz, 1H, H-1'), 7.20 (s, 2H, NH <sub>2</sub> ), 8.00 (d, $J$ = 7.6 Hz, 1H, NH (amide)), 8.07 (s, 1H, H-2), 8.20 (s, 1H, H-8) ppm.
<b><sup>13</sup>C-NMR (101 MHz, DMSO-<i>d</i><sub>6</sub>)</b>	$\delta$ = 19.6(q, CH <sub>3</sub> (aliphatic linker)), 26.1 (s, diazirine), 29.9 (t, -CH <sub>2</sub> -CH <sub>2</sub> -CONH-), 30.2 (t, -CH <sub>2</sub> -CH <sub>2</sub> -CONH-), 58.7 (d, C-2'), 60.1 (t, C-5'), 70.8 (d, C-3'), 82.6 (d, C-1'), 83.8 (d, C-4'), 119.1(s, C-5), 140.3 (d, C-8), 149.8 (s, C-4), 152.9 (d, C-2), 156.5 (s, C-6), 171.7 (s, carbonyl (amide)) ppm.
<b>Optical rotation</b>	$[\alpha]_D^{20}$ = -81.9 (c = 0.23, MeOH)

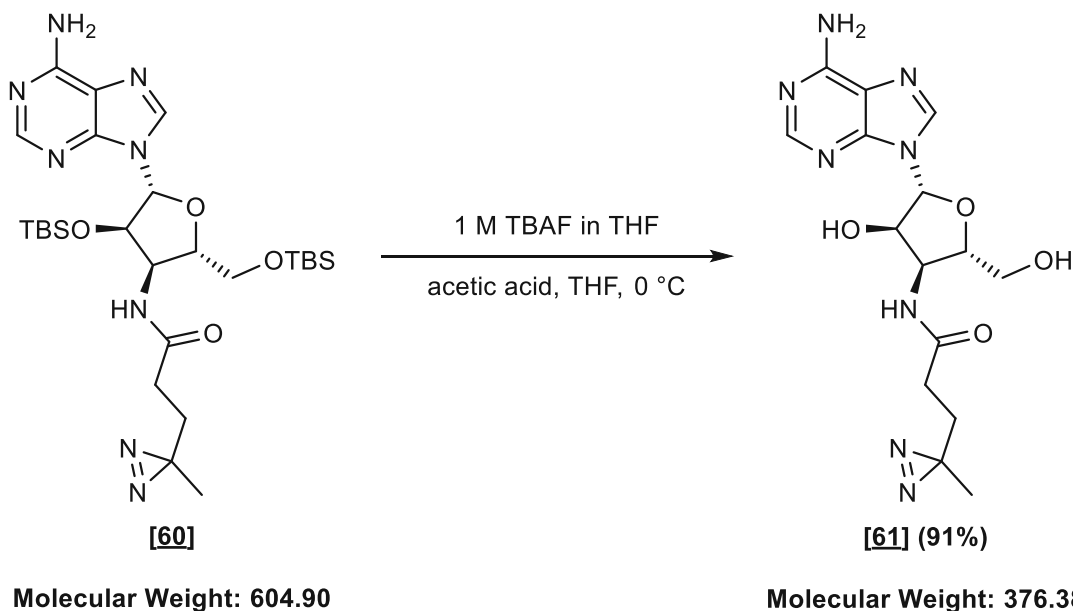
**E IV.9.28 N-((2R,3S,4S,5R)-2-(6-amino-9H-purin-9-yl)-4-hydroxy-5-(hydroxymethyl)tetrahydrofuran-3-yl)-4-(3-(trifluoromethyl)-3H-diazirin-3-yl)benzamide [73]**



N-((2R,3S,4S,5R)-2-(6-amino-9H-purin-9-yl)-4-hydroxy-5-(hydroxymethyl)tetrahydrofuran-3-yl)-4-(3-(trifluoromethyl)-3H-diazirin-3-yl)benzamide [73] was synthesized according to general procedure C using protected adenosine [72] (1.80 g, 2.50 mmol, 1.00 equiv.). The pure product was obtained after purification by flash column chromatography (silica gel/crude material = 100/1, solid load) using MeOH in DCM (5% 5 min; 4-10% 10 min; 10% 10 min) as eluent.

<b>Yield</b>	57% (676 mg, 1.41 mmol)
<b>Appearance</b>	colorless crystals
<b>Melting point</b>	> 211.0 °C (decomposition; formation of bubbles and color change to brown)
<b>TLC</b>	R <sub>f</sub> (DCM/MeOH = 9/1) = 0.19
<b>Sum formula</b>	C <sub>19</sub> H <sub>17</sub> F <sub>3</sub> N <sub>8</sub> O <sub>4</sub>
<b>HR-MS</b>	[M+H] <sup>+</sup> : calculated: 479.1398 Da, found: 479.1411 Da, difference: 2.71 ppm
<b><sup>1</sup>H-NMR (400 MHz, DMSO-<i>d</i><sub>6</sub>)</b>	δ = 3.70 (dd, <i>J</i> = 12.3, 3.2 Hz, 1H, H-5'b), 3.82 (dd, <i>J</i> = 12.4, 2.3 Hz, 1H, H-5'a), 3.85 – 3.94 (m, 1H, H-4'), 4.59 (t, <i>J</i> = 7.5 Hz, 1H, H-3'), 4.73 (td, <i>J</i> = 7.7, 7.7, 6.4 Hz, 1H, H-2'), 5.47 (s, 1H, OH-5'), 5.63 (s, 1H, OH-3'), 6.44 (d, <i>J</i> = 6.4 Hz, 1H, H-1'), 7.16 (s, 2H, NH <sub>2</sub> -C6), 7.23 – 7.30 (m, 2H, H-3ar & H-5ar), 7.55 (d, <i>J</i> = 8.7 Hz, 2H, H-2ar & H-6ar), 8.02 (s, 1H, H-2), 8.27 (s, 1H, H-8), 8.71 (d, <i>J</i> = 7.5 Hz, 1H, NH (amide)) ppm.
<b><sup>13</sup>C-NMR (101 MHz, DMSO-<i>d</i><sub>6</sub>)</b>	δ = 28.0 (s/q, <sup>2</sup> <i>J</i> <sub>CF</sub> = 40.2 Hz, diazirine), 58.8 (d, C-2'), 59.7 (t, C-5'), 70.5 (d, C-3'), 82.3 (d, C-1'), 83.6 (d, C-4'), 118.3 (s, C-5), 121.7 (s/q, <sup>1</sup> <i>J</i> <sub>CF</sub> = 275.1 Hz, CF <sub>3</sub> ), 126.3 (d, C-3ar & C-5ar), 127.9 (d, C-2ar & C-6ar), 130.3 (s, C-1ar), 135.4 (s, C-4ar), 139.6 (d, C-8), 149.2 (s, C-4), 152.4 (d, C-2), 155.8 (s, C-6), 165.6 (s, carbonyl (amide)) ppm.
<b>Optical rotation</b>	[α] <sub>D</sub> <sup>20</sup> = -6.2 (c = 0.5, MeOH)

**E IV.9.29 *N*-((2*S*,3*S*,4*R*,5*R*)-5-(6-Amino-9*H*-purin-9-yl)-4-hydroxy-2-(hydroxymethyl)tetrahydrofuran-3-yl)-3-(3-methyl-3*H*-diazirin-3-yl)propanamide [61]**



*N*-((2*S*,3*S*,4*R*,5*R*)-5-(6-Amino-9*H*-purin-9-yl)-4-hydroxy-2-(hydroxymethyl)tetrahydrofuran-3-yl)-3-(3-methyl-3*H*-diazirin-3-yl)propanamide [61] was synthesized according to general procedure D using protected adenosine [60] (1.35 g, 2.23 mmol, 1.00 equiv.). The pure product was obtained after purification by flash column chromatography (silica gel/crude material = 100/1, solid load) using MeOH in DCM (4% 5 min; 4-10% 10 min; 10% 10 min) as eluent.

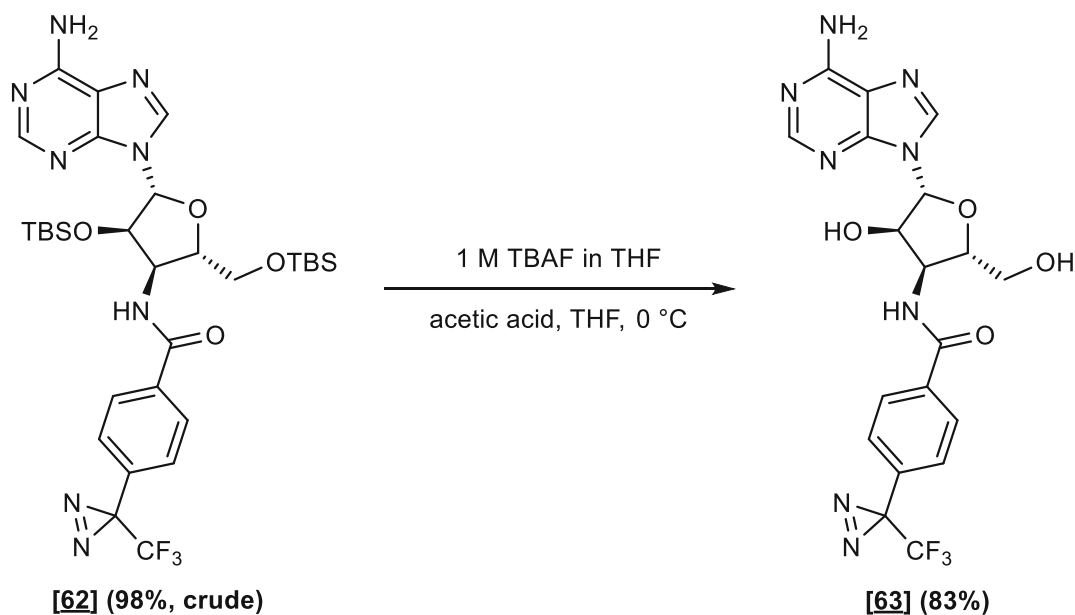
<b>Yield</b>	91% (765 mg, 2.03 mmol)
<b>Appearance</b>	off-white solid
<b>Melting point</b>	> 161 °C (decomposition)
<b>TLC</b>	R <sub>f</sub> (CHCl <sub>3</sub> /MeOH = 9/1) = 0.2
<b>Sum formula</b>	C <sub>15</sub> H <sub>20</sub> N <sub>8</sub> O <sub>4</sub>
<b>HR-MS</b>	[M+H] <sup>+</sup> : calculated: 377.1681 Da, found: 377.1689 Da, difference: 2.39 ppm
<b><sup>1</sup>H-NMR (400 MHz, DMSO-<i>d</i><sub>6</sub>)</b>	δ = 1.00 (s, 3H, CH <sub>3</sub> (aliphatic linker)), 1.57 (td, <i>J</i> = 7.5, 7.1, 1.6 Hz, 2H, -CH <sub>2</sub> -CH <sub>2</sub> -CONH-), 2.00 – 2.18 (m, 2H, -CH <sub>2</sub> -CH <sub>2</sub> -CONH-), 3.53 (ddd, <i>J</i> = 12.2, 6.0, 4.1 Hz, 1H, H-5'b), 3.71 (ddd, <i>J</i> = 12.1, 5.0, 2.4 Hz, 1H, H-5'a), 3.99 (ddd, <i>J</i> = 6.8, 4.0, 2.4 Hz,

1H, H-4'), 4.43 – 4.50 (m, 2H, H-2' & H-3'), 5.19 (dd,  $J = 5.9, 5.0$  Hz, 1H, OH-5'), 5.95 (d,  $J = 2.5$  Hz, 2H, H-1' & OH-2'), 7.31 (s, 2H, NH<sub>2</sub>-C6), 8.02 (d,  $J = 7.3$  Hz, 1H, NH (amide)), 8.15 (s, 1H, H-2), 8.40 (s, 1H, H-8) ppm.

<sup>13</sup>C-NMR (101 MHz, DMSO-*d*<sub>6</sub>)  $\delta = 19.3$ (q, CH<sub>3</sub> (aliphatic linker)), 25.8 (s, diazirine), 29.7 (t, -CH<sub>2</sub>-CH<sub>2</sub>-CONH-), 29.9 (t, -CH<sub>2</sub>-CH<sub>2</sub>-CONH-), 50.4 (d, C-3'), 60.9 (t, C-5'), 73.1 (d, C-2'), 83.2 (d, C-4'), 89.3 (d, C-1'), 119.1 (s, C-5), 139.0 (d, C-8), 148.9 (s, C-4), 152.5 (d, C-2), 156.1 (s, C-6), 171.3 (s, carbonyl (amide)) ppm.

Optical rotation  $[\alpha]_D^{20} = -14.6$  ( $c = 0.5$ , MeOH)

### E IV.9.30 *N*-((2*S*,3*S*,4*R*,5*R*)-5-(6-Amino-9*H*-purin-9-yl)-4-hydroxy-2-(hydroxymethyl)tetrahydrofuran-3-yl)-4-(3-(trifluoromethyl)-3*H*-diazirin-3-yl)benzamide [63]



Molecular Weight: 706.92

Molecular Weight: 478.40

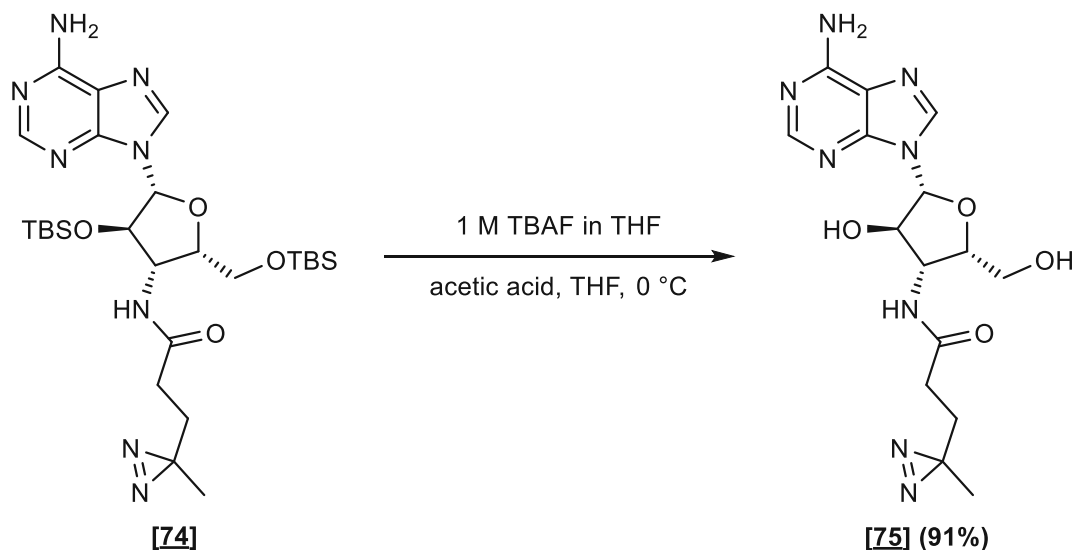
*N*-((2*S*,3*S*,4*R*,5*R*)-5-(6-Amino-9*H*-purin-9-yl)-4-hydroxy-2-(hydroxymethyl)tetrahydrofuran-3-yl)-4-(3-(trifluoromethyl)-3*H*-diazirin-3-yl)benzamide [63] was synthesized according to general procedure D using protected adenosine [62] (1.33 g, 1.88 mmol, 1.00 equiv.). The pure product was obtained after purification by flash column



chromatography (silica gel/crude material = 100/1, solid load) using MeOH in DCM (5% 5 min; 4-10% 10 min; 10% 10 min) as eluent.

<b>Yield</b>	83% (745 mg, 1.56 mmol)
<b>Appearance</b>	colorless crystals
<b>Melting point</b>	> 148 °C (decomposition: formation of bubbles and color change)
<b>TLC</b>	R <sub>f</sub> (CHCl <sub>3</sub> /MeOH = 9/1) = 0.55
<b>Sum formula</b>	C <sub>19</sub> H <sub>17</sub> F <sub>3</sub> N <sub>8</sub> O <sub>4</sub>
<b>HR-MS</b>	[M+H] <sup>+</sup> : calculated: 479.1398 Da, found: 479.1407 Da, difference: 1.97 ppm
<b><sup>1</sup>H-NMR (400 MHz, DMSO-<i>d</i><sub>6</sub>)</b>	δ = 3.58 (dd, <i>J</i> = 12.4, 4.8 Hz, 1H, H-5'b), 3.74 (dd, <i>J</i> = 12.8, 3.5 Hz, 1H, H-5'a), 4.25 (ddd, <i>J</i> = 7.6, 3.8, 2.5 Hz, 1H, H-4'), 4.57 (dd, <i>J</i> = 6.1, 3.5 Hz, 1H, H-2'), 4.68 (td, <i>J</i> = 7.8, 7.8, 5.9 Hz, 1H, H-3'), 5.27 (s, 1H, OH-5'), 5.95 (d, <i>J</i> = 6.2 Hz, 1H, OH-2'), 6.01 (d, <i>J</i> = 3.5 Hz, 1H, H-1'), 7.31 (s, 2H, NH <sub>2</sub> -C6), 7.39 (d, <i>J</i> = 8.1 Hz, 2H, H-3ar & H5ar), 8.00 – 8.03 (m, 2H, H-2ar & H-6ar), 8.14 (s, 1H, H-2), 8.43 (s, 1H, H-8), 8.60 (d, <i>J</i> = 8.0 Hz, 1H, NH (amide)) ppm.
<b><sup>13</sup>C-NMR (101 MHz, DMSO-<i>d</i><sub>6</sub>)</b>	δ = 28.1 (s/q, <sup>2</sup> <i>J</i> <sub>CF</sub> = 40.1 Hz, diazirine), 51.2 (d, C-3'), 60.9 (t, C-5'), 73.2 (d, C-2'), 82.4 (d, C-4'), 89.2 (d, C-1'), 119.1 (s, C-5), 121.8 (s/q, <sup>1</sup> <i>J</i> <sub>CF</sub> = 274.9 Hz, CF <sub>3</sub> ), 126.3 (d, C-3ar & C-5ar), 128.5 (d, C-2ar & C-6ar), 130.3 (s, C-1ar), 135.9 (s, C-4ar), 139.0 (d, C-8), 149.0 (s, C-4), 152.6 (d, C-2), 156.1 (s, C-6), 165.6 (s, carbonyl (amide)) ppm.
<b><sup>19</sup>F NMR (376 MHz, DMSO-<i>d</i><sub>6</sub>)</b>	δ = -64.46 ppm.
<b>Optical rotation</b>	[α] <sub>D</sub> <sup>20</sup> = -20.8 (c = 0.5, MeOH)

**E IV.9.31 *N*-((2*S*,3*R*,4*R*,5*R*)-5-(6-Amino-9*H*-purin-9-yl)-4-hydroxy-2-(hydroxymethyl)tetrahydrofuran-3-yl)-3-(3-methyl-3*H*-diazirin-3-yl)propanamide [75]**



**Molecular Weight: 604.90**

**Molecular Weight: 376.38**

*N*-((2*S*,3*R*,4*R*,5*R*)-5-(6-Amino-9*H*-purin-9-yl)-4-hydroxy-2-(hydroxymethyl)tetrahydrofuran-3-yl)-3-(3-methyl-3*H*-diazirin-3-yl)propanamide [75] was synthesized according to general procedure D using protected adenosine [74] (1.75 g, 2.89 mmol, 1.00 equiv.). The pure product was obtained after purification by flash column chromatography (silica gel/crude material = 100/1, solid load) using MeOH in DCM (4% 5 min; 4-10% 10 min; 10% 10 min) as eluent.

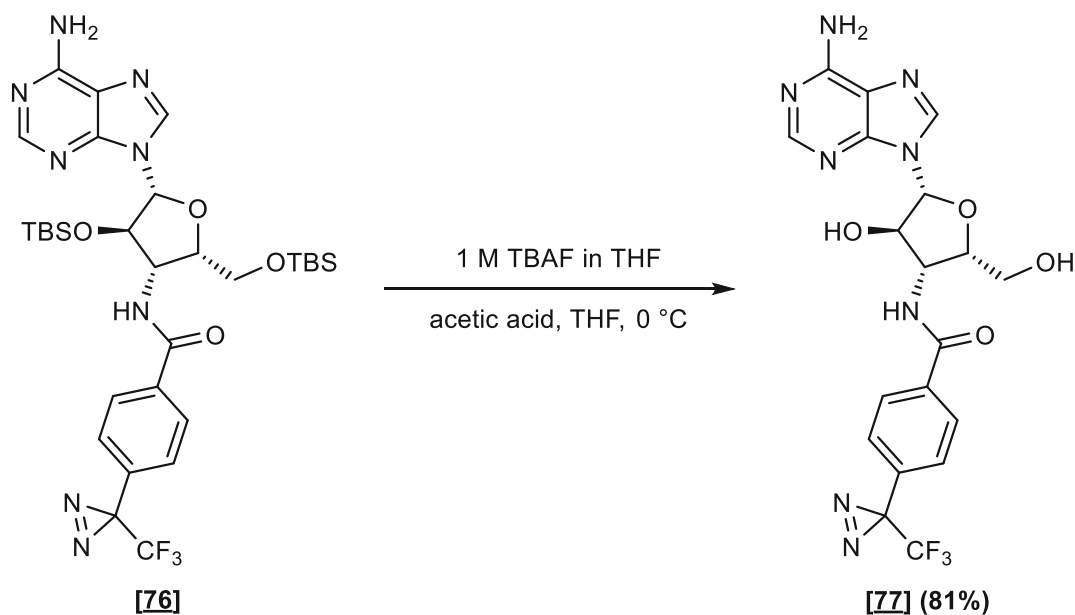
<b>Yield</b>	91% (992 mg, 2.64 mmol)
<b>Appearance</b>	colorless crystals
<b>Melting point</b>	> 118 °C (decomposition, formation of bubbles)
<b>TLC</b>	R <sub>f</sub> (CHCl <sub>3</sub> /MeOH = 9/1) = 0.16
<b>Sum formula</b>	C <sub>15</sub> H <sub>20</sub> N <sub>8</sub> O <sub>4</sub>
<b>HR-MS</b>	[M+Na] <sup>+</sup> : calculated: 399.1500 Da, found: 399.1508 Da, difference: 2.06 ppm
<b><sup>1</sup>H-NMR (400 MHz, DMSO-<i>d</i><sub>6</sub>)</b>	δ = 1.01 (s, 3H, CH <sub>3</sub> (aliphatic linker)), 1.61 (t, <i>J</i> = 7.9 Hz, 2H, -CH <sub>2</sub> -CH <sub>2</sub> -CONH-), 2.07 – 2.16 (m, 2H, -CH <sub>2</sub> -CH <sub>2</sub> -CONH-), 3.45 – 3.66 (m, 2H, H-5'a & H-5'b), 4.21 (ddd, <i>J</i> = 7.1, 4.4, 3.1 Hz, 1H, H-4'), 4.40 (dt, <i>J</i> = 7.9, 6.5 Hz, 1H, H-3'), 4.64 (q, <i>J</i> = 5.5

Hz, 1H, H-2'), 5.39 (dd,  $J = 7.6, 4.3$  Hz, 1H, OH-5'), 5.78 (d,  $J = 5.5$  Hz, 1H, H-1'), 5.86 (d,  $J = 5.4$  Hz, 1H, OH-2'), 7.45 (s, 2H, NH<sub>2</sub>-C6), 8.17 (s, 1H, H-2), 8.34 (s, 1H, H-8), 8.62 (d,  $J = 8.0$  Hz, 1H, NH (amide)) ppm.

<sup>13</sup>C-NMR (101 MHz, DMSO-*d*<sub>6</sub>)  $\delta = 19.9$  (q, CH<sub>3</sub> (aliphatic linker), ), 26.4 (s, diazirine), 30.4 (t, -CH<sub>2</sub>-CH<sub>2</sub>-CONH-), 30.4 (t, -CH<sub>2</sub>-CH<sub>2</sub>-CONH-), 56.5 (d, C-3'), 61.0 (t, C-5'), 77.2 (d, C-2'), 80.3 (d, C-4'), 89.6 (d, C-1'), 120.1 (s, C-5), 141.1 (d, C-8), 149.1 (s, C-4), 152.8 (d, C-2), 157.0 (s, C-6), 171.8 (s, carbonyl (amide)) ppm.

Optical rotation  $[\alpha]_D^{20} = -22.1$  ( $c = 0.5$ , MeOH)

## E IV.9.32 *N*-((2*S*,3*R*,4*R*,5*R*)-5-(6-Amino-9*H*-purin-9-yl)-4-hydroxy-2-(hydroxymethyl)tetrahydrofuran-3-yl)-4-(3-(trifluoromethyl)-3*H*-diazirin-3-yl)benzamide [77]



Molecular Weight: 706.92

Molecular Weight: 478.40

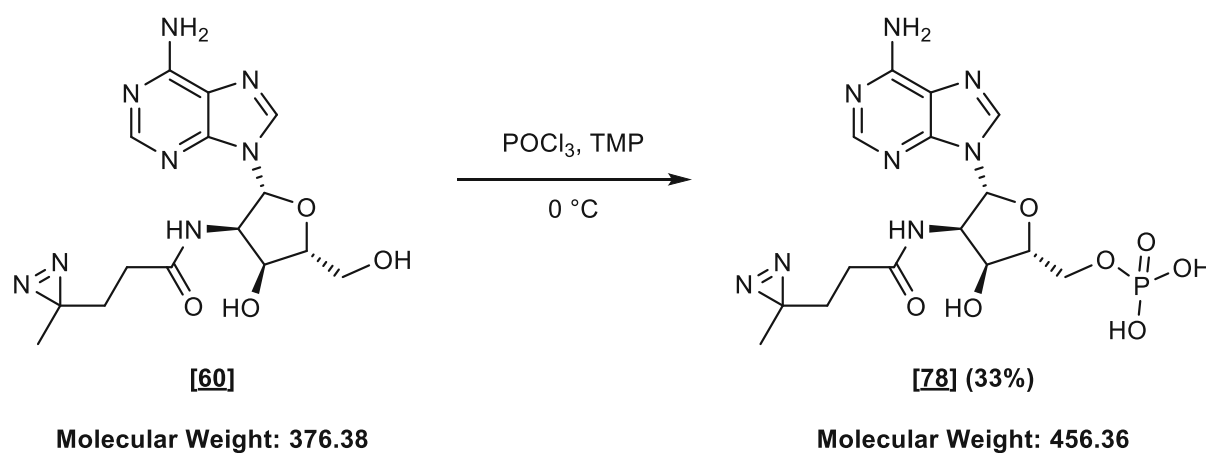
*N*-((2*S*,3*R*,4*R*,5*R*)-5-(6-Amino-9*H*-purin-9-yl)-4-hydroxy-2-(hydroxymethyl)tetrahydrofuran-3-yl)-4-(3-(trifluoromethyl)-3*H*-diazirin-3-yl)benzamide [77] was synthesized according to general procedure D using protected adenosine [76] (1.60 g, 2.26 mmol, 1.00 equiv.). The pure product was obtained after purification by flash column

chromatography (silica gel/crude material = 100/1, solid load) using MeOH in DCM (5% 5 min; 4-10% 10 min; 10% 10 min) as eluent.

<b>Yield</b>	81% (900 mg, 1.88 mmol)
<b>Appearance</b>	colorless solid
<b>Melting point</b>	> 110 °C (decomposition, formation of bubbles)
<b>TLC</b>	R <sub>f</sub> (CHCl <sub>3</sub> /MeOH = 9/1) = 0.28
<b>Sum formula</b>	C <sub>19</sub> H <sub>17</sub> F <sub>3</sub> N <sub>8</sub> O <sub>4</sub>
<b>HR-MS</b>	[M+H] <sup>+</sup> : calculated: 479.1398 Da, found: 479.1411 Da, difference: 2.75 ppm
<b><sup>1</sup>H-NMR (400 MHz, DMSO-<i>d</i><sub>6</sub>)</b>	δ = 3.51 (ddd, <i>J</i> = 12.1, 7.0, 5.1 Hz, 1H, H-5'b), 3.65 (ddd, <i>J</i> = 12.2, 4.7, 3.3 Hz, 1H, H-5'a), 4.29 – 4.35 (m, 1H, H-4'), 4.63 (ddd, <i>J</i> = 8.1, 6.1, 4.8 Hz, 1H, H-3'), 4.78 (q, <i>J</i> = 4.9 Hz, 1H, H-2'), 5.28 (dd, <i>J</i> = 6.9, 4.7 Hz, 1H, OH-5'), 5.85 (d, <i>J</i> = 4.8 Hz, 1H, H-1'), 5.99 (d, <i>J</i> = 5.1 Hz, 1H, OH-2'), 7.43 – 7.51 (m, 4H, NH <sub>2</sub> -C6 & H-3ar & H-5ar), 7.98 (d, <i>J</i> = 8.5 Hz, 2H, H-2ar & H-6ar), 8.05 (s, 1H, H-2), 8.39 (s, 1H, H-8), 9.45 (d, <i>J</i> = 8.1 Hz, 1H, NH (amide)) ppm.
<b><sup>13</sup>C-NMR (101 MHz, DMSO-<i>d</i><sub>6</sub>)</b>	δ = 28.1 (s/q, <sup>2</sup> <i>J</i> <sub>CF</sub> = 39.9 Hz, diazirine), 57.2 (d, C-3'), 60.3 (t, C-5'), 77.4 (d, C-2'), 80.1 (d, C-4'), 89.7 (d, C-1'), 119.6 (s, C-5), 121.8 (s/q, <sup>2</sup> <i>J</i> <sub>CF</sub> = 274.7 Hz, CF <sub>3</sub> ), 126.7 (d, C-3ar & C-5ar), 128.2 (d, C-2ar & C-6ar), 130.5 (s, C-1ar), 136.0 (s, C-4ar), 140.7 (d, C-8), 148.4 (s, C-4), 152.3 (d, C-2), 156.4 (s, C-6), 165.7 (s, carbonyl (amide)) ppm.
<b><sup>19</sup>F NMR (376 MHz, DMSO-<i>d</i><sub>6</sub>)</b>	δ -64.45 ppm.
<b>Optical rotation</b>	[α] <sub>D</sub> <sup>20</sup> = +20.7 (c = 0.5, MeOH)

## E IV.10 Synthesis of modified adenosine monophosphates—Amides

### E IV.10.1 ((2*R*,3*S*,4*R*,5*R*)-5-(6-Amino-9*H*-purin-9-yl)-3-hydroxy-4-(3-(3-methyl-3*H*-diazirin-3-yl)propanamido)tetrahydrofuran-2-yl)methyl dihydrogen phosphate [78]



((2*R*,3*S*,4*R*,5*R*)-5-(6-Amino-9*H*-purin-9-yl)-3-hydroxy-4-(3-(3-methyl-3*H*-diazirin-3-yl)propanamido)tetrahydrofuran-2-yl)methyl dihydrogen phosphate [78] was synthesized according to general procedure E using unprotected adenosine [60] (640 mg, 1.70 mmol, 1.00 equiv.). The pure product was obtained after purification by preparative reverse-phase HPLC (C18-column, MilliQ water + 0.1% formic acid [Solvent A]/acetonitrile [Solvent B]) and lyophilization as a colorless powder.

<b>Yield</b>	33% (256 mg, 0.56 mmol)
<b>Appearance</b>	colorless powder
<b>Melting point</b>	> 151 °C (decomposition; formation of bubbles and color change)
<b>Sum formula</b>	C <sub>15</sub> H <sub>21</sub> N <sub>8</sub> O <sub>7</sub> P
<b>HR-MS</b>	[M+H] <sup>+</sup> : calculated: 457.1344 Da, found: 457.1351 Da, difference: 1.73 ppm
<b><sup>1</sup>H-NMR (400 MHz, D<sub>2</sub>O)</b>	δ = 0.83 (s, 3H, CH <sub>3</sub> (aliphatic linker)), 1.42 – 1.72 (m, 2H, -CH <sub>2</sub> -CH <sub>2</sub> -CONH-), 1.94 – 2.39 (m, 2H, -CH <sub>2</sub> -CH <sub>2</sub> -CONH-), 4.19 (dd, <i>J</i> = 5.0, 3.4 Hz, 2H, H-5'a & H-5'b), 4.48 – 4.52 (m, 1H, H-4'), 4.55 – 4.59 (m, 1H, H-3'), 5.11 (dd, <i>J</i> = 8.3, 5.4 Hz, 1H, H-2'),

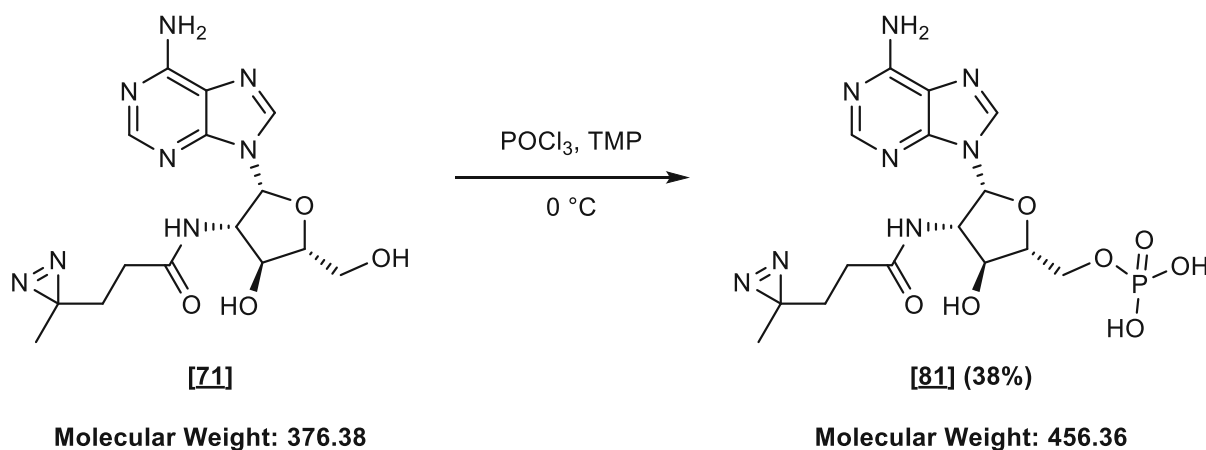
6.25 (d,  $J = 8.3$  Hz, 1H, H-1'), 8.44 (s, 1H, H-2), 8.71 (s, 1H, H-8) ppm.

$^{13}\text{C-NMR}$  (151 MHz,  $\text{D}_2\text{O}$ )  $\delta = 18.5$  (q,  $\text{CH}_3$  (aliphatic linker)), 26.0 (s, diazirine), 29.3 (t,  $-\text{CH}_2-\text{CH}_2-\text{CONH}-$ ), 29.8 (t,  $-\text{CH}_2-\text{CH}_2-\text{CONH}-$ ), 56.9 (d, C-2'), 65.1 (t/d,  $^2J_{\text{CP}} = 5.2$  Hz, C-5'), 70.9 (d, C-3'), 86.3 (d/d,  $^3J_{\text{CP}} = 8.9$  Hz, C-4'), 86.4 (d, C-1'), 118.7 (s, C-5), 142.8 (d, C-8), 145.1 (d, C-2), 148.8 (d, C-4), 150.2 (s, C-6), 175.7 (s, carbonyl (amide)) ppm.

$^{31}\text{P-NMR}$  (162 MHz,  $\text{D}_2\text{O}$ )  $\delta = 0.19$  ppm.

Optical rotation  $[\alpha]_{\text{D}}^{20} = -22.2$  ( $c = 0.5$ ,  $\text{H}_2\text{O}$ )

### E IV.10.2 ((2*R*,3*S*,4*S*,5*R*)-5-(6-Amino-9*H*-purin-9-yl)-3-hydroxy-4-(3-(3-methyl-3*H*-diazirin-3-yl)propanamido)tetrahydrofuran-2-yl)methyl dihydrogen phosphate [81]



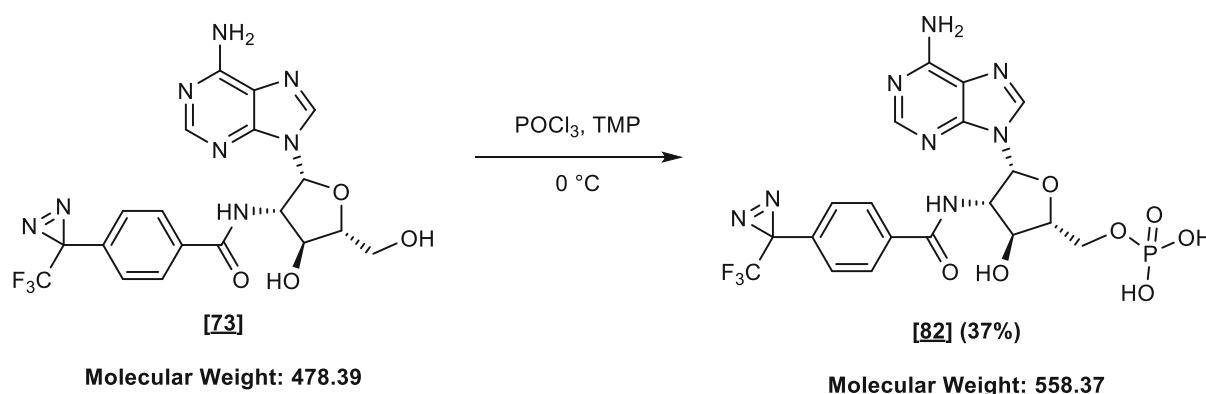
((2*R*,3*S*,4*S*,5*R*)-5-(6-Amino-9*H*-purin-9-yl)-3-hydroxy-4-(3-(3-methyl-3*H*-diazirin-3-yl)propanamido)tetrahydrofuran-2-yl)methyl dihydrogen phosphate **[81]** was synthesized according to general procedure E using unprotected adenosine **[71]** (800 mg, 2.13 mmol, 1.00 equiv.). The pure product was obtained after purification by preparative reverse-phase HPLC (C18-column, water + 0.1% formic acid [Solvent A]/acetonitrile [Solvent B]) and lyophilization as a colorless powder.

**Yield** 38% (372 mg, 0.82 mmol)

**Appearance** colorless powder

<b>Melting point</b>	> 80 °C (decomposition)
<b>Sum formula</b>	C <sub>15</sub> H <sub>21</sub> N <sub>8</sub> O <sub>7</sub> P
<b>HR-MS</b>	[M+H] <sup>+</sup> : calculated: 457.1344 Da, found: 457.1344 Da, difference: 0.18 ppm
<b><sup>1</sup>H-NMR (400 MHz, D<sub>2</sub>O)</b>	δ = 0.78 (s, 3H, CH <sub>3</sub> (aliphatic linker)), 1.23 (ddd, <i>J</i> = 15.1, 8.4, 6.9 Hz, 12H, -CH <sub>2</sub> -CH <sub>2</sub> -CONH-), 1.42 (dt, <i>J</i> = 15.0, 6.8 Hz, 1H, -CH <sub>2</sub> -CH <sub>2</sub> -CONH-), 1.74 (ddd, <i>J</i> = 15.3, 8.3, 6.8 Hz, 1H, -CH <sub>2</sub> -CH <sub>2</sub> -CONH-), 1.96 (dt, <i>J</i> = 15.4, 6.8 Hz, 1H, -CH <sub>2</sub> -CH <sub>2</sub> -CONH-), 4.18 – 4.26 (m, 2H, H-4' & H-5'b), 4.26 – 4.35 (m, 1H, H-5'a), 4.64 – 4.73 (m, 1H, C-3'), 6.65 (d, <i>J</i> = 6.8 Hz, 1H, H-1'), 8.39 (s, 1H, H-2), 8.52 (s, 1H, H-8) ppm.
<b><sup>13</sup>C-NMR (151 MHz, D<sub>2</sub>O)</b>	δ = 18.4 (q, CH <sub>3</sub> (aliphatic linker)), 25.6 (s, diazirine), 28.8 (t, -CH <sub>2</sub> -CH <sub>2</sub> -CONH-), 29.1 (t, -CH <sub>2</sub> -CH <sub>2</sub> -CONH-), 58.3 (d, C-2'), 62.5 (t/d, <sup>2</sup> <i>J</i> <sub>CP</sub> Hz, C-5'), 70.0 (d, C-3'), 81.1 (d, C-4'), 82.9 (d, C-1'), 118.2 (s, C-5), 142.4 (d, C-8), 146.5 (d, C-2), 148.2 (s, C-4), 151.2 (s, C-6), 175.4 (s, carbonyl (amide)) ppm.
<b><sup>31</sup>P-NMR (243 MHz, D<sub>2</sub>O)</b>	δ = 0.27 ppm
<b>Optical rotation</b>	[α] <sub>D</sub> <sup>20</sup> = -59.1 (c = 0.5, H <sub>2</sub> O)
<b>Comment</b>	The H-2'-peak is below the D <sub>2</sub> O-peak.

### E IV.10.3((2*R*,3*S*,4*S*,5*R*)-5-(6-Amino-9*H*-purin-9-yl)-3-hydroxy-4-(4-(3-(trifluoromethyl)-3*H*-diazirin-3-yl)benzamido)tetrahydrofuran-2-yl)methyl dihydrogen phosphate [82]



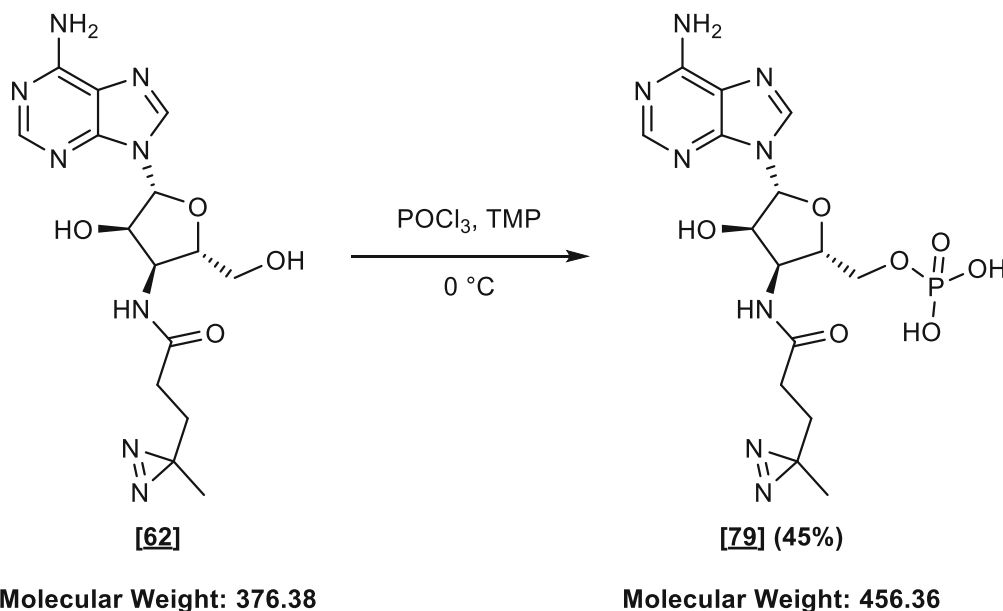
((2*R*,3*S*,4*S*,5*R*)-5-(6-Amino-9*H*-purin-9-yl)-3-hydroxy-4-(4-(3-(trifluoromethyl)-3*H*-diazirin-3-yl)benzamido)tetrahydrofuran-2-yl)methyl dihydrogen phosphate [82] was synthesized according to general procedure E using unprotected adenosine [73] (400 mg, 0.84

mmol, 1.00 equiv.). The pure product was obtained after purification by preparative reverse-phase HPLC (C18-column, MilliQ water + 0.1% formic acid [Solvent A]/acetonitrile [Solvent B]) and lyophilization as colorless crystals.

<b>Yield</b>	37% (173 mg, 0.31 mmol)
<b>Appearance</b>	colorless crystals
<b>Melting point</b>	> 198 °C (decomposition)
<b>Sum formula</b>	C <sub>19</sub> H <sub>18</sub> F <sub>3</sub> N <sub>8</sub> O <sub>7</sub> P
<b>HR-MS</b>	[M+H] <sup>+</sup> : calculated: 559.1061 Da, found: 559.1065 Da, difference: 0.76 ppm
<b><sup>1</sup>H-NMR (400 MHz, D<sub>2</sub>O)</b>	$\delta = 4.29$ (dddd, $J = 17.0, 11.9, 5.0, 2.5$ Hz, 2H, H-4' & H5'b), 4.38 (ddd, $J = 11.8, 4.5, 1.9$ Hz, 1H, H-5'a), 5.08 (dd, $J = 9.3, 6.7$ Hz, 1H, H-2'), 6.70 (d, $J = 6.7$ Hz, 1H, H-1'), 7.21 – 7.27 (m, 2H, H-3ar & H-5ar), 7.32 – 7.37 (m, 2H, H-2ar & H-6ar), 8.20 (s, 1H, H-2), 8.65 (s, 1H, H-8) ppm.
<b><sup>13</sup>C-NMR (151 MHz, D<sub>2</sub>O)</b>	$\delta = 28.2$ (s/q, $^2J_{CF} = 40.7$ Hz, diazirine), 58.7 (d, C-2'), 62.3 (t, C-5'), 68.7 (d, C-3'), 81.3 (d, C-4'), 83.4 (d, C-1'), 118.2 (s, C-5), 121.64 (s/q, $^1J_{CF} = 274.5$ Hz, CF <sub>3</sub> ), 126.6 (d, C-3ar & C-5ar), 126.9 (s, C-1ar), 127.1 (d, C-2ar & C-6ar), 127.7 (s, C-4ar), 142.0 (d, C-8), 146.8 (d, C-2), 148.0 (s, C-4), 151.5 (s, C-6), 170.2 (s, carbonyl (amide)) ppm.
<b><sup>19</sup>F NMR (565 MHz, D<sub>2</sub>O)</b>	$\delta = -65.43$ ppm
<b><sup>31</sup>P NMR (243 MHz, D<sub>2</sub>O)</b>	$\delta = 0.30$ ppm.
<b>Optical rotation</b>	$[\alpha]_D^{20} = -38.2$ (c = 0.25, H <sub>2</sub> O)



**E IV.10.4((2*S*,3*S*,4*R*,5*R*)-5-(6-Amino-9*H*-purin-9-yl)-4-hydroxy-3-(3-(3-methyl-3*H*-diazirin-3-yl)propanamido)tetrahydrofuran-2-yl)methyl dihydrogen phosphate [79]**



((2*S*,3*S*,4*R*,5*R*)-5-(6-Amino-9*H*-purin-9-yl)-4-hydroxy-3-(3-(3-methyl-3*H*-diazirin-3-yl)propanamido)tetrahydrofuran-2-yl)methyl dihydrogen phosphate [79] was synthesized according to general procedure E using unprotected adenosine [62] (600 mg, 1.59 mmol, 1.00 equiv.). The pure product was obtained after purification by preparative reverse-phase HPLC (C18-column, MilliQ water + 0.1% formic acid [Solvent A]/acetonitrile [Solvent B]) and lyophilization as a colorless powder.

<b>Yield</b>	45% (325 mg, 0.71 mmol)
<b>Appearance</b>	colorless powder
<b>Melting point</b>	> 161.0 °C (decomposition; formation of bubbles)
<b>Sum formula</b>	C <sub>15</sub> H <sub>21</sub> N <sub>8</sub> O <sub>7</sub> P
<b>HR-MS</b>	[M+H] <sup>+</sup> : calculated: 457.1344 Da, found: 457.13544 Da, difference: 2.19 ppm
<b><sup>1</sup>H-NMR (400 MHz, D<sub>2</sub>O)</b>	δ = 1.04 (s, 3H, CH <sub>3</sub> (aliphatic linker)), 1.73 (td, <i>J</i> = 7.5, 7.4, 1.1 Hz, 2H, -CH <sub>2</sub> -CH <sub>2</sub> -CONH-), 2.29 (t, <i>J</i> = 7.4 Hz, 2H, -CH <sub>2</sub> -CH <sub>2</sub> -CONH-), 4.08 (ddd, <i>J</i> = 11.9, 5.1, 3.7 Hz, 1H, H-5'b), 4.28 (ddd, <i>J</i> = 11.9, 5.1, 2.3 Hz, 1H, H-5'a), 4.46 (ddd, <i>J</i> = 5.7, 3.5, 1.8 Hz,

1H, H-4'), 6.25 (d,  $J = 1.6$  Hz, 1H, H-1'), 8.45 (s, 1H, H-8), 8.65 (s, 1H, H-2) ppm.

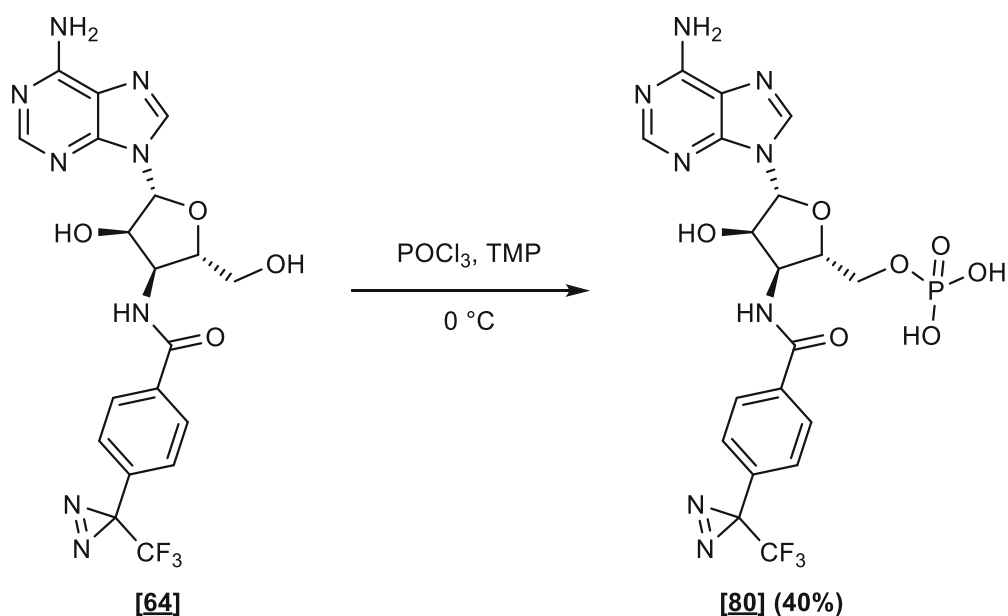
$^{13}\text{C}$ -NMR (101 MHz,  $\text{D}_2\text{O}$ )  $\delta = 18.7$  (q,  $\text{CH}_3$  (aliphatic linker)), 26.3 (s, diazirine), 29.8 (t,  $-\text{CH}_2-\text{CH}_2-\text{CONH}-$ ), 30.1 (t,  $-\text{CH}_2-\text{CH}_2-\text{CONH}-$ ), 50.6 (d, C-3'), 63.8 (t/d,  $^2J_{\text{CP}} = 5.2$  Hz, C-5'), 73.9 (d, C-2'), 81.5 (d/d,  $^3J_{\text{CP}} = 8.6$  Hz, C-4'), 90.3 (d, C-1'), 118.9 (s, C-5), 142.4 (d, C-8), 145.0 (d, C-2), 148.0 (s, C-4), 150.2 (s, C-6), 176.0 (s, carbonyl (amide)) ppm.

$^{31}\text{P}$  NMR (162 MHz,  $\text{D}_2\text{O}$ )  $\delta = 0.12$  ppm.

Optical rotation  $[\alpha]_{\text{D}}^{20} = +14.9$  ( $c = 0.5$ ,  $\text{H}_2\text{O}$ )

Comment The H-2'- and H-3'-peaks are underneath the  $\text{D}_2\text{O}$ -peak.

## E IV.10.5 ((2*S*,3*S*,4*R*,5*R*)-5-(6-Amino-9*H*-purin-9-yl)-4-hydroxy-3-(4-(3-(trifluoromethyl)-3*H*-diazirin-3-yl)benzamido)tetrahydrofuran-2-yl)methyl dihydrogen phosphate [80]



Molecular Weight: 478.39

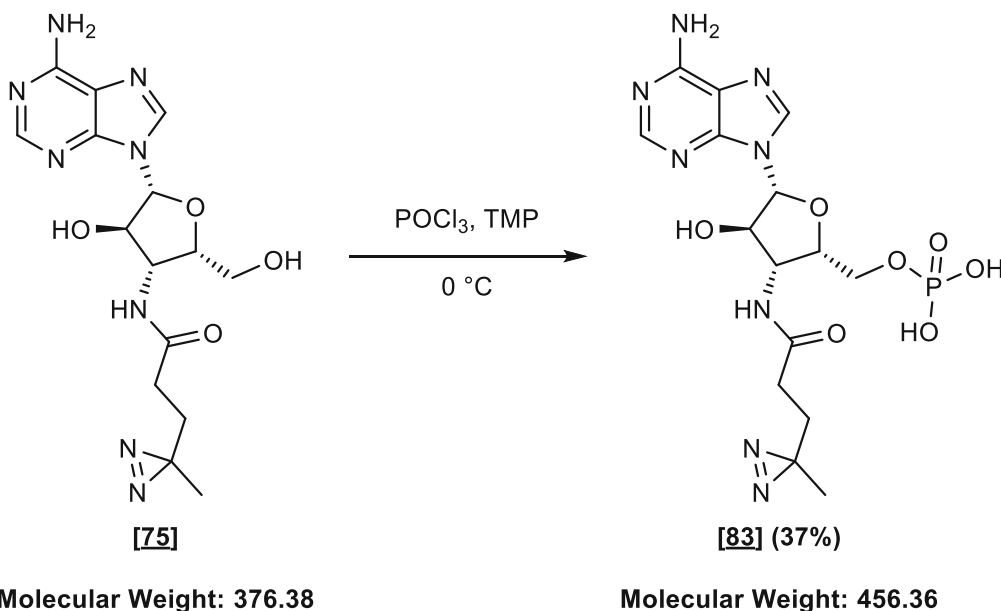
Molecular Weight: 558.37

((2*S*,3*S*,4*R*,5*R*)-5-(6-Amino-9*H*-purin-9-yl)-4-hydroxy-3-(4-(3-(trifluoromethyl)-3*H*-diazirin-3-yl)benzamido)tetrahydrofuran-2-yl)methyl dihydrogen phosphate **[80]** was synthesized according to general procedure E using protected adenosine **[64]** (600 mg, 1.25 mmol, 1.00 equiv.). The pure product was obtained after purification by preparative reverse-

phase HPLC (C18-column, MilliQ water + 0.1% formic acid [Solvent A]/acetonitrile [Solvent B]) and lyophilization as a colorless powder.

<b>Yield</b>	40% (278 mg, 0.50 mmol)
<b>Appearance</b>	colorless powder
<b>Melting point</b>	> 110 °C (decomposition; formation of bubbles and color change)
<b>Sum formula</b>	C <sub>19</sub> H <sub>18</sub> F <sub>3</sub> N <sub>8</sub> O <sub>7</sub> P
<b>HR-MS</b>	[M+Na] <sup>+</sup> : calculated: 581.0880 Da, found: 581.0885 Da, difference: 0.84 ppm
<b><sup>1</sup>H NMR (400 MHz, D<sub>2</sub>O)</b>	$\delta = 3.99 - 4.14$ (m, 1H, H-5'b), $4.17 - 4.27$ (m, 1H, H-5'a), $4.49 - 4.57$ (m, 1H, H-4'), $4.79 - 4.90$ (m, 2H, H-2' & H-3'), $6.22$ (d, $J = 2.3$ Hz, 1H, H-1'), $7.34$ (d, $J = 8.1$ Hz, 2H, C-3ar & C-5ar), $7.80$ (d, $J = 8.5$ Hz, 2H, C-2ar & C-6ar), $8.35$ (s, 1H, H-8), $8.58$ (s, 1H, H-2) ppm.
<b><sup>13</sup>C-NMR</b>	not measured
<b><sup>19</sup>F NMR (376 MHz, D<sub>2</sub>O)</b>	$\delta = -65.35$ ppm.
<b><sup>31</sup>P NMR (162 MHz, D<sub>2</sub>O)</b>	$\delta = 0.21$ ppm.
<b>Comment</b>	A proper <sup>13</sup> C-NMR and the optical rotation could not be measured due to precipitation of the compound in the course of time.

**E IV.10.6((2*S*,3*R*,4*R*,5*R*)-5-(6-Amino-9*H*-purin-9-yl)-4-hydroxy-3-(3-(3-methyl-3*H*-diazirin-3-yl)propanamido)tetrahydrofuran-2-yl)methyl dihydrogen phosphate [83]**



((2*S*,3*R*,4*R*,5*R*)-5-(6-Amino-9*H*-purin-9-yl)-4-hydroxy-3-(3-(3-methyl-3*H*-diazirin-3-yl)propanamido)tetrahydrofuran-2-yl)methyl dihydrogen phosphate **[83]** was synthesized according to general procedure E using protected adenosine **[75]** (644 g, 1.71 mmol, 1.00 equiv.). The pure product was obtained after purification by preparative reverse-phase HPLC (C18-column, MilliQ water + 0.1% formic acid [Solvent A]/acetonitrile [Solvent B]) and lyophilization as a colorless powder.

<b>Yield</b>	37% (290 mg, 0.64 mmol)
<b>Appearance</b>	colorless powder
<b>Melting point</b>	> 191 °C (decomposition)
<b>Sum formula</b>	C <sub>15</sub> H <sub>21</sub> N <sub>8</sub> O <sub>7</sub> P
<b>HR-MS</b>	[M+H] <sup>+</sup> : calculated: 457.1344 Da, found: 457.1338 Da, difference: -1.17 ppm
<b><sup>1</sup>H-NMR (400 MHz, D<sub>2</sub>O)</b>	δ = 1.04 (s, 3H, CH <sub>3</sub> (aliphatic linker)), 1.74 (td, <i>J</i> = 7.5, 7.4, 2.9 Hz, 2H, -CH <sub>2</sub> -CH <sub>2</sub> -CONH-), 2.31 (td, <i>J</i> = 7.3, 7.2, 1.0 Hz, 2H, -CH <sub>2</sub> -CH <sub>2</sub> -CONH-), 4.02 (ddd, <i>J</i> = 12.1, 4.7, 2.3 Hz, 1H, H-5'b), 4.13 (ddd, <i>J</i> = 12.1, 4.4, 2.4 Hz, 1H, H-5'a), 4.70 – 4.75 (m, 1H,

H-4'), 4.84 – 4.91 (m, 2H, H-2' & H-3'), 6.15 – 6.22 (m, 1H, H-1'), 8.45 (s, 1H, H-8), 8.73 (s, 1H, H-2) ppm.

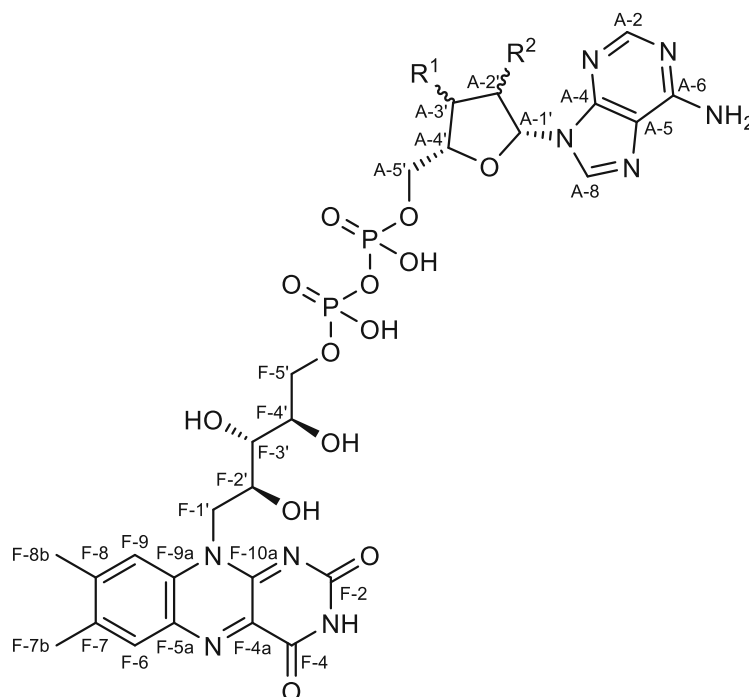
$^{13}\text{C-NMR}$  (151 MHz,  $\text{D}_2\text{O}$ )  $\delta$  = 18.7 (q,  $\text{CH}_3$  (aliphatic linker)), 26.3 (s, diazirine), 29.7 (t,  $-\text{CH}_2-\text{CH}_2-\text{CONH}-$ ), 30.1 (t,  $-\text{CH}_2-\text{CH}_2-\text{CONH}-$ ), 55.2 (d, C-2'), 64.2 (t, C-5'), 76.6 (d, C-3'), 77.9 (d/d,  $^3J_{\text{CP}} = 8.9$  Hz, C-4'), 86.7 (d, C-1'), 118.6 (s, C-4), 142.4 (d, C-8), 145.5 (d, C-2), 148.9 (s, C-4), 150.5 (s, C-6), 176.4 (s, carbonyl (amide)) ppm.

$^{31}\text{P-NMR}$  (162 MHz,  $\text{D}_2\text{O}$ )  $\delta$  = 0.09 ppm.

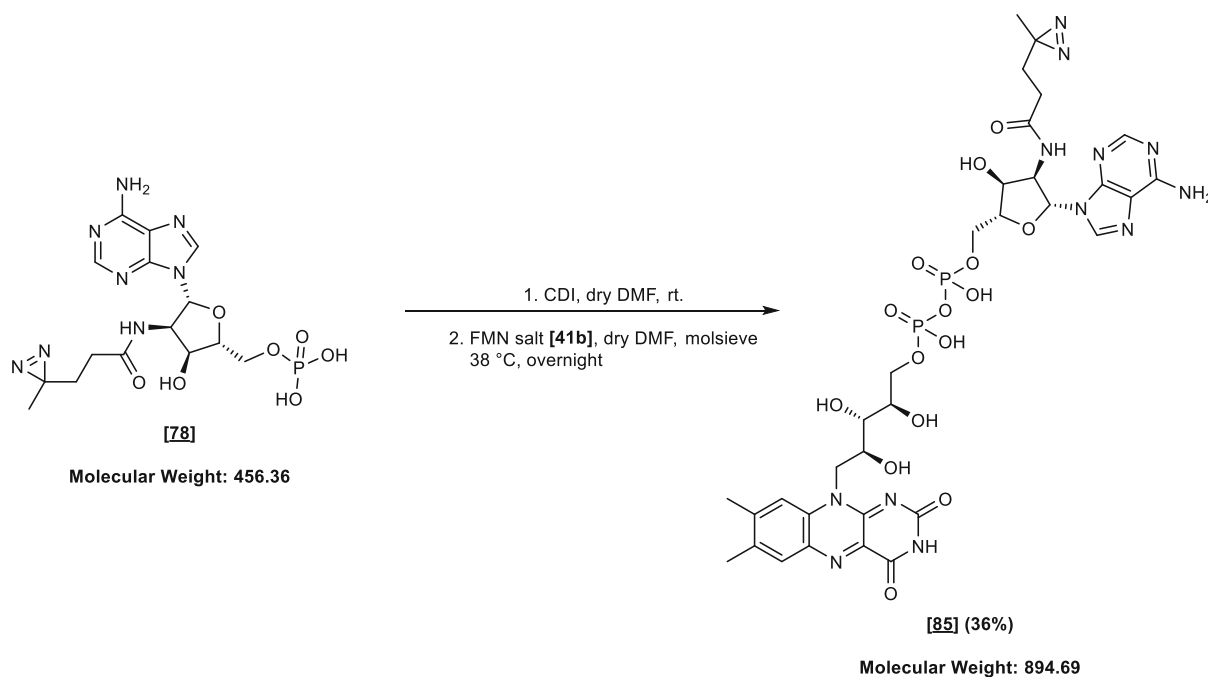
Optical rotation  $[\alpha]_{\text{D}}^{20} = -13.9$  ( $c = 0.5$ ,  $\text{H}_2\text{O}$ )

## E IV.11 Synthesis of modified flavin adenine dinucleotides—Amides

The assignments of protons and carbon atoms in the NMR codes of compounds [85]-[90] were carried out as follows:



## E IV.11.1 ((2*R*,3*S*,4*R*,5*R*)-5-(6-Amino-9*H*-purin-9-yl)-3-hydroxy-4-(3-(3-methyl-3*H*-diazirin-3-yl)propanamido)tetrahydrofuran-2-yl)methyl dihydrogen phosphate [85]



((2*R*,3*S*,4*R*,5*R*)-5-(6-Amino-9*H*-purin-9-yl)-3-hydroxy-4-(3-(3-methyl-3*H*-diazirin-3-yl)propanamido)tetrahydrofuran-2-yl)methyl dihydrogen phosphate [85] was synthesized according to general procedure F using adenosine monophosphate [78] (100 mg, 219  $\mu\text{mol}$ , 1.00 equiv.). The pure product was obtained after purification by preparative reverse-phase HPLC (2.5 mM  $\text{NH}_4^+\text{HCOO}^-$ -buffer [Solvent A]/acetonitrile [Solvent B]) and lyophilization as a yellow-orange powder.

<b>Yield</b>	36% (71 mg, 79 $\mu\text{mol}$ )
<b>Appearance</b>	yellow-orange powder
<b>Melting point</b>	> 175 °C (decomposition)
<b>Sum formula</b>	$\text{C}_{32}\text{H}_{40}\text{N}_{12}\text{O}_{15}\text{P}_2$
<b>HR-MS</b>	[M-H] <sup>-</sup> : calculated: 893.2138 Da, found: 893.2128 Da, difference: -1.20 ppm
<b><sup>1</sup>H-NMR (600 MHz, D<sub>2</sub>O)</b>	$\delta = 0.54$ (s, 3H, CH <sub>3</sub> (aliphatic linker)), 1.19 – 1.36 (m, 2H, -CH <sub>2</sub> -CH <sub>2</sub> -CONH-), 1.85 – 2.02 (m, 2H, -CH <sub>2</sub> -CH <sub>2</sub> -CONH-), 2.29 (s, 2H, CH <sub>3</sub> -CF7), 2.39 (s, 3H, CH <sub>3</sub> -CF8), 3.86 (dd, $J = 7.8, 4.1$ Hz, 1H, H-F3'), 3.97 – 4.06 (m, 1H, H-F4'), 4.21 (dt, $J = 11.1, 6.6$ Hz,

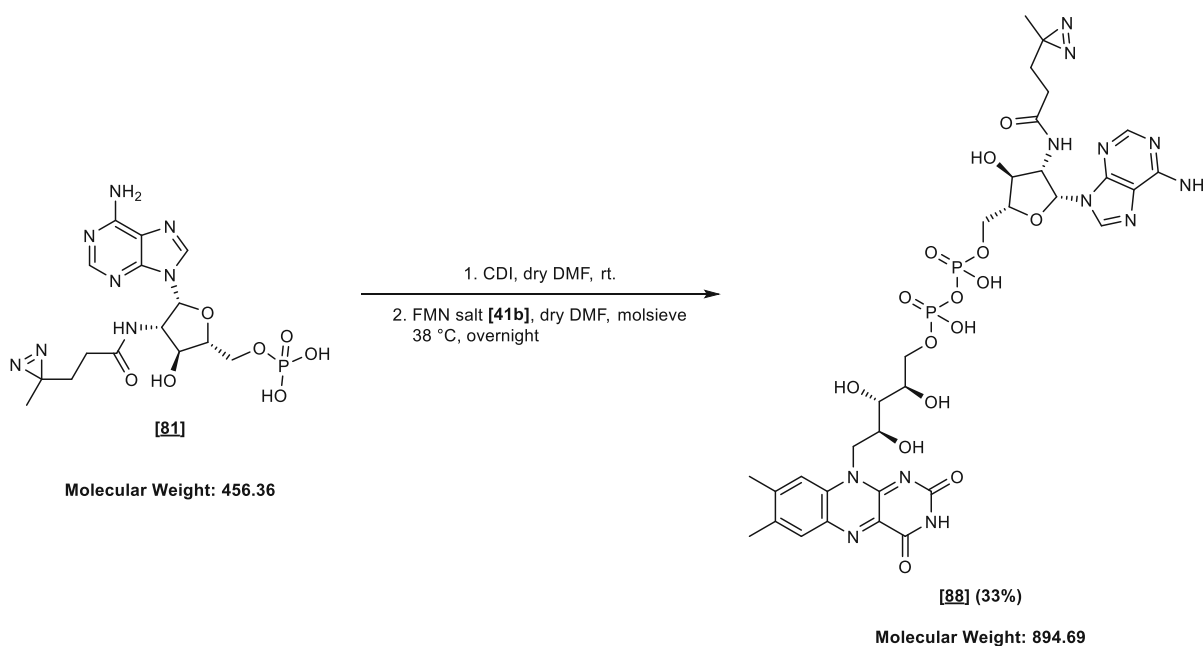
2H, H-A5a' & H-A5b'), 4.25 – 4.32 (m, 2H, H-F2' & H-F5'a), 4.36 (d,  $J = 4.6$  Hz, 1H, H-A4'), 4.38 – 4.44 (m, 2H, H-A3' & H-F1'b), 4.91 (t,  $J = 12.3$  Hz, 1H, H-F1'a), 5.77 (d,  $J = 8.5$  Hz, 1H, H-1A'), 7.55 (s, 1H, H-F9), 7.57 (s, 1H, H-F6), 7.84 (s, 1H, H-A2), 8.33 (s, 1H, H-A8) ppm.

$^{13}\text{C-NMR}$  (151 MHz,  $\text{D}_2\text{O}$ )  $\delta = 18.1$  (q,  $\text{CH}_3$  (aliphatic linker)), 18.6 (q,  $\text{CH}_3$ -F7), 20.7 (q,  $\text{CH}_3$ -F8), 25.5 (s, diazirine), 29.1 (t,  $-\underline{\text{C}}\text{H}_2\text{-CH}_2\text{-CONH-}$ ), 29.5 (t,  $-\text{CH}_2\text{-}\underline{\text{C}}\text{H}_2\text{-CONH-}$ ), 47.3 (d, C-F1'), 56.8 (d, C-A2'), 65.6 (t, C-A5'), 67.7 (t, C-F5'), 69.4 (d, C-F2'), 70.3 (d, C-A3'), 71.2 (d/d,  $^3J_{\text{CP}} = 7.1$  Hz, C-F4'), 72.6 (d, C-F3'), 85.2 (d, C-A1'), 85.4 (d/d,  $^3J_{\text{CP}} = 8.6$  Hz, C-A4'), 116.5 (d, C-F9), 117.7 (s, C-A5), 130.2 (d, C-F6), 131.3 (s, C-F7), 133.9 (s, C-F4a), 134.3 (s, C-F5a), 139.1 (s, C-F9a), 140.0 (d, C-A8), 148.2 (s, C-A4), 149.9 (s, C-F10a), 150.5 (s, C-F8), 150.9 (d, C-A2), 153.9 (s, C-A6), 157.8 (s, C-F2), 161.2 (s, C-F4), 175.1 (s, carbonyl (amide)) ppm.

$^{31}\text{P-NMR}$  (243 MHz,  $\text{D}_2\text{O}$ )  $\delta = -11.23$  (d,  $J_{\text{PP}} = 21.7$  Hz,  $\text{R}^{\text{flavin}}\text{-}\underline{\text{P}}\text{O}_3\text{-O-}\underline{\text{P}}\text{O}_3\text{-R}^{\text{adenosine}}$ ),  $-10.57$  (d,  $J_{\text{PP}} = 21.6$  Hz,  $\text{R}^{\text{flavin}}\text{-}\underline{\text{P}}\text{O}_3\text{-O-}\underline{\text{P}}\text{O}_3\text{-R}^{\text{adenosine}}$ ) ppm.

**Optical rotation**  $[\alpha]_{\text{D}}^{20} = -41.9$  ( $c = 0.5$ ,  $\text{H}_2\text{O}$ )

## E IV.11.2 ((2*R*,3*S*,4*S*,5*R*)-5-(6-Amino-9*H*-purin-9-yl)-3-hydroxy-4-(3-(3-methyl-3*H*-diazirin-3-yl)propanamido)tetrahydrofuran-2-yl)methyl dihydrogen phosphate [88]

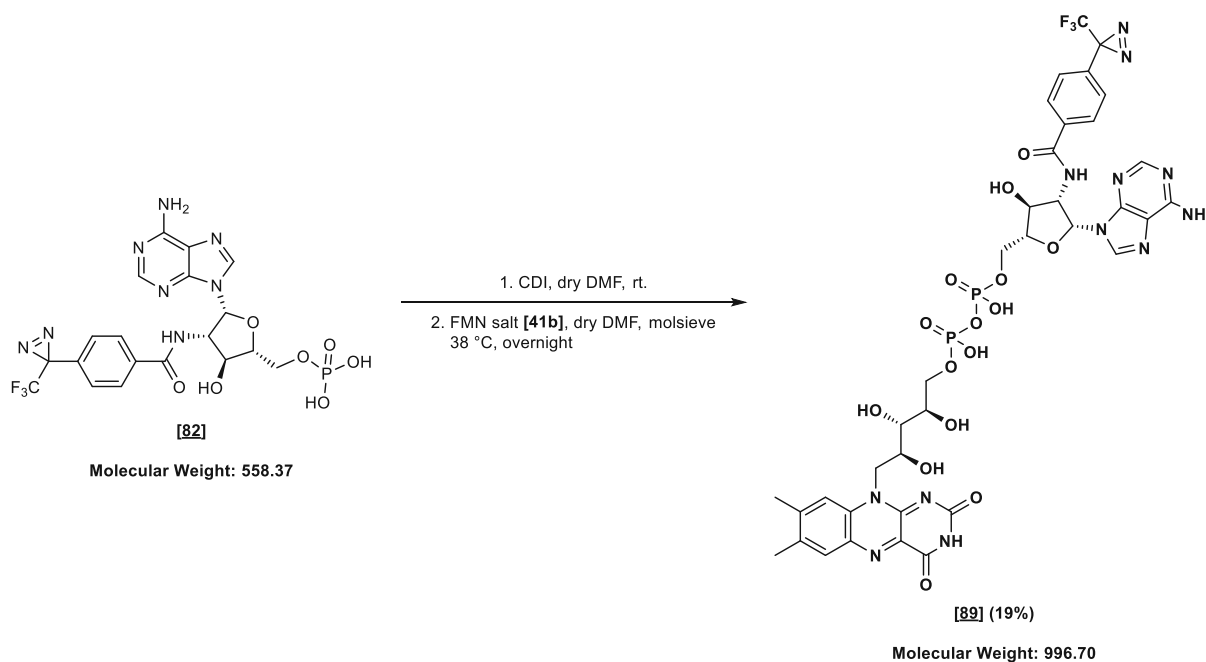


((2*R*,3*S*,4*S*,5*R*)-5-(6-Amino-9*H*-purin-9-yl)-3-hydroxy-4-(3-(3-methyl-3*H*-diazirin-3-yl)propanamido)tetrahydrofuran-2-yl)methyl dihydrogen phosphate **[88]** was synthesized according to general procedure F using protected adenosine **[81]** (100 mg, 219  $\mu\text{mol}$ , 1.00 equiv.). The pure product was obtained after purification by preparative revers-phase HPLC (2.5 mM  $\text{NH}_4^+\text{HCOO}^-$ -buffer [Solvent A]/acetonitrile [Solvent B]) and lyophilization as a yellow-orange powder.

<b>Yield</b>	33% (64 mg, 72 $\mu\text{mol}$ )
<b>Appearance</b>	yellow-orange powder
<b>Melting point</b>	> 199 °C (decomposition)
<b>Sum formula</b>	$\text{C}_{32}\text{H}_{40}\text{N}_{12}\text{O}_{15}\text{P}_2$
<b>HR-MS</b>	[M-H] <sup>-</sup> : calculated: 893.2138 Da, found: 893.2111 Da, difference: -3.11 ppm
<b><sup>1</sup>H-NMR (600 MHz, D<sub>2</sub>O)</b>	$\delta = 0.65$ (s, 3H, CH <sub>3</sub> (aliphatic linker)), 0.91 (dt, $J = 15.2, 7.8$ Hz, 1H, -CH <sub>2</sub> -CH <sub>2</sub> -CONH-), 1.16 (ddd, $J = 14.5, 7.7, 6.6$ Hz, 1H, -CH <sub>2</sub> -CH <sub>2</sub> -CONH-), 1.52 (ddd, $J = 13.5, 8.6, 7.0$ Hz, 1H, -CH <sub>2</sub> -CH <sub>2</sub> -CONH-), 1.75 (ddd, $J = 14.7, 7.9, 6.5$ Hz, 1H, -CH <sub>2</sub> -CH <sub>2</sub> -CONH-), 2.34 (s, 3H, CH <sub>3</sub> -CF7), 2.47 (s, 3H, CH <sub>3</sub> -CF8), 3.96 (dd, $J = 7.8, 3.9$ Hz, 1H, H-F3'), 4.08 – 4.20 (m, 3H, H-A4' & H-F4' & H-F5'b), 4.29 – 4.42 (m, 3H, H-A5'a & H-A5'b & H-F5'a), 4.41 – 4.52 (m, 3H, H-A3' & H-F1'b & H-F2'), 4.68 (dd, $J = 8.9, 6.9$ Hz, 1H, H-A2'), 4.95 (d, $J = 12.3$ Hz, 1H, H-F1'a), 6.15 (d, $J = 7.0$ Hz, 1H, H-A1'), 7.50 (s, 1H, H-F9), 7.62 (s, 1H, H-F6), 7.92 (s, 1H, H-A2), 8.26 (s, 1H, H-A8) ppm.
<b><sup>13</sup>C-NMR (151 MHz, D<sub>2</sub>O)</b>	$\delta = 18.1$ (q, CH <sub>3</sub> (aliphatic linker)), 18.6 (q, CH <sub>3</sub> -F7), 20.8 (q, CH <sub>3</sub> -F8), 25.5 (s, diazirine), 28.9 (t, -CH <sub>2</sub> -CH <sub>2</sub> -CONH-), 29.2 (t, -CH <sub>2</sub> -CH <sub>2</sub> -CONH-), 47.2 (t, C-F1'), 58.0 (d, C-A2'), 63.4 (t/d, $^2J_{CP} = 5.3$ Hz, C-F5'), 67.8 (t, C-A5'), 69.4 (d, C-F2'), 69.9 (d, C-A3'), 71.0 (d, C-F4'), 72.8 (d, C-F3'), 80.67 (d/d, $^3J_{CP}$ d, $J = 8.3$ Hz, C-A4'), 82.3 (d, C-A1'), 116.6 (d, C-F9), 117.6 (s, C-A5), 130.3 (d, C-F6), 131.3 (s, C-F7), 133.8 (s, C-F4a), 134.2 (s, C-F5a), 139.2 (s, C-F9a), 140.3 (d, C-A8), 147.7 (s, C-A4), 149.8 (s, C-F10a), 150.6 (s, C-F8), 151.1 (d, C-A2), 154.0 (s, C-A6), 157.7 (s, C-F2), 161.0 (s, C-F4), 175.1 (s, carbonyl (amide)) ppm.
<b><sup>31</sup>P-NMR (162 MHz, D<sub>2</sub>O)</b>	$\delta = -11.11$ (d, $J_{PP} = 21.7$ Hz, R <sup>flavin</sup> -PO <sub>3</sub> -O-PO <sub>3</sub> -R <sup>adenosine</sup> ), -10.62 (d, $J_{PP} = 21.6$ Hz, R <sup>flavin</sup> -PO <sub>3</sub> -O-PO <sub>3</sub> -R <sup>adenosine</sup> ) ppm.
<b>Optical rotation</b>	$[\alpha]_{\text{D}}^{20} = -70.2$ (c = 0.5, H <sub>2</sub> O)



## E IV.11.3 ((2*R*,3*S*,4*S*,5*R*)-5-(6-Amino-9*H*-purin-9-yl)-3-hydroxy-4-(4-(3-(trifluoromethyl)-3*H*-diazirin-3-yl)benzamido)tetrahydrofuran-2-yl)methyl dihydrogen phosphate [89]



((2*R*,3*S*,4*S*,5*R*)-5-(6-Amino-9*H*-purin-9-yl)-3-hydroxy-4-(4-(3-(trifluoromethyl)-3*H*-diazirin-3-yl)benzamido)tetrahydrofuran-2-yl)methyl dihydrogen phosphate [89] was synthesized according to general procedure F using adenosine monophosphate [82] (160 mg, 287  $\mu\text{mol}$ , 1.00 equiv.). The pure product was obtained after purification by preparative reverse-phase HPLC (2.5 mM  $\text{NH}_4^+\text{HCOO}^-$ -buffer [Solvent A]/acetonitrile [Solvent B]) and lyophilization as a yellow-orange powder.

<b>Yield</b>	19% (53 mg, 53 $\mu\text{mol}$ )
<b>Appearance</b>	yellow-orange powder
<b>Melting point</b>	> 209 °C (decomposition)
<b>Sum formula</b>	$\text{C}_{36}\text{H}_{37}\text{F}_3\text{N}_{12}\text{O}_{15}\text{P}_2$
<b>HR-MS</b>	[M-H] <sup>-</sup> : calculated: 995.1856 Da, found: 995.1856 Da, difference: -0.64 ppm
<b><sup>1</sup>H-NMR (600 MHz, D<sub>2</sub>O)</b>	$\delta$ = 2.35 (s, 3H, CH <sub>3</sub> -F7), 2.44 (s, 3H, CH <sub>3</sub> -F8), 3.90 (dd, $J$ = 8.6, 3.4 Hz, 1H, H-F3'), 4.07 (dt, $J$ = 11.0, 7.5 Hz, 1H, H-F5'b), 4.14 (td, $J$ = 8.7, 7.8, 2.5 Hz, 1H, H-F4'), 4.19 – 4.24 (m, 1H, H-A4'), 4.31 – 4.42 (m, 3H, H-A5'b & H-F5a' & H-F2'), 4.48 (t, $J$ = 14.9

Hz, 2H, H-A5'a & H-F1'b), 4.59 (t,  $J = 8.9$  Hz, 1H, H-A3'), 4.92 (dd,  $J = 9.2, 6.8$  Hz, 2H, H-A2' & H-F1'a), 6.18 (d,  $J = 6.8$  Hz, 1H, H-A1'), 6.96 (d,  $J = 8.5$  Hz, 2H, H-3ar & H-5ar), 6.99 (d,  $J = 8.3$  Hz, 2H, H-2ar & H-6ar), 7.59 (s, 1H, H-F6), 7.60 (s, 1H, H-F9), 7.70 (s, 1H, H-A2), 8.34 (s, 1H, H-A8). ppm.

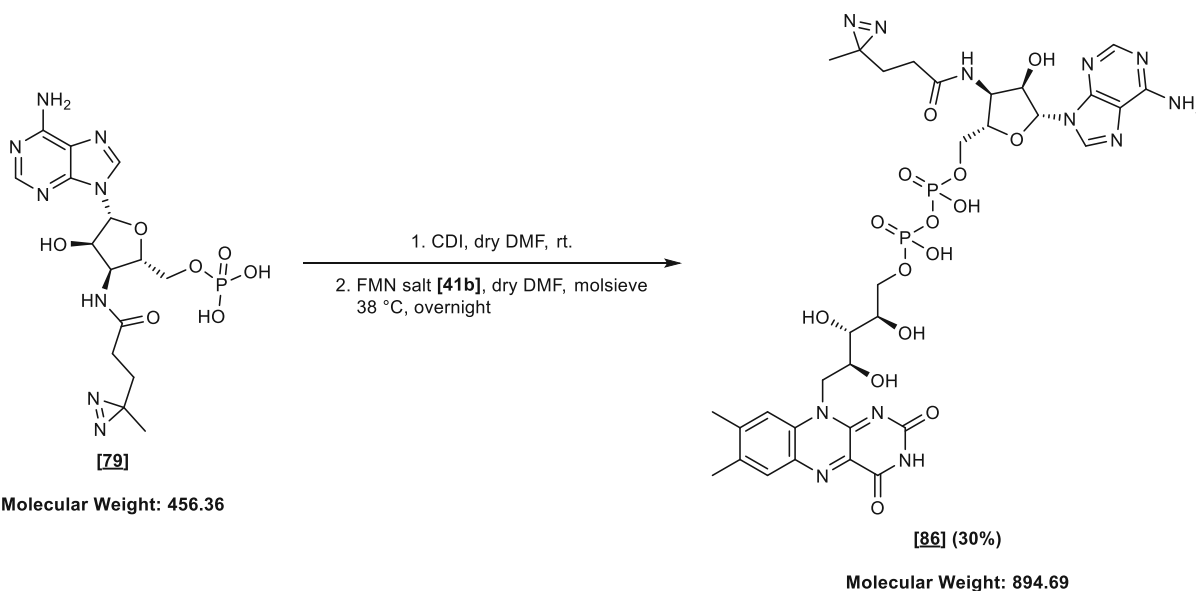
**$^{13}\text{C-NMR}$  (151 MHz,  $\text{D}_2\text{O}$ )**  $\delta = 18.5$  (q,  $\text{CH}_3\text{-F7}$ ), 20.7 (q,  $\text{CH}_3\text{-F8}$ ), 28.1 (s/q,  $^2J_{\text{CF}} = 40.5$ , Hz, diazirine), 47.0 (t, C-F1'), 58.5 (d, C-A2'), 63.2 (t, C-A5'), 68.0 (t/d,  $^2J_{\text{CP}} = 5.0$  Hz, C-F5'), 68.7 (d, C-A3'), 69.3 (d, C-F2'), 70.9 (d/d,  $^3J_{\text{CP}} = 6.3$  Hz, C-F4'), 72.8 (d, C-F3'), 80.9 (d/d,  $^3J_{\text{CP}} = 8.6$  Hz, C-A4'), 82.8 (d, C-A1'), 116.4 (d, C-F9), 117.6 (s, C-A5), 121.5 (s/q,  $^1J_{\text{CF}} = 274.1$  Hz,  $\text{CF}_3$ ), 126.2 (d, C-2ar & C-6ar), 126.8 (d, C-2ar & C-6ar), 130.4 (d, C-F6), 131.4 (s, C-F7), 132.3 (s, C-1ar), 133.2 (s, C-4ar), 134.0 (s, C-F4a), 134.5 (s, C-F5a), 139.1 (s, C-F9a), 139.9 (d, C-A8), 147.6 (s, C-A4), 149.9 (s, C-F10a), 150.6 (s, C-F8), 151.7 (d, C-A2), 154.3 (s, C-A6), 157.8 (s, F-2), 161.40 (s, F-4), 169.6 (s, carbonyl (amide)) ppm.

**$^{19}\text{F NMR}$  (565 MHz,  $\text{D}_2\text{O}$ )**  $\delta = -65.46$  ppm.

**$^{31}\text{P-NMR}$  (162 MHz,  $\text{D}_2\text{O}$ )**  $\delta = -11.13$  (d,  $J_{\text{PP}} = 21.7$  Hz,  $\text{R}^{\text{flavin}}\text{-}\underline{\text{P}}\text{O}_3\text{-O-}\underline{\text{P}}\text{O}_3\text{-R}^{\text{adenosine}}$ ),  $-10.59$  (d,  $J_{\text{PP}} = 21.6$  Hz,  $\text{R}^{\text{flavin}}\text{-}\underline{\text{P}}\text{O}_3\text{-O-}\underline{\text{P}}\text{O}_3\text{-R}^{\text{adenosine}}$ ) ppm.

**Optical rotation**  $[\alpha]_{\text{D}}^{20} = -43.5$  (c = 0.25,  $\text{H}_2\text{O}$ )

**E IV.11.4((2*S*,3*S*,4*R*,5*R*)-5-(6-Amino-9*H*-purin-9-yl)-4-hydroxy-3-(3-(3-methyl-3*H*-diazirin-3-yl)propanamido)tetrahydrofuran-2-yl)methyl dihydrogen phosphate [86]**



((2*S*,3*S*,4*R*,5*R*)-5-(6-Amino-9*H*-purin-9-yl)-4-hydroxy-3-(3-(3-methyl-3*H*-diazirin-3-yl)propanamido)tetrahydrofuran-2-yl)methyl dihydrogen phosphate **[86]** was synthesized according to general procedure F using adenosine monophosphate **[79]** (330 mg, 0.72 mmol, 1.00 equiv.). The pure product was obtained after purification by preparative reverse-phase HPLC (2.5 mM NH<sub>4</sub><sup>+</sup>HCOO<sup>-</sup>-buffer [Solvent A]/acetonitrile [Solvent B]) and lyophilization as a yellow-orange powder.

<b>Yield</b>	30% (194 mg, 217 μmol)
<b>Appearance</b>	yellow-orange powder
<b>Melting point</b>	> 230 °C (decomposition)
<b>Sum formula</b>	C <sub>32</sub> H <sub>40</sub> N <sub>12</sub> O <sub>15</sub> P <sub>2</sub>
<b>HR-MS</b>	[M-H] <sup>-</sup> : calculated: 893.2138 Da, found: 893.2121 Da, difference: -2.02 ppm

<sup>1</sup>H-NMR (600 MHz, D<sub>2</sub>O) δ = 1.02 (s, 3H, CH<sub>3</sub> (aliphatic linker), ), 1.70 (td, *J* = 7.7, 7.6, 3.5 Hz, 2H, -CH<sub>2</sub>-CH<sub>2</sub>-CONH-), 2.27 (h, *J* = 7.6 Hz, 2H, -CH<sub>2</sub>-CH<sub>2</sub>-CONH-), 2.33 (s, 4H, CH<sub>3</sub>-CF<sub>7</sub>), 2.40 (s, 3H, CH<sub>3</sub>-CF<sub>8</sub>), 3.91 (dd, *J* = 7.9, 4.2 Hz, 1H, H-F3'), 4.02 – 4.10 (m, 2H, H-F4' & H-F5'b), 4.22 – 4.38 (m, 3H, H-A5'b & H-F2' & H-F5'a), 4.43 (dd,

$J = 30.5, 11.6$  Hz, 3H, H-A4' & H-A5'a & H-F1'b), 4.55 (dd,  $J = 8.1, 5.6$  Hz, 2H, H-A2' & H-A3'), 4.84 – 4.90 (m, 1H, H-F1'a), 5.85 (d,  $J = 2.6$  Hz, 1H, H-A1'), 7.57 (s, 1H, H-F9), 7.61 (s, 1H, H-F6), 7.88 (s, 1H, H-A2), 8.34 (s, 1H, H-A8) ppm.

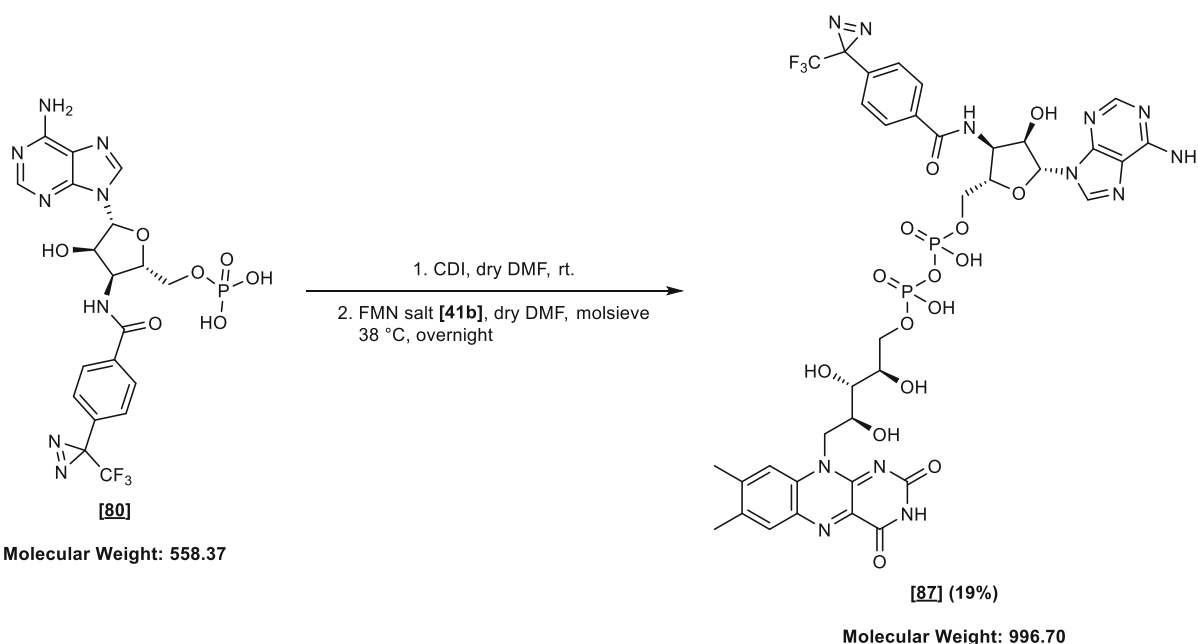
$^{13}\text{C-NMR}$  (151 MHz,  $\text{D}_2\text{O}$ )  $\delta = 18.5$  (q,  $\text{CH}_3\text{-F7}$ ), 18.5 (q,  $\text{CH}_3$  (aliphatic linker)), 20.7 (q,  $\text{CH}_3\text{-F8}$ ), 26.2 (s, diazirine), 29.7 (t,  $-\underline{\text{C}}\text{H}_2\text{-CH}_2\text{-CONH-}$ ), 30.0 (t,  $-\text{CH}_2\text{-}\underline{\text{C}}\text{H}_2\text{-CONH-}$ ), 47.3 (t, C-F1'), 50.9 (d, C-A3'), 65.0 (t, C-A5'), 67.7 (t, C-F5') 69.3 (d, C-F2'), 71.1 (d/d,  $^3J_{\text{CP}} = 6.5$  Hz, C-F4'), 72.4 (d, C-F3'), 73.8 (d, C-A2'), 80.8 (d/d,  $^3J_{\text{CP}} = 8.5$  Hz, C-A4'), 89.3 (d, C-A1'), 116.5 (d, C-F9), 130.4 (d, C-F6), 131.5 (s, C-F7), 133.9 (s, C-F4a), 134.5 (s, C-F5a), 139.0 (s, C-F9a), 139.2 (d, C-A8), 147.5 (s, C-F10a), 149.9 (s, C-F8), 151.6 (d, C-A2), 154.3 (s, C-A6), 157.7 (s, C-F2), 161.2 (s, C-F4), 175.7 (s, carbonyl (amide)) ppm.

$^{31}\text{P-NMR}$  (162 MHz,  $\text{D}_2\text{O}$ )  $\delta = -11.25$  (d,  $J_{\text{PP}} = 21.7$  Hz,  $\text{R}^{\text{flavin}}\text{-}\underline{\text{P}}\text{O}_3\text{-O-}\underline{\text{P}}\text{O}_3\text{-R}^{\text{adenosine}}$ ),  $-10.53$  (d,  $J_{\text{PP}} = 21.6$  Hz,  $\text{R}^{\text{flavin}}\text{-}\text{P}\text{O}_3\text{-O-}\underline{\text{P}}\text{O}_3\text{-R}^{\text{adenosine}}$ ) ppm.

**Optical rotation**  $[\alpha]_{\text{D}}^{20} = -9.7$  ( $c = 0.5$ ,  $\text{H}_2\text{O}$ )

**Comment** The C-A5 peak was not detected in the ATP spectrum.

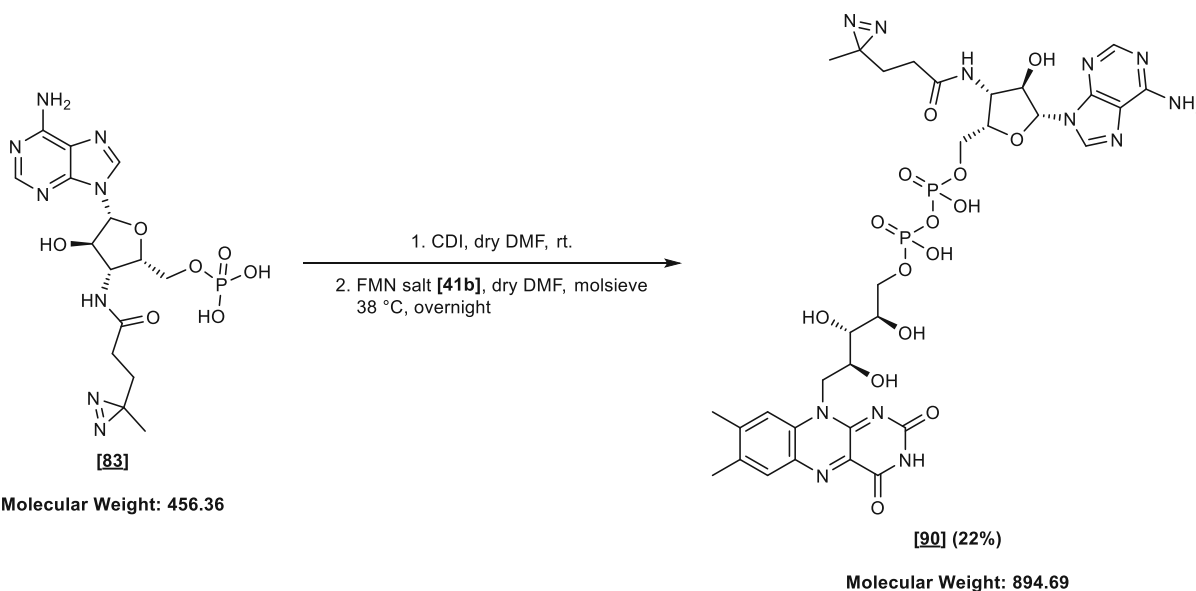
## E IV.11.5 ((2*S*,3*S*,4*R*,5*R*)-5-(6-Amino-9*H*-purin-9-yl)-4-hydroxy-3-(4-(3-(trifluoromethyl)-3*H*-diazirin-3-yl)benzamido)tetrahydrofuran-2-yl)methyl dihydrogen phosphate [87]



((2*S*,3*S*,4*R*,5*R*)-5-(6-Amino-9*H*-purin-9-yl)-4-hydroxy-3-(4-(3-(trifluoromethyl)-3*H*-diazirin-3-yl)benzamido)tetrahydrofuran-2-yl)methyl dihydrogen phosphate [87] was synthesized according to general procedure F using adenosine monophosphate [80] (140 mg, 0.25 mmol, 1.00 equiv.). The pure product was obtained after purification by preparative reverse-phase HPLC (2.5 mM NH<sub>4</sub><sup>+</sup>HCOO<sup>-</sup>-buffer [Solvent A]/acetonitrile [Solvent B]) and lyophilization as a yellow-orange powder.

<b>Yield</b>	19% (47 mg, 47 μmol)
<b>Appearance</b>	yellow-orange powder
<b>Melting point</b>	> 214 °C (decomposition)
<b>Sum formula</b>	C <sub>36</sub> H <sub>37</sub> F <sub>3</sub> N <sub>12</sub> O <sub>15</sub> P <sub>2</sub>
<b>HR-MS</b>	[M-H] <sup>-</sup> : calculated: 995.1856 Da, found: 995.1862 Da, difference: 0.64 ppm
<b><sup>1</sup>H-NMR (600 MHz, D<sub>2</sub>O)</b>	δ = 2.31 (s, 3H, CH <sub>3</sub> -C-F7), 2.40 (s, 3H, CH <sub>3</sub> -C-F8), 3.93 (dd, <i>J</i> = 7.9, 4.4 Hz, 1H, H-F3'), 4.03 – 4.08 (m, 1H, H-F4'), 4.08 – 4.13 (m, 1H, H-F5'b), 4.27 – 4.37 (m, 3H, H-A5'b & H-F2' & H-F5'a), 4.40 – 4.44 (m, 1H, H-A5'a), 4.49 (d, <i>J</i> = 13.8 Hz, 1H, H-F1'b), 4.59 (s, 1H, H-A4'), 4.90 (s, 1H, H-F1'), 6.03 (d, <i>J</i> = 2.5 Hz, 1H, H-A1'), 7.16 (d, <i>J</i> = 8.0 Hz, 2H, H-3ar & H-5ar), 7.60 (s, 1H, C-F6), 7.62 (s, 1H, C-F9), 7.70 (d, <i>J</i> = 8.2 Hz, 2H, H-2ar & H-6ar), 8.10 (s, 1H, H-A2), 8.47 (s, 1H, H-A8).ppm.
<b><sup>13</sup>C-NMR (151 MHz, D<sub>2</sub>O)</b>	δ = 18.7 (q, CH <sub>3</sub> -F7), 20.8 (q, CH <sub>3</sub> -F8), 28.3 (s/q, <sup>2</sup> <i>J</i> <sub>CF</sub> = 40.6 Hz, diazirine), 47.4 (t, C-F1'), 52.1 (d, C-A3'), 65.4 (t, C-A5'), 67.7 (t/d, <sup>2</sup> <i>J</i> <sub>CP</sub> = 4.6 Hz, C-F5'), 69.4 (d, C-F2'), 71.3 (d/d, <sup>3</sup> <i>J</i> <sub>CP</sub> = 7.1 Hz, C-F4'), 72.6 (d, C-F3'), 74.0 (d, C-A2'), 81.1 (d/d, <sup>3</sup> <i>J</i> <sub>CP</sub> = 8.7 Hz, C-A4'), 89.4 (d, C-A1'), 116.7 (d, C-F9), 118.3 (s, C-A5), 121.8 (s/q, <sup>1</sup> <i>J</i> <sub>CF</sub> = 274.4 Hz, CF <sub>3</sub> ), 126.4 (d, C-3ar & C-5ar), 127.8 (d, C-2ar & C-6ar), 130.5 (d, C-F6), 131.7 (s, C-F7), 132.5 (s, C-1ar), 134.0 (s, C-4ar), 134.0 (s, C-F4a), 134.3 (s, C-F5a), 139.2 (s, C-F9a), 140.5 (d, C-A8), 147.9 (s, C-A4), 149.4 (d, C-A2), 150.0 (s, C-F4a), 150.6 (s, C-F10a), 152.9 (s, C-A6), 157.8 (s, C-F2), 161.2 (s, C-F4), 169.7 (s, carbonyl (amide)) ppm.
<b><sup>19</sup>F NMR (565 MHz, D<sub>2</sub>O)</b>	δ = -65.21 ppm.
<b><sup>31</sup>P-NMR (243 MHz, D<sub>2</sub>O)</b>	δ = -11.26 (d, <i>J</i> <sub>PP</sub> = 18.7 Hz, R <sup>flavin</sup> -P <sub>3</sub> -O-P <sub>3</sub> -R <sup>adenosine</sup> ), -10.52 (d, <i>J</i> <sub>PP</sub> = 20.6 Hz, R <sup>flavin</sup> -P <sub>3</sub> -O-P <sub>3</sub> -R <sup>adenosine</sup> ) ppm.
<b>Optical rotation</b>	[α] <sub>D</sub> <sup>20</sup> = -54.0 (c = 0.25, H <sub>2</sub> O)

## E IV.11.6((2*S*,3*R*,4*R*,5*R*)-5-(6-Amino-9*H*-purin-9-yl)-4-hydroxy-3-(3-(3-methyl-3*H*-diazirin-3-yl)propanamido)tetrahydrofuran-2-yl)methyl dihydrogen phosphate [90]



((2*S*,3*R*,4*R*,5*R*)-5-(6-Amino-9*H*-purin-9-yl)-4-hydroxy-3-(3-(3-methyl-3*H*-diazirin-3-yl)propanamido)tetrahydrofuran-2-yl)methyl dihydrogen phosphate **[90]** was synthesized according to general procedure F using protected adenosine **[83]** (250 mg, 0.55 mmol, 1.00 equiv.). The pure product was obtained after purification by preparative reverse-phase HPLC (2.5 mM NH<sub>4</sub><sup>+</sup>HCOO<sup>-</sup>-buffer [Solvent A]/acetonitrile [Solvent B]) and lyophilization as a yellow-orange powder.

<b>Yield</b>	22% (110 mg, 123 μmol)
<b>Appearance</b>	yellow-orange powder
<b>Melting point</b>	> 205 °C (decomposition; at > 158 °C color change to black)
<b>Sum formula</b>	C <sub>32</sub> H <sub>40</sub> N <sub>12</sub> O <sub>15</sub> P <sub>2</sub>
<b>HR-MS</b>	[M-H] <sup>-</sup> : calculated: 893.2138 Da, found: 893.2119 Da, difference: -2.18 ppm

**<sup>1</sup>H-NMR (600 MHz, D<sub>2</sub>O)** δ = 1.02 (s, 3H, CH<sub>3</sub> (aliphatic linker)), 1.71 (td, *J* = 7.4, 7.3, 1.7 Hz, 2H, -CH<sub>2</sub>-CH<sub>2</sub>-CONH-), 2.16 – 2.42 (m, 8H, -CH<sub>2</sub>-CH<sub>2</sub>-CONH- & CH<sub>3</sub>-C-F8 & CH<sub>3</sub>-C-F7), 3.95 (dd, *J* = 7.5, 4.7 Hz, 1H, H-F3'), 4.02 (s, 1H, H-F4'), 4.08 – 4.15 (m, 2H, H-A5'b & H-F5'b), 4.17 – 4.22 (m, 1H, H-A5'a), 4.23 – 4.29 (m, 1H, H-F5'a), 4.33 (dd, *J* = 6.4, 3.5 Hz, 1H, H-F2'), 4.48 (d, *J* = 14.3 Hz, 1H, H-F1'b), 4.64 (dd, *J* = 8.1, 2.6 Hz, 1H, H-A4'), 4.70 – 4.77 (m, 2H,

H-A2' & H-A3'), 4.85 (d,  $J = 4.6$  Hz, 1H, H-F1'a), 5.88 (d,  $J = 6.5$  Hz, 1H, H-A1'), 7.48 (s, 1H, H-F9), 7.57 (s, 1H, H-F6), 7.96 (d,  $J = 1.3$  Hz, 1H, H-A2), 8.42 (s, 1H, H-A8) ppm.

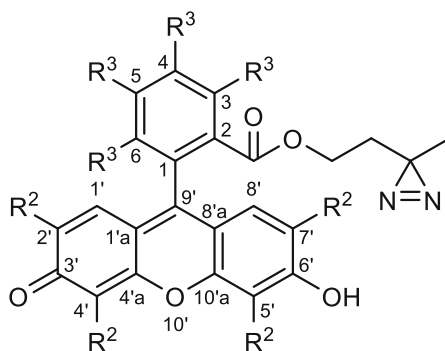
$^{13}\text{C-NMR}$  (151 MHz,  $\text{D}_2\text{O}$ )  $\delta = 18.7$  (q,  $\text{CH}_3$  (aliphatic linker)), 18.7 (q,  $\text{CH}_3\text{-CF7}$ ), 20.8 (1,  $\text{CH}_3\text{-CF8}$ ), 26.3 (s, diazirine), 29.8 (t,  $\text{-CH}_2\text{-CH}_2\text{-CONH-}$ ), 30.2 (t,  $\text{-CH}_2\text{-CH}_2\text{-CONH-}$ ), 47.7 (t, C-F1'), 55.2 (d, C-A3'), 64.8 (t/d,  $^2J_{\text{CP}} = 5.4$  Hz, C-A5'), 67.4 (t/d,  $^2J_{\text{CP}} = 5.6$  Hz, C-F5'), 69.4 (d, C-F2'), 71.2 (d/d,  $^3J_{\text{CP}} = 7.4$  Hz, C-F4'), 72.6 (d, C-F3'), 76.8 (d, C-A3'), 77.5 (d/d,  $^3J_{\text{CP}} = 9.1$  Hz, C-A4'), 86.4 (d, C-A1'), 116.7 (d, C-F9), 117.9 (s, C-A5), 130.3 (d, C-F6), 131.5 (s, C-F7), 133.8 (s, C-F4a), 134.3 (s, C-F5a), 139.2 (s, C-F9a), 140.2 (d, C-A8), 148.5 (s, C-A4), 149.9 (s, C-F10a), 150.6 (s, C-F8), 151.3 (d, C-A2), 154.0 (s, C-A6), 157.6 (s, C-F2), 161.0 (s, C-F4), 176.3 (s, carbonyl (amide)) ppm.

$^{31}\text{P-NMR}$  (243 MHz,  $\text{D}_2\text{O}$ )  $\delta = -11.16$  (d,  $J_{\text{PP}} = 20.5$  Hz,  $\text{R}^{\text{flavin}}\text{-PO}_3\text{-O-PO}_3\text{-R}^{\text{adenosine}}$ ),  $-10.38$  (d,  $J_{\text{PP}} = 20.6$  Hz,  $\text{R}^{\text{flavin}}\text{-PO}_3\text{-O-PO}_3\text{-R}^{\text{adenosine}}$ ) ppm.

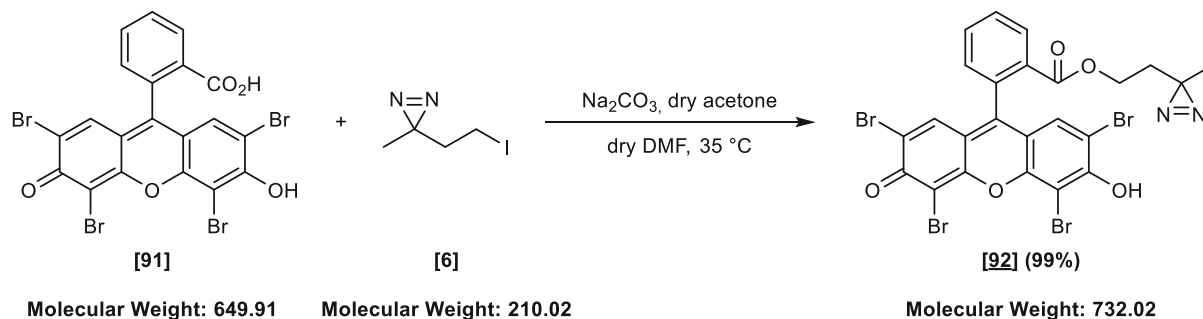
Optical rotation  $[\alpha]_{\text{D}}^{20} = -9.7$  ( $c = 0.5$ ,  $\text{H}_2\text{O}$ )

## E IV.12 Synthesis of fluorescent dyes containing a diazirine linker

The assignments of protons and carbon atoms in the NMR codes of compounds [92] and [94] were carried out as follows:



## E IV.12.1 2-(3-Methyl-3*H*-diazirin-3-yl)ethyl (2,4,5,7-tetrabromo-3,6-dihydroxy-9*H*-xanthen-9-yl)benzoate [92]



2-(3-Methyl-3*H*-diazirin-3-yl)ethyl 2-(2,4,5,7-tetrabromo-3,6-dihydroxy-9*H*-xanthen-9-yl)benzoate [92] was synthesized in analogy to a modified literature procedure.<sup>408</sup> An oven-dried 100 mL Schlenk-flask was flushed with argon using standard Schlenk technique. Eosin Y [91] (280.4 mg, 432.9  $\mu\text{mol}$ , 1.00 equiv.), dry DMF (30 mL) and dry acetone (50 mL) were added followed by the addition of  $\text{Na}_2\text{CO}_3$  (69 mg, 649.3  $\mu\text{mol}$ , 1.50 equiv.) and iodine [6] (100 mg, 476.2  $\mu\text{mol}$ , 1.10 equiv.). The reaction mixture was stirred overnight at room temperature in the dark, and the reaction progress was monitored by TLC analysis. After TLC analysis indicated full conversion of the starting material, the volatiles were removed, excess of 2 N aq. HCl solution was added and extracted with EtOAc (3 times, 100 mL). The combined organic phases were washed with water, dried over  $\text{MgSO}_4$ , filtrated, and evaporated to obtain the crude material, which was further purified by flash column chromatography (silica gel, solid load) using a gradient of MeOH in DCM (10% 5min; 10-20% 10 min; 20% 10min).

<b>Yield</b>	99% (314 mg, 430.1 $\mu\text{mol}$ )
<b>Appearance</b>	red/green crystals
<b>Melting point</b>	> 295 °C (decomposition; formation of bubbles and color change to black)
<b>TLC</b>	$R_f(\text{CHCl}_3/\text{MeOH} = 8/2) = 0.25$
<b>Sum formula</b>	$\text{C}_{24}\text{H}_{16}\text{Br}_4\text{N}_2\text{O}_5$
<b>HR-MS</b>	$[\text{M}+\text{H}]^+$ : calculated: 730.7670 Da, found: 730.7679 Da, difference: -1.2 ppm
<b><sup>1</sup>H-NMR (600 MHz, DMSO)</b>	$\delta = 0.87$ (s, 3H, $\text{CH}_3$ (aliphatic linker)), 1.51 (dd, $J = 6.3, 5.6$ Hz, 2H, $-\text{CH}_2-\text{CH}_2-\text{COOR}$ ), 3.90 (dd, $J = 6.3, 5.6$ Hz, 2H, $-\text{CH}_2-\text{CH}_2-\text{COOR}$ ), 6.94 (s, 2H, H-1' & H-8'), 7.52 (dd, $J = 7.6, 1.3$ Hz, 1H,





10-20% 10 min; 20% 10min) to obtain 2-(3-methyl-3*H*-diazirin-3-yl)ethyl 2,3,4,5-tetrachloro-6-(6-hydroxy-2,4,5,7-tetraiodo-3-oxo-9,9a-dihydro-3*H*-xanthen-9-yl)benzoate [94] as dark purple crystals.

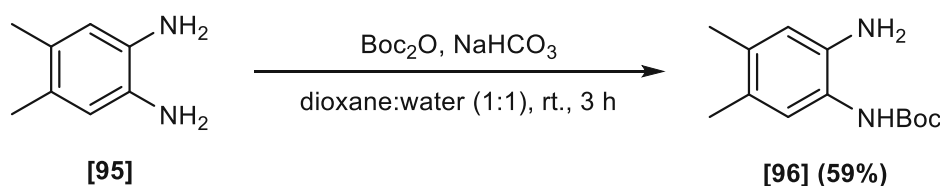
<b>Yield</b>	87% (397 mg, 374.84 mmol)
<b>Appearance</b>	dark purple crystals
<b>Melting point</b>	> 183 °C (decomposition; color change to black)
<b>TLC</b>	$R_f(\text{CHCl}_3/\text{MeOH} = 8/2) = 0.51$
<b>Sum formula</b>	$\text{C}_{24}\text{H}_{12}\text{Cl}_4\text{I}_4\text{N}_2\text{O}_5$
<b>HR-MS</b>	$[\text{M}+\text{H}]^+$ : calculated: 1056.5569 Da, found: 1056.5570 Da, difference: 0.1 ppm

**$^1\text{H-NMR}$  (600 MHz, DMSO)**  $\delta = 0.84$  (s, 3H,  $\text{CH}_3$  (aliphatic linker)), 1.35 (t,  $J = 6.2$  Hz, 2H,  $-\underline{\text{C}}\text{H}_2-\text{CH}_2-\text{COOR}$ ), 3.78 (t,  $J = 6.2$  Hz, 2H,  $-\text{CH}_2-\underline{\text{C}}\text{H}_2-\text{COOR}$ ), 7.49 (s, 2H, H-1' & H-8') ppm.

**$^{13}\text{C-NMR}$  (151 MHz, DMSO)**  $\delta = 19.3$  (q,  $\text{CH}_3$  (aliphatic linker)), 23.7 (s, diazirine), 32.2 (t,  $-\underline{\text{C}}\text{H}_2-\text{CH}_2-\text{COOR}$ ), 61.5 (t,  $-\text{CH}_2-\underline{\text{C}}\text{H}_2-\text{COOR}$ ), 76.0 (s, C-4' & C-5'), 97.4 (s, C-9'), 110.2 (s, C-1'a & C-8'a), 128.8 (s, C-2 or C-3 or C-4 or C-5 or C-6 or C-2' & C-7'), 130.0 (s, C-2 or C-3 or C-4 or C-5 or C-6 or C-2' & C-7'), 132.0 (s, C-2 or C-3 or C-4 or C-5 or C-6 or C-2' & C-7'), 133.4 (s, C-2 or C-3 or C-4 or C-5 or C-6 or C-2' & C-7'), 134.4 (s, C-2 or C-3 or C-4 or C-5 or C-6 or C-2' & C-7'), 135.1 (s, C-2 or C-3 or C-4 or C-5 or C-6 or C-2' & C-7'), 136.1 (d, C-1' & C-8'), 139.3 (s, C-1), 157.1 (s, C-4'a & C-10'a), 163.1 (s, carbonyl (ester)), 171.8 (s, C-3' & C-6') ppm.

## E IV.13 Synthesis of modified ribityl building block

### E IV.13.1 *tert*-Butyl (2-amino-4,5-dimethylphenyl)carbamate [96]



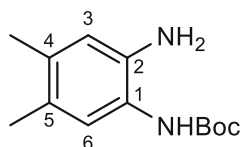
Molecular Weight: 136.20

Molecular Weight: 236.32

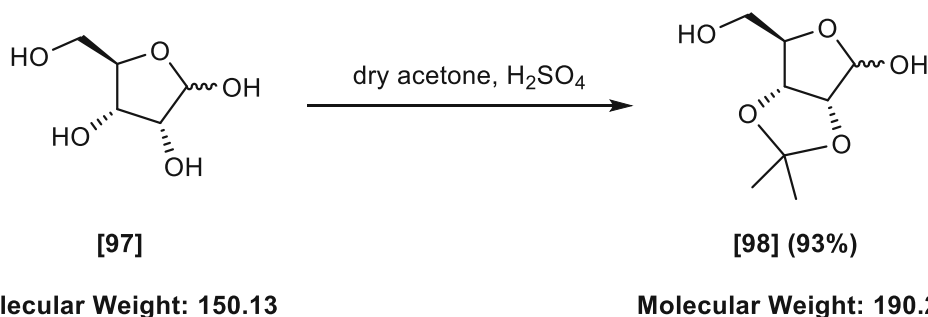
*tert*-Butyl (2-amino-4,5-dimethylphenyl)carbamate [96] was synthesized in analogy to a literature procedure. 4,5-Dimethylbenzene-1,2-diamine [95] (10.00 g, 73.00 mmol), di-*tert*-butyldicarbonate (16.00 g, 73.00 mmol, 1.0 equiv.) and NaHCO<sub>3</sub> (6.2 g, 83.40 mmol, 1.15 equiv.) were dissolved in a mixture of dioxane and water (1:1, total volume 1000 mL). The mixture was stirred for three hours at room temperature before dilution with additional water (1000 mL) and extraction into dichloromethane (200 mL, three times). Combined organic layers were washed with saturated aq. NaHCO<sub>3</sub> (500 mL) and brine (500 mL) and dried over MgSO<sub>4</sub>. The solvent was removed under reduced pressure, and the crude product was purified by flash column chromatography (silica, solid load; gradient of EtOAc in PE, 20-60% 30 min) yielding *tert*-butyl (2-amino-4,5-dimethylphenyl)carbamate [96] as a red-orange solid (10.18 g, 43.07 mmol, 59%).

<b>Yield</b>	59% (10.18 g, 43.07 mmol)
<b>Appearance</b>	red-orange solid
<b>TLC</b>	R <sub>f</sub> (PE/EtOAc = 4/1) = 0.20
<b>Melting point</b>	150 °C – 151 °C (Lit. <sup>374</sup> : 153 °C – 155 °C)
<b>Sum formula</b>	C <sub>13</sub> H <sub>20</sub> N <sub>2</sub> O <sub>2</sub>
<b><sup>1</sup>H-NMR (400 MHz, CDCl<sub>3</sub>)</b>	δ = 1.51 (s, 9H, <i>tert</i> butyl), 2.14 (d, <i>J</i> = 3.5 Hz, 6H, CH <sub>3</sub> -C4 & CH <sub>3</sub> -C5), 3.56 (s, 2H, NH <sub>2</sub> ), 6.16 (s, 1H, NHBoc), 6.58 (s, 1H, H-3), 7.03 (s, 1H, H-6) ppm.
<b><sup>13</sup>C-NMR (101 MHz, CDCl<sub>3</sub>)</b>	δ = 18.8 (q, CH <sub>3</sub> -C4 or CH <sub>3</sub> -C5), 19.3 (q, CH <sub>3</sub> -C4 or CH <sub>3</sub> -C5), 28.4 (q, C(CH <sub>3</sub> ) <sub>3</sub> ), 80.3 (s, C(CH <sub>3</sub> ) <sub>3</sub> ), 119.2 (d, C-3), 122.4 (s, C-1), 125.8 (s, C-5), 127.8 (d, C-6), 134.5 (s, C-4), 137.5 (s, C-2), 154.0 (s, carbonyl (Boc)) ppm.

The assignments of protons and carbon atoms in the NMR codes of compound [96] were carried out as follows:



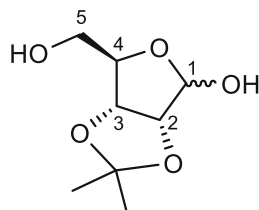
## E IV.13.2 (3a*R*,6*R*,6a*R*)-6-(Hydroxymethyl)-2,2-dimethyltetrahydrofuro[3,4-*d*][1,3]dioxol-4-ol [98]



(3a*R*,6*R*,6a*R*)-6-(Hydroxymethyl)-2,2-dimethyltetrahydrofuro[3,4-*d*][1,3]dioxol-4-ol [98] was prepared following a literature procedure.<sup>445</sup> D-ribose [97] (5.00 g, 33.30 mmol, 1.00 equiv.) was placed in a 250 mL three-neck-round bottom flask, and dry acetone (130 mL) was added. The resulting suspension was cooled to 0 °C using an ice bath and conc. sulfuric acid (90 μL) was added. The reaction mixture was stirred for 10 min at 0 °C and was then allowed to warm up to room temperature. After TLC indicated full conversion of the starting material (3 hours), solid sodium bicarbonate was added in portions to adjust the pH to neutral. The resulting solids were filtered over a short pad of celite, and the filter cake was washed with acetone. The volatiles were further removed under reduced pressure to obtain (3a*S*,6a*S*)-6-(hydroxymethyl)-2,2-dimethyltetrahydrofuro[3,4-*d*][1,3]dioxol-4-ol [98] as a slightly yellow viscous oil (5.90 g, 93%).

<b>Yield</b>	93% (5.90 g, 31.02 mmol)
<b>Appearance</b>	pale yellow viscous oil
<b>TLC</b>	R <sub>f</sub> (PE/EtOAc = 1/1) = 0.3
<b>Sum formula</b>	C <sub>8</sub> H <sub>14</sub> O <sub>5</sub>
<b><sup>1</sup>H-NMR (400 MHz, CDCl<sub>3</sub>)</b>	δ = 1.33 (s, 3H, CH <sub>3</sub> ), 1.49 (s, 3H, CH <sub>3</sub> ), 3.76 (dd, <i>J</i> = 10.8, 2.6 Hz, 2H, H-5'a & H-5'b), 4.42 (t, <i>J</i> = 2.4 Hz, 1H, H-4'), 4.60 (d, <i>J</i> = 5.9 Hz, 1H, H-2'), 4.86 (d, <i>J</i> = 5.9 Hz, 1H, H-3'), 5.43 (s, 1H, H-1') ppm.
<b><sup>13</sup>C-NMR (101 MHz, CDCl<sub>3</sub>)</b>	δ = 24.9 (q, CH <sub>3</sub> ), 26.5 (q, CH <sub>3</sub> ), 64.0 (d, C-5'), 81.9 (d, C-3'), 87.1 (d, C-2'), 88.1 (d, C-4'), 103.4 (d, C-1'), 112.3 (s, C(CH <sub>3</sub> ) <sub>2</sub> ) ppm.
<b>Comment</b>	Spectral data are in accordance with the literature. <sup>446</sup>

The assignments of protons and carbons in the NMR codes of compound [98] were carried out as follows:



# F Appendix

# F I Curriculum vitae



## Clemens Maximilian Cziegler

\*26.10.1991

📍 Feldmühlgasse 15, 1130 Wien

☎ +43 660 4911804

✉ clemens.cziegler@tuwien.ac.at



### Education

#### Skills

Problem Solving

Teamwork

Innovative ability

Time management

#### Chemistry

Organic synthesis

Purification methods

Analysis (NMR, HPLC, GC)

Biocatalysis

Biotransformation

Protein expression

Protein purification

#### Languages

German

English

#### Computing

MS Office

Origin

ChemDoodle

ChemDraw

MestreNova

AdobePhotoshop

#### Other Matters / Interests

Driving license B / Cycling,  
Tennis, Hiking, Cooking,  
Photography



### Employment History

- 09/2022-10/2018 Ph.D. Chemistry, TU Wien, in the Bioorganic Synthetic Chemistry group of Prof. Mihovilovic and Assoc. Prof. Rudroff
- 09/2018-04/2016 MSc. Chemistry, TU Wien
  - Focus: bioorganic synthesis
  - Master thesis: *Synthesis of perillic acid derivatives – putative novel bioactive compounds* in cooperation with BRAIN AG.
- 04/2016-10/2011 BSc. Chemistry, TU Wien
  - Focus: organic synthesis
  - Bachelor thesis: *Synthesis and characterization of arylazo-2-thiophenes*
- 07/2010-10/2001 BG BRG BORG Oberpullendorf, Burgenland
  - Focus: informatics
- 09/2022-10/2018 Project assistant/University assistant at TU Wien
  - WWTF Project: *Diazirine FAD – A stable cofactor for biocatalysis and a molecular probe*
- 08/2016 Internship at Shire
  - Technical service
- 08/2015 Internship at Baxalta
  - Technical service
- 08/2014 Internship at Baxter AG
  - Technical service
- 03/2011-08/2010 Alternative service at the hospital Oberpullendorf

## F II List of abbreviations

aq.	aqueous	HSQC	heteronuclear	single
CDI	1,1'-carbonyldiimidazole		quantum coherence	
COSY	correlated spectroscopy	KMNO <sub>4</sub>	potassium permanganate	
CrO <sub>3</sub>	chromium trioxide	MeOH	methanol	
DCC	<i>N,N'</i> - dicyclohexylcarbodiimide	MeCN	acetonitrile	
DCM	dichloromethane	NaH	sodium hydride	
DIPEA	<i>N,N</i> -diisopropylethylamine	NaOH	sodium hydroxide	
4-DMAP	4-dimethylaminopyridine	NMR	nuclear magnetic resonance	
DMF	dimethylformamide	PE	petroleum ether	
EDCI·HCl	1-ethyl-3-(3- dimethylaminopropyl)carbo diimide hydrochloride	rt	room temperature	
		sat.	saturated	
		THF	tetrahydrofuran	
		TLC	thin layer chromatography	
equiv.	molar equivalents			
EtOAc	ethyl acetate			
EtOH	ethanol			
Et <sub>2</sub> O	diethyl ether			
Et <sub>3</sub> N	trimethylamine			
HCl	hydrochloric acid			
HOBt	hydroxybenzotriazole			
HPLC	high-performance liquid chromatography			
HR-MS	high resolution mass spectrometry			



# F III References

- 1 Hauer, B. Embracing Nature's Catalysts: A Viewpoint on the Future of Biocatalysis. *ACS Catalysis* **10**, 8418-8427 (2020). <https://doi.org:10.1021/acscatal.0c01708>
- 2 Timson, D. J. Four Challenges for Better Biocatalysts. *Fermentation* **5**, 39 (2019).
- 3 Kumar, D., Savitri, T. N., Verma, R. & Bhalla, T. Microbial proteases and application as laundry detergent additive. *Res J Microbiol* **3**, 661-672 (2008).
- 4 Singh, R., Kumar, M., Mittal, A. & Mehta, P. K. Microbial enzymes: industrial progress in 21st century. *3 Biotech* **6**, 174 (2016). <https://doi.org:10.1007/s13205-016-0485-8>
- 5 Choi, J.-M., Han, S.-S. & Kim, H.-S. Industrial applications of enzyme biocatalysis: Current status and future aspects. *Biotechnology Advances* **33**, 1443-1454 (2015). <https://doi.org:https://doi.org/10.1016/j.biotechadv.2015.02.014>
- 6 Meghwanshi, G. K. *et al.* Enzymes for pharmaceutical and therapeutic applications. *Biotechnology and Applied Biochemistry* **67**, 586-601 (2020). <https://doi.org:https://doi.org/10.1002/bab.1919>
- 7 Muthusamy, C. & Bahkali, A. 67-98 (2015).
- 8 Vinod Kumar, N. Enzyme Based Biosensors for Detection of Environmental Pollutants-A Review. *J. Microbiol. Biotechnol.* **25**, 1773-1781 (2015). <https://doi.org:10.4014/jmb.1504.04010>
- 9 Polizzi, K. M., Bommaris, A. S., Broering, J. M. & Chaparro-Riggers, J. F. Stability of biocatalysts. *Current Opinion in Chemical Biology* **11**, 220-225 (2007). <https://doi.org:https://doi.org/10.1016/j.cbpa.2007.01.685>
- 10 Poppe, L. & Vértessy, B. G. The Fourth Wave of Biocatalysis Emerges— The 13 th International Symposium on Biocatalysis and Biotransformations. *ChemBioChem* **19**, 284-287 (2018). <https://doi.org:https://doi.org/10.1002/cbic.201700687>
- 11 Damerow, P.
- 12 McGovern, P. E. *et al.* Fermented beverages of pre- and proto-historic China. *Proceedings of the National Academy of Sciences* **101**, 17593-17598 (2004). <https://doi.org:doi:10.1073/pnas.0407921102>
- 13 Armstrong, E. F. Enzymes: A Discovery and its Consequences. *Nature* **131**, 535-537 (1933). <https://doi.org:10.1038/131535a0>
- 14 zu Heidelberg, N.-M. V. *Verhandlungen des Naturhistorisch-Medizinischen Vereins zu Heidelberg.* (Winter, 1965).
- 15 Bornscheuer, U. T. & Buchholz, K. Highlights in Biocatalysis – Historical Landmarks and Current Trends. *Engineering in Life Sciences* **5**, 309-323 (2005). <https://doi.org:https://doi.org/10.1002/elsc.200520089>
- 16 Heckmann, C. M. & Paradisi, F. Looking Back: A Short History of the Discovery of Enzymes and How They Became Powerful Chemical Tools. *ChemCatChem* **12**, 6082-6102 (2020). <https://doi.org:https://doi.org/10.1002/cctc.202001107>
- 17 Sumner, J. Nobel Lecture: The Chemical Nature of Enzymes. *The Nobel Foundation, Amersterdam* (1946).
- 18 Hildebrandt, G. & Klavehn, W. Manufacture of laevo-1-phenyl-2-methylaminopropanol. *US1956950* (1934).
- 19 Fischer, E. Einfluss der Configuration auf die Wirkung der Enzyme. *Berichte der deutschen chemischen Gesellschaft* **27**, 2985-2993 (1894). <https://doi.org:https://doi.org/10.1002/cber.18940270364>
- 20 Koshland, D. E. Application of a Theory of Enzyme Specificity to Protein Synthesis. *Proceedings of the National Academy of Sciences* **44**, 98-104 (1958). <https://doi.org:doi:10.1073/pnas.44.2.98>
- 21 Sanger, F. & Tuppy, H. The amino-acid sequence in the phenylalanyl chain of insulin. 1. The identification of lower peptides from partial hydrolysates. *Biochemical Journal* **49**, 463-481 (1951). <https://doi.org:10.1042/bj0490463>
- 22 Perutz, M. F. *et al.* Structure of Hæmoglobin: A Three-Dimensional Fourier Synthesis at 5.5-Å. Resolution, Obtained by X-Ray Analysis. *Nature* **185**, 416-422 (1960). <https://doi.org:10.1038/185416a0>
- 23 Blake, C. C. F. *et al.* Structure of Hen Egg-White Lysozyme: A Three-dimensional Fourier Synthesis at 2 Å Resolution. *Nature* **206**, 757-761 (1965). <https://doi.org:10.1038/206757a0>
- 24 Reeke, G. N. *et al.* THE STRUCTURE OF CARBOXYPEPTIDASE A, VI. SOME RESULTS AT 2.0-Å RESOLUTION, AND THE COMPLEX WITH GLYCYL-TYROSINE AT 2.8-Å RESOLUTION. *Proceedings of the National Academy of Sciences* **58**, 2220-2226 (1967). <https://doi.org:doi:10.1073/pnas.58.6.2220>
- 25 Johnson, L. N. & Petsko, G. A. David Phillips and the origin of structural enzymology. *Trends in Biochemical Sciences* **24**, 287-289 (1999). [https://doi.org:https://doi.org/10.1016/S0968-0004\(99\)01423-1](https://doi.org:https://doi.org/10.1016/S0968-0004(99)01423-1)
- 26 Dawes, H. The quiet revolution. *Current Biology* **14**, R605-R607 (2004). <https://doi.org:https://doi.org/10.1016/j.cub.2004.07.038>
- 27 Watson, J. D. & Crick, F. H. C. Molecular Structure of Nucleic Acids: A Structure for Deoxyribose Nucleic Acid. *Nature* **171**, 737-738 (1953). <https://doi.org:10.1038/171737a0>
- 28 Jackson, D. A., Symons, R. H. & Berg, P. Biochemical Method for Inserting New Genetic Information into DNA of Simian Virus 40: Circular SV40 DNA Molecules Containing Lambda Phage Genes and the Galactose Operon of *Escherichia coli*. *Proceedings of the National Academy of Sciences* **69**, 2904-2909 (1972). <https://doi.org:doi:10.1073/pnas.69.10.2904>
- 29 Johnson, I. S. Human Insulin from Recombinant DNA Technology. *Science* **219**, 632-637 (1983). <https://doi.org:doi:10.1126/science.6337396>
- 30 Hutchison, C. A. *et al.* Mutagenesis at a specific position in a DNA sequence. *Journal of Biological Chemistry* **253**, 6551-6560 (1978). [https://doi.org:https://doi.org/10.1016/S0021-9258\(19\)46967-6](https://doi.org:https://doi.org/10.1016/S0021-9258(19)46967-6)
- 31 Fisher, C. L. & Pei, G. K. Modification of a PCRBased Site-Directed Mutagenesis Method. *BioTechniques* **23**, 570-574 (1997). <https://doi.org:10.2144/97234bm01>
- 32 Khorana, H. G. Nucleic acid synthesis. *Pure and Applied Chemistry* **17**, 349-382 (1968). <https://doi.org:doi:10.1351/pac196817030349>
- 33 Gillam, S., Rottman, F., Jahnke, P. & Smith, M. Enzymatic synthesis of oligonucleotides of defined sequence: synthesis of a segment of yeast iso-1-cytochrome c gene. *Proceedings of the National Academy of Sciences* **74**, 96-100 (1977). <https://doi.org:10.1073/pnas.74.1.96>
- 34 Saiki, R. K. *et al.* Enzymatic Amplification of Globin Genomic Sequences and Restriction Site Analysis for Diagnosis of Sickle Cell Anemia. *Science* **230**, 1350-1354 (1985). <https://doi.org:doi:10.1126/science.2999980>
- 35 Chen, K. & Arnold, F. H. Tuning the activity of an enzyme for unusual environments: sequential random mutagenesis of subtilisin E for catalysis in dimethylformamide. *Proceedings of the National Academy of Sciences* **90**, 5618-5622 (1993). <https://doi.org:doi:10.1073/pnas.90.12.5618>
- 36 Porto de Souza Vandenberghe, L. *et al.* in *Biomass, Biofuels, Biochemicals* (eds Sudhir P. Singh *et al.*) 11-30 (Elsevier, 2020).

- 37 McDonald, A. G. & Tipton, K. F. Fifty-five years of enzyme classification: advances and difficulties. *The FEBS Journal* **281**, 583-592 (2014). <https://doi.org/10.1111/febs.12530>
- 38 Prier, C. K. & Arnold, F. H. Chemomimetic Biocatalysis: Exploiting the Synthetic Potential of Cofactor-Dependent Enzymes To Create New Catalysts. *Journal of the American Chemical Society* **137**, 13992-14006 (2015). <https://doi.org/10.1021/jacs.5b09348>
- 39 Richter, M. Functional diversity of organic molecule enzyme cofactors. *Natural Product Reports* **30**, 1324-1345 (2013). <https://doi.org/10.1039/C3NP70045C>
- 40 Wittung-Stafshede, P. Role of Cofactors in Protein Folding. *Accounts of Chemical Research* **35**, 201-208 (2002). <https://doi.org/10.1021/ar010106e>
- 41 Harden, A., Young, W. J. & Martin, C. J. The alcoholic ferment of yeast-juice. Part II. The cofermment of yeast-juice. *Proceedings of the Royal Society of London. Series B, Containing Papers of a Biological Character* **78**, 369-375 (1906). <https://doi.org/10.1098/rspb.1906.0070>
- 42 von Euler, H. & Myrbäck, K. Co-Zymase. XVII. (1930).
- 43 Warburg, O. & Christian, W. Pyridin, der wasserstoffübertragende Bestandteil von Gärungsfermenten. *Helvetica Chimica Acta* **19**, E79-E88 (1936). <https://doi.org/10.1002/hlca.193601901199>
- 44 Snell, E. E. The Vitamin B6 Group. I. Formation of Additional Members from Pyridoxine and Evidence Concerning their Structure. *Journal of the American Chemical Society* **66**, 2082-2088 (1944). <https://doi.org/10.1021/ja01240a024>
- 45 Baddiley, J. & Todd, A. R. 122. Nucleotides. Part I. Muscle adenylic acid and adenosine diphosphate. *Journal of the Chemical Society (Resumed)*, 648-651 (1947). <https://doi.org/10.1039/JR9470000648>
- 46 Baddiley, J., Michelson, A. M. & Todd, A. R. 124. Nucleotides. Part II. A synthesis of adenosine triphosphate. *Journal of the Chemical Society (Resumed)*, 582-586 (1949). <https://doi.org/10.1039/JR9490000582>
- 47 Christie, S. M. H., Kenner, G. W. & Todd, A. R. Total Synthesis of Flavin-adenine-dinucleotide. *Nature* **170**, 924-924 (1952). <https://doi.org/10.1038/170924a0>
- 48 Hodgkin, D. C. *et al.* Structure of Vitamin B12: The Crystal Structure of the Hexacarboxylic Acid derived from B12 and the Molecular Structure of the Vitamin. *Nature* **176**, 325-328 (1955). <https://doi.org/10.1038/176325a0>
- 49 Hodgkin, D. C. *et al.* Structure of Vitamin B12. *Nature* **178**, 64-66 (1956). <https://doi.org/10.1038/178064a0>
- 50 McNaught, A. D. & Wilkinson, A. *Compendium of chemical terminology*. Vol. 1669 (Blackwell Science Oxford, 1997).
- 51 Fischer, J. D., Holliday, G. L., Rahman, S. A. & Thornton, J. M. The Structures and Physicochemical Properties of Organic Cofactors in Biocatalysis. *Journal of Molecular Biology* **403**, 803-824 (2010). <https://doi.org/10.1016/j.jmb.2010.09.018>
- 52 Hashim, O. H. & Adnan, N. A. Coenzyme, cofactor and prosthetic group — Ambiguous biochemical jargon. *Biochemical Education* **22**, 93-94 (1994). [https://doi.org/10.1016/0307-4412\(94\)90088-4](https://doi.org/10.1016/0307-4412(94)90088-4)
- 53 Andreini, C., Bertini, I., Cavallaro, G., Holliday, G. L. & Thornton, J. M. Metal ions in biological catalysis: from enzyme databases to general principles. *JBC Journal of Biological Inorganic Chemistry* **13**, 1205-1218 (2008). <https://doi.org/10.1007/s00775-008-0404-5>
- 54 Tainer, J. A., Getzoff, E. D., Richardson, J. S. & Richardson, D. C. Structure and mechanism of copper, zinc superoxide dismutase. *Nature* **306**, 284-287 (1983). <https://doi.org/10.1038/306284a0>
- 55 Hart, P. J. *et al.* A Structure-Based Mechanism for Copper-Zinc Superoxide Dismutase. *Biochemistry* **38**, 2167-2178 (1999). <https://doi.org/10.1021/bi982284u>
- 56 Scrutton, N. S. *et al.* Electron transfer in trimethylamine dehydrogenase and electrontransferring flavoprotein. *Biochemical Society Transactions* **27**, 196-201 (1999). <https://doi.org/10.1042/bst0270196>
- 57 Fitzpatrick, P. F. Tetrahydropterin-Dependent Amino Acid Hydroxylases. *Annual Review of Biochemistry* **68**, 355-381 (1999). <https://doi.org/10.1146/annurev.biochem.68.1.355>
- 58 Blaszczyk, J., Shi, G., Yan, H. & Ji, X. Catalytic center assembly of HPPK as revealed by the crystal structure of a ternary complex at 1.25 Å resolution. *Structure* **8**, 1049-1058 (2000). [https://doi.org/10.1016/s0969-2126\(00\)00502-5](https://doi.org/10.1016/s0969-2126(00)00502-5)
- 59 Li, Y. *et al.* Is the critical role of loop 3 of Escherichia coli 6-hydroxymethyl-7,8-dihydropterin pyrophosphokinase in catalysis due to loop-3 residues arginine-84 and tryptophan-89? Site-directed mutagenesis, biochemical, and crystallographic studies. *Biochemistry* **44**, 8590-8599 (2005). <https://doi.org/10.1021/bi0503495>
- 60 Carpenter, E. P., Hawkins, A. R., Frost, J. W. & Brown, K. A. Structure of dehydroquininate synthase reveals an active site capable of multistep catalysis. *Nature* **394**, 299-302 (1998). <https://doi.org/10.1038/28431>
- 61 Christianson, D. W. & Fierke, C. A. Carbonic Anhydrase: Evolution of the Zinc Binding Site by Nature and by Design. *Accounts of Chemical Research* **29**, 331-339 (1996). <https://doi.org/10.1021/ar950123z>
- 62 Lesburg, C. A., Zhai, G., Cane, D. E. & Christianson, D. W. Crystal Structure of Pentalenene Synthase: Mechanistic Insights on Terpenoid Cyclization Reactions in Biology. *Science* **277**, 1820-1824 (1997). <https://doi.org/10.1126/science.277.5333.1820>
- 63 Essen, L.-O. *et al.* Structural Mapping of the Catalytic Mechanism for a Mammalian Phosphoinositide-Specific Phospholipase C. *Biochemistry* **36**, 1704-1718 (1997). <https://doi.org/10.1021/bi962512p>
- 64 Haft, D. H. *et al.* Mycofactacin-associated mycobacterial dehydrogenases with non-exchangeable NAD cofactors. *Scientific Reports* **7**, 41074 (2017). <https://doi.org/10.1038/srep41074>
- 65 Morey, A. V. & Juni, E. Studies on the Nature of the Binding of Thiamine Pyrophosphate to Enzymes. *Journal of Biological Chemistry* **243**, 3009-3019 (1968). [https://doi.org/10.1016/S0021-9258\(18\)93372-7](https://doi.org/10.1016/S0021-9258(18)93372-7)
- 66 Chu, X.-Y. & Zhang, H.-Y. Cofactors as Molecular Fossils To Trace the Origin and Evolution of Proteins. *ChemBioChem* **21**, 3161-3168 (2020). <https://doi.org/10.1002/cbic.202000027>
- 67 Goldman, A. D. & Kacar, B. Cofactors are Remnants of Life's Origin and Early Evolution. *Journal of Molecular Evolution* **89**, 127-133 (2021). <https://doi.org/10.1007/s00239-020-09988-4>
- 68 White, H. B., 3rd. Coenzymes as fossils of an earlier metabolic state. *J Mol Evol* **7**, 101-104 (1976). <https://doi.org/10.1007/bf01732468>
- 69 Szathmáry, E. The origin of the genetic code: amino acids as cofactors in an RNA world. *Trends Genet* **15**, 223-229 (1999). [https://doi.org/10.1016/s0168-9525\(99\)01730-8](https://doi.org/10.1016/s0168-9525(99)01730-8)
- 70 Kirschning, A. Coenzymes and Their Role in the Evolution of Life. *Angewandte Chemie International Edition* **60**, 6242-6269 (2021). <https://doi.org/10.1002/anie.201914786>
- 71 Jadhav, V. R. & Yarus, M. Coenzymes as coribozymes. *Biochimie* **84**, 877-888 (2002). [https://doi.org/10.1016/S0300-9084\(02\)01404-9](https://doi.org/10.1016/S0300-9084(02)01404-9)
- 72 Pimviriyakul, P. & Chaiyen, P. in *The Enzymes* Vol. 47 (eds Pimchai Chaiyen & Fuyuhiko Tamanoi) 1-36 (Academic Press, 2020).
- 73 Joosten, V. & van Berkel, W. J. H. Flavoenzymes. *Current Opinion in Chemical Biology* **11**, 195-202 (2007). <https://doi.org/10.1016/j.cbpa.2007.01.010>

- 74 Hefti, M. H., Vervoort, J. & Van Berkel, W. J. H. De flavination and reconstitution of flavoproteins: Tackling fold and function. *European Journal of Biochemistry* **270**, 4227-4242 (2003). <https://doi.org/10.1046/j.1432-1033.2003.03802.x>
- 75 Fraaije, M. W., van den Heuvel, R. H., van Berkel, W. J. & Mattevi, A. Covalent flavinylation is essential for efficient redox catalysis in vanillyl-alcohol oxidase. *The Journal of biological chemistry* **274**, 35514-35520 (1999). <https://doi.org/10.1074/jbc.274.50.35514>
- 76 Abbas, C. A. & Sibirny, A. A. Genetic control of biosynthesis and transport of riboflavin and flavin nucleotides and construction of robust biotechnological producers. *Microbial Mol Biol Rev* **75**, 321-360 (2011). <https://doi.org/10.1128/MMBR.00030-10>
- 77 Winkler, A., Hartner, F., Kutchan, T. M., Glieder, A. & Macheroux, P. Biochemical evidence that berberine bridge enzyme belongs to a novel family of flavoproteins containing a bi-covalently attached FAD cofactor. *The Journal of biological chemistry* **281**, 21276-21285 (2006). <https://doi.org/10.1074/jbc.M603267200>
- 78 Huang, C.-H. et al. Crystal Structure of Glucooligosaccharide Oxidase from *Acremonium strictum*: A NOVEL FLAVINYLIATION OF 6-S-CYSTEINYLYL, 8 $\alpha$ -N1-HISTIDYL FAD\*. *Journal of Biological Chemistry* **280**, 38831-38838 (2005). <https://doi.org/https://doi.org/10.1074/jbc.M506078200>
- 79 Heuts, Dominic P. H. M., Winter, Remko T., Damsma, Gerke E., Janssen, Dick B. & Fraaije, Marco W. The role of double covalent flavin binding in chito-oligosaccharide oxidase from *Fusarium graminearum*. *Biochemical Journal* **413**, 175-183 (2008). <https://doi.org/10.1042/bj20071591>
- 80 Koetter, J. W. A. & Schulz, G. E. Crystal Structure of 6-Hydroxy-d-nicotine Oxidase from *Arthrobacter nicotinovorans*. *Journal of Molecular Biology* **352**, 418-428 (2005). <https://doi.org/https://doi.org/10.1016/j.jmb.2005.07.041>
- 81 Hassan-Abdallah, A., Bruckner, R. C., Zhao, G. & Jorns, M. S. Biosynthesis of Covalently Bound Flavin: Isolation and in Vitro Flavinylation of the Monomeric Sarcosine Oxidase Apoprotein. *Biochemistry* **44**, 6452-6462 (2005). <https://doi.org/10.1021/bi047271x>
- 82 Lienhart, W.-D., Gudipati, V. & Macheroux, P. The human flavoproteome. *Archives of Biochemistry and Biophysics* **535**, 150-162 (2013). <https://doi.org/https://doi.org/10.1016/j.abb.2013.02.015>
- 83 Macheroux, P., Kappes, B. & Ealick, S. E. Flavogenomics – a genomic and structural view of flavin-dependent proteins. *The FEBS Journal* **278**, 2625-2634 (2011). <https://doi.org/https://doi.org/10.1111/j.1742-4658.2011.08202.x>
- 84 Fraaije, M. W. & Mattevi, A. Flavoenzymes: diverse catalysts with recurrent features. *Trends in Biochemical Sciences* **25**, 126-132 (2000). [https://doi.org/https://doi.org/10.1016/S0968-0004\(99\)01533-9](https://doi.org/https://doi.org/10.1016/S0968-0004(99)01533-9)
- 85 Smith, D. R. M., Grünschow, S. & Goss, R. J. M. Scope and potential of halogenases in biosynthetic applications. *Current Opinion in Chemical Biology* **17**, 276-283 (2013). <https://doi.org/https://doi.org/10.1016/j.cbpa.2013.01.018>
- 86 Walsh, C. T. & Wencewicz, T. A. Flavoenzymes: Versatile catalysts in biosynthetic pathways. *Natural Product Reports* **30**, 175-200 (2013). <https://doi.org/10.1039/C2NP20069D>
- 87 Mukherjee, A. & Schroeder, C. M. Flavin-based fluorescent proteins: emerging paradigms in biological imaging. *Current Opinion in Biotechnology* **31**, 16-23 (2015). <https://doi.org/https://doi.org/10.1016/j.copbio.2014.07.010>
- 88 Baker Dockrey, S. A. & Narayan, A. R. H. Flavin-dependent biocatalysts in synthesis. *Tetrahedron* **75**, 1115-1121 (2019). <https://doi.org/https://doi.org/10.1016/j.tet.2019.01.008>
- 89 Torres Pazmiño, D. E., Dudek, H. M. & Fraaije, M. W. Baeyer–Villiger monooxygenases: recent advances and future challenges. *Current Opinion in Chemical Biology* **14**, 138-144 (2010). <https://doi.org/https://doi.org/10.1016/j.cbpa.2009.11.017>
- 90 Barile, M. et al. Biosynthesis of Flavin Cofactors in Man: Implications in Health and Disease. *Current Pharmaceutical Design* **19**, 2649-2675 (2013). <https://doi.org/http://dx.doi.org/10.2174/1381612811319140014>
- 91 Huerta, C., Borek, D., Machius, M., Grishin, N. V. & Zhang, H. Structure and Mechanism of a Eukaryotic FMN Adenylyltransferase. *Journal of Molecular Biology* **389**, 388-400 (2009). <https://doi.org/https://doi.org/10.1016/j.jmb.2009.04.022>
- 92 Iamurri, S. M., Daugherty, A. B., Edmondson, D. E. & Lutz, S. Truncated FAD synthetase for direct biocatalytic conversion of riboflavin and analogs to their corresponding flavin mononucleotides. *Protein Engineering, Design and Selection* **26**, 791-795 (2013). <https://doi.org/10.1093/protein/gzt055>
- 93 Manstein, D. J. & Pai, E. F. Purification and characterization of FAD synthetase from *Brevibacterium ammoniagenes*. *Journal of Biological Chemistry* **261**, 16169-16173 (1986). [https://doi.org/https://doi.org/10.1016/S0021-9258\(18\)66693-1](https://doi.org/https://doi.org/10.1016/S0021-9258(18)66693-1)
- 94 Pedrolli, D. B. et al. in *Flavins and Flavoproteins: Methods and Protocols* (eds Stefan Weber & Erik Schleicher) 41-63 (Springer New York, 2014).
- 95 Lee, E. R., Blount, K. F. & Breaker, R. R. Roseoflavin is a natural antibacterial compound that binds to FMN riboswitches and regulates gene expression. *RNA Biol* **6**, 187-194 (2009). <https://doi.org/10.4161/rna.6.2.7727>
- 96 DiMarco, A. A., Bobik, T. A. & Wolfe, R. S. Unusual coenzymes of methanogenesis. *Annu Rev Biochem* **59**, 355-394 (1990). <https://doi.org/10.1146/annurev.bi.59.070190.002035>
- 97 White, R. H. Biosynthesis of the methanogenic cofactors. *Vitam Horm* **61**, 299-337 (2001). [https://doi.org/10.1016/s0083-6729\(01\)61010-0](https://doi.org/10.1016/s0083-6729(01)61010-0)
- 98 Fagan, R. L. & Palfey, B. A. in *Comprehensive Natural Products II* (eds Hung-Wen Liu & Lew Mander) 37-113 (Elsevier, 2010).
- 99 Massey, V. & Palmer, G. On the Existence of Spectrally Distinct Classes of Flavoprotein Semiquinones. A New Method for the Quantitative Production of Flavoprotein Semiquinones\*. *Biochemistry* **5**, 3181-3189 (1966). <https://doi.org/10.1021/bi00874a016>
- 100 Edwards, A. M. in *Flavins and Flavoproteins: Methods and Protocols* (eds Stefan Weber & Erik Schleicher) 3-13 (Springer New York, 2014).
- 101 Piano, V., Palfey, B. A. & Mattevi, A. Flavins as Covalent Catalysts: New Mechanisms Emerge. *Trends in Biochemical Sciences* **42**, 457-469 (2017). <https://doi.org/https://doi.org/10.1016/j.tibs.2017.02.005>
- 102 Walsh, C. Flavin coenzymes: at the crossroads of biological redox chemistry. *Accounts of Chemical Research* **13**, 148-155 (1980). <https://doi.org/10.1021/ar50149a004>
- 103 Valentino, H. & Sobrado, P. in *Methods in Enzymology* Vol. 620 (ed Bruce A. Palfey) 51-88 (Academic Press, 2019).
- 104 Knaus, T., Toogood, H. S. & Scrutton, N. S. in *Green Biocatalysis* 473-488 (2016).
- 105 Atta-Asafo-Adjei, E., Lawton, M. P. & Philpot, R. Cloning, sequencing, distribution, and expression in *Escherichia coli* of flavin-containing monooxygenase 1C1. Evidence for a third gene subfamily in rabbits. *Journal of Biological Chemistry* **268**, 9681-9689 (1993).
- 106 Alfieri, A., Malito, E., Orru, R., Fraaije, M. W. & Mattevi, A. Revealing the moonlighting role of NADP in the structure of a flavin-containing monooxygenase. *Proceedings of the National Academy of Sciences* **105**, 6572-6577 (2008).
- 107 Fraaije, M. W., Kamerbeek, N. M., van Berkel, W. J. & Janssen, D. B. Identification of a Baeyer–Villiger monooxygenase sequence motif. *FEBS letters* **518**, 43-47 (2002).
- 108 Velikogne, S., Breukelaar, W. B., Hamm, F., Glabonjat, R. A. & Kroutil, W. C=C-Ene-Reductases Reduce the C=N Bond of Oximes. *ACS Catalysis* **10**, 13377-13382 (2020). <https://doi.org/10.1021/acscatal.0c03755>



- 109 Huijbers, M. M. E., Montersino, S., Westphal, A. H., Tischler, D. & van Berkel, W. J. H. Flavin dependent monooxygenases. *Archives of Biochemistry and Biophysics* **544**, 2-17 (2014). <https://doi.org/10.1016/j.abb.2013.12.005>
- 110 Bučko, M. et al. Baeyer-Villiger oxidations: biotechnological approach. *Applied Microbiology and Biotechnology* **100**, 6585-6599 (2016). <https://doi.org/10.1007/s00253-016-7670-x>
- 111 Weichold, V., Milbredt, D. & van Pée, K. H. Specific enzymatic halogenation—from the discovery of halogenated enzymes to their applications *in vitro* and *in vivo*. *Angewandte Chemie International Edition* **55**, 6374-6389 (2016).
- 112 Gvozdev, A. R., Tukhvatullin, I. A. & Gvozdev, R. I. Quinone-dependent alcohol dehydrogenases and FAD-dependent alcohol oxidases. *Biochemistry (Moscow)* **77**, 843-856 (2012). <https://doi.org/10.1134/S0006297912080056>
- 113 Dijkman, W. P., de Gonzalo, G., Mattevi, A. & Fraaije, M. W. Flavoprotein oxidases: classification and applications. *Applied Microbiology and Biotechnology* **97**, 5177-5188 (2013). <https://doi.org/10.1007/s00253-013-4925-7>
- 114 Abreia, A. T., Sützl, L. & Haltrich, D. Pyranose oxidase: A versatile sugar oxidoreductase for bioelectrochemical applications. *Bioelectrochemistry* **132**, 107409 (2020). <https://doi.org/10.1016/j.bioelechem.2019.107409>
- 115 Okuda-Shimazaki, J., Yoshida, H. & Sode, K. FAD dependent glucose dehydrogenases - discovery and engineering of representative glucose sensing enzymes. *Bioelectrochemistry* **132**, 1-13 (2020).
- 116 Bankar, S. B., Bule, M. V., Singhal, R. S. & Ananthanarayan, L. Glucose oxidase — An overview. *Biotechnology Advances* **27**, 489-501 (2009). <https://doi.org/10.1016/j.biotechadv.2009.04.003>
- 117 Robbins, J. M. & Ellis, H. R. in *Methods in Enzymology* Vol. 620 (ed Bruce A. Palfey) 399-422 (Academic Press, 2019).
- 118 Pitsawong, W., Hoben, J. P. & Miller, A.-F. Understanding the Broad Substrate Repertoire of Nitroreductase Based on Its Kinetic Mechanism\*. *Journal of Biological Chemistry* **289**, 15203-15214 (2014). <https://doi.org/10.1074/jbc.M113.547117>
- 119 Pimviriyakul, P. & Chaiyen, P. A complete bioconversion cascade for dehalogenation and denitration by bacterial flavin-dependent enzymes. *Journal of Biological Chemistry* **293**, 18525-18539 (2018). <https://doi.org/10.1074/jbc.RA118.005538>
- 120 Deller, S., Macheroux, P. & Sollner, S. Flavin-dependent quinone reductases. *Cellular and Molecular Life Sciences* **65**, 141 (2007). <https://doi.org/10.1007/s00018-007-7300-y>
- 121 Ross, D. Quinone reductases multitasking in the metabolic world. *Drug Metabolism Reviews* **36**, 639-654 (2004). <https://doi.org/10.1081/DMR-200033465>
- 122 Prosser, G. A. et al. Discovery and evaluation of *Escherichia coli* nitroreductases that activate the anti-cancer prodrug CB1954. *Biochemical Pharmacology* **79**, 678-687 (2010). <https://doi.org/10.1016/j.bcp.2009.10.008>
- 123 Cavener, D. R. GMC oxidoreductases: A newly defined family of homologous proteins with diverse catalytic activities. *Journal of Molecular Biology* **223**, 811-814 (1992). [https://doi.org/10.1016/0022-2836\(92\)90992-5](https://doi.org/10.1016/0022-2836(92)90992-5)
- 124 Kiess, M., Hecht, H.-J. & Kalisz, H. M. Glucose oxidase from *Penicillium amagasakiense*. *European Journal of Biochemistry* **252**, 90-99 (1998). <https://doi.org/10.1046/j.1432-1327.1998.2520090.x>
- 125 Roth, J. P. & Klinman, J. P. Catalysis of electron transfer during activation of O<sub>2</sub> by the flavoprotein glucose oxidase. *Proceedings of the National Academy of Sciences* **100**, 62-67 (2003). <https://doi.org/10.1073/pnas.252644599>
- 126 Romero, E. & Gadda, G. Alcohol oxidation by flavoenzymes. *Biomolecular Concepts* **5**, 299-318 (2014). <https://doi.org/10.1515/bmc-2014-0016>
- 127 Romero, E., Ferreira, P., Martínez, Á. T. & Martínez, M. J. New oxidase from *Bjerkandera arthroconidial* anamorph that oxidizes both phenolic and nonphenolic benzyl alcohols. *Biochimica et Biophysica Acta (BBA) - Proteins and Proteomics* **1794**, 689-697 (2009). <https://doi.org/10.1016/j.bbapap.2008.11.013>
- 128 Dijkman, W. P. & Fraaije, M. W. Discovery and Characterization of a 5-Hydroxymethylfurfural Oxidase from *Methylovorus* sp. Strain MP688. *Applied and Environmental Microbiology* **80**, 1082-1090 (2014). <https://doi.org/10.1128/AEM.03740-13>
- 129 Menon, V., Hsieh, C. T. & Fitzpatrick, P. F. Substituted Alcohols as Mechanistic Probes of Alcohol Oxidase. *Bioorganic Chemistry* **23**, 42-53 (1995). <https://doi.org/10.1006/bioo.1995.1004>
- 130 Fernandez, I. S. et al. Novel structural features in the GMC family of oxidoreductases revealed by the crystal structure of fungal aryl-alcohol oxidase. *Acta Crystallographica Section D* **65**, 1196-1205 (2009). <https://doi.org/10.1107/S0907444909035860>
- 131 Martin Hallberg, B., Henriksson, G., Pettersson, G. & Divne, C. Crystal structure of the flavoprotein domain of the extracellular flavocytochrome cellobiose dehydrogenase11Edited by D. Rees. *Journal of Molecular Biology* **315**, 421-434 (2002). <https://doi.org/10.1006/jmbi.2001.5246>
- 132 Yue, Q. K., Kass, I. J., Sampson, N. S. & Vrieland, A. Crystal Structure Determination of Cholesterol Oxidase from *Streptomyces* and Structural Characterization of Key Active Site Mutants. *Biochemistry* **38**, 4277-4286 (1999). <https://doi.org/10.1021/bi982497i>
- 133 Salvi, F. & Gadda, G. Human choline dehydrogenase: Medical promises and biochemical challenges. *Archives of Biochemistry and Biophysics* **537**, 243-252 (2013). <https://doi.org/10.1016/j.abb.2013.07.018>
- 134 Salvi, F., Wang, Y.-F., Weber, I. T. & Gadda, G. Structure of choline oxidase in complex with the reaction product glycine betaine. *Acta Crystallographica Section D* **70**, 405-413 (2014). <https://doi.org/10.1107/S1399004713029283>
- 135 Wohlfahrt, G. et al. 1.8 and 1.9 Å resolution structures of the *Penicillium amagasakiense* and *Aspergillus niger* glucose oxidases as a basis for modelling substrate complexes. *Acta Crystallographica Section D* **55**, 969-977 (1999). <https://doi.org/10.1107/S0907444999003431>
- 136 Tan, T. C. et al. The 1.6 Å Crystal Structure of Pyranose Dehydrogenase from *Agaricus meleagris* Rationalizes Substrate Specificity and Reveals a Flavin Intermediate. *PLOS ONE* **8**, e53567 (2013). <https://doi.org/10.1371/journal.pone.0053567>
- 137 Martin Hallberg, B., Leitner, C., Haltrich, D. & Divne, C. Crystal Structure of the 270 kDa Homotetrameric Lignin-degrading Enzyme Pyranose 2-Oxidase. *Journal of Molecular Biology* **341**, 781-796 (2004). <https://doi.org/10.1016/j.jmb.2004.06.033>
- 138 Mugo, A. N. et al. Crystal structure of pyridoxine 4-oxidase from *Mesorhizobium loti*. *Biochimica et Biophysica Acta (BBA) - Proteins and Proteomics* **1834**, 953-963 (2013). <https://doi.org/10.1016/j.bbapap.2013.03.004>
- 139 Roth, J. P. & Klinman, J. P. Catalysis of electron transfer during activation of O<sub>2</sub> by the flavoprotein glucose oxidase. *Proceedings of the National Academy of Sciences of the United States of America* **100**, 62-67 (2003). <https://doi.org/10.1073/pnas.252644599>
- 140 Wong, C. M., Wong, K. H. & Chen, X. D. Glucose oxidase: natural occurrence, function, properties and industrial applications. *Applied Microbiology and Biotechnology* **78**, 927-938 (2008). <https://doi.org/10.1007/s00253-008-1407-4>
- 141 Müller, D. Oxidation von Glukose mit Extrakten aus *Aspegillus niger*. *Biochem. z* **199**, 136-170 (1928).
- 142 Swoboda, B. E. P. & Massey, V. Purification and Properties of the Glucose Oxidase from *Aspergillus niger*. *Journal of Biological Chemistry* **240**, 2209-2215 (1965). [https://doi.org/10.1016/S0021-9258\(18\)97448-X](https://doi.org/10.1016/S0021-9258(18)97448-X)
- 143 Hecht, H. J., Kalisz, H. M., Hendle, J., Schmid, R. D. & Schomburg, D. Crystal Structure of Glucose Oxidase from *Aspergillus niger* Refined at 2.3 Å Reslution. *Journal of Molecular Biology* **229**, 153-172 (1993). <https://doi.org/10.1006/jmbi.1993.1015>

- 144 Wohlfahrt, G. *et al.* 1.8 and 1.9 Å resolution structures of the *Penicillium amagasakiense* and *Aspergillus niger* glucose oxidases as a basis for modelling substrate complexes. *Acta Crystallographica Section D: Biological Crystallography* **55**, 969-977 (1999). <https://doi.org:10.1107/S0907444999003431>
- 145 Sriwaiyaphram, K., Punthong, P., Sucharitakul, J. & Wongnate, T. in *The Enzymes* Vol. 47 (eds Pimchai Chaiyen & Fuyuhiko Tamanoi) 193-230 (Academic Press, 2020).
- 146 Leskovic, V., Trivić, S., Wohlfahrt, G., Kandrač, J. & Peričin, D. Glucose oxidase from *Aspergillus niger*: the mechanism of action with molecular oxygen, quinones, and one-electron acceptors. *The International Journal of Biochemistry & Cell Biology* **37**, 731-750 (2005). <https://doi.org:https://doi.org/10.1016/j.biocel.2004.10.014>
- 147 Steffolani, M. E., Ribotta, P. D., Pérez, G. T. & León, A. E. Effect of glucose oxidase, transglutaminase, and pentosanase on wheat proteins: Relationship with dough properties and bread-making quality. *Journal of Cereal Science* **51**, 366-373 (2010). <https://doi.org:https://doi.org/10.1016/j.jcs.2010.01.010>
- 148 Dubey, M. K. *et al.* Improvement Strategies, Cost Effective Production, and Potential Applications of Fungal Glucose Oxidase (GOD): Current Updates. *Frontiers in Microbiology* **8** (2017). <https://doi.org:10.3389/fmicb.2017.01032>
- 149 Yadav, P., Chauhan, A. K., Singh, R. B., Khan, S. & Halabi, G. in *Functional Foods and Nutraceuticals in Metabolic and Non-Communicable Diseases* (eds Ram B. Singh, Shaw Watanabe, & Adrian A. Isaza) 325-337 (Academic Press, 2022).
- 150 Heller, A. & Feldman, B. Electrochemical Glucose Sensors and Their Applications in Diabetes Management. *Chemical Reviews* **108**, 2482-2505 (2008). <https://doi.org:10.1021/cr068069y>
- 151 Wang, H.-C. & Lee, A.-R. Recent developments in blood glucose sensors. *Journal of Food and Drug Analysis* **23**, 191-200 (2015). <https://doi.org:https://doi.org/10.1016/j.jfda.2014.12.001>
- 152 Yildiz, H. B., Kiralp, S., Toppare, L. & Yağci, Y. Immobilization of glucose oxidase in conducting graft copolymers and determination of glucose amount in orange juices with enzyme electrodes. *International Journal of Biological Macromolecules* **37**, 174-178 (2005). <https://doi.org:https://doi.org/10.1016/j.ijbiomac.2005.10.004>
- 153 Bobrowski, T. & Schuhmann, W. Long-term implantable glucose biosensors. *Current Opinion in Electrochemistry* **10**, 112-119 (2018). <https://doi.org:https://doi.org/10.1016/j.coelec.2018.05.004>
- 154 Westermark, U. & Eriksson, K. E.
- 155 HENRIKSSON, G., PETTERSSON, G., JOHANSSON, G., RUIZ, A. & UZCATEGUI, E. Cellobiose oxidase from *Phanerochaete chrysosporium* can be cleaved by papain into two domains. *European journal of biochemistry* **196**, 101-106 (1991).
- 156 Csarman, F., Wohlschlager, L. & Ludwig, R. in *The Enzymes* Vol. 47 (eds Pimchai Chaiyen & Fuyuhiko Tamanoi) 457-489 (Academic Press, 2020).
- 157 Igarashi, K., Samejima, M. & Eriksson, K. E. L. Cellobiose dehydrogenase enhances *Phanerochaete chrysosporium* cellobiohydrolase I activity by relieving product inhibition. *European Journal of Biochemistry* **253**, 101-106 (1998). <https://doi.org:10.1046/j.1432-1327.1998.2530101.x>
- 158 Ander, P., Mishra, C., Farrell, R. L. & Eriksson, K.-E. L. Redox reactions in lignin degradation: interactions between laccase, different peroxidases and cellobiose: quinone oxidoreductase. *Journal of Biotechnology* **13**, 189-198 (1990). [https://doi.org:https://doi.org/10.1016/0168-1656\(90\)90104-J](https://doi.org:https://doi.org/10.1016/0168-1656(90)90104-J)
- 159 Vaaje-Kolstad, G. *et al.* An Oxidative Enzyme Boosting the Enzymatic Conversion of Recalcitrant Polysaccharides. *Science* **330**, 219-222 (2010). <https://doi.org:doi:10.1126/science.1192231>
- 160 Zarattini, M. *et al.* LPMO-oxidized cellulose oligosaccharides evoke immunity in *Arabidopsis* conferring resistance towards necrotrophic fungus *B. cinerea*. *Communications Biology* **4**, 727 (2021). <https://doi.org:10.1038/s42003-021-02226-7>
- 161 Beeson, W. T., Phillips, C. M., Cate, J. H. D. & Marletta, M. A. Oxidative Cleavage of Cellulose by Fungal Copper-Dependent Polysaccharide Monooxygenases. *Journal of the American Chemical Society* **134**, 890-892 (2012). <https://doi.org:10.1021/ja210657t>
- 162 Kracher, D. *et al.* Extracellular electron transfer systems fuel cellulose oxidative degradation. *Science* **352**, 1098-1101 (2016). <https://doi.org:doi:10.1126/science.aaf3165>
- 163 Hallberg, B. M. *et al.* A new scaffold for binding haem in the cytochrome domain of the extracellular flavocytochrome cellobiose dehydrogenase. *Structure* **8**, 79-88 (2000).
- 164 Hallberg, B. M., Henriksson, G., Pettersson, G. & Divne, C. Crystal structure of the flavoprotein domain of the extracellular flavocytochrome cellobiose dehydrogenase. *Journal of molecular biology* **315**, 421-434 (2002).
- 165 Rotsaert, F. A. J., Li, B., Renganathan, V. & Gold, M. H. Site-Directed Mutagenesis of the Heme Axial Ligands in the Hemoflavoenzyme Cellobiose Dehydrogenase. *Archives of Biochemistry and Biophysics* **390**, 206-214 (2001). <https://doi.org:https://doi.org/10.1006/abbi.2001.2362>
- 166 Hallberg, B. M., Henriksson, G., Pettersson, G., Vasella, A. & Divne, C. Mechanism of the Reductive Half-reaction in Cellobiose Dehydrogenase\*. *Journal of Biological Chemistry* **278**, 7160-7166 (2003). <https://doi.org:https://doi.org/10.1074/jbc.M210961200>
- 167 Kracher, D. & Ludwig, R. Cellobiose dehydrogenase: An essential enzyme for lignocellulose degradation in nature—A review/Cellobiosedehydrogenase: Ein essentielles Enzym für den Lignozelluloseabbau in der Natur—Eine Übersicht. *Die Bodenkultur: Journal of Land Management, Food and Environment* **67**, 145-163 (2016).
- 168 Bao, W. & Renganathan, V. Cellobiose oxidase of *Phanerochaete chrysosporium* enhances crystalline cellulose degradation by cellulases. *FEBS Letters* **302**, 77-80 (1992). [https://doi.org:https://doi.org/10.1016/0014-5793\(92\)80289-5](https://doi.org:https://doi.org/10.1016/0014-5793(92)80289-5)
- 169 Hildén, L. *et al.* Do the extracellular enzymes cellobiose dehydrogenase and manganese peroxidase form a pathway in lignin biodegradation? *FEBS Letters* **477**, 79-83 (2000). [https://doi.org:https://doi.org/10.1016/S0014-5793\(00\)01757-9](https://doi.org:https://doi.org/10.1016/S0014-5793(00)01757-9)
- 170 Barr, D. P. & Aust, S. D. Mechanisms white rot fungi use to degrade pollutants. *Environmental science & technology* **28**, 78A-87A (1994).
- 171 Harms, H., Schlosser, D. & Wick, L. Y. Untapped potential: exploiting fungi in bioremediation of hazardous chemicals. *Nature Reviews Microbiology* **9**, 177-192 (2011). <https://doi.org:10.1038/nrmicro2519>
- 172 Nyanhongo, G. S., Thallinger, B. & Guebitz, G. M. Cellobiose dehydrogenase-based biomedical applications. *Process Biochemistry* **59**, 37-45 (2017). <https://doi.org:https://doi.org/10.1016/j.procbio.2017.02.023>
- 173 Alonso, S., Rendueles, M. & Díaz, M. Bio-production of lactobionic acid: Current status, applications and future prospects. *Biotechnology Advances* **31**, 1275-1291 (2013). <https://doi.org:https://doi.org/10.1016/j.biotechadv.2013.04.010>
- 174 Ludwig, R. *et al.* Cellobiose dehydrogenase modified electrodes: advances by materials science and biochemical engineering. *Analytical and Bioanalytical Chemistry* **405**, 3637-3658 (2013).
- 175 Scheiblbrandner, S. & Ludwig, R. Cellobiose dehydrogenase: Bioelectrochemical insights and applications. *Bioelectrochemistry* **131**, 107345 (2020).
- 176 van Berkel, W. J., Kamerbeek, N. M. & Fraaije, M. W. Flavoprotein monooxygenases, a diverse class of oxidative biocatalysts. *J Biotechnol* **124**, 670-689 (2006). <https://doi.org:10.1016/j.jbiotec.2006.03.044>

- 177 Fraaije, M. W., Kamerbeek, N. M., van Berkel, W. J. H. & Janssen, D. B. Identification of a Baeyer–Villiger monooxygenase sequence motif. *FEBS Letters* **518**, 43–47 (2002). [https://doi.org/10.1016/S0014-5793\(02\)02623-6](https://doi.org/10.1016/S0014-5793(02)02623-6)
- 178 Riebel, A. *et al.* Expanding the set of rhodococcal Baeyer–Villiger monooxygenases by high-throughput cloning, expression and substrate screening. *Applied Microbiology and Biotechnology* **95**, 1479–1489 (2012). <https://doi.org/10.1007/s00253-011-3823-0>
- 179 Malito, E., Alfieri, A., Fraaije, M. W. & Mattevi, A. Crystal structure of a Baeyer–Villiger monooxygenase. *Proceedings of the National Academy of Sciences* **101**, 13157–13162 (2004).
- 180 Orru, R. *et al.* Snapshots of enzymatic Baeyer–Villiger catalysis: oxygen activation and intermediate stabilization. *Journal of Biological Chemistry* **286**, 29284–29291 (2011).
- 181 Fürst, M. J. L. J., Gran-Scheuch, A., Aalbers, F. S. & Fraaije, M. W. Baeyer–Villiger Monooxygenases: Tunable Oxidative Biocatalysts. *ACS Catalysis* **9**, 11207–11241 (2019). <https://doi.org/10.1021/acscatal.9b03396>
- 182 Chen, Y., Peoples, O. & Walsh, C. Acinetobacter cyclohexanone monooxygenase: gene cloning and sequence determination. *Journal of Bacteriology* **170**, 781–789 (1988).
- 183 Donoghue, N. A., Norris, D. B. & Trudgill, P. W. The purification and properties of cyclohexanone oxygenase from *Nocardia globerula* CL1 and *Acinetobacter* NCIB 9871. *European Journal of Biochemistry* **63**, 175–192 (1976).
- 184 Morii, S. *et al.* Steroid Monooxygenase of *Rhodococcus rhodochrous*: Sequencing of the Genomic DNA, and Hyperexpression, Purification, and Characterization of the Recombinant Enzyme. *The Journal of Biochemistry* **126**, 624–631 (1999).
- 185 Brzostowicz, P. C., Gibson, K. L., Thomas, S. M., Blasko, M. S. & Rouvière, P. E. Simultaneous identification of two cyclohexanone oxidation genes from an environmental *Brevibacterium* isolate using mRNA differential display. *Journal of bacteriology* **182**, 4241–4248 (2000).
- 186 Kamerbeek, N. M. *et al.* 4-Hydroxyacetophenone monooxygenase from *Pseudomonas fluorescens* ACB: A novel flavoprotein catalyzing Baeyer–Villiger oxidation of aromatic compounds. *European Journal of Biochemistry* **268**, 2547–2557 (2001).
- 187 Kostichka, K., Thomas, S. M., Gibson, K. J., Nagarajan, V. & Cheng, Q. Cloning and characterization of a gene cluster for cyclododecanone oxidation in *Rhodococcus ruber* SC1. *Journal of Bacteriology* **183**, 6478–6486 (2001).
- 188 Nelson, K. *et al.* Complete genome sequence and comparative analysis of the metabolically versatile *Pseudomonas putida* KT2440. *Environmental microbiology* **4**, 799–808 (2002).
- 189 Van Beilen, J. B. *et al.* Cloning of Baeyer–Villiger monooxygenases from *Comamonas*, *Xanthobacter* and *Rhodococcus* using polymerase chain reaction with highly degenerate primers. *Environmental Microbiology* **5**, 174–182 (2003).
- 190 Cheng, Q., Thomas, S. M., Kostichka, K., Valentine, J. R. & Nagarajan, V. Genetic analysis of a gene cluster for cyclohexanol oxidation in *Acinetobacter* sp. strain SE19 by *in vitro* transposition. *Journal of Bacteriology* **182**, 4744–4751 (2000).
- 191 Bramucci, M. in *Chem. Abstr.* 233997.
- 192 Brzostowicz, P. C., Walters, D. M., Thomas, S. M., Nagarajan, V. & Rouviere, P. E. mRNA differential display in a microbial enrichment culture: simultaneous identification of three cyclohexanone monooxygenases from three species. *Applied and environmental microbiology* **69**, 334–342 (2003).
- 193 Fraaije, M. W., Kamerbeek, N. M., Heidekamp, A. J., Fortin, R. & Janssen, D. B. The prodrug activator EtaA from *Mycobacterium tuberculosis* is a Baeyer–Villiger monooxygenase. *Journal of Biological Chemistry* **279**, 3354–3360 (2004).
- 194 Fraaije, M. W. *et al.* Discovery of a thermostable Baeyer–Villiger monooxygenase by genome mining. *Applied Microbiology and Biotechnology* **66**, 393–400 (2005).
- 195 Kotani, T., Yurimoto, H., Kato, N. & Sakai, Y. Novel acetone metabolism in a propane-utilizing bacterium, *Gordonia* sp. strain TY-5. *Journal of bacteriology* **189**, 886–893 (2007).
- 196 Kirschner, A., Altenbuchner, J. & Bornscheuer, U. T. Cloning, expression, and characterization of a Baeyer–Villiger monooxygenase from *Pseudomonas fluorescens* DSM 50106 in *E. coli*. *Applied microbiology and biotechnology* **73**, 1065–1072 (2007).
- 197 Onaca, C., Kieninger, M., Engesser, K.-H. & Altenbuchner, J. Degradation of alkyl methyl ketones by *Pseudomonas veronii* MEK700. *Journal of bacteriology* **189**, 3759–3767 (2007).
- 198 Rehdorf, J., Zimmer, C. L. & Bornscheuer, U. T. Cloning, expression, characterization, and biocatalytic investigation of the 4-hydroxyacetophenone monooxygenase from *Pseudomonas putida* JD1. *Applied and environmental microbiology* **75**, 3106–3114 (2009).
- 199 Jiang, J. *et al.* Genome mining in *Streptomyces avermitilis*: A biochemical Baeyer–Villiger reaction and discovery of a new branch of the pentalenolactone family tree. *Biochemistry* **48**, 6431–6440 (2009).
- 200 Mirza, I. A. *et al.* Crystal structures of cyclohexanone monooxygenase reveal complex domain movements and a sliding cofactor. *Journal of the American Chemical Society* **131**, 8848–8854 (2009).
- 201 Seo, M.-J., Zhu, D., Endo, S., Ikeda, H. & Cane, D. E. Genome mining in streptomyces. Elucidation of the role of Baeyer–Villiger monooxygenases and non-heme iron-dependent dehydrogenase/oxygenases in the final steps of the biosynthesis of pentalenolactone and neopentalenolactone. *Biochemistry* **50**, 1739–1754 (2011).
- 202 Leisch, H. *et al.* Cloning, Baeyer–Villiger Biooxidations, and Structures of the Camphor Pathway 2-Oxo- $\beta$ -keto- $\gamma$ -butyrolactone-4,5,5-Trimethylcyclopentenylacetyl-Coenzyme A Monooxygenase of *Pseudomonas putida* ATCC 17453. *Applied and Environmental Microbiology* **78**, 2200–2212 (2012). <https://doi.org/10.1128/AEM.07694-11>
- 203 Weiss, M., Denger, K., Huhn, T. & Schleheck, D. Two enzymes of a complete degradation pathway for linear alkylbenzenesulfonate (LAS) surfactants: 4-sulfoacetophenone Baeyer–Villiger monooxygenase and 4-sulfophenylacetate esterase in *Comamonas testosteroni* KF-1. *Applied and environmental microbiology* **78**, 8254–8263 (2012).
- 204 Leipold, F., Wardenga, R. & Bornscheuer, U. T. Cloning, expression and characterization of a eukaryotic cycloalkanone monooxygenase from *Cylindrocarpum radicolica* ATCC 11011. *Applied microbiology and biotechnology* **94**, 705–717 (2012).
- 205 Iwaki, H. *et al.* Camphor pathway redux: functional recombinant expression of 2, 5- and 3, 6-diketocamphane monooxygenases of *Pseudomonas putida* ATCC 17453 with their cognate flavin reductase catalyzing Baeyer–Villiger reactions. *Applied and environmental microbiology* **79**, 3282–3293 (2013).
- 206 Hwang, W. C., Xu, Q., Wu, B. & Godzik, A. Crystal Structure of a Baeyer–Villiger Flavin-containing Monooxygenase from *Staphylococcus Aureus* MRSA Strain MU50. *Proteins* **86**, 269 (2018).
- 207 Ferroni, F., Smit, M. & Opperman, D. Functional divergence between closely related Baeyer–Villiger monooxygenases from *Aspergillus flavus*. *Journal of Molecular Catalysis B: Enzymatic* **107**, 47–54 (2014).
- 208 Romero, E., Castellanos, J. R. G., Mattevi, A. & Fraaije, M. W. Characterization and crystal structure of a robust cyclohexanone monooxygenase. *Angewandte Chemie International Edition* **55**, 15852–15855 (2016).
- 209 De Gonzalo, G., Fürst, M. J. & Fraaije, M. W. Polycyclic ketone monooxygenase (PockeMO): a robust biocatalyst for the synthesis of optically active sulfoxides. *Catalysts* **7**, 288 (2017).



- 210 Ceccoli, R. D., Bianchi, D. A., Fink, M. J., Mihovilovic, M. D. & Rial, D. V. Cloning and characterization of the Type I Baeyer–Villiger monooxygenase from *Leptospira biflexa*. *AMB Express* **7**, 1-13 (2017).
- 211 Fiorentini, F. *et al.* (2017).
- 212 Gran-Scheuch, A., Trajkovic, M., Parra, L. & Fraaije, M. W. Mining the Genome of *Streptomyces leeuwenhoekii*: Two New Type I Baeyer–Villiger Monooxygenases From Atacama Desert. *Frontiers in microbiology* **9**, 1609 (2018).
- 213 Zhang, Y. *et al.* Discovery of Two Native Baeyer–Villiger Monooxygenases for Asymmetric Synthesis of Bulky Chiral Sulfoxides. *Applied and Environmental Microbiology* **84**, e00638-00618 (2018). <https://doi.org/doi:10.1128/AEM.00638-18>
- 214 Liu, Y.-Y., Li, C.-X., Xu, J.-H. & Zheng, G.-W. Efficient Synthesis of Methyl 3-Acetoxypropionate by a Newly Identified Baeyer–Villiger Monooxygenase. *Applied and Environmental Microbiology* **85**, e00239-00219 (2019). <https://doi.org/doi:10.1128/AEM.00239-19>
- 215 Baeyer, A. & Villiger, V. Einwirkung des caro'schen reagens auf ketone. *Berichte der deutschen chemischen Gesellschaft* **32**, 3625-3633 (1899).
- 216 Sheng, D., Ballou, D. P. & Massey, V. Mechanistic Studies of Cyclohexanone Monooxygenase: Chemical Properties of Intermediates Involved in Catalysis. *Biochemistry* **40**, 11156-11167 (2001). <https://doi.org/10.1021/bi011153h>
- 217 Sucharitakul, J., Prongjit, M., Haltrich, D. & Chaiyen, P. Detection of a C4a-Hydroperoxyflavin Intermediate in the Reaction of a Flavoprotein Oxidase. *Biochemistry* **47**, 8485-8490 (2008). <https://doi.org/10.1021/bi801039d>
- 218 Chaiyen, P., Fraaije, M. W. & Mattevi, A. The enigmatic reaction of flavins with oxygen. *Trends in Biochemical Sciences* **37**, 373-380 (2012). <https://doi.org/https://doi.org/10.1016/j.tibs.2012.06.005>
- 219 Schmidt, S. & Bornscheuer, U. T. in *The Enzymes* Vol. 47 (eds Pimchai Chaiyen & Fuyuhiko Tamanoi) 231-281 (Academic Press, 2020).
- 220 Holtmann, D. & Hollmann, F. The Oxygen Dilemma: A Severe Challenge for the Application of Monooxygenases? *ChemBioChem* **17**, 1391-1398 (2016). <https://doi.org/https://doi.org/10.1002/cbic.201600176>
- 221 Beier, A. *et al.* Switch in Cofactor Specificity of a Baeyer–Villiger Monooxygenase. *ChemBioChem* **17**, 2312-2315 (2016). <https://doi.org/https://doi.org/10.1002/cbic.201600484>
- 222 Balke, K., Beier, A. & Bornscheuer, U. T. Hot spots for the protein engineering of Baeyer–Villiger monooxygenases. *Biotechnology Advances* **36**, 247-263 (2018). <https://doi.org/https://doi.org/10.1016/j.biotechadv.2017.11.007>
- 223 Malito, E., Alfieri, A., Fraaije, M. W. & Mattevi, A. Crystal structure of a Baeyer–Villiger monooxygenase. *Proceedings of the National Academy of Sciences* **101**, 13157-13162 (2004). <https://doi.org/doi:10.1073/pnas.0404538101>
- 224 Orru, R. *et al.* Snapshots of Enzymatic Baeyer–Villiger Catalysis: OXYGEN ACTIVATION AND INTERMEDIATE STABILIZATION\*. *Journal of Biological Chemistry* **286**, 29284-29291 (2011). <https://doi.org/https://doi.org/10.1074/jbc.M111.255075>
- 225 Mirza, I. A. *et al.* Crystal Structures of Cyclohexanone Monooxygenase Reveal Complex Domain Movements and a Sliding Cofactor. *Journal of the American Chemical Society* **131**, 8848-8854 (2009). <https://doi.org/10.1021/ja9010578>
- 226 Doukyu, N. & Ogino, H. Organic solvent-tolerant enzymes. *Biochemical engineering journal* **48**, 270-282 (2010).
- 227 Bong, Y. K. *et al.* Baeyer–Villiger monooxygenase-mediated synthesis of esomeprazole as an alternative for kagan sulfoxidation. *The Journal of organic chemistry* **83**, 7453-7458 (2018).
- 228 Baldwin, C. V., Wohlgenuth, R. & Woodley, J. M. The first 200-L scale asymmetric Baeyer–Villiger oxidation using a whole-cell biocatalyst. *Organic Process Research & Development* **12**, 660-665 (2008).
- 229 Woo, J.-M. *et al.* Improving catalytic activity of the Baeyer–Villiger monooxygenase-based *Escherichia coli* biocatalysts for the overproduction of (Z)-11-(heptanoyloxy) undec-9-enoic acid from ricinoleic acid. *Scientific reports* **8**, 1-11 (2018).
- 230 Delgove, M. A. *et al.* A prospective life cycle assessment (LCA) of monomer synthesis: comparison of biocatalytic and oxidative chemistry. *ChemSusChem* **12**, 1349-1360 (2019).
- 231 Sattler, J. H. *et al.* Back Cover: Introducing an In Situ Capping Strategy in Systems Biocatalysis To Access 6-Aminohexanoic acid (Angew. Chem. Int. Ed. 51/2014). *Angewandte Chemie International Edition* **53**, 14274-14274 (2014).
- 232 van Beek, H. L., Romero, E. & Fraaije, M. W. Engineering cyclohexanone monooxygenase for the production of methyl propanoate. *ACS chemical biology* **12**, 291-299 (2017).
- 233 Milker, S., Fink, M. J., Rudroff, F. & Mihovilovic, M. D. Non-hazardous biocatalytic oxidation in Nylon-9 monomer synthesis on a 40 g scale with efficient downstream processing. *Biotechnology and Bioengineering* **114**, 1670-1678 (2017).
- 234 Zhang, Y. *et al.* Engineering of Cyclohexanone Monooxygenase for the Enantioselective Synthesis of (S)-Omeprazole. *ACS Sustainable Chemistry & Engineering* **7**, 7218-7226 (2019). <https://doi.org/10.1021/acssuschemeng.9b00224>
- 235 Mihovilovic, Marko D., Müller, B. & Stanetty, P. Monooxygenase-Mediated Baeyer–Villiger Oxidations. *European Journal of Organic Chemistry* **2002**, 3711-3730 (2002). [https://doi.org/https://doi.org/10.1002/1099-0690\(200211\)2002:22<3711::AID-EJOC3711>3.0.CO;2-5](https://doi.org/https://doi.org/10.1002/1099-0690(200211)2002:22<3711::AID-EJOC3711>3.0.CO;2-5)
- 236 van Beek, H. L., Wijma, H. J., Fromont, L., Janssen, D. B. & Fraaije, M. W. Stabilization of cyclohexanone monooxygenase by a computationally designed disulfide bond spanning only one residue. *FEBS Open Bio* **4**, 168-174 (2014). <https://doi.org/https://doi.org/10.1016/j.fob.2014.01.009>
- 237 Schmidt, S., Genz, M., Balke, K. & Bornscheuer, U. T. The effect of disulfide bond introduction and related Cys/Ser mutations on the stability of a cyclohexanone monooxygenase. *Journal of biotechnology* **214**, 199-211 (2015).
- 238 Engel, J., Mthethwa, K. S., Opperman, D. J. & Kara, S. Characterization of new Baeyer–Villiger monooxygenases for lactonizations in redox-neutral cascades. *Molecular Catalysis* **468**, 44-51 (2019).
- 239 Mansouri, H. R. *et al.* Mutations Increasing Cofactor Affinity, Improve Stability and Activity of a Baeyer–Villiger Monooxygenase. *ACS Catalysis* **12**, 11761-11766 (2022). <https://doi.org/10.1021/acscatal.2c03225>
- 240 Rudroff, F., Rydz, J., Ogink, F. H., Fink, M. & Mihovilovic, M. D. Comparing the stereoselective biooxidation of cyclobutanones by recombinant strains expressing bacterial Baeyer–Villiger monooxygenases. *Advanced Synthesis & Catalysis* **349**, 1436-1444 (2007).
- 241 Opperman, D. J. & Reetz, M. T. Towards practical Baeyer–Villiger-monoxygenases: Design of cyclohexanone monooxygenase mutants with enhanced oxidative stability. *ChemBioChem* **11**, 2589-2596 (2010).
- 242 Eijsink, V. G. H., Gåseidnes, S., Borchert, T. V. & van den Burg, B. Directed evolution of enzyme stability. *Biomolecular Engineering* **22**, 21-30 (2005). <https://doi.org/https://doi.org/10.1016/j.bioeng.2004.12.003>
- 243 Brissos, V., Gonçalves, N., Melo, E. P. & Martins, L. O. Improving Kinetic or Thermodynamic Stability of an Azoreductase by Directed Evolution. *PLOS ONE* **9**, e87209 (2014). <https://doi.org/10.1371/journal.pone.0087209>
- 244 Kearney, E. B. & Singer, T. P. On the prosthetic group of succinic dehydrogenase. *Biochimica et Biophysica Acta* **17**, 596-597 (1955). [https://doi.org/https://doi.org/10.1016/0006-3002\(55\)90432-7](https://doi.org/https://doi.org/10.1016/0006-3002(55)90432-7)
- 245 Kearney, E. B. & With the technical assistance of Paul, B. Studies on Succinic Dehydrogenase: XII. FLAVIN COMPONENT OF THE MAMMALIAN ENZYME. *Journal of Biological Chemistry* **235**, 865-877 (1960). [https://doi.org/https://doi.org/10.1016/S0021-9258\(19\)67952-4](https://doi.org/https://doi.org/10.1016/S0021-9258(19)67952-4)

- 246 Walker, W. H., Singer, T. P., Ghisla, S. & Hemmerich, P. Studies on Succinate Dehydrogenase. *European Journal of Biochemistry* **26**, 279-289 (1972). <https://doi.org/10.1111/j.1432-1033.1972.tb01766.x>
- 247 Heuts, D. P. H. M., Scrutton, N. S., McIntire, W. S. & Fraaije, M. W. What's in a covalent bond? *The FEBS Journal* **276**, 3405-3427 (2009). <https://doi.org/10.1111/j.1742-4658.2009.07053.x>
- 248 Huang, C.-H. et al. Crystal structure of glucooligosaccharide oxidase from *Acremonium strictum*: a novel flavinylation of 6-S-cysteinylyl, 8 $\alpha$ -N1-histidyl FAD. *Journal of Biological Chemistry* **280**, 38831-38838 (2005).
- 249 Heuts, D. P., Winter, R. T., Damsma, G. E., Janssen, D. B. & Fraaije, M. W. The role of double covalent flavin binding in chito-oligosaccharide oxidase from *Fusarium graminearum*. *Biochemical Journal* **413**, 175-183 (2008).
- 250 Winkler, A., Hartner, F., Kutchan, T. M., Glieder, A. & Macheroux, P. Biochemical evidence that berberine bridge enzyme belongs to a novel family of flavoproteins containing a bi-covalently attached FAD cofactor. *Journal of Biological Chemistry* **281**, 21276-21285 (2006).
- 251 Rand, T., Qvist, K. B., Walter, C. P. & Poulsen, C. H. Characterization of the flavin association in hexose oxidase from *Chondrus crispus*. *The FEBS journal* **273**, 2693-2703 (2006).
- 252 Alexeev, I., Sultana, A., Mäntsälä, P., Niemi, J. & Schneider, G. Aclacinomycin oxidoreductase (AknOx) from the biosynthetic pathway of the antibiotic aclacinomycin is an unusual flavoenzyme with a dual active site. *Proceedings of the National Academy of Sciences* **104**, 6170-6175 (2007).
- 253 Taura, F., Sirikantaramas, S., Shoyama, Y., Shoyama, Y. & Morimoto, S. Phytocannabinoids in *Cannabis sativa*: Recent Studies on Biosynthetic Enzymes. *Chemistry & Biodiversity* **4**, 1649-1663 (2007). <https://doi.org/10.1002/cbdv.200790145>
- 254 Fraaije, M. W., van den Heuvel, R. H. H., van Berkel, W. J. H. & Mattevi, A. Covalent Flavinylation Is Essential for Efficient Redox Catalysis in Vanillyl-alcohol Oxidase\*. *Journal of Biological Chemistry* **274**, 35514-35520 (1999). <https://doi.org/10.1074/jbc.274.50.35514>
- 255 Coulombe, R., Yue, K. Q., Ghisla, S. & Vrielink, A. Oxygen Access to the Active Site of Cholesterol Oxidase through a Narrow Channel Is Gated by an Arg-Glu Pair\*. *Journal of Biological Chemistry* **276**, 30435-30441 (2001). <https://doi.org/10.1074/jbc.M104103200>
- 256 Forneris, F. et al. Structural Analysis of the Catalytic Mechanism and Stereoselectivity in *Streptomyces coelicolor* Alditol Oxidase. *Biochemistry* **47**, 978-985 (2008). <https://doi.org/10.1021/bi701886t>
- 257 Malito, E., Coda, A., Bilyeu, K. D., Fraaije, M. W. & Mattevi, A. Structures of Michaelis and Product Complexes of Plant Cytokinin Dehydrogenase: Implications for Flavoenzyme Catalysis. *Journal of Molecular Biology* **341**, 1237-1249 (2004). <https://doi.org/10.1016/j.jmb.2004.06.083>
- 258 Jin, J., Mazon, H., van den Heuvel, R. H. H., Janssen, D. B. & Fraaije, M. W. Discovery of a eugenol oxidase from *Rhodococcus* sp. strain RHA1. *The FEBS Journal* **274**, 2311-2321 (2007). <https://doi.org/10.1111/j.1742-4658.2007.05767.x>
- 259 Kenney, W. C. et al. Identification of the covalently bound flavin of L-gulonolactone oxidase. *Biochemical and Biophysical Research Communications* **71**, 1194-1200 (1976). [https://doi.org/10.1016/0006-291X\(76\)90780-4](https://doi.org/10.1016/0006-291X(76)90780-4)
- 260 Shimizu, M., Murakawa, S. & Takahashi, T. The Covalently Bound Flavin Prosthetic Group of D-Gluconolactone Dehydrogenase of *Penicillium cyaneo-fulvum*. *Agricultural and Biological Chemistry* **41**, 2107-2108 (1977). <https://doi.org/10.1271/bbb1961.41.2107>
- 261 Kenney, W. C. et al. Identification of the covalently-bound flavin of l-galactonolactone oxidase from yeast. *FEBS Letters* **97**, 40-42 (1979). [https://doi.org/10.1016/0014-5793\(79\)80047-2](https://doi.org/10.1016/0014-5793(79)80047-2)
- 262 Huh, W.-K. et al. Characterisation of D-Arabinono-1,4-Lactone Oxidase from *Candida albicans* ATCC 10231. *European Journal of Biochemistry* **225**, 1073-1079 (1994). <https://doi.org/10.1111/j.1432-1033.1994.1073b.x>
- 263 Hiraga, K., Kitazawa, M., Kaneko, N. & Oda, K. Isolation and Some Properties of Sorbitol Oxidase from *Streptomyces* sp. H-7775. *Bioscience, Biotechnology, and Biochemistry* **61**, 1699-1704 (1997). <https://doi.org/10.1271/bbb.61.1699>
- 264 Yamashita, M. et al. Isolation, characterization, and molecular cloning of a thermostable xylitol oxidase from *Streptomyces* sp. IKD472. *Journal of Bioscience and Bioengineering* **89**, 350-360 (2000). [https://doi.org/10.1016/S1389-1723\(00\)88958-6](https://doi.org/10.1016/S1389-1723(00)88958-6)
- 265 Carter, C. J. & Thornburg, R. W. Tobacco Nectarin V Is a Flavin-Containing Berberine Bridge Enzyme-Like Protein with Glucose Oxidase Activity. *Plant Physiology* **134**, 460-469 (2004). <https://doi.org/10.1104/pp.103.027482>
- 266 Müller, F. *Chemistry and biochemistry of flavoenzymes*. Vol. 3 (CRC Press, 1991).
- 267 Halada, P., Leitner, C., Sedmera, P., Haltrich, D. & Volc, J. Identification of the covalent flavin adenine dinucleotide-binding region in pyranose 2-oxidase from *Trametes multicolor*. *Analytical biochemistry* **314**, 235-242 (2003).
- 268 Kujawa, M. et al. Properties of pyranose dehydrogenase purified from the litter-degrading fungus *Agaricus xanthoderma*. *The FEBS journal* **274**, 879-894 (2007).
- 269 Walker, W. H., Singer, T. P., Ghisla, S. & Hemmerich, P. Studies on Succinate Dehydrogenase: 8 $\alpha$ -Histidyl-FAD as the Active Center of Succinate Dehydrogenase. *European Journal of Biochemistry* **26**, 279-289 (1972).
- 270 Leys, D., Basran, J. & Scrutton, N. S. Channelling and formation of 'active' formaldehyde in dimethylglycine oxidase. *The EMBO journal* **22**, 4038-4048 (2003).
- 271 Chiribau, C. B., Sandu, C., Fraaije, M., Schiltz, E. & Brandsch, R. A novel  $\gamma$ -N-methylaminobutyrate demethylating oxidase involved in catabolism of the tobacco alkaloid nicotine by *Arthrobacter nicotinovorans* pAO1. *European journal of biochemistry* **271**, 4677-4684 (2004).
- 272 Mathews, F. S., Chen, Z. W., Bellamy, H. D. & McIntire, W. S. Three-dimensional structure of p-cresol methylhydroxylase (flavocytochrome c) from *Pseudomonas putida* at 3.0-Å resolution. *Biochemistry* **30**, 238-247 (1991).
- 273 Edmondson, D. E., Binda, C. & Mattevi, A. The FAD binding sites of human monoamine oxidases A and B. *Neurotoxicology* **25**, 63-72 (2004).
- 274 Zhou, B. P., Lewis, D. A., Kwan, S.-W. & Abell, C. W. Flavinylation of Monoamine Oxidase B (\*). *Journal of Biological Chemistry* **270**, 23653-23660 (1995).
- 275 Ferri, S. et al. Cloning and expression of fructosyl-amine oxidase from marine yeast *Pichia* species N1-1. *Marine Biotechnology* **6**, 625-632 (2004).
- 276 Wagner, M. A., Khanna, P. & Jorns, M. S. Structure of the flavocoenzyme of two homologous amine oxidases: Monomeric sarcosine oxidase and N-methyltryptophan oxidase. *Biochemistry* **38**, 5588-5595 (1999).
- 277 Ilari, A. et al. The X-ray structure of N-methyltryptophan oxidase reveals the structural determinants of substrate specificity. *Proteins: Structure, Function, and Bioinformatics* **71**, 2065-2075 (2008).
- 278 Goyer, A. et al. Characterization and metabolic function of a peroxisomal sarcosine and piperolate oxidase from *Arabidopsis*. *Journal of Biological Chemistry* **279**, 16947-16953 (2004).



- 279 Carrell, C. J. *et al.* NikD, an unusual amino acid oxidase essential for nikkomycin biosynthesis: Structures of closed and open forms at 1.15 and 1.90 Å resolution. *Structure* **15**, 928-941 (2007).
- 280 Chen, Z.-w. *et al.* The structure of flavocytochrome c sulfide dehydrogenase from a purple phototrophic bacterium. *Science* **266**, 430-432 (1994).
- 281 Driessche, G. V. *et al.* Covalent structure of the flavoprotein subunit of the flavocytochrome c: sulfide dehydrogenase from the purple phototrophic bacterium *Chromatium vinosum*. *Protein science* **5**, 1753-1764 (1996).
- 282 Liaw, S.-H., Lee, D. Y., Chow, L.-P., Lau, G.-X. & Su, S.-N. Structural characterization of the 60-kDa bermuda grass pollen isoallergens, a covalent flavoprotein. *Biochemical and Biophysical Research Communications* **280**, 738-743 (2001).
- 283 Willie, A., Edmondson, D. E. & Jorns, M. S. Sarcosine oxidase contains a novel covalently bound FMN. *Biochemistry* **35**, 5292-5299 (1996).
- 284 Thiemer, B., Andreesen, J. R. & Schröder, T. The NADH-dependent reductase of a putative multicomponent tetrahydrofuran mono-oxygenase contains a covalently bound FAD. *European Journal of Biochemistry* **268**, 3774-3782 (2001).
- 285 Li, Y.-S. *et al.* A unique flavin mononucleotide-linked primary alcohol oxidase for glycopeptide A40926 maturation. *Journal of the American Chemical Society* **129**, 13384-13385 (2007).
- 286 Bandejas, T. M., Salgueiro, C., Kletzin, A., Gomes, C. M. & Teixeira, M. Acidianus ambivalens type-II NADH dehydrogenase: genetic characterisation and identification of the flavin moiety as FMN. *FEBS letters* **531**, 273-277 (2002).
- 287 STEENKAMP, D. J. & WC, K. Structure of the covalently bound coenzyme of trimethylamine dehydrogenase. Evidence for a 6-substituted flavin. (1978).
- 288 Yang, C. C., Packman, L. C. & Scrutton, N. S. The primary structure of *Hyphomicrobium* X dimethylamine dehydrogenase: relationship to trimethylamine dehydrogenase and implications for substrate recognition. *European journal of biochemistry* **232**, 264-271 (1995).
- 289 Fujieda, N., Tsuse, N., Satoh, A., Ikeda, T. & Kano, K. Production of completely flavinylated histamine dehydrogenase, unique covalently bound flavin, and iron-sulfur cluster-containing enzyme of *Nocardioides simplex* in *Escherichia coli*, and its properties. *Bioscience, biotechnology, and biochemistry* **69**, 2459-2462 (2005).
- 290 Hayashi, M. *et al.* FMN is covalently attached to a threonine residue in the NqrB and NqrC subunits of Na<sup>+</sup>-translocating NADH-quinone reductase from *Vibrio alginolyticus*. *FEBS letters* **488**, 5-8 (2001).
- 291 Heuts, D. P. H. M., Janssen, D. B. & Fraaije, M. W. Changing the substrate specificity of a chitoooligosaccharide oxidase from *Fusarium graminearum* by model-inspired site-directed mutagenesis. *FEBS Letters* **581**, 4905-4909 (2007). [https://doi.org:https://doi.org/10.1016/j.febslet.2007.09.019](https://doi.org/https://doi.org/10.1016/j.febslet.2007.09.019)
- 292 Leferink, N. G. H., Heuts, D. P. H. M., Fraaije, M. W. & van Berkel, W. J. H. The growing VAO flavoprotein family. *Archives of Biochemistry and Biophysics* **474**, 292-301 (2008). [https://doi.org:https://doi.org/10.1016/j.abb.2008.01.027](https://doi.org/https://doi.org/10.1016/j.abb.2008.01.027)
- 293 Fraaije, M. W., van Berkel, W. J. H., Benen, J. A. E., Visser, J. & Mattevi, A. A novel oxidoreductase family sharing a conserved FAD-binding domain. *Trends in Biochemical Sciences* **23**, 206-207 (1998). [https://doi.org:https://doi.org/10.1016/S0968-0004\(98\)01210-9](https://doi.org/https://doi.org/10.1016/S0968-0004(98)01210-9)
- 294 Fraaije, M. W., van den Heuvel, R. H., van Berkel, W. J. & Mattevi, A. Covalent flavinylation is essential for efficient redox catalysis in vanillyl-alcohol oxidase. *Journal of Biological Chemistry* **274**, 35514-35520 (1999).
- 295 Nandigama, R. K. & Edmondson, D. E. Influence of FAD Structure on Its Binding and Activity with the C406A Mutant of Recombinant Human Liver Monoamine Oxidase A \*. *Journal of Biological Chemistry* **275**, 20527-20532 (2000). <https://doi.org:10.1074/jbc.M002132200>
- 296 Caldinelli, L. *et al.* Dissecting the Structural Determinants of the Stability of Cholesterol Oxidase Containing Covalently Bound Flavin \*. *Journal of Biological Chemistry* **280**, 22572-22581 (2005). <https://doi.org:10.1074/jbc.M500549200>
- 297 Starbird, C. A., Maklashina, E., Cecchini, G. & Iverson, T. in *eLS* 1-11.
- 298 Cecchini, G., Schröder, I., Gunsalus, R. P. & Maklashina, E. Succinate dehydrogenase and fumarate reductase from *Escherichia coli*. *Biochimica et Biophysica Acta (BBA) - Bioenergetics* **1553**, 140-157 (2002). [https://doi.org:https://doi.org/10.1016/S0005-2728\(01\)00238-9](https://doi.org/https://doi.org/10.1016/S0005-2728(01)00238-9)
- 299 Ackrell, B. A., Cochran, B. & Cecchini, G. Interactions of oxaloacetate with *Escherichia coli* fumarate reductase. *Archives of biochemistry and biophysics* **268**, 26-34 (1989).
- 300 Sucheta, A., Cammack, R., Weiner, J. & Armstrong, F. A. Reversible electrochemistry of fumarate reductase immobilized on an electrode surface. Direct voltammetric observations of redox centers and their participation in rapid catalytic electron transport. *Biochemistry* **32**, 5455-5465 (1993).
- 301 Heering, H. A., Weiner, J. H. & Armstrong, F. A. Direct detection and measurement of electron relays in a multicentered enzyme: Voltammetry of electrode-surface films of *E. coli* fumarate reductase, an iron-sulfur flavoprotein. *Journal of the American Chemical Society* **119**, 11628-11638 (1997).
- 302 Heffron, K. *Studies of the redox and catalytic properties of the anaerobic respiratory enzymes of Escherichia coli*, University of Oxford, (2001).
- 303 Turner, K. *et al.* Redox properties of flavocytochrome c 3 from *Shewanella frigidimarina* NCIMB400. *Biochemistry* **38**, 3302-3309 (1999).
- 304 Tomasiak, T. M., Maklashina, E., Cecchini, G. & Iverson, T. M. A Threonine on the Active Site Loop Controls Transition State Formation in *Escherichia coli* Respiratory Complex II \*. *Journal of Biological Chemistry* **283**, 15460-15468 (2008). <https://doi.org:10.1074/jbc.M801372200>
- 305 Blaut, M. *et al.* Fumarate Reductase Mutants of *Escherichia coli* That Lack Covalently Bound Flavin. *Journal of Biological Chemistry* **264**, 13599-13604 (1989). [https://doi.org:10.1016/S0021-9258\(18\)80039-4](https://doi.org:10.1016/S0021-9258(18)80039-4)
- 306 Bertsova, Y. V. *et al.* Alternative pyrimidine biosynthesis protein ApbE is a flavin transferase catalyzing covalent attachment of FMN to a threonine residue in bacterial flavoproteins. *Journal of Biological Chemistry* **288**, 14276-14286 (2013).
- 307 Deka, R. K., Brautigam, C. A., Liu, W. Z., Tomchick, D. R. & Norgard, M. V. Molecular insights into the enzymatic diversity of flavin-trafficking protein (Ftp; formerly ApbE) in flavoprotein biogenesis in the bacterial periplasm. *MicrobiologyOpen* **5**, 21-38 (2016). <https://doi.org:https://doi.org/10.1002/mbo3.306>
- 308 MACHEROUX, P., PLATTNER, H. J., ROMAGUERA, A. & DIEKMANN, H. FAD and substrate analogs as probes for lysine N6-hydroxylase from *Escherichia coli* EN 222. *European Journal of Biochemistry* **213**, 995-1002 (1993). [https://doi.org:https://doi.org/10.1111/j.1432-1033.1993.tb17846.x](https://doi.org/https://doi.org/10.1111/j.1432-1033.1993.tb17846.x)
- 309 Moore, E. G., Cardemil, E. & Massey, V. Production of a covalent flavin linkage in lipoamide dehydrogenase. Reaction with 8-Cl-FAD. *Journal of Biological Chemistry* **253**, 6413-6422 (1978).
- 310 Massey, V. & Hemmerich, P. Active-site probes of flavoproteins. *Biochemical Society Transactions* **8**, 246-257 (1980).

- 311 Raibekas, A. A., Fukui, K. & Massey, V. Design and properties of human span class="smallcaps smallerCapital">d</span>-amino acid oxidase with covalently attached flavin. *Proceedings of the National Academy of Sciences* **97**, 3089-3093 (2000). <https://doi.org/doi:10.1073/pnas.97.7.3089>
- 312 Raibekas, A. A., Fukui, K. & Massey, V. Design and properties of human amino acid oxidase with covalently attached flavin. *Proceedings of the National Academy of Sciences* **97**, 3089-3093 (2000). <https://doi.org/doi:10.1073/pnas.97.7.3089>
- 313 Negri, A. *et al.* Covalent Flavinylation of L-Aspartate Oxidase from *Escherichia coli* Using N<sup>6</sup>-(6-Carboxyhexyl)-FAD Succinimidoester. *Journal of Protein Chemistry* **18**, 671-676 (1999). <https://doi.org/10.1023/A:1020606323716>
- 314 Singh, A., Thornton, E. R. & Westheimer, F. H. The Photolysis of Diazoacetylchymotrypsin. *Journal of Biological Chemistry* **237**, PC3006-PC3008 (1962). [https://doi.org/https://doi.org/10.1016/S0021-9258\(18\)60265-0](https://doi.org/https://doi.org/10.1016/S0021-9258(18)60265-0)
- 315 Ruoho, A. E., Kiefer, H., Roeder, P. E. & Singer, S. J. The Mechanism of Photoaffinity Labeling. *Proceedings of the National Academy of Sciences of the United States of America* **70**, 2567-2571 (1973).
- 316 Burton, N. R., Kim, P. & Backus, K. M. Photoaffinity labelling strategies for mapping the small molecule–protein interactome. *Organic & Biomolecular Chemistry* **19**, 7792-7809 (2021). <https://doi.org/10.1039/D1OB01353J>
- 317 Park, J., Koh, M., Koo, J. Y., Lee, S. & Park, S. B. Investigation of Specific Binding Proteins to Photoaffinity Linkers for Efficient Deconvolution of Target Protein. *ACS Chemical Biology* **11**, 44-52 (2016). <https://doi.org/10.1021/acscchembio.5b00671>
- 318 Sakurai, K., Ozawa, S. & Yamaguchi, T. Photoaffinity labeling studies of the carbohydrate-binding proteins with different affinities. *Bioorganic & Medicinal Chemistry* **23**, 5319-5325 (2015). <https://doi.org/https://doi.org/10.1016/j.bmc.2015.07.065>
- 319 Fleet, G. W. J., Porter, R. R. & Knowles, J. R. Affinity Labelling of Antibodies with Aryl Nitrene as Reactive Group. *Nature* **224**, 511-512 (1969). <https://doi.org/10.1038/224511a0>
- 320 Kiefer, H., Lindstrom, J., Lennox, E. S. & Singer, S. J. Photo-Affinity Labeling of Specific Acetylcholine-Binding Sites on Membranes. *Proceedings of the National Academy of Sciences* **67**, 1688-1694 (1970). <https://doi.org/doi:10.1073/pnas.67.4.1688>
- 321 Galardy, R. E., Craig, L. C., Jamieson, J. D. & Printz, M. P. Photoaffinity labeling of peptide hormone binding sites. *The Journal of biological chemistry* **249**, 3510-3518 (1974).
- 322 Paulsen, S. 3,3-Dialkyl-diazacyclopenten-(1). *Angewandte Chemie* **72**, 781-782 (1960).
- 323 Ge, S.-S. *et al.* Current advances of carbene-mediated photoaffinity labeling in medicinal chemistry. *RSC Advances* **8**, 29428-29454 (2018). <https://doi.org/10.1039/C8RA03538E>
- 324 A. Fleming, S. Chemical reagents in photoaffinity labeling. *Tetrahedron* **51**, 12479-12520 (1995). [https://doi.org/https://doi.org/10.1016/0040-4020\(95\)00598-3](https://doi.org/https://doi.org/10.1016/0040-4020(95)00598-3)
- 325 Wang, J., Kubicki, J., Peng, H. & Platz, M. S. Influence of Solvent on Carbene Intersystem Crossing Rates. *Journal of the American Chemical Society* **130**, 6604-6609 (2008). <https://doi.org/10.1021/ja711385t>
- 326 Song, M.-G. & Sheridan, R. S. Regiochemical Substituent Switching of Spin States in Aryl(trifluoromethyl)carbenes. *Journal of the American Chemical Society* **133**, 19688-19690 (2011). <https://doi.org/10.1021/ja209613u>
- 327 O'Brien, J. G. K., Jemas, A., Asare-Okai, P. N., am Ende, C. W. & Fox, J. M. Probing the Mechanism of Photoaffinity Labeling by Dialkyldiazirines through Bioorthogonal Capture of Diazoalkanes. *Organic Letters* **22**, 9415-9420 (2020). <https://doi.org/10.1021/acs.orglett.0c02714>
- 328 Preston, G. W., Radford, S. E., Ashcroft, A. E. & Wilson, A. J. Analysis of Amyloid Nanostructures Using Photo-cross-linking: In Situ Comparison of Three Widely Used Photo-cross-linkers. *ACS Chemical Biology* **9**, 761-768 (2014). <https://doi.org/10.1021/cb400731s>
- 329 Sakurai, K., Ozawa, S., Yamada, R., Yasui, T. & Mizuno, S. Comparison of the Reactivity of Carbohydrate Photoaffinity Probes with Different Photoreactive Groups. *ChemBioChem* **15**, 1399-1403 (2014). <https://doi.org/https://doi.org/10.1002/cbic.201402051>
- 330 Hill, J. R. & Robertson, A. A. B. Fishing for Drug Targets: A Focus on Diazirine Photoaffinity Probe Synthesis. *Journal of Medicinal Chemistry* **61**, 6945-6963 (2018). <https://doi.org/10.1021/acs.jmedchem.7b01561>
- 331 Smith, R. A. G. & Knowles, J. R. Aryldiazirines. Potential reagents for photolabeling of biological receptor sites. *Journal of the American Chemical Society* **95**, 5072-5073 (1973). <https://doi.org/10.1021/ja00796a062>
- 332 Brunner, J., Senn, H. & Richards, F. M. 3-Trifluoromethyl-3-phenyldiazirine. A new carbene generating group for photolabeling reagents. *Journal of Biological Chemistry* **255**, 3313-3318 (1980). [https://doi.org/https://doi.org/10.1016/S0021-9258\(19\)85701-0](https://doi.org/https://doi.org/10.1016/S0021-9258(19)85701-0)
- 333 Blencowe, A. & Hayes, W. Development and application of diazirines in biological and synthetic macromolecular systems. *Soft Matter* **1**, 178-205 (2005). <https://doi.org/10.1039/B501989C>
- 334 Das, J. Aliphatic Diazirines as Photoaffinity Probes for Proteins: Recent Developments. *Chemical Reviews* **111**, 4405-4417 (2011). <https://doi.org/10.1021/cr100272z>
- 335 Hashimoto, M. & Hatanaka, Y. Recent Progress in Diazirine-Based Photoaffinity Labeling. *European Journal of Organic Chemistry* **2008**, 2513-2523 (2008). <https://doi.org/https://doi.org/10.1002/ejoc.200701069>
- 336 Shah, N. P. *et al.* Overriding Imatinib Resistance with a Novel ABL Kinase Inhibitor. *Science* **305**, 399-401 (2004). <https://doi.org/doi:10.1126/science.1099480>
- 337 Shi, H., Zhang, C.-J., Chen, G. Y. J. & Yao, S. Q. Cell-Based Proteome Profiling of Potential Dasatinib Targets by Use of Affinity-Based Probes. *Journal of the American Chemical Society* **134**, 3001-3014 (2012). <https://doi.org/10.1021/ja208518u>
- 338 Gao, J., Mfuh, A., Amako, Y. & Woo, C. M. Small Molecule Interactome Mapping by Photoaffinity Labeling Reveals Binding Site Hotspots for the NSAIDs. *Journal of the American Chemical Society* **140**, 4259-4268 (2018). <https://doi.org/10.1021/jacs.7b11639>
- 339 Stewart, D. S. *et al.* p-(4-Azipentyl)propofol: A Potent Photoreactive General Anesthetic Derivative of Propofol. *Journal of Medicinal Chemistry* **54**, 8124-8135 (2011). <https://doi.org/10.1021/jm200943f>
- 340 Jayakar, S. S., Dailey, W. P., Eckenhoff, R. G. & Cohen, J. B. Identification of Propofol Binding Sites in a Nicotinic Acetylcholine Receptor with a Photoreactive Propofol Analog\*. *Journal of Biological Chemistry* **288**, 6178-6189 (2013). <https://doi.org/https://doi.org/10.1074/jbc.M112.435909>
- 341 Hall, M. A. *et al.* m-Azipropofol (AziPm) a Photoactive Analogue of the Intravenous General Anesthetic Propofol. *Journal of Medicinal Chemistry* **53**, 5667-5675 (2010). <https://doi.org/10.1021/jm100407z>
- 342 Yip, G. M. S. *et al.* A propofol binding site on mammalian GABAA receptors identified by photolabeling. *Nature Chemical Biology* **9**, 715-720 (2013). <https://doi.org/10.1038/nchembio.1340>
- 343 Development of a Cannabinoid-Based Photoaffinity Probe to Determine the Δ<sup>8</sup>/9-Tetrahydrocannabinol Protein Interaction Landscape in Neuroblastoma Cells. *Cannabis and Cannabinoid Research* **3**, 136-151 (2018). <https://doi.org/10.1089/can.2018.0003>
- 344 Horning, B. D. *et al.* Chemical Proteomic Profiling of Human Methyltransferases. *Journal of the American Chemical Society* **138**, 13335-13343 (2016). <https://doi.org/10.1021/jacs.6b07830>
- 345 Anderson, L. N. *et al.* Live Cell Discovery of Microbial Vitamin Transport and Enzyme-Cofactor Interactions. *ACS Chemical Biology* **11**, 345-354 (2016). <https://doi.org/10.1021/acscchembio.5b00918>

- 346 Romine, M. F. *et al.* Elucidation of roles for vitamin B<sub>12</sub> in regulation of folate, ubiquinone, and methionine metabolism. *Proceedings of the National Academy of Sciences* **114**, E1205-E1214 (2017). <https://doi.org/doi:10.1073/pnas.1612360114>
- 347 Jelcic, M. *et al.* A Photo-clickable ATP-Mimetic Reveals Nucleotide Interactors in the Membrane Proteome. *Cell Chemical Biology* **27**, 1073-1083.e1012 (2020). <https://doi.org/https://doi.org/10.1016/j.chembiol.2020.05.010>
- 348 Šileikytė, J., Sundalam, S., David, L. L. & Cohen, M. S. Chemical Proteomics Approach for Profiling the NAD Interactome. *Journal of the American Chemical Society* **143**, 6787-6791 (2021). <https://doi.org/10.1021/jacs.1c01302>
- 349 Lam, A. T. *et al.* A Bifunctional NAD<sup>+</sup> for Profiling Poly-ADP-Ribosylation-Dependent Interacting Proteins. *ACS Chemical Biology* **16**, 389-396 (2021). <https://doi.org/10.1021/acscchembio.0c00937>
- 350 Christie, S. M. H., Kenner, G. W. & Todd, A. R. Nucleotides. Part XXV. A synthesis of flavin-adenine dinucleotide. *Journal of the Chemical Society (Resumed)*, 46-52 (1954). <https://doi.org/10.1039/JR9540000046>
- 351 DeLuca, C. & Kaplan, N. O. LARGE SCALE SYNTHESIS AND PURIFICATION OF FLAVIN ADENINE DINUCLEOTIDE. *Journal of Biological Chemistry* **223**, 569-576 (1956). [https://doi.org/https://doi.org/10.1016/S0021-9258\(18\)65165-8](https://doi.org/https://doi.org/10.1016/S0021-9258(18)65165-8)
- 352 Huennekens, F. M. & Kilgour, G. L. A NEW CHEMICAL SYNTHESIS OF FLAVIN-ADENINE-DINUCLEOTIDE AND ANALOGS1,2. *Journal of the American Chemical Society* **77**, 6716-6717 (1955). <https://doi.org/10.1021/ja01629a136>
- 353 Frago, S., Martínez-Júlviz, M., Serrano, A. & Medina, M. Structural analysis of FAD synthetase from *Corynebacterium ammoniagenes*. *BMC Microbiol* **8**, 160-160 (2008). <https://doi.org/10.1186/1471-2180-8-160>
- 354 Mishanina, T. V. & Kohen, A. Synthesis and application of isotopically labeled flavin nucleotides. *Journal of Labelled Compounds and Radiopharmaceuticals* **58**, 370-375 (2015). <https://doi.org/doi:10.1002/ilcr.3313>
- 355 Sebastián, M. *et al.* The FAD synthetase from the human pathogen *Streptococcus pneumoniae*: a bifunctional enzyme exhibiting activity-dependent redox requirements. *Scientific Reports* **7**, 7609 (2017). <https://doi.org/10.1038/s41598-017-07716-5>
- 356 Thorpe, C. & Massey, V. Flavin analog studies of pig kidney general acyl-CoA dehydrogenase. *Biochemistry* **22**, 2972-2978 (1983).
- 357 Yoshikawa, M., Kato, T. & Takenishi, T. A novel method for phosphorylation of nucleosides to 5'-nucleotides. *Tetrahedron Letters* **8**, 5065-5068 (1967). [https://doi.org/https://doi.org/10.1016/S0040-4039\(01\)89915-9](https://doi.org/https://doi.org/10.1016/S0040-4039(01)89915-9)
- 358 Stocker, A., Hecht, H.-J. & Bückmann, A. F. Synthesis, Characterization and Preliminary Crystallographic Data of N6-(6-carbamoylhexyl)-FAD-d-amino-acid Oxidase from Pig Kidney, a Semi-Synthetic Oxidase. *European Journal of Biochemistry* **238**, 519-528 (1996). <https://doi.org/https://doi.org/10.1111/j.1432-1033.1996.0519z.x>
- 359 Saleh, A., Compernelle, F. & Janssen, G. An Improved Synthesis of N6-(6-Aminoethyl)FAD. *Nucleosides and Nucleotides* **14**, 689-692 (1995). <https://doi.org/10.1080/1525779508012450>
- 360 김범태, 김승기, Lee, S.-J. & Hwang, K.-J. A Convenient and Versatile Synthesis of 2' (and 3')-Amino (and azido)-2' (and 3')-deoxyadenosine as Diverse Synthetic Precursors of Cyclic Adenosine Diphosphate Ribose (cADPR). *Bulletin of the Korean Chemical Society* **25**, 243-248 (2004). <https://doi.org/10.5012/BKCS.2004.25.2.243>
- 361 Karpeisky, A. *et al.* Scalable and efficient synthesis of 2'-deoxy-2'-N-phthaloyl nucleoside phosphoramidites for oligonucleotide synthesis. *Bioorganic & Medicinal Chemistry Letters* **12**, 3345-3347 (2002). [https://doi.org/https://doi.org/10.1016/S0960-894X\(02\)00744-8](https://doi.org/https://doi.org/10.1016/S0960-894X(02)00744-8)
- 362 Chapuis, H. & Strazewski, P. Shorter puromycin analog synthesis by means of an efficient Staudinger-Villars coupling. *Tetrahedron* **62**, 12108-12115 (2006). <https://doi.org/https://doi.org/10.1016/j.tet.2006.09.045>
- 363 Klinchan, C., Hsu, Y.-L., Lo, L.-C., Pluempunapat, W. & Chuawong, P. Synthesis of non-hydrolyzable substrate analogs for Aspartyl-tRNA synthetase. *Tetrahedron Letters* **55**, 6204-6207 (2014). <https://doi.org/https://doi.org/10.1016/j.tetlet.2014.09.060>
- 364 Bockman, M. R. *et al.* Targeting Mycobacterium tuberculosis Biotin Protein Ligase (MtBPL) with Nucleoside-Based Bisubstrate Adenylation Inhibitors. *Journal of Medicinal Chemistry* **58**, 7349-7369 (2015). <https://doi.org/10.1021/acs.jmedchem.5b00719>
- 365 Murthy, Y. V. S. N. & Massey, V. Chemical Modification of the N-10 Ribityl Side Chain of Flavins EFFECTS ON PROPERTIES OF FLAVOPROTEIN DISULFIDE OXIDOREDUCTASES (\*). *Journal of Biological Chemistry* **270**, 28586-28594 (1995). <https://doi.org/10.1074/jbc.270.48.28586>
- 366 Engst, S., Vock, P., Wang, M., Kim, J.-J. P. & Ghisla, S. Mechanism of Activation of Acyl-CoA Substrates by Medium Chain Acyl-CoA Dehydrogenase: Interaction of the Thioester Carbonyl with the Flavin Adenine Dinucleotide Ribityl Side Chain. *Biochemistry* **38**, 257-267 (1999). <https://doi.org/10.1021/bi9815041>
- 367 Kuhn, R., Reinemund, K., Weygand, F. & Ströbele, R. Über die Synthese des Lactoflavins (Vitamin B<sub>2</sub>). *Berichte der deutschen chemischen Gesellschaft (A and B Series)* **68**, 1765-1774 (1935). <https://doi.org/https://doi.org/10.1002/cber.19350680922>
- 368 Karrer, P., Schöpp, K., Benz, F. & Pfähler, K. Synthesen von Flavinen (Vorläuf. Mitteil.). *Berichte der deutschen chemischen Gesellschaft (A and B Series)* **68**, 216-219 (1935).
- 369 Karrer, P. & Meerwein, H. Modified flavin synthesis. *Helvetica Chimica Acta* **18**, 1130-1134 (1935).
- 370 Karrer, P. & Meerwein, H. F. Improved synthesis of lactoflavin and 6: 7-dimethyl-9-(l'-arabityl)-zso-alloxazin. *Helvetica Chimica Acta* **19**, 264-269 (1936).
- 371 Mansurova, M., Koay, M. S. & Gärtner, W. Synthesis and Electrochemical Properties of Structurally Modified Flavin Compounds. *European Journal of Organic Chemistry* **2008**, 5401-5406 (2008). <https://doi.org/https://doi.org/10.1002/ejoc.200800504>
- 372 Neti, S. S. & Poulter, C. D. Site-Selective Synthesis of 15N- and 13C-Enriched Flavin Mononucleotide Coenzyme Isotopologues. *The Journal of Organic Chemistry* **81**, 5087-5092 (2016). <https://doi.org/10.1021/acs.joc.6b00640>
- 373 Courjean, O. *et al.* A two-step synthesis of 7,8-dichloro-riboflavin with high yield. *RSC Advances* **2**, 2700-2701 (2012). <https://doi.org/10.1039/C2RA01211A>
- 374 Wood, A. C., Knight, D. W. & Richter, G. Rational improvement of the synthesis of 1-deazariboflavin. *Tetrahedron* **71**, 1679-1683 (2015). <https://doi.org/https://doi.org/10.1016/j.tet.2015.01.053>
- 375 Tishler, M., Pfister 3rd, K., Babson, R., Ladenburg, K. & Fleming, A. J. The reaction between o-aminoazo compounds and barbituric acid. A new synthesis of riboflavin. *Journal of the American Chemical Society* **69**, 1487-1492 (1947).
- 376 Kambe, T., Correia, B. E., Niphakis, M. J. & Cravatt, B. F. Mapping the Protein Interaction Landscape for Fully Functionalized Small-Molecule Probes in Human Cells. *Journal of the American Chemical Society* **136**, 10777-10782 (2014). <https://doi.org/10.1021/ja505517t>
- 377 Appel, R. Tertiary Phosphane/Tetrachloromethane, a Versatile Reagent for Chlorination, Dehydration, and P-N Linkage. *Angewandte Chemie International Edition in English* **14**, 801-811 (1975). <https://doi.org/https://doi.org/10.1002/anie.197508011>
- 378 Horne, J. E. *et al.* Rapid Mapping of Protein Interactions Using Tag-Transfer Photocrosslinkers. *Angewandte Chemie International Edition* **57**, 16688-16692 (2018). <https://doi.org/https://doi.org/10.1002/anie.201809149>
- 379 Sun, R. *et al.* Simple Light-Triggered Fluorescent Labeling of Silica Nanoparticles for Cellular Imaging Applications. *Chemistry – A European Journal* **23**, 13893-13896 (2017). <https://doi.org/https://doi.org/10.1002/chem.201703653>



- 380 Kumar, A. B. & Manetsch, R. Ammonia-free synthesis of 3-trifluoromethyl-3-phenyldiaziridine. *Synthetic Communications* **48**, 626-631 (2018). <https://doi.org/10.1080/00397911.2017.1354026>
- 381 Tamura, Y., Minamikawa, J., Sumoto, K., Fujii, S. & Ikeda, M. Synthesis and some properties of O-acyl- and O-nitrophenylhydroxylamines. *The Journal of Organic Chemistry* **38**, 1239-1241 (1973). <https://doi.org/10.1021/jo00946a045>
- 382 Chalker, J. M. *et al.* Methods for converting cysteine to dehydroalanine on peptides and proteins. *Chemical Science* **2**, 1666-1676 (2011). <https://doi.org/10.1039/C1SC00185J>
- 383 Glachet, T. *et al.* Iodonitrene in Action: Direct Transformation of Amino Acids into Terminal Diazirines and 15N2-Diazirines and Their Application as Hyperpolarized Markers. *Journal of the American Chemical Society* (2019). <https://doi.org/10.1021/jacs.9b07035>
- 384 Ibert, Q. *et al.* One-Pot Synthesis of Diazirines and 15N2-Diazirines from Ketones, Aldehydes and Derivatives: Development and Mechanistic Insight. *Advanced Synthesis & Catalysis* **363**, 4390-4398 (2021). <https://doi.org/https://doi.org/10.1002/adsc.202100679>
- 385 Markiewicz, W. & Wiewiórowski, M. A new type of silyl protecting groups in nucleoside chemistry. *Nucleic Acids Research* **5**, s185-s190 (1978).
- 386 Garegg, P. J. & Samuelsson, B. Oxidation of primary and secondary alcohols in partially protected sugars with the chromium trioxide-pyridine complex in the presence of acetic anhydride. *Carbohydrate Research* **67**, 267-270 (1978). [https://doi.org/https://doi.org/10.1016/S0008-6215\(00\)83749-0](https://doi.org/https://doi.org/10.1016/S0008-6215(00)83749-0)
- 387 Sugihara, Y., Tatsumi, S. & Kobori, A. Development of Novel Photoresponsive Oligodeoxyribonucleotides with a 2'-O-Diazirine-conjugated Adenosine for DNA Interstrand Crosslinking. *Chemistry Letters* **46**, 236-239 (2017). <https://doi.org/10.1246/cl.160998>
- 388 Neises, B. & Steglich, W. Simple Method for the Esterification of Carboxylic Acids. *Angewandte Chemie International Edition in English* **17**, 522-524 (1978). <https://doi.org/https://doi.org/10.1002/anie.197805221>
- 389 Pfleiderer, W. *et al.* Model Studies Towards the Automated Synthesis of tRNAs. *Nucleosides and Nucleotides* **10**, 377-382 (1991). <https://doi.org/10.1080/07328319108046483>
- 390 Rangelov, M. A., Vayssilov, G. N. & Petkov, D. D. Quantum chemical model study of the acyl migration in 2'(3')-formyl nucleosides. *International Journal of Quantum Chemistry* **106**, 1346-1356 (2006). <https://doi.org/https://doi.org/10.1002/qua.20892>
- 391 Griffin, B. E., Jarman, M., Reese, C. B., Sulston, J. E. & Trentham, D. R. Some Observations Relating to Acyl Mobility in Aminoacyl Soluble Ribonucleic Acids\*. *Biochemistry* **5**, 3638-3649 (1966). <https://doi.org/10.1021/bi00875a037>
- 392 Kremisky, J. N. & Sinha, N. D. Facile deprotection of silyl nucleosides with potassium fluoride/18-crown-6. *Bioorganic & Medicinal Chemistry Letters* **4**, 2171-2174 (1994).
- 393 Shimshock, S. J., Waltermire, R. E. & DeShong, P. A total synthesis of (+)-tiramdamycin B. *Journal of the American Chemical Society* **113**, 8791-8796 (1991).
- 394 Oltvoort, J. J., Kloosterman, M. & van Boom, J. H. Selective allylation of sugar derivatives containing the 1,1,3,3-tetraisopropylidisiloxane-1,3-diyl protective group. *Recueil des Travaux Chimiques des Pays-Bas* **102**, 501-505 (1983). <https://doi.org/https://doi.org/10.1002/recl.19831021201>
- 395 Nicolaou, K. & Webber, S. Stereocontrolled total synthesis of lipoxins B. *Synthesis* **1986**, 453-461 (1986).
- 396 Zhu, C. *et al.* Fully Automated Continuous Meso-flow Synthesis of 5'-Nucleotides and Deoxynucleotides. *Organic Process Research & Development* **18**, 1575-1581 (2014). <https://doi.org/10.1021/op5002066>
- 397 Cramer, F. & Neunhoeffer, H. Zur Chemie der „energiereichen Phosphate“, XV1) Reaktionen von Adenosin-5'-phosphorsäureimidazolid—eine neue Synthese von Adenosindiphosphat und Flavin-adenin-dinucleotid. *Chemische Berichte* **95**, 1664-1669 (1962). <https://doi.org/10.1002/cber.19620950714>
- 398 Smith, E. C. & Metzler, D. E. The Photochemical Degradation of Riboflavin. *Journal of the American Chemical Society* **85**, 3285-3288 (1963). <https://doi.org/10.1021/ja00903a051>
- 399 Holzer, W. *et al.* Photo-induced degradation of some flavins in aqueous solution. *Chemical Physics* **308**, 69-78 (2005). <https://doi.org/https://doi.org/10.1016/j.chemphys.2004.08.006>
- 400 Chen, L., Rejman, D., Bonnac, L., Pankiewicz, K. W. & Patterson, S. E. Nucleoside-5'-Phosphoimidazolides: Reagents for Facile Synthesis of Dinucleoside Pyrophosphates. *Current Protocols in Nucleic Acid Chemistry* **23**, 13.14.11-13.14.10 (2005). <https://doi.org/10.1002/0471142700.nc1304s23>
- 401 Saxon, E. & Bertozzi, C. R. Cell Surface Engineering by a Modified Staudinger Reaction. *Science* **287**, 2007-2010 (2000). <https://doi.org/doi:10.1126/science.287.5460.2007>
- 402 Saxon, E., Armstrong, J. I. & Bertozzi, C. R. A "Traceless" Staudinger Ligation for the Chemoselective Synthesis of Amide Bonds. *Organic Letters* **2**, 2141-2143 (2000). <https://doi.org/10.1021/ol006054v>
- 403 Omura, K. & Swern, D. Oxidation of alcohols by "activated" dimethyl sulfoxide. a preparative, steric and mechanistic study. *Tetrahedron* **34**, 1651-1660 (1978). [https://doi.org/https://doi.org/10.1016/0040-4020\(78\)80197-5](https://doi.org/https://doi.org/10.1016/0040-4020(78)80197-5)
- 404 Kim, B.-H. *et al.* Catenation of 1,1-dichlorotertaphenylsilole and 1,1-dichlorotetraphenylgermole to optoelectronic polymers. *Molecular Crystals and Liquid Crystals* **425**, 243-248 (2004). <https://doi.org/10.1080/15421400490506883>
- 405 Ahad, A. M., Jensen, S. M. & Jewett, J. C. A Traceless Staudinger Reagent To Deliver Diazirines. *Organic Letters* **15**, 5060-5063 (2013). <https://doi.org/10.1021/ol402404n>
- 406 Haraguchi, K. *et al.* Novel Stereoselective Entry to 2'-β-Carbon-Substituted 2'-Deoxy-4'-thionucleosides from 4-Thiofuranoid Glycols. *Organic Letters* **6**, 2645-2648 (2004). <https://doi.org/10.1021/ol040035u>
- 407 Chen, Y. & Topp, E. M. Quantitative Analysis of Peptide-Matrix Interactions in Lyophilized Solids Using Photolytic Labeling. *Molecular Pharmaceutics* **15**, 2797-2806 (2018). <https://doi.org/10.1021/acs.molpharmaceut.8b00283>
- 408 Amat-Guerri, F., López-González, M. M. C., Martínez-Utrilla, R. & Sastre, R. Synthesis and Spectroscopic Properties of New Rose Bengal and Eosin Y Derivatives. *Dyes and Pigments* **12**, 249-272 (1990). [https://doi.org/https://doi.org/10.1016/0143-7208\(90\)85017-1](https://doi.org/https://doi.org/10.1016/0143-7208(90)85017-1)
- 409 Insińska-Rak, M. & Sikorski, M. Riboflavin Interactions with Oxygen—A Survey from the Photochemical Perspective. *Chemistry – A European Journal* **20**, 15280-15291 (2014). <https://doi.org/https://doi.org/10.1002/chem.201403895>
- 410 Baptista, M. S. *et al.* Type I and Type II Photosensitized Oxidation Reactions: Guidelines and Mechanistic Pathways. *Photochemistry and Photobiology* **93**, 912-919 (2017). <https://doi.org/https://doi.org/10.1111/php.12716>
- 411 Gonçalves, L. C. P. *et al.* Boosting photobioredox catalysis by morpholine electron donors under aerobic conditions. *Catalysis Science & Technology* **9**, 2682-2688 (2019). <https://doi.org/10.1039/C9CY00496C>
- 412 Gonçalves, L. C. P. *et al.* Morpholine-based buffers activate aerobic photobiocatalysis via spin-correlated ion pair formation. *Catalysis Science & Technology* **9**, 1365-1371 (2019). <https://doi.org/10.1039/C8CY02524J>
- 413 Gonçalves, L. C. P. *et al.* Mutagenesis-Independent Stabilization of Class B Flavin Monooxygenases in Operation. *Advanced Synthesis & Catalysis* **359**, 2121-2131 (2017). <https://doi.org/10.1002/adsc.201700585>

- 414 Rial, D. V. *et al.* (Wiley Online Library, 2008).
- 415 Su, Q., Boucher, P. A. & Rokita, S. E. Conversion of a Dehalogenase into a Nitroreductase by Swapping its Flavin Cofactor with a 5-Deazaflavin Analogue. *Angewandte Chemie International Edition* **56**, 10862-10866 (2017). <https://doi.org/https://doi.org/10.1002/anie.201703628>
- 416 Grenga, P. N., Sumbler, B. L., Beland, F. & Prierer, R. Reductive amination agents: comparison of Na(CN)BH<sub>3</sub> and Si-CBH. *Tetrahedron Letters* **50**, 6658-6660 (2009). <https://doi.org/https://doi.org/10.1016/j.tetlet.2009.09.076>
- 417 Abdel-Magid, A. F., Carson, K. G., Harris, B. D., Maryanoff, C. A. & Shah, R. D. Reductive Amination of Aldehydes and Ketones with Sodium Triacetoxyborohydride. Studies on Direct and Indirect Reductive Amination Procedures 1. *The Journal of Organic Chemistry* **61**, 3849-3862 (1996). <https://doi.org/10.1021/jo960057x>
- 418 Chen, G. *et al.* Asymmetric oxidations at sulfur catalyzed by engineered strains that overexpress cyclohexanone monooxygenase. *New Journal of Chemistry* **23**, 827-832 (1999). <https://doi.org/10.1039/A902283J>
- 419 Swoboda, B. E. P. The relationship between molecular conformation and the binding of flavin-adenine dinucleotide in glucose oxidase. *Biochimica et Biophysica Acta (BBA) - Protein Structure* **175**, 365-379 (1969). [https://doi.org/https://doi.org/10.1016/0005-2795\(69\)90014-2](https://doi.org/https://doi.org/10.1016/0005-2795(69)90014-2)
- 420 Werner, W., Rey, H.-G. & Wielinger, H. Über die Eigenschaften eines neuen Chromogens für die Blutzuckerbestimmung nach der GOD/POD-Methode. *Fresenius' Zeitschrift für analytische Chemie* **252**, 224-228 (1970).
- 421 Baminger, U., Subramaniam, S. S., Renganathan, V. & Haltrich, D. Purification and characterization of cellobiose dehydrogenase from the plant pathogen *Sclerotium (Athelia) rolfsii*. *Applied and environmental microbiology* **67**, 1766-1774 (2001).
- 422 Bao, W. J., Usha, S. N. & Renganathan, V. Purification and Characterization of Cellobiose Dehydrogenase, a Novel Extracellular Hemoflavoenzyme from the White-Rot Fungus *Phanerochaete chrysosporium*. *Archives of Biochemistry and Biophysics* **300**, 705-713 (1993). <https://doi.org/https://doi.org/10.1006/abbi.1993.1098>
- 423 Syeda, S. S. *et al.* The Fungal Sexual Pheromone Sirenin Activates the Human CatSper Channel Complex. *ACS Chemical Biology* **11**, 452-459 (2016). <https://doi.org/10.1021/acschembio.5b00748>
- 424 König, W. & Geiger, R. Eine neue Methode zur Synthese von Peptiden: Aktivierung der Carboxylgruppe mit Dicyclohexylcarbodiimid unter Zusatz von 1-Hydroxy-benzotriazolen. *Chemische Berichte* **103**, 788-798 (1970). <https://doi.org/https://doi.org/10.1002/cber.19701030319>
- 425 Sun, D., Xu, H., Wijerathna, S. R., Dealwis, C. & Lee, R. E. Structure-Based Design, Synthesis, and Evaluation of 2'-(2-Hydroxyethyl)-2'-deoxyadenosine and the 5'-Diphosphate Derivative as Ribonucleotide Reductase Inhibitors. *ChemMedChem* **4**, 1649-1656 (2009). <https://doi.org/https://doi.org/10.1002/cmdc.200900236>
- 426 Smith, A. B. & Ott, G. R. Total synthesis of (-)-macrolactin A. *Journal of the American Chemical Society* **118**, 13095-13096 (1996).
- 427 Wallrodt, S. Synthesis and Characterisation of NAD<sup>+</sup> Analogues for the Cellular Imaging of Poly(ADP-Ribos)ylation. (2017).
- 428 Admas, T. H., Bernat, V., Heinrich, M. R. & Tschammer, N. Development of Photoactivatable Allosteric Modulators for the Chemokine Receptor CXCR3. *ChemMedChem* **11**, 575-584 (2016). <https://doi.org/10.1002/cmdc.201500573>
- 429 Längle, D. *et al.* Unique photoaffinity probes to study TGF $\beta$  signaling and receptor fates. *Chemical Communications* **55**, 4323-4326 (2019). <https://doi.org/10.1039/C9CC00929A>
- 430 Baughman, T. W., Sworen, J. C. & Wagener, K. B. The facile preparation of alkenyl metathesis synthons. *Tetrahedron* **60**, 10943-10948 (2004). <https://doi.org/https://doi.org/10.1016/j.tet.2004.09.021>
- 431 Luo, Y. & Hu, Y. Synthesis and Antifungal Activity of 2-Aryl-1,2,4-triazolo[1,5-a]pyridine Derivatives. *Archiv der Pharmazie* **339**, 262-266 (2006). <https://doi.org/https://doi.org/10.1002/ardp.200500227>
- 432 Lin, Y. A., Chalker, J. M., Floyd, N., Bernardes, G. J. L. & Davis, B. G. Allyl Sulfides Are Privileged Substrates in Aqueous Cross-Metathesis: Application to Site-Selective Protein Modification. *Journal of the American Chemical Society* **130**, 9642-9643 (2008). <https://doi.org/10.1021/ja8026168>
- 433 Ambroise, Y., Pillon, F., Mioskowski, C., Valleix, A. & Rousseau, B. Synthesis and Tritium Labeling of New Aromatic Diazirine Building Blocks for Photoaffinity Labeling and Cross-Linking. *European Journal of Organic Chemistry* **2001**, 3961-3964 (2001). [https://doi.org/https://doi.org/10.1002/1099-0690\(200110\)2001:20<3961::AID-EJOC3961>3.0.CO;2-R](https://doi.org/https://doi.org/10.1002/1099-0690(200110)2001:20<3961::AID-EJOC3961>3.0.CO;2-R)
- 434 Nassal, M. 4-(1-Azi-2, 2, 2-trifluoroethyl) benzoic acid, a highly photolabile carbene generating label readily fixable to biochemical agents. *Liebigs Annalen der Chemie* **1983**, 1510-1523 (1983).
- 435 Robins, M. J., Wilson, J. S. & Hansske, F. Nucleic acid related compounds. 42. A general procedure for the efficient deoxygenation of secondary alcohols. Regiospecific and stereoselective conversion of ribonucleosides to 2'-deoxynucleosides. *Journal of the American Chemical Society* **105**, 4059-4065 (1983). <https://doi.org/10.1021/ja00350a052>
- 436 Smicic, R. & Engels, J. W. Preparation of Zwitterionic Ribonucleoside Phosphoramidites for Solid-Phase siRNA Synthesis. *The Journal of Organic Chemistry* **73**, 4994-5002 (2008). <https://doi.org/10.1021/jo800451m>
- 437 Mechoulam, R., Danieli, N. & Mazur, Y. The structure and synthesis of oleuropeic acid. *Tetrahedron Letters* **3**, 709-712 (1962). [https://doi.org/https://doi.org/10.1016/S0040-4039\(00\)70937-3](https://doi.org/https://doi.org/10.1016/S0040-4039(00)70937-3)
- 438 Eldrup, A. B. *et al.* Structure-Activity Relationship of Purine Ribonucleosides for Inhibition of Hepatitis C Virus RNA-Dependent RNA Polymerase. *Journal of Medicinal Chemistry* **47**, 2283-2295 (2004). <https://doi.org/10.1021/jm030424e>
- 439 Ling Chwang, T., Williams, R. D. & Schieber, J. E. Synthesis of 2'-o-nitro-9- $\beta$ -d-arabinofuranosyladenine and 2'-o-nitro-9- $\beta$ -d-arabinofuranosylhypoxanthine. *Tetrahedron Letters* **24**, 3183-3186 (1983). [https://doi.org/https://doi.org/10.1016/S0040-4039\(00\)88130-7](https://doi.org/https://doi.org/10.1016/S0040-4039(00)88130-7)
- 440 福川, 清., 上田, 亨. & 平野, 孝. Synthesis of 2'-Substituted Derivatives of Neplanocin A (Nucleosides and Nucleotides. XLIV). *CHEMICAL & PHARMACEUTICAL BULLETIN* **31**, 1582-1592 (1983). <https://doi.org/10.1248/cpb.31.1582>
- 441 Van Calenberg, S. *et al.* Synthesis and Conformational Analysis of 2'-Deoxy-2'-(3-methoxybenzamido)adenosine, a rational-designed inhibitor of trypanosomal glyceraldehyde phosphate dehydrogenase (GAPDH). *Helvetica Chimica Acta* **77**, 631-644 (1994). <https://doi.org/https://doi.org/10.1002/hlca.19940770306>
- 442 Bressi, J. C. *et al.* Adenosine Analogues as Selective Inhibitors of Glyceraldehyde-3-phosphate Dehydrogenase of Trypanosomatidae via Structure-Based Drug Design. *Journal of Medicinal Chemistry* **44**, 2080-2093 (2001). <https://doi.org/10.1021/jm000472o>
- 443 MORISAWA, H., UTAGAWA, T., YAMANAKA, S. & YAMAZAKI, A. A New Method for the Synthesis of 2'-Amino-2'-deoxyguanosine and adenosine and Their Derivatives. *Chemical and Pharmaceutical Bulletin* **29**, 3191-3195 (1981).
- 444 Hobbs, J., Sternbach, H., Sprinzl, M. & Eckstein, F. Polynucleotides containing 2'-amino-2'-deoxyribose and 2'-azido-2'-deoxyribose. *Biochemistry* **12**, 5138-5145 (1973). <https://doi.org/10.1021/bi00749a018>
- 445 Song, W.-S., Liu, S.-X. & Chang, C.-C. Synthesis of l-Deoxyribonucleosides from d-Ribose. *The Journal of Organic Chemistry* **83**, 14923-14932 (2018). <https://doi.org/10.1021/acs.joc.8b02002>

- 446 Heinrich, M. *et al.* Chagosensine: A Riddle Wrapped in a Mystery Inside an Enigma. *Journal of the American Chemical Society* **142**, 6409-6422 (2020). <https://doi.org/10.1021/jacs.0c01700>